ACSP · Analog Circuits And Signal Processing

Hercules G. Dimopoulos

Analog Electronic Filters

Theory, Design and Synthesis

Springer

VISIT…

Analog Electronic Filters

ANALOG CIRCUITS AND SIGNAL PROCESSING

Series Editors:
Mohammed Ismail. *The Ohio State University*
Mohamad Sawan. *École Polytechnique de Montréal*

For further volumes:
www.springer.com/series/7381

Hercules G. Dimopoulos

Analog Electronic Filters

Theory, Design and Synthesis

Springer

Dr. Hercules G. Dimopoulos
Department Electronics
Technol. Educ. Inst. of Piraeus (T.E.I.)
P. Ralli & Thivon 250
Egaleo 12244
Greece
hdimop@teipir.gr

Series Editors:
Mohammed Ismail
205 Dreese Laboratory
Department of Electrical Engineering
The Ohio State University
2015 Neil Avenue
Columbus, OH 43210, USA

Mohamad Sawan
Electrical Engineering Department
École Polytechnique de Montréal
Montréal, QC, Canada

ISBN 978-94-007-2189-0 e-ISBN 978-94-007-2190-6
DOI 10.1007/978-94-007-2190-6
Springer Dordrecht Heidelberg London New York

Library of Congress Control Number: 2011938013

© Springer Science+Business Media B.V. 2012
No part of this work may be reproduced, stored in a retrieval system, or transmitted in any form or by any means, electronic, mechanical, photocopying, microfilming, recording or otherwise, without written permission from the Publisher, with the exception of any material supplied specifically for the purpose of being entered and executed on a computer system, for exclusive use by the purchaser of the work.

Cover design: VTeX UAB, Lithuania

Printed on acid-free paper

Springer is part of Springer Science+Business Media (www.springer.com)

To my beloved wife Kalliope for her affection, patience and wisdom

Preface

Filters are essential subsystems in a huge variety of electronic systems. Filter applications are innumerable; they are used for noise reduction, demodulation, signal detection, multiplexing, sampling, sound and speech processing, transmission line equalization and image processing, to name just a few. In practice, no electronic system can exist without filters. They can be found in everything from power supplies to mobile phones and hard disk drives and from loudspeakers and MP3 players to home cinema systems and broadband Internet connections.

This textbook introduces basic concepts and methods and the associated mathematical and computational tools employed in electronic filter theory, synthesis and design. Since the approximation problem must be solved before a filter can be designed, a significant part of the book is concerned with approximations in a manner that allows deep understanding and easy generalization. The approximation procedure uses the filter specifications to derive a circuit function, from which the electronic filter circuit can then be synthesized. The synthesis method to be used in order to derive an electronic circuit from a mathematical circuit function depends on the technology which is to be employed for the final implementation of the filter. Synthesis methods are therefore dependent on the technologies currently available and change as technology evolves. In this book, synthesis methods have been restricted to the classical passive and active-RC cases, which are excellent robust paradigms with high didactic value. More recent technologies like OTA-C, log-domain, current conveyors based circuits and so on are not presented as they are overly specialized for a general filter textbook which is aimed mainly at supporting students of undergraduate filter courses.

Most of the material of the book can be taught as part of undergraduate courses on filters. Chapter 1 is a general introduction to filter concepts and design methods and provides a basic background to these as well as the common language for filter synthesis and design. Chapter 2 deals with the classical polynomial approximations (Butterworth and Chebyshev) that lead to all-pole lowpass transfer functions without zeros. It also introduces the recently documented Pascal approximation. In Chap. 3, rational approximations are presented. Rational approximations, such as the inverse Chebyshev, lead to lowpass transfer functions with $j\omega$-axis zeros and gain or attenuation ripple in the stopband. Chapter 4 is exclusively devoted to a special rational approximation, the elliptic approximation, not only for its importance, but also because it has not been given the full attention it deserves in the literature due to the

complicated mathematics involved. In this chapter, all mathematical formulae are provided and the corresponding computational tools are explicitly presented.

Chapters 2–4 apply to lowpass filters. Chapter 5 presents the transformations that can be used for other types of filters, i.e. highpass, bandpass and band-reject filters. Chapter 6 provides an introduction to passive filters, while the actual design of such filters is dealt with in Chap. 7. The active-RC simulation of passive ladder filters is presented in Chap. 8.

Operational amplifiers and first and second order circuits are presented in Chaps. 9 and 10, while in Chap. 11 some specific filter synthesis mathematics is presented. Finally, Chap. 12 covers the synthesis of RLCM one-port circuits, used extensively in passive filter design.

I would like to express my gratitude to laboratory staff, Dr. Elena Sarri and Mr. Makis Zigiris for their help in preparing the manuscript and for drawing most of the figures. Special thanks are due to Mr. Miltos Poulizos for his assistance in drawing part of the figures. Finally, I would like to thank all my friends and colleagues for encouraging me to write this textbook and for all of the stimulating discussions we have had during the process.

Athens, Greece Hercules G. Dimopoulos

Contents

1 Introduction to Filter Concepts 1
1.1 Gain and Attenuation Functions 1
1.2 Ideal Transmission 4
1.2.1 Ideal Filters 5
1.3 Real Electronic Filters 7
1.3.1 Realizable Lowpass Filters 8
1.3.2 Realizable Highpass (HP) Filters 10
1.3.3 Realizable Bandpass (BP) Filters 11
1.3.4 Realizable Band-Reject (BR) Filters 11
1.4 Filter Technologies 12
1.5 Designing a Filter 16
1.5.1 Scaling and Normalization: Smart Simplification 17
1.5.2 Approximation: The Heart of Filter Design 18
1.6 Scaling and Normalization 22
1.6.1 Impedance Scaling 23
1.6.2 Frequency Scaling 24
1.6.3 Full Normalization 25
1.6.4 Prototype Filters 29
1.7 Circuit Order 30
1.8 Problems 33
References 34

2 All-Pole Approximations 37
2.1 Filter Specifications and Approximations 37
2.1.1 All-Pole Transfer Functions and Approximations 39
2.2 The Butterworth Approximation 41
2.2.1 Optimization Using β as a Design Parameter 44
2.2.2 The 3 dB Frequency of Butterworth Filters 46
2.2.3 The Cut-off Rate 47
2.2.4 The Normalized Butterworth Lowpass Transfer Function . 49
2.2.5 Table of Prototype Butterworth Filters 53
2.3 The Chebyshev Approximation 59
2.3.1 Chebyshev Polynomials 60

2.3.2 The All-Pole Chebyshev Approximation 61
2.3.3 The 3-dB Frequency and The Cut-off Rate 70
2.3.4 The Transfer Function 71
2.4 The Pascal Approximation 77
2.4.1 Optimizing the Pascal Approximation 84
2.4.2 Order Calculation 86
2.4.3 The Transfer Function 86
2.4.4 Design Examples 88
2.4.5 Comparison to Other Polynomial Approximations 91
2.5 Chebyshev and Pascal Design Tables 94
2.5.1 Table: Chebyshev Approximation 94
2.6 Problems 99
References 102

3 Rational Approximations 103
3.1 Introduction 103
3.2 Rational Approximations 104
3.3 The Inverse Chebyshev Approximation 110
3.3.1 Gain Analysis 113
3.3.2 Ripple Factor and Order Calculation 116
3.3.3 Optimization 118
3.4 The Inverse Pascal Approximation 130
3.4.1 The Pascal Rational Function $F_P(\Omega)$ 134
3.4.2 Definition of the Inverse Pascal Approximation 137
3.4.3 Gain Analysis 139
3.4.4 Filter Design Using the Inverse Pascal Approximation . . . 139
3.4.5 The Order Inequality and the Order Nomograph 141
3.4.6 The Transfer Function of the Inverse Pascal Filters 146
3.5 Inverse Pascal Tables 153
3.6 Problems 162
References 163

4 The Elliptic (Cauer) Approximation 165
4.1 Introduction 165
4.2 Calculation of $K(x)$ and $\mathrm{sn}(u, x)$ 169
4.2.1 The AGM and the Complete Elliptic Integral $K(x)$ 170
4.2.2 The Jacobi Nome q (Modular Constant) 170
4.2.3 Theta Functions and the Jacobi Elliptic Sine $\mathrm{sn}(u, x)$ 171
4.3 The Elliptic Approximation and the Elliptic Rational Function . . . 172
4.4 Properties of the Elliptic Rational Function $R_N(\Omega_S, \Omega)$ 173
4.5 Calculations 176
4.6 Specifications and the Order of the Elliptic Approximation 180
4.7 Elliptic Filter Design Optimization 184
4.7.1 Stopband Optimization $\Omega_{S\max}$ 187
4.8 The Transfer Function 190
4.9 Elliptic Filter Design Aids 204

4.9.1 The Order Nomograph . . . 204
4.9.2 Transfer Function Tables . . . 206
4.9.3 Computer Aided Elliptic Filter Design . . . 210
4.10 Problems . . . 211
References . . . 211

5 Frequency Transformations . . . 213
5.1 The Lowpass to Highpass (LP-HP) Frequency Transformation . . . 213
5.1.1 The LP-HP Frequency Transformation at Transfer Function Level . . . 215
5.1.2 The LP-HP Frequency Transformation at Component Level 217
5.2 The Lowpass to Bandpass (LP-BP) Frequency Transformation . . . 227
5.2.1 The LP-BP Frequency Transformation at Transfer Function Level . . . 232
5.2.2 The LP-BP Frequency Transformation at Component Level 234
5.3 The Lowpass to Band-Reject (LP-BR) Frequency Transformation . 237
5.3.1 The LP-BR Frequency Transformation at Transfer Function Level . . . 242
5.3.2 The LP-BR Frequency Transformation at Component Level 245
5.4 Problems . . . 247
References . . . 251

6 Passive Filters: Basic Theory and Concepts . . . 253
6.1 Power and Maximum Power Transfer . . . 254
6.2 Insertion (Transmission or Effective) Parameters . . . 261
6.2.1 The Effective Attenuation . . . 263
6.2.2 The Reflected Power and the Reflection Coefficient . . . 265
6.2.3 The Transmission Function $T(s)$ and the Characteristic Function $K(s)$ . . . 267
6.2.4 Relationship Between $\rho(s)$ and $T(s)$ or $H(s)$ . . . 268
6.3 The Passive Filters Design Procedure . . . 270
6.4 Determination of $Z_1(s)$ of a Lowpass Filter . . . 271
6.4.1 Determination of $Z_1(s)$ via $\rho(s)$ . . . 273
6.4.2 Determination of $Z_1(s)$ via $ABCD$ Two-Port Parameters . 275
6.5 Problems . . . 283
References . . . 287

7 Synthesis and Design of Passive Filters . . . 289
7.1 Preliminaries . . . 289
7.2 The Butterworth Approximation in Passive Filter Design . . . 291
7.2.1 Butterworth Filter Design by Analysis . . . 304
7.3 The Chebyshev Approximation in Passive Filter Design . . . 309
7.3.1 Even Order Passive Chebyshev Filters . . . 313
7.3.2 The Modified Chebyshev Approximation . . . 317
7.3.3 The Synthesis of Passive Chebyshev Filters . . . 321
7.4 The Pascal Approximation in Passive Filter Design . . . 332
7.4.1 Even Order Passive Pascal Filters . . . 339

7.4.2 The Modified Pascal Approximation . . . 349
7.5 The Elliptic Approximation in Passive Filter Design . . . 351
7.5.1 Odd Order Elliptic Passive Filters . . . 354
7.5.2 Even Order Elliptic Passive Filters . . . 359
7.6 Problems . . . 362
References . . . 363

8 Active Simulation of Passive Ladder Filters . . . 365
8.1 Inductance Simulation . . . 366
8.1.1 Riordan's Simulated Inductor . . . 366
8.1.2 Antoniou's Simulated Inductor . . . 369
8.1.3 Floating Simulated Inductors . . . 370
8.1.4 A General Approach . . . 373
8.1.5 A Single Op Amp Simulated Inductor . . . 375
8.2 Frequency Dependent Impedance Scaling . . . 380
8.3 Linear Transformation Active Filters . . . 383
8.3.1 Connection of Linearly Transformed Two-Ports . . . 387
8.3.2 Input Termination . . . 388
8.3.3 Output Termination . . . 390
8.3.4 Wave Active Filters . . . 394
8.3.5 Leap-Frog Filters . . . 395
8.4 Problems . . . 397
References . . . 402

9 Operational Amplifiers . . . 403
9.1 Introduction . . . 403
9.2 Operational Amplifier Models . . . 404
9.2.1 Voltage-Mode Operational Amplifiers . . . 404
9.2.2 Current-Mode Operational Amplifiers . . . 411
9.3 Basic Operational Amplifier Circuits . . . 416
9.3.1 Voltage Follower or Buffer . . . 416
9.3.2 Inverting Amplifier Circuits . . . 417
9.3.3 Circuits with Non-inverting Voltage Amplifier . . . 427
9.4 Integrators Revisited . . . 435
9.4.1 Inverting Integrators . . . 436
9.4.2 Non-inverting Integrators . . . 440
9.5 Operational Amplifier Imperfections . . . 442
9.5.1 The Frequency Dependent Finite Open-Loop Gain . . . 442
9.5.2 Other Imperfections . . . 443
9.5.3 Linear and Non-linear Operation . . . 444
9.6 Problems . . . 446
References . . . 447

10 Second Order Functions and Circuits . . . 449
10.1 Introduction . . . 449
10.2 Second Order Functions . . . 451

10.2.1 Second Order Lowpass (LP) Transfer Functions 451
10.2.2 Second Order Highpass (HP) Transfer Functions 456
10.2.3 Second Order Bandpass (BP) Transfer Functions 459
10.2.4 Second Order Band-Reject (BR) Transfer Functions . . . 461
10.2.5 Second Order Allpass (AP) Transfer Functions 462
10.3 Second Order Active-RC Circuits 464
10.3.1 Impedance and Frequency Scaling 464
10.3.2 The RC-CR or LP-HP Transformation 466
10.4 Sallen-Key Circuits 468
10.4.1 Sallen and Key Second Order Lowpass Filter 468
10.4.2 Sallen and Key Second Order Highpass Filter 470
10.4.3 Sallen and Key Second Order Bandpass Filter 471
10.5 Deliyannis Circuits 473
10.5.1 The Generalized Deliyannis Circuit 474
10.5.2 Friend's Biquad 476
10.6 Multiple Feedback (MF) Circuits 477
10.6.1 The Lowpass Multiple Feedback Circuit 477
10.6.2 The Highpass Multiple Feedback Circuit 478
10.6.3 The Bandpass Multiple Feedback Circuit 479
10.6.4 The Band-Reject Multiple Feedback Circuit 480
10.6.5 The Boctor Circuits 481
10.7 Current Generalized Immittance Converter (CGIC) Circuits . . . 482
10.7.1 The Basic CGIC Biquad 483
10.7.2 The Generalized (or 2-OA) CGIC Biquad 485
10.8 Biquads with 3 Operational Amplifiers 493
10.8.1 The Tow-Thomas Biquad 493
10.8.2 The State Variable or KHN Circuit 496
10.8.3 The Universal Circuit 497
10.8.4 The 3-OA CGIC Biquad 501
10.8.5 The Bainter 3-OA Circuit 503
10.9 Creation of Zeros 504
10.10 Problems 506
References 507

11 Some Filter Design Mathematics 509
11.1 Polynomials 509
11.1.1 Even and Odd Part of Polynomials 512
11.1.2 The Polynomial $P(-s)$ 512
11.2 Hurwitz Polynomials 513
11.2.1 The Continued-Fraction Property 514
11.3 Strictly Hurwitz Polynomials—Routh's Criterion 517
11.4 Rational Functions 519
11.5 Sturm's Theorem 520
11.6 Retrieving Polynomial $P(s)$ from $|P(j\omega)|$ 524
11.7 Partial Fractions Expansion—Pole Residues 528

11.8 Positive Real (PR) Functions . . . 529
11.8.1 Positive Real Functions: Definition I . . . 529
11.8.2 Positive Real Functions: Definition II . . . 530
11.8.3 Positive Real Functions: Definition III . . . 532
11.9 Problems . . . 535
References . . . 536

12 Synthesis of RLCM One-Port Circuits . . . 537
12.1 Pole Removals . . . 537
12.1.1 Removal of Pole at $s = 0$ . . . 538
12.1.2 Removal of Pole at $s = \infty$ . . . 540
12.1.3 Removal of a Conjugate Pole Pair at $s = \pm j\omega_1$ . . . 542
12.1.4 Partial Pole Removal . . . 544
12.1.5 Removal of a Constant . . . 545
12.2 Minimum Positive Real Functions . . . 546
12.3 Synthesis of Minimum Positive Real Functions . . . 551
12.3.1 Brune's Method with $X_1 < 0$ . . . 551
12.3.2 Brune's Method with $X_1 > 0$ . . . 556
12.4 Synthesis of LC One-Ports . . . 561
12.4.1 Properties of the LC Functions . . . 561
12.4.2 Foster Realizations . . . 563
12.4.3 Cauer Realizations . . . 565
12.5 Problems . . . 570
References . . . 572

Index . . . 573

Introduction to Filter Concepts

1

1.1 Gain and Attenuation Functions

An electric circuit can be represented by a diagram as shown in Fig. 1.1 and referred to as a block diagram. In the frequency (Laplace) domain, the voltage excitation and response, $E(s)$ and $V_2(s)$ respectively, will produce the voltage transfer function $H(s) = \frac{V_2(s)}{E(s)}$, which in turn yields the magnitude and phase frequency responses $G(\omega)$ and $\phi(\omega)$ respectively given for $s = j\omega$ as:

$$G(\omega) = |H(j\omega)| = \left|\frac{V_2(j\omega)}{E(j\omega)}\right| \qquad \phi(\omega) = \sphericalangle H(j\omega) \tag{1.1}$$

In the above equation, $\sphericalangle z$ denotes the *argument* of z.

The magnitude frequency response is commonly referred to as *plain gain* function or simply as *gain function* of the circuit. The corresponding *logarithmic gain* function $G_{dB}(\omega)$ is defined as

$$G_{dB}(\omega) = 20\log(G(\omega)) = 20\log\left(\frac{|V_2(j\omega)|}{|E(j\omega)|}\right) \text{ (dB)} \tag{1.2}$$

Both $G(\omega)$ and $G_{dB}(\omega)$ are real functions of ω. The plain gain function assumes non negative values only. The logarithmic gain, of course, can take any positive or negative value depending on whether the value of the plain gain is greater or less than unity. A negative value for $G_{dB}(\omega)$ simply means that the magnitude of the output is less than the magnitude of the input. The logarithmic gain can be positive or negative. Logarithmic gain should not be confused with *attenuation*, which is another term often used, based on the magnitude characteristic and defined as

$$A(\omega) = 20\log\left(\frac{|E(j\omega)|}{|V_2(j\omega)|}\right) = 20\log\left(\frac{1}{G(\omega)}\right) = -G_{dB}(\omega) \text{ (dB)} \tag{1.3}$$

Clearly attenuation is measured in dB and is the opposite of the logarithmic gain. Thus, it assumes positive and negative values. A negative value of the dB-gain simply means that the output is smaller than the input in which case the corresponding

H.G. Dimopoulos, *Analog Electronic Filters*, Analog Circuits and Signal Processing,
DOI 10.1007/978-94-007-2190-6_1, © Springer Science+Business Media B.V. 2012

Fig. 1.1 Block representation of a circuit

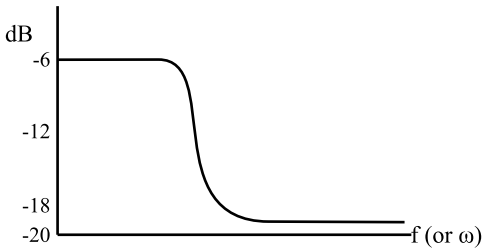

Fig. 1.2 Gain or attenuation?

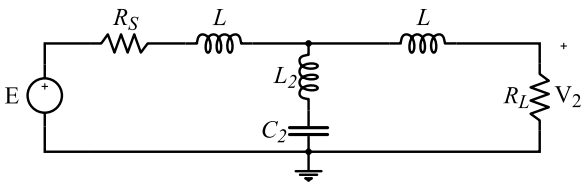

Fig. 1.3 A 3rd order passive elliptic lowpass filter

attenuation is positive. Therefore, a dB plot like the one shown in Fig. 1.2 is meaningless since it describes completely different situations if it represents a gain plot or an attenuation plot. If it is a gain plot, it describes a lowpass filter. If it is an attenuation plot, it describes a highpass filter.

It is observed that both $G_{dB}(\omega)$ and $A(\omega)$ are real functions of ω and have computational and plotting problems at those frequency points at which the plain gain $G(\omega)$ becomes zero, i.e. at those zeros of the transfer function $H(s)$ located on the $j\omega$-axis (known as transmission zeros). At these frequencies, the plain gain is zero, the logarithmic gain G_{dB} becomes $-\infty$ and the corresponding attenuation becomes ∞.

Example 1.1 Calculate and plot the voltage gain function of the circuit of Fig. 1.3 with $R_S = R_L = 1$, $L = 2.1819$, $L_2 = 0.0294$ and $C_2 = 0.9317$.

The voltage transfer function of the passive ladder circuit of Fig. 1.3 can be calculated using any circuit analysis method (e.g mesh or nodal analysis) to yield:

$$H(s) = \frac{R_L(s^2 L_2 C_2 + 1)}{s^3(2L_2 + L)LC_2 + s^2(R_S + R_L)(L + L_2)C_2 + s(2L + R_S R_L C_2) + R_S + R_L}$$

Using the given element values, the transfer function takes the numerical form:

$$H(s) = \frac{0.02739s^2 + 1}{4.55506s^3 + 4.12054s^2 + 5.2955s + 2}$$

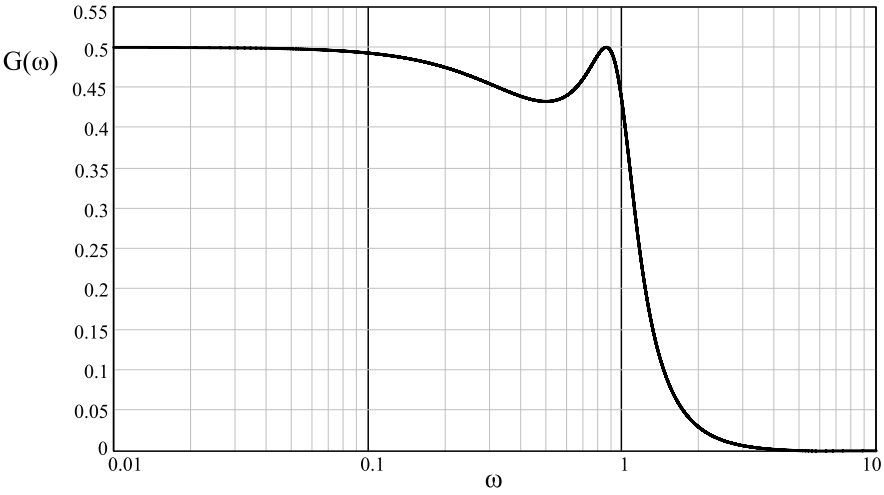

Fig. 1.4 Plain gain plot

For the plain gain $G(\omega)$ plot, we calculate the magnitude of $H(s)$ for $s = j\omega$:

$$G(\omega) = |H(j\omega)| = \frac{|1 - 0.02739\omega^2|}{|2 - 4.12054\omega^2 + j\omega(5.2955 - 4.5551\omega^2)|}$$
$$= \frac{|1 - 0.02739\omega^2|}{\sqrt{(2 - 4.12054\omega^2)^2 + \omega^2(5.2955 - 4.5551\omega^2)^2}}$$

In order to acquire an insight into the plot of $G(\omega)$ we need some typical values. It is clear that $G(0) = 0.5$ and that $G(6.0421) = 0$, since the numerator of ω becomes zero at $s = j6.0421$. It is also obvious that $G(\omega)$ tends to zero as ω tends to ∞ since the order of the denominator is higher than the order of the numerator. For a finer plot the calculation of several additional points is necessary, for which Mathcad or MATLAB could be conveniently used. The plot is shown in Fig. 1.4, where we have chosen to use a logarithmic frequency scale from $\omega = 0.01$ to $\omega = 10$.

It is not evident from this plot that the gain becomes zero at $\omega = 6.0421$ because of the neighboring low values. However, if we plot the logarithmic gain $G_{dB}(\omega) = 20\log(G(\omega))$, as we have done in Fig. 1.5, this important feature is highlighted. This aspect lends support for the use of logarithmic gain plots.

The plot of the attenuation

$$A(\omega) = -G_{dB}(\omega)$$
$$= -20\log\left(\frac{|1 - 0.02739\omega^2|}{\sqrt{(2 - 4.12054\omega^2)^2 + \omega^2(5.2955 - 4.5551\omega^2)^2}}\right)$$

is shown in Fig. 1.6.

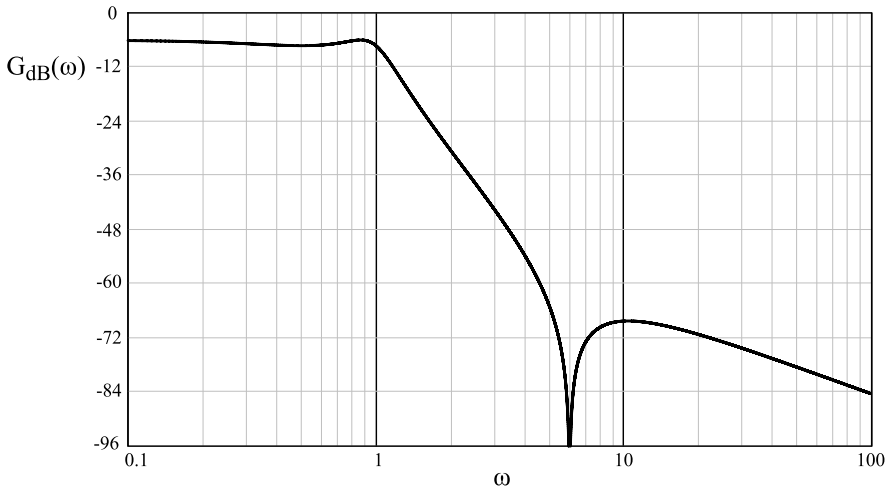

Fig. 1.5 Logarithmic gain plot

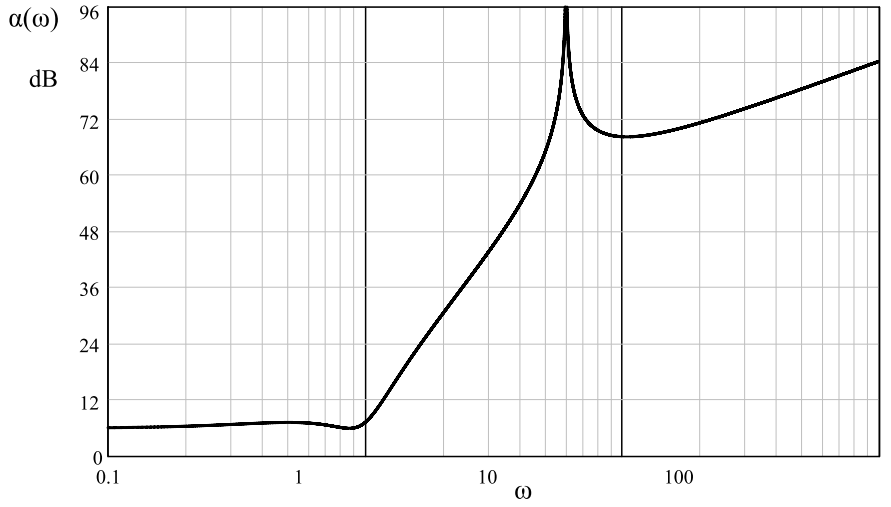

Fig. 1.6 Attenuation plot

1.2 Ideal Transmission

The gain $G(\omega) = |H(j\omega)|$ of a circuit depends in general on frequency and does not remain constant for all frequencies (in fact it can be shown that it can never be exactly constant over a non-zero segment of the frequency axis). As a result, the frequencies contained in a signal pass through a circuit and will have their amplitudes modified according to this gain to produce an output that differs from the input signal. This is called *amplitude distortion*. In addition, from the phase response of

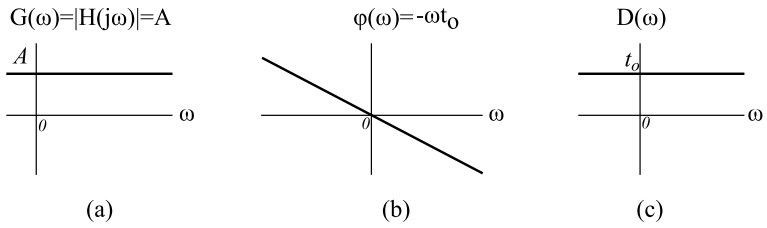

Fig. 1.7 Ideal transmission characteristics

the circuit $\phi(\omega) = \sphericalangle H(j\omega)$ is not in general directly proportional to frequency, i.e. $\phi(\omega) \neq t_o\omega$, and this will lead to different delay times for different frequencies, thereby producing a group delay distortion. The group delay is the time required for each frequency to pass through the system, since delay is given by:

$$D(\omega) = -\frac{d}{d\omega}\phi(\omega) \text{ (s)} \tag{1.4}$$

Thus, even if there is no amplitude distortion, frequencies that constitute the input signal will pass through the circuit with different delays producing an output signal which is different from the input signal. This is called *group delay distortion*, which is directly related to *phase distortion*.

It is apparent that if a signal is to pass through a system without any distortion, the gain function must be constant with frequency, i.e. $G(\omega) = |H(j\omega)| = A$ and the phase function must be linear of the form $\phi(\omega) = t_o\omega$. This is illustrated in Fig. 1.7.

The transfer function of such an ideal system is $H(j\omega) = Ae^{-j\omega t_o}$ and its corresponding impulse response is $h(t) = A\delta(t - t_o)$. This ideal system that performs the *ideal* or *distortionless* transmission will have an input-output relationship $y(t) = Ax(t - t_o)$, that is to say its output in time is identical to the input but scaled by A and shifted by t_o. Such a system is of no use in filtering applications where the objective is to shape the spectrum of the input signal.

1.2.1 Ideal Filters

The *ideal lowpass filter* is an ideal transmission system with transfer function:

$$H(j\omega) = \begin{cases} e^{-j\omega t_o} & \text{for } |\omega| \leq \omega_C \\ 0 & \text{for } |\omega| > \omega_C \end{cases} \tag{1.5}$$

or $H(j\omega) = e^{-j\omega t_o}[u(\omega + \omega_C) - u(\omega - \omega_C)]$.

Frequency ω_C is called *cut-off frequency*. For the ideal lowpass filter, we have $|H(j\omega)| = 1$ for $|\omega| \leq \omega_C$ and $|H(j\omega)| = 0$ for $|\omega| > \omega_C$. Moreover, the phase is $\phi(\omega) = \sphericalangle H(j\omega) = -\omega t_o$. The constant gain allows all frequencies from $-\omega_C$ to $+\omega_C$ to pass with the same gain while the linear phase ensures that these frequencies

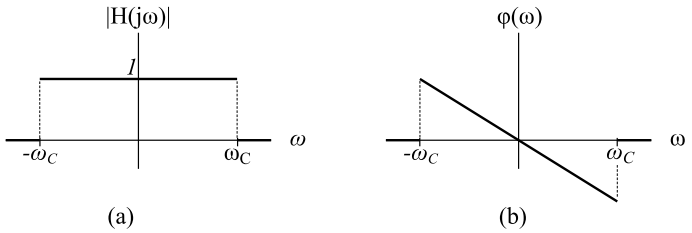

Fig. 1.8 Ideal lowpass filter characteristics

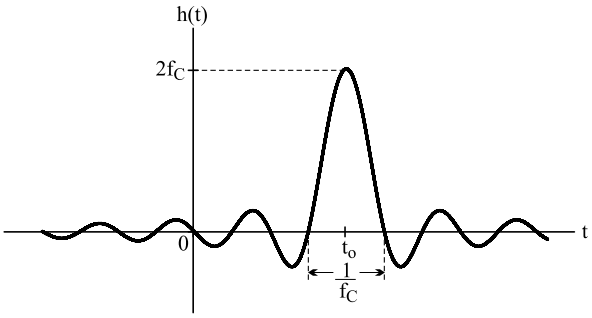

Fig. 1.9 The impulse response of the ideal lowpass filter

pass with constant delay t_o. Frequencies with $|\omega| > \omega_C$ are completely removed. Figure 1.8 shows graphically the gain and phase characteristics of the ideal lowpass filter, which as is shown below, cannot be realized by a causal system.

The impulse response of the ideal lowpass filter with the transfer function of (1.5) can be determined by using the inverse Fourier transform of $H(j\omega)$:

$$\begin{aligned} h(t) &= \frac{1}{2\pi}\int_{-\infty}^{\infty} H(j\omega)e^{j\omega t}\,d\omega = \frac{1}{2\pi}\int_{-\omega_C}^{\omega_C} |H(j\omega)|e^{-j\omega t_o}e^{j\omega t}\,d\omega \\ &= \frac{1}{2\pi}\int_{-\omega_C}^{\omega_C} e^{j\omega(t-t_o)}\,d\omega = \frac{\omega_C}{\pi}\frac{\sin(\omega_C(t-t_o))}{(t-t_o)\omega_C} \\ &= 2f_C\,\mathrm{sinc}(2f_C(t-t_o)) \quad \text{where } f_C = \frac{\omega_C}{2\pi} \end{aligned} \tag{1.6}$$

The time plot of the impulse response $h(t) = 2f_C\,\mathrm{sinc}[2f_C(t-t_o)]$ of the ideal lowpass filter is shown in Fig. 1.9. It is evident that the ideal lowpass filter produces a response to the impulse excitation for $t < 0$, that is to say before the excitation is applied, as if it can predict that $\delta(t)$ will be applied at $t = 0$. This makes the ideal lowpass filter *non causal*. Such systems are not realizable with physical components.

It can be demonstrated in a similar manner that the ideal highpass, bandpass and band-reject filters are also not realizable. However, as an aside, and under very careful convergence conditions, it can be observed that as the cut-off frequency $f_C \to \infty$, the ideal lowpass filter becomes an ideal allpass filter. Its impulse response $h(t)$ becomes zero everywhere except for $t = t_o$, i.e. it is a delta function

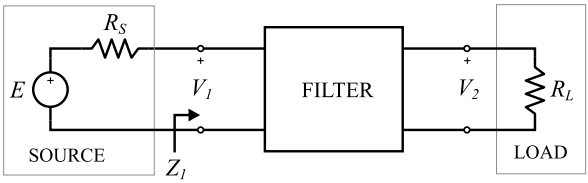

Fig. 1.10 The filter model

at t_o. This specific impulse response can be produced by a causal system and therefore this singular case of an ideal allpass filter can exist. In fact, it represents a system that simply shifts the excitation by t_o.

1.3 Real Electronic Filters

A filter is inserted between two sections of an electronic system in order to control the power transferred from one to the other in a desired way that depends on frequency. Such power control is achieved by shaping the spectrum of the input signal (Parseval's theorem) by leaving the frequencies of the passband almost unaffected (introducing zero or low and tolerable attenuation) and by eliminating or reducing the rest of the spectrum, through the introduction of high attenuation which may be occasionally infinite on a finite set of frequency points. The section of the system that provides the power to be controlled by the filter is usually represented by its Thevenin equivalent and represents the *source* of the filter with source resistance R_S. The section that follows the filter is the *load* of the filter and is represented by a resistor R_L. This is shown in Fig. 1.10.

The voltage transfer function of the complete system is

$$H(s) = \frac{V_2(s)}{E(s)} \tag{1.7}$$

and the corresponding *transmission function*

$$T(s) = \frac{1}{H(s)} = \frac{E(s)}{V_2(s)} \tag{1.8}$$

The associated gain functions are

$$G(\omega) = |H(j\omega)| = \frac{|V_2(j\omega)|}{|E(j\omega)|} \qquad G_{dB}(\omega) = 20\log(G(\omega)) \tag{1.9}$$

and the attenuation function

$$A(\omega) = 20\log(|T(j\omega)|) = 20\log\left(\frac{1}{|H(j\omega)|}\right) = -20\log(G(\omega))\ \text{dB} \tag{1.10}$$

Filters are designed to satisfy such magnitude specifications firstly by relaxing the stringent equality requirements for the gain and secondly by neglecting the phase or delay characteristics. In some filter design applications, the filter requirements im-

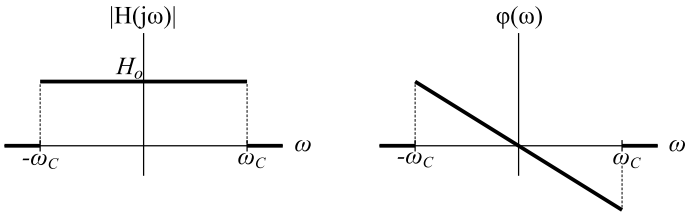

Fig. 1.11 Gain and phase characteristics of the ideal lowpass filter

pose not only magnitude specifications, but also some phase or delay requirements. In these cases, filter designers prefer to design the filter in two stages. The first is concerned with satisfying the magnitude specifications while the second stage involves the design of a cascaded additional filter which minimally disturbs the gain and improves the phase response to the required form. The design of filters from phase or delay specifications is a very specialized and rare task beyond the scope of this book.

When a filter is inserted between source and load, as in Fig. 1.10, it introduces the specified frequency dependent gain. This frequency dependence is often called *selectivity*. In the ideal case, selectivity is expressed by constant zero gain (infinite attenuation) in some frequency bands, referred to as *stopbands*, and constant zero attenuation in other frequency bands, called *passbands*. Unfortunately, keeping absolutely constant magnitude characteristics in a frequency band cannot be achieved by causal (realizable) systems which, in addition to this physical constraint, have magnitude characteristics that are expressed by continuous functions and cannot "jump" instantly from one value to another.

1.3.1 Realizable Lowpass Filters

According to Sect. 1.2.1, the ideal lowpass filter is described by the gain and phase characteristics of Fig. 1.11, which correspond to the transfer function

$$H(j\omega) = \begin{cases} H_o e^{-j\omega t_o} & \text{for } |\omega| \le \omega_C \\ 0 & \text{for } |\omega| > \omega_C \end{cases} \tag{1.11}$$

The gain function $|H(j\omega)|$ and the phase function $\phi(\omega) = \sphericalangle H(j\omega)$ of a circuit are in fact the magnitude and phase spectra respectively of its impulse response $h(t)$. As such, for systems with real components, $|H(j\omega)|$ is an even function of ω and $\phi(\omega)$ is an odd function of ω. In the study of signals, double sided spectra, like those in Fig. 1.11 are preferred, showing the functions for $-\infty < \omega < \infty$. In circuit theory and design, however, where we deal with real and positive frequencies, we prefer the single-sided spectra like those in Fig. 1.12, i.e. plots for $\omega \ge 0$. These plots are not called spectra any more (although they are), but *magnitude* and *phase response* respectively.

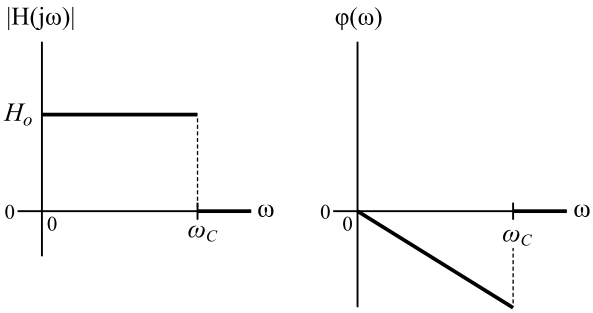

Fig. 1.12 Gain and phase characteristics of the ideal lowpass filter

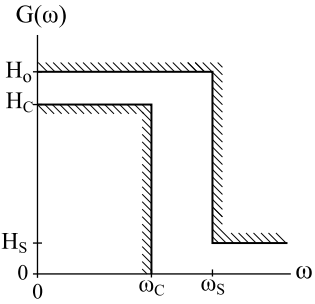

Fig. 1.13 Specifications of a realizable lowpass filter

An ideal lowpass filter which is non-causal is non-realizable. We can perceive the non-realizability as being due to two reasons: The first is that the gain of electric circuits cannot be kept absolutely constant over a frequency band. The second reason is that gain functions are continuous functions of ω and cannot exhibit a jump from H_o down to 0 at the cut-off frequency of Fig. 1.12.

However, the ideal lowpass filter characteristics can be relaxed through allowing certain tolerable deviations from their ideal behavior, as shown in Fig. 1.13. Thus in the passband, for frequencies $0 \leq \omega_C$, the gain can take values from H_o to H_C, a value very near H_o. The value H_C indicates the minimum allowed gain in the passband.

Since the gain cannot jump from its higher values to lower values, in real filters the stopband does not start at ω_C, but at a higher frequency ω_S. A new band, called the transition band, is created to allow the gain fall from its high to low values from ω_C to ω_S. In the stopband, starting now at ω_S, the *stopband edge frequency*, the gain is not zero, but less than a value H_S that is much smaller than H_o and H_C and expresses the maximum allowed value of the gain in the stopband. These three quantities, H_C, H_S and ω_S, determine the tolerances of the approximation of the strict characteristics of the ideal lowpass filter, which correspond to $H_C = H_o$, $H_S = 0$ and $\omega_S = \omega_C$. It will be proven later that the complexity of the filter circuit depends heavily on the strictness of these tolerances.

The five quantities H_o, H_C, H_S, ω_C and ω_S constitute the magnitude specifications of the realizable lowpass filter and are dictated by the requirements of the system in which the filter will be used.

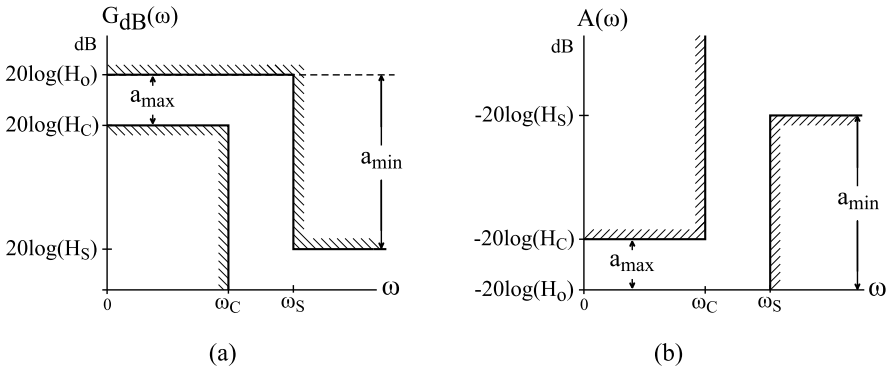

Fig. 1.14 Specifications in terms of (**a**) logarithmic gain (**b**) attenuation

Filter specifications can also be given in terms of the logarithmic gain or the attenuation function, as shown in Fig. 1.14.

If Figs. 1.13 and 1.14a describe the same filter, then

$$G_o = 20\log(H_o), \qquad G_C = 20\log(H_C), \qquad G_S = 20\log(H_S)$$
$$\text{and } H_o = 10^{\frac{G_o}{20}},\ H_C = 10^{\frac{G_C}{20}},\ H_S = 10^{\frac{G_S}{20}} \tag{1.12}$$

Very often, filter specifications are described by two positive numbers $\alpha_{\max}$ (or α_{MAX} or α_p) and $\alpha_{\min}$ (or α_{MIN} or α_s) that correspond to the allowed fluctuation of the logarithmic gain (or the attenuation) in dB in the passband and the stopband respectively (see Fig. 1.14a and b). These positive $\alpha_{\max}$ and $\alpha_{\min}$ are related to the plain gain specifications through the following relationships:

$$\alpha_{\max} = 20\log\left(\frac{H_o}{H_C}\right) \qquad \alpha_{\min} = 20\log\left(\frac{H_o}{H_S}\right) \tag{1.13}$$

$$\frac{H_o}{H_C} = 10^{\frac{\alpha_{\max}}{20}} \qquad \frac{H_o}{H_S} = 10^{\frac{\alpha_{\min}}{20}} \tag{1.14}$$

From the two positive numbers $\alpha_{\max}$ and $\alpha_{\min}$ (in dB), we see that the passband gain can vary from its maximum value $G_o = 20\log(H_o)$ down to $G_o - \alpha_{\max}$ and in the stopband, the gain must remain under $G_o - \alpha_{\min}$. This is shown in Fig. 1.14. If the value of G_o is not given, it can be taken equal to 0, a value that corresponds to $H_o = 1$.

1.3.2 Realizable Highpass (HP) Filters

Figure 1.15a shows the plot of the plain gain $G(\omega) = |H(j\omega)|$ of the ideal highpass filter with zero gain in the stopband 0–ω_C and constant gain H_o in the passband $\omega > \omega_C$. The realizable highpass specifications are shown in Fig. 1.15b. Note that

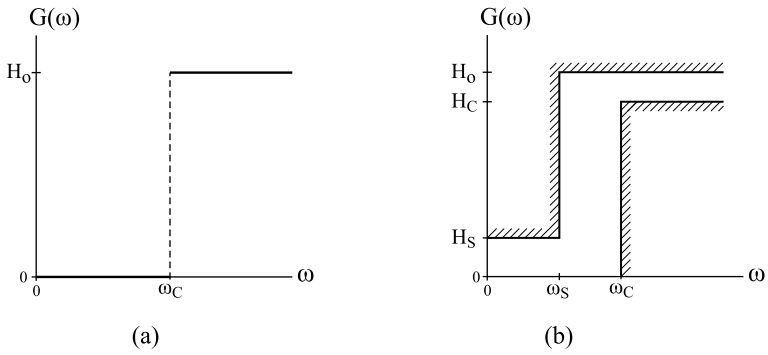

Fig. 1.15 Highpass filter specifications

in the case of highpass filters, the stopband edge frequency ω_S is smaller than the cutoff frequency ω_C. Figures 1.15c and show the specifications of highpass filters in terms of the logarithmic gain and attenuation respectively.

1.3.3 Realizable Bandpass (BP) Filters

Figure 1.16a shows the plain gain $G(\omega) = |H(j\omega)|$ of the ideal bandpass filter with zero gain in the stopbands 0–ω_{C1} and $\omega > \omega_{C2}$. For the passband $\omega_{C1} \leq \omega \leq \omega_{C2}$, the gain remains constant at H_o. The corresponding realizable bandpass specifications are shown in Fig. 1.16b. The width of the passband is referred to as bandwidth BW of the bandpass filter with $BW = \omega_{C2} - \omega_{C1}$. The geometric mean ω_o of ω_{C1} and ω_{C2}, i.e. $\omega_o = \sqrt{\omega_{C1}\omega_{C2}}$, is referred to as the *center frequency* of the bandpass filter. Figures 1.16c and d show the specifications of bandpass filters in terms of the logarithmic gain and attenuation respectively.

1.3.4 Realizable Band-Reject (BR) Filters

Figure 1.17a shows the plain gain $G(\omega) = |H(j\omega)|$ of the ideal *band-reject* or *band-stop* filter with zero gain in the stopband $\omega_{C1} < \omega < \omega_{C2}$. For the passbands 0–$\omega_{C1}$ and $\omega > \omega_{C2}$ the gain remains constant H_o. The corresponding realizable band-reject specifications are shown in Fig. 1.17b.

The frequency width $BW = \omega_{C2} - \omega_{C1}$ of the passbands is referred to as bandwidth BW of the band-reject filter. The width $BW_S = \omega_{S2} - \omega_{S1}$ of the stopband defines BW_S, which is very important in the BR filter design. The geometric mean ω_o of ω_{S1} and ω_{S2}, i.e. $\omega_o = \sqrt{\omega_{S1}\omega_{S2}}$, is referred to as the *center frequency* of the band-reject filter. Figures 1.17c and d show the specifications of the real band-reject filters in terms of the logarithmic gain and attenuation respectively.

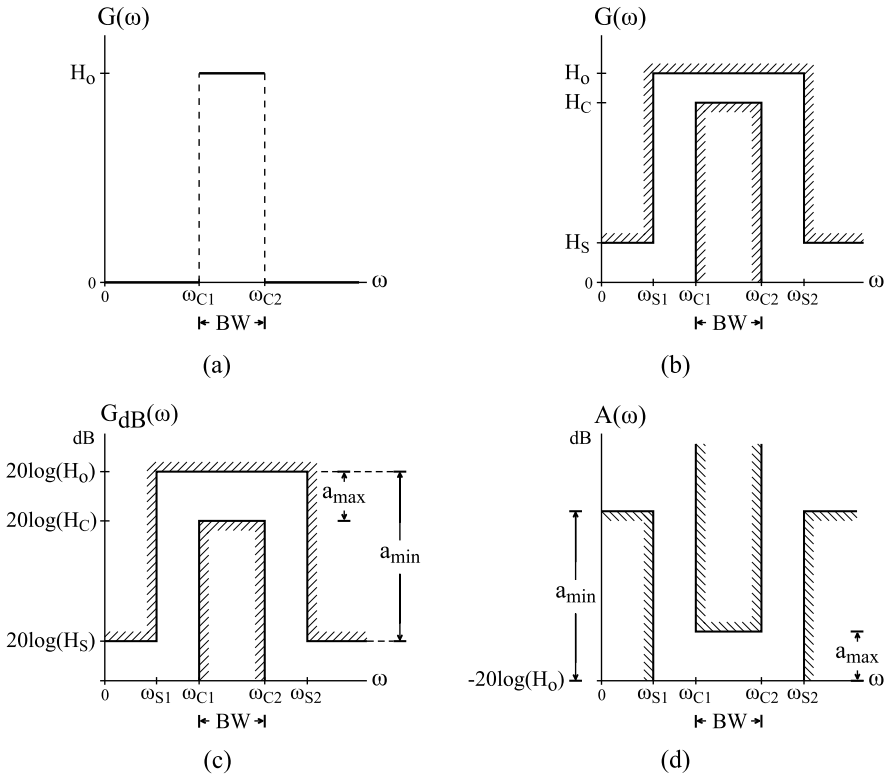

Fig. 1.16 Bandpass filter specifications

1.4 Filter Technologies

Filters process and shape the spectra of the electric signals. As such, filters are very important subsystems in many electronic systems and especially in communications systems. Filter applications are innumerable and filters are used for noise reduction, demodulation, signal detection, multiplexing, sampling, sound and speech processing, transmission line equalization, image processing, to name some. In practice, there is no electronic system without filters. We find them from power supplies to mobile phones and hard disk drives and from loudspeakers and MP3 players to home cinema systems and broadband Internet connections.

A filter takes a signal in its input, and creates the desirable output according to its characteristics. Filters can be classified in three major categories in relation to their input signal, their internal signals and the output signals:

i. Continuous-time (CT)
ii. Sampled-data and
iii. Discrete-time

Continuous-time signals are those that exist in any time and can be described by functions of time t for any value of t.

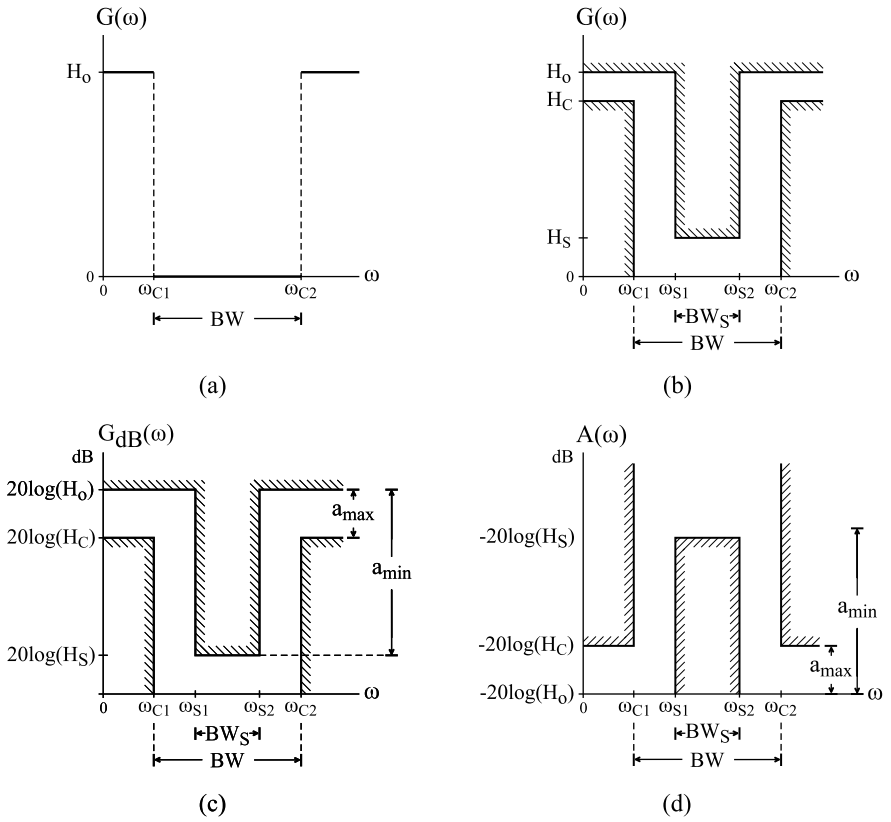

Fig. 1.17 Band-reject filter specifications

Discrete-time signals are defined only in discrete time instants and can be described by a function $f(nT)$ with $n_1 \leq n \leq n_2$ where $n_1 > -\infty$ and $n_2 < \infty$. The value of discrete-time signals for $nT < t < (n+1)T$ can be zero or undefined, for as far as the processing system is concerned, it is in general indifferent to this value. The frequency spectrum of discrete-time signals is given by z-transform on the unity circle $|z|$ in the z-plane.

Sampled-data signals are expressed with impulse signals as

$$f_S(t) = \sum_{n=-\infty}^{\infty} f(nT)\delta(t - nT)$$

where $f(t)$ is a continuous time signal and T the sampling period. The sampled signals $f_S(t)$ have zero value for $nT < t < (n+1)T$ and their frequency spectrum is given by the Fourier transform, as in case of continuous time signals.

The characterization *analogue* or *digital* refers to the signals for which the appropriate filters have been designed. In the case of analogue filters, the filters are designed for continuous-time electric signals, voltages or currents. In digital filters, the signals are coded into a digital form. Filters that deal with continuous time or sampled-data signals are analogue. Filters that handle discrete-time signals can be analogue or digital.

A general classification of analogue electronic filters could be as follows:

1. Passive RLCM filters that are realized using resistors, inductors, capacitors and ideal transformers.
2. Active-RC filters realized using operational amplifiers, resistors and capacitors.
3. Integrated MOS-C filters that are in fact active-RC filters where resistors have been replaced by suitably connected and biased MOSFETs.
4. Integrated OTA-C or $g_m - C$ filters. These use operational transducer amplifiers (OTA) instead of operational amplifiers. OTAs in fact convert voltages into currents and can be realized with simple and easily integrated circuits and can operate at higher frequencies than the operational amplifier.
5. Current-mode integrated filters.
6. Active switched capacitor filters designed for discrete-time signals and realized using operational amplifiers, capacitors and switches.
7. Microwave filters with distributed parameters (waveguides) and microwave filters based on microwave resonators and cavities.
8. Crystal filters based on piezoelectric resonators that behave like resonant LC circuits.
9. Mechanical and electromechanical filters based on mechanical and electromechanical resonators.

Microwave, crystal, mechanical, electromechanical filters, as well as some very special cases such as acoustic delay line filters, ultrasonic filters and surface acoustic filters etc. are beyond the scope of this textbook.

Each of the above category of analogue filters refers to the technology used to implement the transfer function which satisfies given specifications. The technology depends mainly on the operating frequency, the need for integration and the environment the filter is to operate within.

Figure 1.18 shows an approximate diagram of the frequency range in which each analogue filter technology can be used. Upper and lower limits are indicative and change as filters are still a "hot" research subject due to the constantly increasing need for highly selective, high frequency and low power consumption filter circuits.

The revision of filter design methodology is the most recent development in the area. Instead of treating the filter as handling voltage signals and implemented using voltage described sections, current logic has been introduced. This has led to the employment of current-handling sections which have proved to be very effective since current-mode building blocks can be implemented with simpler and more easily integrated circuits, and can perform much better at high frequencies than their voltage-mode counterparts. In this filter category fall, for example, the current-mode dual output-OTA-C filters, current conveyors filters (CCI, CCII, CCII+) as well as Log Domain filters.

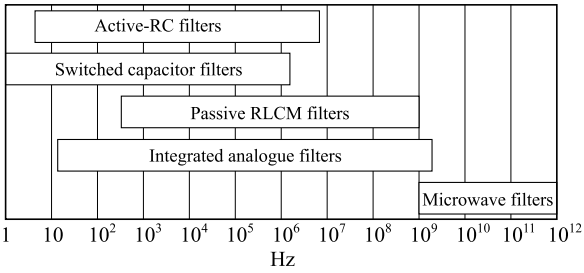

Fig. 1.18 Indicative frequency range for some filter technologies

Operating frequency is not the unique criterion for the choice of technology and in most cases there are more filter technologies that can be employed. In the MHz region for example, passive, active-RC, switched capacitor and integrated filters can be used. For decisions regarding use, some other factors must be taken into account, such as the availability of DC power, the kind of signals to be processed by the filter (sampled or not), the need for integrating the filter as a part of the total system and finally the cost.

The diagram of Fig. 1.18 shows that analogue integrated filters cover a wide range of operating frequencies. The design of such filters is based on the design of active-RC filters, which in turn may require the active simulation of a passive RLCM filter. This means that in order to design an analogue integrated filter it may be necessary to design a passive RLC filter in the first place and simulate it with an active-RC circuit. Bearing this in mind, passive RLC and active-RC filter design becomes very important and is the main scope of this textbook.

In passive filter design, the passive elements that are used to influence the selectivity of a circuit are, by and large, the inductor and the capacitor (LC circuits). Resistors may be used to reduce selectivity to a desirable or tolerable level in order to improve, for example, the time domain or group delay performance of a circuit. These LC circuits:

(a) can satisfy any practical filter specifications, no matter how strict they are
(b) need a minimum number of components
(c) can be designed so that they can maximize the power transferred from source to load in some frequencies in their passband.

This last feature has been proved to be essential in ensuring the low sensitivity in highly-selective high-precision filters.

Two circuit topologies are used in passive-LC filter design, the lattice and the ladder, shown in Fig. 1.19a and b respectively.

The lattice structure is inserted between source and load, and its component impedances $Z_A(s)$ and $Z_B(s)$ can be determined to satisfy a given set of filter specifications. However, the lattice does present some disadvantages when compared to the ladder topology. Specifically, firstly for a given set of requirements, it needs more lossless elements than the corresponding ladder, and secondly it presents high sensitivity to component changes. This is due to the fact that in order to realize a transmission zero, a bridge equilibrium is required with $|Z_A(j\omega)| = |Z_B(j\omega)|$. Moreover, the two branches Z_A must be absolutely identical and this requires many

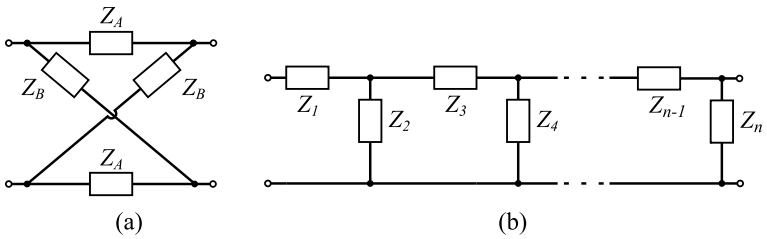

Fig. 1.19 (**a**) Lattice. (**b**) Ladder structure

and very precise components. The same is true for the two branches Z_B, thereby raising the cost and making tuning of such filters very difficult. These disadvantages limit the use of the lattice topology to electromechanical filters mainly due to the inherent ability to exploit the properties of the electromechanical resonators. Lattice-LC circuits are also used as phase shifting circuits.

The ladder-LC circuit topology can be used to satisfy any filter specifications employing a low number of lossless elements and without the problems of the lattice. In Fig. 1.19b, the horizontal branches are called *series arms* and the vertical branches, *shunt arms*. All branches Z_k of the LC ladder are LC combinations, and ladder-LC circuits are used almost exclusively in the design of passive filters presenting minimum sensitivity in the passband. If there is a transmission zero at ω_z in the stopband, it is created either by one series arm whose admittance becomes zero at that frequency, or by a shunt arm, whose impedance becomes zero at ω_z. This fact makes filter tuning simpler than in the case of lattice circuits. Finally, an nth order transfer function can be realized with lossless ladder circuits with n lossless arms.

1.5 Designing a Filter

Suppose we are asked to design a lowpass filter with the following specifications:
(a) For $0 \leq f \leq 1.0$ kHz the gain is $G(f) = 4$
(b) For $f > 1.0$ kHz the gain is $G(f) = 0.7$
It is apparent that this filter is not realizable for three reasons, although only one would suffice to make it non-realizable:
1. the gain cannot be absolutely constant in the passband
2. the gain cannot be absolutely constant in the stopband
3. the gain cannot jump from 4 to 0

For the filter to be realizable, some tolerance should be given in the passband gain, the stopband gain and the transition from high to low gain, as shown in Fig. 1.20b where:
(a) For $0 \leq f \leq 1.0$ kHz the gain may vary $G(f) \leq 3.9$
(b) for 1.0 kHz $\leq f \leq 3.0$ kHz the gain must be $G(f) \leq 3.9$
(c) For $f > 3.0$ kHz the gain must be $G(f) \leq 0.7$

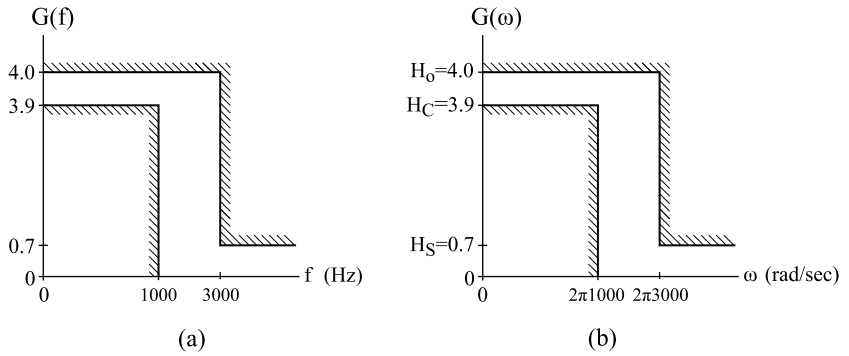

Fig. 1.20 Lowpass specifications

In Fig. 1.20b, these specifications are simply given in terms of the angular frequency $\omega = 2\pi f$. Filter specifications define the frame in which the gain function of the filter should be limited. In our case, the cutoff frequency, which is the end of the passband, is $\omega_C = 2\pi 1000$ rad/s and the stopband edge frequency, which is the beginning of the stopband, is $\omega_S = 2\pi 3000$ rad/s. The band from ω_C to ω_S is defined as the *transition band*. The maximum gain allowed in the passband is $H_o = 4$ and the minimum allowed gain in the passband is $H_C = 3.9$. The maximum allowed gain in the stopband is $H_S = 0.7$.

1.5.1 Scaling and Normalization: Smart Simplification

If a circuit has a characteristic frequency at ω_o and we wish to move it to another frequency ω_x, then we can *scale* the frequency by $\gamma = \frac{\omega_x}{\omega_o}$. All circuit functions will then be frequency-scaled by the same factor γ. For example, if before scaling the transfer function is $H(s)$ and the gain function $G(\omega)$, the new frequency-scaled transfer function will be $H(\gamma s)$ and the new gain function $G(\gamma\omega)$. When using $\omega_x = 1$, i.e. when we want the characteristic frequency to move from $\omega = \omega_o$ to $\omega = 1$, this particular frequency scaling is called *frequency normalization*. In frequency normalization, frequency is scaled (divided) by a characteristic frequency ω_o so as to make this characteristic frequency equal to 1. The new scaled frequency $\frac{\omega}{\omega_o} = \Omega$ is the *normalized frequency*. In filter design, the characteristic frequency used for frequency normalization is the cutoff frequency ω_C, and therefore the normalized cutoff frequency becomes equal to 1 and the normalized stopband edge frequency becomes $\Omega_S = \frac{\omega_S}{\omega_C} > 1$.

In our design example, angular frequencies are normalized using $2\pi 1000$ rad/s and as a result the normalized cutoff frequency is $\Omega_C = 1$ and the normalized stopband edge frequency becomes $\Omega_S = \frac{2\pi 3000}{2\pi 1000} = 3$. In Sect. 1.6, it will be shown that frequency scaling and normalization does not affect the magnitude characteristics (gain or attenuation), and therefore the frequency-normalized specifications plots retain the vertical axis without any change, as shown in Fig. 1.21b.

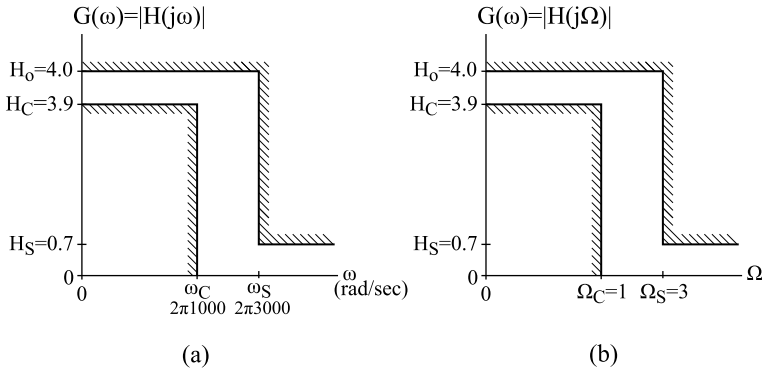

Fig. 1.21 (**a**) LP specifications. (**b**) Frequency normalized LP specifications

A frequency-normalized filter, i.e. a filter which satisfies normalized specifications, can be easily denormalized so that the cutoff frequency takes any desirable value, without affecting gain and attenuation characteristics.

1.5.2 Approximation: The Heart of Filter Design

Lowpass filter design from given normalized specifications starts from finding a gain function $G(\Omega)$ (or $G_{dB}(\Omega)$ or $A(\Omega)$) which satisfies the specifications, i.e. for our example, its frequency plot lies in the allowed region of the normalized specifications diagram of Fig. 1.21. The mathematical procedure necessary for finding the function $G(\Omega)$ is called *approximation* and theoretically yields an infinite number of solutions of which only a subset satisfy the realizability conditions for stable linear time invariant electronic circuits. As an example, consider the gain function

$$G(\Omega) = \frac{10.292}{\sqrt{\Omega^5 + 1.235\Omega^3 - 3.567\Omega^2 + 1.524\Omega + 6.77}} \tag{1.15}$$

which satisfies the specifications of our example in the manner shown in Fig. 1.22. However, this is not enough since the gain function must satisfy some more realizability conditions.

$G(\Omega)$, i.e. the magnitude of the transfer function $H(s)$ of a linear time invariant circuit for $s = j\Omega$, is an even function of Ω and $G^2(\Omega)$ is an even rational function. In addition, we know that the poles of $H(s)$ must be located in the left-hand half s-plane. These fundamental necessary conditions for $G(\Omega)$ and $H(s)$ limit the number of possible solutions. The gain function of (1.15) is not an even function, nor is its square, and this implies that there is no linear time invariant circuit with this gain function. It will be shown later that $G(\Omega)$ must be of the form:

$$G(\Omega) = \frac{A}{\sqrt{1 + k^2 P^2(\Omega)}} \tag{1.16}$$

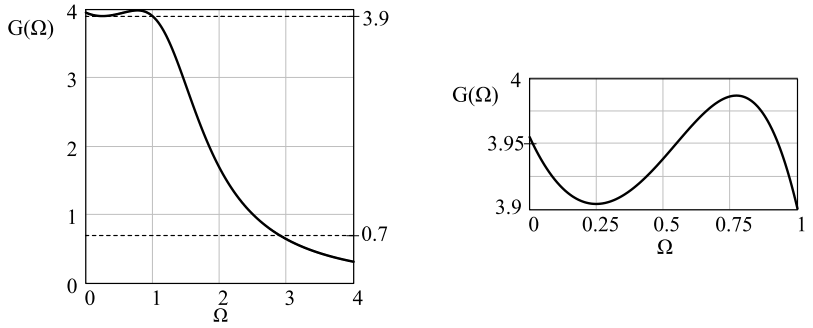

Fig. 1.22 Plot (**a**) from 0 to 4 (**b**) from 0 to 1

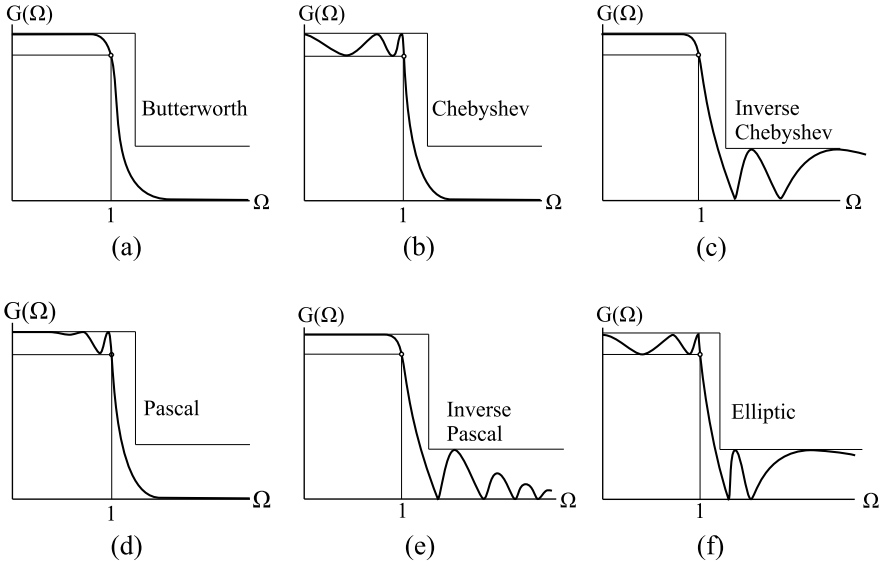

Fig. 1.23 The gain plot of several approximations

where k is a constant and $P(\Omega)$ is a polynomial or a rational function of Ω.

Fortunately, there are long-established approximations, each corresponding to a certain approximating function $P(\Omega)$. Although many other approximations exist (Bessel, Legendre, Papoulis etc.), the corresponding gain functions of some of them, namely Butterworth, Chebyshev, Pascal and Elliptic, are shown in Fig. 1.23. These approximations lead with certainty to realizable transfer functions and the filter designer simply chooses one of them, rather than trying to discover a new approximation.

Two of the next chapters deal with approximations and the subject will be covered in depth in these.

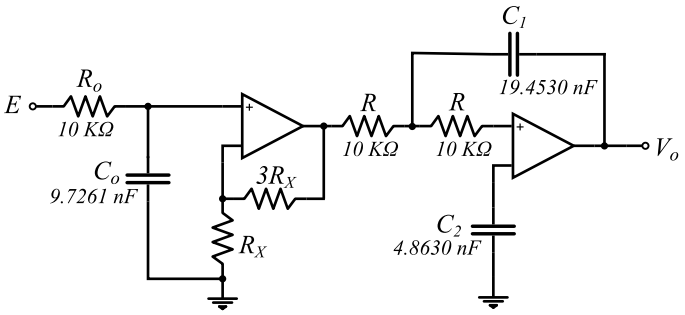

Fig. 1.24 Denormalized active-RC Butterworth filter

The design of a filter is based on the transfer function $H(s)$. Approximation gives the gain function $G(\Omega) = |H(j\Omega)|$, i.e. the magnitude of $H(s)$ for $s = j\Omega$. The transfer function is then calculated, as we will see later, using simple mathematics and exploiting the realizability conditions of the gain and transfer functions.

Returning to our design example with specifications of Fig. 1.21, if the Butterworth approximation is to be used, the gain function will be

$$G_{BUn}(\Omega) = \frac{4}{\sqrt{1 + 0.2279^2\Omega^6}} \tag{1.17}$$

from which the corresponding transfer function can be calculated as

$$H_{BUn}(s) = \frac{17.5514}{s^3 + 3.2743s^2 + 5.3604s + 4.3878}. \tag{1.18}$$

For the moment, let us not worry about how these functions have been determined, nor how the denormalized active-RC filter which realizes the transfer function of (1.18), shown in Fig. 1.24 is designed. These will be presented later. Note only that the gain response of the denormalized filter, shown in Fig. 1.25, satisfies the specifications in a monotonic manner.

If the Chebyshev approximation had been preferred, the gain function would have been

$$G_{CHn}(\Omega) = \frac{4}{\sqrt{1 + 0.2279^2(4\Omega^2 - 3)^2\Omega^2}} \tag{1.19}$$

in which case the corresponding transfer function is

$$H_{CHn}(s) = \frac{4.38784}{s^3 + 1.588677s^2 + 2.011947s + 1.09696} \tag{1.20}$$

The denormalized active-RC filter which realizes the transfer function of equation (1.20) is shown in Fig. 1.26. The gain response of the denormalized filter is shown in Fig. 1.27.

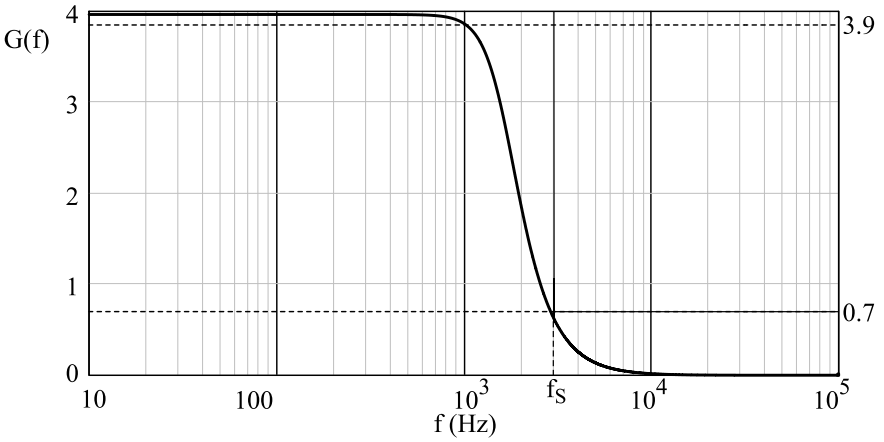

Fig. 1.25 Frequency response of the denormalized active-RC Butterworth filter

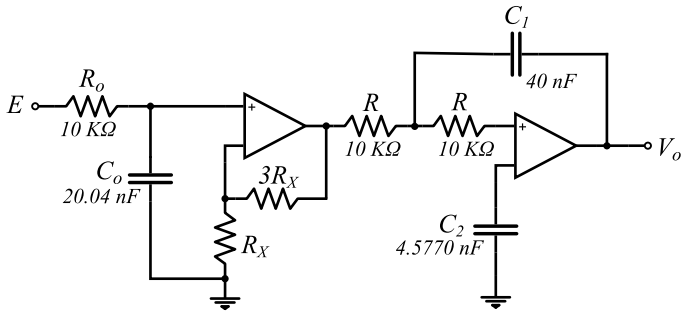

Fig. 1.26 Denormalized active-RC Chebyshev filter

It is observed that in both cases, the transfer functions have the same form with different coefficients and that the filter circuits structures are identical, with different component values. Moreover, it can be observed that the Chebyshev filter can satisfy the strictest specifications (e.g. $H_S = 0.3$).

The usage of approximations, the calculation of the corresponding transfer functions and the synthesis of the filter circuits is the nucleus of this book and will be presented in the next chapters. For the moment, the general filter design procedure should be understood as follows:

(i) Frequency is scaled using ω_C so that the normalized cutoff frequency becomes 1 and the stopband edge frequency $\Omega_S = \frac{\omega_S}{\omega_C}$.
(ii) Using one of the known approximations, the corresponding transfer function $H(s)$ is calculated, whose frequency response $|H(j\Omega)| = G(\Omega)$ satisfies the specifications.
(iii) The normalized filter circuit is synthesized from $H(s)$.
(iv) The filter is denormalized to the desired frequency and impedance level.

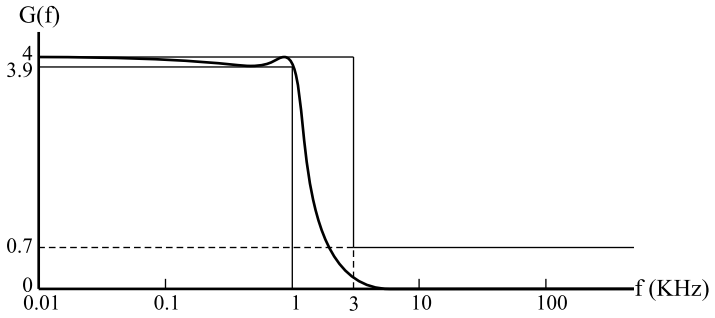

Fig. 1.27 Frequency response of the denormalized active-RC Chebyshev filter

All approximations and filter design procedures refer exclusively to normalized lowpass filters. The problem of designing a filter of a type other than lowpass (e.g. highpass or bandpass) is transformed initially to a normalized lowpass filter design problem which, in the end, is transformed to the desired type using the corresponding frequency transformation.

The realization of a circuit from its transfer function depends on the technology in mind. In the active-RC case for example, it is possible to design circuit sections that can operate independently from the previous and following ones. This is mainly due to the inherent properties of the operational amplifiers. If, however, the filter is to be realized using only passive components, the design procedure is more complicated since all filter sections, including the source and load impedances, are involved. This complication is the reason for presenting passive filter design in a later chapter, following the active filter design.

The implementation of a transfer function using active-RC circuits can be faced in various manners, one of which is to analyze the transfer function into first and second order factors related to its poles and to cascade the corresponding circuits that realize these factors. This simple method has been used in our example and although it does not lead to the optimum result, it is very popular due to its simplicity. A completely different method is the active-RC simulation of passive filters, where a passive filter is designed first and then simulated using active-RC circuits employing one of the many methods that have been proposed and will be presented in later chapters.

1.6 Scaling and Normalization

The values of the quantities involved in the analysis of a circuit may vary from very small (e.g. $C = 1$ pF $= 10^{-12}$ F) to very high, of the order of 10^{12} (e.g. GHz). This enormous spread makes calculations not only difficult, but also prone to inaccuracy. The problem is overcome by using impedance and frequency scaling, which facilitates calculations and in general the design procedures.

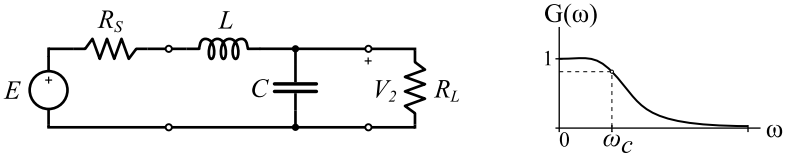

Fig. 1.28 A simple circuit and its gain plot

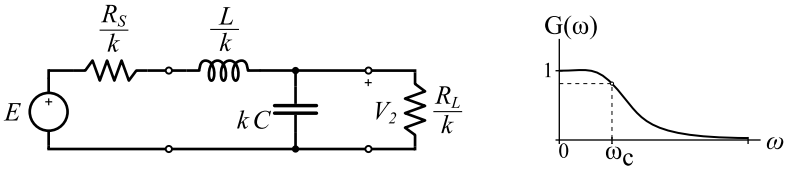

Fig. 1.29 The circuit with its impedances scaled by k

1.6.1 Impedance Scaling

The voltage transfer function $H(s)$ of the circuit of the simple Fig. 1.28, calculated using any analysis method, is:

$$H(s) = \frac{1/LC}{s^2 + (\frac{R_S}{L} + \frac{1}{R_L C})s + \frac{1+R_S/R_L}{LC}} \tag{1.21}$$

The input driving point impedance is

$$Z(s) = \frac{s^2 + (\frac{R_S}{L} + \frac{1}{R_L C})s + \frac{1+(R_S/R_L)}{LC}}{s + \frac{1}{R_L C}} L \tag{1.22}$$

If all impedances of the circuit are divided (scaled) by k, the load resistance will become $R_{Ln} = \frac{R_L}{k}$ and the resistor R_S will take the value $R_{Sn} = \frac{R_S}{k}$. The impedance sL of the inductor will become $s\frac{L}{k}$, which corresponds to the scaled inductance $L_n = \frac{L}{k}$. Similarly, the impedance $\frac{1}{sC}$ of the capacitor will become $\frac{1}{sCk}$, which corresponds to a capacitor $C_n = kC$. Figure 1.29 shows the circuit after scaling the impedances by k.

Substituting the scaled values in (1.21), it becomes obvious that impedance scaling has no effect whatsoever on the transfer function $H(s)$ and the circuit of Fig. 1.29 has exactly the same voltage transfer function and frequency response as the initial circuit of Fig. 1.28. Substituting the new scaled values in (1.22), it can be seen that for the input driving point impedance $Z_n(s)$ of the scaled circuit, we have $Z_n(s) = \frac{Z(s)}{k}$. Although these conclusions come from a simple example, it can be proved that, in general, impedance scaling does not affect the transfer functions of the circuit and simply scales the driving point impedance functions by k.

If the scaling factor k is a dimensionless number, the scaled circuit elements simply change their values.

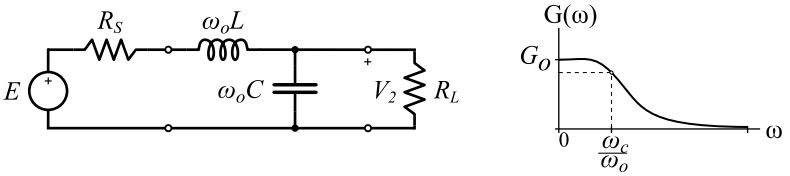

Fig. 1.30 Frequency scaled circuit

1. A resistor $R = 1200\ \Omega$, if scaled with $k = 600$, becomes a resistor with $R_n = \frac{1200\ \Omega}{600} = 2\ \Omega$
2. An inductor with $L = 120$ mH, if scaled with $k = 600$, becomes an inductor with $L_n = \frac{120\ \text{mH}}{600} = 0.2$ mH.
3. A capacitor with $C = 5$ nF, if scaled with $k = 600$, becomes a capacitor with $C_n = \frac{5\ \text{nF}}{600} = 3\ \mu\text{F}$.

If the scaling factor k is chosen to have dimensions of resistance, e.g. $k = R_o = 600\ \Omega$, the scaled resistors will be dimensionless quantities, pure numbers. In our example circuit of Fig. 1.28, the scaled quantities $R_{Sn} = \frac{R_S}{R_o}$ and $R_{Ln} = \frac{R_L}{R_o}$ will be dimensionless. The same is true for the scaled impedances of the inductor and the capacitor $s\frac{L}{R_o}$ and $\frac{1}{sCR_o}$ respectively, although the scaled quantities $L_n = \frac{L}{R_o}$ and $C_n = R_o C$, in this case have time dimensions and are both measured in seconds! The impedance scaled circuit with $k = R_o\Omega$ is no more a real circuit, but a model of the initial circuit which has the same transfer function. The usefulness lies in the fact that from a scaled circuit, the real circuit is instantly retrieved by simply multiplying all scaled resistances and inductances by R_o and dividing all scaled capacitances by R_o.

When the scaling resistance R_o is selected to be equal to a characteristic resistance of the circuit (e.g. the load resistance) so that after scaling this characteristic resistance becomes equal to 1, impedance scaling is referred to as *impedance normalization*.

1.6.2 Frequency Scaling

Let us now examine what will happen to the transfer function of the circuit of Fig. 1.28 if all inductances and capacitances are multiplied by ω_o, a quantity with dimensions of angular frequency (rad/s), as shown in Fig. 1.30. This simple operation is called frequency scaling for reasons that will become clear below. The frequency scaled inductance will be $L_n = \omega_o L$ and the frequency scaled capacitance $C_n = \omega_o C$.

Setting $L = \omega_o L$ and $C = \omega_o C$, the frequency scaled values, in (1.21) we get

$$H_n(s) = \frac{1}{LC(\omega_o s)^2 + (R_S C + \frac{L}{R_L})\omega_o s + 1 + \frac{R_S}{R_L}} = H(\omega_o s) \tag{1.23}$$

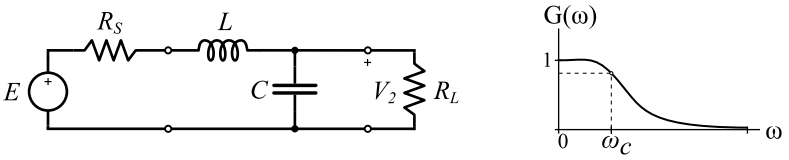

Fig. 1.31 A simple circuit and its gain plot

It is clear that the frequency scaling procedure simply multiplies the independent variable s by ω_o. This means that whatever happens to the initial circuit for s, will happen in the frequency scaled by ω_o circuit for $\frac{s}{\omega_o}$, and whatever happens to the initial circuit for ω will happen in the frequency scaled by ω_o circuit for $\Omega = \frac{\omega}{\omega_o}$.

Although frequency scaling was presented using a simple circuit, it can be shown that, in general, by multiplying all impedances and capacitances of a circuit by ω_o all circuit functions $F(s)$ are simply frequency scaled, becoming $F(\omega_o s)$.

All functions $F_n(s)$ of a frequency scaled circuit can be "descaled" simply by dividing the independent variable by the desired frequency ω_o: $F(s) = F_n(\frac{s}{\omega_o})$

When the scaling frequency ω_o is selected to be equal to a characteristic frequency of the circuit (e.g. the cutoff frequency) so that after scaling the characteristic frequency becomes equal to 1, impedance scaling is referred to as *frequency normalization*.

1.6.3 Full Normalization

Impedance and frequency scaling can be applied simultaneously on a circuit. Remember that after impedance scaling using R_o (in Ω), the scaled resistors are dimensionless and the scaled inductances and capacitances are measured in s. If the impedance scaled circuit is then frequency scaled using ω_o in rad/s, it is obvious that these awkward elements will be dimensionless numbers.

If the example circuit of Fig. 1.31 with load resistor R_L and cutoff frequency ω_C is impedance scaled using $R_o = R_L$ and frequency scaled using $\omega_o = \omega_C$, the normalized circuit will have all resistances divided by R_L, all inductances divided by R_L and multiplied by ω_C and all capacitances multiplied by $R_L\omega_C$. The dimensionless normalized values will be:

$$\boxed{R_n = \frac{R}{R_L} \qquad L_n = \frac{\omega_C}{R_L}L \qquad C_n = \omega_L R_C C} \tag{1.24}$$

The normalized dimensionless angular frequency, time and frequency are given by

$$\boxed{\Omega = \frac{\omega}{\omega_C} \qquad t_n = \frac{\omega_C}{2\pi}t \qquad F_n = \frac{2\pi}{\omega_C}f} \tag{1.25}$$

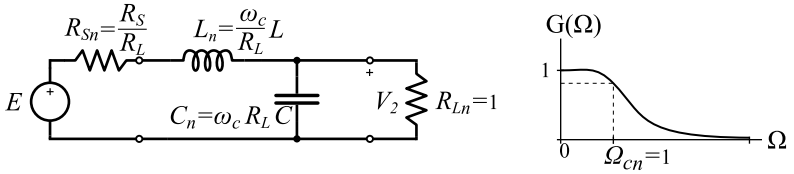

Fig. 1.32 The normalized circuit

The transfer function of the example circuit of Fig. 1.31 with load resistance R_L and cutoff frequency ω_C has been previously calculated (see (1.21)):

$$H(s) = \frac{1/LC}{s^2 + (\frac{R_S}{L} + \frac{1}{R_L C})s + \frac{1+R_S/R_L}{LC}} \tag{1.26}$$

Normalization of the circuit using R_L and ω_C results to the normalized circuit of Fig. 1.32 with $R_{Ln} = 1$, cutoff frequency $\Omega_C = 1$ and the element values:

$$\boxed{R_{Sn} = \frac{R_S}{R_L} \qquad R_{Ln} = \frac{R_L}{R_L} = 1 \qquad L_n = \frac{\omega_C}{R_L}L \qquad C_n = \omega_C R_L C} \tag{1.27}$$

The transfer function $H_n(s)$ of the normalized circuit is

$$H_n(s) = \frac{1/(L_n C_n)}{s^2 + (\frac{R_{Sn}}{L_n} + \frac{1}{R_{Ln}C_n})s + \frac{1+(R_{Sn}/R_{Ln})}{L_n C_n}} = H(\omega_C s)$$

Frequency or full normalization scales not only the transfer function, but also the gain and attenuation functions and the corresponding phase functions:

$$\begin{aligned} &\text{If} \quad G(\omega) = |H(j\omega)| \quad \Longrightarrow \quad G_n(\omega) = |H(j\omega_C\omega)| = G(\omega_C\omega), \quad \text{and} \\ &\text{If} \quad \phi(\omega) = \sphericalangle H(j\omega) \quad \Longrightarrow \quad \phi_n(\omega) = \sphericalangle H_n(j\omega) = \phi(\omega_C\omega) \end{aligned} \tag{1.28}$$

The normalized circuit element values can be denormalized for any desirable load resistance level R_L and any desirable cutoff frequency ω_C as follows:

$$\boxed{R = R_L R_n \qquad L = \frac{R_L}{\omega_C}L_n \qquad C = \frac{1}{\omega_C R_L}C_n} \tag{1.29}$$

As an example, if we are given a normalized filter like the one shown in Fig. 1.33 with unit load and normalized cutoff frequency $\Omega_C = 1$, in order to make the load $R_L = 600\ \Omega$ and the cutoff frequency $\omega_C = 2\pi 7500$ rad/s (i.e. $f_C = 7500$ Hz), we must denormalize using (1.29) with $R_L = 600\ \Omega$ and $\omega_C = 2\pi 7500$ rad/s. If we want the load to be 300 Ω and the cutoff frequency 3000 Hz, then we must denormalize using (1.29) with $R_L = 300\ \Omega$ and $\omega_C = 2\pi 3000$ rad/s.

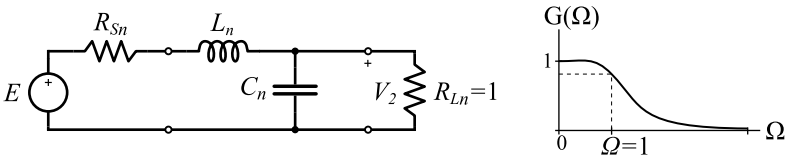

Fig. 1.33 A normalized filter

Fig. 1.34 A 3rd order passive lowpass filter table

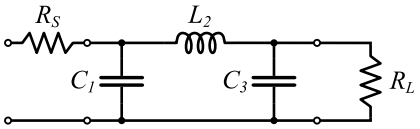

	R_S	R_L	ω_c	a_{max}	C_1	L_2	C_3
1							
2							
3							
4							
⋮							
10^8							

Normalized filters have unit load and unit angular cutoff frequency and can be easily denormalized for any desired load and cutoff frequency. Normalization facilitates the creation of filter tables as will become apparent from the following example.

Suppose that the transfer function of the 3rd order passive filter of Fig. 1.34 with cutoff frequency $f_C \rightarrow \omega_C = 2\pi \cdot f_C$ and passband tolerance determined by $\alpha_{\max}$ is given by:

$$H(s) = \frac{\omega_C^3 \frac{R_L}{\beta(R_S+R_L)}}{(s+\omega_C\beta^{-\frac{1}{3}})(s^2+\omega_C\beta^{-\frac{1}{3}}+\omega_C\beta^{-\frac{2}{3}})} \quad \text{with } \beta = \sqrt{10^{\frac{\alpha_{\max}}{10}}-1} \quad (1.30)$$

Using certain synthesis methods that will be presented later in this book, we can calculate the values of the capacitances C_1, C_3 and the inductor L_2 as functions of R_S, R_L, ω_C and $\alpha_{\max}$, i.e. $C_1(R_S, R_L, \omega_C, \alpha_{\max})$, $L_2(R_S, R_L, \omega_C, \alpha_{\max})$ and $C_3(R_S, R_L, \omega_C, \alpha_{\max})$. In order to create a table giving the values of C_1, L_2 and C_3 for given R_S, R_L, ω_C and $\alpha_{\max}$, a table like the one shown in Fig. 1.34 will be necessary.

For the table to be useful, at least 100 R_S values and 100 R_L values are necessary. For the cutoff frequency more than 1000 entries, if not many more, will be needed. Finally, for $\alpha_{\max}$, we will limit the table values to only 10. This will require $10^2 \cdot 10^2 \cdot 10^3 \cdot 10^1 = 10^8$ (100 million) entries in the table, to accommodate all possible value combinations in approximately one million pages!

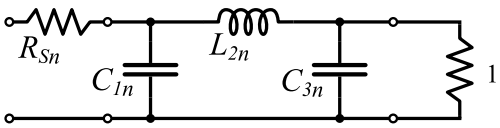

Fig. 1.35 A 3rd order normalized passive lowpass filter table

	R_{Sn}	a_{max}	C_{1n}	L_{2n}	C_{3n}
1					
2					
3	1	0.5	0.7043	1.4085	0.7043
4					
⋮					
10^3					

Using impedance and frequency normalization using R_L and ω_C so that the load resistance and the cutoff frequency become equal to 1, the corresponding columns of the table are not needed any more and the number of the entries drops spectacularly from 10^8 to 10^3, requiring only 10 pages instead of one million pages. The form of such a table giving the normalized element values of the 3rd order passive filter is shown in Fig. 1.35.

We shall see in Sect. 1.6.4 that the size of the table can be reduced further to 100 series fitting in one page.

To demonstrate the use of such a table, let us design a passive lowpass filter with $R_S = R_L = 1$ kOhm, $f_C = 1$ kHz, $\alpha_{\max} = 0.5$ dB, $f_S = 4$ kHz and $\alpha_{\min} = 25$ dB. To design the filter, we first normalize the specifications with $R_L = 10^3$ Ohm and $\omega_C = 2\pi\,10^3$ rad/s. The normalized specifications will be: $R_{Sn} = 1$, $R_{Ln} = 1$, $\Omega_C = 1$, $\Omega_S = 4$, $\alpha_{\max} = 0.5$ dB and $\alpha_{\min} = 25$ dB.

A normalized filter with these specifications is that of Fig. 1.36a, as we will see later. Although complete synthesis methods would have revealed the element values, this can be avoided if we have the table of Fig. 1.35, from which, with $R_{Sn} = 1$, we can take the normalized values $C_{1n} = 0.7043$, $L_{2n} = 1.4085$ and $C_{3n} = 0.7043$ of the normalized filter with $R_{Ln} = 1$, $\Omega_C = 1$ and $\alpha_{\max} = 0.5$.

To make the load from $1 \to 10^3$ Ohm and the cutoff angular frequency from $1 \to 2\pi\,10^3$ rad/s, the normalized element values must be denormalized using $R_L = 10^3$ Ohm and $\omega_C = 2\pi\,10^3$ rad/s:

$$C_1 = C_3 = \frac{C_n}{\omega_C R_L} = \frac{0.7043}{2\pi \cdot 10^3 \cdot 10^3} = 112 \text{ nF}$$

$$L_2 = \frac{L_n R_L}{\omega_C} = \frac{1.4085 \cdot 10^3}{2\pi \cdot 10^3} = 224.2 \text{ mH}$$

$$R_L = R_{Ln} \cdot 10^3 = 1000 \text{ Ohm} \qquad R_S = R_{Sn} \cdot 10^3 = 1000 \text{ Ohm}$$

The denormalized filter is shown in Fig. 1.36b.

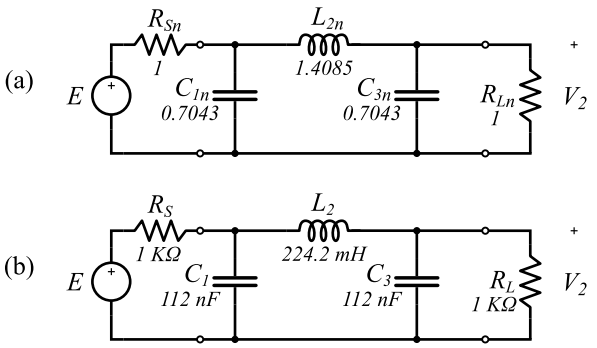

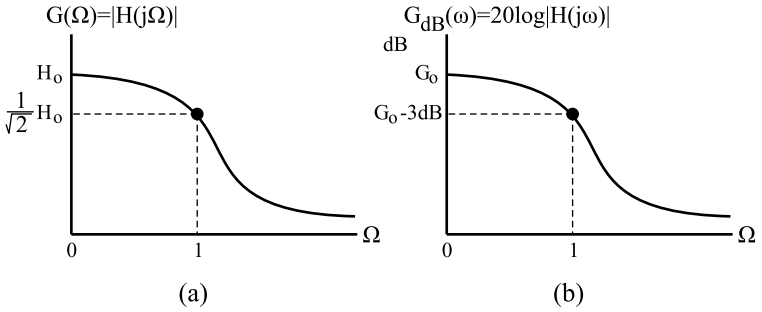

Fig. 1.36 (**a**) Normalized (**b**) denormalized filter

Fig. 1.37 Prototype lowpass filter specifications

1.6.4 Prototype Filters

The number of entries of Table II in Fig. 1.35 can be further reduced if we assume that $G(1) = \frac{\sqrt{2}}{2}H_o$, as shown in Fig. 1.37a. This corresponds to $\alpha_{\max} = 3$ dB as shown in Fig. 1.37b. Normalized filters with $G(1) = \frac{\sqrt{2}}{2}H_o$ are referred to as *prototype filters*.

Prototype filters are related to normalized filters that have $G(1) = H_C \neq \frac{\sqrt{2}}{2}H_o$ via frequency scaling. In the prototype filter, gain H_C is assumed at a frequency $\Omega_x < 1$, as shown in Fig. 1.38a and we want this frequency equal to 1. This can be done by frequency scaling the prototype filter using Ω_x. If the transfer function of the prototype filter is $H_p(s)$, the transfer function of the filter with $G(1) = H_C$ will be $H(s) = H_p(\Omega_x \cdot s)$. This frequency scaling does not affect the values of resistors, but only the values of inductors and capacitors which are divided by Ω_x.

Since from a prototype filter we can get a normalized filter with $G(1) = H_C$, the column $\alpha_{\max}$ of the table of Fig. refTableExampleN is not required for prototype filters with $\alpha_{\max} = 3$ dB. This leads to a prototype filter table like similar to that of Fig. 1.39, with only 100 entries fitting on a single page. Remember that we started from a table with one million pages, we reduced it to a table with 10 pages using normalization and finally we have a table that fits on a single page. The table of

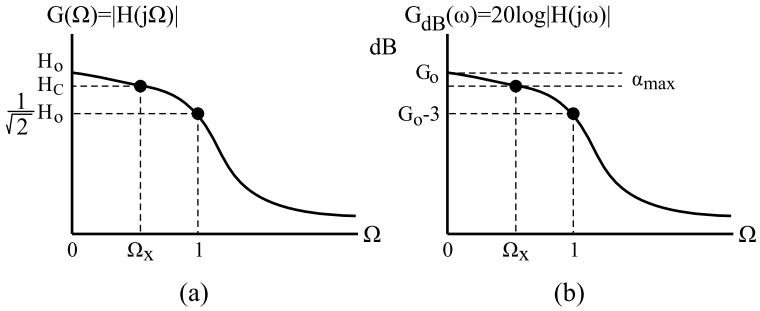

Fig. 1.38 Prototype lowpass filter specifications

Fig. 1.39 Prototype filter table

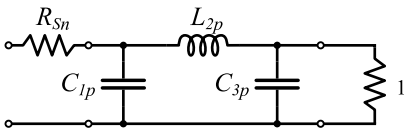

	R_{Sn}	C_{1p}	L_{2p}	C_{3p}
1	1.0000	1.0000	2.0000	1.0000
2	0.9900			
⋮				
11	0.9000	0.8082	1.6332	1.000
⋮				
51	0.5000	1.1811	0.7789	3.2612
⋮				
91	0.1000	5.1672	0.1377	15.4554
⋮				
100	0.0100	···	···	···

Fig. 1.39 is valid only for the 3rd order passive ladder filter but there exist similar tables for any order. When the design procedure shows that a filter of order n can satisfy the specifications, the values of the lossless elements of the prototype filter can be taken from the entry of the appropriate table that correspond to the normalized R_{Sn}. These values are then divided by Ω_x to give the normalized values of the filter with $G(1) = H_C$. The filter can then be denormalized for the specified load resistance and cutoff frequency. It will be seen later that frequency Ω_x, for which the gain of the prototype filter is $G_p(\Omega) = H_C$, emerges from the design procedure.

1.7 Circuit Order

The order of a linear circuit is the degree of its characteristic differential equation and is therefore the higher order of s that appears in any of the related circuit functions, e.g. the transfer function or any driving-point function. This means that given a

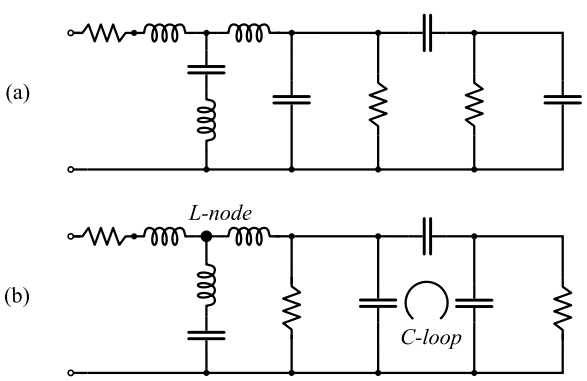

Fig. 1.40 (**a**) A passive circuit. (**b**) Rearranged

circuit, the calculation of the differential equation or of a circuit function is required so as to determine its order. The order of a circuit is a measure of its complexity, and in filters, the order is a measure of their selectivity.

In the case of RLC circuits, the order can be determined directly from their topology by inspection, and is directly proportional to the number of lossless elements L and C, after combining in series or in parallel any elements of the same kind. In fact, the total count of inductors and capacitors determine the maximum order that can be expected from the circuit. Resistors do not directly affect the order of linear circuits.

The maximum order as the sum of the inductors and capacitors count is reduced if L or C-nodes exist in the circuit structure, i.e. nodes with only inductors or capacitors connected to them. A further reduction is due to the existence of closed paths (loops) consisting exclusively of inductors (L-loops) or capacitors (C-loops). In fact each L-node, C-node, L-loop or C-loop reduces the order by 1. In the circuit of Fig. 1.40a, there are one L-node and one C-loop. If this is not obvious, see the circuit of Fig. 1.40b, which is the same circuit redrawn to make the L-node and the C-loop apparent. Since the number of reactive elements is 7 (3 inductors and 4 capacitors), the order of the circuit will be $n = 7 - 1 - 1 = 5$, which is independent of the element values. All functions of the circuit will have a polynomial of maximum degree 5. For example, if all element values are set to 1, the driving-point input impedance will be:

$$Z_1(s) = \frac{6s^5 + 12s^4 + 14s^3 + 9s^2 + 6s + 1}{4s^4 + 8s^3 + 8s^2 + 5s + 2} \tag{1.31}$$

The order of the circuit of Fig. 1.41 is obviously $n = 3$ since it has 2 capacitors and 1 inductor in a topology without identical element loops or nodes. This is confirmed by determining the transfer function $H(s) = V_2(s)/E(s)$:

$$H(s) = \frac{L_1C_1s^2 + 1}{L_1C_1C_2R_1s^3 + [L_1C_1 + L_1C_1(1 + \frac{R_1}{R})]s^2 + (R_1C_2 + \frac{L_1}{R})s + 1 + \frac{R_1}{R}} \tag{1.32}$$

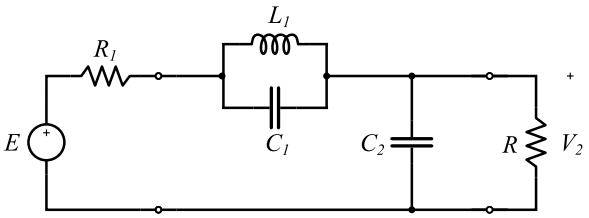

Fig. 1.41 A circuit of order $n = 3$

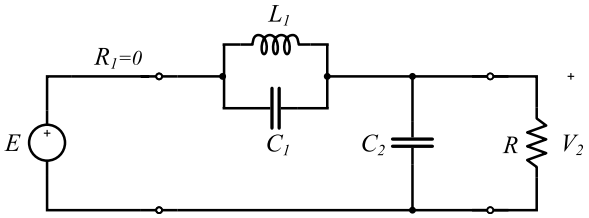

Fig. 1.42 The circuit is now of order $n = 2$

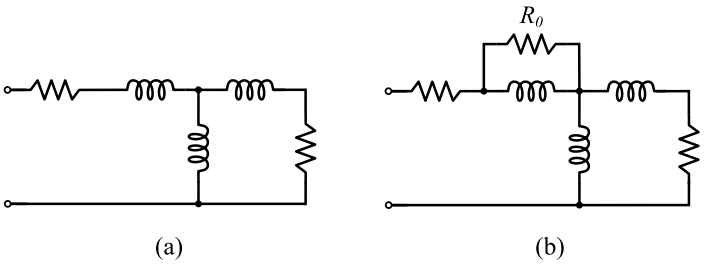

Fig. 1.43 (**a**) A circuit with one L-node and $n = 2$. (**b**) The circuit without the L-node has $n = 3$

Removing resistor R_1, the circuit becomes that of Fig. 1.42, and since resistors do not affect the order, it is expected that the order will remain $n = 3$. However, calculation of the same transfer function by any analysis method or by setting $R_1 = 0$ in (1.32) gives:

$$H(s) = \frac{L_1 C_1 s^2 + 1}{s^2 + L_1(C_1 + C_1)s + \frac{L_1}{R} + 1} \tag{1.33}$$

This implies that by removing the resistor R_1, the order is $n = 2$ and not $n = 3$ as expected. The explanation is that by removing R_1, capacitors C_1 and C_2 form a C-loop through the ideal voltage source. Therefore, resistors may not affect the order in a direct manner but they may prevent the formation of identical element nodes or loops. Consider as a second example, the circuit of Fig. 1.43a, the order of which is $n = 3 - 1 = 2$ due to the obvious L-node. By adding the resistor R_o, as we have done in Fig. 1.43b, the circuit does not have an L-node any more and its order is $n = 3$.

Circuits of order n with exactly n reactive (lossless) elements are referred to as *canonic*. Circuits of Figs. 1.40 and 1.41 are not canonic. Canonic circuits do not have L-nodes, C-nodes, L-loops or C-loops.

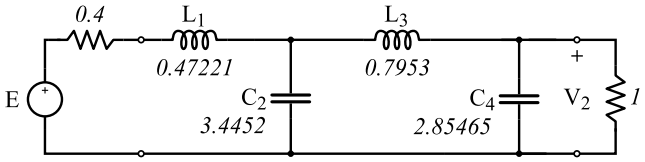

Fig. 1.44 A normalized passive lowpass filter

In active-RC (inductorless) filter design, the order of the circuits depends only on the number of capacitors. If an active-RC circuit is of order n, then it has at least n capacitors. A canonic active-RC circuit has exactly as many capacitors as its order. It is, however, very common for active-RC circuits to have more capacitors than their order and there is no simple and direct way to determine their order by inspection.

In filter design, the calculation of the order of the filter is one of the fundamental tasks and as we shall see, it is determined from the specifications. Since on the one hand higher order means higher complexity and on the other it implies higher selectivity, designers seek the minimum order to ensure the desired selectivity.

1.8 Problems

1.1 Determine the impulse response of the ideal highpass filter in order to show that it is a non-realizable system.

1.2 Show that the magnitude response of $H_{BUn}(\Omega)$ of (1.18) is given by (1.17).

1.3 Calculate and plot the logarithmic gain from $H_{BUn}(\Omega)$ of (1.18).

1.4 Show that the magnitude response of $H_{CHn}(\Omega)$ of (1.20) is given by (1.19).

1.5 The circuit of Fig. 1.44 is a normalized passive lowpass filter. Calculate its element values in order to be used with load resistance $R_L = 1.5$ kOhm and cutoff frequency $f_C = 2.0$ kHz.

1.6 The circuit of Fig. 1.45 is a passive lowpass filter with cutoff frequency $f_C = 5.0$ kHz. Calculate its element values in order to be used with load resistance $R_L = 600$ Ohm and cutoff frequency $f_C = 3.0$ kHz.

1.7 The circuit of Fig. 1.46 is an active normalized lowpass filter. Taking into account that in real active filters resistance values must be in the 10 kOhm region, calculate its element values in order to have cutoff frequency $f_C = 5.0$ kHz.

1.8 Prove that the voltage transfer function of the circuit of Fig. 1.47 is:

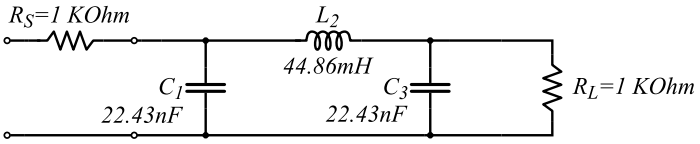

Fig. 1.45 Lowpass filter for Problem 1.6

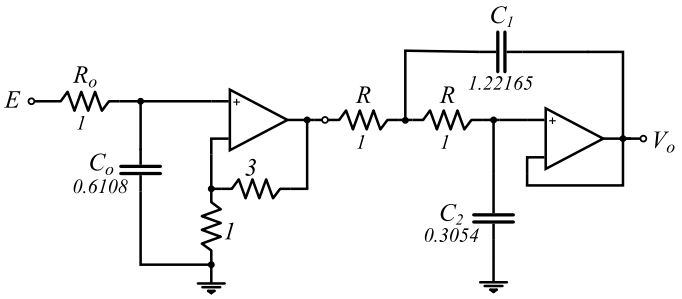

Fig. 1.46 Circuit for Problem 1.7

Fig. 1.47 Circuit for Problems 1.8 and 1.9

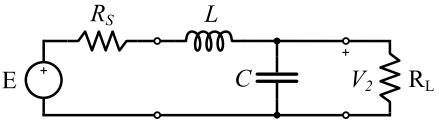

$$H(s) = \frac{V_2(s)}{E(s)} = \frac{1/LC}{s^2 + (\frac{R_S}{L} + \frac{1}{R_L C})s + \frac{1+R_S/R_L}{LC}}$$

1.9 Prove that the driving-point input impedance function of the circuit of Fig. 1.47 is:

$$Z(s) = \frac{s^2 + (\frac{R_S}{L} + \frac{1}{R_L C})s + \frac{1+(R_S/R_L)}{LC}}{s + \frac{1}{R_L C}} L$$

1.10 Determine how the step and impulse responses of a circuit are affected by frequency scaling.

References[1]

1. Ananda Mohan, P.V.: Current-Mode VLSI Analog Filters Design and Applications. Birkhauser, Boston (2003)

[1] All references, whether or not cited within the text, are recommended for further reading.

2. Antoniou, A.: Digital Filters Analysis Design and Applications, 2nd edn. McGraw-Hill, New York (1993)
3. Chen, W.-K.: Passive and Active Filters—Theory and Implementations. Wiley, New York (1986)
4. Chen, W.-K.: Passive, Active and Digital Filters. The Circuits and Filters Handbook, vol. V. CRC Press, Boca Raton (2009)
5. Chirlian, P.M.: Signals and Filters. Springer, Berlin (1994)
6. Deliyannis, T., Sun, Y., Fidler, J.K.: Continuous-Time Active Filter Design. CRC Press, Boca Raton (1999)
7. Papoulis, A.: Circuits and Systems—A Modern Approach. Holt, Rinehart and Winston, New York (1980)
8. Schaumann, R., Van Valkenburg, M.E.: Design of Analog Filters. Oxford University Press, London (2001)
9. Sun, Y. (ed.): Design of High Frequency Integrated Analogue Filters. The Institution of Electrical Engineers (2002)
10. Wanhammar, L.: Analog Filters Using MATLAB. Springer, Berlin (2009)
11. Williams, A., Taylor, F.: Electronic Filter Design Handbook. McGraw-Hill, New York (2006)

All-Pole Approximations

2

2.1 Filter Specifications and Approximations

The behavior of analogue filters can be described in the time or in the frequency domain and filters can be designed from time or frequency domain specifications. However, it is more often the case that filters are designed from frequency domain specifications from either amplitude or phase requirements.

Filter specifications are usually given in terms of magnitude characteristics and describe the desirable gain or attenuation in the passband and stopband within specified tolerances. As we will see and prove, the complexity of the transfer function of the filter and of the filter itself depends heavily on these tolerances and increases as these become stricter.

All filter approximations, tables and nomographs refer to normalized lowpass specifications (see Sect. 1.6) since they are not only easily denormalized but can be transformed to any other filter type, such as highpass, band-reject and bandpass filters.

Approximations are mathematical procedures used to translate given magnitude specifications into realizable transfer functions. Employment of well known approximations like Butterworth, Chebyshev, elliptic etc. to determine the transfer function of a filter ensures that the magnitude response will satisfy the specifications and will be realizable with passive or active circuits.

The synthesis of a normalized lowpass filter with given magnitude specifications starts with finding a gain function $G(\Omega)$ that satisfies the specifications with $G(\Omega)^2$ being a rational even function of Ω. This procedure, *the approximation*, yields theoretically infinite solutions and some of these are not suitable since they do not satisfy certain realizability conditions. This means that simply finding a mathematical function, the plot of which does not violate the specifications, does not necessarily assure its realizability as a gain function of a realizable circuit.

Fortunately, as it has been mentioned in Chap. 1, the filter designer can choose from some established approximations that lead to realizable transfer functions. Among these, the most popular are the Butterworth, Chebyshev and Cauer (or elliptic) approximations. The manner in which each of them approximates the ideal

H.G. Dimopoulos, *Analog Electronic Filters*, Analog Circuits and Signal Processing,
DOI 10.1007/978-94-007-2190-6_2, © Springer Science+Business Media B.V. 2012

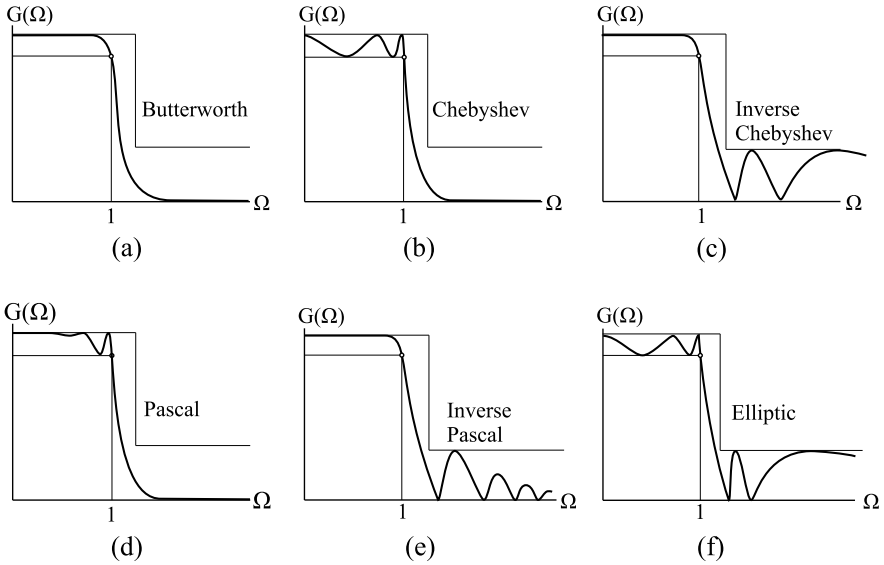

Fig. 2.1 Butterworth, Chebyshev, Pascal and elliptic approximations

lowpass gain specifications is shown in Fig. 2.1. From these approximations, Butterworth, Chebyshev and Pascal, (a), (b) and (d) in Fig. 2.1 are monotonic in the stopband. Inverse Chebyshev (Fig. 2.1c), inverse Pascal (Fig. 2.1e) and Cauer (Fig. 2.1f) have transmission zeros, i.e. frequencies at which the plain gain becomes zero.

In order to synthesize and finally implement a passive or active filter from magnitude specifications, it is necessary to calculate its transfer function $H(s) = \frac{X_{out}(s)}{X_{in}(s)}$. The approximation gives the gain function $G(\omega) = |H(s)|_{s=j\omega}$. The poles and zeros of the required and stable transfer function are obtained by a factorization process, the basis of which is as indicated in (2.1)

$$H(s)H(-s) = |H(j\omega)|^2_{\omega=-js} = |H(j\omega)|^2_{\omega^2=-s^2} \tag{2.1}$$

The approximation procedure is completed when we have constructed the transfer function $H(s)$, the magnitude of which $|H(s)|_{s=j\omega} = G(\omega)$ satisfies the filter specifications.

If the lowpass filter specifications are not normalized with $\Omega_C = 1$, as in Fig. 2.2a, they can be normalized by scaling the angular frequencies by the given ω_C so that the normalized stopband edge frequency becomes $\Omega_S = \frac{\omega_S}{\omega_C} > 1$ (Fig. 2.2b).

As shown in Chap. 1, frequency scaling does not affect the magnitude characteristics (gain or attenuation). Moreover, a filter designed with normalized specifications can easily be made to operate at any desired frequency, within the operational frequency range of the devices used in the implementation, by denormalizing accordingly the circuit elements.

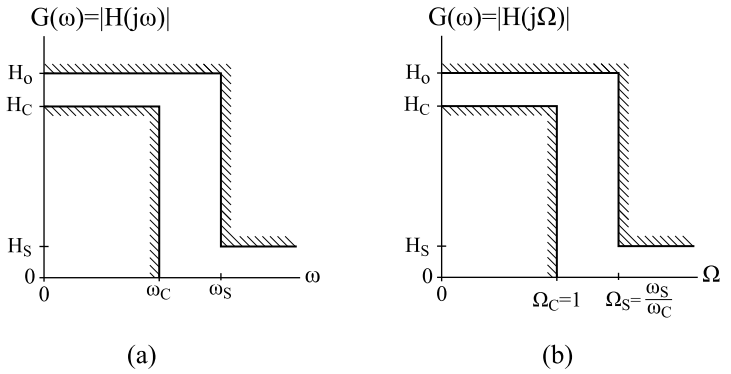

Fig. 2.2 The lowpass specifications and the normalized lowpass specifications

2.1.1 All-Pole Transfer Functions and Approximations

The term *all-pole* refers to transfer functions with constant numerators of the form $H(s) = \frac{k}{D(s)}$, where $D(s)$ is in general a polynomial in s of degree N:

$$H(s) = \frac{k}{D(s)} = \frac{k}{s^N + B_{N-1}s^{N-1} + \cdots + B_1 s + B_0} \tag{2.2}$$

Filter transfer functions have to be stable with all their poles in the left hand half s-plane. Poles on the $j\omega$-axis would make the transfer function *marginally stable* and would create infinite gain at their frequencies, a situation which is neither desirable nor useful in filter applications. Therefore, the only acceptable kinds of poles in the filter transfer functions are negative real poles $s_p = -c$ $(c > 0)$ and complex conjugate pole pairs $s_p = -a \pm jb$, with negative real part, i.e. $a > 0$. This means that only terms of the form $(s + c)$ and $(s^2 + 2as + a^2 + b^2)$ will be present in the denominator polynomial $D(s)$ of (2.2) which, due to the exclusive presence of such terms, will be complete, i.e. without missing terms.

From (2.2) we get

$$H(j\Omega) = \frac{k}{D(j\Omega)}$$

$$\rightarrow \quad |H(j\Omega)| = \frac{|k|}{\sqrt{1 + [|D(j\Omega)|^2 - 1]}} = \frac{|k|}{\sqrt{1 + Q(\Omega)}} \tag{2.3}$$

This is the general form of the magnitude response of all-pole lowpass filters with a constant numerator and a denominator which is the square root of a factor of the form $1 + [|D(j\Omega)|^2 - 1]$. The term $|D(j\Omega)|$, as a magnitude function, is an even function of Ω and therefore, the bracketed term

$$\left[|D(j\Omega)|^2 - 1\right] = Q(\Omega) \tag{2.4}$$

is a real even polynomial in Ω of even degree $2N$ of the form:

$$Q(\Omega) = \Omega^{2N} + b_{2N-2}\Omega^{2N-2} + b_{2N-4}\Omega^{2N-4} + \cdots + b_2\Omega^2 + b_0 \tag{2.5}$$

with all $b_i \neq 0$, except the constant term b_0, which can be zero only in the case when the constant term B_0 of $D(s)$ is equal to 1, i.e. only if $D(0) = 1$.

The term *complete polynomial* is used for a polynomial of order N in which all coefficients are $\neq 0$. The terms *complete odd* and *complete even* polynomial will also be used for odd and even polynomials respectively with no missing terms. In complete even polynomials, the constant term can be zero but in any case they can be expressed as polynomials in $\Omega_{sq} = \Omega^2$:

$$\begin{aligned} & Q(\Omega) = \Omega^{2N} + b_{2N-2}\Omega^{2N-2} + \cdots + b_2\Omega^2 + b_0 \\ \Rightarrow \quad & Q(\Omega) = Q(\Omega_{sq}) = \Omega_{sq}^N + b_{2N-2}\Omega_{sq}^{N-1} + \cdots + b_2\Omega_{sq} + b_0 \end{aligned}$$

Bearing in mind the expression (2.3) for the magnitude response of all-pole transfer functions as well as that $Q(\Omega)$ is a complete even polynomial, in all polynomial approximations the gain is expressed with a similar function of the form

$$G(\Omega) = |H(j\Omega)| = \frac{H_o}{\sqrt{1 + P_a(\Omega)}} \tag{2.6}$$

where $P_a(\Omega)$ must meet the conditions set for $Q(\Omega)$, i.e. it must be a complete even polynomial, as defined above. In fact any complete even polynomial can be used in (2.6) in order to express the lowpass gain characteristics, provided it assumes low values in the passband and high values in the stopband.

Equation (2.6) is the basis of the all-pole approximations which differ only in the polynomial used. In fact, all known all-pole approximations use (2.6) with $P_a(\Omega) = \gamma^2 P_N^2(\Omega)$:

$$G(\Omega) = \frac{H_o}{\sqrt{1 + \gamma^2 P_N^2(\Omega)}} \tag{2.7}$$

with $P_N(\Omega)$ being the *approximating polynomial* (complete even or odd) and γ a design parameter.

Although it is not necessary, $P_a(\Omega)$ is taken to be equal to the square of an even or odd polynomial of degree N, i.e. $P_a(\Omega) = \gamma^2 P_N^2(\Omega)$ in order to simplify the related mathematical complexity.

For lowpass gain characteristics to be achieved, $P_N(\Omega)$ must assume low values for $0 \leq \Omega \leq 1$ and high values for $\Omega > 1$. For practical reasons, the approximating polynomial $P_N(\Omega)$ is made to assume unity value at $\Omega = 1$, i.e. $P_N(1) = 1$.

In the Butterworth approximation, $P_N(\Omega) = \Omega^N$ is used, as will be seen in the next section. If Chebyshev polynomials are used instead, the Chebyshev approximation is derived. In a similar way, Pascal, Legendre or Bessel polynomials can be used to produce the approximation with the corresponding name and properties.

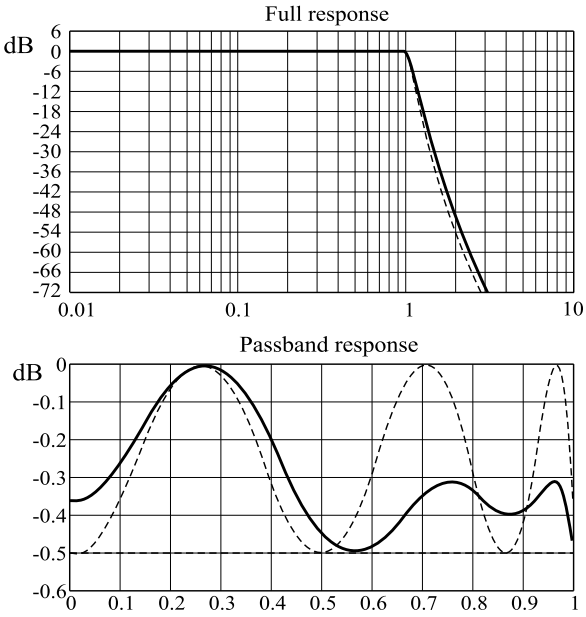

Fig. 2.3 Logarithmic gain of a 6th order non-square approximation compared to the corresponding Chebyshev response (*dotted*)

All-pole approximations are also referred to as *polynomial approximations* due to the fact that the approximating functions are polynomials.

It should be noted that all-pole approximations using in (2.6) a complete even polynomial $P_a(\Omega)$ of order $2N$ which is not the square of another polynomial of degree N have not been reported in the related literature. For example, the polynomial of degree $2 \cdot 6 = 12$

$$P_a(\Omega) = 47.346554 \prod_{m=1}^{6} (\Omega^2 - \Omega_{zm}^2) \quad \text{where } \Omega_{zm} = \frac{m-1}{0.725806(m+1)}$$

which is not the square of another polynomial of degree $N = 6$ can be used in (2.6) with $H_o = 0.958833$ to give the logarithmic gain shown in Fig. 2.3. The figure also shows the corresponding 6th order Chebyshev filter with 0.5 dB passband ripple, for comparison. This approximation exhibits a non-equiripple behavior in the passband and its advantage over the corresponding Chebyshev response might be the inherent diminishing ripple [11] and the lower pole Qs.

2.2 The Butterworth Approximation

Assuming that the type of response is selected a priori (e.g. Butterworth type etc.) the following four parameters describe the filter transfer function completely:

$$\{H_o, H_C, H_S, \Omega_S\} \qquad (\Omega_C = 1)$$

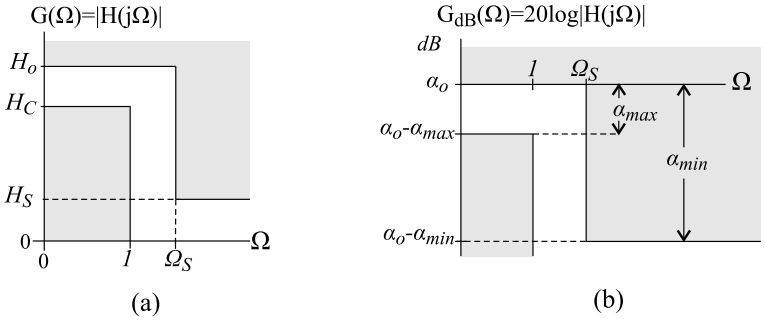

Fig. 2.4 Normalized lowpass specifications: (**a**) Plain gain. (**b**) Logarithmic gain

In terms of logarithmic gain, the normalized lowpass specifications can be described by

$$\{\alpha_o, \alpha_{\max}, \alpha_{\min}, \Omega_S\} \qquad (\Omega_C = 1)$$

where $\alpha_o = 20\log(H_o)$, $\alpha_{\max} = 20\log(H_o/H_C)$ and $\alpha_{\min} = 20\log(H_o/H_S)$.

The parameter H_o can be taken equal to 1 (i.e. $\alpha_o = 0$ dB) without loss of generality and therefore the filter requirements can in practice be determined by three parameters:

$$\Omega_S \quad \text{and} \quad \{H_C, H_S\} \quad \text{or} \quad \{a_{\max}, \alpha_{\min}\} \tag{2.8}$$

referred to as the normalized lowpass filter specifications.

Thus, the design process seeks to find a function $G(\Omega)$ which stays within the limits defined by the specifications. In other words, the response does not stray into the dashed areas of Fig. 2.4. S. Butterworth proposed [1] the monotonic function:

$$G(\Omega) = \frac{H_o}{\sqrt{1+\beta^2\Omega^{2N}}} \tag{2.9}$$

with N, the *order* of the approximation, a positive integer, and β a design parameter related to the passband tolerance. Notice that the Butterworth gain function of (2.9) is in accordance with (2.7) with $P_N(\Omega) = \Omega^N$ with $Q_{2N}(\Omega) = \beta^2\Omega^{2N}$.

Equation (2.9) for $\Omega = 0$ gives by definition $G(0) = H_o$ while the *integer order* N and the design parameter β remain to be determined.

The order N is selected to be the lowest integer consistent with the specifications. Its selection will be examined shortly. For the present we select β such that

$$G(1) = \frac{H_o}{\sqrt{1+\beta^2}} \geq H_C \quad \Leftrightarrow \quad \beta^2 \leq (H_o/H_C)^2 - 1$$

$$\Leftrightarrow \quad \beta \leq \beta_{\max} = \sqrt{\left(\frac{H_o}{H_C}\right)^2 - 1} = \sqrt{10^{\frac{a_{\max}}{10}} - 1} \tag{2.10}$$

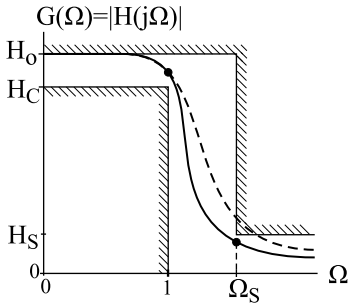

Fig. 2.5 Butterworth approximation stopband scenarios

Thus any value of $\beta \leq \beta_{\max}$ ensures that the gain for $0 \leq \Omega \leq 1$ will remain $\geq H_C$. For $\beta = \beta_{\max}$ we make the gain $G(1) = H_C$ and the gain curve passes from the point $\{1, H_C\}$. It is almost exclusively the case in the literature that β is taken to be $\beta_{\max}$ and only in [5] is it allowed to be a design parameter and can assume any value $\beta_{\min} \leq \beta \leq \beta_{\max}$. The minimum value $\beta_{\min}$ depends on the order N which must be first calculated. Before the order calculation, let us examine the derivative of the Butterworth gain function of (2.9).

$$\frac{d}{d\Omega}G(\Omega) = \frac{d}{d\Omega}\left(\frac{H_o}{\sqrt{1+\beta^2\Omega^{2N}}}\right) = -\frac{N\beta^2 H_o \Omega^{2N-1}}{(1+\beta^2\Omega^{2N})^{\frac{3}{2}}} \tag{2.11}$$

The derivative is non-positive and henceforth $G(\Omega)$ is monotonically decaying. It can also be shown that all $(N-1)$ derivatives of $G(\Omega)$ assume zero value for $\Omega = 0$ and for this reason Butterworth approximation is called *maximally flat*.

The Butterworth gain function of (2.9) with $\beta \leq \beta_{\max}$ satisfies the passband specifications ($0 \leq \Omega \leq 1$) but may violate the specifications for $\Omega \geq 1$ as shown in Fig. 2.5 with a dashed curve.

In order for the monotonic gain function to satisfy the specifications for $\Omega \geq 1$, it is sufficient to ensure that $G(\Omega_S) \leq H_S$. This will lead to the calculation of the order N of the approximation:

$$G(\Omega_S) = \frac{H_o}{\sqrt{1+\beta^2\Omega_S^{2N}}} \leq H_S \quad \Leftrightarrow \quad \Omega_S^{2N} \geq \frac{(H_o/H_S)^2 - 1}{\beta^2}$$

$$\Leftrightarrow \quad 2N \log \Omega_S \geq \log\left(\frac{(H_o/H_S)^2 - 1}{\beta^2}\right)$$

$$\Leftrightarrow \quad N \geq \frac{\log(\frac{(H_o/H_S)^2-1}{\beta^2})}{2\log\Omega_S}$$

From the above relation, it can be concluded that the integer order N of the approximation must be greater than the *fractional order* N_d of the approximation:

$$N \geq N_d = \frac{\log(\frac{(H_o/H_S)^2-1}{\beta^2})}{2\log\Omega_S} \tag{2.12}$$

Since N must be integer, it is taken as the minimum integer that satisfies $N \geq N_d$, i.e. the integer that results from rounding up N_d. The complexity of a filter is directly proportional to the order of the approximation, and for this reason we try to keep N as low as possible. The fractional order N_d, if seen as a function of β, assumes its minimum value for $\beta = \beta_{\max}$ and the *order equation* (2.12) becomes:

$$n_{f\,\min} = \frac{\log(\frac{\frac{H_o^2}{H_S^2}-1}{\frac{H_o^2}{H_C^2}-1})}{2\log\Omega_S} = \frac{\log(\frac{10^{\frac{a_{\min}}{10}}-1}{10^{\frac{a_{\max}}{10}}-1})}{2\log\Omega_S} \tag{2.13}$$

The order equation gives the fractional order of the approximation as a function of the specifications. The integer order N of the approximation will of course be the next integer value greater than N_d. It is clear from (2.13) that the order is increasing as Ω_S approaches unity and becomes infinite for $\Omega_S = 1$. This means that as we try to make a narrow transition band, we increase the order or that higher order filters realize narrower transition bands. The order also increases as the passband tolerance decreases (H_C approaches H_o) and as the maximum allowed stopband gain H_S decreases. Thus, as we try to make the response closer to the ideal brick wall characteristic the order becomes increasingly large until it becomes infinite for the ideal case.

Filters designed to have the monotonic maximally flat gain function of (2.9) are referred to as Butterworth filters and the name implies only that they realize this type of response, no matter how they are implemented. Butterworth filters can be implemented under any suitable technology.

2.2.1 Optimization Using β as a Design Parameter

Returning to (2.12), we saw that N_d is minimized for $\beta = \beta_{\max}$. Decreasing β from its maximum value, the fractional order increases until it takes integer value and $G(\Omega_S) = H_S$. This minimum value of β is given by

$$\beta_{\min} = \frac{\sqrt{(H_o/H_S)^2-1}}{\Omega_S^N} = \frac{\sqrt{10^{\frac{a_{\min}}{10}}-1}}{\Omega_S^N} \tag{2.14}$$

Decreasing β to a value lower than $\beta_{\min}$, N_d exceeds the integer order N and the new integer order of the filter will increase by 1. This is shown in Fig. 2.6 for a filter designed with normalized specifications $H_o = 1$, $H_C = 0.95$, $H_S = 0.05$ and $\Omega_S = 2.7$ which give $N_d = 4.135 \Rightarrow N = 5$.

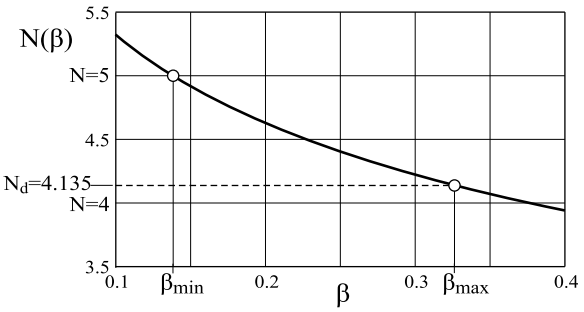

Fig. 2.6 Plot of N_d as a function of β

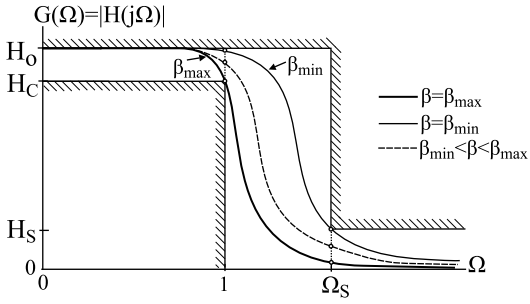

Fig. 2.7 Butterworth gain plot for the various values of β

When the minimum fractional order N_d has been calculated from (2.13) and has been rounded up to the next integer value N, the coefficient β becomes a design parameter and its value can be selected from

$$\beta_{\min} = \frac{\sqrt{\frac{H_o^2}{H_S^2} - 1}}{\Omega_S^N} \leq \beta \leq \sqrt{\frac{H_o^2}{H_C^2} - 1} = \beta_{\max} \tag{2.15}$$

or, in terms of logarithmic gain specifications

$$\beta_{\min} = \frac{\sqrt{10^{\frac{\alpha_{\min}}{10}} - 1}}{\Omega_S^N} \leq \beta \leq \sqrt{10^{\frac{\alpha_{\max}}{10}} - 1} = \beta_{\max} \tag{2.16}$$

For the calculated N, any value of β within the permitted range $\beta_{\min} \leq \beta \leq \beta_{\max}$ leads to a Butterworth gain function $G(\Omega) = \frac{H_o}{\sqrt{1+\beta^2\Omega^{2N}}}$ which satisfies the specifications in a different manner, as shown in Fig. 2.7.

2.2.1.1 Case I: $\beta = \beta_{\max}$

Using $\beta = \beta_{\max}$ in (2.9) we get $G(1) = H_C$ and $G(\Omega_S) < H_S$. In this case, the passband tolerance is fully used and the gain is optimized at the stopband edge frequency Ω_S, where it takes the value

$$H_{S\min} = G(\Omega_S) = \frac{H_o}{\sqrt{1+\beta_{\max}^2 \Omega_S^{2N}}} \leq H_S \tag{2.17}$$

This case is referred to as *stopband edge frequency gain optimized*.

2.2.1.2 Case II: $\beta = \beta_{\min}$

Using $\beta = \beta_{\min}$ in (2.9), we get $G(\Omega_S) = H_S$ and $G(1) = H_{C\max} > H_C$. In this case, the stopband tolerance is fully used with $G(\Omega_S) = H_S$ and the gain is optimized in the passband, where it varies from H_o down to $H_{C\max} > H_C$:

$$H_{C\max} = G(1) = \frac{H_o}{\sqrt{1+\beta_{\min}^2}} = \frac{H_o}{\sqrt{1+\frac{(H_o/H_S)^2-1}{\Omega_S^{2N}}}} > H_C \tag{2.18}$$

This case, in which β takes the minimum value, is referred to as *passband gain optimized*.

2.2.1.3 Case III: $\beta_{\min} \leq \beta \leq \beta_{\max}$

Using any other permitted value of β in (2.9), the specifications are satisfied with $G(1) \geq H_C$ and $G(\Omega_S) \leq H_S$, namely

$$G(\Omega_S) = \frac{H_o}{\sqrt{1+\beta^2\Omega_S^{2N}}} < H_S \quad \text{and} \quad G(1) = \frac{H_o}{\sqrt{1+\beta^2}} > H_C \tag{2.19}$$

2.2.2 The 3 dB Frequency of Butterworth Filters

The characteristic frequency Ω_{3dB} of Fig. 2.8 at which the gain drops by 3 dB from H_o to $H_o/\sqrt{2}$ is such that:

$$G(\Omega_{3dB}) = \frac{H_o}{\sqrt{1+\beta^2\Omega_{3dB}^{2N})}} = \frac{H_o}{\sqrt{2}} \quad \Leftrightarrow \quad \beta\Omega_{3dB}^N = 1 \quad \Leftrightarrow \quad \Omega_{3dB}^N = \frac{1}{\beta}$$

$$\Omega_{3dB} = \left(\frac{1}{\beta}\right)^{\frac{1}{N}} = \beta^{-\frac{1}{N}} \tag{2.20}$$

The Ω_{3dB} frequency is shown in Fig. 2.8.

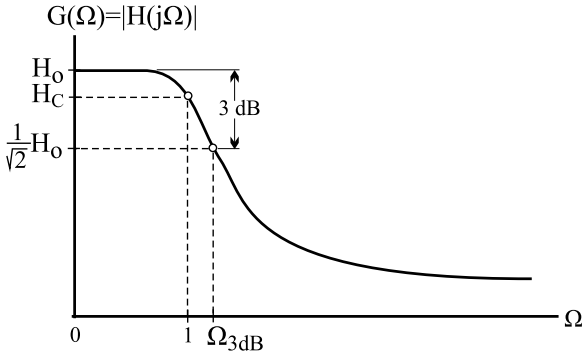

Fig. 2.8 The 3 dB frequency Ω_{3dB}

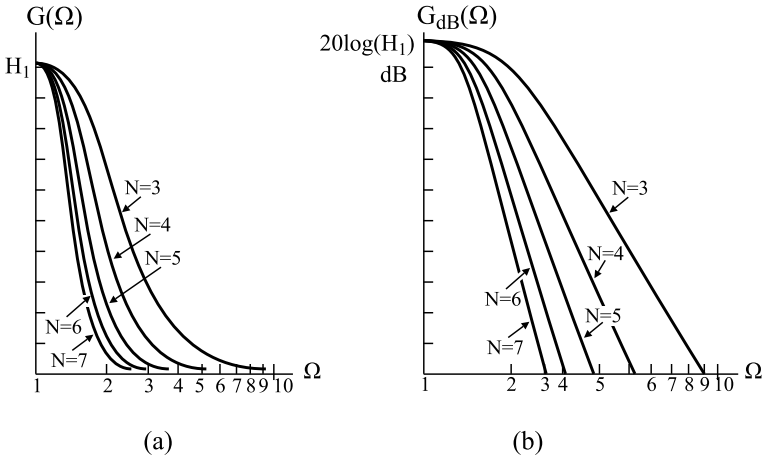

Fig. 2.9 Plots of plain and logarithmic Butterworth gain

2.2.3 The Cut-off Rate

Figure 2.9 shows the gain plots of Butterworth approximation for various values of N and $\Omega \geq 1$. The normalized frequency Ω is plotted in logarithmic scale and it is obvious that the curves become almost straight lines for $\Omega \gg 1$. The slope of these lines increases with N and it will be shown that it depends only on N. The slope of the logarithmic gain curves is measured in dB/octave. The slope of the logarithmic gain at frequencies where it is constant ($\Omega \gg 1$) is referred to as *cut-off rate* and can be determined by taking the difference of the logarithmic gain at a frequency Ω_1 and at the double frequency $2\Omega_1$:

$$r = 20\log(G(\Omega_1)) - 20\log(G(2\Omega_1)) = 20\log\left(\frac{\sqrt{1+\beta^2 2^{2N}\Omega_1^{2N}}}{\sqrt{1+\beta^2\Omega_1^{2N}}}\right)$$

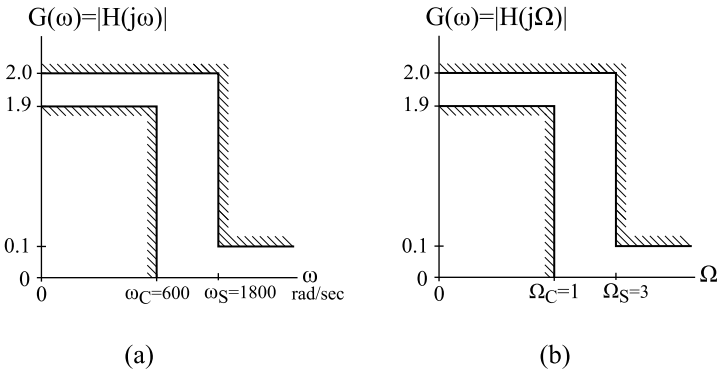

Fig. 2.10 Filter specifications of Example 2.1

$$\text{since } \Omega_1 \gg 1 \Rightarrow \beta^2 \Omega_1^{2n} \gg 1 \quad \text{and}$$

$$r \approx 20\log\left(\frac{\sqrt{\beta^2 2^{2N} \Omega_1^{2N}}}{\sqrt{\beta^2 \Omega_1^{2N}}}\right) = 20\log(2^N) = N20\log(2) \approx 6N \text{ dB/octave}$$

This means that in the stopband, the logarithmic gain falls at a rate of $6N$ dB for every frequency doubling (one octave). The above relationship between the order of the filter and the cutoff rate explains the curves of Fig. 2.9b.

Often, instead of giving H_S and Ω_S in the specifications, the cut-off rate is given, from which the order N can be calculated (e.g. given $r = 24$ dB/octave, the order is $N = 24/6 = 4$).

Example 2.1 Determine the Butterworth gain function $G_\alpha(\omega)$ that satisfies the specifications shown in Fig. 2.10a.

We identify the specifications:

$$\omega_C = 600 \text{ rad/s}, \qquad \omega_S = 1800 \text{ rad/s},$$
$$H_o = 2, \qquad H_C = 1.9 \quad \text{and} \quad H_S = 0.1$$

Normalizing with $\omega_C = 600$ rad/s we get the normalized specifications of Fig. 2.10b with $\Omega_C = 1$ and $\Omega_S = 3$. In order to use (2.9), we need a value for β and the order N which will be calculated from (2.13).

$$\beta_{\max} = \sqrt{\left(\frac{H_o}{H_C}\right)^2 - 1} = \sqrt{\left(\frac{2.0}{1.90}\right)^2 - 1} = 0.3286837 \quad \beta_{\max}^2 = 0.1080329$$

$$N_d = \frac{\log\left(\frac{(H_o/H_S)^2-1}{\beta_{\max}^2}\right)}{2\log\Omega_S} = \frac{\log\left(\frac{\frac{2.0^2}{0.1^2}-1}{0.1080329}\right)}{2\log(3)} = 3.7385$$

The integer order will be the rounded up N_d, i.e. $N = 4$. Now $\beta_{\min}$ can be calculated:

$$\beta_{\min} = \frac{\sqrt{\frac{H_o^2}{H_S^2} - 1}}{\Omega_S^N} = \frac{\sqrt{\frac{2^2}{0.1^2} - 1}}{3^4} = 0.246605 \quad \text{and} \quad \beta_{\min}^2 = 0.0608$$

For $\beta = \beta_{\max}$ the normalized gain function will be

$$G_{\max}(\Omega) = \frac{2}{\sqrt{1 + 0.108033\Omega^8}}$$

For $\beta = \beta_{\min}$, the normalized gain function will be

$$G_{\min}(\Omega) = \frac{2}{\sqrt{1 + 0.0608\Omega^8}}$$

The corresponding denormalized gain functions for $\omega_C = 600$ rad/s will be

$$G_{1\max}(\omega) = G\left(\frac{\omega}{\omega_C}\right) = \frac{2}{\sqrt{1 + 0.108033(\frac{\omega}{600})^8}}$$

$$G_{1\min}(\omega) = G\left(\frac{\omega}{\omega_C}\right) = \frac{2}{\sqrt{1 + 0.0608(\frac{\omega}{600})^8}}$$

2.2.4 The Normalized Butterworth Lowpass Transfer Function

The gain function $G(\Omega) = |H(s)|_{s=j\Omega}$ of (2.9) is well determined after the calculation of the order N and the selection of the design parameter β. In fact, we now have the following relation:

$$|H(s)|_{s=j\Omega}^2 = \frac{H_o^2}{1 + \beta^2\Omega^{2N}} \tag{2.21}$$

From (2.21) and the fact that the denominator of the transfer function $H(s)$ is a Hurwitz polynomial, with no roots in the right hand half-plane, $H(s)$ can be determined from

$$H(s)H(-s) = |H(j\Omega)|_{\Omega^2=-s^2}^2 = G(\Omega)^2|_{\Omega^2=-s^2}$$

$$(\Omega^2 = -s^2 \text{ or } \Omega = -js \text{ are used equivalently}) \tag{2.22}$$

On letting $|H(j\Omega)| = \frac{H_o}{\sqrt{1+\beta^2\Omega^{2N}}}$ in (2.22) we get

$$H(s)H(-s) = \frac{H_o^2}{1 + \beta^2\Omega^{2N}}\bigg|_{\Omega^2=-s^2} = \frac{H_o^2}{1 + \beta^2(-s^2)^N} = \frac{\frac{H_o^2}{\beta^2}}{\frac{1}{\beta^2} + (-s^2)^N} \tag{2.23}$$

The denominator of (2.23) is a binomial of the form $x^N + \frac{1}{\beta^2}$ with $x = -s^2$. The roots of this binomial expression are of course the roots of the equation

$$x^N + \left(\frac{1}{\beta^2}\right) = 0 \quad \Leftrightarrow \quad x^N - \frac{1}{\beta^2} e^{j(2k+1)\pi} = 0$$

and henceforth the roots are

$$x_k = \sqrt[N]{\frac{1}{\beta^2}} e^{j\frac{2k+1}{N}\pi} \quad \text{for } k = 0, 1, 2, \ldots, (N-1)$$

Since we have set $x = s^2$, for the roots s_k we have:

$$s_k^2 = -\sqrt[N]{\frac{1}{\beta^2}} e^{j\frac{2k+1}{N}\pi} = \sqrt[N]{\frac{1}{\beta^2}} e^{j(\frac{2k+1}{N}\pi+\pi)} \quad \text{with } k = 0, 1, 2, \ldots, (N-1) \tag{2.24}$$

Finally, the roots of $\frac{1}{\beta^2} + (-s^2)^N = 0$ are given below:

$$\begin{aligned} s_{k+} &= \sqrt[N]{\frac{1}{\beta}} e^{j(\frac{2k+1}{2N}\pi+\frac{\pi}{2})} \quad \text{and} \\ s_{k-} &= \sqrt[N]{\frac{1}{\beta}} e^{j(\frac{2k+1}{2N}\pi-\frac{\pi}{2})} \quad k = 0, 1, 2, \ldots, N-1 \end{aligned} \tag{2.25}$$

The roots s_{k+} and s_{k-} are the poles of $H(s)H(-s)$. It should be noticed from (2.25) that these do not lie on the $j\omega$-axis, i.e. their real part

$$\cos\left(\frac{2k+1}{2N}\pi \pm \frac{\pi}{2}\right)$$

cannot become zero since this would require

$$\frac{2k+1}{2N}\pi \pm \frac{\pi}{2} = \lambda\frac{\pi}{2} \quad \text{with } \lambda \text{ odd}$$

Working out this condition, we find that it requires $2k = N(\lambda \pm 1) - 1$, which is never true since $2k$ is even and $N(\lambda \pm 1) - 1$ is always odd.

$$\begin{aligned} \text{Moreover, real roots exist} \quad &\Leftrightarrow \quad \sin\left(\frac{2k+1}{2N}\pi \pm \frac{\pi}{2}\right) = 0 \\ &\Leftrightarrow \quad \frac{2k+1}{2N}\pi \pm \frac{\pi}{2} = \lambda\pi \text{ where } \lambda \text{ is an integer} \\ &\Leftrightarrow \quad N(2\lambda+1) - 1 \text{ must be even} \\ &\Leftrightarrow \quad N(2\lambda+1) \text{ is odd} \quad \Leftrightarrow \quad N \text{ is odd} \end{aligned}$$

For odd values of N, there exists a pair of real roots with value $\pm\sqrt[N]{\frac{1}{\beta}} = \pm\beta^{-\frac{1}{N}}$.

The N roots s_{k+} are all located in the left hand half-plane since

$$\frac{\pi}{2} < \frac{2k+1}{2N}\pi + \frac{\pi}{2} < \frac{3\pi}{2} \quad \text{for all } k = 0, 1, 2, \ldots, (N-1)$$

whilst all N roots s_{k-} of (2.25) are located in the right hand half-plane and are one-by-one opposite to s_{k+}.

In view of all of these properties, (2.23) gives:

$$H(s)H(-s) = \frac{\frac{H_o^2}{\beta^2}}{\frac{1}{\beta^2} + (-s^2)^N} = \underbrace{\frac{\frac{H_o}{\beta}}{\prod_{k=0}^{N-1}(s - s_{k+})}}_{\substack{\text{poles} \\ \text{in the LHP}}} \times \underbrace{\frac{\frac{H_o}{\beta}}{\prod_{k=0}^{N-1}(s - s_{k-})}}_{\substack{\text{poles} \\ \text{in the RHP}}}$$

from which $H(s)$ can be identified as:

$$H_{BUT}(s) = \frac{\frac{H_o}{\beta}}{\prod_{k=0}^{N-1}(s - s_{k+})} \tag{2.26}$$

The poles of $H_{BUT}(s)$ are given by

$$s_k = \sqrt[N]{\frac{1}{\beta}} e^{j\left(\frac{2k+1}{2N}\pi + \frac{\pi}{2}\right)} \quad k = 0, 1, 2, \ldots, (N-1) \tag{2.27}$$

and are located in the s-plane on a circle with radius

$$\sqrt[N]{\frac{1}{\beta}} = \beta^{-\frac{1}{N}} \tag{2.28}$$

It should be noted that the radius given in (2.28) is the magnitude of the poles and is equal to the 3 dB frequency of (2.20). Parameter β in (2.28) has a value given by (2.15), namely

$$\beta_{\min} = \frac{\sqrt{(H_o/H_S)^2 - 1}}{\Omega_S^N} \le \beta \le \sqrt{(H_o/H_C)^2 - 1} = \beta_{\max}$$

For $k = 0$ the first pole is obtained with phase angle $\frac{\pi}{2} + \frac{\pi}{2N}$ and the next poles are at a distance $\frac{\pi}{N}$, as shown in Fig. 2.11. Figure 2.12 shows the poles of the transfer function for $N = 3$ and $N = 4$.

By adjusting the index k in (2.27) so that it varies from $k = 1$ to N, we get

$$H_{BUT}(s) = \frac{\frac{H_o}{\beta}}{\prod_{k=1}^{N}(s - s_k)} \tag{2.29}$$

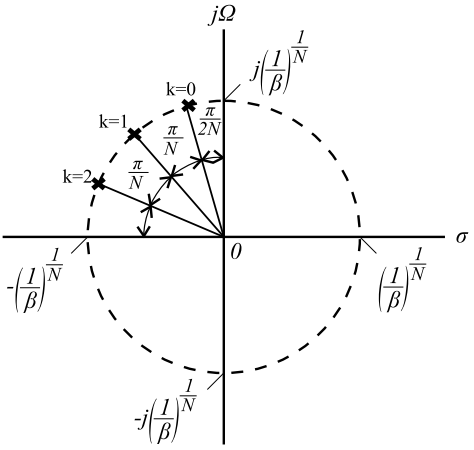

Fig. 2.11 Pole location of normalized Butterworth transfer function

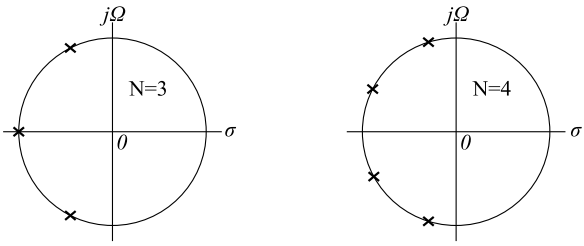

Fig. 2.12 Poles for $N = 3$ and $N = 4$

where

$$s_k = \sqrt[N]{\frac{1}{\beta}}\, e^{j\left(\frac{2k+N-1}{2N}\pi\right)} \quad \text{for } k = 1, 2, \ldots, N \tag{2.30}$$

or

$$s_k = \beta^{-\frac{1}{N}}\left[\cos\left(\frac{2k+N-1}{2N}\pi\right) + j\sin\left(\frac{2k+N-1}{2N}\pi\right)\right]$$
$$\text{for } k = 1, 2, \ldots, N \tag{2.31}$$

The poles of the transfer function of (2.30) for given N, depend only on the design parameter β, and each choice $\beta_{\min} \le \beta \le \beta_{\max}$ from (2.15) leads to a different set of poles of the transfer function, the corresponding gain function $|H(j\Omega)|$ of which satisfies the specifications in its own way according to Sect. 2.2.1 and Fig. 2.7.

It will be shown later in this book that the all-pole Butterworth lowpass transfer function can be realized not only with active circuits but also with doubly terminated passive ladder two-port LC circuits like the one in Fig. 2.13. Such a circuit, with the proper calculation of the element values, can realize a Butterworth response with

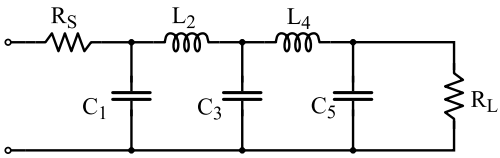

Fig. 2.13 Typical structure of a passive-LC doubly terminated lowpass filter

$N = 5$. The total number of lossless elements in this case (inductors and capacitors) equals the order N of the approximation.

2.2.5 Table of Prototype Butterworth Filters

The approximation of prototype specifications of Fig. 1.37 with $G(1) = \frac{1}{\sqrt{2}} H_o$ or $\alpha_{\max} = 3$ dB requires that $\beta = 1$. In this case *the prototype Butterworth lowpass transfer function* is given by (2.32).

$$H_{pBUT}(s) = \frac{H_o}{[s - e^{j(\frac{\pi}{2N} + \frac{\pi}{2})}][s - e^{j(\frac{3\pi}{2N} + \frac{\pi}{2})}] \cdots [s - e^{j(\frac{(2N-1)\pi}{2N} + \frac{\pi}{2})}]} \tag{2.32}$$

Since the only parameter in (2.32) is the order N, a table of prototype Butterworth lowpass transfer functions can be created.

If the normalized lowpass filter specifications require $G(1) = H_C \neq \frac{1}{\sqrt{2}} H_o$ ($a_{\max} \neq 3dB$), the corresponding normalized transfer functions will simply be frequency scaled with Ω_{3dB} of (2.20), i.e.

$$H_n(s) = H_{pBUT}\left(\frac{s}{\Omega_{3dB}}\right) = \frac{H_o}{D_p(\frac{s}{\Omega_{dB}})} \quad \text{where } \Omega_{3dB} = \left(\frac{1}{\beta}\right)^{\frac{1}{N}} = \beta^{-\frac{1}{N}} \tag{2.33}$$

Example 2.2 Calculate the transfer function of a normalized lowpass Butterworth filter of order $N = 3$ with $G(0) = 4$ and $G(1) = 3.9$.

Obviously, since Ω_S and H_S are not specified, only $\beta_{\max}$ can be calculated. From Table 2.1, we have for the 3rd order prototype Butterworth filter

$$H_{pBUT}(s) = \frac{H_o}{D(s)} = \frac{4}{s^3 + 2s^2 + 2s + 1}$$

that has $G(1) = 0.7071 \times 4 = 2.8284$ while we require $G(1) = 3.9$.

For the specified $H_o = G(0) = 4$ and $H_C = G(1) = 3.9$, the 3 dB frequency can be calculated:

$$\Omega_{3dB} = \left(\frac{1}{\beta_{\max}}\right)^{\frac{1}{N}} = \left(\frac{1}{\sqrt{\frac{G(0)^2}{G(1)^2} - 1}}\right)^{\frac{1}{3}} = 1.63713$$

Table 2.1 Denominator of the prototype Butterworth lowpass transfer functions

Denominator of the prototype Butterworth lowpass transfer functions $H_{pBUT}(s)=\frac{H_o}{D_p(s)}\|H_{pBUT}(j\Omega)\|=\frac{H_o}{\sqrt{1+\beta^2\Omega^{2N}}}$ with $G(1)=\frac{\sqrt{2}}{2}H_o$	
N	$D_p(s)$
1	$s+1$
2	$s^2+\sqrt{2}s+1$
3	$(s+1)(s^2+s+1)=s^3+2s^2+2s+1$
4	$(s^2+0.765367s+1)(s^2+1.847759s+1)=s^4+2.613126s^3+3.414214s^2+2.613126s+1$
5	$(s+1)(s^2+0.618034s+1)(s^2+1.618034s+1)$ $=s^5+3.236068s^4+5.236068s^3+5.236068s^2+3.236068s+1$
6	$(s^2+0.517638s+1)(s^2+(\sqrt{2}/2)s+1)(s^2+1.931852s+1)$ $=s^6+3.863703s^5+7.464102s^4+9.141620s^3+7.464102s^2+3.863703s+1$
7	$(s+1)(s^2+0.445042s+1)(s^2+1.246980s+1)(s^2+1.801938s+1)$ $=s^7+4.493959s^6+10.097835s^5+14.591794s^4+14.591794s^3$ $+10.097835s^2+4.493959s+1$
8	$(s^2+0.390181s+1)(s^2+1.11114s+1)(s^2+1.662939s+1)(s^2+1.961571s+1)$ $=s^8+5.125831s^7+13.137071s^6+21.846151s^5+25.688356s^4+21.846151s^3$ $+13.137071s^2+5.125831s+1$
9	$(s+1)(s^2+s+1)(s^2+0.347296s+1)(s^2+1.532089s+1)(s^2+1.879385s+1)$ $=s^9+5.758770s^8+16.581719s^7+31.163437s^6+41.986386s^5+41.986386s^4$ $+31.163437s^3+16.581719s^2+5.758770s+1$

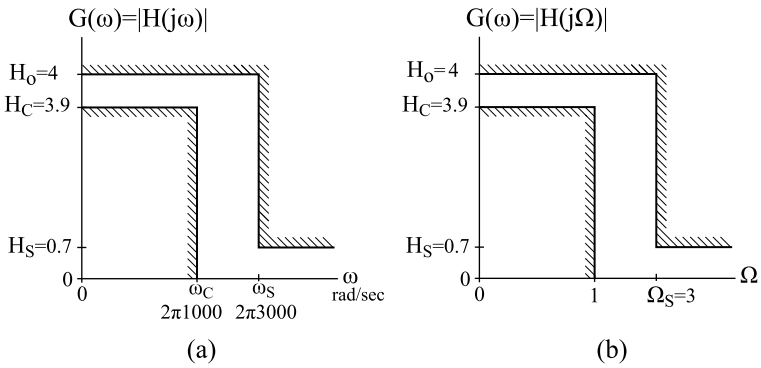

Fig. 2.14 Filter specifications of application Example 2.3

and the transfer function will be:

$$H(s)=H_{nBUT}\left(\frac{s}{1.63713}\right)=\frac{H_o}{D_p(\frac{s}{1.63713})}=\frac{17.5514}{s^3+3.27426s^2+5.3604s+4.3878}$$

Example 2.3 Calculate the transfer function of a lowpass filter with Butterworth response with the specifications given in Fig. 2.14a.

By normalizing the given specifications with $\omega_C = 2\pi 1000$ rad/s, we get the normalized specifications of Fig. 2.14b. The normalized stopband edge frequency is $\Omega_S = \frac{2\pi 3000}{2\pi 1000} = 3$. We next calculate $\beta_{\max}$ from (2.10) or (2.15):

$$\beta_{\max} = \sqrt{\left(\frac{H_o}{H_C}\right)^2 - 1} = \sqrt{\left(\frac{4}{3.9}\right)^2 - 1} = 0.2279$$

From (2.13), the fractional order of the approximation is calculated:

$$N_d = \frac{\log(\frac{\frac{H_o^2}{H_S^2} - 1}{\beta_{\max}^2})}{2\log\Omega_S} = \frac{\log(\frac{\frac{4^2}{0.7^2} - 1}{0.2279^2})}{2\log(3)} = 2.918$$

The integer order of the approximation will be taken $N = 3$. With this value of N, we can now calculate the minimum value of β from (2.15):

$$\beta_{\min} = \frac{\sqrt{\frac{H_o^2}{H_S^2} - 1}}{\Omega_S^N} = \frac{\sqrt{\frac{4^2}{0.7^2} - 1}}{3^3} = 0.208374 \quad \text{and} \quad \beta_{\min}^2 = 0.04342$$

According to (2.29) and (2.30), the transfer function of the filter will be:

$$H_{BUT}(s) = \frac{\frac{H_o}{\beta}}{\prod_{k=1}^{3}(s - s_{k+})} \quad \text{with } s_{k+} = \sqrt[3]{\frac{1}{\beta}} e^{j(\frac{2k+3-1}{2\times 3}\pi)} \quad \text{for } k = 1, \ldots, 3$$

If for our calculations we use $\beta = \beta_{\min} = 0.208374$, the poles of the transfer function of the normalized filter are found to be -1.686755 and $-0.843377 \pm j1.46077$ and the transfer function of the normalized filter:

$$H_{\min}(s) = \frac{19.196228}{(s + 1.686755)(s^2 + 1.686755s + 2.845143)}$$

If $\beta = \beta_{\max} = 0.2279$ is used, the poles will be -1.637132 and $-0.818566 \pm j1.4178$ and for the transfer function of the normalized filter we find:

$$\begin{aligned} H(s) &= \frac{17.5514}{(s + 1.63713)(s^2 + 1.63713s + 2.6802)} \\ &= \frac{17.5514}{s^3 + 3.2743s^2 + 5.3604s + 4.3878} \end{aligned} \tag{2.34}$$

The second form of the transfer function, with the denominator as a formal polynomial, is not particularly useful and the factored form is preferred.

Alternatively, since we know the order N of the approximation, we can take the transfer function of the prototype filter with $N = 3$ from Table 2.1 and use (2.33). From the table with $N = 3$, we get

$$H_{pBUT} = \frac{H_o}{(s + 1)(s^2 + s + 1)} \quad \text{with } H_o = 4$$

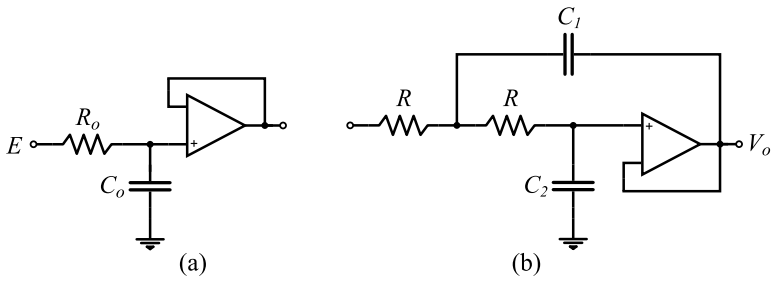

Fig. 2.15 (**a**) Lossy integrator. (**b**) Lowpass Sallen–Key circuit

Since in the prototype filters $G(1) = |H_{nBUT}(j1)| = \frac{1}{\sqrt{2}}H_o$, the transfer function for our specifications with different value $G(1) = H_C = 3.9$ (i.e. $\beta = \beta_{\max} = 0.2279$), will be

$$H(s) = H_{pBUT}\left(\frac{s}{\Omega_{3dB}}\right) = \frac{H_o}{(\frac{s}{\Omega_{3dB}}+1)[(\frac{s}{\Omega_{3dB}})^2 + (\frac{s}{\Omega_{3dB}})+1]}$$

$$\text{where } \Omega_{3dB} = \left(\frac{1}{\beta_{\max}}\right)^{\frac{1}{N}} = \left(\frac{1}{0.2279}\right)^{\frac{1}{3}} = 1.637132$$

Finally, the transfer function of the normalized filter will be:

$$H(s) = \frac{17.5514}{(s+1.63713)(s^2+1.63713s+2.6802)}$$

As expected, the transfer function is identical to the previously calculated (2.34). All transfer functions determined in this example refer to the normalized filter which satisfies the normalized specifications of Fig. 2.14b. The corresponding transfer functions that meet the specifications of Fig. 2.14a will be simply frequency scaled by $\omega_C = 2\pi\,1000$, i.e. $H(\frac{s}{\omega_C})$.

Example 2.4 The transfer function calculated in Example 2.3 using $\beta = \beta_{\max}$, can be factored as follows:

$$H(s) = \frac{A_1}{s+1.63713} \times \frac{A_2}{s^2+1.63713s+2.6802} \tag{2.35}$$

where $A_1 A_2 = 17.5514$. The first term can be realized using a first order circuit like the one shown in Fig. 2.15a. The circuit is a lossy integrator and the voltage follower (buffer) is used to isolate the circuit from the next section. The second term can be realized with a lowpass Sallen–Key circuit like the one shown in Fig. 2.15b.

The transfer function of the first order circuit of Fig. 2.15a is

$$H_1(s) = \frac{\frac{1}{R_oC_o}}{s+\frac{1}{R_oC_o}} \quad \text{with } R_oC_o = \frac{1}{1.63713} = 0.6108 \text{ and } A_1 = 1.63713$$

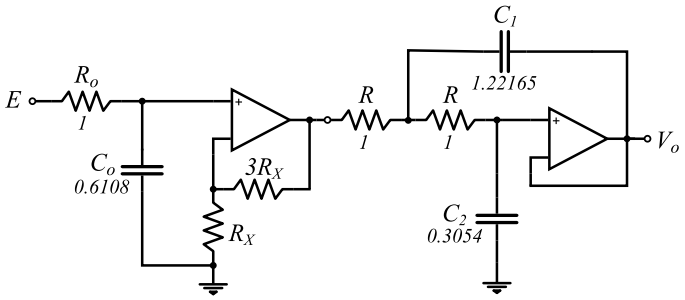

Fig. 2.16 Cascade connection of the two circuits

Choosing $R_o = 1$, we get $C_o = 0.6108$. This choice is not unique and any other would be acceptable as long as it satisfies $R_o C_o = 0.6108$.

The second term $\frac{A_2}{s^2+1.63713s+2.6802}$ of (2.35) is a 2nd order lowpass function of the form $\frac{A_2}{s^2+\frac{\omega_o}{Q}s+\omega_o^2}$ with

$$\omega_o = \sqrt{2.6802} = 1.63713 \quad \text{and} \quad Q = \sqrt{\frac{2.6802}{1.63713}} = 1$$

and can be realized with the unity gain ($k = 1$) Sallen–Key lowpass circuit of Fig. 2.15b (see Chap. 10). This circuit has the following transfer function:

$$H(s) = \frac{\frac{1}{R^2C_1C_2}}{s^2 + s(\frac{2}{RC_1}) + \frac{1}{R^2C_1C_2}}$$

from which, with known Q and ω_o, we find

$$C_1 = \frac{2Q}{\omega_o R} \quad \text{and} \quad C_2 = \frac{1}{2\omega_o RQ}$$

In this circuit, $A_2 = \frac{1}{R^2C_1C_2} = \omega_o^2 = 2.6802$.

We can now choose any value for R, e.g. $R = 1$ (do not forget that we design a normalized filter from a normalized transfer function!), in which case:

$$C_1 = \frac{2Q}{\omega_o R} = \frac{2}{1.63713} = 1.22165 \quad \text{and} \quad C_2 = \frac{1}{2 \cdot 1.63713} = 0.3054$$

When cascading the two circuits, they have

$$A_1 A_2 = \frac{\omega_o^2}{R_o C_o} = 4.3878$$

Consequently, if we wish $A_1 A_2 = 17.5514$, we must add a unit with gain $A = \frac{17.5514}{4.3878} = 4$, as we have done in Fig. 2.16, by replacing the buffer with a non-inverting voltage amplifier with gain 4.

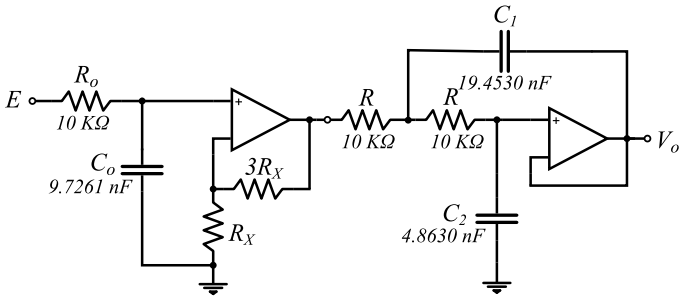

Fig. 2.17 Final denormalized circuit

This filter satisfies the normalized frequency specifications with $\Omega_C = 1$ and can be denormalized simply by dividing the capacitors by the specified $\omega_C = 2\pi \times 1000$. A resistor level adjustment, which does not affect the transfer function and the frequency response, is achieved by multiplying all resistors by R_n and dividing all capacitors by R_n. The value of R_n is so selected as to lead to reasonable resistor values of the order of 10 kOhm. In our case we select $R_n = 10^4$ Ohm.

$$R_o = 1 \times 10^4\ \Omega = 10\ \text{k}\Omega \qquad C_o = \frac{0.6108}{2\pi \times 10^3 \times 10^4} = 9.7261\ \text{nF}$$

$$R = 1 \times 10^4\ \Omega = 10\ \text{k}\Omega \qquad C_1 = \frac{1.22165}{2\pi \times 10^3 \times 10^4} = 19.4530\ \text{nF}$$

$$C_2 = \frac{0.3054}{2\pi \times 10^3 \times 10^4} = 4.8630\ \text{nF}$$

The values of resistors R_x and $3R_x$ are not important, provided that they keep the correct ratio value to realize gain 4. Resistors in active circuits must be kept at high levels, e.g. 10 kOhm, and therefore R_x could be 10 kOhm and $3R_x = 30$ kOhm. Figure 2.17 shows the final filter circuit and Fig. 2.18 the corresponding gain response.

The section ordering is theoretically neither important nor obligatory and the final circuit can be that of Fig. 2.19. However, the circuit of Fig. 2.17 is preferred as it obeys the rule that sections are ordered according to the distance of the pole(s) they realize from the $j\omega$-axis and sections that realize distant poles go first [10, 12].

A designer's creativity is only limited by the number of the circuits available for the realization of the various sections. The first order circuit, for example, can be realized using the inverting lossy integrator of Fig. 2.20a, and for the second order section a multiple feedback 2nd order lowpass circuit like the one in Fig. 2.20b can be used (see Chap. 10).

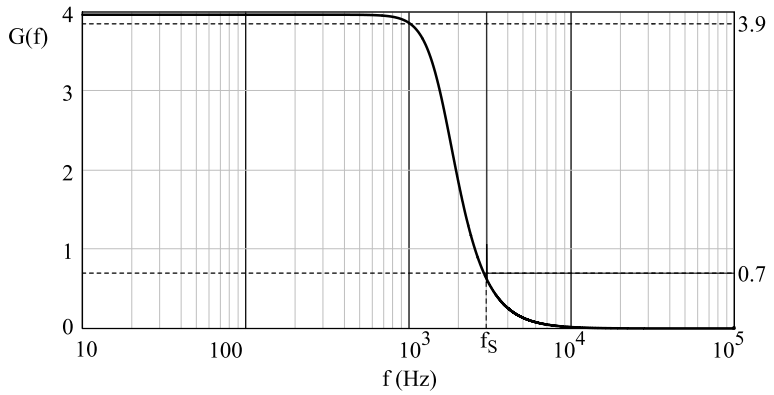

Fig. 2.18 Frequency response

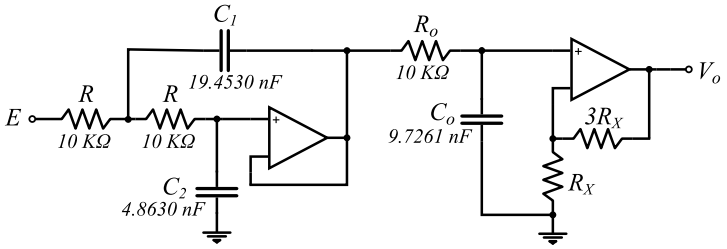

Fig. 2.19 Alternative connection

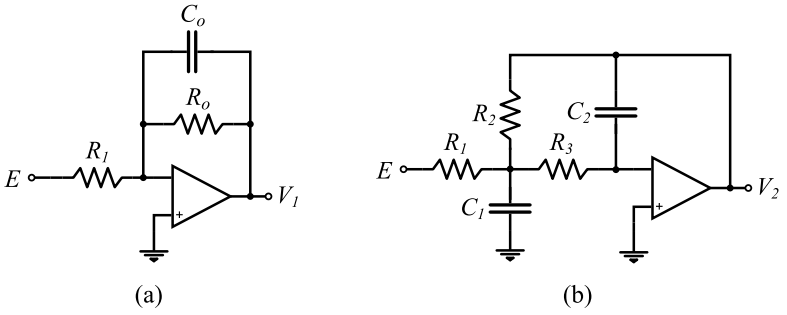

Fig. 2.20 Alternative circuits

2.3 The Chebyshev Approximation

According to Sect. 2.1.1, all approximations use a gain expression of the form of (2.7):

$$G(\Omega) = |H(j\Omega)| = \frac{H_o}{\sqrt{1 + \gamma^2 P_N^2(\Omega)}} \tag{2.36}$$

It should be remembered that the approximating polynomial $P_N(\Omega)$ of degree N must be a complete even or odd polynomial in Ω and that in order to achieve low-pass gain characteristics, $P_N(\Omega)$ must assume low values for $0 \leq \Omega \leq 1$ and high values for $\Omega > 1$.

Due to the form of the gain of (2.36), certain characteristics of the approximating polynomial are inherited to the gain function. If, for example, $P_N(\Omega)$ is monotonically increasing for $\Omega > 1$, then $G(\Omega)$ will be monotonically decreasing in the same interval, as in the Butterworth case with $P(N, \Omega) = \Omega^N$. If $P_N(\Omega)$ assumes zero values at certain frequencies, the related gain $G(\Omega)$ will be maximized at these frequencies, and at the frequencies of any extrema of $P_N(\Omega)$, the gain in (2.36) will be minimized. Such polynomials with roots and extrema in the passband are the Chebyshev polynomials [2] and when used in (2.36) lead to non-monotonic passband gain functions.

2.3.1 Chebyshev Polynomials

The general form of the Chebyshev polynomial of order N is

$$C_N(\Omega) = \cos(N \cos^{-1}(\Omega)) \quad \text{or} \quad C_N(\Omega) = \cosh(N \cosh^{-1}(\Omega)) \tag{2.37}$$

This definition does not indicate that $C_N(\Omega)$ is a polynomial. It will be seen shortly, however, that this is the case. Clearly,

$$C_0(\Omega) = 1 \quad \text{and} \quad C_1(\Omega) = \Omega \tag{2.38}$$

Moreover, by using trigonometric relationships it can be shown that the Chebyshev polynomial of degree N is related to the polynomials of degrees $(N-1)$ and $(N-2)$ by the recursive formula:

$$C_N(\Omega) = 2\Omega C_{N-1}(\Omega) C_{N-2}(\Omega) \tag{2.39}$$

Equation (2.39) provides a way to calculate any Chebyshev polynomial of degree N recursively as follows:

$$C_2(\Omega) = 2\Omega C_1(\Omega) - C_0(\Omega) = 2\Omega^2 - 1$$
$$C_3(\Omega) = 2\Omega C_2(\Omega) - C_1(\Omega) = 2\Omega(2\Omega^2 - 1) - \Omega = 4\Omega^3 - 3\Omega$$

The parameter η, which will be used extensively in this chapter to allow unified expressions, is defined by:

$$\eta = \begin{cases} 0 & \text{for } N \text{ even} \\ 1 & \text{for } N \text{ odd} \end{cases} \tag{2.40}$$

Table 2.2 Chebyshev polynomials

Chebyshev Polynomials for $N = 0$–9	
N	$C_N(\Omega) = \cos(N\cos^{-1}(\Omega)) = \cosh(N\cosh^{-1}(\Omega))$
0	1
1	Ω
2	$2\Omega^2 - 1$
3	$4\Omega^3 - 3\Omega$
4	$8\Omega^4 - 8\Omega^2 + 1$
5	$16\Omega^5 - 20\Omega^3 + 5\Omega$
6	$32\Omega^6 - 48\Omega^4 + 18\Omega^2 - 1$
7	$64\Omega^7 - 112\Omega^5 + 56\Omega^3 - 7\Omega$
8	$128\Omega^8 - 256\Omega^6 + 160\Omega^4 - 32\Omega^2 + 1$
9	$256\Omega^9 - 576\Omega^7 + 432\Omega^5 - 120\Omega^3 + 9\Omega$

Table 2.3 Properties of the Chebyshev polynomials

Fundamental properties of Chebyshev polynomials	
N odd	$C_N(0) = 0,\ C_N(1) = 1,\ C_N(-\Omega) = -C_N(\Omega)$
N even	$C_N(0) = \pm 1,\ C_N(1) = 1,\ C_N(-\Omega) = C_N(\Omega)$
All N	$\Omega = [-1, 1] \rightarrow$ ripple between -1 and 1
	For $\Omega > 1$ polynomials increase monotonically.
	$C_N^2(\Omega) = \frac{1}{2}(C_{2N}(\Omega) + 1)$

Using η, the general form of the Chebyshev polynomial of degree N will be given by

$$C_N(\Omega) = c_N\Omega^N + c_{N-2}\Omega^{N-2} + \cdots + c_\eta\Omega^\eta$$
$$\text{with: } c_N = 2^{N-1} \text{ and } c_\eta = N^\eta(-1)^{\frac{N+3\eta}{2}} \tag{2.41}$$

Table 2.2 has been created using the recursive formula of (2.39).

Some easily demonstrable important and characteristic properties of the Chebyshev polynomials are tabulated in Table 2.3. These properties are visualized in the graphs shown in Fig. 2.21.

2.3.2 The All-Pole Chebyshev Approximation

As a reminder, the parameters

$$\{H_o, H_C, H_S, \Omega_S\} \qquad (\Omega_C = 1)$$

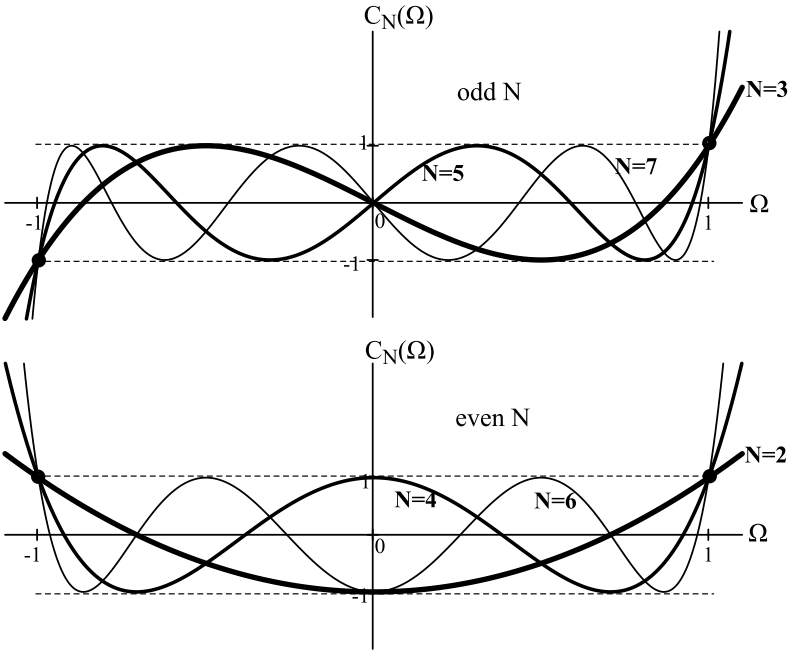

Fig. 2.21 Graphs of odd and even Chebyshev polynomials

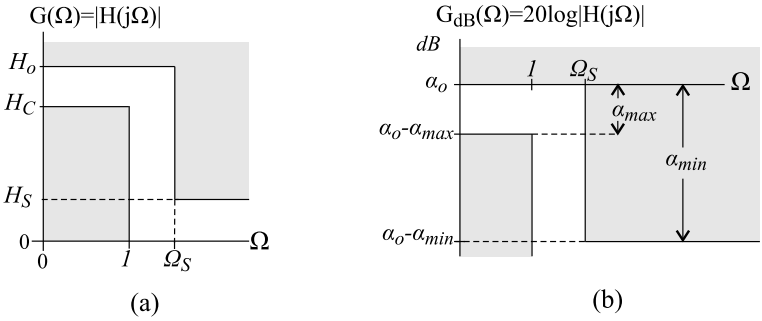

Fig. 2.22 Normalized lowpass specifications. (**a**) Plain gain (**b**). Logarithmic gain

specify the normalized lowpass gain specifications (Fig. 2.22). In logarithmic gain terms, the specifications are of course

$$\{\alpha_o, \alpha_{\max}, \alpha_{\min}, \Omega_S\} \qquad (\Omega_C = 1)$$

where $\alpha_o = 20\log(H_o)$, $\alpha_{\max} = 20\log(H_o/H_C)$ and $\alpha_{\min} = 20\log(H_o/H_S)$.

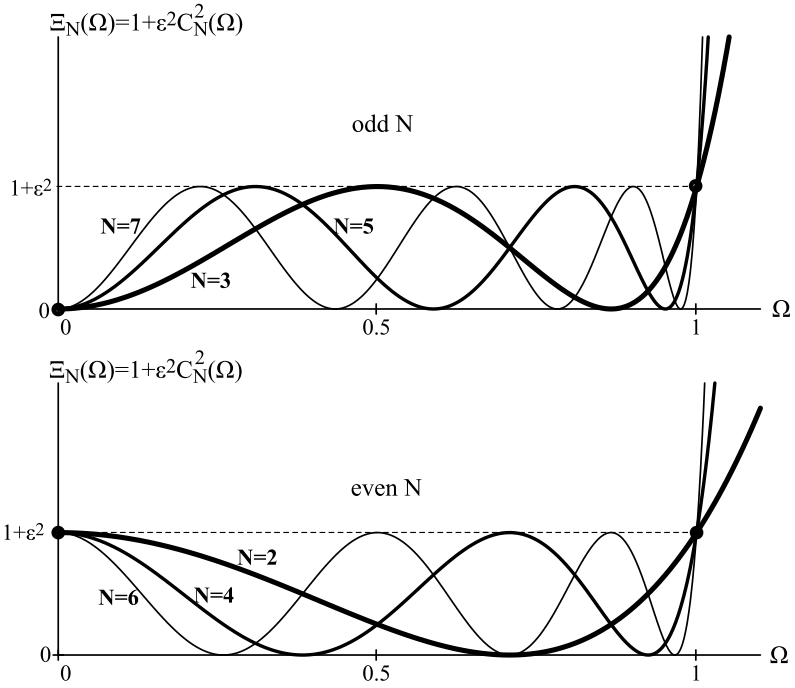

Fig. 2.23 The $\Xi_n(\Omega)$ function

H_o can be taken equal to 1 (i.e. $\alpha_o = 0$ dB) without loss of generality and therefore the filter requirements are determined by three parameters:

$$\Omega_S \quad \text{and} \quad \{H_C, H_S\} \quad \text{or} \quad \{\alpha_{\max}, \alpha_{\min}\} \tag{2.42}$$

referred to as the normalized lowpass filter specifications.

Since Chebyshev polynomials $C_N(\Omega)$ are even or odd, they can be used as approximating functions in (2.7) or (2.36) so as to derive the Chebyshev approximation:

$$G_{CH}(\Omega) = \frac{H_o}{\sqrt{1+\varepsilon^2 C_N^2(\Omega)}} \tag{2.43}$$

The *ripple factor* ε and order N are so chosen to keep the response $G_{CH}(\Omega)$ within the specifications.

In the interval from $\Omega = 0$ to $\Omega = 1$ the function $\Xi_N(\Omega) = 1 + \varepsilon^2 C_N^2(\Omega)$ assumes values which vary from 1 to $1 + \varepsilon^2$ and $\Xi_N(1) = 1 + \varepsilon^2$ since $C_N(\Omega) = 1$ for odd and even N (Fig. 2.23). Therefore, $\frac{H_o}{\sqrt{\Xi_N(\Omega)}} = \frac{H_o}{\sqrt{1+\varepsilon^2 C_N^2(\Omega)}}$ assumes values from 1 to $\frac{H_o}{\sqrt{1+\varepsilon^2}}$ in the same interval [0, 1] and for $\Omega = 1$ takes the value $\frac{H_o}{\sqrt{1+\varepsilon^2}}$.

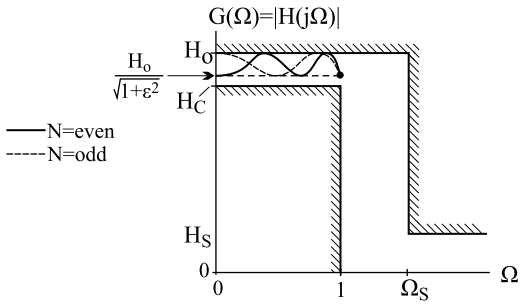

Fig. 2.24 Passband approximation

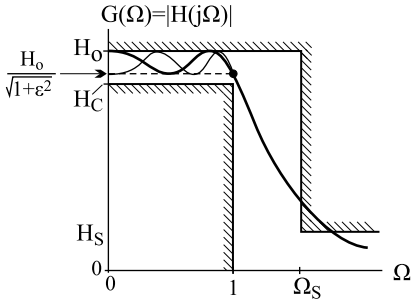

Fig. 2.25 Violation of the specifications in the stopband

For $\Omega > 1$, function $\Xi_N(\Omega)$ is positive and monotonically increasing and therefore $\frac{H_o}{\sqrt{\Xi_N(\Omega)}}$ is positive and monotonically decreasing to zero as $\Omega \to \infty$.

The ripple factor ε can be so selected as to ensure that $\frac{H_o}{\sqrt{1+\varepsilon^2}} \geq H_C$, i.e.

$$\varepsilon \leq \sqrt{\frac{H_o^2}{H_C^2} - 1} = \sqrt{10^{\frac{\alpha_{\max}}{10}} - 1} = \varepsilon_{\max} \tag{2.44}$$

For values of $\varepsilon \leq \varepsilon_{\max}$, the gain $G_{CH}(\Omega)$ will vary in the passband between H_o and $\frac{H_o}{\sqrt{1+\varepsilon^2}} \geq H_C$ and for $\Omega = 1$ it will assume the value $G_{CH}(1) = \frac{H_o}{\sqrt{1+\varepsilon^2}} \geq H_C$. These properties are shown in Fig. 2.24.

As far as the value $G_{CH}(0)$ is concerned, we note that

$$G_{CH}(0) = H_o \quad \text{for odd } N \quad \text{and} \quad G_{CH}(0) = \frac{H_o}{\sqrt{1+\varepsilon^2}} \quad \text{for even } N \tag{2.45}$$

Finally, the Chebyshev gain of (2.43) with $\varepsilon \leq \varepsilon_{\max}$ satisfies the passband specifications according to Fig. 2.24 and (2.45) for $G_{CH}(0)$. Keep in mind that for $\varepsilon = \varepsilon_{\max}$, from (2.44) $\rightarrow G_{CH}(1) = H_C$. However, the stopband specifications might not necessarily be satisfied as shown in Fig. 2.25.

Since Chebyshev polynomials are monotonically increasing for $\Omega > 1$, the gain $G_{CH}(\Omega)$ is monotonically decreasing for the same interval and therefore if we ensure that $G_{CH}(\Omega_S) \leq H_S$, the stopband requirements will be met. This is done

below.

$$G_{CH}(\Omega_s) = \frac{H_o}{\sqrt{1+\varepsilon^2 C_N^2(\Omega_S)}} \leq H_S$$

$$\Leftrightarrow \quad C_N^2(\Omega_S) \geq \frac{(H_o/H_S)^2 - 1}{\varepsilon^2}$$

$$\Leftrightarrow \quad N\cosh^{-1}(\Omega_S) \geq \cosh^{-1}\sqrt{\frac{(H_o/H_S)^2 - 1}{\varepsilon^2}}$$

From the above equation, we get for the order N:

$$N \geq N_d = \frac{\cosh^{-1}(\sqrt{\frac{(H_o/H_S)^2-1}{\varepsilon^2}})}{\cosh^{-1}(\Omega_S)} \tag{2.46}$$

The quantity N_d is in general a non-integer number referred to as the *decimal order* of the approximation. As mentioned in the Butterworth approximation, the complexity of a filter is directly proportional to the order of the approximation and this is the reason we try to keep N as low as possible. The decimal order N_d, if seen as a function of ε, assumes its minimum value for $\varepsilon = \varepsilon_{\max}$. Since normally we are looking for the minimum possible N, the maximum value of ε from (2.44) must be used in (2.46) and finally the order equation is given below

$$N \geq N_d = \frac{\cosh^{-1}(\sqrt{\frac{(H_o/H_S)^2-1}{\varepsilon_{\max}^2}})}{\cosh^{-1}(\Omega_S)} = \frac{\cosh^{-1}(\sqrt{\frac{(H_o/H_S)^2-1}{(H_o/H_C)^2-1}})}{\cosh^{-1}(\Omega_S)} \tag{2.47}$$

In terms of the logarithmic gain specifications, the order equation (2.47) becomes:

$$N \geq N_d = \frac{\cosh^{-1}(\sqrt{\frac{10^{\frac{\alpha_{\min}}{10}}-1}{10^{\frac{\alpha_{\max}}{10}}-1}})}{\cosh^{-1}(\Omega_S)} \tag{2.48}$$

The integer order of the approximation will be the minimum integer N that satisfies $N \geq N_d$, i.e. N_d rounded up to the next integer.

It is apparent from equations (2.47) and (2.48) that the order increases as Ω_S approaches unity and becomes infinite for $\Omega_S = 1$. In other words, the order increases as we try to make the transition band as narrow as possible. In effect, we also say that higher order filters can realize narrower transition bands. The order also increases as the passband tolerance decreases (H_C approaches H_o or $\alpha_{\max}$ approaches zero) and as the maximum allowed stopband gain H_S decreases ($\alpha_{\min}$ increases). Thus, as we try to make the specifications closer and closer to the ideal ones, the order becomes larger and larger, finally becoming infinite. This is another way of saying that the ideal specifications are unrealizable.

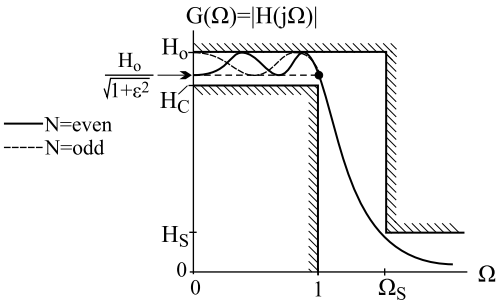

Fig. 2.26 Ripple factor lower than the maximum value

Filters designed with the Chebyshev approximation as above are referred to as Chebyshev filters. Chebyshev filters can be implemented using any suitable technology, e.g. as passive, active or digital filters.

Finally, the Chebyshev gain function

$$G_{CH}(\Omega) = \frac{H_o}{\sqrt{1+\varepsilon^2 C_N^2(\Omega)}} \quad \text{with}$$

$$\varepsilon \le \varepsilon_{\max} = \sqrt{(H_o/H_C)^2 - 1} = \sqrt{10^{\frac{\alpha_{\max}}{10}} - 1} \quad \text{and} \quad N \ge N_d \quad \text{(from (2.48))}$$

satisfies the magnitude specifications in the manner shown in Fig. 2.26.

Passband tolerance is reached only when $\varepsilon = \varepsilon_{\max}$, in which case, $G_{CH}(1) = H_C$ and $G_{CH}(\Omega_S) < H_S$. As far as the DC gain is concerned, it is $G_{CH}(0) = H_C$ when N is odd and $G_{CH}(0) = \frac{H_o}{\sqrt{1+\varepsilon^2}}$ when N is even. In both cases, $G_{CH}(1) = \frac{H_o}{\sqrt{1+\varepsilon^2}}$.

It should be noted that the number of extrema in the passband is equal to the integer order N, including the extremum at $\Omega = 0$.

When the order N has been determined from (2.47) or (2.48), the minimum value of the ripple factor ε can be calculated since

$$N \ge \frac{\cosh^{-1}\left(\sqrt{\frac{(H_o/H_S)^2-1}{\varepsilon^2}}\right)}{\cosh^{-1}(\Omega_S)}$$

from which we get

$$\varepsilon \ge \frac{\sqrt{(H_o/H_S)^2 - 1}}{C_N(\Omega_s)} = \varepsilon_{\min} \tag{2.49}$$

The specifications are satisfied for any value of ε

$$\varepsilon_{\min} = \frac{\sqrt{H_o^2/H_S^2 - 1}}{C_N(\Omega_s)} \le \varepsilon \le \sqrt{H_o^2/H_C^2 - 1} = \varepsilon_{\max} \tag{2.50}$$

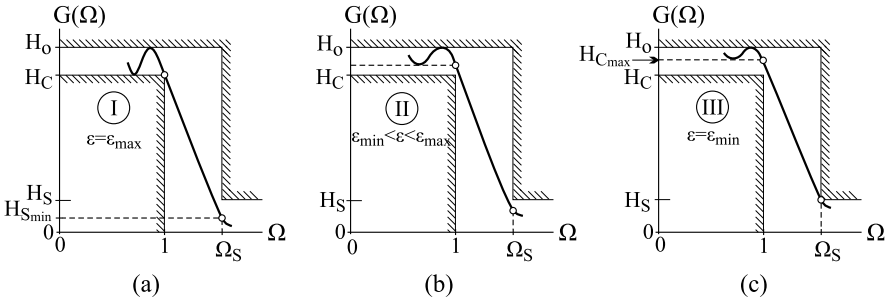

Fig. 2.27 Three choices of the ripple factor ε

or in terms of logarithmic gain

$$\varepsilon_{\min} = \frac{\sqrt{10^{\frac{\alpha_{\min}}{10}} - 1}}{C_N(\Omega_s)} \leq \varepsilon \leq \sqrt{10^{\frac{\alpha_{\max}}{10}} - 1} = \varepsilon_{\max} \tag{2.51}$$

Figure 2.27 shows the manner in which the specifications are met for three choices of the value of the ripple factor.

Case I: $\varepsilon = \varepsilon_{\max}$ When the maximum value of the ripple factor $\varepsilon = \varepsilon_{\max}$ is used, the gain ripple exhausts the passband tolerance with $G_{CH}(1) = H_C$. However, the gain at the stopband edge frequency Ω_S is

$$H_{S\min} = G(\Omega_S) \leq H_S$$

$$H_{S\min} = \frac{H_o}{\sqrt{1 + ((H_o/H_C)^2 - 1)C_N^2(\Omega_S)}} = \frac{H_o}{\sqrt{1 + (10^{\frac{\alpha_{\max}}{10}} - 1)C_N^2(\Omega_S)}} \tag{2.52}$$

This is the minimum gain achieved with a Chebyshev filter of order N at the specified Ω_S and with the specified passband tolerance. Filters designed with $\varepsilon = \varepsilon_{\max}$ are referred to as *stopband edge frequency gain optimized*.

Case II: $\varepsilon_{\min} < \varepsilon < \varepsilon_{\max}$ When the ripple factor ε is not selected to have neither the maximum nor the minimum value, neither passband nor stopband tolerances are exhausted.

Case III: $\varepsilon = \varepsilon_{\min}$ When the minimum value of the ripple factor $\varepsilon = \varepsilon_{\min}$ is used, the gain ripple reaches the stopband tolerance with $G_{CH}(\Omega_S) = H_S$. The gain at $\Omega = 1$ is

$$H_{C\max} = G(1) > H_C$$

$$H_{C\max} = \frac{H_o}{\sqrt{1 + \frac{(H_o/H_S)^2 - 1}{C_N^2(\Omega_S)}}} = \frac{H_o}{\sqrt{1 + \frac{10^{\frac{\alpha_{\min}}{10}} - 1}{C_N^2(\Omega_S)}}} > H_C \tag{2.53}$$

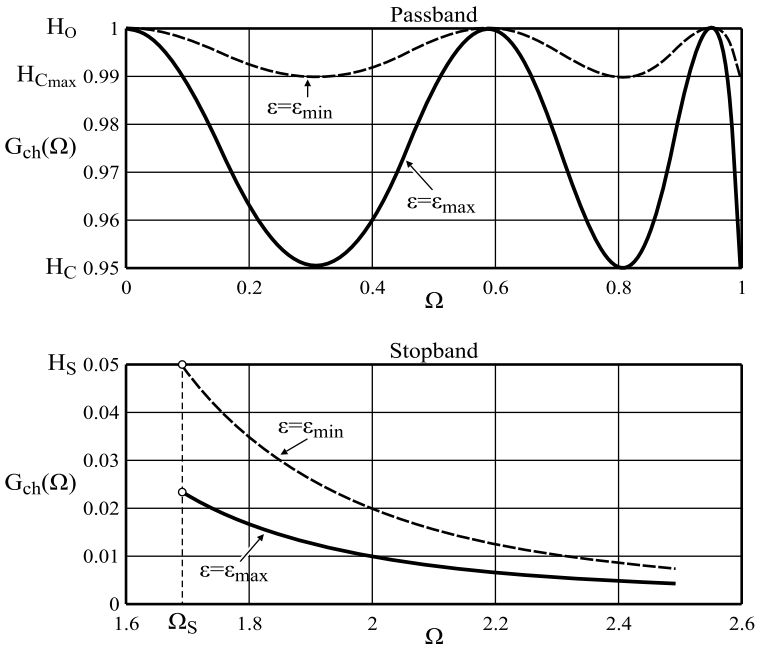

Fig. 2.28 Passband and stopband gain for the maximum and minimum value of the ripple factor

This is the minimum passband ripple that can be achieved with a Chebyshev filter of order N and with the specified stopband tolerance and Ω_S. Filters designed with $\varepsilon = \varepsilon_{\min}$ are referred to as *passband gain optimized* (Fig. 2.27c).

Example 2.5 For $H_o = 1$, $H_C = 0.95$, $H_S = 0.05$ and $\Omega_S = 1.7$, the order can be calculated from (2.47) as $N = 5$. From (2.50), we find $\varepsilon_{\min} = 0.14536$ and $\varepsilon_{\max} = 0.328684$. If $\varepsilon = \varepsilon_{\max} = 0.328684$ is chosen, the ripple will be from $H_o = 1$ to $H_C = 0.95$ and $G_{CH}(1.7) = H_{S\min} = 0.0221$. If $\varepsilon = \varepsilon_{\min} = 0.14536$ is chosen, the ripple will be from $H_o = 1$ to $H_{C\max} = 0.9896$ and $G_{CH}(1.7) = H_S = 0.05$. Figure 2.28 shows these two cases.

Example 2.6 Calculate the stopband edge frequency gain optimized Chebyshev gain function $G_{CH}(\Omega)$ with the specifications given in Fig. 2.29.

First, we identify the specifications: $\omega_C = 600$ rad/s, $\omega_S = 1800$ rad/s, $H_o = 2$, $H_C = 1.9$, and $H_S = 0.1$. Normalizing with $\omega_C = 600$ rad/s, the normalized specifications, shown in Fig. 2.6b will be: $\Omega_C = 1$, $\Omega_S = 3$, $H_o = 2$, $H.C = 1.9$, and $H_S = 0.1$.

Since the stopband edge frequency gain optimized filter is required, $\varepsilon_{\max}$ must be used. From (2.50) we have:

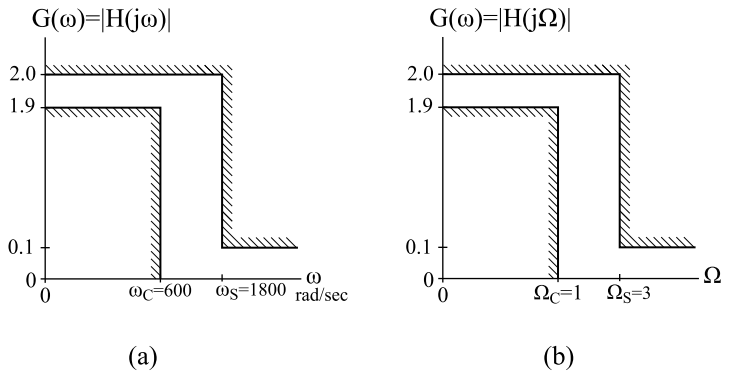

Fig. 2.29 Specifications for Example 2.6a

$$\varepsilon_{\max} = \sqrt{\left(\frac{H_o}{H_C}\right)^2 - 1} = \sqrt{\left(\frac{2.0}{1.90}\right)^2 - 1} = 0.3286837$$

From (2.47), the decimal order N_d and the integer order N can be calculated:

$$N_d = \frac{\cosh^{-1}\left(\sqrt{\frac{\frac{H_o^2}{H_S^2}-1}{\frac{H_o^2}{H_C^2}-1}}\right)}{\cosh^{-1}(\Omega_S)} = \frac{\cosh^{-1}\left(\sqrt{\frac{\frac{2.0^2}{0.1^2}-1}{\frac{2.0^2}{1.9^2}-1}}\right)}{\cosh^{-1}(3)} = 2.723146$$

Therefore $N = 3$ and

$$G_{CH}(\Omega) = \frac{2}{\sqrt{1 + 0.108033C_3^2(\Omega)}} = \frac{2}{\sqrt{1 + 0.108033(4\Omega^3 - 3\Omega)^2}}$$

This is the normalized gain, and the gain which satisfies the specifications of Fig. 2.29a with $\omega_C = 600$ rad/s will be

$$G_{CH}(\omega) = \frac{2}{\sqrt{1 + 0.108033(4\frac{\omega^3}{\omega_C^3} - 3\frac{\omega}{\omega_C})^2}}$$

It should be noted that the Butterworth approximation with the same specifications (see Example 2.1) led to $N = 4$. This is not accidental. In general, for a given set of specifications, the Chebyshev approximation leads to a lower degree than all other all-pole approximations.

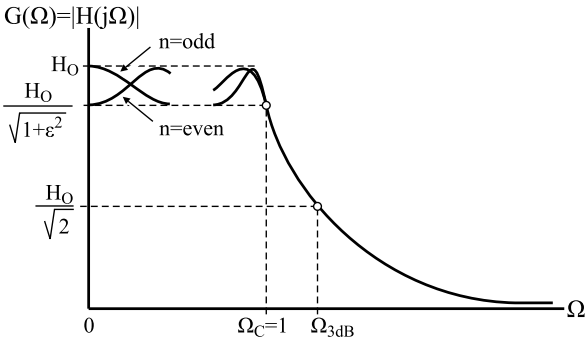

Fig. 2.30 The 3-dB frequency Ω_{3dB}

2.3.3 The 3-dB Frequency and The Cut-off Rate

The frequency Ω_{3dB} at which the gain drops by 3 dB from its maximum value in the passband corresponds to that value at which the gain falls from its maximum value H_o to the value $\frac{1}{\sqrt{2}}H_o$ as shown in Fig. 2.30.

The frequency Ω_{3dB} is determined as follows:

$$\begin{aligned} G_{CH}(\Omega_{3dB}) &= \frac{H_o}{\sqrt{1+\varepsilon^2 C_N(\Omega_{3dB})}} = \frac{\sqrt{2}}{2}H_o \\ \Leftrightarrow \quad & \varepsilon C_N(\Omega_{3dB}) = 1 \\ \Leftrightarrow \quad & \cosh(N\cosh^{-1}(\Omega_{3dB})) = \frac{1}{\varepsilon} \end{aligned}$$

from which we get

$$\Omega_{3dB} = \cosh\left[\frac{1}{N}\cosh^{-1}\left(\frac{1}{\varepsilon}\right)\right] \tag{2.54}$$

It is apparent that for given order N, frequency Ω_{3dB} depends only on the choice of the ripple factor ε.

Another characteristic quantity of polynomial filters is the *cut-off rate* at frequencies $\Omega \gg 1$.

Figure 2.31 shows the plain and logarithmic gain of Chebyshev approximation for $\Omega > 1$ and for a range of orders $N = 3$–7. In the logarithmic gain plot versus logarithmic Ω axis, the gain curves become almost straight lines with increasing constant slope for higher N. This slope can be expressed in dB/octave and is referred to as *cut-off rate* and for $\Omega_1 \gg 1$ can be calculated as follows:

$$\begin{aligned} r &= 20\log(G(\Omega_1)) - 20\log(G(2\Omega_1)) = 20\log\left(\frac{G(\Omega_1}{G(2\Omega_1)}\right) \\ &= 20\log\left(\sqrt{\frac{1+\varepsilon^2 C_N^2(2\Omega_1)}{\sqrt{1+\varepsilon^2 C_N^2(\Omega_1)}}}\right) \approx 20\log\left(\sqrt{\frac{\varepsilon^2 C_N^2(2\Omega_1)}{\sqrt{\varepsilon^2 C_N^2(\Omega_1)}}}\right) \end{aligned}$$

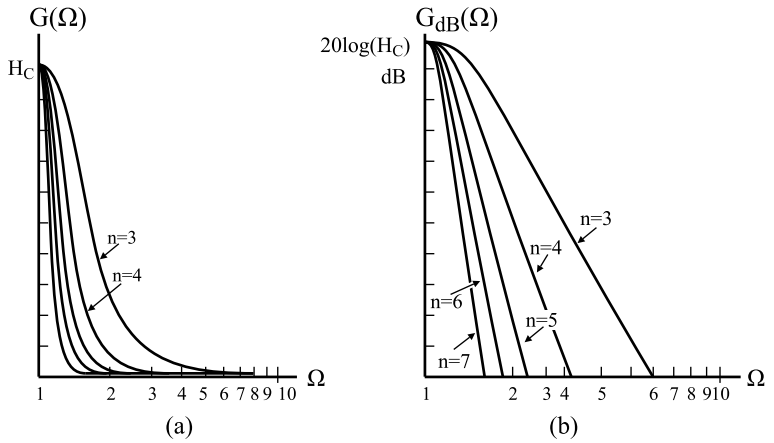

Fig. 2.31 Chebyshev plain and logarithmic gain for $\Omega > 1$

$$= 20\log\left(\frac{C_N(2\Omega_1)}{C_N(\Omega_1)}\right) = 20\log\left(\frac{c_N(2\Omega_1)^N + \cdots}{c_N(\Omega_1)^N + \cdots}\right)$$

$$\text{which for } \Omega_1 \gg 1 \Rightarrow r \approx 20\log(2^N) \approx 6N \text{ dB/octave}$$

This means that the logarithmic gain in the stopband decreases at a rate $6N$ dB/octave, i.e. $6N$ dB for every frequency doubling. If the cut-off rate r is specified, then the order is $N = \frac{r}{6}$.

2.3.4 The Transfer Function

In order to synthesize the filter, the transfer function itself is required.

Thus far, the approximation process yields $G_{CH}(\Omega) = |H(s)|_{s=j\Omega}$. Now we seek to determine a transfer function $H_{CH}(s) = \frac{N(s)}{D_N(s)}$ for which we know its magnitude G_{CH} and that the denominator polynomial $D_N(s)$ is a Hurwitz polynomial. As we have done in the case of Butterworth filters, from

$$H_{CH}(s)H_{CH}(-s) = \frac{N(s)N(-s)}{D_N(s)D_N(-s)} = |G_{CH}(j\Omega)|^2_{\Omega=-js}$$

$$= \frac{H_o^2}{1 + \varepsilon^2 C_N^2(\Omega)|_{\Omega=-js}} \tag{2.55}$$

we set

$$N(s)N(-s) = H_o^2 \quad \Rightarrow \quad N(s) = H_o \tag{2.56}$$

and

$$D_N(s)D_N(-s) = 1 + \varepsilon^2 C_N^2(\Omega)|_{\Omega=-js} \tag{2.57}$$

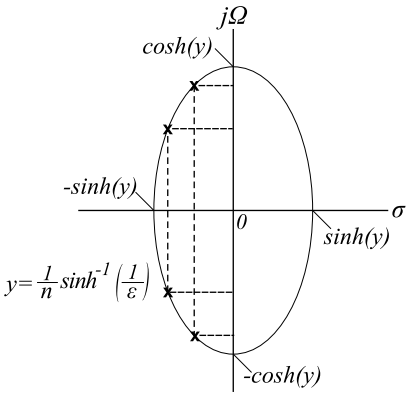

Fig. 2.32 Poles location of the transfer function of Chebyshev approximation

For a specific order N and ripple factor ε, the denominator polynomial $D_N(s)$ has N roots $s_k = \sigma_k + j\Omega_k$ in the left half s-plane given by

$$\begin{aligned} ChebPoles - 1 &= \sin\left(\frac{(2n+2k-1)\pi}{2N}\right)\sinh\left[\frac{1}{N}\sinh^{-1}\left(\frac{1}{\varepsilon}\right)\right] \\ \Omega_k &= \cos\left(\frac{(2n+2k-1)\pi}{2N}\right)\cosh\left[\frac{1}{N}\sinh^{-1}\left(\frac{1}{\varepsilon}\right)\right] \\ k &= 1, 2, \ldots, N \end{aligned} \tag{2.58}$$

For the values of σ_k and Ω_k given by (2.58), it can be easily shown that:

$$\frac{\sigma_k^2}{\sinh^2[\frac{1}{N}\sinh^{-1}(\frac{1}{\varepsilon})]} + \frac{\Omega_k^2}{\cosh^2[\frac{1}{N}\sinh^{-1}(\frac{1}{\varepsilon})]} = 1 \tag{2.59}$$

This implies that the poles of the Chebyshev transfer function lie on an ellipse with the major axis on the $j\Omega$-axis and the minor on the real axis of the s-plane, as shown in Fig. 2.32. This should be compared to the Butterworth case, in which the poles are all located on a circle.

When N is odd, there is a real pole given by (2.58) for $k_o = \frac{N+1}{2}$:

$$s_{k_o} = -\sinh\left[\frac{1}{N}\sinh^{-1}\left(\frac{1}{\varepsilon}\right)\right] + j0 \tag{2.60}$$

It should be noted that there are no poles on the imaginary axis since this would require $\sin(\frac{(2N+2k-1)\pi}{2N}) = 0$, i.e. the positive integer k needs to be $k = \frac{1}{2} - N$ which is impossible.

Finally, the transfer function is given in (2.61)

$$\left\{\begin{array}{l} H_{CH}(s)=\dfrac{H_o/(\varepsilon c_N)}{\prod_{k=1}^{N}(s-s_k)} \quad \text{with } s_k=\sigma_k+j\Omega_k \text{ and} \\ \sigma_k=\sin\left(\dfrac{(2N+2k-1)\pi}{2N}\right)\sinh\left[\dfrac{1}{N}\sinh^{-1}\left(\dfrac{1}{\varepsilon}\right)\right] \\ \Omega_k=\cos\left(\dfrac{(2N+2k-1)\pi}{2N}\right)\cosh\left[\dfrac{1}{N}\sinh^{-1}\left(\dfrac{1}{\varepsilon}\right)\right] \\ k=1,2,\ldots,N \end{array}\right\} \tag{2.61}$$

The coefficient c_N in (2.61) is the coefficient of the highest order term Ω^N in $C_N(\Omega)$, taken from Table 2.2 or calculated as

$$c_N=2^{N-1}$$

The all-pole Chebyshev transfer functions can be implemented using active-RC or passive circuits. The complexity of the implementation depends on the order N and this is the main reason why we want it minimized. Since both Butterworth and Chebyshev filters have all-pole transfer functions, they are realized with similar circuits but of element values.

At the end of this chapter a table is given for the denominator polynomial $D_N(s)$ of the transfer function of the prototype Chebyshev filters with $\Omega_{3dB}=1$. Unfortunately, a separate table is required for each value of the ripple factor. Tables are given for $\alpha_{\max}=0.1$, 0.5, 1.0, 2.0 and 3.0 dB where

$$\alpha_{\max}=20\log\left(\frac{H_o}{H_C}\right)=20\log\sqrt{1+\varepsilon^2}\ (\text{dB})$$

Example 2.7 Calculate the transfer function of the filter of Example 2.6.

In Example 2.6, the order of the filter was found $N=3$ and the 3rd order Chebyshev polynomial is $C_3(\Omega)=4\Omega^3-3\Omega$. Therefore, $c_N=c_3=2^{3-1}=4$. From the specifications, $H_o=2$ and $\varepsilon=\varepsilon_{\max}=0.3286837$. According to (2.61), the transfer function will be

$$H_{CH}(s)=\frac{H_o/(\varepsilon c_N)}{\prod_{k=1}^{N}(s-s_k)}=\frac{2/(0.3286837\cdot 4)}{\prod_{k=1}^{3}(s-s_k)}$$

with $s_k=\sigma_k+j\Omega_k$ and

$$\sigma_k=\sin\left(\frac{(6+2k-1)\pi}{6}\right)\sinh\left[\frac{1}{3}\sinh^{-1}\left(\frac{1}{0.3286837}\right)\right]$$

$$\Omega_k=\cos\left(\frac{(6+2k-1)\pi}{6}\right)\cosh\left[\frac{1}{3}\sinh^{-1}\left(\frac{1}{0.3286837}\right)\right]$$

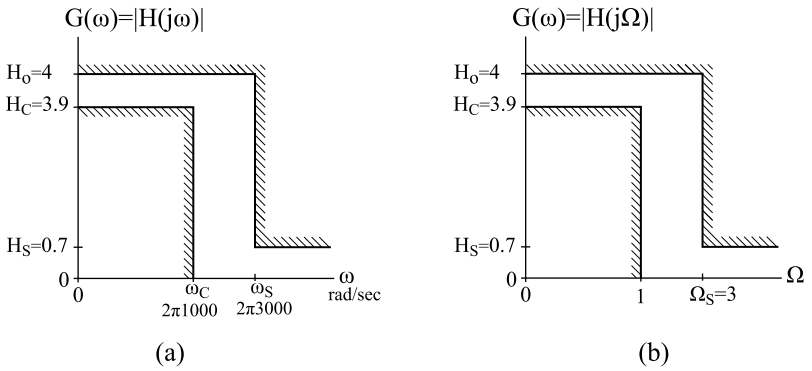

Fig. 2.33 Specifications for Example 2.8

The poles are calculated for $k = 1, \ldots, 3$:

$$s_1 = -0.3246 - j1.0325 \qquad s_2 = -0.6492 \qquad s_3 = -0.3246 + j1.0325$$

The transfer function can then be calculated as

$$H(s) = \frac{2/(4 \cdot 0.32868)}{(s + 0.6492)(s^2 + 2 \cdot 0.3246 \cdot s + 0.3246^2 + 1.0325^2)}$$

This is the normalized transfer function. The transfer function which corresponds to $\omega_C = 600$ and $\omega_S = 1800$ rad/s will be the following

$$H_o(s) = H(s/600)$$

Example 2.8 Find the Chebyshev transfer function from the specifications of Fig. 2.33a.

First, the specifications are identified and normalized as in Fig. 2.33b. The maximum value of the ripple factor is then calculated:

$$\varepsilon_{\max} = \sqrt{\left(\frac{H_o}{H_C}\right)^2 - 1} = \sqrt{\left(\frac{4}{3.9}\right)^2 - 1} = 0.2279$$

The decimal order N_d is calculated from (2.47)

$$N_d = \frac{\cosh^{-1}\left(\sqrt{\frac{\frac{4^2}{0.7^2} - 1}{\frac{4^2}{3.9^2} - 1}}\right)}{\cosh^{-1}(3)} = 2.2119$$

The integer order N of the approximation and the filter will of course be $N = 3$. The transfer function will be:

$$H_{CH}(s) = \frac{H_o/(\varepsilon c_3)}{\prod_{k=1}^{3}(s - s_k)} \quad \text{with } s_k = \sigma_k + j\Omega_k$$

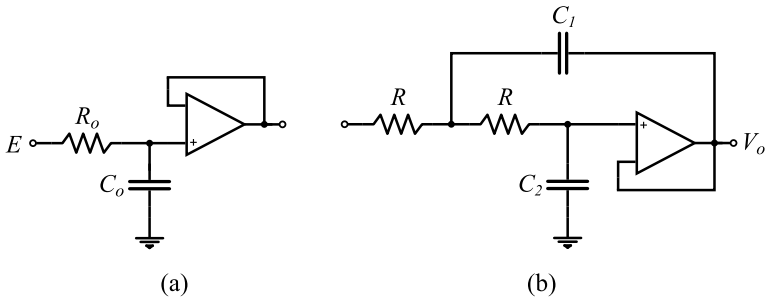

Fig. 2.34 (**a**) Lossy integrator. (**b**) A Sallen-Key 2nd order LP circuit

where

$$\sigma_k = \sin\left(\frac{(2\cdot 3+2k-1)\pi}{2\cdot 3}\right)\sinh\left[\frac{1}{3}\sinh^{-1}\left(\frac{1}{\varepsilon}\right)\right]$$

$$\Omega_k = \cos\left(\frac{(2\cdot 3+2k-1)\pi}{2\cdot 3}\right)\cosh\left[\frac{1}{3}\sinh^{-1}\left(\frac{1}{\varepsilon}\right)\right]$$

Since the order is $N=3 \Rightarrow c_N = c_3 = 4$ (from Table 2.2). If the table is not available, c_N can be calculated from $c_N = 2^{N-1}$.

Selecting the maximum ripple factor value $\varepsilon = \varepsilon_{\max} = 0.2279$, the poles can be calculated for $k = 1\ldots 3$:

$$s_1 = -0.397169 - j1.05997 \qquad s_2 = -0.794339 \qquad s_3 = -0.397169 + j1.05997$$

The transfer function is calculated from (2.61):

$$H_{CH}(s) = \frac{4.38784}{(s+0.794339)(s^2+0.794339s+1.38097375)}$$
$$= \frac{4.38784}{s^3+1.588677s^2+2.011947s+1.09696}$$

Example 2.9 $H_{CH}(s)$ of Example 2.8 can be factorized as follows:

$$H_{CH}(s) = \frac{A_1}{s+0.794339} \times \frac{A_2}{s^2+0.79433s+1.38097375}$$

where $A_1 A_2 = 4.38784$. The first factor $\frac{A_1}{s+0.794339}$ can be realized using a lossy integrator (Fig. 2.34a). The second order factor $\frac{A_2}{s^2+0.79433s+1.38097375}$ can be realized using a Sallen–Key second order lowpass circuit (Fig. 2.34b) with

$$\omega_o = \sqrt{1.38097375} = 1.1751483 \quad \text{and} \quad Q = \sqrt{\frac{1.38097375}{0.794339}} = 1.4794047$$

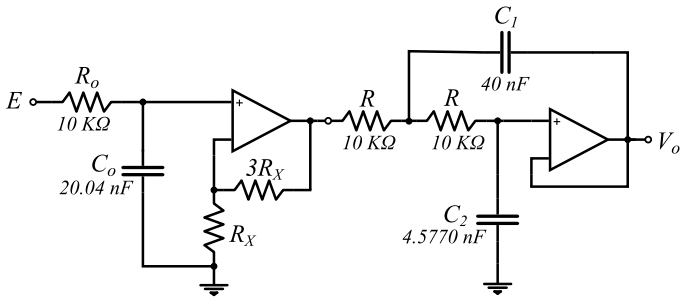

Fig. 2.35 Denormalized circuit

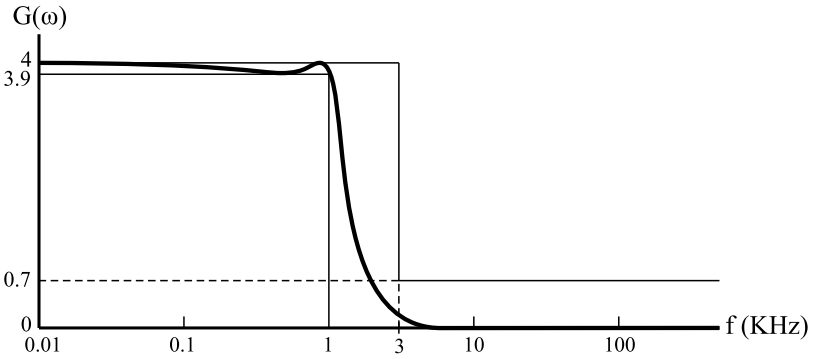

Fig. 2.36 Frequency response of the denormalized circuit

It is observed that the value of the required quality factor Q is higher than the Q required for the 3rd order Butterworth filter of Example 2.4, which meets the same specifications. However, the Chebyshev filter can meet stricter specifications, for which a higher order Butterworth filter is required.

The element values can be calculated as in Example 2.4:

$$R_o = 1 \qquad C_o = 1.25891 \qquad R = 1 \qquad C_1 = 2.5178178 \qquad C_2 = 0.2876$$

Next, the normalized element values are denormalized using $R_n = 10$ kOhm and $\omega_C = 2\pi 10^3$ rad/s (in order to shift the unity cut-off frequency from 1 to ω_C), i.e. $G(2\pi 10^3) = 3.9$:

$$R_o = R = 10 \text{ kOhm} \qquad C_o = 20.04 \text{ nF} \qquad C_1 = 40 \text{ nF} \qquad C_2 = 4.5770 \text{ nF}$$

The denormalized filter is shown in Fig. 2.35. Figure 2.36 shows the plot of the plain gain of the denormalized filter from its PSpice simulation.

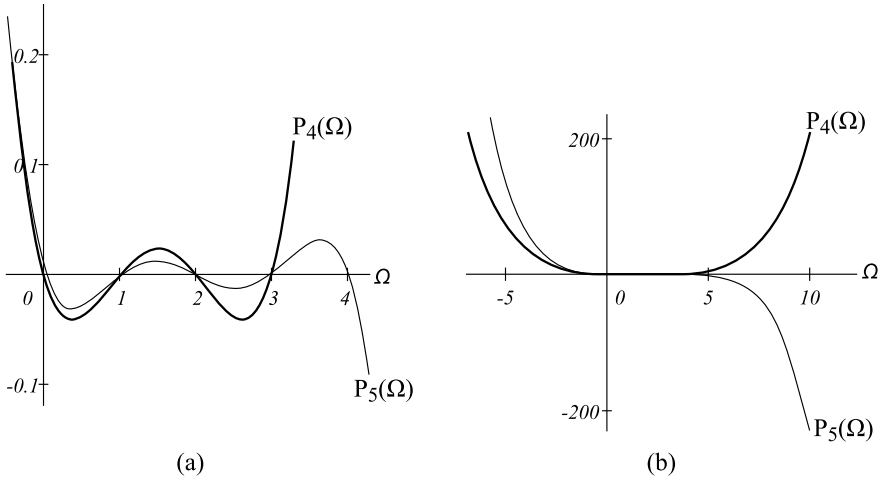

Fig. 2.37 Plot of Pascal polynomials

2.4 The Pascal Approximation

According to (2.7), the approximating polynomial $P_N(\Omega)$ must be an even or odd polynomial in order to lead to a realizable transfer function.

Another set of polynomials are sometimes used in the approximation procedure, the so called Pascal polynomials. The Pascal polynomial [6] of degree N is given by

$$P_o(N,\Omega) = \frac{(-1)^N}{N!}\Omega(\Omega-1)(\Omega-2)\cdots(\Omega-N+1) \tag{2.62}$$

or equivalently

$$P_o(N,\Omega) = \frac{(-1)^N}{N!}\prod_{k=1}^{N}(\Omega-k+1) \tag{2.63}$$

These polynomials, plotted for several orders in Fig. 2.37(a), assume extremely low values for $0 \le \Omega \le N-1$ and very high values for $\Omega \le N-1$. It is clear that they do not satisfy the required symmetry in this form since they are neither odd nor even. However, if they are appropriately shifted this condition can be satisfied.

The Symmetric Shifted Pascal Polynomial $P(N,\Omega)$ The shifted version $P(N,\Omega)$ of the Pascal polynomial $P_o(N,\Omega)$

$$P(N,\Omega) = P_o\left(N,\Omega+\frac{N-1}{2}\right) = \frac{(-1)^N}{N!}\prod_{k=1}^{N}\left(\Omega+\frac{N-1}{2}-k+1\right) \tag{2.64}$$

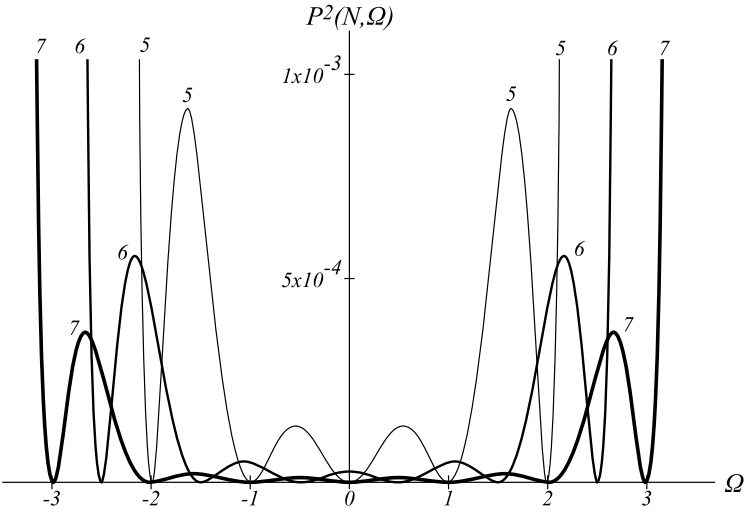

Fig. 2.38 Plot of shifted Pascal polynomials

or equivalently

$$P(N,\Omega)=\frac{(-1)^{\eta}}{N!}\cdot\Omega^{\eta}\cdot\prod_{k=1}^{\frac{N-\eta}{2}}\left[\Omega^2-\left(\frac{N+1}{2}-k\right)^2\right]$$

$$\eta=\begin{cases}1 & \text{for } N \text{ odd}\\ 0 & \text{for } N \text{ even}\end{cases} \tag{2.65}$$

is even when the degree N is even and odd when the degree N is odd and therefore $P^2(N,\Omega)$ is an even polynomial. Moreover, it can be shown that this shifted Pascal polynomial possesses the property

$$P\left(N,\frac{N+1}{2}\right)=\pm 1 \quad\Rightarrow\quad P^2\left(N,\frac{N+1}{2}\right)=1 \tag{2.66}$$

Figure 2.38 shows the plot of $P^2(N,\Omega)$ for $N=5$–7.

It can be shown analytically that the higher local maximum $P^2_{\max}$ of $P^2(N,\Omega)$ occurs for Ω_m between the higher roots of the symmetric polynomial $P(N,\Omega)$, i.e.:

$$\frac{N-1}{2}-1<\Omega_m<\frac{N+1}{2}-1$$

Since $P^2(N,\Omega)$ is an even function, this absolute maximum $P^2_{\max}$ occurs also at $-\Omega_m$.

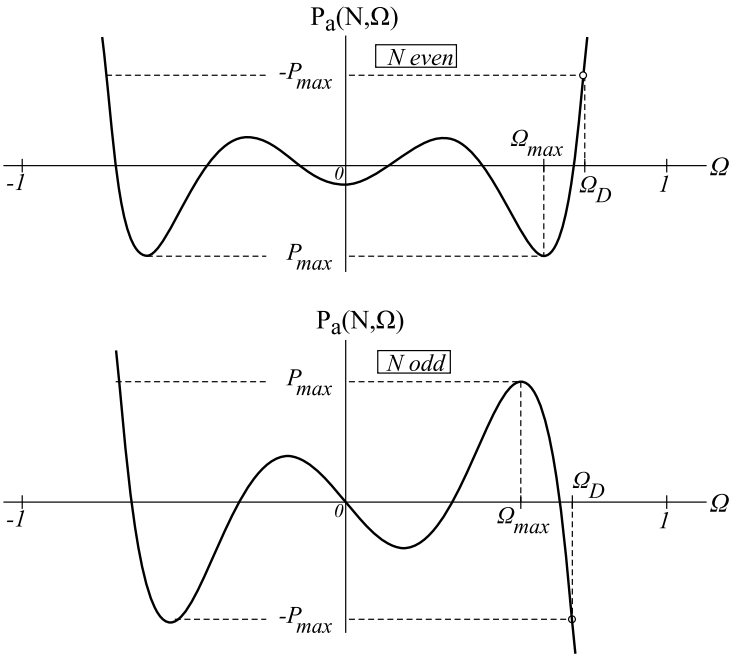

Fig. 2.39 Detailed plot of $P_a(\Omega)$ polynomials

The Shifted and Scaled Symmetric Pascal Polynomial $P_a(N, \Omega)$ If we wish to maintain the condition $|P(N, 1)| = 1$, the property of (2.66) implies that a frequency scaling by $(N + 1)/2$ is required. We denote this symmetric Pascal polynomial by $P_a(N, \Omega)$:

$$P_a(N, \Omega) = P\left(N, \frac{N+1}{2}\Omega\right) = \frac{(-1)^N}{N!}\prod_{k=1}^{N}\left(\frac{N+1}{2}\Omega + \frac{N-1}{2} - k + 1\right) \quad (2.67)$$

or

$$P_a(N, \Omega) = \frac{(-1)^\eta}{N!} \cdot \left(\frac{N+1}{2}\Omega\right)^\eta \cdot \prod_{k=1}^{\frac{N-\eta}{2}}\left[\left(\frac{N+1}{2}\Omega\right)^2 - \left(\frac{N+1}{2} - k\right)^2\right] \quad (2.68)$$

where $\eta = \begin{cases} 1 \text{ for } N \text{ odd} \\ 0 \text{ for } N \text{ even} \end{cases}$.

The highest maximum $P_{\max}$ of $P_a(N, \Omega)$, an indicative plot of which is shown in Fig. 2.39, occurs for $\Omega_{\max}$ between the higher roots of $P_a(N, \Omega)$ i.e.:

$$\frac{N-3}{N+1} < \Omega_{\max} < \frac{N-1}{N+1}$$

Table 2.4 Characteristic values of $P_a(N, \Omega)$

N	$\Omega_{\max}$	$P_{\max}$	Ω_D
2	0.00000000	−0.12500000	0.47140452
3	0.28867513	+0.06415003	0.57735029
4	0.44721360	−0.04166667	0.65289675
5	0.54814429	+0.03026194	0.70639006
6	0.61812758	−0.02347346	0.74582512
7	0.66950940	+0.01901625	0.77599290
8	0.70882772	−0.01588792	0.79978194
9	0.73987600	+0.01358345	0.81900877
10	0.76500826	−0.01182234	0.83486553
11	0.78576311	+0.01043707	0.84816452
12	0.80318872	−0.00932176	0.85947728
13	0.81802376	+0.00840640	0.86921746
14	0.83080378	−0.00764299	0.87769147
15	0.84192645	+0.00699753	0.88513110

Since $P_a^2(N, \Omega)$ is an even polynomial, this highest maximum $P_{\max}^2$ occurs also at $-\Omega_{\max}$. Therefore, the absolute extremum $P_{\max}$ of $P_a(N, \Omega)$ occurs at $\pm\Omega_{\max}$. This extreme value $P_{\max}$ of $P_a(N, \Omega)$ is negative when N is even and positive when it is odd, as shown in Fig. 2.39. It can be shown that there is always a frequency Ω_D in the range $\Omega_{\max} < \Omega_D < 1$ at which the polynomial assumes the value $-P_{\max}$, as indicated in Fig. 2.39. If $P_a(N, \Omega)$ is used to approximate the normalized lowpass filter specifications in a manner described by (2.7), the minimum passband gain will occur at $\Omega_{\max}$ and Ω_D.

Due to the nature of Pascal polynomials, $P_{\max}$ and the related frequencies $\Omega_{\max}$ and Ω_D cannot be determined analytically. These characteristic values, calculated using mathematical software, are tabulated in Table 2.4 for $N = 2$–15 with reference to Fig. 2.39.

The "Filter-Appropriate" Modified Symmetric Pascal Polynomial $P_D(N, \Omega)$

It is desirable to have the value $-P_{\max}$ at $\Omega = 1$ instead of Ω_D. This would ensure that at $\Omega = 1$ the gain will be exactly equal to the minimum gain in the passband which is due to the absolute extreme value $-P_{\max}$ of $P_a(N, \Omega)$. To move Ω_D to 1, we simply scale the polynomial $P_a(N, \Omega)$ of (2.67) and (2.68) by $\Omega_D < 1$, so defining $P_D(N, \Omega)$:

$$P_D(N, \Omega) = P_a(N, \Omega_D \Omega) = \frac{(-1)^N}{N!} \prod_{k=1}^{N} \left(\frac{N+1}{2} \Omega_D \Omega + \frac{N-1}{2} - k + 1 \right) \quad (2.69)$$

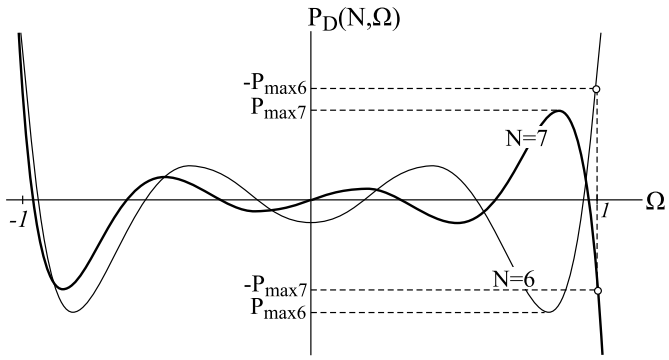

Fig. 2.40 Plot of filter-appropriate $P_D(\Omega)$ polynomials

From (2.69), it is clear that $P_D(N, \Omega)$ has $(N - \eta)/2$ positive non-zero roots ρ_k given by

$$\rho_k = \frac{(N+1) - 2k}{(N+1)\Omega_D} < 1 \quad \text{for } k = 1, \ldots, \frac{N-\eta}{2} \tag{2.70}$$

and $(N - \eta)/2$ negative real roots $-\rho_k$. Parameter Ω_D depends only on N and can be taken from Table 2.4. Equation (2.69) can therefore be written as

$$P_D(\Omega) = \frac{(-1)^\eta}{N!}\left(\frac{N+1}{2}\Omega_D\right)^N \Omega^\eta \prod_{k=1}^{\frac{N-\eta}{2}} [\Omega^2 - \rho_k^2] \tag{2.71}$$

where ρ_k are the positive roots of $P_D(N, \Omega)$ given in (2.70).

The symmetric polynomial $P_D(N, \Omega)$ is related to the original Pascal polynomial $P_o(N, \Omega)$ of (2.63) by the relationship:

$$P_D(N, \Omega) = P_o\left(N, \frac{N+1}{2}\Omega_D\Omega + \frac{N-1}{2}\right) \tag{2.72}$$

The absolute extremum of $P_D(N, \Omega)$ has the same value $P_{\max}$ and occurs at $\Omega_{\max}/\Omega_D < 1$. The property of $P_D(N, \Omega)$ which makes it "filter-appropriate" can be expressed as

$$|P_D(N, 1)| = \left|P_D\left(N, \frac{\Omega_{\max}}{\Omega_D}\right)\right| = |P_{\max}| \tag{2.73}$$

The polynomial $P_D(N, \Omega)$ is so constructed as to assume the value $\pm P_{\max}$ at $\Omega = 1$ and to decrease monotonically from $\Omega_{\max}/\Omega_D < 1$. Both characteristic frequencies, as well as $P_{\max}$, can be taken from Table 2.4. An indicative plot of $P_D(N, \Omega)$ for $N = 6$ and $N = 7$ is shown in Fig. 2.40.

Table 2.5 Roots of the filter-appropriate Pascal polynomial $P_D(\Omega)$

N	ρ_1	ρ_2	ρ_3	ρ_4	ρ_5	ρ_6	ρ_7
2	0.70710678						
3	0.8660254						
4	0.91898144	0.30632715					
5	0.94376568	0.47188284					
6	0.95771207	0.57462724	0.19154241				
7	0.96650368	0.64433579	0.32216789				
8	0.97248731	0.69463379	0.41678027	0.13892676			
9	0.97679052	0.73259289	0.48839526	0.24419763			
10	0.98001629	0.76223489	0.54445349	0.32667210	0.10889070		
11	0.98251382	0.78601105	0.58950829	0.39300553	0.19650276		
12	0.98449821	0.80549854	0.62649886	0.44749919	0.26849951	0.08949984	
13	0.98610865	0.82175721	0.65740577	0.49305432	0.32870288	0.16435144	
14	0.98743887	0.83552520	0.68361153	0.53169786	0.37978418	0.22787051	0.07595684
15	0.98855417	0.84733215	0.70611012	0.56488810	0.42366607	0.28244405	0.14122202

Referring to the definition of $P_D(N, \Omega)$ of (2.71), its non-zero roots are given by

$$\pm\frac{(N+1)-2k}{(N+1)\Omega_D} \quad \text{for } k = 1, \ldots, \frac{N-\eta}{2}$$

The $(N-\eta)/2$ positive roots ρ_k of interest are given by

$$\rho_k = \frac{(N+1)-2k}{(N+1)\Omega_D} \quad \text{for } k = 1, \ldots, \frac{N-\eta}{2}, \ \eta = \begin{cases} 1 & \text{for } N \text{ odd} \\ 0 & \text{for } N \text{ even} \end{cases} \tag{2.74}$$

(Frequency Ω_D depends only on N and can be taken from Table 2.4.)

It is observed from (2.71) that for odd N, in which case $\eta = 1$, there will also exist a root at $\Omega = 0$. Table 2.5 gives the positive roots of $P_D(\Omega)$ for $N = 1$–15.

While for odd degree polynomials we have $P_D(N, 0) = 0$, even degree polynomials assume a very low value $P_D(N, 0)$ at $\Omega = 0$ given by:

$$\begin{aligned} P_D(N,0) &= \frac{N-1}{2\pi \cdot N!}\sin\left(\frac{N+1}{2}\pi\right)\Gamma\left(\frac{N+1}{2}\right)\Gamma\left(\frac{N-1}{2}\right) \quad \text{or} \\ P_D(N,0) &= \frac{1}{\pi \cdot N!}\sin\left(\frac{N+1}{2}\pi\right)\Gamma^2\left(\frac{N+1}{2}\right) \end{aligned} \tag{2.75}$$

$\Gamma(x)$ is the Gamma function [7]. Table 2.6 gives $P_D(N, 0)$ for the even $N = 2$–16.

Table 2.6 Values $P_D(N, 0)$

N	$P_D(N, 0)$
2	$-125 \cdot 10^{-3}$
4	$+23.4375 \cdot 10^{-3}$
6	$-4.882812 \cdot 10^{-3}$
8	$+1.068115 \cdot 10^{-3}$
10	$-240.325928 \cdot 10^{-6}$
12	$+55.074692 \cdot 10^{-6}$
14	$-12.785196 \cdot 10^{-6}$
16	$+2.99653 \cdot 10^{-6}$

Table 2.7 Polynomial coefficients of $P_D(N, \Omega)$ for $N = 2$–7

$P_D(N, \Omega) = a_N \Omega^N + a_{N-1} \Omega^{N-1} + \cdots + a_1 \Omega + a_0$

$N \rightarrow$	2	3	4	5	6	7
a_0	−0.125000	0	0.023438	0	−0.004882	0
a_1	0	0.192450	0	−0.070639	0	0.022171
a_2	0.250000	0	−0.277522	0	0.153199	0
a_3		−0.256600	0	0.396539	0	−0.2907494
a_4			0.295751	0	−0.564281	0
a_5				−0.356162	0	0.800362
a_6					0.439438	0
a_7						−0.550800

The coefficients of the polynomial $P_D(N, \Omega)$ for $N = 2$–7 are tabulated in Table 2.7.

For the coefficients of the highest and lowest order terms of $P_D(N, \Omega)$, analytic formulae can be derived from the definition equations:

$$a_N = \frac{(-1)^N}{N!} \cdot \left(\frac{N+1}{2} \Omega_D \right)^N \tag{2.76}$$

$$a_\eta = \frac{(-1)^{\frac{N+\eta}{2}}}{N!} \left(\frac{N+1}{2} \Omega_D \right)^\eta \cdot \prod_{k=1}^{(N-\eta)/2} \left(\frac{N+1}{2} - k \right)^2 \tag{2.77}$$

or

$$a_\eta = \frac{(-1)^{\frac{N+\eta}{2}}}{2^N N!} (N+1)^\eta \Omega_D^\eta \cdot \prod_{k=1}^{(N-\eta)/2} (N+1-2k)^2 \tag{2.78}$$

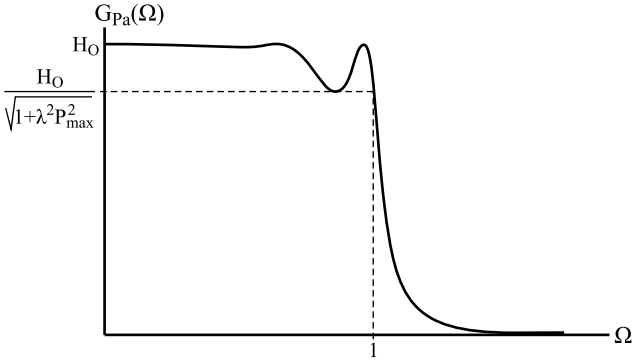

Fig. 2.41 The Pascal approximation gain

2.4.1 Optimizing the Pascal Approximation

The polynomial $P_D(N, \Omega)$ is symmetric and therefore can be used for the definition of the Pascal approximation:

$$G_{Pa}(\Omega) = \frac{H_o}{\sqrt{1 + \lambda^2 P_D^2(N, \Omega)}} \tag{2.79}$$

The non-equiripple nature of the Pascal polynomials appears in the gain of the Pascal approximation, as shown in Fig. 2.41. The minimum passband gain depends only on the order N, occurs at $\Omega = \frac{\Omega_{\max}}{\Omega_D}$ and its value is $\frac{H_o}{\sqrt{1+P_{\max}^2}}$. The gain takes the same value at $\Omega = 1$.

The constant factor λ, corresponding to the ripple factor ε of the Chebyshev approximation, is calculated next from the normalized lowpass filter specifications Ω_S and $\{H_C, H_S\}$ or $\{\alpha_{\max}, \alpha_{\min}\}$.

The plot of $G_{Pa}(\Omega)$ of (2.79) must not enter the shaded areas of Fig. 2.42a. The gain at $\Omega = 1$, $G_{Pa}(1) = \frac{H_o}{\sqrt{1+\lambda^2 P_D(1)}}$, equals the gain at $(\Omega_{\max}/\Omega_D) < 1$ which is the absolute passband minimum and decreases monotonically for $\Omega > 1$. Therefore, as far as the passband is concerned, the gain will remain in the permitted area by selecting λ to satisfy

$$G_{Pa}(1) = \frac{H_o}{\sqrt{1 + \lambda^2 P_D^2(N, 1)}} \geq H_C \tag{2.80}$$

The term $P_D^2(N, 1) = P_{\max}^2$ and therefore

$$\lambda \leq \lambda_{\max} = \frac{\sqrt{\frac{H_o^2}{H_C^2} - 1}}{|P_{\max}|} = \frac{\sqrt{10^{\frac{\alpha_{\max}}{10}} - 1}}{|P_{\max}|} \tag{2.81}$$

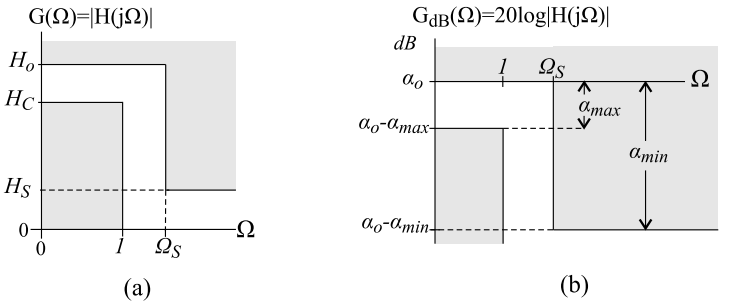

Fig. 2.42 Normalized lowpass specifications: (**a**) Plain gain. (**b**) Logarithmic gain

Using the maximum value for the λ parameter we get the stopband edge optimized response:

$$\lambda = \lambda_{\max} \quad \Rightarrow \quad G_{Pa}(1) = G_{Pa}\left(\frac{\Omega_{\max}}{\Omega_D}\right) = H_C$$

and

$$G_{Pa}(\Omega_S) = \frac{H_o}{\sqrt{1 + (10^{\frac{\alpha_{\max}}{10}} - 1)(\frac{P_D(N,\Omega_S)}{P_D(N,1)})^2}} < H_S \tag{2.82}$$

It will be shown that parameter λ has also a lower boundary value $\lambda_{\min}$ derived from the stopband requirement:

$$G_{Pa}(\Omega_S) = \frac{H_o}{\sqrt{1 + \lambda^2 P_D^2(N, \Omega_S)}} \leq H_S \tag{2.83}$$

This implies that

$$\lambda \geq \lambda_{\min} = \frac{\sqrt{\frac{H_o^2}{H_S^2} - 1}}{|P_D(N, \Omega_S)|} = \frac{\sqrt{10^{\frac{\alpha_{\min}}{10}} - 1}}{|P_D(N, \Omega_S)|} \tag{2.84}$$

The passband optimized response is derived by selecting

$$\lambda = \lambda_{\min} \quad \Rightarrow \quad G_{Pa}(\Omega_S) = H_S$$

and

$$G_{Pa}(1) = \frac{H_o}{\sqrt{1 + (10^{\frac{\alpha_{\min}}{10}} - 1)(\frac{P_D(N,1)}{P_D(N,\Omega_S)})^2}} > H_C \tag{2.85}$$

Finally, the ripple factor λ can be selected from (2.81) in view of (2.84), or from their combined expression:

$$\frac{\sqrt{10^{\frac{\alpha_{\min}}{10}}-1}}{|P_D(N,\Omega_S)|} = \lambda_{\min} \le \lambda \le \lambda_{\max} = \frac{\sqrt{10^{\frac{\alpha_{\max}}{10}}-1}}{|P_D(N,1)|}$$
$$\text{with } |P_D(N,1)| = |P_{\max}| \tag{2.86}$$

2.4.2 Order Calculation

So far, the order N has not been known, but can be calculated from (2.80) by setting $\lambda = \lambda_{\min}$ or from (2.83) by setting $\lambda = \lambda_{\max}$. In both cases, we end up with the order inequality

$$\left|\frac{P_D(N,1)}{P_D(N,\Omega_S)}\right| = \left|\frac{P_{\max}}{P_D(N,\Omega_S)}\right| \le g = \sqrt{\frac{\frac{H_o^2}{H_C^2}-1}{\frac{H_o^2}{H_S^2}-1}} = \sqrt{\frac{10^{\frac{\alpha_{\max}}{10}}-1}{10^{\frac{\alpha_{\min}}{10}}-1}} \ll 1 \tag{2.87}$$

In this inequality, the only unknown is the order N since the quantity g depends on the gain specifications. Therefore, for the calculation of the order, inequality (2.87) must be solved for N, but due to the nature of the Pascal polynomials, an analytic expression cannot be derived. However, the nomograph shown in Fig. 2.43 can be derived by using a mathematical software package.

The nomograph works as follows: We draw a vertical line from the point of the horizontal axis which corresponds to the specified Ω_S. We then draw a horizontal line from the point of the vertical axis that corresponds to HP:

$$HP = 20 \cdot \log\left(\frac{1}{g}\right) \tag{2.88}$$

The two lines intersect at a point. The order N is the number of the curve that lies above this point.

As an example, let us find the order if the specifications of the filter are $\Omega_S = 1.5$, $\alpha_{\max} = 0.5$ dB and $\alpha_{\min} = 40$ dB. Equation (2.88) gives $HP = 49.14$ and from the nomograph we get $N = 8$, since the point is located above curve 7.

2.4.3 The Transfer Function

The poles and the transfer function can, in theory, be calculated from

$$H(s)H(-s) = G_{Pa}^2(\Omega)|_{\Omega^2=-s^2}$$
$$= \frac{H_o^2}{1+\lambda^2 P_D^2(N,\Omega)}\bigg|_{\Omega^2=-s^2} = G_{Pa}^2(js) = G_{Pa}^2(-js) \tag{2.89}$$

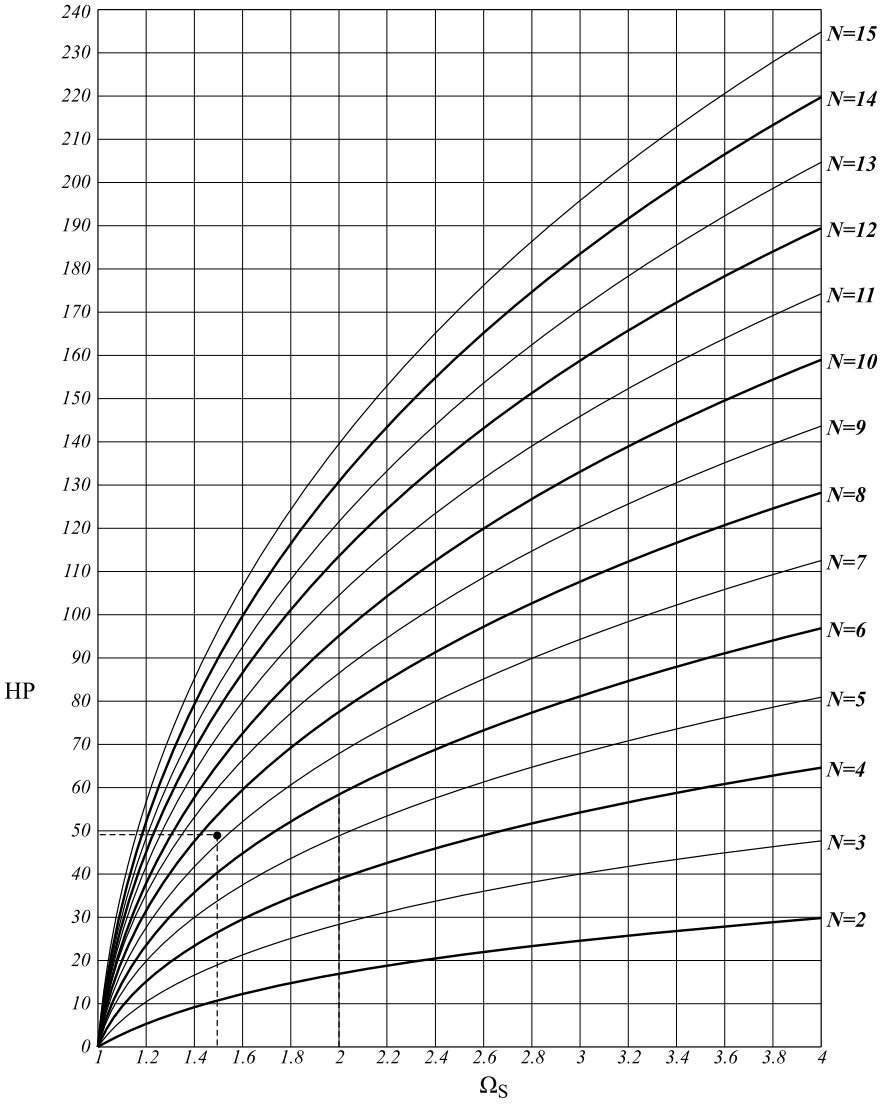

Fig. 2.43 Nomograph for the calculation of the order of the Pascal approximation

Since we have a polynomial approximation, the transfer function is expected to be all-pole of the form:

$$H(s) = \frac{C}{\prod_{k=1}^{N}(s - s_k)} = \frac{C}{(s + s_R)^{\eta} \prod_{k=1}^{\frac{N-\eta}{2}} (s^2 + 2\,\mathrm{Re}[s_k] + |s_k|^2)}$$

$$\text{with } \eta = \begin{cases} 1 & \text{for } N \text{ odd} \\ 0 & \text{for } N \text{ even} \end{cases} \tag{2.90}$$

where $s_k = \sigma_k \pm j\Omega_k$ are the $(N-\eta)/2$ conjugate pole pairs of $H(s)$ and s_R the real pole when N is odd.

The constant C of (2.90) can be calculated by letting

$$P_D(N, \Omega) = a_N \Omega^N + \cdots + a_\eta \Omega^\eta$$

in (2.89), which after some manipulation yields:

$$C = \frac{H_o}{\lambda \cdot |\alpha_N|} \tag{2.91}$$

where α_N is the coefficient of Ω^N in the polynomial $P_D(N, \Omega)$ taken from Table 2.7 or calculated from (2.76).

It seems again that no analytic expressions can be found for the poles and the use of numerical methods is inevitable in order to calculate the poles from equation (2.89). Note that α_N depends only on the order N, and the ripple factor $\lambda_{\max}$ depends on N and the specified $\alpha_{\max}$. In view of (2.89), the poles are therefore functions of N and $\alpha_{\max}$, and a table giving the constant C and the poles can be created for all values of order N and all values of $\alpha_{\max}$. Tabulation for $\lambda = \lambda_{\min}$ would require separate tables for values of Ω_S since $\lambda_{\min}$ depends on Ω_S according to (2.84).

Tables 2.8 at the end of this chapter give the constant C and the poles of the transfer function for $N = 2$–9 and $\alpha_{\max} = 0.01$, 0.1, 0.5, 1.0, 1.25 and 1.5 dB. All tables have been created for the stopband edge optimized case with $\lambda = \lambda_{\max}$. For any other value $\lambda_{\min} < \lambda < \lambda_{\max}$, a mathematical software package must be used.

2.4.4 Design Examples

Given the normalized specifications Ω_S and $\{H_C, H_S\}$ or $\{\alpha_{\max}, \alpha_{\min}\}$, the complete design procedure can be outlined as follows:

1. Calculate HP from (2.88) and find the order N of the filter from the nomograph of Fig. 2.43. If the transfer function of the stopband edge optimized filter ($\lambda = \lambda_{\max}$) is required, skip to step 4.
2. Get $P_{\max}$ and Ω_D from Table 2.4 for the calculated order N.
3. Calculate the limits of the ripple factor λ. If the stopband edge optimized filter is to be designed, $\lambda_{\max}$ can be calculated from (2.86). If the passband optimized filter is required, $L(N, \Omega_S) = P_D(N, \Omega_S)$ can be calculated from (2.69) or (2.71) and $\lambda_{\min}$ from (2.86). At this point, all necessary information for the gain is available.
4. If the stopband edge optimized filter is to be designed with $\lambda = \lambda_{\max}$, the transfer function can be calculated using the tables at the end of the chapter. For any other value $\lambda_{\min} < \lambda < \lambda_{\max}$, the coefficient C and the poles of the transfer function can be calculated from (2.89) using a mathematical software package.

Example 2.10 As an example, a Pascal filter transfer function with specifications $H_o = 1$, $\Omega_S = 2$, $\alpha_{\max} = 1.25$ dB and $\alpha_{\min} = 40$ dB will be calculated and compared to the Butterworth and Chebyshev transfer functions with the same specifications.

From (2.88), we find $HP = 44.77$. Using this value, the order of the filter can be found from the nomograph: $N = 5$ ($N_{But} = 8$, $N_{Che} = 5$). For the stopband edge optimized filter, the ripple factor, although unnecessary, is calculated from (2.86) $\lambda_{\max} = 19.083796$

From Table 2.4 for $N = 5$, we get $P_{\max} = 0.03026194$ and $\Omega_D = 0.70639006$. From Tables 2.8 for $N = 5$ and $\alpha_{\max} = 1.25$, we get $C = 0.147125$, real pole -0.383466 and two conjugate pole pairs:

$$\begin{aligned} -0.286033 \pm j0.558421 \quad &\rightarrow \quad \Omega_1 = 0.62741472, \qquad Q_1 = 1.09675171 \\ -0.094300 \pm j0.982733 \quad &\rightarrow \quad \Omega_2 = 0.98724656, \qquad Q_2 = 5.23459125 \end{aligned}$$

Knowing C and the poles, the transfer function is calculated from (2.90):

$$H(s) = \frac{0.147125}{(s + 0.383466)(s^2 + \frac{\Omega_1}{Q_1}s + \Omega_1^2)(s^2 + \frac{\Omega_2}{Q_2}s + \Omega_2^2)}$$

The plot of the gain function $G(\Omega) = |H(j\Omega)|$ is shown in Fig. 2.44 (thick curve) together with the corresponding gain plots for the Butterworth design ($N_{But} = 8$, dotted curve) and Chebyshev design ($N_{Che} = 5$, thin curve).

Example 2.11 As a second example, let us design a Pascal filter with specifications $\Omega_S = 1.5$, $\alpha_{\max} = 0.5$ dB and $\alpha_{\min} = 40$ dB.

From (2.88), $HP = 49.14$. Using this value, the order of the filter can be found from the nomograph: $N = 8$ ($N_{But} = 14$, $N_{Che} = 7$). For the stopband edge optimized filter $\lambda = \lambda_{\max}$, the ripple factor is calculated from (2.86) as $\lambda_{\max} = 21.985965$.

From Table 2.4 for $N = 8$, we get $P_{\max} = -0.01588792$ and $\Omega_D = 0.79978194$. From Tables 2.8 for $N = 8$ and $\alpha_{\max} = 0.5$, we get $C = 0.06514816$ and four conjugate pole pairs:

$$\begin{aligned} -0.43824049 \pm j0.18275053 \quad &\rightarrow \quad \Omega_1 = 0.4748184, \qquad Q_1 = 0.54173266 \\ -0.35480472 \pm j0.52718634 \quad &\rightarrow \quad \Omega_2 = 0.6354619, \qquad Q_2 = 0.89550936 \\ -0.20803356 \pm j0.81122122 \quad &\rightarrow \quad \Omega_3 = 0.8374711, \qquad Q_3 = 2.01282686 \\ -0.06129275 \pm j1.00838152 \quad &\rightarrow \quad \Omega_4 = 1.0102419, \qquad Q_4 = 8.24261602 \end{aligned}$$

Therefore, the transfer function will be

$$H(s) = \frac{0.06514816}{\prod_{k=1}^{4}(s^2 + \frac{\Omega_k}{Q_k}s + \Omega_k^2)}$$

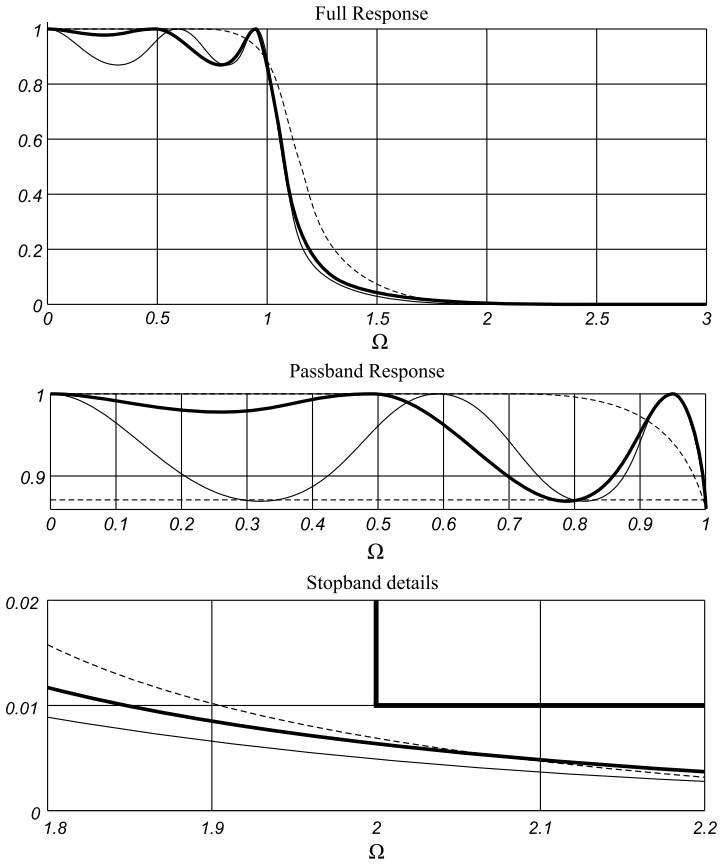

Fig. 2.44 Gain plot of design Example 2.10

Figure 2.45 shows the gain response $G(\Omega) = |H(j\Omega)|$ (thick curve) against the corresponding responses of the Butterworth ($N_{But} = 14$, dotted curve) and Chebyshev ($N_{Che} = 7$, thin curve) responses.

Example 2.12 In order to design the passband optimized filter with the same specifications and $G_{Pa}(\Omega_S) = H_S$, the minimum value $\lambda = \lambda_{\min}$ must be used. Calculation of the value $P_D(N, \Omega_S) = P_D(8, 1.5)$ must firstly be performed from (2.69) or (2.71), and then $\lambda_{\min}$ can be found from (2.86): $\lambda_{\min} = 13.414$. In this case, Tables 2.8 for the transfer function constant C and the poles cannot be used. Using a mathematical software package, we find $C = 0.10677611$ and the four new conjugate pole pairs:

$$-0.4962400 \pm j0.1898488 \quad \rightarrow \quad \Omega_1 = 0.531316, \qquad Q_1 = 0.53534173$$
$$-0.4060296 \pm j0.5468592 \quad \rightarrow \quad \Omega_2 = 0.681113, \qquad Q_2 = 0.83874807$$

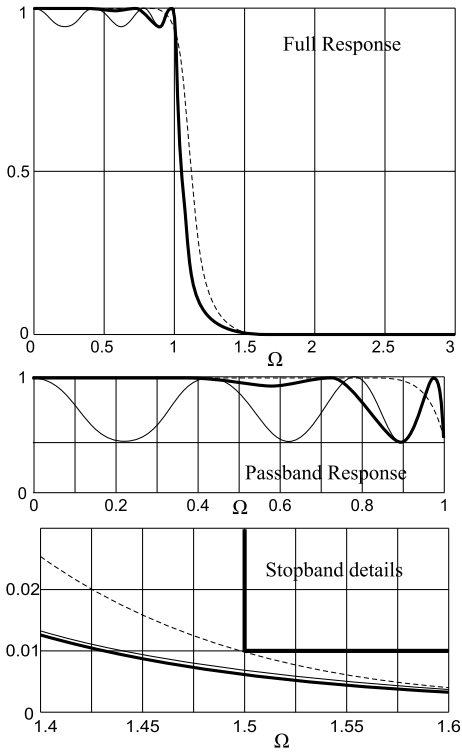

Fig. 2.45 Gain plot of design Example 2.11

$$-0.2468183 \pm j0.8389962 \quad \rightarrow \quad \Omega_3 = 0.874548, \qquad Q_3 = 1.77164396$$
$$-0.0769663 \pm j1.0296597 \quad \rightarrow \quad \Omega_4 = 1.032532, \qquad Q_4 = 6.70772459$$

The transfer function will in this case be:

$$H(s) = \frac{0.10677611}{\prod_{k=1}^{4}(s^2 + \frac{\omega_k}{Q_k}s + \omega_k^2)}$$

It should be observed that the passband optimized design with $\lambda = \lambda_{\min}$ leads to lower Q values. The gain response of the passband optimized filter is shown in Fig. 2.46 (thick curve).

2.4.5 Comparison to Other Polynomial Approximations

If the order of a Chebyshev filter which meets certain specifications is N_{Cheb}, then the order N of the Pascal filter that meets the same specifications is usually for low orders N_{Cheb}, as in Example 2.10. For higher orders, due to narrow transition bands (Ω_S close to 1), the order of the Pascal filter can be, in the worst case $N_{Cheb} + 2$.

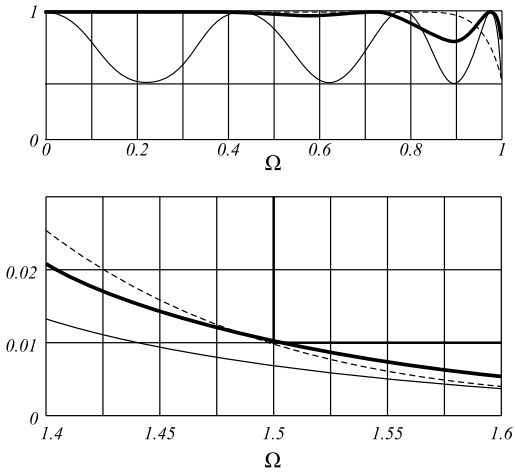

Fig. 2.46 Gain plot of design Example 2.12

This statement cannot be proved analytically but can be demonstrated and verified by constructing combined Pascal-Chebyshev order nomographs [6]. It should be noticed that the order of the Butterworth filters in these cases can even be as high as $2N_{Cheb}$, as in Example 2.11.

As far as the pole-Qs are concerned, Pascal filters seem to exhibit lower values, even when the Chebyshev filter that meets the same specifications is of lower order. In Example 2.10, Pascal filter with $N = 5$ has $Q_1 = 1.1$ and $Q_2 = 5.23$. The corresponding Chebyshev filter with $N_{Cheb} = 5$ has $Q_1 = 1.5$ and $Q_2 = 6.0$. In Example 2.11, Pascal filter with $N = 8$ has $Q_1 = 0.54$, $Q_2 = 0.89$, $Q_3 = 2.01$ and $Q_4 = 8.24$. The corresponding Chebyshev filter with $N_{Cheb} = 7$ has $Q_1 = 1.1$, $Q_2 = 2.58$ and $Q_3 = 8.84$. It should be noticed that the passband optimized Pascal filter of Example 2.12 has even lower Q values: $Q_1 = 0.54$, $Q_2 = 0.84$, $Q_3 = 1.77$ and $Q_4 = 6.70$.

Group delay must be compared for filters that meet the same specifications, and not for filters having the same order. Under this principle, Fig. 2.47 shows the group delay plots for the three design examples.

In Fig. 2.47(a), the order of the Pascal and the Chebyshev filter is $N_{Pa} = N_{Cheb} = 5$, and the group delay of the Pascal filter (thick curve) seems to be slightly better and still comparable to the Butterworth delay (dotted).

In Fig. 2.47(b), the group delay of the Pascal filter is smoother and absolutely comparable to that of Chebyshev, although $N_{Pa} = 8$ and $N_{Cheb} = 7$. The group delay of the Butterworth filter (dotted) that meets the same specifications with $N_{But} = 14$ is slightly better.

In Fig. 2.47(c), the group delay of the passband optimized Pascal filter is better than that of the Chebyshev filter and comparable to that of the Butterworth filter which meets the same specifications with $N_{But} = 14$.

The classical polynomial approximations such as Butterworth and Chebyshev, leading to all-pole transfer functions, are extensively used in analogue and IIR digital filter design. In this chapter, the Pascal approximation was also presented based

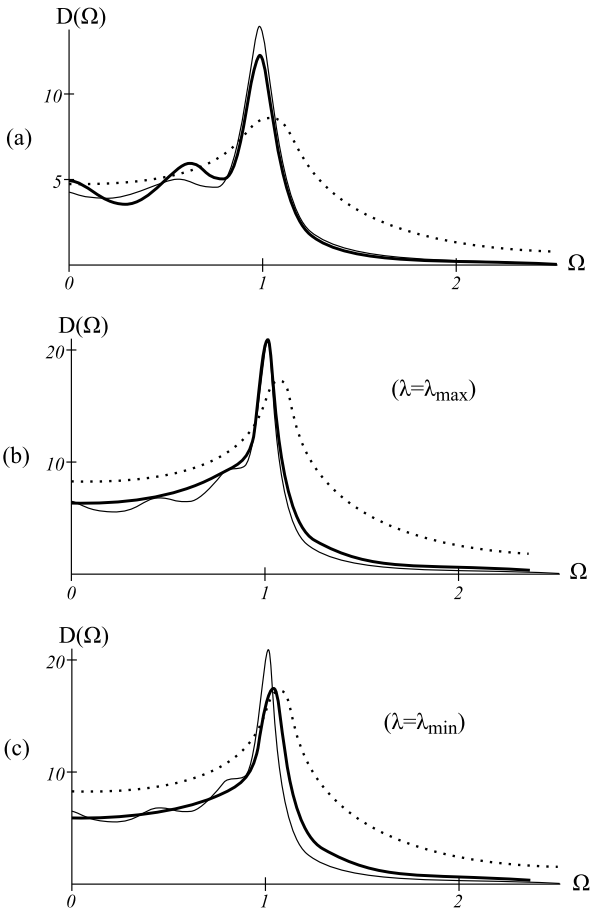

Fig. 2.47 Group delay:
(**a**) Design Example 2.10.
(**b**) Design Example 2.11.
(**c**) Design Example 2.12

on a suitably modified symmetric Pascal polynomial, $P_D(N, \Omega)$. The optimization and the application of the Pascal approximation was demonstrated by several design examples. The mathematical complexity involved due to the nature of the Pascal polynomials do not allow the analytical expression of the order equation and the transfer function poles and for this reason an exact nomograph is used for the order calculation and detailed tables for the transfer function constant and poles. The order of the so derived Pascal filters was found to be comparable to that of Chebyshev filters which meet the same specifications with the lowest possible order as compared to all other known polynomial approximations. The Pascal filters were found to require lower pole-Q values than their Chebyshev counterparts and exhibit slightly improved group delay performance comparable, in some cases, to that of the Butterworth filters designed to meet the same specifications.

In all cases, for Butterworth, Chebyshev and Pascal approximations, once the transfer function is available, passive, active, or IIR digital filters can be realized using the classic well-established methods that will be presented in the next chap-

ters. For analogue high frequency integrated filters, a passive LC ladder filter can be initially designed, which can then be properly simulated to derive active structures suitable for integrated realizations.

2.5 Chebyshev and Pascal Design Tables

Design tables for the Chebyshev and Pascal approximations are presented in the following pages.

2.5.1 Table: Chebyshev Approximation

Denominator $D_N(s)$ of $H_{CH}(s) = \frac{H_o/(\varepsilon c_N)}{D_N(s)}$ of *normalized* lowpass Chebyshev filters ($c_N = 2^{N-1}$ is the coefficient of Ω^N in $C_N(\Omega)$)

$$\Omega_C = 1 \qquad G_{CH}(1) = \frac{H_o}{\sqrt{1+\varepsilon^2}} \qquad D_N(s) = \prod_{k=1}^{N}(s - s_k) \quad s_k = \sigma_k + j\Omega_k$$

$$\sigma_k = \sin(x)\sinh(y),\ \ \Omega_k = \cos(x)\cosh(y),\ \ x = \frac{(2N+2k-1)\pi}{2N}$$

$$y = \frac{1}{N}\sinh^{-1}\left(\frac{1}{\varepsilon}\right)$$

$$G_{CH}(\Omega) = |H_{CH}(j\Omega)| = \frac{H_o}{\sqrt{1+\varepsilon^2 C_N^2(\Omega)}} \qquad \Omega_{3dB} = \cosh\left[\frac{1}{N}\cosh^{-1}\left(\frac{1}{\varepsilon}\right)\right]$$

N	Ripple 0.1 dB ($\varepsilon = 0.152620$)	εc_N	Ω_{3dB}
1	$s + 6.552203$	0.15262	6.552203
2	$s^2 + 2.372356s + 3.314037$	0.305241	1.943219
3	$(s + 0.969406)(s^2 + 0.969406s + 1.689747)$	0.610482	1.388995
4	$(s^2 + 0.528313s + 1.330031)(s^2 + 1.27546s + 0.622925)$	1.220963	1.213099
5	$(s + 0.538914)(s^2 + 0.333067s + 1.194937)(s^2 + 0.871982s + 0.63592)$	2.441927	1.134718
N	Ripple 0.5 dB ($\varepsilon = 0.349311$)	εc_N	Ω_{3dB}
1	$s + 2.862775$	0.349311	2.862775
2	$s^2 + 1.425625s + 1.516203$	0.698623	1.389744
3	$(s + 0.626456)(s^2 + 0.626456s + 1.42448)$	1.397246	1.167485
4	$(s^2 + 0.350706s + 1.063519)(s^2 + 0.84668s + 0.356412)$	2.794491	1.093102
5	$(s + 0.36232)(s^2 + 0.223926s + 1.035784)(s^2 + 0.586245s + 0.476767)$	5.588982	1.059259

N	Ripple 1.0 dB ($\varepsilon = 0.508847$)	εc_N	Ω_{3dB}
1	$s + 1.965227$	0.508847	1.965227
2	$s^2 + 1.097734s + 1.10251$	1.017694	1.217626
3	$(s + 0.494171)(s^2 + 0.494171s + 0.994205)$	2.03589	1.094868
4	$(s^2 + 0.279072s + 0.986505)(s^2 + 0.673739s + 0.279398)$	4.070777	1.053002
5	$(s + 0.289493)(s^2 + 0.178917s + 0.988315)(s^2 + 0.46841s + 0.429298)$	8.141554	1.033815
N	Ripple 2.0 dB ($\varepsilon = 0.764783$)	εc_N	Ω_{3dB}
1	$s + 1.30756$	0.764783	1.30756
2	$s^2 + 0.803816s + 0.82306$	1.529566	1.074142
3	$(s + 0.368911)(s^2 + 0.368911s + 0.886095)$	3.059132	1.032729
4	$(s^2 + 0.209775s + 0.928675)(s^2 + 0.50644s + 0.221568)$	6.118265	1.018367
5	$(s + 0.218308)(s^2 + 0.134922s + 0.952167)(s^2 + 0.35323s + 0.39315)$	12.23653	1.011742
N	Ripple 3.0 dB ($\varepsilon = 0.997628$)	εc_N	Ω_{3dB}
1	$s + 1.002377$	0.997628	1.002377
2	$s^2 + 0.6449s + 0.707948$	1.995257	1.000594
3	$(s + 0.29862)(s^2 + 0.29862s + 0.839174)$	3.990513	1.000264
4	$(s^2 + 0.170341s + 0.903087)(s^2 + 0.411239s + 0.19598)$	7.981027	1.000149
5	$(s + 0.17753)(s^2 + 0.10972s + 0.936025)(s^2 + 0.28725s + 0.377009)$	15.962054	1.000095

Pascal Tables 2.8 (see (2.90) and (2.91)) $\lambda = \lambda_{\max}$

N	C	Real s_R	Pair 1	Pair 2	Pair 3	Pair 4
$\alpha_{\max} = 0.01$						
2	10.413869		-2.227764 $\pm j2.337292$ $Q = 0.724698$			
3	5.206936	-1.589371	-0.794685 $\pm j1.626215$ $Q = 1.138815$			
4	2.934297		-1.044855 $\pm j0.565886$ $Q = 0.568622$	-0.429585 $\pm j1.376373$ $Q = 1.678195$		
5	1.769666	-0.929117	-0.744100 $\pm j0.768710$ $Q = 0.718895$	-0.279541 $\pm j1.259329$ $Q = 2.307319$		

Pascal Tables 2.8 (Continued)

N	C	Real s_R	Pair 1	Pair 2	Pair 3	Pair 4
6	1.112555		-0.787056 $\pm j0.311634$ $Q = 0.537767$	-0.564546 $\pm j0.860564$ $Q = 0.911542$	-0.201501 $\pm$j1.193811 $Q = 3.004193$	
7	0.719074	-0.747272	-0.667122 $\pm j0.497552$ $Q = 0.623748$	-0.448356 $\pm j0.908832$ $Q = 1.130140$	-0.154870 $\pm$j1.152746 $Q = 3.755102$	
8	0.473977		-0.685759 $\pm j0.214871$ $Q = 0.523970$	-0.571780 $\pm j0.616491$ $Q = 0.735273$	-0.368266 $\pm j0.936914$ $Q = 1.366801$	-0.124349 $\pm j1.124942$ $Q = 4.550879$
9	0.317021	-0.667452	-0.622821 $\pm j0.367348$ $Q = 0.580491$	-0.496350 $\pm j0.696974$ $Q = 0.861941$	-0.310304 $\pm j0.954500$ $Q = 1.617242$	-0.103048 $\pm j1.105038$ $Q = 5.385007$
$\alpha_{\max} = 0.1$						
2	3.276101		-1.186178 $\pm j1.380948$ $Q = 0.767359$			
3	1.638051	-0.969406	-0.484703 $\pm j1.206155$ $Q = 1.340928$			
4	0.923101		-0.687948 $\pm j0.457626$ $Q = 0.600520$	-0.278303 $\pm j1.131224$ $Q = 2.092963$		
5	0.556720	-0.652393	-0.513602 $\pm j0.655532$ $Q = 0.810717$	-0.187406 $\pm j1.093326$ $Q = 2.959545$		
6	0.349999		-0.576657 $\pm j0.272841$ $Q = 0.553142$	-0.402354 $\pm j0.758765$ $Q = 1.067273$	-0.138125 $\pm j1.071182$ $Q = 3.909688$	
7	0.226213	-0.569057	-0.503758 $\pm j0.445436$ $Q = 0.667431$	-0.327070 $\pm j0.819700$ $Q = 1.349165$	-0.107841 $\pm j1.056909$ $Q = 4.925736$	
8	0.149108		-0.536721 $\pm j0.194964$ $Q = 0.531966$	-0.441631 $\pm j0.561055$ $Q = 0.808387$	-0.273459 $\pm j0.858899$ $Q = 1.648108$	-0.087613 $\pm j1.047051$ $Q = 5.996295$
9	0.099732	-0.535685	-0.497623 $\pm j0.337401$ $Q = 0.604094$	-0.390185 $\pm j0.642298$ $Q = 0.963038$	-0.233680 $\pm j0.885749$ $Q = 1.960065$	-0.073275 $\pm j1.039887$ $Q = 7.113384$

Pascal Tables 2.8 (Continued)

N	C	Real s_R	Pair 1	Pair 2	Pair 3	Pair 4
$\alpha_{\max} = 0.5$						
2	1.431388		-0.712812 $\pm j1.004043$ $Q = 0.863721$			
3	0.715694	-0.626457	-0.313228 $\pm j1.021928$ $Q = 1.706189$			
4	0.403319		-0.473019 $\pm j0.399956$ $Q = 0.654778$	-0.185811 $\pm j1.018171$ $Q = 2.785057$		
5	0.243241	-0.479538	-0.367266 $\pm j0.591875$ $Q = 0.948309$	-0.127497 $\pm j1.014480$ $Q = 4.009746$		
6	0.152921		-0.441502 $\pm j0.250192$ $Q = 0.574702$	-0.295576 $\pm j0.699381$ $Q = 1.284398$	-0.095139 $\pm j1.011785$ $Q = 5.340876$	
7	0.098837	-0.452860	-0.396560 $\pm j0.414208$ $Q = 0.723012$	-0.245068 $\pm j0.766314$ $Q = 1.641479$	-0.074938 $\pm j1.009831$ $Q = 6.756307$	
8	0.065148		-0.438240 $\pm j0.182751$ $Q = 0.541733$	-0.354805 $\pm j0.527186$ $Q = 0.895509$	-0.208034 $\pm j0.811221$ $Q = 2.012827$	-0.061288 $\pm j1.008378$ $Q = 8.241702$
9	0.043575	-0.447883	-0.413955 $\pm j0.318731$ $Q = 0.631040$	-0.318420 $\pm j0.608385$ $Q = 1.078254$	-0.179934 $\pm j0.843059$ $Q = 2.395455$	-0.051527 $\pm j1.007266$ $Q = 9.786973$
$\alpha_{\max} = 1.0$						
2	0.982613		-0.548867 $\pm j0.895129$ $Q = 0.956520$			
3	0.491307	-0.494171	-0.247085 $\pm j0.965999$ $Q = 2.017720$			
4	0.276869		-0.385603 $\pm j0.377784$ $Q = 0.699974$	-0.148193 $\pm j0.983002$ $Q = 3.354099$		
5	0.166979	-0.407030	-0.305853 $\pm j0.566511$ $Q = 1.052470$	-0.102338 $\pm j0.989590$ $Q = 4.860703$		

Pascal Tables 2.8 (Continued)

N	C	Real s_R	Pair 1	Pair 2	Pair 3	Pair 4
6	0.104977		-0.383801 $\pm j0.241065$ $Q = 0.590447$	-0.249813 $\pm j0.675152$ $Q = 1.440849$	-0.076689 $\pm j0.992848$ $Q = 6.492463$	
7	0.067849	-0.402818	-0.350205 $\pm j0.401443$ $Q = 0.760595$	-0.209387 $\pm j0.744156$ $Q = 1.845995$	-0.060590 $\pm j0.994713$ $Q = 8.223764$	
8	0.044723		-0.395505 $\pm j0.177699$ $Q = 0.548148$	-0.316890 $\pm j0.513188$ $Q = 0.951660$	-0.179237 $\pm j0.791172$ $Q = 2.262982$	-0.049668 $\pm j0.995890$ $Q = 10.037888$
9	0.029913	-0.409609	-0.377413 $\pm j0.310934$ $Q = 0.647831$	-0.286839 $\pm j0.594246$ $Q = 1.150213$	-0.156064 $\pm j0.824921$ $Q = 2.689774$	-0.041834 $\pm j0.996687$ $Q = 11.923013$
$\alpha_{\max} = 1.25$						
2	0.865781		-0.499894 $\pm j0.865964$ $Q = 1.000106$			
3	0.432891	-0.453133	-0.226566 $\pm j0.950787$ $Q = 2.157005$			
4	0.243950		-0.357779 $\pm j0.370834$ $Q = 0.720123$	-0.136308 $\pm j0.973361$ $Q = 3.605295$		
5	0.147125	-0.383466	-0.286033 $\pm j0.558421$ $Q = 1.096752$	-0.094300 $\pm j0.982733$ $Q = 5.234591$		
6	0.092495		-0.364884 $\pm j0.238135$ $Q = 0.597062$	-0.234913 $\pm j0.667338$ $Q = 1.505827$	-0.070751 $\pm j0.987613$ $Q = 6.997370$	
7	0.059782	-0.386340	-0.334920 $\pm j0.397324$ $Q = 0.775785$	-0.197697 $\pm j0.736954$ $Q = 1.929747$	-0.055947 $\pm j0.990524$ $Q = 8.866478$	
8	0.039405		-0.381389 $\pm j0.176063$ $Q = 0.550706$	-0.304335 $\pm j0.508654$ $Q = 0.973840$	-0.169760 $\pm j0.784617$ $Q = 2.364431$	-0.045892 $\pm j0.992424$ $Q = 10.824132$
9	0.026356	-0.396944	-0.365311 $\pm j0.308401$ $Q = 0.654350$	-0.276347 $\pm j0.589650$ $Q = 1.178221$	-0.148181 $\pm j0.818964$ $Q = 2.808264$	-0.038673 $\pm j0.993746$ $Q = 12.857736$

Pascal Tables 2.8 (Continued)

N	C	Real s_R	Pair 1	Pair 2	Pair 3	Pair 4
$\alpha_{\max} = 1.5$						
2	0.778464		-0.461089 $\pm j0.844158$ $Q = 1.043049$			
3	0.389232	-0.420112	-0.210056 $\pm j0.939346$ $Q = 2.291162$			
4	0.219346		-0.335093 $\pm j0.365204$ $Q = 0.739560$	-0.126673 $\pm j0.966086$ $Q = 3.845942$		
5	0.132287	-0.364010	-0.269761 $\pm j0.551805$ $Q = 1.138443$	-0.087756 $\pm j0.977549$ $Q = 5.592095$		
6	0.083166		-0.349191 $\pm j0.235725$ $Q = 0.603264$	-0.222628 $\pm j0.660911$ $Q = 1.566289$	-0.065902 $\pm j0.983651$ $Q = 7.479746$	
7	0.053753	-0.372639	-0.322204 $\pm j0.393930$ $Q = 0.789742$	-0.188031 $\pm j0.731006$ $Q = 2.007118$	-0.052147 $\pm j0.987350$ $Q = 9.480258$	
8	0.035431		-0.369634 $\pm j0.174714$ $Q = 0.553040$	-0.293868 $\pm j0.504909$ $Q = 0.993987$	-0.161907 $\pm j0.779188$ $Q = 2.457679$	-0.042796 $\pm j0.989795$ $Q = 11.574823$
9	0.023698	-0.386388	-0.355221 $\pm j0.306307$ $Q = 0.660220$	-0.267586 $\pm j0.585850$ $Q = 1.203477$	-0.141638 $\pm j0.814018$ $Q = 2.916757$	-0.036079 $\pm j0.991514$ $Q = 13.750098$

2.6 Problems

2.1 Show that all $N - 1$ derivatives of the Butterworth gain function $G(\Omega)$ of (2.9) assume zero value at $\Omega = 0$.

2.2 Verify that $G_{1\max}(\omega)$ and $G_{2\max}(\omega)$ of Example 2.1 satisfy the specifications of Fig. 2.10a.

2.3 Calculate the transfer function of the normalized Butterworth lowpass filter with the specifications given in Fig. 2.48 without using Table 2.1.

2.4 Use Table 2.1 to calculate the transfer function of the normalized Butterworth lowpass filter with the specifications given in Fig. 2.48.

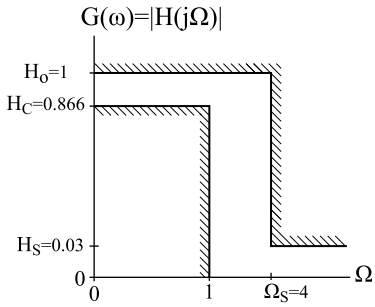

Fig. 2.48 Filter specifications for Problems 2.3 and 2.4

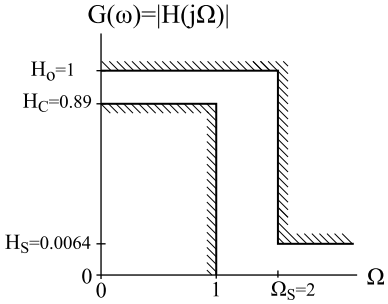

Fig. 2.49 Filter specifications for Problems 2.7–2.9

2.5 Follow Example 2.4 to realize the normalized transfer function of Problem 2.3 or 2.4.

2.6 Verify the results of Example 2.5.

2.7 Calculate the order of the Butterworth and the Chebyshev filter which satisfy the specifications of Fig. 2.49.

2.8 Calculate the transfer function $H(s)$ of the normalized stopband edge frequency gain optimized Chebyshev lowpass filter with the specifications given in Fig. 2.49 and design an active-RC circuit with voltage transfer function $H(s)$.

2.9 Calculate the transfer function $H(s)$ of the normalized passband optimized Chebyshev lowpass filter with the specifications given in Fig. 2.49 and design an active-RC circuit with voltage transfer function $H(s)$.

2.10 Figure 2.50 shows the plot of the logarithmic voltage gain of a normalized lowpass Butterworth filter. Determine the corresponding voltage transfer function.

2.11 Figure 2.51 shows the plot of the stopband logarithmic voltage gain of a normalized lowpass Chebyshev filter with 2 dB passband ripple. Determine the corresponding voltage transfer function.

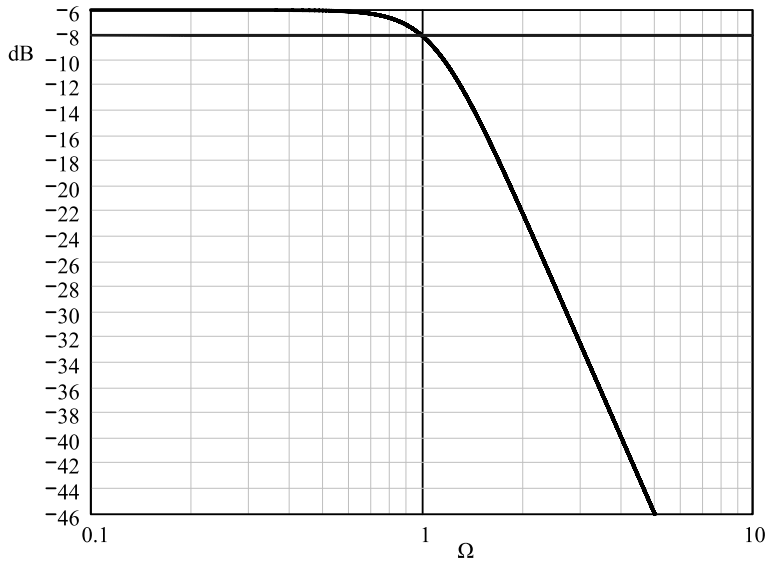

Fig. 2.50 Gain plot for Problem 2.10

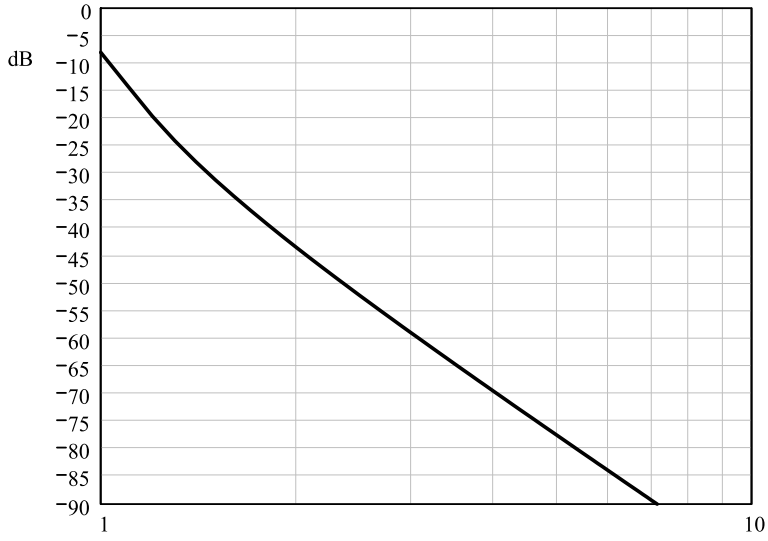

Fig. 2.51 Stopband gain plot for Problem 2.11

2.12 Calculate the poles of Pascal design Example 2.10 directly from equation (2.89) using mathematical software, e.g. MATLAB, Mathematica or Mathcad. Use $\lambda = \lambda_{\max}$.

2.13 Repeat Pascal design Example 2.10 with $\alpha_{max} = 1.5$ and $\alpha_{min} = 24$ dB. Determine the order of the Pascal filter from the nomograph of Fig. 2.43 and try to calculate the constant C of the transfer function and the poles using a mathematical software package with $\lambda = \lambda_{max}$. Finally, compare your results with the corresponding values from the tables.

References[1]

1. Butterworth, S.: On the theory of filter amplifiers. Wirel. Eng. **7**, 536–541 (1930)
2. Chebyshev, P.L.: Theorie des mechanisms connus sous le nom de parallelogrammes. Oeuvres, vol. I, St. Petersburg (1899)
3. Chen, W.-K.: Passive, Active and Digital Filters. The Circuits and Filters Handbook, vol. 5. CRC Press, Boca Raton (2009)
4. Chirlian, P.M.: Signals and Filters. Springer, Berlin (1994)
5. Dimopoulos, H.G.: Optimal use of some classical approximations in filter design. IEEE Trans. Circuits Syst. II, Analog Digit. Signal Process. **54**(9), 780–784 (2007)
6. Dimopoulos, H.G., Sarri, E.: The modified pascal polynomial approximation and filter design method. Int. J. Circuit Theory Appl. (2010). doi:10.1002/cta.711
7. Oldham, K.B., Spanier, J.: The Fractional Calculus. Dover, New York (2002)
8. Schaumann, R., Van Valkenburg, M.E.: Design of Analog Filters. Oxford University Press, London (2001)
9. Temes, G.C., LaPatra, J.W.: Introduction to Circuit Synthesis and Design. McGraw-Hill, Boca Raton (1977)
10. Van Valkenburg, M.E.: Analog Filter Design. Oxford University Press, London (1982)
11. Wanhammar, L.: Analog Filters Using MATLAB. Springer, Berlin (2009)
12. Williams, A., Taylor, F.: Electronic Filter Design Handbook. McGraw-Hill, New York (2006)

[1] All references, whether or not cited within the text, are recommended for further reading.

Rational Approximations

3

3.1 Introduction

The approximations presented in the previous chapter are referred to as all-pole because they lead to all-pole transfer functions, i.e. transfer functions of the form $H(s) = K/D(s)$ with constant numerator, without finite zeros. The absence of finite zeros ensures that the gain is monotonically decreasing for $\Omega > 1$. These approximations are also called *polynomial approximations* due to the fact that the approximating function is in polynomial form.

This chapter deals with some more complicated approximations which lead to transfer functions with $j\Omega$-axis finite zeros. This means that in the numerator polynomial of the transfer function, there exist factors $(s^2 + \Omega_{Zk}^2)$ and therefore the magnitude response, the plain gain, becomes zero at the real frequencies Ω_{Zk} (transmission zeros). Approximations with transmission zeros are also referred to as *rational approximations* since the approximating functions are rational functions. Figure 3.1 shows the three rational approximations which will be presented in details in this and the next chapter.

The gain shown in Fig. 3.1a is monotonic in the passband and transition band and exhibits equiripple behavior in the stopband. Such a gain is obtained by the inverse Chebyshev (or Chebyshev II) approximation. A similar gain curve is shown in Fig. 3.1b, but with non-equal stopband gain maxima. Such a stopband gain behavior can be obtained by the inverse Pascal approximation. The gain of the elliptic approximation shown in Fig. 3.1c exhibits equiripple behavior in both passband and stopband. Elliptic approximation can meet given specifications with the minimum order as compared to all other approximations.

Approximations with transmission zeros require higher design effort than all-pole approximations but possess certain desirable characteristics that are sometimes required by the filter application.

H.G. Dimopoulos, *Analog Electronic Filters*, Analog Circuits and Signal Processing,
DOI 10.1007/978-94-007-2190-6_3, © Springer Science+Business Media B.V. 2012

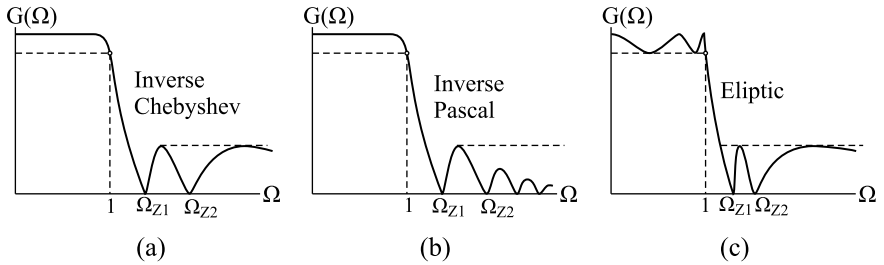

Fig. 3.1 (**a**) Inverse Chebyshev. (**b**) Inverse Pascal. (**c**) Elliptic

3.2 Rational Approximations

As we have seen, the gain of the ideal normalized lowpass filter is generally approximated using a gain expression of the form:

$$G(\Omega) = |H(j\Omega)| = \frac{H_o}{\sqrt{1+\gamma^2 F^2(\Omega)}} \tag{3.1}$$

where Ω is the normalized angular frequency.

When $F(\Omega)$ is a polynomial of order N, as in the Butterworth, Chebyshev and Pascal cases of the previous chapter, the related transfer function takes the all-pole form

$$H(s) = \frac{A}{\prod_{k=1}^{N}(s - s_k)} \tag{3.2}$$

and the poles s_k are given by the corresponding formulae in each case.

In rational approximations, $F(\Omega)$ takes the form

$$F_R(\Omega) = \frac{N_R(\Omega)}{D_R(\Omega)}$$

where $N_R(\Omega)$ and $D_R(\Omega)$ are real polynomials of order N and n_p respectively:

$$N_R(\Omega) = A_N\Omega^N + A_{N-1}\Omega^{N-1} + A_{N-2}\Omega^{N-2} + \cdots \tag{3.3}$$

$$D_R(\Omega) = B_{n_p}\Omega^{n_p} + B_{n_p-1}\Omega^{n_p-1} + B_{n_p-2}\Omega^{n_p-2} + \cdots \tag{3.4}$$

Substituting $F(\Omega)$ with $F_R(\Omega)$ in (3.1) yields

$$G(\Omega) = |H(j\Omega)| = \frac{H_o}{\sqrt{1+\gamma^2 F_R^2(\Omega)}} = \frac{H_o}{\sqrt{1+\gamma^2 \frac{N_R^2(\Omega)}{D_R^2(\Omega)}}} \tag{3.5}$$

and

$$G^2(\Omega) = |H(j\Omega)|^2 = \frac{H_o^2}{1+\gamma^2 \frac{N_R^2(\Omega)}{D_R^2(\Omega)}} = \frac{H_o^2 D_R^2(\Omega)}{D_R^2(\Omega)+\gamma^2 N_R^2(\Omega)} \tag{3.6}$$

The gain function $G(\Omega)$ is the magnitude of the transfer function for $s = j\Omega$, i.e. $G(\Omega) = |H(j\Omega)|$, and therefore is an even function of Ω.

In order for $G(\Omega)$ of (3.5) to be even, $F_R^2(\Omega) = \frac{N_R^2(\Omega)}{D_R^2(\Omega)}$ must be even and this requires both polynomials $N_R(\Omega)$ and $D_R(\Omega)$ to be either odd or even.

On the other hand, the denominator polynomial $D_R(\Omega)$ must be even, otherwise, according to (3.5) or (3.6), it would introduce a transmission zero at $\Omega = 0$, which is not expected in lowpass filters.

Finally, in $F_R(\Omega)$ of (3.5), $N_R(\Omega)$ is an even or odd polynomial of degree N, and $D_R(\Omega)$ an even polynomial of degree n_p. To ensure the expected lowpass behavior for $\Omega \to \infty$, the degree N of the numerator must be equal or greater than the degree n_p of the denominator, i.e. $N \geq n_p$. When $N > n_p$, then $\lim_{\Omega\to\infty} F_R(\Omega) = \infty$ and from (3.1) $\Rightarrow G(\infty) = 0$. When $N = n_p$ (even), $\lim_{\Omega\to\infty} F_R(\Omega) = \frac{A_N}{B_{n_p}} = K$ where A_N and B_{n_p} are the coefficients of the highest order terms in $N_R(\Omega)$ and $D_R(\Omega)$ respectively. In this case, the gain for $\Omega \to \infty$ will be $G(\infty) = \frac{H_o}{\sqrt{1+\gamma^2 K^2}} > 0$, and $K = \frac{A_N}{B_{n_p}}$ must be as high as necessary in order to satisfy the stopband gain specifications.

The corresponding transfer function $H(s) = \frac{N_{TF}(s)}{D_{TF}(s)}$ can be determined from

$$H(s)H(-s) = |H(j\Omega)|^2_{\Omega^2=-s^2} = \frac{N_{TF}(s)}{D_{TF}(s)} \cdot \frac{N_{TF}(-s)}{D_{TF}(-s)} \tag{3.7}$$

and therefore from (3.6) and (3.7) we get:

$$\begin{aligned} H(s)H(-s) &= \frac{N_{TF}(s)}{D_{TF}(s)} \cdot \frac{N_{TF}(-s)}{D_{TF}(-s)} \\ &= \frac{H_o^2 D_R^2(\Omega)|_{\Omega^2=-s^2}}{D_R^2(\Omega)|_{\Omega^2=-s^2} + \gamma^2 N_R^2(\Omega)|_{\Omega^2=-s^2}} \end{aligned} \tag{3.8}$$

Both $N_{TF}(s)$ and $D_{TF}(s)$ polynomials must have real coefficients and the degree of $N_{TF}(s)$ cannot exceed the degree of $D_{TF}(s)$ [6]. This is ensured by the conclusion of the previous paragraph, where it has been shown that $N \geq n_p$.

The numerator of (3.8), as the square of an even polynomial of degree n_p, is also an even polynomial of degree $2n_p$ and when Ω^2 is replaced by $-s^2$ becomes an even polynomial in s of degree $2n_p$, contributing n_p zeros z_k $(k = 1, 2, \ldots, n_p)$ to the transfer function. Moreover, since $D_R(\Omega)$ is an even polynomial of degree n_p, and $N_R(\Omega)$ is an even or odd polynomial of degree $N \geq n_p$, $D_R^2(\Omega)$ and $N_R^2(\Omega)$ are even polynomials. When Ω^2 is replaced by $-s^2$, the denominator of (3.8) becomes an even polynomial of s of degree $2N$ and contributes N poles p_k to the transfer

function. It should be remembered that N is the degree of $N_R(\Omega)$. Therefore, the transfer function in the case of rational approximations will be of the general form:

$$H(s) = A\frac{\prod_{k=1}^{n_p}(s - z_k)}{\prod_{k=1}^{N}(s - p_k)} \quad \text{with } n_p \text{ even and } N \geq n_p \tag{3.9}$$

From the mathematical point of view, any rational function $F_R(\Omega) = \frac{N_R(\Omega)}{D_R(\Omega)}$ with $D_R(\Omega)$ an even polynomial of degree n_p and $N_R(\Omega)$ an even or odd polynomial of degree $N \geq n_p$ can be used as approximating function $F_R(\Omega)$ in (3.5), provided that it assumes low values for the region $0 \leq \Omega \leq 1$ and high values for $\Omega > 1$, in order for (3.5) to exhibit lowpass behavior.

We will next show that, in addition to these necessary conditions ($D_R(\Omega)$ even, $N_R(\Omega)$ odd or even of degree $N \geq n_p$), the n_p roots of the even polynomial $D_R(\Omega)$ must be real or imaginary.

Suppose that the even polynomial $D_R(\Omega)$ had a complex conjugate root pair $\rho_k = a_k \pm jb_k$. Then, since $D_R(\Omega)$ is even, $-\rho_k = -a_k \pm jb_k$ would also be roots and $D_R(\Omega)$ would contain the term

$$(\Omega^2 - 2a_k\Omega + a_k^2 + b_k^2)(\Omega^2 + 2a_k\Omega + a_k^2 + b_k^2)$$

and $D_R^2(\Omega)|_{\Omega^2=-s^2}$ in (3.8) would then contain the term

$$(-s^2 + j2a_ks + a_k^2 + b_k^2)^2(-s^2 - j2a_ks + a_k^2 + b_k^2)^2$$

To separate $H(s)$ and $H(-s)$ using (3.7),

$$\text{either} \quad (-s^2 + j2a_ks + a_k^2 + b_k^2)^2 \quad \text{or} \quad (-s^2 - j2a_ks + a_k^2 + b_k^2)^2$$

should be allocated to the numerator $N_{TF}(s)$ of $H(s)$, which would have complex coefficients. Since all coefficients of $N_{TF}(s)$ must be real, a_k must be zero. This implies that the even polynomial $D_R(\Omega)$ cannot have complex conjugate root pairs of the form $\rho_k = a_k \pm jb_k$ but either imaginary conjugate or real symmetric root pairs:

$$\rho_k = \pm j\Omega_{zk} \quad \text{or} \quad \rho_k = \pm\Omega_{zk} \quad \text{with real } \Omega_{zk} \geq 0 \tag{3.10}$$

All known rational approximations are based on rational functions $F_R(\Omega)$ with denominator polynomials with real root pairs $\rho_k = \pm\Omega_{zk}$. The cases of polynomials $D_R(\Omega)$ with imaginary root pairs or imaginary and real root pairs have not been reported and their investigation is beyond the scope of this textbook. However, two examples are given below.

Example 3.1 Consider the rational function

$$F_R(\Omega) = \frac{N_R(\Omega)}{D_R(\Omega)} = \frac{3\Omega^3}{\Omega^2 + 2} \quad \text{with } N_R(\Omega) = 3\Omega^3 \text{ and } D_R(\Omega) = \Omega^2 + 2$$

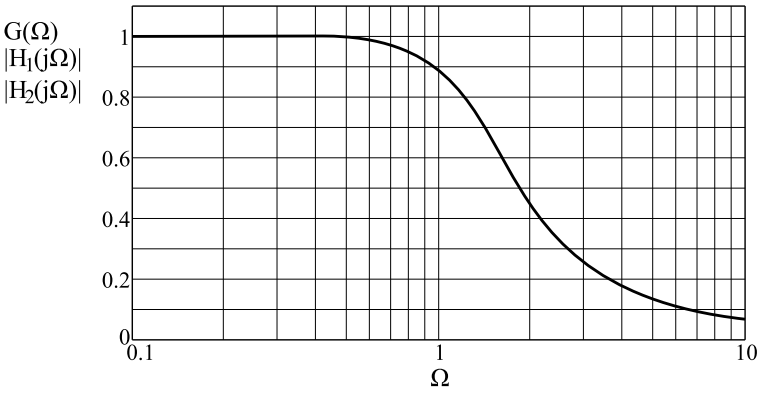

Fig. 3.2 Plain gain plot for Example 3.1

in which the roots of $D_R(\Omega)$ are $\pm j\sqrt{2}$. According to (3.5), the corresponding gain function will be

$$G(\Omega) = \frac{H_o}{\sqrt{1+\gamma^2 F_R^2(\Omega)}} = \frac{H_o}{\sqrt{1+\gamma^2 \frac{9\Omega^6}{(\Omega^2+2)^2}}} \tag{3.11}$$

For $\gamma = 0.5$, this example rational approximation leads to the following transfer functions from (3.7)

$$H_1(s) = \frac{\frac{2}{3}(s^2-2)}{(s+0.917439)(s^2+1.584106s+1.453322)}$$

or

$$H_2(s) = \frac{\frac{2}{3}(s+\sqrt{2})^2}{(s+0.917439)(s^2+1.584106s+1.453322)}$$

The plain gain plot from (3.11) and as $|H_1(j\Omega)|$ and $|H_2(j\Omega)|$ is shown in Fig. 3.2.

Example 3.2 Consider the following rational function in which $D_R(\Omega)$ has real and imaginary root pairs ± 4 and $\pm j8$

$$F_R(\Omega) = \frac{N_R(\Omega)}{D_R(\Omega)} = \frac{975 \cdot \Omega^5}{(\Omega^2-16)(\Omega^2+64)}$$

According to (3.5), the corresponding gain function will be

$$G(\Omega) = \frac{H_o}{\sqrt{1+\gamma^2 F_R^2(\Omega)}} = \frac{H_o}{\sqrt{1+\gamma^2 \frac{975^2 \cdot \Omega^{10}}{(\Omega^2-16)^2(\Omega^2+64)^2}}} \tag{3.12}$$

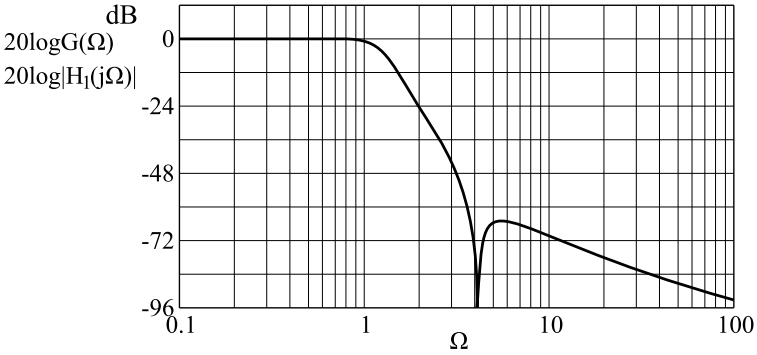

Fig. 3.3 Logarithmic gain plot for Example 3.2

For $\gamma = 0.5$, using (3.7), this example rational approximation leads to the transfer function shown below:

$$H_1(s) = \frac{2.051282 \cdot 10^{-3}(s^2 - 8^2)(s^2 + 4^2)}{(s + 1.174231)(s^2 + 1.868734s + 1.35714)(s^2 + 0.692452s + 1.318096)}$$

The logarithmic gain plot, both from (3.12) and $20\log|H_1(j\Omega)|$, is shown in Fig. 3.3.

If the roots of the even polynomial $D_R(\Omega)$ are real pairs of the form $\rho_k = \pm\Omega_{zk}$, the polynomial will contain the term $\prod_{k=1}^{n_p/2}(\Omega^2 - \Omega_{zk}^2)$ and the numerator of $H(s)H(-s)$ of (3.8) will contain the term $\prod_{k=1}^{n_p/2}(s^2 + \Omega_{zk}^2)^2$. If we limit our attention to this case, considering that the even polynomial $D_R(\Omega)$ of even degree n_p has $\frac{n_p}{2}$ real symmetric root pairs $\pm\Omega_{zk}$, then $D_R(\Omega)$ will be of the form:

$$D_R(\Omega) = B_{n_p}\prod_{k=1}^{\frac{n_p}{2}}(\Omega^2 - \Omega_{zk}^2) \quad \Rightarrow \quad D_R^2(\Omega) = B_{np}^2\prod_{k=1}^{\frac{n_p}{2}}(\Omega^2 - \Omega_{zk}^2)^2 \tag{3.13}$$

where B_{np} is the coefficient of the highest order term of $D_R(\Omega)$. Therefore, from (3.8):

$$N_{TF}(s)N_{TF}(-s) = H_o^2 \cdot B_{n_p}^2 \cdot \prod_{k=1}^{\frac{n_p}{2}}(s^2 + \Omega_{zk}^2)^2 \tag{3.14}$$

$$\Rightarrow \quad N_{TF}(s) = N_{TF}(-s) = H_o \cdot |B_{n_p}| \cdot \prod_{k=1}^{\frac{n_p}{2}}(s^2 + \Omega_{zk}^2) \tag{3.15}$$

Finally, the general form of the transfer function of rational approximations when $D_R(\Omega)$ has only real roots $\pm\Omega_{zk}$ is given below:

$$H(s) = \frac{H_o \cdot |B_{n_p}| \cdot \prod_{k=1}^{\frac{n_p}{2}} (s^2 + \Omega_{zk}^2)}{B \cdot \prod_{k=1}^{N} (s - p_k)} \quad \text{with } n_p \text{ even and } N \geq n_p \tag{3.16}$$

B_{n_p} is the coefficient of the highest order term in $D_R(\Omega)$, and B will be discussed later.

The $n_p/2$ conjugate pair zeros $\pm j\Omega_{zk}$ of $H(s)$ have been contributed by the $n_p/2$ real pair roots $\pm\Omega_{zk}$ of the real even polynomial $D_R(\Omega)$ of the denominator of the approximating rational function $F_R(\Omega)$. The poles p_k of $H(s)$ are the LH half s-plane roots of the even denominator polynomial of (3.8):

$$\begin{aligned} &D_{TF}(s)D_{TF}(-s) = D_R^2(\Omega)|_{\Omega^2=-s^2} + \gamma^2 N_R^2(\Omega)|_{\Omega^2=-s^2} = 0 \quad \text{or} \\ &D_{TF}(s)D_{TF}(-s) = B_{np}^2 \cdot \prod_{k=1}^{\frac{n_p}{2}} (s^2 + \Omega_{zk}^2)^2 + \gamma^2 N_R^2(\Omega)|_{\Omega^2=-s^2} = 0 \end{aligned} \tag{3.17}$$

The calculation of the poles is the most laborious task in all approximations and in many cases they cannot be expressed analytically. However since $D_{TF}(s)D_{TF}(-s)$ is an even polynomial, half of its roots are located in the left half s-plane and can always be allocated as poles to a realizable transfer function.

The symmetric numerator polynomial $N_R(\Omega)$ of order N takes the general form:

$$\begin{aligned} N_R(\Omega) &= A_N\Omega^N + A_{N-2}\Omega^{N-2} + \cdots + A_0 \quad \text{when } N \text{ is even} \\ N_R(\Omega) &= A_N\Omega^N + A_{N-2}\Omega^{N-2} + \cdots + A_1\Omega \quad \text{when } N \text{ is odd} \end{aligned}$$

The order of the polynomial of (3.17) is $2N$ and if $N > n_p$, the coefficient g_{2N} of the highest order term is $g_{2N} = \gamma^2 A_N^2$ where A_N is the coefficient of the highest order term of $N_R(\Omega)$. If $N = n_p$ (even), then it is clear from (3.17) that $g_{2N} = \gamma^2 A_N^2 + B_{n_p}^2$. Therefore, the coefficient B in (3.16) will be

$$B = \begin{cases} \gamma |A_N| & \text{when } N > n_p \\ \sqrt{\gamma^2 A_N^2 + B_{n_p}^2} & \text{when } N = n_p \text{ (even)} \end{cases} \tag{3.18}$$

and finally the transfer function will be

$$H(s) = H_o \cdot C \cdot \frac{\prod_{k=1}^{\frac{n_p}{2}} (s^2 + \Omega_{zk}^2)}{\prod_{k=1}^{N} (s - p_k)} \quad \text{with } n_p \text{ even and } N \geq n_p \tag{3.19}$$

where

$$C = \frac{B_{n_p}}{\gamma |A_N|} \quad \text{when } N > n_p \tag{3.20}$$

$$C = \frac{B_{n_p}}{\sqrt{\gamma^2 A_N^2 + B_{n_p}^2}} \quad \text{when } N = n_p \text{ (even)} \tag{3.21}$$

The above analysis sets the necessary conditions for the selection of a rational approximating function $F_R(\Omega) = \frac{N_R(\Omega)}{D_R(\Omega)}$ for use in (3.5):

i. The numerator polynomial $N_R(\Omega)$ of degree N must be symmetric (even or odd). Moreover, in order to maintain lowpass characteristics for $\Omega \to \infty$, the order N of the numerator polynomial $N_R(\Omega)$ must be equal or higher than the order n_p of the denominator polynomial $D_R(\Omega)$.
ii. The denominator polynomial $D_R(\Omega)$ must be an even polynomial of even degree n_p.
iii. The even polynomial $D_R(\Omega)$ can have imaginary root pairs $\pm j\Omega_{zk}$ or/and real root pairs $\pm\Omega_{zk}$. If $D_R(\Omega)$ has only real roots, frequencies Ω_{zk} must be located in the stopband, i.e. $\Omega_{zk} > \Omega_S$ in order to ensure lowpass behavior.

When all roots of $D_R(\Omega)$ are real, (3.16) implies that the corresponding transfer functions will have only $j\Omega$-axis zeros $\pm j\Omega_{zk}$, i.e. real transmission zeros at Ω_{zk}.

The necessary conditions i–iii can also be proved sufficient, i.e. when met by $F_R(\Omega)$, the corresponding transfer function is realizable.

Several rational functions $F_R(\Omega)$ have been successfully deployed leading to realizable transfer functions and filters with distinct and different characteristics. However, all known rational approximations use $D_R(\Omega)$ with all roots to be real in the approximating rational function $F_R(\Omega) = \frac{N_R(\Omega)}{D_R(\Omega)}$, as for example the elliptic and the inverse Chebyshev approximations.

3.3 The Inverse Chebyshev Approximation

Equation (3.5) with $\gamma = \epsilon^{-1}$ and the rational function

$$F_R(\Omega) = \frac{1}{C_N(\frac{\Omega_S}{\Omega})} \tag{3.22}$$

defines the gain of the inverse Chebyshev or Chebyshev II approximation:

$$G_{ICH}(\Omega) = \frac{H_o}{\sqrt{1 + \frac{1}{\epsilon^2 C_N^2(\frac{\Omega_S}{\Omega})}}} = \frac{\epsilon H_o |C_N(\frac{\Omega_s}{\Omega})|}{\sqrt{1 + \epsilon^2 C_N^2(\frac{\Omega_s}{\Omega})}} \tag{3.23}$$

It should be noted that in contrast to the polynomial approximations, the approximating rational function $F_R(\Omega)$ depends on Ω_S, the specified stopband edge frequency.

The Chebyshev polynomial $C_N(x)$ of degree N used in (3.22) and (3.23) can be expressed as

$$C_N(x) = \cosh(N \cosh^{-1}(x)) = c_N x^N + c_{N-2} x^{N-2} + \cdots + c_\eta x^\eta \tag{3.24}$$

where the coefficients of the highest and lowest order terms are given by

$$c_N = 2^{N-1} \quad \text{and} \quad c_\eta = N^\eta (-1)^{\frac{N+3\eta}{2}} \tag{3.25}$$

Parameter η, which will be used extensively in this chapter to allow unified expressions, is given by:

$$\eta = \begin{cases} 0 & \text{when } N \text{ is even} \\ 1 & \text{when } N \text{ is odd} \end{cases} \tag{3.26}$$

Taking into account (3.24) and (3.26), (3.22) yields:

$$\begin{aligned} F_R(\Omega) &= \frac{1}{C_N(\frac{\Omega_S}{\Omega})} = \frac{\Omega^N}{\Omega^N C_N(\frac{\Omega_S}{\Omega})} \\ \Rightarrow \quad F_R(\Omega) &= \frac{\Omega^N}{c_N\Omega_S^N + c_{N-2}\Omega_S^{N-2}\Omega^2 + \cdots + c_\eta \Omega_S^\eta \Omega^{N-\eta}} \\ &= \frac{N_R(\Omega)}{D_R(\Omega)} \end{aligned} \tag{3.27}$$

From (3.27) it becomes clear that

$$\begin{aligned} N_R(\Omega) &= \Omega^N \quad \text{and} \\ D_R(\Omega) &= \Omega^N C_N\left(\frac{\Omega_S}{\Omega}\right) = c_N\Omega_S^N + c_{N-2}\Omega_S^{N-2}\Omega^2 \\ &\qquad + \cdots + c_\eta \Omega_S^\eta \Omega^{N-\eta} \end{aligned} \tag{3.28}$$

The order of $D_R(\Omega)$ is $n_p = N - \eta$, always even.

The three realizability conditions are satisfied in the case of the inverse Chebyshev approximation with the approximating rational function of (3.27):

i. The numerator polynomial $N_R(\Omega) = \Omega^N$ of degree N is symmetric (even or odd) and $N \geq n_p = N - \eta$, ensuring lowpass characteristics for $\Omega \to \infty$.
ii. The denominator polynomial $D_R(\Omega)$, given in (3.28), is an even polynomial since $(N - \eta)$ is always even.
iii. It is shown below that the even polynomial $D_R(\Omega)$ has $(N-\eta)/2$ real root pairs $\pm\Omega_{zk}$ with $|\Omega_{zk}| > \Omega_S$.

Chebyshev polynomials $C_N(\Omega)$ of degree N have $(N-\eta)/2$ positive roots given by

$$\rho_k = \cos\left(\frac{2k-1}{2N}\pi\right) \quad k = 1, 2, \ldots, \frac{N-\eta}{2} \tag{3.29}$$

and $(N - \eta)/2$ negative roots $-\rho_k$. Therefore, the roots Ω_{zk} of $D_R(\Omega) = \Omega^N C_N(\frac{\Omega_S}{\Omega})$ will be $\Omega_{zk} = \pm\frac{\Omega_S}{\rho_k}$. For $\Omega = 0$, from (3.28) we have $D_R(0) = c_N\Omega_S^N = 2^{N-1}\Omega_S^N > 0$.

According to (3.13), the even denominator polynomial $D_R(\Omega)$ can be expressed as:

$$D_R(\Omega) = |c_\eta|\Omega_S^\eta \prod_{k=1}^{(N-\eta)/2} (\Omega^2 - \Omega_{zk}^2)$$

$$\text{where } \Omega_{zk} = \frac{\Omega_S}{\rho_k} = \frac{\Omega_S}{\cos(\frac{2k-1}{2N}\pi)}$$
$$(\eta \text{ from (3.26) and } c_\eta \text{ from (3.25)}) \tag{3.30}$$

with $|\Omega_{zk}| > \Omega_S$, since from (3.29), $\rho_k < 1$. Taking (3.30) into account, the approximating rational function of the inverse Chebyshev approximation of (3.22) yields:

$$F_R(\Omega) = \frac{\Omega^N}{|c_\eta|\Omega_S^\eta \prod_{k=1}^{\frac{N-\eta}{2}} (\Omega^2 - \frac{\Omega_S^2}{\rho_k^2})}$$
$$\text{where } \rho_k = \cos\left(\frac{2k-1}{2N}\pi\right) \text{ and } c_\eta = N^\eta(-1)^{\frac{N+3\eta}{2}} \text{ (from (3.25))} \tag{3.31}$$

The gain of the inverse Chebyshev approximation can be found from (3.1) using $\gamma = \epsilon^{-1}$ and $F_R(\Omega)$ of (3.31)

$$G_{ICH}(\Omega) = \frac{H_o|c_\eta|\epsilon\Omega_S^\eta \prod_{k=1}^{\frac{N-\eta}{2}} (\Omega^2 - \frac{\Omega_S^2}{\rho_k^2})}{\sqrt{\Omega^{2N} + c_\eta^2\epsilon^2\Omega_S^{2\eta} \prod_{k=1}^{\frac{N-\eta}{2}} (\Omega^2 - \frac{\Omega_S^2}{\rho_k^2})^2}}$$
$$\rho_k = \cos\left(\frac{2k-1}{2N}\pi\right) \text{ and } c_\eta = N^\eta(-1)^{\frac{N+3\eta}{2}} \text{ (from (3.25))} \tag{3.32}$$

Equation (3.19) with $\gamma = \epsilon^{-1}$, $n_p = N - \eta$, $A_N = 1$ and $B_{n_p} = |c_\eta|\Omega_S^\eta$ yields the transfer function of the inverse Chebyshev approximation:

$$H(s) = \frac{H_o K \prod_{k=1}^{\frac{N-\eta}{2}} (s^2 + \Omega_{zk}^2)}{\prod_{k=1}^{N} (s - p_k)} \tag{3.33}$$

where $\Omega_{zk} = \frac{\Omega_S}{\rho_k} = \Omega_S/\cosh(\frac{2k-1}{2N}\pi)$ and coefficient K can be taken from (3.20) and (3.21) which can be expressed in a unified form using η:

$$K = \frac{\epsilon|c_\eta|\Omega_S^\eta}{\sqrt{1 + \epsilon^2 c_\eta^2 \Omega_S^{2\eta}(1-\eta)}} \tag{3.34}$$

In the above equations, c_η is the coefficient of the lowest term of the Chebyshev polynomial $C_N(\Omega)$ taken from (3.25): $c_\eta = N^\eta(-1)^{\frac{N+3\eta}{2}}$.

In (3.33), p_k are the left hand half s-plane roots of the even polynomial of order $2N$

$$s^{2N} + (-1)^N \epsilon^2 c_\eta^2 \Omega_S^{2\eta} \prod_{k=1}^{\frac{N-\eta}{2}} \left(s^2 + \frac{\Omega_S^2}{\rho_k^2}\right)^2 \tag{3.35}$$

which will be calculated next.

The gain function of the inverse Chebyshev approximation of (3.23) is repeated here for convenience:

$$G_{ICH}(\Omega) = \frac{H_o}{\sqrt{1 + \frac{1}{\epsilon^2 C_N^2(\frac{\Omega_s}{\Omega})}}} = \frac{\epsilon H_o |C_N(\frac{\Omega_s}{\Omega})|}{\sqrt{1 + \epsilon^2 C_N^2(\frac{\Omega_s}{\Omega})}} \tag{3.36}$$

Since the denominator has the same form $\sqrt{1+\epsilon^2 C_n^2(x)}$ as in the Chebyshev case, the poles of $H_{ICH}(\frac{\Omega_S}{s})$ will be those of $H_{CH}(s)$ for $s = \frac{\Omega_S}{s}$. The poles of $H_{CH}(s)$ have been given in the previous chapter in (2.61), from which we get:

$$\begin{aligned}
&\frac{\Omega_S}{p_k} = \sigma_k + j\Omega_k \quad \text{where} \\
&\sigma_k = \sin\left(\frac{2N+2k-1}{2N}\pi\right)\sinh\left[\frac{1}{N}\sinh^{-1}\left(\frac{1}{\epsilon}\right)\right] \\
&\Omega_k = \cos\left(\frac{2N+2k-1}{2N}\pi\right)\cosh\left[\frac{1}{N}\sinh^{-1}\left(\frac{1}{\epsilon}\right)\right] \\
&k = 1, 2, \ldots, N
\end{aligned} \tag{3.37}$$

The poles p_k of $H_{ICH}(s)$ can be calculated from (3.37):

$$\left\{\begin{aligned}
&p_k = \sigma_{ki} + j\Omega_{ki} = \frac{\Omega_S \sigma_k}{\sigma_k^2 + \Omega_k^2} - j\frac{\Omega_S \Omega_k}{\sigma_k^2 + \Omega_k^2} \quad \text{with} \\
&\sigma_k = \sin\left(\frac{2N+2k-1}{2N}\pi\right)\sinh\left[\frac{1}{N}\sinh^{-1}\left(\frac{1}{\epsilon}\right)\right] \\
&\Omega_k = \cos\left(\frac{2N+2k-1}{2N}\pi\right)\cosh\left[\frac{1}{N}\sinh^{-1}\left(\frac{1}{\epsilon}\right)\right] \\
&k = 1, 2, \ldots, N
\end{aligned}\right\} \tag{3.38}$$

Equation (3.33) fully defines the transfer function of the inverse Chebyshef approximation with K from (3.34) and the poles p_k from (3.38). However, the order N and the ripple factor ϵ are still unknown and will be calculated in the next sections.

3.3.1 Gain Analysis

The gain of the inverse Chebyshev approximation of (3.23) can also be expressed as

$$G_{ICH}(\Omega) = H_o\sqrt{1 - \frac{1}{1 + \epsilon^2 C_N^2(\frac{\Omega_s}{\Omega})}} \tag{3.39}$$

A more detailed form can be derived using (3.31) in (3.5) with $\gamma = \epsilon^{-1}$:

$$G_{ICH}(\Omega) = \frac{H_o}{\sqrt{1 + \frac{N_R^2(\Omega)}{\epsilon^2 D_R^2(\Omega)}}} = \frac{H_o \epsilon |c_\eta| \Omega_S^\eta \prod_{k=1}^{\frac{N-\eta}{2}} (\Omega^2 - \frac{\Omega_S^2}{\rho_k^2})}{\sqrt{\Omega^{2N} + \epsilon^2 c_\eta^2 \Omega_S^{2\eta} \prod_{k=1}^{\frac{N-\eta}{2}} (\Omega^2 - \frac{\Omega_S^2}{\rho_k^2})^2}} \tag{3.40}$$

where from (3.25), $c_\eta = N^\eta (-1)^{\frac{N+3\eta}{2}}$ is the coefficient of the lowest term of $C_N(\Omega)$ and η as defined in (3.26). Next, it will be shown that:

1. The function $G_{ICH}(\Omega)$ is monotonically decreasing in the interval $0 \le \Omega \le \Omega_S$.
2. In the stopband, there exist $(N - \eta)/2$ maxima with values equal to $G_{ICH}(\Omega_S)$

If the above two conditions hold, then in order to satisfy the specifications it is sufficient to ensure that $G_{ICH}(1) \ge H_C$ and $G_{ICH}(\Omega_S) \le H_S$.

Defining

$$\Xi_N(x) = 1 + \epsilon^2 C_N^2(x),$$

the following properties can easily be shown and are visualized in Fig. 3.4:

i. $\Xi_N(1) = 1 + \epsilon^2 C_N^2(1) = 1 + \epsilon^2$ for all N.

ii. $\Xi_N(0) = 1 + \epsilon^2 C_N^2(0) = 1 + (1 - \eta)\epsilon^2 = \begin{cases} 1 & \text{for } N = \text{odd} \\ 1 + \epsilon^2 & \text{for } N = \text{even} \end{cases}$

iii. For $x > 1$, $\Xi_N(x) = 1 + \epsilon^2 C_N^2(x)$ is increasing monotonically following $C_N^2(x)$

iv. For $0 < x < 1$, $\Xi_N(x)$ presents equal ripple from 1 to $1 + \epsilon^2$

Therefore the function $\Xi_{No}(\Omega) = \Xi_N(\Omega_S/\Omega) = 1 + \epsilon^2 C_N^2(\Omega_S/\Omega)$ has the following basic properties:

i. $\Xi_{No}(\Omega_S) = \Xi_N(1) = 1 + \epsilon^2 C_N^2(1) = 1 + \epsilon^2$ for all N.

ii. $\Xi_{No}(\infty) = \Xi_N(0) = \begin{cases} 1 & \text{for } N = \text{odd} \\ 1 + \epsilon^2 & \text{for } N = \text{even} \end{cases}$

iii. $\Xi_{No}(\Omega) = \Xi_N(\Omega_S/\Omega) = 1 + \epsilon^2 C_N^2(\Omega_S/\Omega)$ is decreasing monotonically for $0 < \Omega < \Omega_S$

iv. For $\Omega > \Omega_S$, $\Xi_{No}(\Omega) = \Xi_N(\Omega_S/\Omega)$ presents equal ripple between 1 to $1 + \epsilon^2$.

Taking these properties into account, the inverse Chebyshev gain of (3.36) and (3.39) is repeated in (3.41).

$$G_{ICH}(\Omega) = H_o \sqrt{1 - \frac{1}{1 + \epsilon^2 C_N^2(\frac{\Omega_s}{\Omega})}} = \frac{\epsilon H_o |C_N(\frac{\Omega_s}{\Omega})|}{\sqrt{1 + \epsilon^2 C_N^2(\frac{\Omega_s}{\Omega})}} \tag{3.41}$$

$G_{ICH}(\Omega)$ is monotonically decreasing for $0 \le \Omega \le \Omega_S$, since $\Xi_N(\Omega_S/\Omega) = 1 + \epsilon^2 C_N^2(\Omega_S/\Omega)$ is monotonically decreasing in this interval, as shown in Fig. 3.5. For $\Omega \ll 1$, $1 + \epsilon^2 C_N^2(\Omega_S/\Omega)$ assumes very large values, and therefore $G_{ICH}(\Omega)$ assumes values very near H_o. For $\Omega_S/\Omega = 1$, i.e. for $\Omega = \Omega_S$

$$\Xi_N(\Omega_S/\Omega)_{\Omega=\Omega_S} = \Xi_N(1) = 1 + \epsilon^2 C_N(1) = 1 + \epsilon^2$$

and therefore

$$G_{ICH}(\Omega_S) = \frac{\epsilon H_o}{\sqrt{1 + \epsilon^2}} \tag{3.42}$$

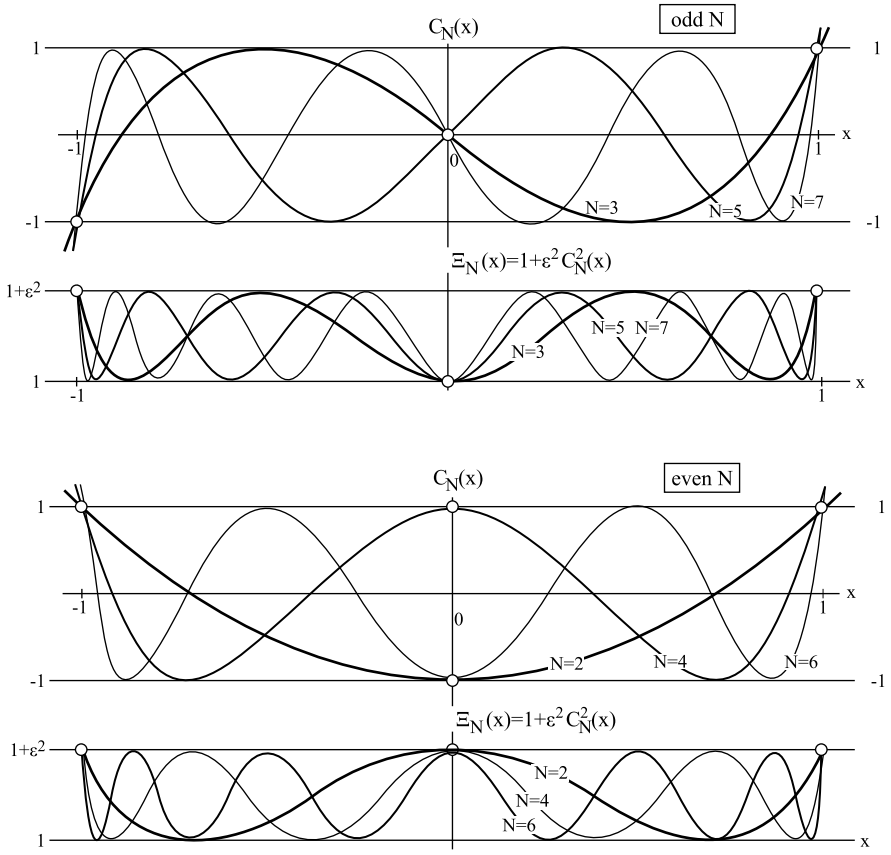

Fig. 3.4 Plots of $C_N(x)$ and $\Xi_N(x) = 1 + \epsilon^2 C_N^2(x)$ for odd and even N

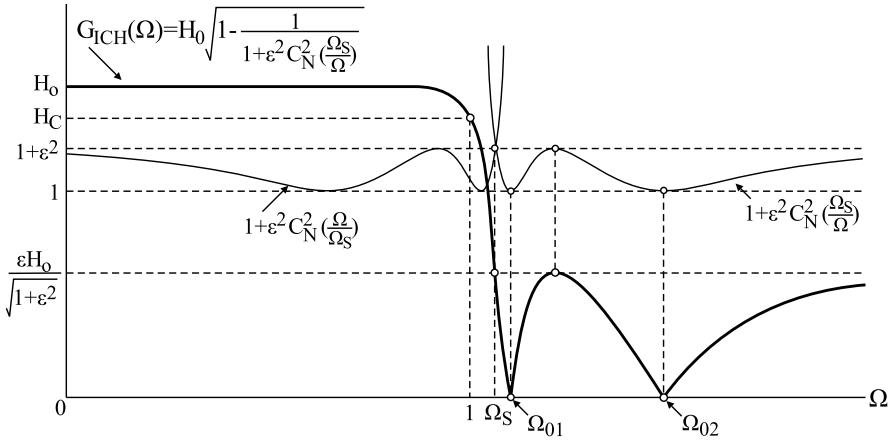

Fig. 3.5 Plots of $\Xi_N(x)$ and $\Xi_N(1/x)$ with $x = \Omega/\Omega_S$

By definition, $G_{ICH}(\Omega)$ becomes zero when $C_N^2(\Omega_S/\Omega) = 0$. Moreover, since

$$C_N(\Omega_S\Omega) = \cos[N\cos^{-1}(\Omega_S/\Omega)]$$

$C_N(\frac{\Omega_S}{\Omega})$ becomes zero when $N\cos^{-1}(\Omega_S/\Omega)$ is an odd multiple of $\pi/2$, i.e. when $N\cos^{-1}(\frac{\Omega_S}{\Omega}) = (2k-1)\frac{\pi}{2}$. From this result, the $(N-\eta/2)$ discrete values which make $G_{ICH}(\Omega) = 0$ can be obtained:

$$\Omega_{zk} = \frac{\Omega_S}{\cos(\frac{2k-1}{2N}\pi)} \quad \text{for } k = 1,\ldots,\frac{N-\eta}{2},\ \eta \text{ from (3.26)} \tag{3.43}$$

Notice that this is the same result expressed in (3.31).

For $\Omega > 1$, when $C_N(\Omega_S/\Omega) = \pm 1$, the expression $1+\epsilon^2 C_N^2(\Omega_S/\Omega)$ assumes its maximum value $1+\epsilon^2$, and the gain $G_{ICH}(\Omega)$ assumes also maximum value $\frac{\epsilon H_o}{\sqrt{1+\epsilon^2}}$. Therefore, the stopband maxima have the same value $\frac{\epsilon H_o}{\sqrt{1+\epsilon^2}}$ with $G_{ICH}(\Omega_S)$.

$C_N(\Omega_S/\Omega)$ assumes the value $= \pm 1$ when $N\cos^{-1}(\frac{\Omega_S}{\Omega})$ is an even multiple of π, i.e. when $N\cos^{-1}(\frac{\Omega_S}{\Omega}) = 2k\pi$, from which we get $(N-\eta/2)$ discrete values of Ω_{MAXk}, for which the gain becomes maximum in the stopband:

$$\Omega_{MAXk} = \frac{\Omega_S}{\cos(\frac{2k}{N}\pi)} \quad k = 1\ldots\left(\frac{N-\eta}{2}\right),\ \eta = \begin{cases} 1 & \text{for } N \text{ odd} \\ 0 & \text{for } N \text{ even} \end{cases} \tag{3.44}$$

3.3.2 Ripple Factor and Order Calculation

Having all the details of the gain function of the inverse Chebyshev approximation, we can now deal with the ripple factor ϵ and the order N. Let us start from the stopband, for which it has been found that the maxima have the value $\frac{\epsilon H_o}{\sqrt{1+\epsilon^2}} = G_{ICH}(\Omega_S)$.

Requiring that $\frac{\epsilon H_o}{\sqrt{1+\epsilon^2}} \le H_S$, a first estimate of ϵ can be obtained:

$$\epsilon \le \epsilon_{\max} = \frac{1}{\sqrt{(H_o^2/H_S^2)-1}} = \frac{1}{\sqrt{10^{\frac{a_{\min}}{10}}-1}} \tag{3.45}$$

It should be noted that the maximum value $\epsilon_{\max}$ of the ripple factor depends only on H_o and H_S (or only on $\alpha_{\min}$). If this maximum value $\epsilon = \epsilon_{\max}$ is selected, the stopband tolerance is fully reached with $G_{ICH}(\Omega_S) = H_S$ and all maxima at H_S.

In the monotonic passband $0 \le \Omega \le 1$, we have from (3.41) that $G_{ICH}(0) = H_o$ and it is required that

$$G_{ICH}(1) = H_o\sqrt{1-\frac{1}{1+\epsilon_{\max}^2 C_N^2(\Omega_s)}} \ge H_C \tag{3.46}$$

from which we find

$$N \geq N_d = \frac{\cosh^{-1}\left(\frac{\sqrt{(H_o/H_S)^2-1}}{\epsilon_{\max}}\right)}{\cosh^{-1}(\Omega_S)} = \frac{\cosh^{-1}\left(\frac{1}{g}\right)}{\cosh^{-1}(\Omega_S)}$$

$$\text{where } g = \sqrt{\frac{(H_o/H_C)^2-1}{(H_o/H_S)^2-1}} = \sqrt{\frac{10^{\frac{\alpha_{\max}}{10}}-1}{10^{\frac{\alpha_{\min}}{10}}-1}} \tag{3.47}$$

In terms of the logarithmic gain specifications, the above order equation (3.47) becomes:

$$N \geq N_d = \frac{\cosh^{-1}\left(\sqrt{\frac{10^{\frac{\alpha_{\min}}{10}}-1}{10^{\frac{\alpha_{\max}}{10}}-1}}\right)}{\cosh^{-1}(\Omega_S)} \tag{3.48}$$

The non-integer order N_d in general takes a decimal value. The integer order of the approximation will be the minimum integer N that satisfies $N \geq N_d$, i.e. N_d rounded up to the next integer value.

It should be noted that the order equation (3.47) and (3.48) of the inverse Chebyshev approximation is identical to the order equation (2.47) in the case of the Chebyshev approximation.

From (3.47) and (3.48), it is apparent that the order increases as Ω_S approaches unity and becomes infinite for $\Omega_S = 1$. This means that the order increases as we try to make the transition band as narrow as possible. It also means that higher order filters can realize narrower transition bands. The order also increases as the passband tolerance decreases (H_C approaches H_o or $\alpha_{\max}$ approaches zero) and as the maximum allowed stopband gain H_S decreases ($\alpha_{\min}$ increases).

Filters designed with the inverse Chebyshev approximation are referred to as inverse Chebyshev filters and the name implies only that they realize this type of response, no matter how they are implemented. Inverse Chebyshev filters can be implemented using any suitable technology, e.g. as passive, active or digital IIR filters.

Since $\cosh^{-1}(x)$ is an increasing function of x, $N_d(\epsilon)$ decreases as ϵ increases and therefore $N_d(\epsilon_{\max})$ is the minimum value for all permissible values $\epsilon \leq \epsilon_{\max}$. Figure 3.6 shows this situation.

It is clear from Fig. 3.6 that there is a value $\epsilon_{\min}$ for which $N_d(\epsilon_{\min})$ becomes equal to the integer order N. For $\epsilon < \epsilon_{\min}$, higher order is required. Given the integer order N, the minimum value of ϵ can be determined from (3.47) setting

$$\frac{\cosh^{-1}\left(\frac{1}{g}\right)}{\cosh^{-1}(\Omega_s)} = N \quad g \text{ (from (3.47))}$$

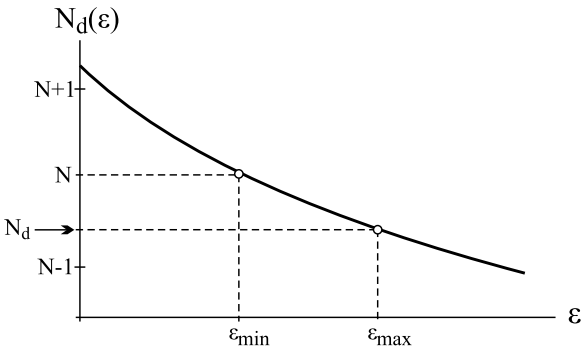

Fig. 3.6 N_d as a function of ϵ

from which we find

$$\epsilon_{\min} = \frac{1}{C_N(\Omega_S)\sqrt{\frac{H_o^2}{H_C^2} - 1}} = \frac{1}{C_N(\Omega_S)\sqrt{10^{\frac{\alpha_{\max}}{10}} - 1}} \tag{3.49}$$

For a specific order N, the minimum value of the ripple factor depends not only on the passband tolerance, but also on the stopband edge frequency Ω_S.

Finally, when the order N of the approximation has been determined, the ripple factor can be chosen from the interval given below.

$$\epsilon_{\min} = \frac{1}{C_N(\Omega_S)\sqrt{\frac{H_o^2}{H_C^2} - 1}} \leq \epsilon \leq \frac{1}{\sqrt{\frac{H_o^2}{H_S^2} - 1}} = \epsilon_{\max} \tag{3.50}$$

or, in terms of logarithmic gain

$$\epsilon_{\min} = \frac{1}{C_N(\Omega_S)\sqrt{10^{\frac{\alpha_{\max}}{10}} - 1)}} \leq \epsilon \leq \frac{1}{\sqrt{10^{\frac{\alpha_{\min}}{10}} - 1}} = \epsilon_{\max} \tag{3.51}$$

3.3.3 Optimization

Given the specifications Ω_S and $\{H_o, H_C, H_S\}$ or $\{\alpha_o, \alpha_{\max}, \alpha_{\min}\}$, the order of the approximation can be determined from the order equation (3.47) or (3.48), and inverse Chebyshev approximation can be optimized as to meet certain criteria and exhibit different characteristics.

3.3.3.1 Optimization Using the Ripple Factor

The boundary values of the ripple factor ϵ depend only on the filter specifications and can be calculated as soon as the order N has been determined from the order equation (3.47) or (3.48). Different gain characteristics are obtained for each selection of $\epsilon_{\min} \leq \epsilon \leq \epsilon_{\max}$.

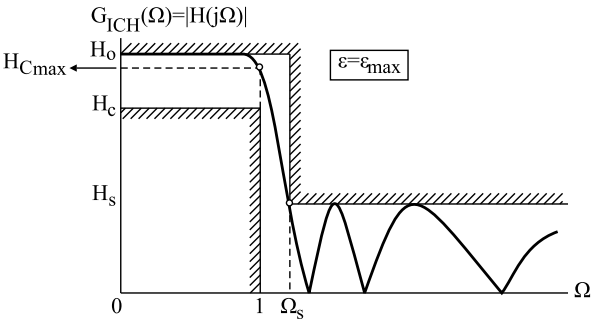

Fig. 3.7 Case A: $\epsilon = \epsilon_{\max}$ (passband optimization)

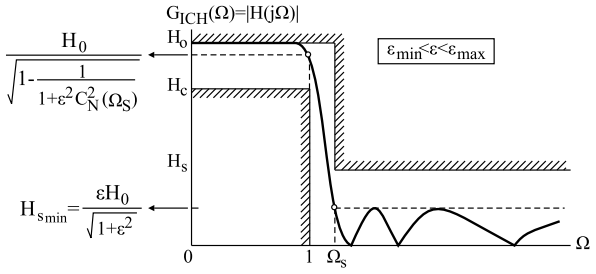

Fig. 3.8 Case B: $\epsilon_{\min} < \epsilon < \epsilon_{\max}$

Case A: $\epsilon = \epsilon_{\max}$ (Passband Optimization) Choosing $\epsilon = \epsilon_{\max}$, the maxima of the stopband gain become exactly equal to the specified minimum stopband gain, and in addition $G_{ICH}(\Omega_S) = H_S$. In this case, shown in Fig. 3.7, the plain gain at $\Omega = 1$ assumes the value

$$H_{C\max} = G_{ICH}(1) = \frac{H_o \epsilon_{\max} |C_N(\Omega_S)|}{\sqrt{1 + \epsilon_{\max}^2 C_N^2(\Omega_S)}} = \frac{H_o |C_N(\Omega_S)|}{\sqrt{\frac{H_o^2}{H_S^2} - 1 + C_N^2(\Omega_S)}} > H_C \quad (3.52)$$

and the logarithmic passband ripple becomes minimum

$$\alpha_{C\min} = 20 \log\left(\frac{H_o}{H_{C\max}}\right)$$

Case B: $\epsilon_{\min} < \epsilon < \epsilon_{\max}$ For a value $\epsilon_{\min} < \epsilon < \epsilon_{\max}$, the specifications are satisfied as shown in Fig. 3.8 with $G_{ICH}(1) \geq H_C$, and the stopband gain maxima assume the value $G_{ICH}(\Omega_S) \leq H_S$.

Case C: $\epsilon = \epsilon_{\min}$ (Stopband Edge Frequency Gain Optimization) For $\epsilon = \epsilon_{\min}$, passband tolerance is reached with $G_{ICH}(1) = H_C$. The maxima of the stopband gain in this case assume the value $H_{S\min} = G_{ICH}(\Omega_S) \leq H_S$ (see Fig. 3.9).

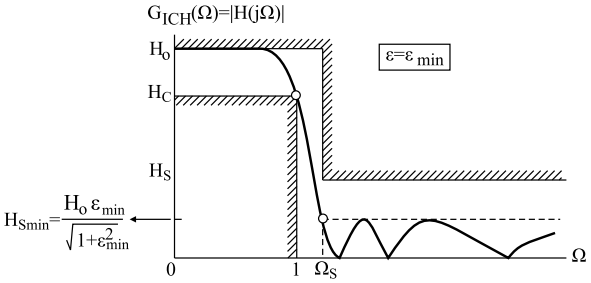

Fig. 3.9 Case C: $\epsilon = \epsilon_{\min}$ (stopband edge frequency gain optimization)

$$H_{S\min} = G_{ICH}(\Omega_S) = \frac{H_o\epsilon_{\min}}{\sqrt{1+\epsilon_{\min}^2}} = \frac{H_o}{\sqrt{1+C_n^2(\Omega_S)(\frac{H_o^2}{H_C^2}-1)}} \le H_S \tag{3.53}$$

The frequency Ω_{Hs} at which $G_{ICH}(\Omega_{Hs}) = H_S$ is given by

$$\Omega_{Hs} = \frac{\Omega_S}{\cosh[\frac{1}{N}\cosh^{-1}(gC_N(\Omega_S))]} \quad \text{where } g = \sqrt{\frac{(H_o/H_C)^2-1}{(H_o/H_S)^2-1}} \tag{3.54}$$

3.3.3.2 Transition Band Optimization $\Omega_{S\min}$

If we require that $G_{ICH}(1) = H_C$ and $G_{ICH}(\Omega_S) = H_S$, as shown in Fig. 3.10, then $\epsilon_{\min}$ and $\epsilon_{\max}$ must become equal:

$$\epsilon_{\min} = \frac{1}{C_N(\Omega_S)\sqrt{\frac{H_o^2}{H_C^2}-1}} = \frac{1}{\sqrt{\frac{H_o^2}{H_S^2}-1}} = \epsilon_{\max} \tag{3.55}$$

This can only happen if there is a frequency $\Omega_{S\min}$ at which $C_N(\Omega_{S\min})$ takes the value:

$$C_N(\Omega_{S\min}) = \sqrt{\frac{(H_o/H_S)^2-1}{(H_o/H_C)^2-1}} \tag{3.56}$$

from which we find

$$\Omega_{S\min} = \cosh\left(\frac{1}{N}\cosh^{-1}\sqrt{\frac{(H_o/H_S)^2-1}{(H_o/H_C)^2-1}}\right) \le \Omega_S \tag{3.57}$$

This means that the filter can be designed with stricter transition band specifications ($\Omega_{S\min} < \Omega_S$). For the given magnitude specifications, the filter designed with $\Omega_{S\min} < \Omega_S$ has the steepest gain in the transition band and is referred to as *transition band optimized*. Figure 3.10 shows the gain plot of a filter designed with $\Omega_{S\min}$ instead of the specified Ω_S. It should be noted that $\Omega_{S\min}$ given in (3.57) is such that the order remains N as if it has been calculated using the specified Ω_S. In fact, the use of $\Omega_{S\min}$ in (3.47) or (3.48) leads to integer $N_d = N$.

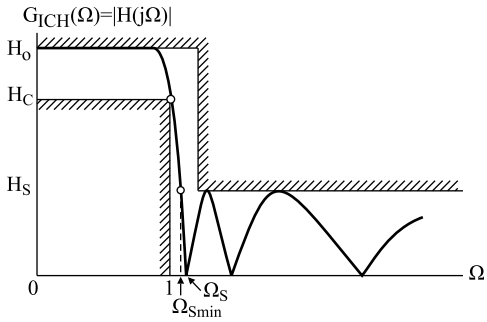

Fig. 3.10 Transition band optimization $\Omega_{S\min}$

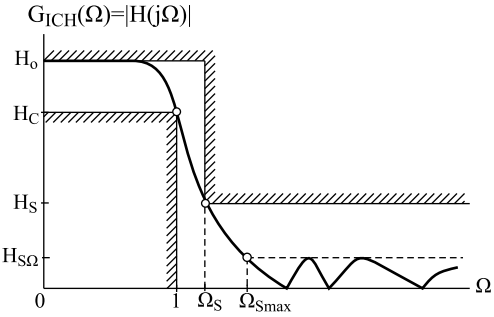

Fig. 3.11 Stopband optimization $\Omega_{S\max}$

3.3.3.3 Stopband Optimization $\Omega_{S\max}$

One more optimization can be performed in the inverse Chebyshev approximation. Let us suppose that we have the stopband edge frequency gain optimized design with $\epsilon = \epsilon_{\min}$ of Case C (Fig. 3.9), where the stopband maxima and $G_{ICH}(\Omega_S)$ assume equal values $H_{S\min}$ (see (3.53)), lower than the specified H_S. The frequency Ω_{Hs} at which $G_{ICH}(\Omega_{Hs}) = H_S$ is given by (3.54):

$$\Omega_{Hs} = \frac{\Omega_S}{\cosh[\frac{1}{N}\cosh^{-1}(gC_N(\Omega_S))]} < \Omega_S \quad \text{where } g = \sqrt{\frac{(H_o/H_C)^2 - 1}{(H_o/H_S)^2 - 1}}$$

If we drag Ω_{Hs} to the right until the curve touches the point $\{\Omega_S, H_S\}$, the frequency at which the gain becomes equal to the stopband maxima moves to a frequency $\Omega_{S\max} > \Omega_S$. Moreover, the stopband maxima will decrease, as can be seen from (3.53) for $\Omega_S = \Omega_{S\max}$. This situation is shown in Fig. 3.11 and frequency $\Omega_{S\max}$ can be calculated from

$$\Omega_S = \frac{\Omega_{S\max}}{\cosh[\frac{1}{N}\cosh^{-1}(gC_N(\Omega_{S\max}))]} \quad \text{where } g = \sqrt{\frac{(H_o/H_C)^2 - 1}{(H_o/H_S)^2 - 1}} \tag{3.58}$$

Therefore, if minimum stopband ripple is required, the filter can be designed using $\Omega_{S\max}$ instead of the specified Ω_S without change of the order. However, the solution of (3.58) for $\Omega_{S\max}$ is not an easy task. In fact, the following equation must

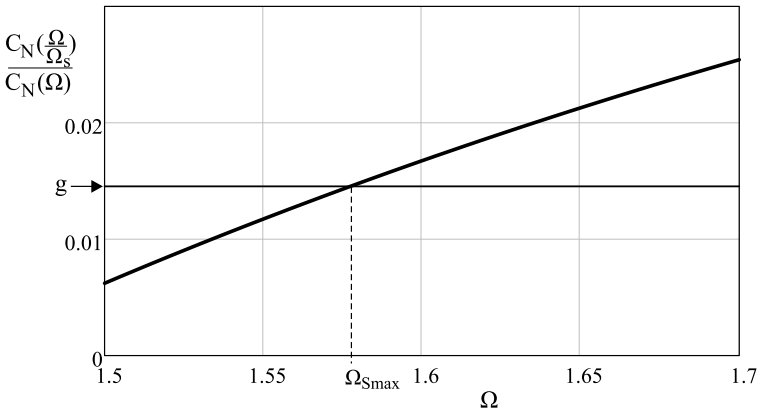

Fig. 3.12 Graphical calculation of $\Omega_{S\max}$

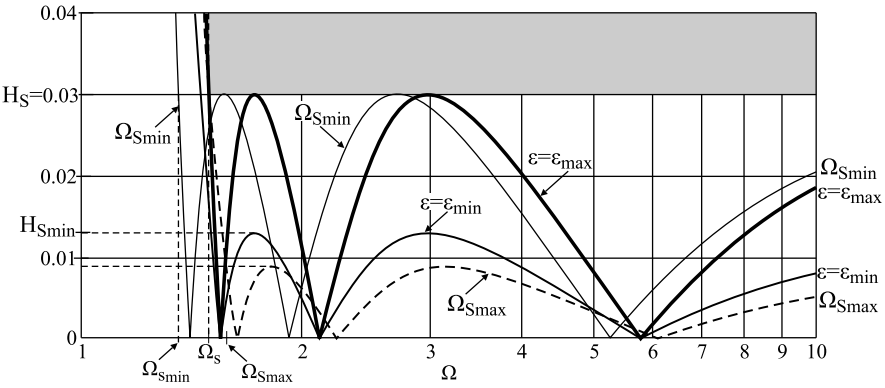

Fig. 3.13 Stopband details of the four optimized designs

be solved,

$$C_N\left(\frac{\Omega_{S\max}}{\Omega_S}\right) = g \cdot C_N(\Omega_{S\max}) \tag{3.59}$$

which cannot be solved analytically, and the use of numerical methods is inevitable. Figure 3.12 shows a way to calculate $\Omega_{S\max}$ graphically for $N = 6$, $\Omega_S = 1.5$, $H_o = 1$, $H_C = 0.9$ and $H_S = 0.03$ to find $\Omega_{S\max} = 1.5774$.

Figure 3.13 shows the stopband details of the four optimized designs for a filter with specifications $\Omega_S = 1.5$, $H_o = 1$, $H_C = 0.9$ and $H_S = 0.03$ from which $N = 6$.

Inverse Chebyshev transfer functions can be realized using various technologies, e.g. active-RC or passive. When they are realized with doubly terminated passive ladders, they may look like the circuits of Fig. 3.14, with parallel resonant LC circuits in the series arms to realize the transmission zeros.

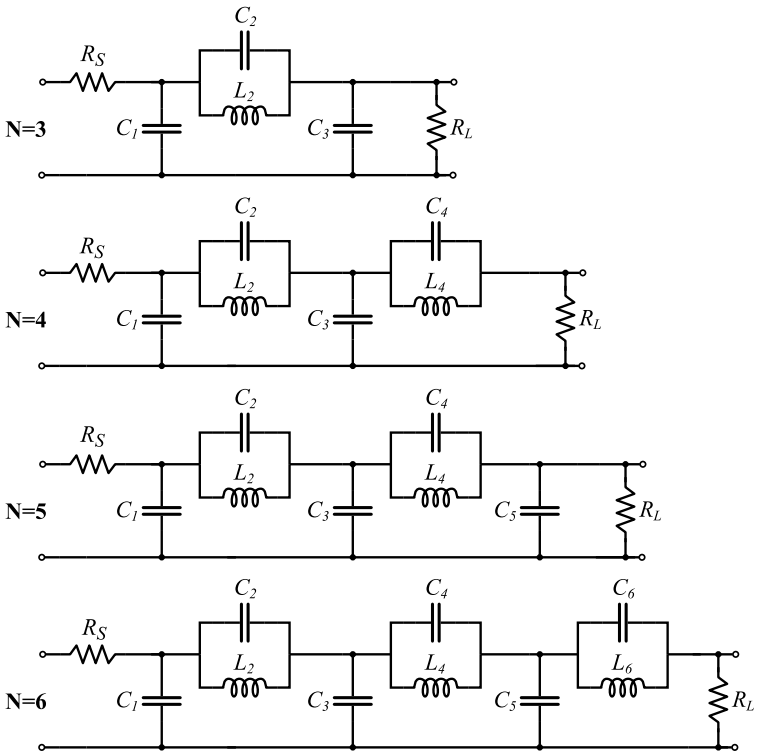

Fig. 3.14 The structure of passive inverse Chebyshev filters

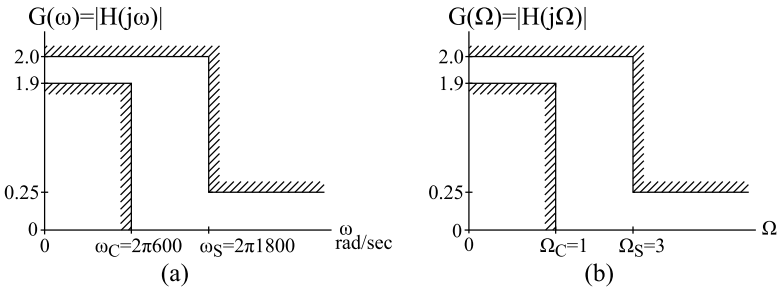

Fig. 3.15 (**a**) Lowpass filter specifications. (**b**) Normalized specifications

Example 3.3 Find the inverse Chebyshev plain gain function $G_{ICH}(\Omega)$ and the corresponding transfer function $H_{ICH}(s)$ from the plain gain specifications of Fig. 3.15.

The specifications are identified as follows:

$$\omega_C = 2\pi\,600 \text{ rad/s}, \qquad \omega_S = 2\pi\,1800 \text{ rad/s},$$

$$H_o = 2, \qquad H_C = 1.9, \quad \text{and} \quad H_S = 0.25$$

The normalized specifications shown in Fig. 3.15b will be

$$\Omega_C = 1, \qquad \Omega_S = 3, \qquad H_o = 2, \qquad H_C = 1.9, \quad \text{and} \quad H_S = 0.25$$

In order to calculate the normalized gain

$$G_{ICH}(\Omega) = H_o \frac{\epsilon |C_N(\frac{\Omega_S}{\Omega})|}{\sqrt{1 + \epsilon^2 C_N^2(\frac{\Omega_S}{\Omega})}}$$

which meets the normalized specifications, $\epsilon_{\max}$ will be first calculated from (3.50):

$$\epsilon_{\max} = \frac{1}{\sqrt{\frac{H_o^2}{H_S^2} - 1}} = \frac{1}{\sqrt{\frac{2^2}{0.1^2} - 1}} = 0.125988$$

The decimal order N_d is then calculated from (3.47):

$$N_d = \frac{\cosh^{-1}\left(\sqrt{\frac{\frac{H_o^2}{H_S^2} - 1}{\frac{H_o^2}{H_C^2} - 1}}\right)}{\cosh^{-1}(\Omega_S)} = \frac{\cosh^{-1}\left(\sqrt{\frac{\frac{2^2}{0.25^2} - 1}{\frac{2^2}{1.9^2} - 1}}\right)}{\cosh^{-1}(3)} = 2.1993$$

and the integer order will be $N = 3$. Having N, the minimum value of the ripple factor can be calculated from (3.50) for $N = 3$ and $\Omega_S = 3$:

$$C_3(3) = 4 \cdot 3^3 - 3 \cdot 3 \quad \Rightarrow \quad C_3(3) = 99.0$$

$$\epsilon_{\min} = \frac{1}{C_N(\Omega_S)\sqrt{(H_o/H_C)^2 - 1}} = \frac{1}{99.0\sqrt{(2^2/1.9^2) - 1}} = 0.03073167$$

Finally, for $N = 3$ and $\Omega_S = 3$, the gain will be

$$G_{ICH}(\Omega) = H_o \sqrt{1 - \frac{1}{1 + \epsilon^2 C_3^2(\frac{3}{\Omega})}} = \frac{\epsilon H_o |C_3(\frac{3}{\Omega})|}{\sqrt{1 + \epsilon^2 C_3^2(\frac{3}{\Omega})}}$$

$$\text{where } \epsilon_{\min} \le \epsilon \le \epsilon_{\max} \text{ and } C_3(x) = 4x^3 - 3x$$

The gain function $G_{ICH}(\Omega)$ satisfies the normalized specifications and its plot is shown in Fig. 3.16 for the two boundary values of the ripple factor ϵ. The value of ϵ does not affect the position of the transmission zero, but mainly the value of the gain at $\Omega = \Omega_S$ and $\Omega = 1$.

For $N = 3$, the unique, since $(N - \eta)/2 = 1$, zero of the transfer function is given by (3.29):

$$\pm j \frac{3}{\cos(\frac{2 \cdot 1 - 1}{2 \cdot 3}\pi)} = 3.464$$

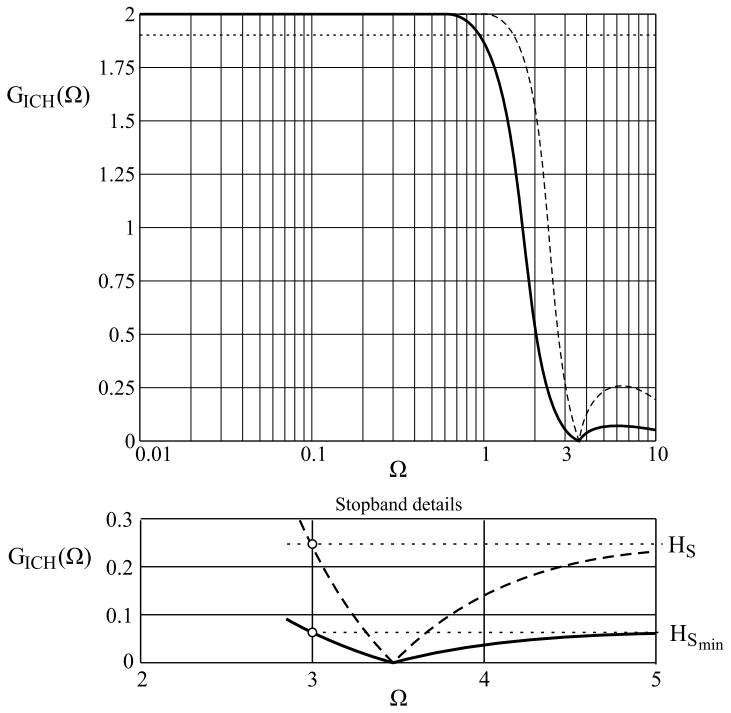

Fig. 3.16 Gain plot of $G_{ICH}(\Omega)$ for $\epsilon = \epsilon_{\min}$ and $\epsilon = \epsilon_{\max}$ (*dashed*)

The constant K is determined from (3.34) and the poles p_k of the transfer function from (3.38) for $k = 1, \ldots, 3$:

For $\epsilon = \epsilon_{\max} = 0.125988$, we find $K = 1.1338934$ and

$$p_1 = -0.8487 - j2.021273 \qquad p_2 = -2.831293$$
$$p_3 = -0.8487 + j2.021273$$
$$\Rightarrow \quad H_1(s) = \frac{2 \cdot 1.1338934 \cdot (s^2 + 3.464^2)}{(s + 2.831293)(s^2 + 2 \cdot 0.8487s + 0.8487^2 + 2.021273^2)}$$

For $\epsilon = \epsilon_{\min} = 0.03073167$, we find $K = 0.2765849$ and

$$p_1 = -0.656601 - j1.287085 \qquad p_2 = -1.589787$$
$$p_3 = -6566 + j1.287085$$
$$\Rightarrow \quad H_2(s) = \frac{2 \cdot 0.2765849 \cdot (s^2 + 3.464^2)}{(s + 1.589787)(s^2 + 2 \cdot 0.656601s + 0.656601^2 + 1.287085^2)}$$

The plots of $G_{HICH}(\Omega, \epsilon_{\max}) = |H_1(j\Omega)|$ and $G_{HICH}(\Omega, \epsilon_{\min}) = |H_2(j\Omega)|$ are shown in Fig. 3.17. The plots are of course identical with those of Fig. 3.16.

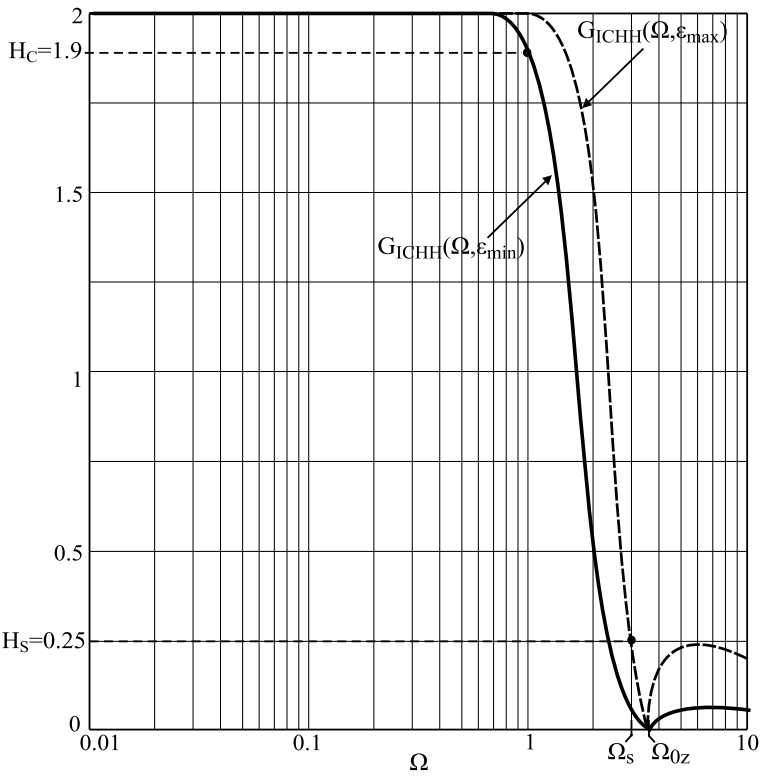

Fig. 3.17 Gain plot of $G_{HICH}(\Omega)$ from the transfer functions

If $H_{ICH}(s)$ satisfies the normalized specifications, the transfer function that satisfies the specifications with $\omega_C = 2\pi 600$ rad/s ($f_C = 600$ Hz) will be simply $H_{ICH}(s/\omega_C)$ and the corresponding gain function will be $|H_{ICH}(j\omega/\omega_C)| = |H_{ICH}(jf/f_C)|$. Figure 3.18 shows the denormalized plain gain plots and Fig. 3.19 the corresponding logarithmic gain plots, where the stopband details are better visualized.

Example 3.4 Find the gain function $G_{ICH}(\Omega)$ and the transfer function $H_{ICH}(s)$ so as to satisfy the plain gain specifications of Fig. 3.20.

The specifications are identified as follows:

$$\omega_C = 2\pi 1000 \text{ rad/s}, \qquad \omega_S = 2\pi 1500 \text{ rad/s},$$
$$H_o = 1, \qquad H_C = 0.9, \quad \text{and} \quad H_S = 0.03$$

The normalized specifications shown in Fig. 3.20b will be

$$\Omega_C = 1, \qquad \Omega_S = 1.5, \qquad H_o = 1, \qquad H_C = 0.9, \quad \text{and} \quad H_S = 0.03$$

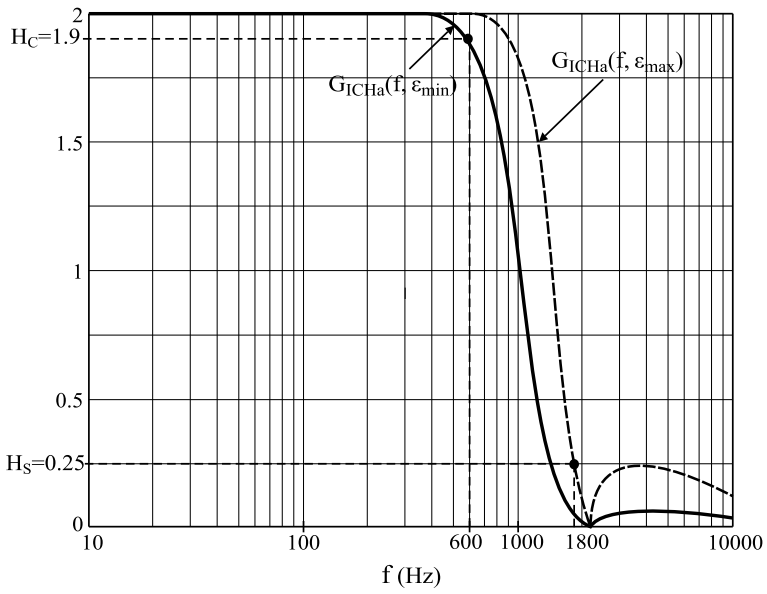

Fig. 3.18 Gain plot of denormalized $G_{ICHa}(\Omega)$

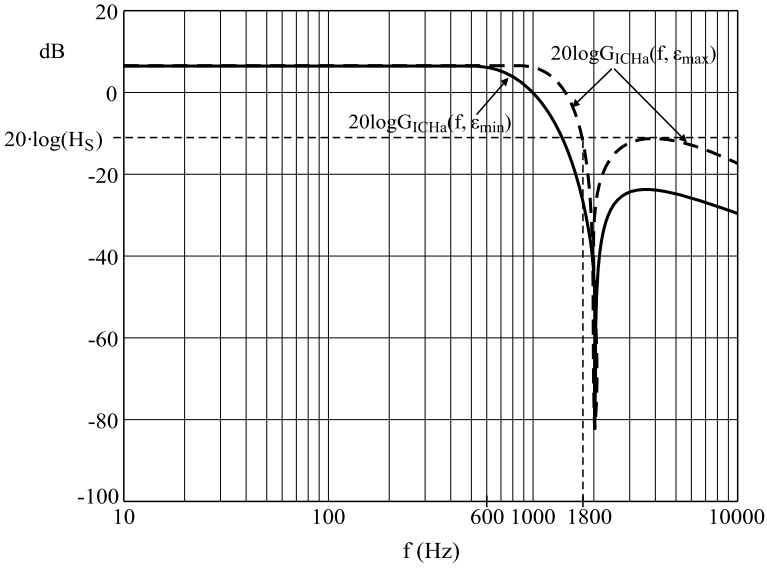

Fig. 3.19 Logarithmic gain plot of denormalized $G_{ICHa}(\Omega)$

In order to calculate the normalized gain, the maximum value of the ripple factor $\epsilon_{\max}$ is first calculated from (3.50): $\epsilon_{\max} = 0.03001351$. The decimal order N_d is then calculated from (3.47): $N_d = 5.116465 \Rightarrow N = 6$.

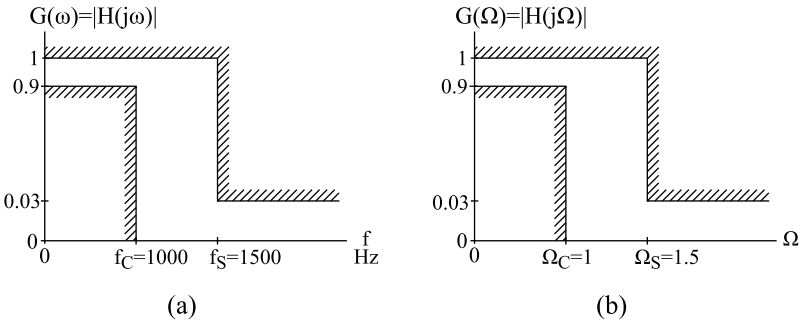

Fig. 3.20 (**a**) Lowpass filter specifications. (**b**) Normalized specifications

The minimum value of the ripple factor can be calculated from (3.50) for $N = 6$ and $\Omega_S = 1.5$: $\epsilon_{\min} = 0.01282448$.

Figure 3.21 shows the gain plot from (3.23) with $N = 6$, $\Omega_S = 1.5$, for $\epsilon = \epsilon_{\min}$ and $\epsilon = \epsilon_{\max}$. The value of ϵ does not affect the position of the transmission zero, but mainly the value of the gain at $\Omega = \Omega_S$ and $\Omega = 1$.

For $N = 6$ ($\eta = 0$), the $(N - \eta)/2 = 3$ conjugate imaginary zero pairs of the transfer function are calculated from (3.29):

$$\Omega_{z1} = \pm j1.552914 \qquad \Omega_{z2} = \pm j2.12132 \qquad \Omega_{z3} = \pm j5.795555$$

The constant K is calculated from (3.34) and the poles p_k of the transfer function from (3.38) for $k = 1, \ldots, 6$:

For $\epsilon = \epsilon_{\max} = 0.125988$, we find $K = 0.3$ and

$$p_1 = p_6^* = -0.19523 - j1.20567 \qquad p_2 = p_5^* = -0.74816 - j1.23803$$
$$p_3 = p_4^* = -1.71103 + j0.75866$$
$$H_1(s) = \frac{0.03 \cdot (s^2 + 1.5529^2)(s^2 + 2.1213^2)(s^2 + 5.7956^2)}{(s^2 + 0.3905s + 1.4918)(s^2 + 1.4963s + 2.0925)(s^2 + 3.4221s + 3.5032)}$$

For $\epsilon = \epsilon_{\min} = 0.03073167$, we find $K = 0.012823$ and

$$p_1 = p_6^* = -0.20091 - j1.09198 \qquad p_2 = p_5^* = -0.71963 - j1.04803$$
$$p_3 = p_4^* = -1.42685 + j0.55679$$
$$H_2(s) = \frac{0.012823 \cdot (s^2 + 1.5529^2)(s^2 + 2.1213^2)(s^2 + 5.7956^2)}{(s^2 + 0.4018s + 1.2328)(s^2 + 1.4393s + 1.6162)(s^2 + 2.8537s + 2.3459)}$$

If $H_{ICH}(s)$ satisfies the normalized specifications, the transfer function that satisfies the specifications with $\omega_C = 2\pi 1000$ rad/s ($f_C = 1000$ Hz) will be simply $H_{ICH}(s/\omega_C)$ and the corresponding gain function will be $|H_{ICH}(j\omega/\omega_C)| = |H_{ICH}(jf/f_C)|$. Figure 3.22 shows the denormalized plain and logarithmic gain plots for the two boundary values of the ripple factor.

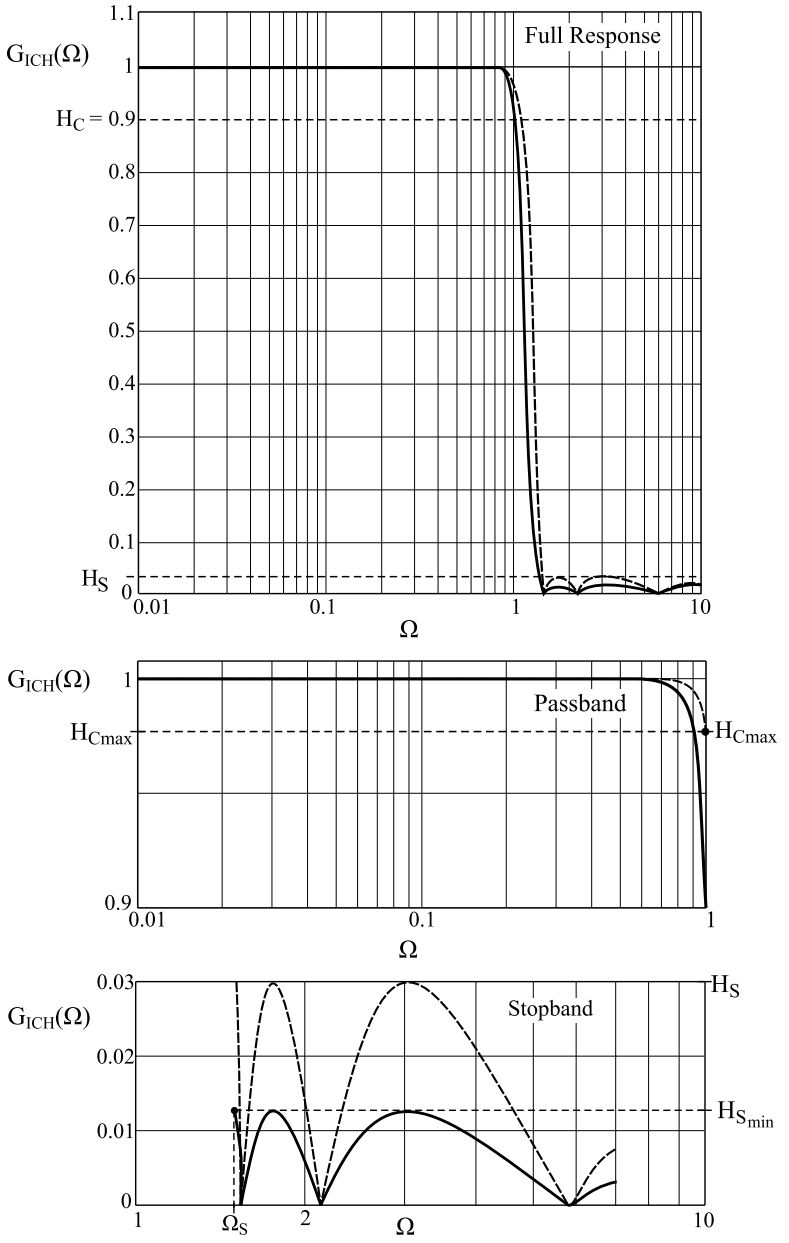

Fig. 3.21 Gain plots of Example 3.4 for $\epsilon_{\min}$ and $\epsilon_{\max}$ (*dashed*)

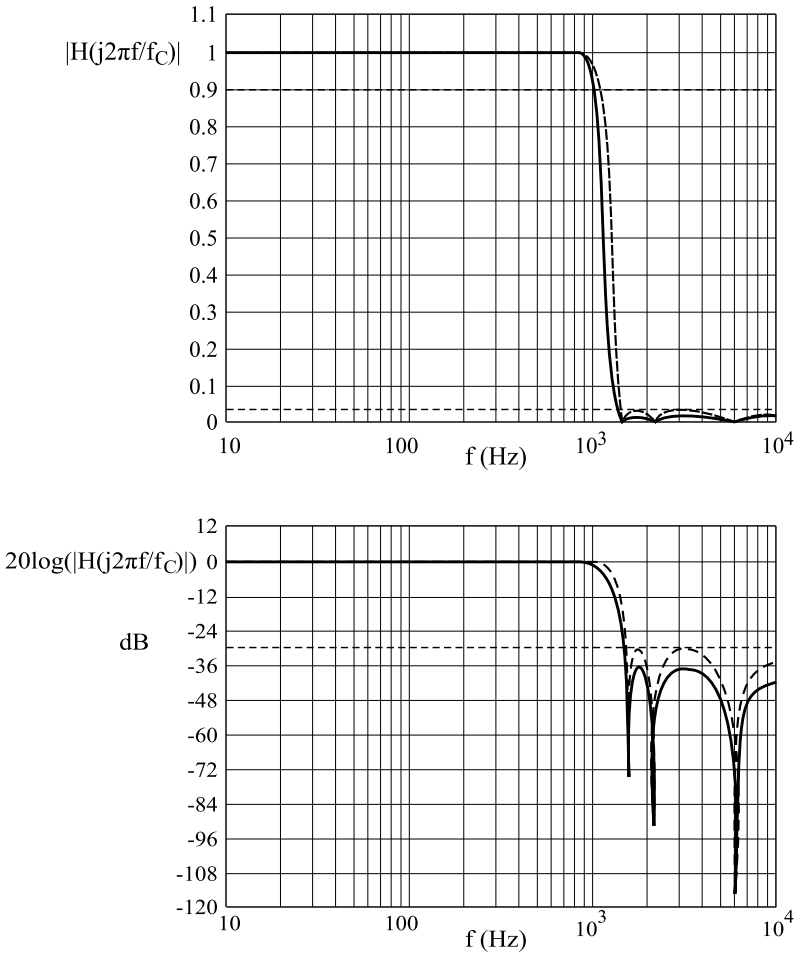

Fig. 3.22 Plain and logarithmic gain plots of Example 3.4 for $\epsilon_{\min}$ and $\epsilon_{\max}$ (*dashed*)

3.4 The Inverse Pascal Approximation

Inverse Pascal approximation is based on the properly modified Pascal polynomials [4] of Sect. 2.4 of the previous chapter and leads to monotonic passband gain, like its inverse Chebyshev counterpart. The stopband response is similar to that of the inverse Chebyshev and elliptic approximations but is non-equiripple as shown in Fig. 3.23.

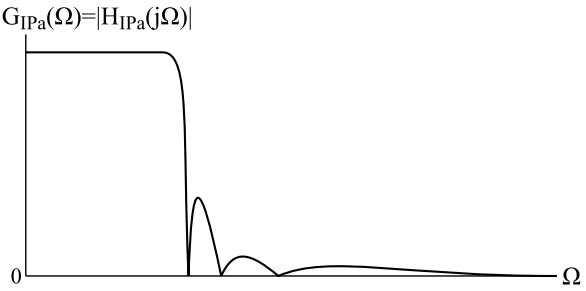

Fig. 3.23 Typical inverse Pascal magnitude response

The filter-appropriate Pascal polynomial denoted as $P_D(\Omega)$ has been introduced in the previous chapter ((2.69) and (2.71)) and its definition is repeated here for convenience:

$$P_D(\Omega) = \frac{(-1)^N}{N!} \prod_{k=1}^{N} \left(\frac{N+1}{2} \Omega_D \Omega + \frac{N-1}{2} - k + 1 \right) \tag{3.60}$$

or equivalently

$$P_D(\Omega) = \frac{(-1)^\eta}{N!} \left(\frac{N+1}{2} \Omega_D \right)^\eta \Omega^\eta \prod_{k=1}^{\frac{N-\eta}{2}} \left[\left(\frac{N+1}{2} \Omega_D \Omega \right)^2 - \left(\frac{N+1}{2} - k \right)^2 \right] \tag{3.61}$$

or

$$P_D(\Omega) = \frac{(-1)^\eta}{N!} \left(\frac{N+1}{2} \Omega_D \right)^N \Omega^\eta \prod_{k=1}^{\frac{N-\eta}{2}} \left[\Omega^2 - \left(\frac{N+1-2k}{(N+1)\Omega_D} \right)^2 \right] \tag{3.62}$$

where η is used again in order to unify the expressions for even and odd N:

$$\eta = \begin{cases} 0 & \text{when } N \text{ is even} \\ 1 & \text{when } N \text{ is odd} \end{cases} \tag{3.63}$$

Ω_D can be taken from Table 2.4, repeated here for convenience. An indicative plot of $P_D(\Omega)$ for $N = 6$ and $N = 7$ is shown in Fig. 3.24.

From (3.61) or (3.62), it is clear that $P_D(\Omega)$ has $(N - \eta)/2$ positive non-zero roots ρ_k given by

$$\rho_k = \frac{(N+1) - 2k}{(N+1)\Omega_D} < 1 \quad \text{for } k = 1 \ldots \frac{N-\eta}{2} \tag{3.64}$$

and $(N - \eta)/2$ negative roots $-\rho_k$. Parameter Ω_D depends only on N and can be taken from Table 3.1. Table 3.2 gives the positive roots of $P_D(\Omega)$ for $N = 2 - 15$.

Table 3.1 Parameters of $P_D(N, \Omega)$

N	$\Omega_{\max}$	$P_{\max}$	Ω_D
2	0.00000000	−0.12500000	0.47140452
3	0.28867513	+0.06415003	0.57735029
4	0.44721360	−0.04166667	0.65289675
5	0.54814429	+0.03026194	0.70639006
6	0.61812758	−0.02347346	0.74582512
7	0.66950940	+0.01901625	0.77599290
8	0.70882772	−0.01588792	0.79978194
9	0.73987600	+0.01358345	0.81900877
10	0.76500826	−0.01182234	0.83486553
11	0.78576311	+0.01043707	0.84816452
12	0.80318872	−0.00932176	0.85947728
13	0.81802376	+0.00840640	0.86921746
14	0.83080378	−0.00764299	0.87769147
15	0.84192645	+0.00699753	0.88513110

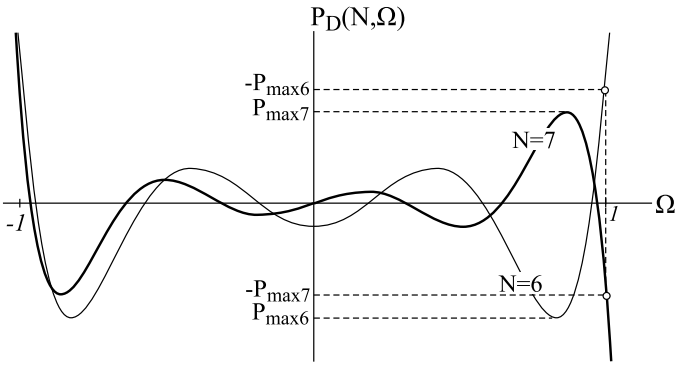

Fig. 3.24 Graph of polynomial $P_D(\Omega)$ for $N = 6$ and $N = 7$

Equation (3.62) can therefore be written as

$$P_D(\Omega) = \frac{(-1)^\eta}{N!}\left(\frac{N+1}{2}\Omega_D\right)^N \Omega^\eta \prod_{k=1}^{\frac{N-\eta}{2}} [\Omega^2 - \rho_k^2] \tag{3.65}$$

where ρ_k are the roots of $P_D(\Omega)$ calculated from (3.64) or taken from Table 3.2.

It should be noted from (3.65) that for odd N, in which case $\eta = 1$, there will also exist a root at $\Omega = 0$, i.e. $P_D(0) = 0$.

Table 3.2 Roots of the filter-appropriate Pascal polynomial $P_D(\Omega)$

N	ρ_1	ρ_2	ρ_3	ρ_4	ρ_5	ρ_6	ρ_7
2	0.70710678						
3	0.86602540						
4	0.91898144	0.30632715					
5	0.94376568	0.47188284					
6	0.95771207	0.57462724	0.19154241				
7	0.96650368	0.64433579	0.32216789				
8	0.97248731	0.69463379	0.41678027	0.13892676			
9	0.97679052	0.73259289	0.48839526	0.24419763			
10	0.98001629	0.76223489	0.54445349	0.32667210	0.10889070		
11	0.98251382	0.78601105	0.58950829	0.39300553	0.19650276		
12	0.98449821	0.80549854	0.62649886	0.44749919	0.26849951	0.08949984	
13	0.98610865	0.82175721	0.65740577	0.49305432	0.32870288	0.16435144	
14	0.98743887	0.83552520	0.68361153	0.53169786	0.37978418	0.22787051	0.07595684
15	0.98855417	0.84733215	0.70611012	0.56488810	0.42366607	0.28244405	0.14122202

Even degree polynomials assume a very low value $P_D(0) \leq 0$ at $\Omega = 0$:

$$\begin{aligned} \text{For odd } N: \quad & P_D(0) = 0 \\ \text{For even } N: \quad & P_D(0) = \frac{(-1)^{\frac{N}{2}}}{N!} \prod_{k=1}^{\frac{N}{2}} \left(\frac{N+1}{2} - k \right)^2 \\ \text{For odd and even } N: \quad & \Omega \to \infty \quad \Rightarrow \quad P_D(\Omega) \to \infty \end{aligned} \tag{3.66}$$

The coefficients a_k of the odd or even polynomial $P_D(\Omega)$ when expressed in their expanded form

$$\begin{aligned} P_D(\Omega) &= a_N \Omega^N + a_{N-2} \Omega^{N-2} + \cdots + a_\eta \Omega^\eta \\ \text{where } \eta &= \begin{cases} 1 & \text{for } N \text{ odd} \\ 0 & \text{for } N \text{ even} \end{cases} \end{aligned} \tag{3.67}$$

are tabulated for $N = 2$–7 in Table 2.7. For the coefficients of the highest and lowest order terms of $P_D(\Omega)$, analytic formulae have been derived in the previous Chapter ((2.76)–(2.78)) from the definition equations and are repeated here:

$$a_N = \frac{(-1)^N}{N!} \cdot \left(\frac{N+1}{2} \Omega_D \right)^N \tag{3.68}$$

$$a_\eta = \frac{(-1)^{\frac{N+\eta}{2}}}{N!}\left(\frac{N+1}{2}\Omega_D\right)^\eta \cdot \prod_{k=1}^{(N-\eta)/2}\left(\frac{N+1}{2}-k\right)^2 \tag{3.69}$$

or

$$a_\eta = \frac{(-1)^{\frac{N+\eta}{2}}}{2^N N!}(N+1)^\eta \Omega_D^\eta \cdot \prod_{k=1}^{(N-\eta)/2}(N+1-2k)^2 \tag{3.70}$$

The absolute extremum of $P_D(\Omega)$ for $0 < \Omega < 1$ assumes the value $P_{\max}$ and occurs at $\Omega_m = \Omega_{\max}/\Omega_D < 1$. Polynomial $P_D(\Omega)$ is so constructed as to assume the value $-P_{\max}$ at $\Omega = 1$ and be monotonic for $\Omega > \Omega_m = \Omega_{\max}/\Omega_D$. The main property of $P_D(\Omega)$, as expressed in Sect. 2.4 of the previous chapter, is:

$$\begin{aligned} &P_D(1) = -P_D(\Omega_m) = P_{\max} \quad \text{or} \\ &|P_D(1)| = |P_D(\Omega_m)| = |P_{\max}| \quad \text{where } \Omega_m = \frac{\Omega_{\max}}{\Omega_D} < 1 \end{aligned} \tag{3.71}$$

Table 3.1 gives the characteristic values $P_{\max}$, $\Omega_{\max}$ and Ω_D.

3.4.1 The Pascal Rational Function $F_P(\Omega)$

Substituting Ω with Ω_S/Ω in (3.62), we obtain:

$$P_D\left(\frac{\Omega_S}{\Omega}\right) = \frac{\frac{(-1)^\eta}{N!}(\frac{N+1}{2}\Omega_D)^N \Omega_S^\eta \prod_{k=1}^{\frac{N-\eta}{2}}(\Omega_S^2 - \rho_k^2\Omega^2)}{\Omega^N} \tag{3.72}$$

Defining the Pascal rational function as

$$F_P(\Omega) = \frac{1}{P_D(\frac{\Omega_S}{\Omega})} \tag{3.73}$$

we get

$$F_P(\Omega) = \frac{N_R(\Omega)}{D_R(\Omega)} = \frac{\Omega^N}{\frac{(-1)^\eta}{N!}(\frac{N+1}{2}\Omega_D)^N \Omega_S^\eta \prod_{k=1}^{\frac{N-\eta}{2}}(\Omega_S^2 - \rho_k^2\Omega^2)} \tag{3.74}$$

where ρ_k are the positive roots of the filter-appropriate Pascal polynomial $P_D(\Omega)$ given in (3.64).

The numerator and denominator polynomials of $F_P(\Omega)$ are given below:

$$N_R(\Omega) = \Omega^N \tag{3.75}$$

$$D_R(\Omega) = \frac{(-1)^\eta}{N!}\left(\frac{N+1}{2}\Omega_D\right)^N \Omega_S^\eta \prod_{k=1}^{\frac{N-\eta}{2}}(\Omega_S^2 - \rho_k^2\Omega^2) \tag{3.76}$$

or

$$D_R(\Omega) = \frac{(-1)^{\frac{N+\eta}{2}}}{N!}\left(\frac{N+1}{2}\Omega_D\right)^N \Omega_S^\eta \prod_{k=1}^{\frac{N-\eta}{2}}(\rho_k^2)\prod_{k=1}^{\frac{N-\eta}{2}}\left(\Omega^2 - \frac{\Omega_S^2}{\rho_k^2}\right) \tag{3.77}$$

The denominator polynomial $D_R(\Omega)$ is always even and, when expanded, will be of the form:

$$D_R(\Omega) = B_{N-\eta}\Omega^{N-\eta} + B_{N-\eta-2}\Omega^{N-\eta-2} + \cdots + B_2\Omega^2 + B_0 \tag{3.78}$$

Using (3.77) and (3.70), the coefficient $B_{N-\eta}$ of the highest order term $\Omega^{N-\eta}$ of $D_R(\Omega)$ can be expressed as:

$$B_{N-\eta} = \frac{(-1)^{\frac{N+\eta}{2}}}{N!}\left(\frac{N+1}{2}\Omega_D\right)^\eta \Omega_S^\eta \prod_{k=1}^{\frac{N-\eta}{2}}\left(\frac{N+1}{2} - k\right)^2 \tag{3.79}$$

or

$$B_{N-\eta} = a_\eta \Omega_S^\eta \tag{3.80}$$

For the constant term B_0 we can find from (3.77) and (3.68):

$$B_0 = \frac{(-1)^\eta}{N!}\left(\frac{N+1}{2}\Omega_D\Omega_S\right)^N \quad \text{or } B_0 = a_N\Omega_S^N \tag{3.81}$$

Quantities a_η (a_0 or a_1) and a_N are the corresponding coefficients of $P_D(\Omega)$ and can be calculated from (3.70) and (3.68) respectively, or taken from Table 2.7 of the previous chapter.

The even polynomial $D_R(\Omega)$ has $(N-\eta)/2$ positive roots

$$\Omega_{zk} = \frac{\Omega_S}{\rho_k} \quad \text{for } k = 1, \ldots, \frac{N-\eta}{2} \tag{3.82}$$

and $(N-\eta)/2$ negative roots $-\Omega_{zk}$. ρ_k are the positive roots of $P_D(\Omega)$ given in (3.64).

Before we continue, it is worth studying the Pascal rational function $F_P(\Omega)$.

i. For $\Omega = 0 \Rightarrow F_P(0) = 0$ since $P_D(\infty) = \infty$
ii. For $\Omega = 1 \Rightarrow F_P(1) = \frac{1}{P_D(\Omega_S)}$. Since $\Omega_S > 1$, $|P_D(\Omega_S)|$ has a value $\gg |P_{\max}|$ and therefore $|F_P(1)| \leq |\frac{1}{P_{\max}}|$.
iii. For $0 \leq \Omega \leq 1$, the Pascal rational function $F_P(\Omega)$ starts from $F_P(0) = 0$ and is monotonically increasing for even N and decreasing for odd N. In both cases the end value $|F_P(1)| = |\frac{1}{P_D(\Omega_S)}|$ is very small, since $|P_D(\Omega_S)| \gg |P_{\max}|$.
iv. For $\Omega \to \infty \Rightarrow \frac{\Omega_S}{\Omega} = 0 \Rightarrow F_P(\infty) = \frac{1}{P_D(0)}$. Since $P_D(0) = 0$ for odd N and assumes a very low value for even N, $|F_P(\infty)|$ becomes infinite when N is odd and assumes a very high value when N is even.
v. For $\Omega = \Omega_S \Rightarrow F_P(\Omega_S) = \frac{1}{P_D(1)} = \frac{1}{P_{\max}}$

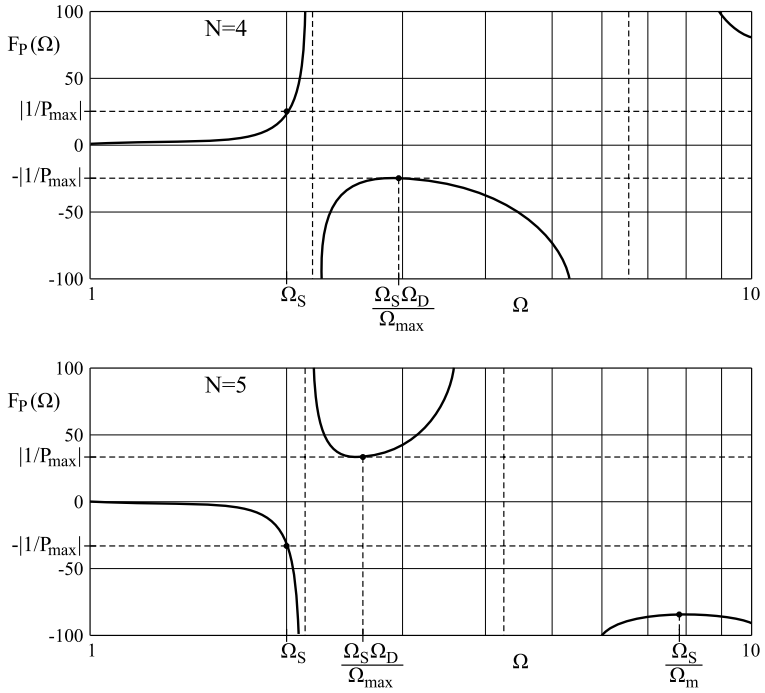

Fig. 3.25 Plot of the rational function $F_P(\Omega)$ for $N = 4$ and $N = 5$

vi. For $\Omega = \frac{\Omega_S \Omega_D}{\Omega_{\max}} \Rightarrow F_P(\frac{\Omega_S \Omega_D}{\Omega_{\max}}) = \frac{1}{P_D(1)} = \frac{1}{P_{\max}}$. These are the frequency and the value of the first local extremum of $F_P(\Omega)$ for $\Omega > \Omega_S$ and corresponds to the last and highest extremum of $P_D(\Omega)$ at $\Omega = \frac{\Omega_{\max}}{\Omega_D} < 1$.

vii. The extrema of $P_D(\Omega)$ for $\Omega_m < \frac{\Omega_{\max}}{\Omega_D} < 1$ are mapped to the extrema of $F_P(\Omega)$ at frequencies $\Omega = \frac{\Omega_S}{\Omega_m} > \frac{\Omega_S \Omega_D}{\Omega_{\max}} > \Omega_S$ with absolute values higher than the value of the first extremum, i.e. $|F_P(\frac{\Omega_S}{\Omega_m})| > |\frac{1}{P_{\max}}|$

viii. If ρ_k are the roots of $P_D(\Omega)$, then from (3.73) and (3.82) $\Rightarrow F_P(\Omega_{zk}) = F_P(\frac{\Omega_S}{\rho_k}) = \infty$

Figure 3.25 shows two indicative plots of $F_P(\Omega)$ for $\Omega \geq 1$ and for $N = 4$ and $N = 5$, and Fig. 3.26 the corresponding plots of $|F_P(\Omega)|$.

The rational function $F_P(\Omega)$ of (3.73) meets the three conditions set in Sect. 3.2:

1. From (3.75), the numerator polynomial is $N_R(\Omega) = \Omega^N$ of degree N and is symmetric (even or odd).
2. The denominator polynomial $D_R(\Omega)$ is given in (3.76) or (3.77) and is clearly an even polynomial.
3. The even denominator polynomial $D_R(\Omega)$ has $(N - \eta)/2$ real root pairs $\pm\frac{\Omega_S}{\rho_k} = \pm\Omega_{zk}$ with $\Omega_{zk} > \Omega_S$.

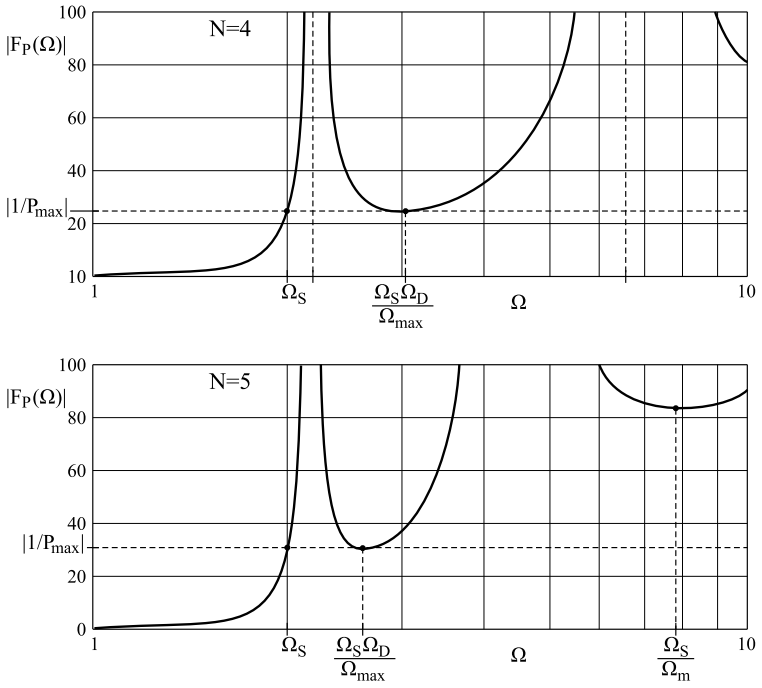

Fig. 3.26 Plot of $|F_P(\Omega)|$ for $N = 4$ and $N = 5$

Therefore, the Pascal rational function $F_P(\Omega) = 1/P_D(\Omega_S/\Omega)$ can be used as an approximating function in (3.5) to derive the inverse Pascal approximation.

3.4.2 Definition of the Inverse Pascal Approximation

The inverse Pascal approximation is defined using the Pascal rational function $F_P(\Omega)$ of (3.73) in (3.5) with $\gamma = \lambda^{-1}$:

$$G_{IPa}(\Omega) = \frac{H_o}{\sqrt{1+\lambda^{-2}F_R^2(\Omega)}} = \frac{H_o}{\sqrt{1+\frac{1}{\lambda^2 P_D^2(\frac{\Omega_S}{\Omega})}}} = \frac{\lambda H_o |P_D(\frac{\Omega_S}{\Omega})|}{\sqrt{1+\lambda^2 P_D^2(\frac{\Omega_S}{\Omega})}} \tag{3.83}$$

Figure 3.27 shows two indicative gain plots of the inverse Pascal approximation for $N = 4$ and $N = 5$ corresponding to $F_P(\Omega)$ of Figs. 3.25 and 3.26.

According to (3.19), the related transfer function will be

$$H(s) = \frac{C\prod_{k=1}^{\frac{N-\eta}{2}}(s^2+\Omega_{zk}^2)}{\prod_{k=1}^{N}(s-s_k)}$$

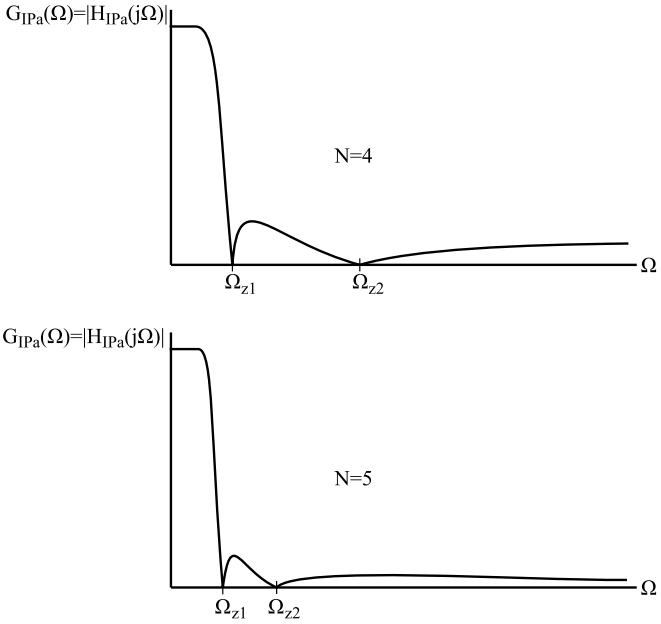

Fig. 3.27 Typical inverse Pascal gain plots

$$C = \frac{H_o \lambda a_\eta \Omega_S^\eta}{\sqrt{(1-\eta)\lambda^2 a_\eta^2 + 1}},\ \Omega_{zk} = \frac{\Omega_S}{\rho_k},\ \rho_k = \frac{N+1-2k}{(N+1)\Omega_D} \tag{3.84}$$

Poles s_k are calculated from (3.17) as the LH half s-plane roots of

$$s^{2N} + (-1)^\eta \lambda^2 a_\eta^2 \Omega_S^{2\eta} \prod_{k=1}^{\frac{N-\eta}{2}} (s^2 + \Omega_{zk}^2)^2 = 0 \tag{3.85}$$

where, from (3.84), $\Omega_{zk} = (\frac{(N+1)\Omega_D \Omega_S}{N+1-2k})$ and a_η can be calculated from (3.69) or (3.70). From (3.84), it becomes apparent that for the calculation of the transfer function of the inverse Pascal approximation, the following are required:

1. The order N and the ripple parameter λ: These both depend on the specifications and the necessary means for their calculation will be provided below.
2. Ω_D: Depends only on N and is taken from Table 3.1, when order N has been determined.
3. Coefficient a_η (a_0 or a_1): Depends only on N and is calculated from (3.69) or (3.70) or taken from Table 2.7 of the previous chapter.
4. The N poles s_k, i.e. the left half s-plane roots of the even polynomial $D_{TF}(s)D_{TF}(-s)$ of degree $2N$ of (3.85). When order N and the ripple parameter λ have been determined, poles s_k can be calculated numerically.

3.4.3 Gain Analysis

The gain function of the inverse Pascal approximation as defined in (3.83) is:

$$G_{IPa}(\Omega) = \frac{H_o}{\sqrt{1+\lambda^{-2}F_P^2(\frac{\Omega_S}{\Omega})}} = \frac{H_o}{\sqrt{1+\frac{1}{\lambda^2 P_D^2(\frac{\Omega_S}{\Omega})}}} \tag{3.86}$$

Following the analysis of the behavior of $F_P(\Omega)$ of Sect. 3.4.1, in the passband, since $|F_P(\Omega)|$ is monotonically increasing, the gain of (3.86) will be monotonically decreasing from

$$G_{IPa}(0) = H_o$$

down to

$$G_{IPa}(1) = \frac{H_o}{\sqrt{1+\frac{1}{\lambda^2 P_D^2(\Omega_S)}}} \tag{3.87}$$

$|F_P(\Omega)|$ is also monotonically increasing for $1 \le \Omega \le \Omega_S$ and at Ω_S it assumes the value $|F_P(\Omega_S)| = \frac{1}{|P_{\max}|}$. Therefore, $G_{IPa}(\Omega)$ will be monotonically decreasing in the transition band and

$$G_{IPa}(\Omega_S) = \frac{\lambda H_o |P_{\max}|}{\sqrt{1+\lambda^2 P_{\max}^2}} \tag{3.88}$$

The same gain value is assumed at the frequency $\frac{\Omega_S \Omega_D}{\Omega_{\max}}$ of the first and highest stopband maximum. Consequent stopband gain maxima assume lower values.

Finally, at the stopband frequencies $\frac{\Omega_S}{\rho_k}$ which correspond to the $(N-\eta)/2$ positive roots ρ_k of $P_D(\Omega)$, the gain will be zero. Roots ρ_k are given by (3.64):

$$\rho_k = \frac{(N+1)-2k}{(N+1)\Omega_D} < 1 \quad \text{for } k = 1, \ldots, \frac{N-\eta}{2} \tag{3.89}$$

3.4.4 Filter Design Using the Inverse Pascal Approximation

The normalized lowpass filter specifications of Fig. 3.28 are given as

$$\Omega_S \quad \text{and} \quad \{H_C, H_S\} \quad \text{or} \quad \{\alpha_{\max}, \alpha_{\min}\} \tag{3.90}$$

In this section, the normalized lowpass filter will be designed from these specifications. The maximum passband gain H_o is usually taken as equal to 1, in which case $\alpha_o = 0$.

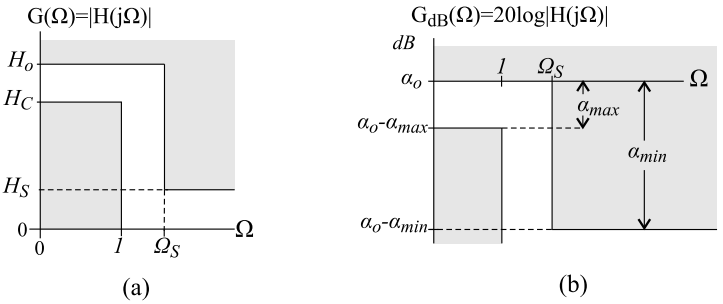

Fig. 3.28 Normalized lowpass specifications: (**a**) Plain gain. (**b**) Logarithmic gain

3.4.4.1 Calculation of the Ripple Parameter λ and Design Optimization

Given the specifications of (3.90), the plot of $G_{IPa}(\Omega)$ of (3.86) must not enter the shaded area of Fig. 3.28. In the passband, where $G_{IPa}(\Omega)$ is monotonic and $G_{IPa}(0) = H_o$, this can be ensured by selecting λ to satisfy

$$G_{IPa}(1) = \frac{H_o}{\sqrt{1 + \lambda^{-2} P_D^{-2}(\Omega_S)}} \geq H_C \tag{3.91}$$

Solving for λ we find:

$$\lambda \geq \frac{1}{|P_D(\Omega_S)|\sqrt{\frac{H_o^2}{H_C^2} - 1}} = \frac{1}{|P_D(\Omega_S)|\sqrt{10^{\frac{\alpha_{\max}}{10}} - 1}} = \lambda_{\min} \tag{3.92}$$

Selecting the minimum value $\lambda_{\min}$ of ripple parameter λ:

$$\lambda = \lambda_{\min} \quad \Rightarrow \quad G_{IPa}(1) = H_C \tag{3.93}$$

It can also be shown that for $\lambda = \lambda_{\min}$ we have $G_{IPa}(\Omega_S) < H_S$, and the so designed filter is referred to as *stopband edge frequency gain optimized* and has the minimum stopband edge frequency gain.

In the stopband we must ensure that

$$G_{IPa}(\Omega_S) = \frac{H_o}{\sqrt{1 + \lambda^{-2} P_D^{-2}(1)}} \leq H_S \tag{3.94}$$

from which we get:

$$\lambda \leq \frac{1}{|P_D(1)|\sqrt{\frac{H_o^2}{H_S^2} - 1}} = \frac{1}{|P_D(1)|\sqrt{10^{\frac{\alpha_{\min}}{10}} - 1}} = \lambda_{\max} \tag{3.95}$$

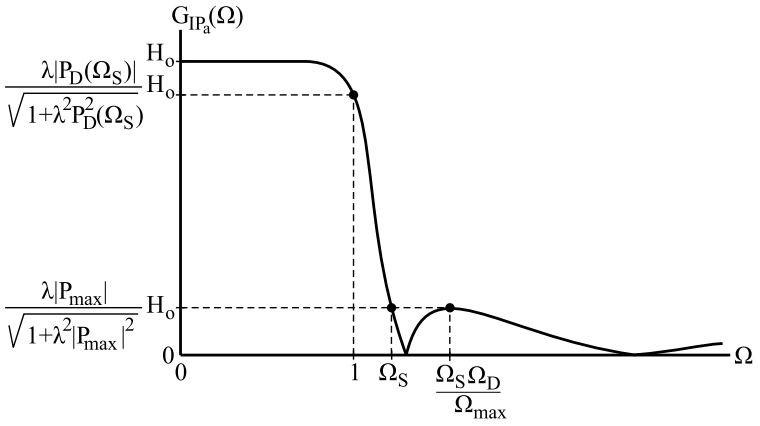

Fig. 3.29 Typical inverse Pascal gain plots

For $\lambda = \lambda_{max}$ of (3.95), the value of the first and highest extremum of the stopband gain which occurs at $\frac{\Omega_S\Omega_D}{\Omega_{max}}$ will be:

$$\lambda = \lambda_{max} \quad \Rightarrow \quad G_{IPa}\left(\frac{\Omega_S\Omega_D}{\Omega_{max}}\right) = G_{IPa}(\Omega_S) = H_S \tag{3.96}$$

It can also be shown that for $\lambda = \lambda_{max}$, the gain at $\Omega = 1$ is $G_{IPa}(1) > H_C$ and the so designed filter is referred to as *passband optimized* and has the minimum passband gain tolerance.

Finally, the ripple parameter λ can be chosen from the following range:

$$\lambda_{min} \leq \lambda \leq \lambda_{max} \tag{3.97}$$

Parameters Ω_D, Ω_{max} and P_{max} depend only on order N and can be taken from Table 3.1. A typical gain plot of the inverse Pascal gain is shown in Fig. 3.29. Remember that $G_{IPa}(\Omega_S)$ assumes the value of the maximum stopband gain and the first transmission zero occurs at Ω_{z1} where $\Omega_S < \Omega_{z1} < \Omega_S\Omega_D/\Omega_{max}$.

3.4.5 The Order Inequality and the Order Nomograph

So far, the order N is not yet known but it can be calculated from (3.91) with $\lambda = \lambda_{min}$ or from (3.94) with $\lambda = \lambda_{max}$. In both cases, we will end up with the following order inequality:

$$\left|\frac{P_D(1)}{P_D(\Omega_S)}\right| \leq g \quad \text{where } g = \sqrt{\frac{H_o^2/H_C^2 - 1}{H_o^2/H_S^2 - 1}} = \sqrt{\frac{10^{\frac{\alpha_{max}}{10}} - 1}{10^{\frac{\alpha_{min}}{10}} - 1}} \ll 1 \tag{3.98}$$

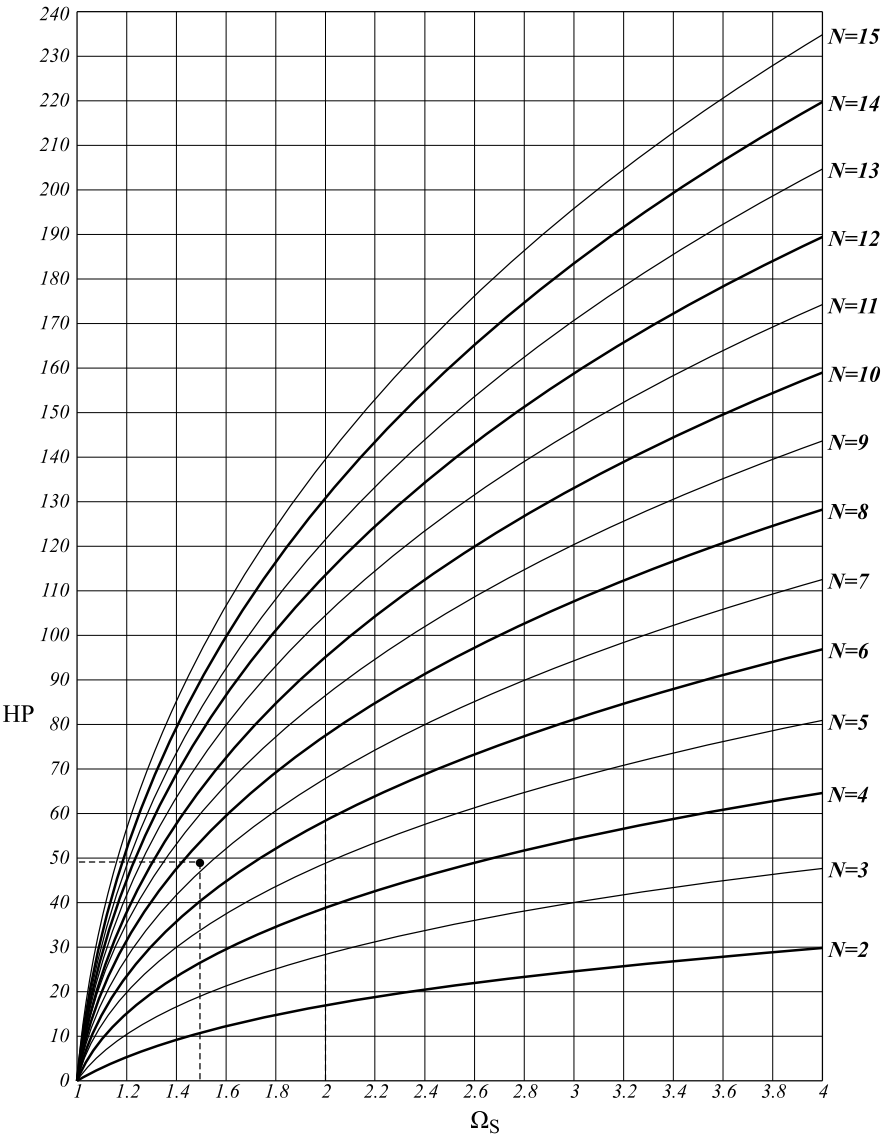

Fig. 3.30 Nomograph for the calculation of the order of the Pascal and inverse Pascal approximation

Polynomial $P_D(\Omega)$ is of degree N, and the minimum N which satisfies (3.98) must be determined. Order inequality (3.98) has the same form as the order inequality in the all-pole Pascal case (see Sect. 2.4.2 in the previous chapter) and must be solved numerically for N. However, since the order inequality (3.98) is identical to the order inequality of the all-pole Pascal approximation, this can be handled using the same nomograph given in Fig. 2.43, repeated for convenience in Fig. 3.30.

The nomograph is used in the same way as in the all-pole Pascal approximation: A vertical line is drawn from the point of the horizontal axis which corresponds to the specified Ω_S. A horizontal line is then drawn from the point of the vertical axis that corresponds to HP:

$$HP = 20 \cdot \log\left(\frac{1}{g}\right) \tag{3.99}$$

The two lines intersect at a point. The order of the approximation is equal to the number of the curve that is above this point. As an example, let us find the order if the specifications of the filter are $\Omega_S = 1.5$, $\alpha_{\max} = 0.5$ dB and $\alpha_{\min} = 40$ dB. Equation (3.99) gives $HP = 49.14$ and from the nomograph we get $N = 8$, since the point is located above the curve 7 and below curve 8.

When order N has been determined from the nomograph, the ripple factor λ can be selected from (3.97), repeated here:

$$\frac{1}{|P_D(\Omega_S)|\sqrt{10^{\frac{\alpha_{\max}}{10}} - 1}} = \lambda_{\min} \leq \lambda \leq \lambda_{\max} = \frac{1}{|P_D(1)|\sqrt{10^{\frac{\alpha_{\min}}{10}} - 1}} \tag{3.100}$$

For the calculation of the boundary values of λ, since $|P_D(1)| = |P_{\max}|$, it can be taken from Table 3.1. $P_D(\Omega_S)$ can be easily calculated from the definition of polynomial $P_D(\Omega)$ given in (3.60)–(3.62).

The order inequality (3.98) is valid for the minimum integer order N calculated from the nomograph or using a mathematical package. The point of intersection of the two lines in the calculation of the order from the nomograph lies between two curves corresponding to two integer orders, N and $N-1$. Selecting the order which corresponds to the upper curve, we in fact turn order inequality into order equation:

$$\left|\frac{P_D(1)}{P_D(\Omega_S)}\right| = \sqrt{\frac{10^{\frac{\alpha_{\max}}{10}} - 1}{10^{\frac{\alpha_{\min}}{10}} - 1}} \ll 1 \tag{3.101}$$

by admitting that the filter with integer order N can satisfy stricter specifications which would have made the intersection point lie on curve N from the beginning. This means that if two of the three $\{\Omega_S, \alpha_{\max}, \alpha_{\min}\}$ are kept as specified, the third could be stricter.

The order equation (3.101) involves four variables: $\{N, \Omega_S, \alpha_{\max}, \alpha_{\min}\}$.

A. When solved for N with given $\{\Omega_S, \alpha_{\max}\}$, order N assumes a non-integer value which becomes integer only by increasing $\alpha_{\min}$. The integer order filter will have exactly $\alpha_{\max}$ passband gain tolerance and at Ω_S, the gain, denoted by $\alpha_{S\max}$, will be lower than the specified $\alpha_{\min}$. This corresponds to the stopband edge

frequency gain optimized filter using $\lambda = \lambda_{\min}$, in which case

$$G_{IPa}(\Omega_S) = H_{S\min} = \frac{H_o}{\sqrt{1 + \frac{P_D^2(\Omega_S)(10^{0.1\cdot\alpha_{\max}}-1)}{P_D^2(1)}}} < H_S$$
$$\alpha_{S\max} = 20\log\left(\frac{H_o}{H_{S\min}}\right) > \alpha_{\min} \tag{3.102}$$

B. When solved for N with given $\{\Omega_S, \alpha_{\min}\}$, order N assumes a non-integer value which becomes integer only by decreasing $\alpha_{\max}$. The integer order filter will have exactly $\alpha_{\min}$ stopband gain tolerance and at $\Omega = 1$ the gain, denoted by $\alpha_{C\min}$, will correspond to lower passband tolerance $\alpha_{\max}$. This corresponds to the passband optimized filter using $\lambda = \lambda_{\max}$, in which case

$$G_{IPa}(1) = H_{C\max} = \frac{H_o}{\sqrt{1 + \frac{P_D^2(1)(10^{0.1\cdot\alpha_{\min}}-1)}{P_D^2(\Omega_S)}}} > H_C$$
$$\alpha_{C\min} = 20\log\left(\frac{H_o}{H_{C\max}}\right) < \alpha_{\max} \tag{3.103}$$

C. When solved for Ω_S with given $\{N, \alpha_{\max}, \alpha_{\min}\}$, Ω_S assumes a value $\Omega_{S\min}$ which is lower than the specified stopband edge frequency. The filter of order N will have exactly the specified $\alpha_{\min}$ and $\alpha_{\min}$ but the stopband edge frequency will be $\Omega_{S\min}$, lower than Ω_S of the specifications. This is the *transition band optimized filter* [3], which satisfies the passband and stopband gain specifications in an exact manner with the minimum stopband edge frequency. Frequency $\Omega_{S\min}$ can only be calculated numerically from

$$P_D^2(\Omega_{S\min}) = \frac{P_D^2(1)}{g^2} = \frac{P_{\max}^2}{g^2} \tag{3.104}$$

Notice that $\Omega_{S\min}$ does not depend on Ω_S and can be determined directly from $\{N, \alpha_{\max}, \alpha_{\min}\}$.

The positive Parameter HP of (3.99)

$$HP = 20\cdot\log\left(\frac{1}{g}\right) = 20\cdot\log\left(\sqrt{\frac{10^{\frac{\alpha_{\min}}{10}}-1}{10^{\frac{\alpha_{\max}}{10}}-1}}\right) \tag{3.105}$$

is an increasing function of $\alpha_{\min}$ and a decreasing function of $\alpha_{\max}$.

When calculating the order from the nomograph using the specified values for $\{\Omega_S, \alpha_{\max}, \alpha_{\min}\}$, point x_0 of intersection of the two lines, lies between two curves corresponding to N and $N-1$. This is shown in Fig. 3.31 and implies that if Ω_S and $\alpha_{\max}$ are kept to the specified values, $\alpha_{\min}$ can be increased to its highest value $\alpha_{S\max}$, which corresponds to point $x_2 = \{\Omega_S, HP_N\}$ on curve N, as shown

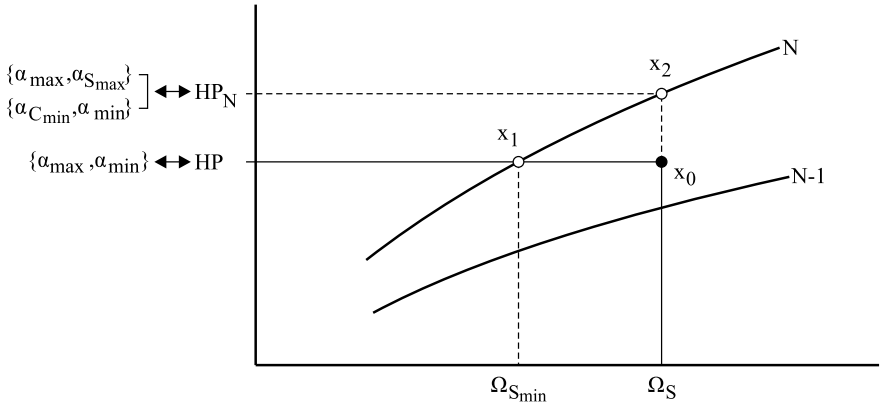

Fig. 3.31 Detail of the Pascal order nomograph

in Fig. 3.31. This is analogous to the traditional rounding up of the calculated decimal order to the next integer value and can also be achieved by keeping $\alpha_{\min}$ to the specified value and decreasing $\alpha_{\max}$ to its lowest value $\alpha_{C\min}$, which corresponds to point $x_2 = \{\Omega_S, HP_N\}$ on curve N of Fig. 3.31.

The first case, where Ω_S and $\alpha_{\max}$ are kept to the specified values and $\alpha_{\min}$ is increased to $\alpha_{S\max}$, corresponds to designing the stopband edge frequency gain optimized filter with $\lambda = \lambda_{\min}$. In this case,

$$G_{IPa}(\Omega_S) = H_{S\min} = \frac{H_o}{\sqrt{1 + \frac{P_D^2(\Omega_S)(10^{0.1\cdot\alpha_{\max}}-1)}{P_D^2(1)}}} < H_S$$
$$\alpha_{S\max} = 20\log\left(\frac{H_o}{H_{S\min}}\right) > \alpha_{\min} \tag{3.106}$$

This can be interpreted in two ways:

a. The gain of the filter of order N at $\Omega = 1$ will be exactly $\alpha_{\max}$ below α_o but at $\Omega = \Omega_S$ will be $\alpha_{S\max} > \alpha_{\min}$ below α_o.
b. The maximum stopband tolerance that can be used with $\{N, \Omega_S, \alpha_{\max}\}$ is $\alpha_{S\max}$.

The second case, where Ω_S and $\alpha_{\min}$ are kept to the specified values and $\alpha_{\max}$ is decreased to $\alpha_{C\min}$, corresponds to designing the passband optimized filter with $\lambda = \lambda_{\max}$. In this case,

$$G_{IPa}(1) = H_{C\max} = \frac{H_o}{\sqrt{1 + \frac{P_D^2(1)(10^{0.1\cdot\alpha_{\min}}-1)}{P_D^2(\Omega_S)}}} > H_C$$
$$\alpha_{C\min} = 20\log\left(\frac{H_o}{H_{C\max}}\right) < \alpha_{\max} \tag{3.107}$$

Again, this can be interpreted in two ways:

a. The gain of the filter of order N at Ω_S will be exactly $\alpha_{\min}$ below α_o but at $\Omega = 1$ will be $\alpha_{C\,\min} < \alpha_{\max}$ below α_o.
b. The minimum passband tolerance that can be used with $\{N, \Omega_S, \alpha_{\min}\}$ is $\alpha_{C\,\min}$.

Point x_0 of Fig. 3.31 can also be moved to point x_1 of curve N by dragging it to the left, i.e. keeping $\alpha_{\max}$ and $\alpha_{\min}$ to the specified values and decreasing Ω_S to its minimum value $\Omega_{S\,\min}$. This is the *transition band optimized filter*, which satisfies the passband and stopband gain specifications in an exact manner with the minimum possible stopband edge frequency. Frequency $\Omega_{S\,\min}$ can be taken from the nomograph and if a more exact value is required, it can be calculated from

$$P_D^2(\Omega_{S\,\min}) = \frac{P_D^2(1)}{g^2} = \frac{P_{\max}^2}{g^2} \tag{3.108}$$

Notice that $\Omega_{S\,\min}$ does not depend on Ω_S and can be determined directly from $\{N, \alpha_{\max}, \alpha_{\min}\}$.

3.4.6 The Transfer Function of the Inverse Pascal Filters

When N and λ have been determined, the transfer function can be calculated from (3.84), repeated here for convenience:

$$H(s) = \frac{C\prod_{k=1}^{\frac{N-\eta}{2}}(s^2 + (\Omega_{zk}^2)^2)}{\prod_{k=1}^{N}(s - s_k)} \quad \text{with } \eta = \begin{cases} 0 & \text{when } N \text{ is even} \\ 1 & \text{when } N \text{ is odd} \end{cases}$$

$$C = \frac{H_o \lambda a_\eta \Omega_S^\eta}{\sqrt{(1-\eta)\lambda^2 a_\eta^2 + 1}} \qquad \Omega_{zk} = \frac{\Omega_S}{\rho_k} \qquad \rho_k = \frac{N+1-2k}{(N+1)\Omega_D} \tag{3.109}$$

a_η from (3.69)–(3.70)

Poles s_k can be calculated solving (3.85) of degree $2N$ for s:

$$s^{2N} + (-1)^\eta \lambda^2 a_\eta^2 \Omega_S^{2\eta} \prod_{k=1}^{\frac{N-\eta}{2}} (s^2 + \Omega_{zk}^2)^2 = 0$$

$$\text{where } \Omega_{zk} = \left(\frac{(N+1)\Omega_D \Omega_S}{N+1-2k}\right) \text{ and } \Omega_D \text{ from Table 3.1} \tag{3.110}$$

If the $2N$ roots of this equation are calculated, the N left half s-plane roots can be allocated as poles of the transfer function $H(s)$.

Therefore, the final problem in inverse Pascal approximation is how to find the roots of the even polynomial of (3.110). As happens in all approximations, this is the most serious and laborious task, and inverse Pascal approximation is no exception.

From (3.109) and (3.110) it is clear that for a specific order N, C and the poles depend on Ω_S (since $\Omega_{zk} = \Omega_S/\rho_k$) and λ. If we use $\lambda = \lambda_{\min}$, then C and the poles will depend on Ω_S and $\alpha_{\max}$ (see (3.97)). If $\lambda = \lambda_{\max}$ is used, then from (3.97) it is clear that C and the poles will depend on Ω_S and $\alpha_{\min}$. If $\Omega_{S\min}$ is calculated from $\{N, \alpha_{\max}, \alpha_{\min}\}$, all transfer function parameters of the filter $\{N, \Omega_{S\min}, \alpha_{\max}, \alpha_{\min}\}$ will depend only on $\alpha_{\max}$ and $\alpha_{\min}$:

A. Design with $\lambda_{\min}$: Poles depend on Ω_S and $\alpha_{\max}$
B. Design with $\lambda_{\max}$: Poles depend on Ω_S and $\alpha_{\min}$
C. Design with $\Omega_{S\min}$: Poles depend on $\alpha_{\max}$ and $\alpha_{\min}$

This means that three sets of tables can be constructed:

A. Design with $\lambda_{\min}$: Poles and C will be given for each order for prescribed values of Ω_S and $\alpha_{\max}$. For each combination $\{N, \Omega_S, \alpha_{\max}\}$, the maximum value of $\alpha_{\min} - \alpha_{S\max}$ that can be achieved can also be given, as calculated from (3.106).
B. Design with $\lambda_{\max}$: Poles and C will be given for each order for prescribed values of Ω_S and $\alpha_{\min}$. For each combination $\{N, \Omega_S, \alpha_{\min}\}$, the minimum value of $\alpha_{\max} = \alpha_{C\min}$ that can be achieved can also be given, as calculated from (3.107).
C. Design with $\Omega_{S\min}$: Poles and C will be given for each order for prescribed values of $\alpha_{\max}$ and $\alpha_{\min}$. For each combination $\{N, \alpha_{\max}, \alpha_{\min}\}$, the minimum value of $\Omega_S = \Omega_{S\min}$ that can be achieved can also be given, as calculated from (3.108).

The indicative tables at the end of the chapter are given for a limited number of entries, namely:

$$\begin{aligned} &N\text{: } 3\text{–}5 \qquad \Omega_S\text{: } 1.5,\ 2.0 \\ &\alpha_{\max}\text{: } 0.1,\ 0.5,\ 1.0,\ 1.5,\ 2.0,\ 2.5\ \text{dB} \\ &\alpha_{\min}\text{: } 12,\ 18,\ 24,\ 30,\ 36, 42\ \text{dB} \end{aligned} \tag{3.111}$$

In all tables, the complex pole pairs are given in terms of their frequency and quality factor whilst the real pole s_R, if N is odd, is given explicitly.

Usage of Tables Set A with Prescribed Ω_S and $\alpha_{\max}$ Tables with prescribed Ω_S and $\alpha_{\max}$, like Tables 3.3 and 3.4, can be used when Ω_S and $\alpha_{\max}$ of the specifications, as well as the order N are included in the tabulated values of (3.111). If this is the case, the corresponding table gives the maximum $\alpha_{S\max}$ that can be achieved with the specified values, the constant C, the zeros and the poles of the transfer function. These tables also give the 3 dB frequency in the last column.

If the specified values of Ω_S and $\alpha_{\max}$ are tabulated, the tables can also be used for the determination of the order: We simply find the lower N that gives $\alpha_{S\max}$ greater than the specified $\alpha_{\min}$. It should finally be noted that filters obtained from the A set of tables, like Tables 3.3 and 3.4, are stopband edge frequency gain optimized, i.e. they have $20\log G_{IPa}(1) = \alpha_o - \alpha_{\max}$ and at Ω_S and at the frequency of the first stopband gain extremum, the gain assumes a value lower than the spec-

ified $\alpha_o - \alpha_{\min}$. The filter with specifications $\{\Omega_S, \alpha_{\max}\alpha_{S\max}\}$ covers in an exact way both specified passband and stopband tolerances $\alpha_{\max}$ and $\alpha_{S\max}$ given in the table.

Usage of Tables Set B with Prescribed Ω_S and $\alpha_{\min}$ Tables with prescribed Ω_S and $\alpha_{\min}$, like Tables 3.5 and 3.6, can be used when Ω_S and $\alpha_{\min}$ of the specifications, as well as the order N are included in the tabulated values of (3.111). If this is the case, the corresponding table gives the minimum $\alpha_{C\min}$ that can be achieved with the specified values, the constant C, the zeros and the poles of the transfer function.

If the specified values of Ω_S and $\alpha_{\min}$ are tabulated, the tables can also be used for the determination of the order: We simply find the lower N that gives $\alpha_{C\min}$ lower than the specified $\alpha_{\max}$. It should finally be noted that filters obtained from the B set of tables are passband gain optimized, i.e. they have $20\log G_{IPa}(1) \geq \alpha_o - \alpha_{\max}$ and at Ω_S and at the frequency of the first stopband gain extremum, the gain assumes a value equal to the specified $\alpha_o - \alpha_{\min}$. The filter with specifications $\{\Omega_S, \alpha_{C\min}\alpha_{\min}\}$ covers in an exact way both specified passband and stopband tolerances $\alpha_{C\min}$ and $\alpha_{\min}$.

Usage of Tables Set C with Prescribed $\alpha_{\max}$ and $\alpha_{\min}$ Tables with prescribed $\alpha_{\max}$ and $\alpha_{\min}$, like Tables 3.7–3.10, can be used when $\alpha_{\max}$ and $\alpha_{\min}$ of the specifications, as well as the order N are included in the tabulated values. The corresponding table gives $\Omega_{S\min} \leq \Omega_S$, at which the logarithmic gain is exactly $\alpha_o - \alpha_{\min}$, the constant C, the zeros and the poles of the transfer function.

If the specified values of $\alpha_{\max}$ and $\alpha_{\min}$ are tabulated, the tables can also be used for the determination of the order: We simply find the lower N that gives $\Omega_{S\min}$ lower than the specified Ω_S. It should finally be noted that filters obtained from the C set of tables fully cover the specified passband and stopband tolerances $\alpha_{\max}$ and $\alpha_{\min}$ with stopband edge frequency $\Omega_{S\min}$ of the table.

Example 3.5 Design a normalized lowpass filter with the following specifications:

$$\{\Omega_S = 2,\ \alpha_o = 0,\ \alpha_{\max} = 0.5\text{ dB},\ \alpha_{\min} = 24\text{ dB}\}$$

We first calculate HP from (3.99):

$$HP = 20 \cdot \log\left(\frac{1}{g}\right) = 20 \cdot \log\left(\frac{\sqrt{10^{\frac{24}{10}}-1}}{\sqrt{10^{\frac{0.5}{10}}-1}}\right) = 33.1184$$

Referring to the nomograph of Fig. 3.30, the point $[\Omega_S = 2, HP = 33.1184]$ lies between curves 3 and 4 and therefore $N = 4$.

Calculation of Parameters Requiring Only N From Table 3.1 for $N = 4$, we get

$$\Omega_{\max} = 0.44721360 \qquad P_{\max} = P_D(1) = -0.04166667 \qquad \Omega_D = 0.65289675$$

and from (3.60)–(3.62), we find:

$$P_D(\Omega_S) = P_D(2) = 3.64537112$$

At this point, having only the order N, the roots of polynomial $P_D(\Omega)$ must be calculated from (3.64):

$$\rho_k = \frac{(N+1) - 2k}{(N+1)\Omega_D} < 1 \quad \text{for } k = 1, \ldots, \frac{N-\eta}{2} \text{ and } \eta = 0$$

which for $N = 4$ yields

$$\rho_1 = 0.91898144 \qquad \rho_2 = 0.30632715$$

The coefficient of the lower order term of $P_D(\Omega)$, α_0 in the case of even N, can be taken from Table 2.7 or can be calculated from (3.70):

$$a_0 = \frac{1}{16 \cdot 24} \cdot \prod_{k=1}^{2} (4 + 1 - 2k)^2 = 0.0234375$$

Calculation of Parameters Requiring N and Ω_S The magnitude of the zeros of the transfer function, according to (3.84) or (3.109), will be: $\Omega_{zk} = \frac{\Omega_S}{\rho_k}$ for $k = 1, \ldots, (N-\eta)/2$:

$$\Omega_{z1} = 2.1763225 \qquad \Omega_{z2} = 6.5289675$$

Calculation of Parameters Requiring $\alpha_{\max}$ and $\alpha_{\min}$ The boundary values of the ripple factor λ can be determined from (3.97), which for $\alpha_{\max} = 0.5$ and $\alpha_{\min} = 24$ yields

$$\frac{1}{|P_D(\Omega_S)|\sqrt{10^{0.1 \cdot 0.5} - 1}} = \lambda_{\min} \le \lambda \le \lambda_{\max} = \frac{1}{|P_{\max}|\sqrt{10^{0.1 \cdot 24} - 1}}$$

$$\lambda_{\min} = 0.7853179 \le \lambda \le 1.5173209 = \lambda_{\max}$$

(i) $\lambda = \lambda_{\min} = 0.78531789$ (Stopband edge frequency gain optimized filter). In this design, the logarithmic gain at $\Omega_S = 2$ will be less than the specified $\alpha_{\min} = 24$ dB, and is given by (3.106): $\alpha_{S\max} = 29.70796251 > \alpha_{\min}$.

Constant C of the transfer function can be calculated from (3.84) with

$$H_o = 1, \qquad \eta = 0, \qquad \lambda = 0.78531789,$$

$$a_\eta = a_0 = 0.0234375, \qquad \Omega_S = 2$$

to find $C = 0.01840277$. Using a mathematical package, the poles are calculated from (3.110) which, for the calculated values $N = 4$, $\eta = 0$, $\lambda_{\min} = 0.7853179$, $a_0 = 0.0234375$, $\Omega_{z1} = 2.1763225$ and $\Omega_{z2} = 6.5289675$, becomes:

$$s^8 + 0.7853179^2 \cdot 0.0234375^2 \cdot (s^2 + 2.1763225^2)^2 (s^2 + 6.5289675^2)^2 = 0$$

$$\Rightarrow \quad s_{1,2} = -1.3357603 \pm j0.690818$$

$$s_{3,4} = -0.3999288 \pm j1.2177887$$

or in terms of pole frequency and Qs

$$\Omega_{p1} = 1.503824 \qquad Q_{p1} = 0.562909$$

$$\Omega_{p2} = 1.281777 \qquad Q_{p2} = 1.602506$$

Finally, the transfer function of the stopband edge frequency gain optimized filter will be

$$H_1(s) = \frac{0.018403(s^2 + 2.176323^2)(s^2 + 6.528968^2)}{(s^2 + \frac{1.503824}{0.562909}s + 1.503824^2)(s^2 + \frac{1.281777}{1.602506}s + 1.281777^2)}$$

(ii) $\lambda = \lambda_{\max} = 1.51732092$ (Passband optimized filter).

In this case, according to (3.107), the passband gain will vary from 0 to $\alpha_{C\,\min} = 0.13968284 < \alpha_{\max} = 0.5$

For the calculation of the filter parameters, the same procedure is followed with $\lambda = \lambda_{\max} = 1.51732092$ to find $C = 0.03553974$ and

$$s_{1,2} = -1.593466 \pm j0.897223 \qquad s_{3,4} = -0.419364 \pm j1.403501$$

or in terms of pole frequency and Qs

$$\Omega_{p1} = 1.828700 \qquad Q_{p1} = 0.573812$$

$$\Omega_{p2} = 1.464814 \qquad Q_{p2} = 1.746472$$

The transfer function of the passband optimized filter will be

$$H_2(s) = \frac{0.03553974(s^2 + 2.176323^2)(s^2 + 6.528968^2)}{(s^2 + \frac{1.8287}{0.573812}s + 1.8287^2)(s^2 + \frac{1.464814}{1.746472}s + 1.464814^2)}$$

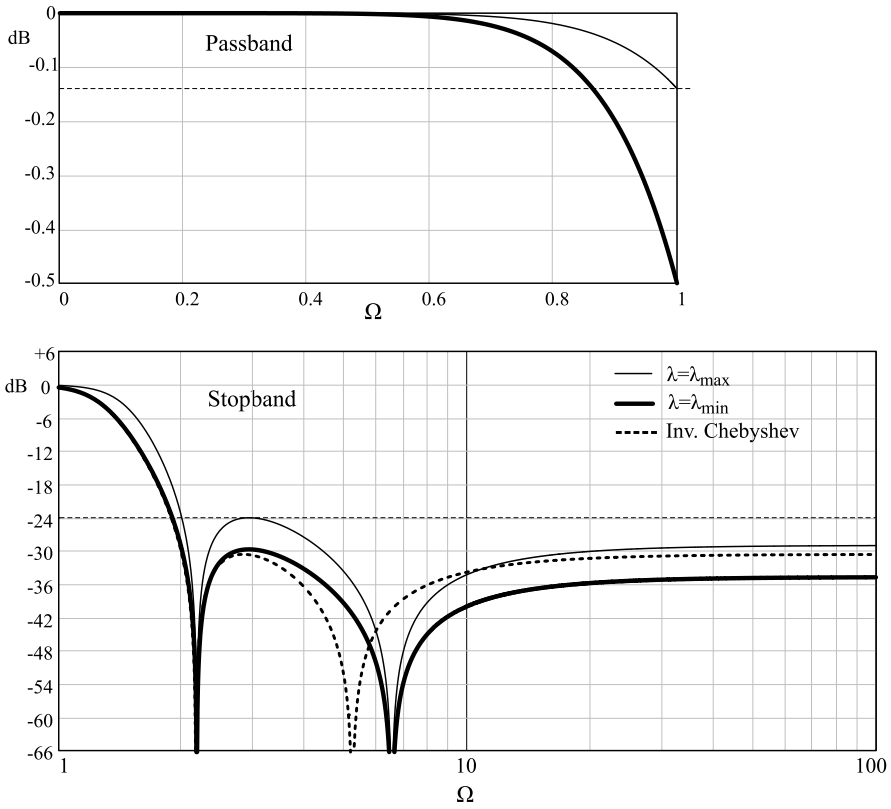

Fig. 3.32 Gain plots with $\lambda_{\min}$ (*thick*), $\lambda_{\max}$ (*thin*), inverse Chebyshev (*dashed*)

The gain plots from $H_1(s)$ and $H_2(s)$ are shown in Fig. 3.32, together with the gain of the corresponding inverse Chebyshev filter (dashed curve).

Design from the Tables Since the specifications Ω_S, $\alpha_{\max}$ and $\alpha_{\min}$ are included in the inverse Pascal design tables at the end of the chapter, all transfer function parameters can be taken from the there.

For the specified $\Omega_S = 2$ and $\alpha_{\max} = 0.5$, Table 3.4 A.2 can be used and this corresponds to designing with $\lambda = \lambda_{\min}$. Below is the related table entry:

$\Omega_S = 2.0$	N	$\alpha_{\max}$	$\alpha_{S\max}$	C	zeros Ω_{zk}	Poles Ω_p	Q_p	Ω_{3dB}
A.1	4	0.5	29.70796251	0.01840277	6.52896753	1.50382360	0.56290922	1.24566806
					2.17632251	1.28177701	1.60250641	

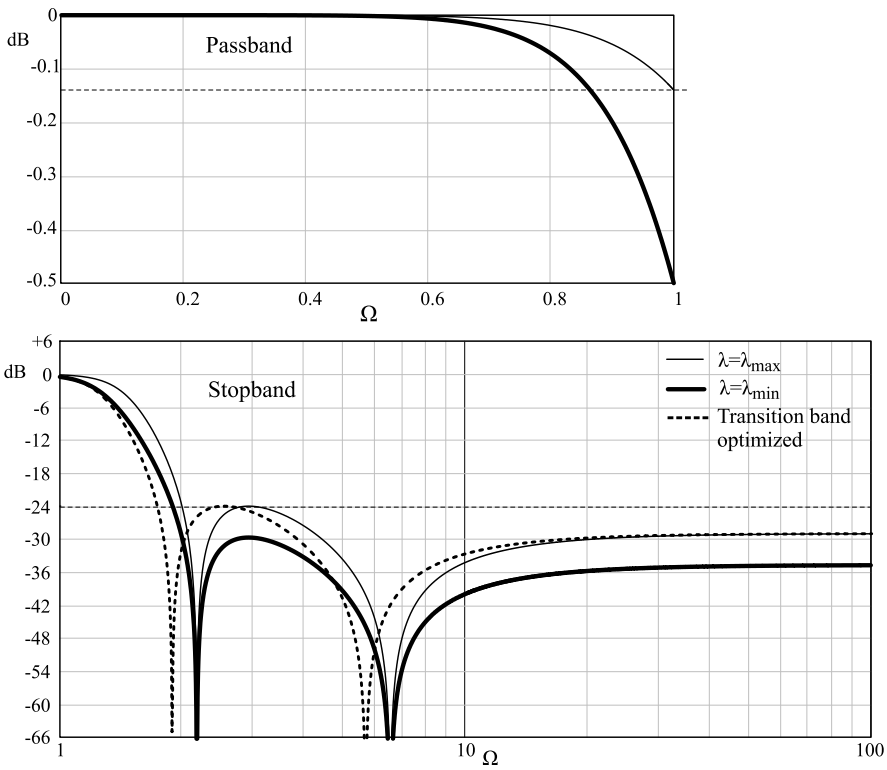

Fig. 3.33 Gain plots with $\lambda_{\min}$ (*thick*), $\lambda_{\max}$ (*thin*), transition band optimized (*dotted*)

$\alpha_{S\max} = 29.70796251$ means that the first stopband gain maximum and the gain at $\Omega_S = 2$ are below the initially specified $\alpha_{\min} = 24$ dB.

For the specified $\Omega_S = 2$ and $\alpha_{\min} = 24$ dB, Table 3.6 B.2 can be used and this corresponds to designing with $\lambda = \lambda_{\max}$. Below is the related table entry:

$\Omega_S = 2.0$	N	$\alpha_{\min}$	$\alpha_{C\max}$	C	zeros Ω_{zk}	Poles	
						Ω_p	Q_p
B.2	4	24	0.13968284	0.03553974	6.52896753	1.82869973	0.57381202
					2.17632251	1.46481408	1.74647165

$\alpha_{C\min} = 0.13968284$ means that in the passband the gain varies from 0 at $\Omega = 1$ to $\alpha_{C\min} = 0.13968284$ at $\Omega = 1$ instead of the initially specified $\alpha_{\max} = 0.5$ dB.

A third design, the transition band optimized, emerges using Table 3.8 with $\alpha_{\max} = 0.5$, $N = 4$ and $\alpha_{\min} = 24$. The related table entry is repeated below:

$\alpha_{\max} = 0.5$	N	$\alpha_{\min}$	$\Omega_{S\min}$	C	zeros Ω_{zk}	Poles	
						Ω_p	Q_p
C.2	4	24	1.73858427	0.03553974	5.67558012	1.58967429	0.57381202
					1.89186004	1.27335135	1.74647165

The table gives $\Omega_{S\min} = 1.73858427$, which implies that with $\alpha_{\max} = 0.5$, $N = 4$ and $\alpha_{\min} = 24$, a filter with steeper gain roll-off is designed, which will have the specified stopband edge frequency gain at $\Omega = \Omega_{S\min} = 1.73858427$ instead of $\Omega_S = 2$. The transfer function of this filter will be

$$H_3(s) = \frac{0.03554(s^2 + 1.891860^2)(s^2 + 5.675580^2)}{(s^2 + \frac{1.589674}{0.573812}s + 1.589674^2)(s^2 + \frac{1.273351}{1.746472}s + 1.273351^2)}$$

The dotted curve in Fig. 3.33 is the logarithmic gain plot of such a filter, i.e. $20\log(H_3(j\Omega))$.

3.5 Inverse Pascal Tables

The indicative tables are given for a limited number of entries, namely:

$$\begin{aligned} &N:\ 3\text{–}5 \qquad \Omega_S:\ 1.5,\ 2.0 \\ &\alpha_{\max}:\ 0.1,\ 0.5,\ 1.0,\ 1.5,\ 2.0,\ 2.5\ \text{dB} \\ &\alpha_{\min}:\ 12,\ 18,\ 24,\ 30,\ 36,\ 42\ \text{dB} \end{aligned} \tag{3.112}$$

In all tables, the complex pole pairs are given in terms of their frequency Ω_p and quality factor Q_p and therefore a pole pair $\{\Omega_p, Q_p\}$ corresponds to a denominator factor

$$s^2 + \frac{\Omega_p}{Q_p}s + \Omega_p^2$$

The real pole s_R is given explicitly and exists only if N is odd, in which case corresponds to a denominator factor $(s - s_R)$. Each zero Ω_{zk} corresponds to a numerator term $(s^2 + \Omega zk^2)$.

Finally, if in the filter specifications $H_o \neq 1$ (i.e. $\alpha_o \neq 0$), then the transfer function constant C of the tables, must be multiplied by H_o.

Table 3.3 A.1 Inverse Pascal parameters for prescribed $\Omega_S = 1.5$ and $\alpha_{\max}$ ($N = 3$–5)

$\Omega_S = 1.5$	N	$\alpha_{\max}$	$\alpha_{S\max}$	C	zeros	Poles		Ω_{3dB}
					Ω_{zk}	Ω_p	Q_p	
A.1	3	0.1	4.604065230	3.27610161	1.73205081	1.58407573	2.47258252	1.44312483
						$s_R = -3.91675797$		
		0.5	10.36768374	1.43138758	1.73205081	1.3763111	1.64713299	1.2625427
						$s_R = -2.26696741$		
		1.0	13.41888533	0.98261336	1.73205081	1.26338344	1.46183507	1.17017601
						$s_R = -1.84685822$		
		1.5	15.36754602	0.77846352	1.73205081	1.19212661	1.3784543	1.1115862
						$s_R = -1.64329205$		
		2.0	16.84633085	0.65378014	1.73205081	1.13899133	1.32736915	1.06746778
						$s_R = -1.51186195$		
		2.5	18.06455611	0.56676397	1.73205081	1.09601425	1.29144195	1.031443
						$s_R = -1.41543878$		
	4	0.1	10.71045721	0.16888233	4.89672565	2.30506534	0.64243159	1.34381243
					1.63224188	1.42494844	2.6284537	
		0.5	17.59335473	0.07465413	4.89672565	1.73512721	0.59497390	1.19928077
					1.63224188	1.25859467	2.02150324	
		1.0	20.82069442	0.05132395	4.89672565	1.53740693	0.58269809	1.12860084
					1.63224188	1.17777276	1.86250945	
		1.5	22.83017498	0.04068074	4.89672565	1.42964841	0.57678534	1.08424668
					1.63224188	1.12760097	1.78540685	
		2.0	24.33963088	0.03417340	4.89672565	1.35523423	0.57300515	1.05094601
					1.63224188	1.09023473	1.73588481	
		2.5	25.57624588	0.02962932	4.89672565	1.29800712	0.57026109	1.0237586
					1.63224188	1.05992239	1.69980676	
	5	0.1	17.49199156	0.4715666	3.17875513	1.75292868	0.79679061	1.28435669
					1.58937756	1.33278902	2.85827096	
						$s_R = -2.20526116$		
		0.5	24.62093626	0.20603591	3.17875513	1.46489733	0.73031489	1.16217332
					1.58937756	1.19704649	2.38660159	
						$s_R = -1.71030989$		
		1.0	27.88049664	0.14143873	3.17875513	1.35094509	0.71027686	1.1042813
					1.58937756	1.13371033	2.24776906	
						$s_R = -1.53906528$		
		1.5	29.90074939	0.11205312	3.17875513	1.28518954	0.70000357	1.06823817
					1.58937756	1.09460934	2.17706999	
						$s_R = -1.44523866$		
		2.0	31.41557071	0.09410602	3.17875513	1.23816743	0.69318153	1.04125123
					1.58937756	1.06549266	2.13027650	
						$s_R = -1.38014913$		
		2.5	32.65538142	0.08158079	3.17875513	1.20107004	0.68808945	1.01923783
					1.58937756	1.04183939	2.09542063	
						$s_R = -1.32989697$		

Table 3.4 A.2 Inverse Pascal parameters for prescribed $\Omega_S = 2.0$ and $\alpha_{\max}$ ($N = 3$–5)

$\Omega_S = 2.0$	N	$\alpha_{\max}$	$\alpha_{S\max}$	C	zeros Ω_{zk}	Poles Ω_p	Q_p	Ω_{3dB}
A.2	3	0.1	12.23912715	1.5120469	2.30940108	1.74262006	1.52389788	1.60775093
						$s_R = -2.65557501$		
		0.5	19.21605721	0.66064042	2.30940108	1.40821239	1.26170953	1.33030738
						$s_R = -1.776755$		
		1.0	22.45595517	0.45351386	2.30940108	1.26487567	1.19521428	1.20693096
						$s_R = -1.51179746$		
		1.5	24.46964697	0.35929085	2.30940108	1.18089075	1.16363219	1.13312443
						$s_R = -1.37412249$		
		2.0	25.98120277	0.30174468	2.30940108	1.12059130	1.14365913	1.07943069
						$s_R = -1.28157448$		
		2.5	27.21906925	0.26158337	2.30940108	1.07300194	1.12929483	1.03664300
						$s_R = -1.21173554$		
	4	0.1	22.53560322	0.04208932	6.52896753	1.92639602	0.57758481	1.45433576
					2.17632251	1.51324110	1.79585606	
		0.5	29.70796251	0.01840277	6.52896753	1.50382360	0.56290922	1.24566806
					2.17632251	1.28177701	1.60250641	
		1.0	32.97299732	0.01263419	6.52896753	1.35027457	0.55859157	1.15440465
					2.17632251	1.18282213	1.54483921	
		1.5	34.99506974	0.01000958	6.52896753	1.26468300	0.55640726	1.09966861
					2.17632251	1.12407192	1.51548818	
		2.0	36.51079543	0.00840651	6.52896753	1.20474244	0.55497034	1.05965413
					2.17632251	1.0813879	1.49610783	
		2.5	37.75114418	0.0072877	6.52896753	1.15816943	0.55390595	1.02759887
					2.17632251	1.04734745	1.48171254	
	5	0.1	32.50727516	0.11064608	4.23834017	1.60725015	0.68867609	1.36248374
					2.11917009	1.39287391	2.09943333	
						$s_R = -1.78101976$		
		0.5	39.69730438	0.04834326	4.23834017	2.02673444	0.66570722	1.19591982
					2.11917009	0.62582875	1.94277481	
						$s_R = -1.44924895$		
		1.0	42.96454972	0.03318649	4.23834017	1.24701592	0.65816627	1.1234406
					2.11917009	1.13976296	1.89148149	
						$s_R = -1.32529184$		
		1.5	44.98735605	0.0262916	4.23834017	1.18791583	0.65416703	1.07985403
					2.11917009	1.09425322	1.86429029	
						$s_R = -1.25525856$		
		2.0	46.50344633	0.02208058	4.23834017	1.14557857	0.65145746	1.04788553
					2.11917009	1.06098226	1.84586912	
						$s_R = -1.20577882$		
		2.5	47.74401194	0.01914172	4.23834017	1.11212772	0.64940558	1.02219208
					2.11917009	1.03430511	1.83191905	
						$s_R = -1.16707157$		

Table 3.5 B.1 Inverse Pascal parameters for prescribed $\Omega_S = 1.5$ and $\alpha_{\min}$ ($N = 3$–5)

$\Omega_S = 1.5$	N	$\alpha_{\min}$	$\alpha_{C\,\min}$	C	zeros Ω_{zk}	Poles Ω_p	Q_p
B.1	3	12	0.73102259	1.16779041	1.73205081	1.31582102	1.53778528
						$s_R = -2.0234502$	
		18	2.47141669	0.57105985	1.73205081	1.09827156	1.29322374
						$s_R = -1.42031086$	
		24	6.11590417	0.28449767	1.73205081	0.90008233	1.17045108
						$s_R = -1.05350233$	
		30	11.24938737	0.14237370	1.73205081	0.72901544	1.10240418
						$s_R = -0.80366966$	
		36	17.00155639	0.07132915	1.73205081	0.58612862	1.06269721
						$s_R = -0.62287725$	
		42	22.93701637	0.03574590	1.73205081	0.46910304w	1.03882581
						$s_R = -0.48731635$	
	4	12	0.1371884	0.14444299	4.89672565	2.17754460	0.63004959
					1.63224188	1.39499121	2.47092004
		18	0.54692551	0.07120131	4.89672565	1.70831428	0.59319617
					1.63224188	1.24843665	1.99855356
		24	1.87727401	0.03553974	4.89672565	1.37152480	0.57381202
					1.63224188	1.09861056	1.74647165
		30	4.99568882	0.01779389	4.89672565	1.11693306	0.56247686
					1.63224188	0.95454994	1.59675106
		36	9.82367782	0.00891579	4.89672565	0.91841941	0.55543701
					1.63224188	0.82173000	1.50240859
		42	15.47185695	0.00446819	4.89672565	0.76029389	0.55088987
					1.63224188	0.70270773	1.44072496
	5	12	0.02716151	0.9086393	3.17875513	2.02068241	0.88771357
					1.58937756	1.42922784	3.53616695
						$s_R = -2.78074245$	
		18	0.11247175	0.44433266	3.17875513	1.73041389	0.79060957
					1.58937756	1.32340199	2.81360870
						$s_R = -2.16268364$	
		24	0.43639767	0.22136315	3.17875513	1.48777431	0.73471166
					1.58937756	1.20909216	2.41724804
						$s_R = -1.74614663$	
		30	1.52925161	0.11077873	3.17875513	1.28205005	0.69953486
					1.58937756	1.09269540	2.17385124
						$s_R = -1.44084245$	
		36	4.28394812	0.05550009	3.17875513	1.10686154	0.67623005
					1.58937756	0.97906603	2.01444358
						$s_R = -1.20628914$	
		42	8.86256579	0.02781332	3.17875513	0.95722135	0.66024403
					1.58937756	0.87142587	1.90561073
						$s_R = -1.02031784$	

Table 3.6 B.2 Inverse Pascal parameters for prescribed $\Omega_S = 2.0$ and $\alpha_{\min}$ ($N = 3$–5)

$\Omega_S = 2.0$	N	$\alpha_{\min}$	$\alpha_{C\,\min}$	C	zeros Ω_{zk}	Poles Ω_p	Q_p
B.2	3	12	0.09436395	1.55705388	2.30940108	1.75442803	1.53778528
						$s_R = -2.6979336$	
		18	0.38166000	0.76141314	2.30940108	1.46436208	1.29322374
						$s_R = -1.89374781$	
		24	1.36752755	0.37933023	2.30940108	1.20010977	1.17045108
						$s_R = -1.40466977$	
		30	3.94068115	0.18983160	2.30940108	0.97202058	1.10240418
						$s_R = -1.07155955$	
		36	8.38072964	0.09510554	2.30940108	0.78150482	1.06269721
						$s_R = -0.83050299$	
		42	13.88166701	0.04766120	2.30940108	0.62547072	1.03882581
						$s_R = -0.64975513$	
	4	12	0.00841691	0.14444299	6.52896753	2.90339279	0.63004959
					2.17632251	1.85998828	2.47092004
		18	0.03509008	0.07120131	6.52896753	2.27775238	0.59319617
					2.17632251	1.66458220	1.99855356
		24	0.13968284	0.03553974	6.52896753	1.82869973	0.57381202
					2.17632251	1.46481408	1.74647165
		30	0.53276223	0.01779389	6.52896753	1.48924408	0.56247686
					2.17632251	1.27273325	1.59675106
		36	1.81837284	0.00891579	6.52896753	1.22455921	0.55543701
					2.17632251	1.09564001	1.50240859
		42	4.87203290	0.00446819	6.52896753	1.01372519	0.55088987
					2.17632251	0.93694365	1.44072496
	5	12	0.00084368	1.21151906	4.23834017	2.69424321	0.88771357
					2.11917009	1.90563712	3.53616695
						$s_R = -3.7076566$	
		18	0.00352705	0.59244355	4.23834017	2.30721852	0.79060957
					2.11917009	1.76453598	2.81360870
						$s_R = -2.88357819$	
		24	0.01419331	0.29515087	4.23834017	1.98369909	0.73471166
					2.11917009	1.61212288	2.41724804
						$s_R = -2.3281955$	
		30	0.05639862	0.14770497	4.23834017	1.70940006	0.69953486
					2.11917009	1.45692720	2.17385124
						$s_R = -1.92112327$	
		36	0.22046862	0.07400012	4.23834017	1.47581539	0.67623005
					2.11917009	1.30542138	2.01444358
						$s_R = -1.60838552$	
		42	0.81834939	0.03708443	4.23834017	1.27629513	0.66024403
					2.11917009	1.16190116	1.90561073
						$s_R = -1.36042379$	

Table 3.7 C.1 Inverse Pascal parameters for prescribed $\alpha_{\max} = 0.1$ and $\alpha_{\min}$ ($N = 3$–5)

$\alpha_{\max} = 0.1$	N	$\alpha_{\min}$	$\Omega_{S\min}$	C	zeros Ω_{zk}	Poles Ω_p	Q_p
C.1	3	12	1.98314818	1.54393427	2.28994227	1.73964538	1.53778528
						$s_R = -2.67520105$	
		18	2.4522782	0.93359842	2.83164696	1.79551161	1.29322374
						$s_R = -2.32199824$	
		24	3.04352365	0.57725026	3.51435840	1.82628124	1.17045108
						$s_R = -2.13757284$	
		30	3.79416067	0.36012579	4.38111937	1.84400113	1.10240418
						$s_R = -2.03283456$	
		36	4.74598779	0.22568486	5.48019466	1.85450618	1.06269721
						$s_R = -1.97077854$	
		42	5.9502797	0.14179873	6.87079117	1.86086286	1.03882581
						$s_R = -1.93311237$	
	4	12	1.54668735	0.14443625	5.04913574	2.24532045	0.63004959
					1.68304525	1.43841017	2.47092004
		18	1.78668168	0.07120130	5.83259335	2.03480923	0.59319617
					1.94419778	1.48703927	1.99855356
		24	2.07574079	0.03553974	6.77622212	1.89795331	0.57381202
					2.25874071	1.52028716	1.74647165
		30	2.42563959	0.01779389	7.91846105	1.80618469	0.56247686
					2.63948702	1.54359608	1.59675106
		36	2.8477511	0.00891579	9.29643723	1.74361992	0.55543701
					3.09881241	1.56005502	1.50240859
		42	3.35495009	0.00446819	10.9521801	1.70049871	0.55088987
					3.6507267	1.57169959	1.44072496
	5	12	1.36218792	0.82482884	2.88670788	1.83503277	0.88771357
					1.44335394	1.29791793	3.53616695
						$s_R = -2.52526251$	
		18	1.51377278	0.44841252	3.20794199	1.74630229	0.79060957
					1.603971	1.33555327	2.81360870
						$s_R = -2.18254109$	
		24	1.69186521	0.24967777	3.58535015	1.67807574	0.73471166
					1.79267507	1.36374731	2.41724804
						$s_R = -1.96949649$	
		30	1.90177793	0.14045104	4.03019090	1.62544966	0.69953486
					2.01509545	1.38537600	2.17385124
						$s_R = -1.82677491$	
		36	2.14803863	0.07947756	4.55205921	1.58505423	0.67623005
					2.27602960	1.40204777	2.01444358
						$s_R = -1.72743711$	
		42	2.43546006	0.04515884	5.16115410	1.5541829	0.66024403
					2.58057705	1.41488193	1.90561073
						$s_R = -1.6566289$	

Table 3.8 C.2 Inverse Pascal parameters for prescribed $\alpha_{\max} = 0.5$ and $\alpha_{\min}$ ($N = 3$–5)

$\alpha_{\max} = 0.5$	N	$\alpha_{\min}$	$\Omega_{S\min}$	C	zeros Ω_{zk}	Poles Ω_p	Q_p
C.2	3	12	1.579787	1.22990674	1.8241809	1.3858113	1.53778528
						$s_R = -2.13108021$	
		18	1.92017843	0.73102454	2.21723107	1.40591824	1.29322374
						$s_R = -1.81816685$	
		24	2.35661905	0.44696842	2.72118929	1.41410078	1.17045108
						$s_R = -1.65513578$	
		30	2.91652474	0.27682428	3.36771269	1.41746104	1.10240418
						$s_R = -1.56261497$	
		36	3.63108027	0.17266792	4.19281035	1.41885338	1.06269721
						$s_R = -1.50781152$	
		42	4.5387883	0.10816204	5.24094129	1.41943959	1.03882581
						$s_R = -1.47455048$	
	4	12	1.33083959	0.14444006	4.34450422	1.93197503	0.63004959
					1.44816807	1.23767301	2.47092004
		18	1.5136098	0.07120131	4.94115461	1.72381416	0.59319617
					1.64705154	1.25976397	1.99855356
		24	1.73858427	0.03553974	5.67558012	1.58967429	0.57381202
					1.89186004	1.27335135	1.74647165
		30	2.01475786	0.0177939	6.57714431	1.50023310	0.56247686
					2.19238144	1.28212466	1.59675106
		36	2.3510392	0.00891579	7.67492931	1.43949336	0.55543701
					2.55830977	1.2879463	1.50240859
		42	2.75764389	0.00446819	9.00228371	1.39774654	0.55088987
					3.00076124	1.29187846	1.44072496
	5	12	1.2222726	0.74035789	2.59020353	1.64654982	0.88771357
					1.29510176	1.16460401	3.53616695
						$s_R = -2.26588354$	
		18	1.34091551	0.39720837	2.84162803	1.54689254	0.79060957
					1.42081401	1.18304683	2.8136087q
						$s_R = -1.93331735$	
		24	1.48367484	0.21895396	3.14415934	1.47158221	0.73471166
					1.57207967	1.19593308	2.41724804
						$s_R = -1.72714255$	
		30	1.65467096	0.12220157	3.50652921	1.41424733	0.69953486
					1.75326460	1.20536757	2.17385124
						$s_R = -1.58941344$	
		36	1.85749585	0.06872746	3.93634965	1.37066048	0.67623005
					1.96817482	1.21240740	2.01444358
						$s_R = -1.49378472$	
		42	2.09604955	0.0388654	4.44188551	1.33758892	0.66024403
					2.22094275	1.21770120	1.90561073
						$s_R = -1.42575784$	

Table 3.9 C.3 Inverse Pascal parameters for prescribed $\alpha_{\max} = 1.0$ and $\alpha_{\min}$ ($N = 3$–5)

$\alpha_{\max} = 1.0$	N	$\alpha_{\min}$	$\Omega_{S\min}$	C	zeros Ω_{zk}	Poles Ω_p	Q_p
C.3	3	12	1.43766193	1.11925855	1.66006901	1.26113719	1.53778528
						$s_R = -1.93935821$	
		18	1.72894461	0.65822056	1.99641328	1.26590047	1.29322374
						$s_R = -1.63709254$	
		24	2.10680123	0.3995867	2.43272451	1.26419637	1.17045108
						$s_R = -1.47968000$	
		30	2.59500855	0.24630731	2.99645777	1.26120086	1.10240418
						$s_R = -1.3903531$	
		36	3.22079750	0.15315784	3.71905660	1.25853439	1.06269721
						$s_R = -1.33744098$	
		42	4.01790565	0.0957491	4.63947782	1.25654117	1.03882581
						$s_R = -1.3053274$	
	4	12	1.25226748	0.14444252	4.08800684	1.81791218	0.63004959
					1.36266895	1.16460141	2.47092004
		18	1.41180787	0.07120131	4.60882388	1.60787437	0.59319617
					1.53627463	1.17503513	1.99855356
		24	1.61098194	0.03553974	5.25902438	1.47300112	0.57381202
					1.75300813	1.17989451	1.74647165
		30	1.85771544	0.01779389	6.06448189	1.38329586	0.56247686
					2.02149396	1.18218811	1.59675106
		36	2.15994543	0.00891579	7.05110678	1.32249053	0.55543701
					2.35036893	1.18326131	1.50240859
		42	2.52683278	0.00446819	8.24880457	1.28075702	0.55088987
					2.74960152	1.18374996	1.44072496
	5	12	1.17042573	0.70899353	2.4803312	1.57670579	0.88771357
					1.2401656	1.11520336	3.53616695
						$s_R = -2.16976835$	
		18	1.27514898	0.37772689	2.70225757	1.47102367	0.79060957
					1.35112878	1.12502313	2.8136087
						$s_R = -1.83849589$	
		24	1.40311931	0.20706595	2.97344847	1.39168325	0.73471166
					1.48672424	1.13100037	2.41724804
						$s_R = -1.63336803$	
		30	1.55797089	0.11506005	3.30160531	1.33159777	0.69953486
					1.65080265	1.13492509	2.17385124
						$s_R = -1.49652706$	
		36	2.15992713	0.02324348	4.57725297	1.59382685	0.67623005
					2.28862649	1.40980753	2.01444358
						$s_R = -1.73699776$	
		42	1.96146382	0.03636988	4.15667545	1.25170336	0.66024403
					2.07833772	1.13951354	1.90561073
						$s_R = -1.33421102$	

Table 3.10 C.4 Inverse Pascal parameters for prescribed $\alpha_{\max} = 2.0$ and $\alpha_{\min}$ ($N = 3$–5)

$\alpha_{\max} = 2.0$	N	$\alpha_{\min}$	$\Omega_{S\min}$	C	zeros Ω_{zk}	Poles Ω_p	Q_p
C.4	3	12	1.30864725	1.01881714	1.51109568	1.14796371	1.53778528
						$s_R = -1.76532169$	
		18	1.55224899	0.59095139	1.79238275	1.13652729	1.29322374
						$s_R = -1.46978407$	
		24	1.87346638	0.35533122	2.16329264	1.12418266	1.17045108
						$s_R = -1.3158008$	
		30	2.29270069	0.21761352	2.64738272	1.11427613	1.10240418
						$s_R = -1.22838266$	
		36	2.83343653	0.13473775	3.27177068	1.10717216	1.06269721
						$s_R = -1.17658876$	
		42	3.52486708	0.08399969	4.07016591	1.10235057	1.03882581
						$s_R = -1.14515023$	
	4	12	1.17963478	0.14444299	3.8508986	1.71247157	0.63004959
					1.28363287	1.09705343	2.47092004
		18	1.31572348	0.07120131	4.29515794	1.49844614	0.59319617
					1.43171931	1.09506494	1.99855356
		24	1.48894011	0.03553974	4.86062082	1.36141219	0.57381202
					1.62020694	1.09051022	1.74647165
		30	1.7062172	0.0177939	5.56991836	1.27048693	0.56247686
					1.85663945	1.08577969	1.59675106
		36	1.97454843	0.00891579	6.44588131	1.20897574	0.55543701
					2.1486271	1.08169713	1.50240859
		42	2.30205073	0.00446819	7.51500724	1.16682341	0.55088987
					2.50500241	1.07844590	1.44072496
	5	12	1.1220115	0.67966795	2.3777332	1.51148593	0.88771357
					1.1888666	1.06907338	3.53616695
						$s_R = -2.08001667$	
		18	1.21233438	0.35911984	2.56914275	1.39856016	0.79060957
					1.28457137	1.06960382	2.8136087
						$s_R = -1.74793049$	
		24	1.32504916	0.19554471	2.80800454	1.31424940	0.73471166
					1.40400227	1.06807103	2.41724804
						$s_R = -1.54248674$	
		30	1.46334014	0.10807132	3.10106665	1.25071686	0.69953486
					1.55053332	1.06599003	2.17385124
						$s_R = -1.40562839$	
		36	1.63003989	0.0603116	3.45433177	1.20281897	0.67623005
					1.72716588	1.06394446	2.01444358
						$s_R = -1.31086628$	
		42	1.82828227	0.03390042	3.87444110	1.16671388	0.66024403
					1.93722055	1.06214165	1.90561073
						$s_R = -1.24361935$	

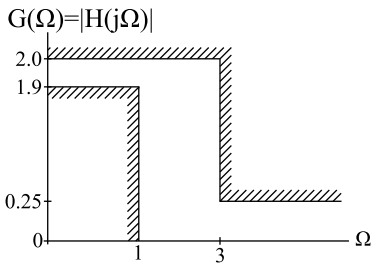

Fig. 3.34 Gain specifications for Problem 3.3

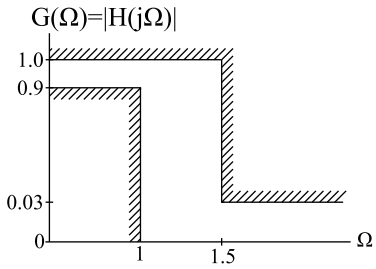

Fig. 3.35 Gain specifications for Problem 3.4

3.6 Problems

3.1 Verify that $H_1(s)$ and $H_2(s)$ of Example 3.1 can be derived from the magnitude response of (3.11)

$$|H(j\Omega)| = G(\Omega) = \frac{1}{\sqrt{1 + \frac{9\Omega^6}{4(\Omega^2+2)^2}}}$$

3.2 Verify that the coefficients of the highest and lowest order terms of the Chebyshev polynomial are given by (3.25):

$$c_N = 2^{N-1} \quad \text{and} \quad c_\eta = N^\eta (-1)^{\frac{N+3\eta}{2}}$$

3.3 Design the transition band optimized inverse Chebyshev filter from the normalized specifications of Fig. 3.34.

3.4 Design the transition band optimized inverse Chebyshev filter from the normalized specifications of Fig. 3.35.

3.5 Use the inverse Pascal design tables A, B and C to determine the order of the normalized inverse Pascal filter that meets the specifications of Fig. 3.36.

3.6 Use the inverse Pascal design tables to determine the order and the transfer function of the stopband edge frequency optimized inverse Pascal filter that meets the specifications of Fig. 3.37a.

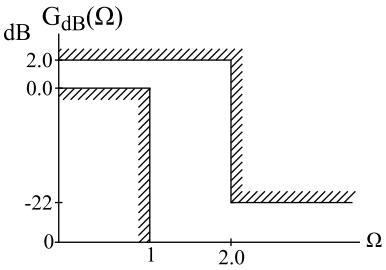

Fig. 3.36 Gain specifications for Problem 3.5

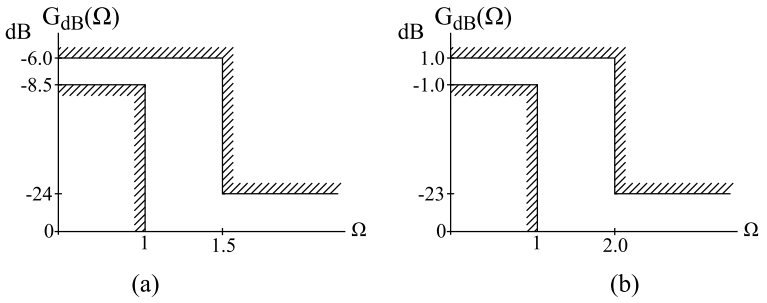

Fig. 3.37 Gain specifications for Problems 3.6 to 3.10

3.7 Use the inverse Pascal design tables to determine the order and the transfer function of the passband optimized inverse Pascal filter that meets the specifications of Fig. 3.37a.

3.8 Use the inverse Pascal design tables to determine the order and the transfer function of the stopband edge frequency optimized inverse Pascal filter that meets the specifications of Fig. 3.37b.

3.9 Use the inverse Pascal design tables to determine the transfer function of the passband optimized inverse Pascal filter that meets the specifications of Fig. 3.37b.

3.10 Use the inverse Pascal design tables to determine the order and the transfer function of the normalized transition band optimized inverse Pascal filter that meets the specifications of Fig. 3.37b. Use mathematical software to plot the logarithmic gain in order to verify your results.

References[1]

1. Chirlian, P.M.: Signals and Filters. Springer, Berlin (1994)

[1] All references, whether or not cited within the text, are recommended for further reading.

2. Daniels, R.W.: Approximation Methods for Electronic Filter Design. McGraw-Hill, New York (1974)
3. Dimopoulos, H.G.: Optimal use of some classical approximations in filter design. IEEE Trans. Circuits Syst. II, Analog Digit. Signal Process. **54**(9), 780–784 (2007)
4. Dimopoulos, H.G., Sarri, E.: The modified Pascal polynomial approximation and filter design method. Int. J. Circuit Theory Appl. (2010). doi:10.1002/cta.711
5. Paarmann, L.D.: Design and Analysis of Analog Filters—A Signal Processing Perspective—With MATLAB Examples. Kluwer Academic, Dordrecht (2001)
6. Temes, G.C., LaPatra, J.W.: Introduction to Circuit Synthesis and Design. McGraw-Hill, New York (1977)
7. Van Valkenburg, M.E.: Analog Filter Design. Oxford University Press, London (1982)
8. Wanhammar, L.: Analog Filters Using MATLAB. Springer, Berlin (2009)
9. Williams, A., Taylor, F.: Electronic Filter Design Handbook. McGraw-Hill, New York (2006)

The Elliptic (Cauer) Approximation

4

Elliptic approximation is a rational approximation, as defined in Chap. 3. Although when the elliptic approximation is used it leads to minimum order filters, the elliptic mathematics involved discourages instructors from including the complete analysis in their syllabi. Moreover, elliptic approximation is usually covered in a simple descriptive manner in filter textbooks. For these reasons, this chapter is devoted to the elliptic approximation alone, which is analytically presented and with all mathematical analyses regarding the design procedures and related formulae given explicitly.

4.1 Introduction

Figure 4.1 shows the plain gain plots of the fifth order ($N = 5$) Butterworth, Chebyshev and inverse Chebyshev approximations, with $H_o = 1$ and $H_C = 0.96828$ ($\alpha_o = 0$, $\alpha_{\max} = 0.28$). Figure 4.2 shows the stopband details where the curves of Chebyshev and inverse Chebyshev approximations intersect at point $\{\Omega = 1.663,\ G(1.663) = 0.033358\}$, implying that the strictest stopband specifications that can be met by the two Chebyshev approximations with $\{N = 5,\ H_o = 1,\ H_C = 0.96828\ (\alpha_{\max} = 0.28\ \text{dB})\}$ are $\{\Omega_S = 1.663,\ H_S = 0.033358\ (\alpha_{\min} = 29.54\ \text{dB})\}$. The plain gain of Butterworth approximation with $N = 5$ at $\Omega = 1.663$ is much higher than 0.033358 and calculation of the Butterworth order with $\{\Omega_S = 1.663,\ H_o = 1,\ H_C = 0.96828,\ H_S = 0.033358\}$ leads to $N = 10$. The Butterworth gain with $N = 10$ is shown in Fig. 4.3.

Therefore, the specifications

$$\begin{aligned} &\{\Omega_S = 1.663, H_o = 1, H_C = 0.96828, H_S = 0.033358\} \quad \text{or} \\ &\{\Omega_S = 1.663, \alpha_{\max} = 0.28\ \text{dB}, \alpha_{\min} = 29.54\ \text{dB}\} \end{aligned} \tag{4.1}$$

can be met by Chebyshev approximations with $N = 5$ and by Butterworth approximation with $N = 10$. Pascal approximations would require $N = 6$. These results are to be expected since, as shown in the previous Chapters, given the specifications, Chebyshev approximations lead to lower orders than Pascal and Butterworth

H.G. Dimopoulos, *Analog Electronic Filters*, Analog Circuits and Signal Processing,
DOI 10.1007/978-94-007-2190-6_4, © Springer Science+Business Media B.V. 2012

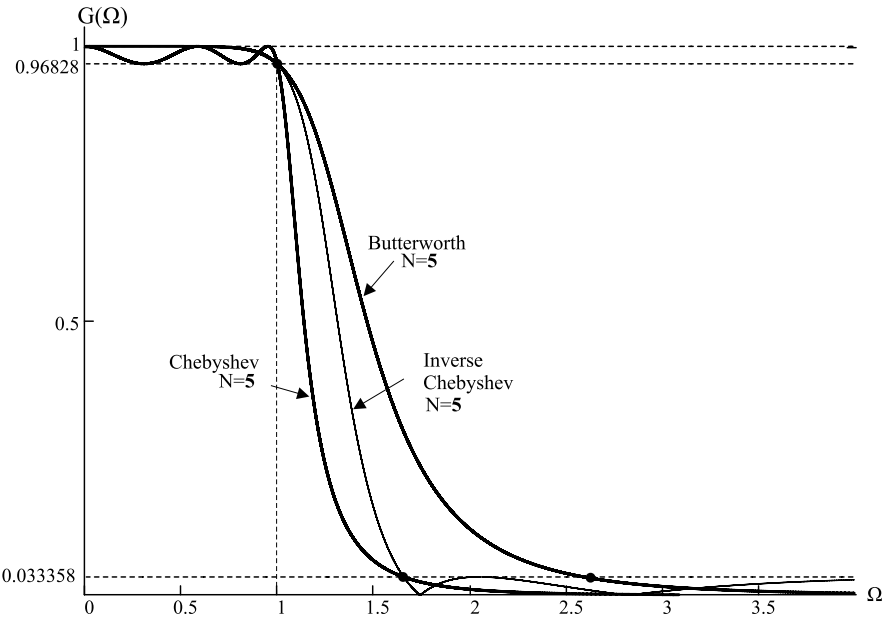

Fig. 4.1 Butterworth and Chebyshev approximations ($N = 5$): Passband and stopband gain plots

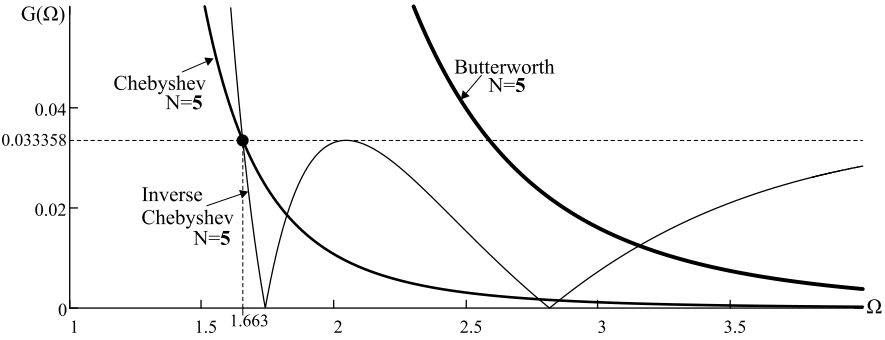

Fig. 4.2 Butterworth and Chebyshev approximations ($N = 5$): Stopband gain plots

approximations. Therefore, the question of whether there is another approximation which would meet the same specifications with even lower order seems reasonable. The answer was given in the late 1920s by Wilhelm Cauer [3, 4], who designed filters using a rational approximation which involves Jacobian elliptic functions.

The gain plot of the elliptic approximation with $N = 5$ and $H_o = 1$, $H_C = 0.96828$ is added in Fig. 4.3 and is shown in Fig. 4.4. Figure 4.5 shows a typical gain plot of the Cauer approximation which is equiripple in both the passband and the stopband. With the same passband characteristics, the gain curve of the elliptic approximation is much steeper in the transition band and can meet even stricter

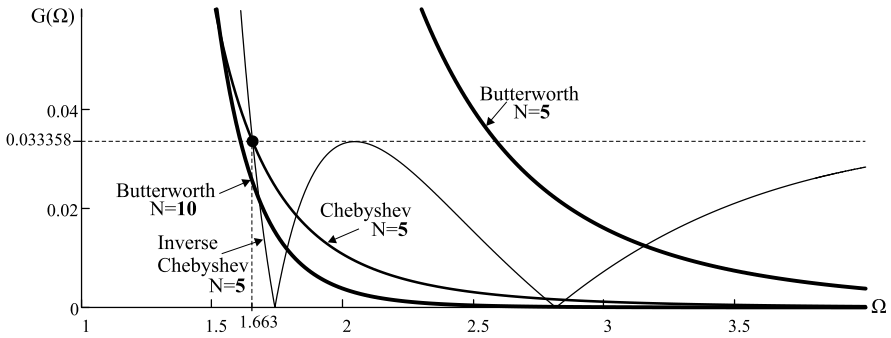

Fig. 4.3 Chebyshev approximations ($N = 5$), Butterworth approximation $N = 5$ and $N = 10$

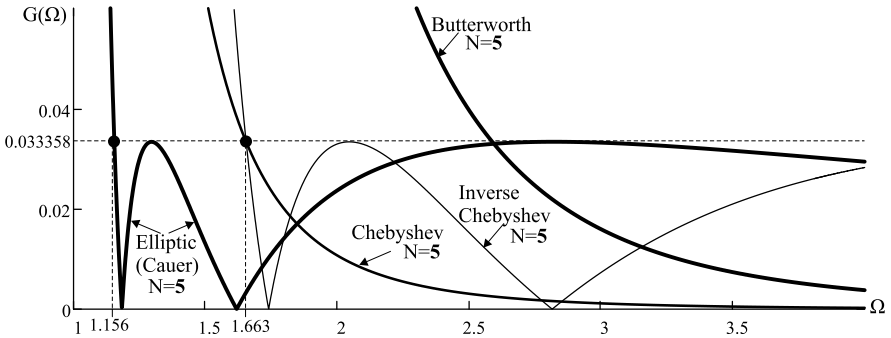

Fig. 4.4 Butterworth, Chebyshev and Elliptic approximations ($N = 5$): Stopband gain plots

stopband specifications, namely $\Omega_S = 1.156$. If we require this same stopband edge frequency for the Chebyshev and for the Butterworth approximations, we will end up with $N_{Ch} = 10$ and $N_{Bu} = 33$ respectively. Pascal approximations would lead to $N_{Pa} = 13$.

The cost of such a very significant order decrease is an increase of the design effort due to the "difficulty" of two elliptic functions.

1. The first is the *complete elliptic integral of the first kind* $K(x)$ [2, 11], which appears in the elliptic approximation always with $x < 1$:

$$K(x) = \int_0^{\pi/2} \frac{1}{\sqrt{1 - x^2 \sin^2(\phi)}} d\phi \tag{4.2}$$

   An indicative plot of $K(x)$ is shown in Fig. 4.6.
2. The second is the *Jacobi elliptic sine* $\mathrm{sn}(u, x)$ of u with modulus x [11]. A plot of $\mathrm{sn}(u, x)$ is shown in Fig. 4.7 for $x = 0.25$ and $x = 0.975$. The Jacobi elliptic sine is a doubly periodic function of u with a real and a complex period both of which depend on the modulus x. The real period is $T(x) = 4K(x)$, where $K(x)$ is the complete elliptic integral of x. For low values of x, $\mathrm{sn}(u, x)$ is very similar to the

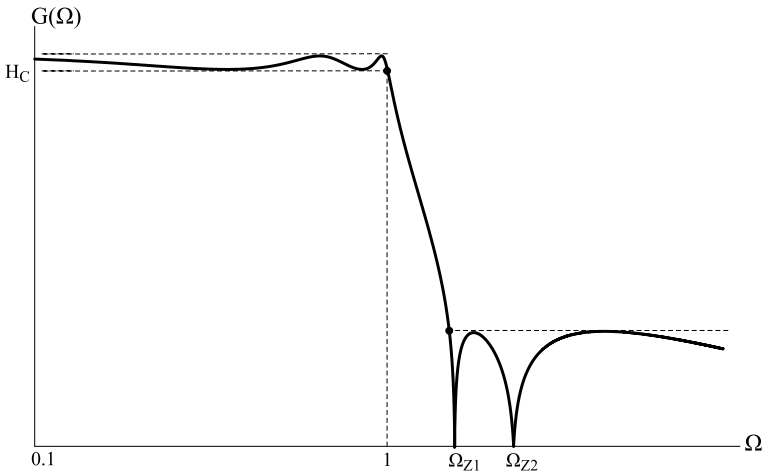

Fig. 4.5 Typical elliptic approximation gain plot

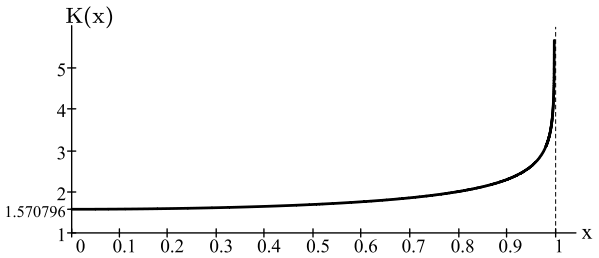

Fig. 4.6 The complete elliptic integral

trigonometric sine, but as x increases the plot is "squared" around its peak values. If θ is the angle for which $\int_0^\theta \frac{1}{\sqrt{1-x^2\sin^2(\phi)}}\,d\phi = u$, then $\mathrm{sn}(u,x) = \sin(\theta)$. This integral with $\theta \neq \pi/2$ is defined as the non-complete elliptic integral with modulus x. A basic property of $\mathrm{sn}(u,x)$ is

$$\mathrm{sn}(K(x),\ x) = 1$$

One of the greatest accomplishments of the Prussian mathematician Carl Gustav Jacob Jacobi (1804–1851) was his *Theory of Elliptic Functions* and their relation to the elliptic theta function.[1] The theory of elliptic functions is indeed complicated but the filter designer is not required to know its details. Functions $K(x)$ and $\mathrm{sn}(u,x)$ can be used as any other conventional function, e.g. $\cos(x)$ or $\cosh^{-1}(x)$, which are considered "easy" mainly because they can be calculated using the corresponding key on any scientific calculator. Instead of intimidating engineers and students by $K(x)$ and $\mathrm{sn}(u,x)$, as is usually done in filter design books, in this present book

[1] Fundamenta nova theoriae functionum ellipticarum, 1829.

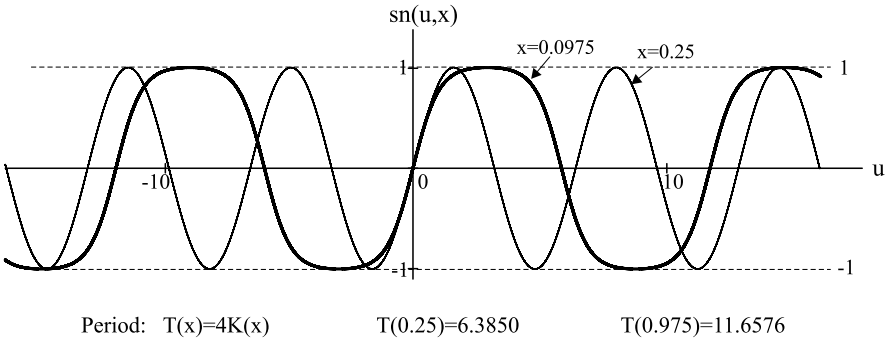

Fig. 4.7 The Jacobi elliptic sine

we prefer to give simple and accurate algorithms for their calculation, which is essentially like having the corresponding keys on your calculator. It will be seen that when the necessary tools have been developed, elliptic approximation is no more difficult than all other approximations. Moreover, it will be demonstrated that the often-used statement that elliptic filters can only be designed from filter tables is not correct. In addition, it will be seen that the designer now has full control over all the parameters related to his filter design needs.

Historical notes[2] will not be used as an excuse for not giving the full details of elliptic filter design or for giving vague and deficient descriptions of the supposed difficulties of elliptic functions. Neither will we give instructions on how to use filter design programs and dedicated functions of a mathematical software package in order to design elliptic filters. In this section, the elliptic approximation and filter design will be demystified and presented in an explicit and useful manner along with all the related mathematics and the relevant design equations for the calculation of the order, the gain function and the transfer function, as has been done with all other approximations.

4.2 Calculation of $K(x)$ and $\mathrm{sn}(u, x)$

The calculation of the complete elliptic integral $K(x)$ and the Jacobi elliptic sine $\mathrm{sn}(u, x)$ which comprise the main difficulty in elliptic filter design, is made very much simpler by the use of the *arithmetic-geometric mean* (AGM) studied initially by Euler and Lagrange and later by Gauss and Legendre, who presented the final theory.

[2] "The world first learned of the Cauer method not through scholarly publication but through a patent disclosure, which eventually reached the Bell Laboratories. Legend has it that the entire Mathematics Department of Bell Laboratories spent the next 2 weeks at the New York Public Library studying elliptic functions. Cauer had studied mathematics under Hilbert at Goettingen, and so elliptic functions and their applications were familiar to him" [16].

4.2.1 The AGM and the Complete Elliptic Integral $K(x)$

If the arithmetic and the geometric mean values of two positive numbers x and y are calculated and then we proceed to find the arithmetic and geometric means of these two values and so on ..., then both sequences of mean values converge very rapidly to the same value $M(x, y)$, defined as the *arithmetic-geometric mean* (AGM) of x and y. In fact, we create two sequences from the two positive numbers x and y:

$$a_n = \frac{a_{n-1} + b_{n-1}}{2} \quad \text{and} \quad b_n = \sqrt{a_{n-1} b_{n-1}} \quad \text{with } a_0 = x \text{ and } b_0 = y \tag{4.3}$$

which converge rapidly to the same number, the arithmetic-geometric mean $AGM(x, y)$ or $M(x, y)$.

Some easily proved properties of the AGM are given below:

1. If $\lambda > 0 \Rightarrow \lambda M(x, y) = M(\lambda x, \lambda y)$
2. $M(x, y) = M(\frac{x+y}{2}, \sqrt{xy})$
3. $M(1, x) = \frac{1+x}{2} M(1, \frac{2\sqrt{2}}{1+x})$
4. $M(1, \sqrt{1-x^2}) = M(1-x, 1+x)$

The AGM as "one of the jewels of classical analysis" [2] becomes more precious in elliptic filter design due to the following facts:

i. The sequences of (4.3) converge rapidly with very high accuracy even with 5–6 iterations. For example for $M(0.25, 3.72)$, the same value 1.428762871307 is found after 5 or 55 or 99 iterations.
ii. The AGM has a strange relationship with numbers and functions that cannot be expressed or calculated analytically, as for example π and the complete elliptic integral $K(x)$, which is of special interest in elliptic filter design. It should be noted that the complete elliptic integral $K(x)$ cannot be expressed analytically and therefore its close relationship with the AGM is more than welcome:

$$K(k) = \int_0^{\pi/2} \frac{1}{\sqrt{1 - k^2 \sin^2(\theta)}} d\theta \tag{4.4}$$

$$\text{For } k < 1: \quad K(k) = \frac{\pi}{2M(1, \sqrt{1-k^2})} = \frac{\pi}{M(1-k, 1+k)} \tag{4.5}$$

4.2.2 The Jacobi Nome q (Modular Constant)

In elliptic filter design, it is also necessary to calculate the elliptic parameters $q(x)$, referred to as *modular constants* or *Jacobi Nome* q defined as follows:

$$q(x) = e^{-\pi \frac{K(\sqrt{1-x^2})}{K(x)}} = e^{-\pi \frac{M(1, \sqrt{1-x^2})}{M(1,x)}} \tag{4.6}$$

From (4.6), it is clear that

$$\ln(q(x)) = -\pi \frac{M(1, \sqrt{1-x^2})}{M(1, x)} \tag{4.7}$$

The Nome $q(x)$ can also be calculated using approximate formulae. A very accurate approximation of $q(x)$ has been known since 1902 [10] and is used in [1] and [5]:

$$q_{app1}(x) = \alpha(x) + 2\alpha^5(x) + 15\alpha^9(x) + 150\alpha^{13}(x) \tag{4.8}$$

with

$$\alpha(x) = 0.5\frac{1-(1-x^2)^{0.25}}{1+(1-x^2)^{0.25}}$$

This is a very accurate approximation, especially if one additional term, namely $1707a^{17}(x)$, is included. A rough approximation of $q(x)$ is also used in the elliptic filter design literature [1, 5, 7]:

$$q(x) \approx q_{app2}(x) = \frac{1}{16}x^2 \tag{4.9}$$

This approximate formula is reasonably accurate only for small values of x (e.g. $x < 0.2$) since the error is considerably high for larger values.

4.2.3 Theta Functions and the Jacobi Elliptic Sine $\mathrm{sn}(u, x)$

The Jacobi theta functions are expressed as fast converging infinite series [2, 11] expressed with conventional functions:

$$\theta_o(z, y) = 1 + 2\sum_{m=1}^{\infty}(-1)^m y^{m^2}\cos(2m\pi z) \tag{4.10}$$

$$\theta_1(z, y) = 2y^{\frac{1}{4}}\sum_{m=0}^{\infty}(-1)^m y^{m(m+1)}\sin((2m+1)\pi z)) \tag{4.11}$$

In fact, less than 10 terms are required for the very precise calculation of the θ functions from (4.10) and (4.11).

The elliptic sine $\mathrm{sn}(u, x)$ is related to theta functions θ_o and θ_1 via

$$\mathrm{sn}(u,x) = \frac{1}{\sqrt{x}}\frac{\theta_1(\frac{u}{2K(x)}, q(x))}{\theta_o(\frac{u}{2K(x)}, q(x))} \quad \text{(Nome } q(x) \text{ from (4.6))} \tag{4.12}$$

or

$$\mathrm{sn}(u,x) = \frac{1}{\sqrt{x}}\frac{\theta_1(u\frac{M(1,\sqrt{1-x^2})}{\pi}, e^{-\pi\frac{M(1,\sqrt{1-x^2})}{M(1,x)}})}{\theta_o(u\frac{M(1,\sqrt{1-x^2})}{\pi}, e^{-\pi\frac{M(1,\sqrt{1-x^2})}{M(1,x)}})} \tag{4.13}$$

and therefore can be calculated from theta functions and the AGMs $M(1,k)$ and $M(1,\sqrt{1-k^2})$. Since theta functions can be calculated using a scientific calculator,

the only missing key on scientific calculators is the one for the calculation of the AGM $M(x, y)$. However, it should be noted that the AGM can be calculated even by hand.

4.3 The Elliptic Approximation and the Elliptic Rational Function

The normalized gain function ($\Omega_C = 1$) of the elliptic approximation is given by the general equation

$$G(\Omega) = \frac{H_o}{\sqrt{1 + \varepsilon^2 R_N^2(\Omega_S, \Omega)}} \tag{4.14}$$

where $R_N(\Omega_S, \Omega)$ is the *elliptic rational function* (ERF) or *Chebyshev rational function* of order N. For the purpose of designing elliptic lowpass filters, $R_N(\Omega_S, \Omega)$ can be defined as follows:

$$R_N(\Omega_S, \Omega) = A_N(\Omega_S)\Omega^\eta \prod_{m=1}^{\frac{N-\eta}{2}} \left(\frac{\Omega^2 - \Omega_{ZR}^2(m)}{\Omega^2 - \frac{\Omega_S^2}{\Omega_{ZR}^2(m)}} \right) \tag{4.15}$$

with $\Omega_S > 1$ and

$$\Omega_{ZR}(m) = \mathrm{sn}\left[\left(\frac{2m-1}{N} + 1 \right) K(k), k \right] < 1 \quad \left(k = \frac{1}{\Omega_S} < 1 \right) \tag{4.16}$$

and

$$A_N(\Omega_S) = \prod_{m=1}^{\frac{N-\eta}{2}} \left(\frac{1 - \frac{\Omega_S^2}{\Omega_{ZR}^2(m)}}{1 - \Omega_{ZR}^2(m)} \right) \quad \text{so that } R_N(\Omega_S, 1) = 1 \tag{4.17}$$

The complete elliptic integral $K(x)$ is given by (4.2): $K(x) = \int_0^{\pi/2} \frac{1}{\sqrt{1-x^2\sin^2(\phi)}}\, d\phi$ and parameter η is defined again as

$$\eta = \begin{cases} 0 & \text{for } N \text{ even} \\ 1 & \text{for } N \text{ odd} \end{cases} \tag{4.18}$$

to allow unified expressions for even and odd N.

The only real difficulty in the above definition of $R_N(\Omega_S, \Omega)$ is the calculation of the roots Ω_{ZR} of the numerator from (4.16) due to the elliptic sine sn(). However, when sn() is expressed in terms of theta functions from (4.13), it can be calculated using a scientific calculator (see also (4.34)).

The elliptic rational function $R_N(\Omega_S, \Omega)$ has real pair roots $\pm\Omega_{ZR}$ in the numerator polynomial and real pair roots $\pm\frac{\Omega_S}{\Omega_{ZR}}$ in the denominator polynomial.

Since $R_N(\Omega_S, \Omega)$ is a rational function, (4.14) defines a rational approximation according to (3.1) and (3.5) with

$$F_R(\Omega) = R_N(\Omega_S, \Omega) = \frac{N_R(\omega)}{D_R(\omega)} \tag{4.19}$$

with the apparent definitions

$$N_R(\Omega) = A_N(\Omega_S)\Omega^\eta \prod_{m=1}^{\frac{N-\eta}{2}} (\Omega^2 - \Omega_{ZR}^2(m)) \quad \text{odd or even} \tag{4.20}$$

$$D_R(\Omega) = \prod_{m=1}^{\frac{N-\eta}{2}} \left(\Omega^2 - \frac{\Omega_S^2}{\Omega_{ZR}^2(m)}\right) \quad \text{always even} \tag{4.21}$$

It is clear that if Ω_{ZR} is a root of $N_R(\Omega)$, then Ω_S/Ω_{ZR} is a root of $D_R(\Omega)$ and therefore $\Omega_{ZR}(m)$ for $m = 1, 2, \ldots, \frac{N-\eta}{2}$, fully determine the ERF for given N and Ω_S.

Example 4.1 The elliptic rational functions for $N = 3, 4, 5$ and 6 are

$$R_3(\Omega_S, \Omega) = \frac{A_3(\Omega_S)\Omega(\Omega^2 - \Omega_{ZR1}^2)}{(\Omega^2 - \frac{\Omega_S^2}{\Omega_{ZR1}^2})}$$

$$R_4(\Omega_S, \Omega) = \frac{A_4(\Omega_S)(\Omega^2 - \Omega_{ZR1}^2)(\Omega^2 - \Omega_{ZR2}^2)}{(\Omega^2 - \frac{\Omega_S^2}{\Omega_{ZR1}^2})(\Omega^2 - \frac{\Omega_S^2}{\Omega_{ZR2}^2})}$$

$$R_5(\Omega_S, \Omega) = \frac{A_5(\Omega_S)\Omega(\Omega^2 - \Omega_{ZR1}^2)(\Omega^2 - \Omega_{ZR2}^2)}{(\Omega^2 - \frac{\Omega_S^2}{\Omega_{ZR1}^2})(\Omega^2 - \frac{\Omega_S^2}{\Omega_{ZR2}^2})}$$

$$R_6(\Omega_S, \Omega) = \frac{A_6(\Omega_S)(\Omega^2 - \Omega_{ZR1}^2)(\Omega^2 - \Omega_{ZR2}^2)(\Omega^2 - \Omega_{ZR3}^2)}{(\Omega^2 - \frac{\Omega_S^2}{\Omega_{ZR1}^2})(\Omega^2 - \frac{\Omega_S^2}{\Omega_{ZR2}^2})(\Omega^2 - \frac{\Omega_S^2}{\Omega_{ZR3}^3})}$$

4.4 Properties of the Elliptic Rational Function $R_N(\Omega_S, \Omega)$

Some properties of the elliptic rational function are presented below.

1. The frequency independent coefficient $A_N(\Omega_S)$, given in (4.17), has been calculated so as to make $R_N(\Omega_S, 1) = 1$. For the sign of $A_N(\Omega_S)$, we have:

$$A_N(\Omega_S): \quad \begin{cases} >0 & \text{for even } (N-\eta)/2 \\ <0 & \text{for odd } (N-\eta)/2 \end{cases}$$

Equation (4.17) gives $A_N(\Omega_S)$ in terms of the roots Ω_{ZR}. Equation (4.35) gives an alternative formula for direct calculation from N and Ω_S:

2. $R_N(\Omega_S, 1) = 1$ makes $G(1) = \frac{H_o}{\sqrt{1+\varepsilon^2}}$ (see (4.14))
3. For the roots of the denominator polynomial $D_R(\Omega)$, we have $|\frac{\Omega_S}{\Omega_{ZR}(m)}| > \Omega_S$ since $|\Omega_{ZR}(m)| < 1$.
4. $R_N(\Omega_S, 0) = 0$ for odd N and ± 1 for even N:

$$R_N(\Omega_S, 0) = \begin{cases} \pm 1 & \text{for even } N \\ 0 & \text{for odd } N \end{cases} \tag{4.22}$$

This makes

$$G(0) = H_o(1+\varepsilon^2)^{\frac{\eta-1}{2}} \quad \Rightarrow \quad G(0) = \begin{cases} H_o & \text{for odd } N \\ H_o/\sqrt{1+\varepsilon^2} & \text{for even } N \end{cases} \tag{4.23}$$

5.

$$R_N(\Omega_S, \Omega) R_N\left(\Omega_S, \frac{\Omega_S}{\Omega}\right) = R_N(\Omega_S, \Omega_S) = L_N(\Omega_S) \tag{4.24}$$

6. The value at $\Omega = \Omega_S$, i.e. $R_N(\Omega_S, \Omega_S)$, denoted as $L_N(\Omega_S)$ and referred to as the *discrimination factor*:

$$L_N(\Omega_s) = R_N(\Omega_S, \Omega_S) \tag{4.25}$$

The discrimination factor is always positive and is given by:

$$L_N(\Omega_S) = R_N(\Omega_S, \Omega_S) = \frac{A_N^2(\Omega_S)}{\Omega_S^{N-2\eta}} \prod_{m=1}^{\frac{N-\eta}{2}} \Omega_{ZR}^4(m) > 0 \tag{4.26}$$

or

$$L_N(\Omega_S) = R_N(\Omega_S, \Omega_S) = \frac{1}{\Omega_S^{N-2\eta}} \prod_{m=1}^{\frac{N-\eta}{2}} \left(\frac{\Omega_S^2 - \Omega_{ZR}^2(m)}{1 - \Omega_{ZR}^2(m)} \right)^2 > 0 \tag{4.27}$$

For even N, it is found that

$$L_N(\Omega_S) = |A_N(\Omega_S)| = \Omega_S^N \prod_{m=1}^{\frac{N-\eta}{2}} \Omega_{ZR}^{-4}(m) \quad \text{(only for even } N) \tag{4.28}$$

Alternative formulae for the calculation of $L_N(\Omega_S)$ are given in (4.36) and (4.37).

7. When $\Omega \to \infty$:

$$\lim_{\Omega \to \infty} R_N(\Omega_S, \Omega) = \begin{cases} \infty & \text{for odd } N \Rightarrow G(\infty) = 0 \\ L_N(\Omega_S) = |A_N(\Omega_S)| & \text{for even } N \end{cases} \tag{4.29}$$

For even $N \Rightarrow G(\infty) = \frac{H_o}{\sqrt{1+\varepsilon^2 L_N^2(\Omega_S)}}$

8. For $1 < \Omega < \Omega_S \Rightarrow R_N(\Omega_S, \Omega)$ is positive and monotonically increasing.
9. Roots Ω_{ZR} have been so defined as to make $R_N(\Omega_S, \Omega)$ possess the equal ripple property in the passband expressed as:

$$\left[\begin{array}{l} \text{For } 0 < \Omega < 1,\ R_N(\Omega_S, \Omega) \text{ exhibits equiripple behavior} \\ \text{with maxima of value } +1 \text{ and minima of value } -1, \\ \text{keeping the passband gain of (4.14) between } H_o \text{ and } \dfrac{H_o}{\sqrt{1+\varepsilon^2}}. \end{array}\right] \tag{4.30}$$

Suppose that such a passband maximum of value 1 occurs at Ω_{pex}. Then from (4.24), we have

$$R_N(\Omega_S, \Omega_{pex}) R_N\left(\Omega_S, \frac{\Omega_S}{\Omega_{pex}}\right) = R_N(\Omega_S, \Omega_S) = L_N(\Omega_S) > 0 \tag{4.31}$$

and since $R_N(\Omega_S, \Omega_{pex}) = 1$

$$\Rightarrow \quad R_N\left(\Omega_S, \frac{\Omega_S}{\Omega_{pex}}\right) = R_N(\Omega_S, \Omega_S) = L_N(\Omega_S) > 0$$

Taking into account that the product of the ERF at Ω_{pex} and at Ω_S/Ω_{pex} is constant, when $R_N(\Omega_S, \Omega_{pex}) = 1$ (maximum), it can be concluded that at Ω_S/Ω_{pex} the ERF has a local stopband minimum, namely $R_N(\Omega_S, \frac{\Omega_S}{\Omega_{pex}}) = L_N(\Omega_S) > 0$. Similarly, if at Ω_{pex} the ERF assumes its minimum passband value -1, at Ω_S/Ω_{pex} it assumes a local maximum value equal to $-L_N(\Omega_S)$. Therefore, for each passband extremum of $R_N(\Omega_S, \Omega)$ at Ω_{pex} with value ± 1, there exists a stopband extremum at Ω_S/Ω_{pex} of value $R_N(\Omega_S, \Omega_S) = \pm L_N(\Omega_S)$. At the frequencies Ω_S/Ω_{pex} of the stopband extrema, the stopband gain takes its maximum value, which equals $G(\Omega_S)$:

$$G(\Omega_S) = \frac{H_o}{\sqrt{1+\varepsilon^2 R_N^2(\Omega_S, \Omega_S)}} = \frac{H_o}{\sqrt{1+\varepsilon^2 L_N^2(\Omega_S)}} \tag{4.32}$$

Figures 4.8 and 4.9 help to visualize the nature of the elliptic rational function and its properties.

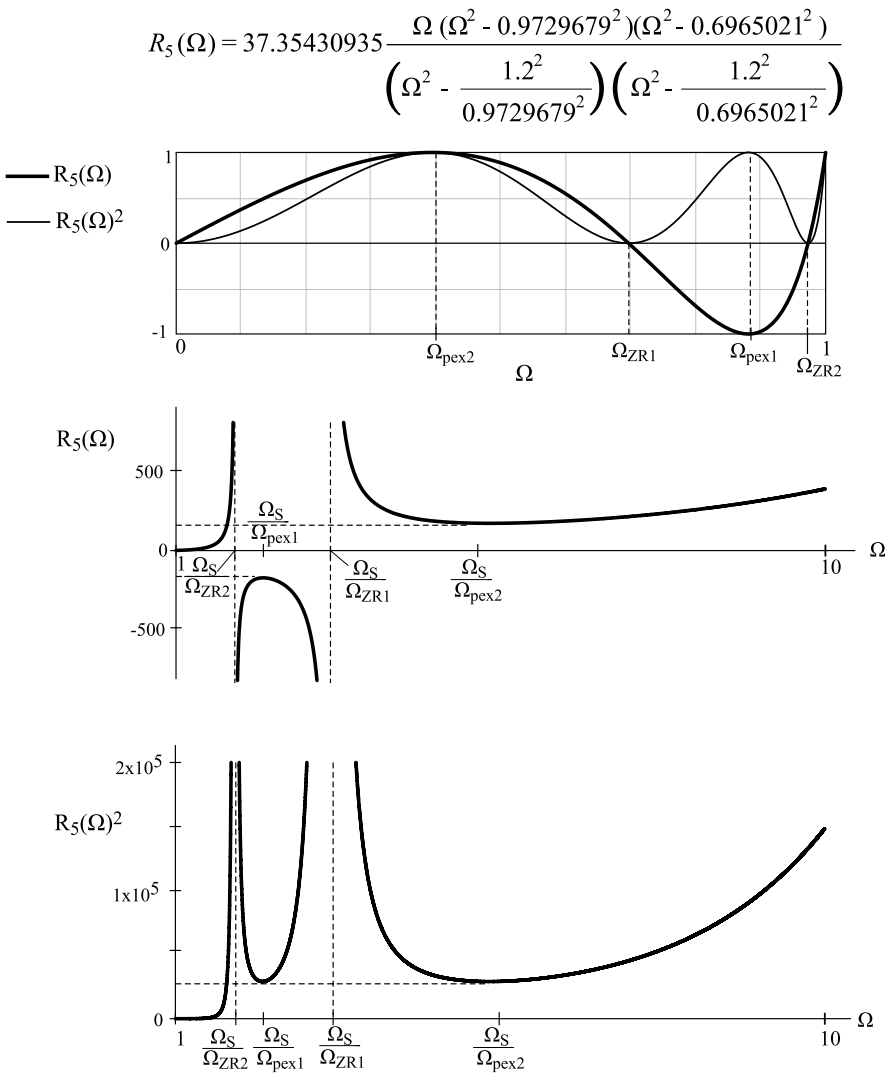

Fig. 4.8 Plots of the elliptic rational function with $N = 5$ and $\Omega_S = 1.2$. Note the Chebyshev-like passband equal ripple of $R_5(\Omega)$ from -1 to 1 and the equal ripple of $R_5^2(\Omega)$ from 0 to 1. Note also the $(N - \eta)/2 = 2$ frequencies at which the ERF and its square assume infinite value and the equal absolute values of the local stopband extrema. This is better described in the plot of $R_5^2(\Omega)$

4.5 Calculations

We saw that the elliptic sine $\mathrm{sn}(u, x)$ can be calculated from (4.12) via the Jacobi theta functions θ_o and θ_1 of (4.10) and (4.11) and the zeros $\Omega_{ZR}(m)$ of the elliptic rational function can be expressed as follows:

$$R_6(\Omega) = \frac{-627.87564(\Omega^2-0.9814215^2)(\Omega^2-0.8025024^2)(\Omega^2-0.3334276^2)}{\left(\Omega^2-\frac{1.2^2}{0.9814215^2}\right)\left(\Omega^2-\frac{1.2^2}{0.8025024^2}\right)\left(\Omega^2-\frac{1.2^2}{0.3334276^2}\right)}$$

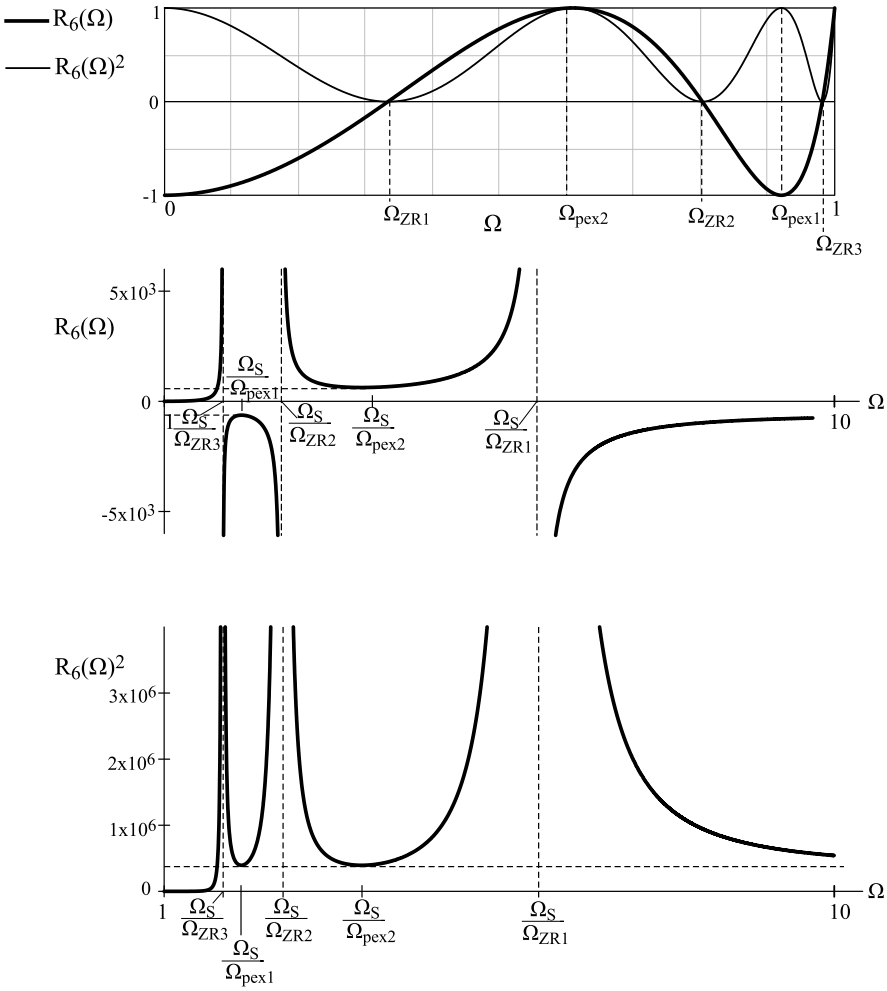

Fig. 4.9 Plots of the elliptic rational function with $N = 6$ and $\Omega_S = 1.2$. Note the Chebyshev-like passband equal ripple of $R_6(\Omega)$ from -1 to 1 and the equal ripple of $R_6^2(\Omega)$ from 0 to 1. Note also the $(N-\eta)/2 = 3$ frequencies at which the ERF and its square assume infinite value and the equal absolute values of the local stopband extrema. This is better described in the plot of $R_6^2(\Omega)$

$$\Omega_{ZR}(m) = \frac{1}{\sqrt{k}} \frac{\theta_1(\frac{2m-1}{2N} + \frac{1}{2}, q(k))}{\theta_o(\frac{2m-1}{2N} + \frac{1}{2}, q(k))} \quad m = 1 \ldots \frac{N-\eta}{2} \tag{4.33}$$

where the Nome $q(1/\Omega_S)$ is given in (4.6) and in the approximate formulae (4.8) and (4.9). Roots Ω_{ZR} can also be expressed in terms of the arithmetic-geometric mean $M(x, y)$, using (4.6):

$$\Omega_{ZR}(m) = \frac{1}{\sqrt{k}} \frac{\theta_1(\frac{2m-1}{2N} + \frac{1}{2}, e^{-\pi(M(1,\sqrt{1-k^2})/M(1,k))})}{\theta_o(\frac{2m-1}{2N} + \frac{1}{2}, e^{-\pi(M(1,\sqrt{1-k^2})/M(1,k))})} \tag{4.34}$$

Having the roots $\Omega_{ZR}(m)$, the coefficient $A_N(\Omega_S)$ can be calculated from (4.17). Alternatively, $A_N(\Omega_S)$ can be calculated without prior knowledge of the roots from:

$$A_N(\Omega_S) = \frac{(-1)^{\frac{N-\eta}{2}}(1/k)^{N-\eta}}{\prod_{m=1}^{\frac{N-\eta}{2}}[\mathrm{sn}^2(\gamma(m)K(k), k)\,\mathrm{sn}^2((\gamma(m) + \frac{\eta}{N})K(k), k)]}$$

$$\text{where } \gamma(m) = \frac{2m-1}{N} + 1 \text{ and } k = \frac{1}{\Omega_S} \tag{4.35}$$

The discrimination factor $L_N(\Omega_S) = R_N(\Omega_S, \Omega_S)$ can be calculated from (4.26) or (4.27). However, it can also be calculated in terms of $\mathrm{sn}(u, x)$, without prior knowledge of the zeros $\Omega_{ZR}(m)$ of the ERF from:

$$L_N(\Omega_S) = \frac{(1/k)^N}{\prod_{m=1}^{(N-\eta)/2} \mathrm{sn}^4((\frac{2m-1+\eta}{N} + 1)K(k), k)} \tag{4.36}$$

$$L_N(\Omega_S) = \frac{1}{k^\eta} \prod_{m=1}^{\frac{N-\eta}{2}} \frac{\theta_o^4[\frac{2m-1+\eta}{2N} + \frac{1}{2}, \mathrm{e}^{-\pi\frac{M(1,\sqrt{1-k^2})}{M(1,k)}}]}{\theta_1^4[\frac{2m-1+\eta}{2N} + \frac{1}{2}, \mathrm{e}^{-\pi\frac{M(1,\sqrt{1-k^2})}{M(1,k)}}]} \tag{4.37}$$

In the above equations (4.33) to (4.37):

$$k = \frac{1}{\Omega_S} \qquad \eta = \begin{cases} 1 & \text{for odd } N \\ 0 & \text{for even } N \end{cases} \qquad m = 1, 2, \ldots, \frac{N-\eta}{2} \tag{4.38}$$

Finally:

1. The calculation of the AGM $M(x, y)$ of two positive numbers x and y can be performed by a 5–6 line program or a simple calculator to make the AGM iteration manually.
2. The theta functions θ_o and θ_1 do not involve any elliptic functions and can be calculated from (4.10) and (4.11) with no more than 9 terms with the aid of a scientific calculator.

Therefore, given N and Ω_S, we can easily calculate:

i. The roots $\Omega_{ZR}(m)$ of the numerator polynomial of $R_N(\Omega_S, \Omega)$ using (4.34)
ii. The coefficient $A_N(\Omega_S)$ using (4.17) (preferably) or (4.35)
iii. The discrimination factor $L_N(\Omega_S)$ from (4.37)

The following example demonstrates the calculation of all parameters of the elliptic approximation.

Example 4.2 Calculate the gain of the elliptic approximation with $N = 6$, $H_o = 1$ and $\Omega_S = 1.2020$ using $\varepsilon = 0.15633$.

$$k = 1/\Omega_S = 0.8319467754 \quad \text{and} \quad \sqrt{1-k^2} = 0.5548554732$$

Let us first calculate the AGM $M(1,k) = M(1, 0.8319467754)$ using a simple calculator. In the first line we write the two positive numbers x and y:

1.0000000000	0.8319467754
0.9159733777	0.9121111530
0.9140422653	0.9140402254
0.9140412454	0.9140412454 $\leftarrow M(1, 0.8319467754)$

In each line after the first, we put the arithmetic and the geometric mean of the two numbers of the proceeding line. It can be seen that the algorithm converges after 2 iterations up to five decimal places and after 3 iterations up to ten decimal places.

We then calculate the AGM $M(1, \sqrt{1-k^2}) = M(1, 0.5548554732)$ with the same method:

1.0000000000	0.5548554732
0.7774277366	0.7448862149
0.7611569758	0.7609830511
0.7610700134	0.7610700084
0.7610700110	0.7610700110 $\leftarrow M(1, 0.5548554732)$

The algorithm converges after 3 iterations up to five digits and after 4 iterations up to ten digits. Finally:

$$M(1,k) = 0.9140412454 \quad \text{and} \quad M(1, \sqrt{1-k^2}) = 0.7610700110$$

and

$$q(k) = e^{-\pi \frac{M(1,\sqrt{1-k^2})}{M(1,k)}} = 0.07310745 \tag{4.39}$$

For the zeros of the ERF, we have from (4.34):

$$\Omega_{ZRm} = \Omega_{ZR}(m) = \sqrt{1.2020}\frac{\theta_1(\frac{N+2m-1}{2N}, 0.07310745)}{\theta_o(\frac{N+2m-1}{2N}, 0.07310745)} \tag{4.40}$$

The theta functions of (4.40) can be calculated from (4.10) and (4.11) using a scientific calculator for $m = 1, 2, 3$ since $(N - \eta)/2 = 3$. Finally, the roots $\Omega_{ZR}(m)$ of the numerator and $\Omega_S/\Omega_{ZR}(m)$ of the denominator are:

$$\Omega_{ZR1} = 0.981344796322 \qquad \Omega_{PR1} = \Omega_S/\Omega_{ZR1} = 1.224849822922$$
$$\Omega_{ZR2} = 0.801964209216 \qquad \Omega_{PR2} = \Omega_S/\Omega_{ZR2} = 1.498820004916$$
$$\Omega_{ZR3} = 0.332940206758 \qquad \Omega_{PR3} = \Omega_S/\Omega_{ZR3} = 3.610257864935$$

From (4.17) (preferably) or (4.35), we can find using a simple scientific calculator:

$$A_6(\Omega_S) = -639.816424030325$$

and from (4.37), in which the second argument of the theta functions has already been calculated (see (4.39)):

$$L_6(\Omega_S) = 639.816424030325 \quad (N \text{ is even } \Rightarrow L_6(\Omega_S) = |A_6(\Omega_S)|)$$

The elliptic rational function with $N = 6$ and $\Omega_S = 1.2020$ will finally be:

$$R_6(\Omega_S, \Omega) = A_6(\Omega_S)\frac{(\Omega^2 - \Omega_{ZR1}^2)(\Omega^2 - \Omega_{ZR2}^2)(\Omega^2 - \Omega_{ZR3}^2)}{(\Omega^2 - \Omega_{PR1}^2)(\Omega^2 - \Omega_{PR2}^2)(\Omega^2 - \Omega_{PR3}^2)} \tag{4.41}$$

The gain function $G(\Omega)$ with $H_o = 1$ and $\varepsilon = 0.15633$ will be:

$$G(\Omega) = \frac{1}{\sqrt{1 + (0.15633)^2 R_6^2(1.202, \Omega)}} \tag{4.42}$$

and will have passband ripple from 1 to $\frac{1}{\sqrt{1+\varepsilon^2}} = 0.988$ and stopband maxima $\frac{1}{\sqrt{1+\varepsilon^2 L_6^2(\Omega_S)}} = 0.01$. The related plots of the plain gain function of (4.42) are shown in Fig. 4.10.

4.6 Specifications and the Order of the Elliptic Approximation

Taking into account that the cutoff frequency Ω_C of the normalized filter is 1 and that H_o is just a reference level usually taken equal to 1 (i.e. $\alpha_o = 20\log(H_o) = 0$ dB), three parameters specify the filter specifications in both cases:

i. The minimum passband gain H_C or the maximum allowed passband dB gain deviation $\alpha_{\max} = 20\log(H_o/H_C)$ from α_o with $\alpha_{\max} > 0$.
ii. The maximum allowed stopband gain H_S or the minimum stopband dB gain deviation $\alpha_{\min} = 20\log(H_o/H_S)$ from α_o with $\alpha_{\min} > 0$.
iii. The normalized stopband edge frequency Ω_S.

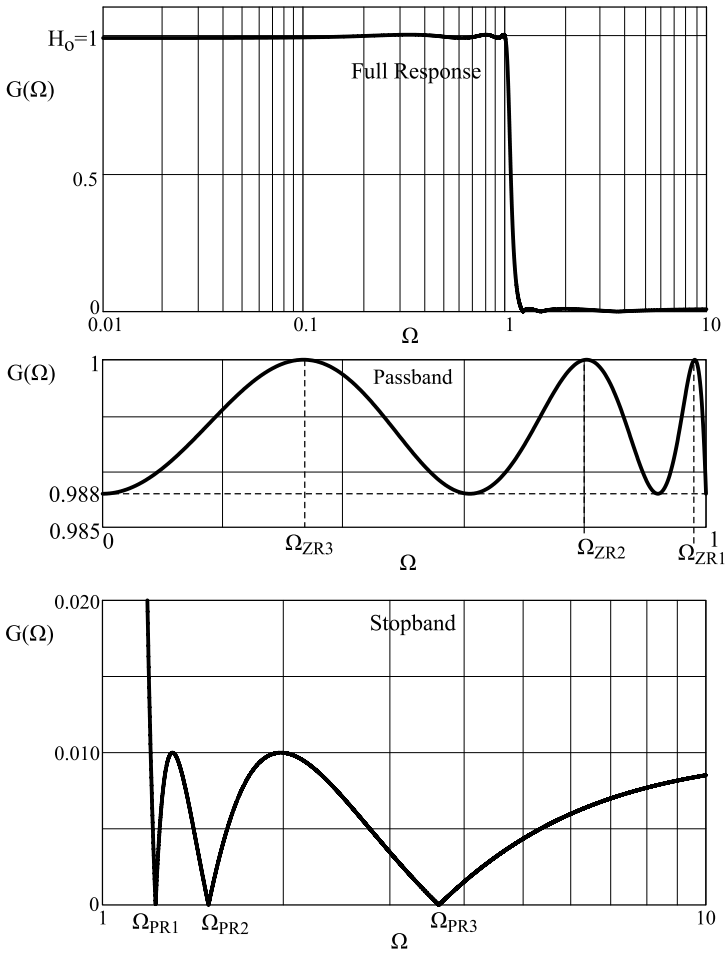

Fig. 4.10 The gain $G(\Omega)$ elliptic approximation of Example 4.2: (**a**) Full response (**b**) passband (**c**) stopband

The normalized lowpass filter specifications are shown in Fig. 4.11.

The gain function of the elliptic approximation has been defined in (4.14) as:

$$G(\Omega) = \frac{H_o}{\sqrt{1 + \varepsilon^2 R_N^2(\Omega_S, \Omega)}} \tag{4.43}$$

Since, by the definition of the elliptic rational function, $R_N(\Omega_S, 1) = 1$, if we require that $G(1) \geq H_C$, the maximum value of ε can be determined:

$$\varepsilon \leq \varepsilon_{\max} = \sqrt{\frac{H_o^2}{H_C^2} - 1} = \sqrt{10^{\frac{\alpha_{\max}}{10}} - 1} \tag{4.44}$$

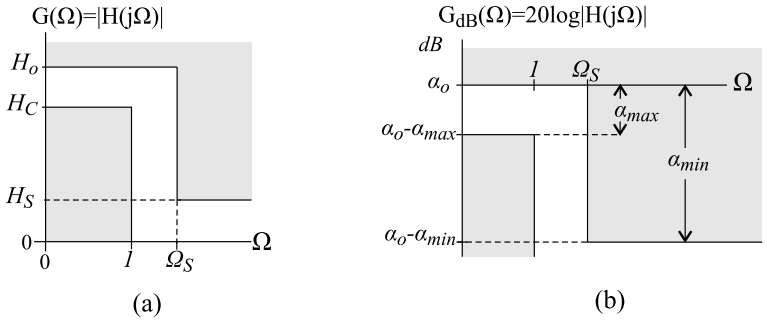

Fig. 4.11 Normalized lowpass specifications: (**a**) Plain gain. (**b**) Logarithmic gain

At the stopband edge frequency Ω_S, we have $R_N(\Omega_S, \Omega_S) = L_N(\Omega_S))$ and the local stopband extrema of $R_N(\Omega_S, \Omega)$ assume the value $\pm L_N(\Omega_S))$. Therefore, in the stopband we have

$$G(\Omega_S) = \frac{H_o}{\sqrt{1 + \varepsilon^2 L_N^2(\Omega_S)}} \tag{4.45}$$

and this is the value of the stopband gain maxima. It is clear from (4.45) that for $\varepsilon = \varepsilon_{\max}$, these maxima assume their minimum value, which can be required to be $\leq H_S$, i.e.:

$$\frac{H_o}{\sqrt{1 + \varepsilon_{\max}^2 L_N^2(\Omega_S)}} \leq H_S \tag{4.46}$$

In this inequality, only N is variable and, if solved for N, yields the order equation. The analytical solution of (4.46) for N is beyond the scope of this textbook but when solved, the decimal order N_d is determined in terms of $K(x)$, the complete elliptic integral of the first kind with modulus x:

$$N \geq N_d = \frac{K(k)}{K(\sqrt{1-k^2})} \cdot \frac{K(\sqrt{1-g^2})}{K(g)} \tag{4.47}$$

where

$$k = \frac{1}{\Omega_S} \quad \text{and} \quad g = \sqrt{\frac{(H_o/H_C)^2 - 1}{(H_o/H_S)^2 - 1}} = \sqrt{\frac{10^{\alpha_{\max}/10} - 1}{10^{\alpha_{\min}/10} - 1}} \tag{4.48}$$

The order equation (4.47) involves the complete elliptic integral $K(x)$ with $x < 1$, and due to (4.5) does not present any calculation difficulty. Under (4.5), the awkward order equation (4.47) for elliptic filters is transformed into an easily computed expression requiring only calculation of four arithmetic-geometric means:

$$N \geq N_d = \frac{M(1, \sqrt{1-g^2}) \cdot M(1, k)}{M(1, g) \cdot M(1, \sqrt{1-k^2})} \tag{4.49}$$

In this equation with $k = 1/\Omega_S < 1$, $g \ll 1$ is given in (4.48) and $M(x, y)$ stands for the AGM of the positive numbers x and y defined in (4.3).

The order equation can also be expressed in terms of the Jacobi Nome $q(x)$ of (4.6). At the beginning of the design, two $q(x)$'s can be calculated directly from the specifications:

$$\begin{aligned} q_k &= q(k) = q\left(\frac{1}{\Omega_S}\right) \\ q_g &= q(g) = q\left(\sqrt{\frac{(H_o/H_C)^2 - 1}{(H_o/H_S)^2 - 1}}\right) = q\left(\sqrt{\frac{10^{\frac{\alpha_{\max}}{10}} - 1}{10^{\frac{\alpha_{\min}}{10}} - 1}}\right) \end{aligned} \tag{4.50}$$

Since $k < 1$ and $g < 1$, (4.6) provides a very straightforward and fast way to calculate them with high accuracy using AGMs.

Using (4.7), the exact order equation (4.47) can also be expressed as:

$$N \geq N_d = \frac{\ln(q_g)}{\ln(q_k)} = \frac{\log(q_g)}{\log(q_k)} \tag{4.51}$$

with q_k and q_g from (4.50).

The calculation of the decimal order N_d using (4.47), (4.49) or (4.51) is exact and involves only calculation of arithmetic-geometric means. However, (4.51) can be simplified by introducing the approximate formulas (4.8) or (4.9) for the calculation of q_g and (4.8) for q_k. Approximation (4.9) cannot be used for q_k since the value of $k = 1/\Omega_S$ is usually higher than 0.6 and the approximation error is very high. Using (4.9) for the numerator and (4.8) for the denominator of (4.51), we get the approximate formula found in the literature [1, 5, 7]:

$$N \geq N_{appr0} = \frac{\log(q_{app2}(g))}{\log(q_{app1}(1/\Omega_S))} = \frac{\log(\frac{1}{16}g^2)}{\log[q_{app1}(1/\Omega_S)]} \tag{4.52}$$

The use of this approximation is vindicated since usually $g < 0.01$ leads to adequately accurate results. Of course, the usage of (4.8) in both the numerator and denominator of (4.51) would give a more accurate result:

$$N \geq N_{appr1} = \frac{\log(q_{app1}(g))}{\log(q_{app1}(1/\Omega_S))} \tag{4.53}$$

To demonstrate the precision of each order calculation formula, we used (4.49), (4.52) and (4.53) in a small program with the normalized LP specifications $\Omega_S = 1.202$, $H_o = 1$, $H_C = 0.988(\alpha_{\max} = 0.104861108$ dB), $H_S = 0.02$ ($\alpha_{\min} = 33.9790$ dB). The results are shown below:

$$\begin{aligned} N_d &= 5.469709951526 \quad \text{from (4.49)} \\ N_{appr0} &= 5.469709951521 \quad \text{from (4.52)} \\ N_{appr1} &= 5.469711820835 \quad \text{from (4.53)} \end{aligned}$$

The order of the filter will of course be rounded up to $N = 6$. It should be noted that the calculation of the four AGMs of (4.49) were performed with less than 5 iterations.

4.7 Elliptic Filter Design Optimization

Now that we have a good insight of the elliptic rational function $R_N(\Omega_S, \Omega)$, we can analyse the gain function of the elliptic approximation given in (4.14) so as to see how it can be made to satisfy certain specifications. Given the specifications Ω_S and $\{H_o, H_C, H_S\}$ or $\{\alpha_o, \alpha_{\max}, \alpha_{\min}\}$, the order of the approximation can be calculated from the order equation (4.47) or the alternative formulae presented in Sect. 4.6. When order N has been calculated from the specifications, elliptic approximation can be optimized so as to meet certain criteria and exhibit different characteristics.

The gain function of the elliptic approximation has been defined in (4.14) as

$$G(\Omega) = \frac{H_o}{\sqrt{1 + \varepsilon^2 R_N^2(\Omega_S, \Omega)}} \tag{4.54}$$

Moreover, the maximum value $\varepsilon_{\max}$ of the ripple factor ε has already been found and is given in (4.44), repeated here for convenience:

$$\varepsilon \le \varepsilon_{\max} = \sqrt{\frac{H_o^2}{H_C^2} - 1} = \sqrt{10^{\frac{\alpha_{\max}}{10}} - 1} \tag{4.55}$$

If we require that $G(\Omega_S)$, and therefore all the stopband maxima, must be below the specified H_S, we get

$$\begin{aligned} G(\Omega_S) &= \frac{H_o}{\sqrt{1 + \varepsilon^2 L_N^2(\Omega_s)}} \le H_S \\ \Rightarrow \quad \varepsilon &\ge \frac{\sqrt{(H_o/H_S)^2 - 1}}{L_N(\Omega_S)} = \varepsilon_{\min} \end{aligned} \tag{4.56}$$

Using the minimum value $\varepsilon_{\min}$, the stopband ripple will be from 0 to H_S and the passband ripple from H_o to $H_{C\max} > H_C$:

$$\varepsilon = \varepsilon_{\min} \quad \Rightarrow \quad G(1) = H_{C\max} = \frac{H_o}{\sqrt{1 + \frac{(H_o/H_S)^2 - 1}{L_N^2(\Omega_S)}}} \ge H_C \tag{4.57}$$

Finally, the ripple factor ε must be selected to satisfy

$$\frac{\sqrt{(H_o/H_S)^2 - 1}}{L_N(\Omega_S)} = \varepsilon_{\min} \le \varepsilon \le \varepsilon_{\max} = \sqrt{\frac{H_o^2}{H_C^2} - 1}$$

or in terms of the logarithmic gain specifications (4.58)

$$\frac{\sqrt{10^{\frac{\alpha_{\min}}{10}}-1}}{L_N(\Omega_S)} = \varepsilon_{\min} \le \varepsilon \le \varepsilon_{\max} = \sqrt{10^{\frac{\alpha_{\max}}{10}}-1}$$

From (4.58) we get

$$L_N(\Omega_S) \ge \frac{1}{g} \quad \Rightarrow \quad L_N(\Omega_S) \ge \sqrt{\frac{10^{\frac{\alpha_{\min}}{10}}-1}{10^{\frac{\alpha_{\max}}{10}}-1}} \tag{4.59}$$

which, for given N, relates the three specified quantities: $\{\Omega_S, \alpha_{\max}, \alpha_{\min}\}$. If we want to investigate the conditions under which the equality holds, i.e.

$$L_N(\Omega_S) = 1/g \quad \Rightarrow \quad L_N(\Omega_S) = \sqrt{\frac{10^{\frac{\alpha_{\min}}{10}}-1}{10^{\frac{\alpha_{\max}}{10}}-1}} \tag{4.60}$$

we can keep two of the three quantities $\{\Omega_S, \alpha_{\max}, \alpha_{\min}\}$ and determine the third so as to make $L_N(\Omega_S) = 1/g$.

Case A. When $\{\Omega_S, \alpha_{\max}\}$ and N are specified, then $\alpha_{\min}$ can be calculated from (4.60) using (4.26) or (4.27) so as to make $L_N(\Omega_S) = 1/g$. If this value is denoted as $\alpha_{\min 0}$, we find

$$\alpha_{\min 0} = 10\log\left[(10^{\alpha_{\max}/10}-1)L_N^2(\Omega_S)+1\right] \ge \alpha_{\min} \tag{4.61}$$

which corresponds to the minimum stopband plain gain ripple that can be achieved with N and $\{\Omega_S, \alpha_{\max}\}$

$$H_{S\min} = G(\Omega_S) = \frac{H_o}{\sqrt{1+(H_o^2/H_C^2-1)L_N^2(\Omega_S)}} \le H_S \tag{4.62}$$

This means that when we are given the specifications $\{\Omega_S, \alpha_{\max}, \alpha_{\min}\}$, a better filter of the same order N can be designed with specifications $\{\Omega_S, \alpha_{\max}, \alpha_{\min 0} > \alpha_{\min}\}$ or, in terms of plain gain, $\{\Omega_S, H_o, H_C, H_{S\min} < H_S\}$. This filter is the *stopband edge frequency gain optimized* [8] and is designed using $\varepsilon = \varepsilon_{\max}$. Figure 4.12 shows the gain plot of this design.

Case B. When $\{\Omega_S, \alpha_{\min}\}$ and N are specified, then $\alpha_{\max}$ can be calculated from (4.60) so as to make $L_N(\Omega_S) = 1/g$. If this value is denoted as $\alpha_{\max 0}$, we find

$$\alpha_{\max 0} = 10\log\left[\frac{10^{\alpha_{\min}/10}-1}{L_N^2(\Omega_S)}+1\right] \le \alpha_{\max} \tag{4.63}$$

This is the minimum passband ripple and corresponds to plain gain variation between H_o and $H_{C\max}$ when Ω_S and $\alpha_{\min}$ are given:

$$H_{C\max} = G(1) = \frac{H_o}{\sqrt{1+\frac{H_o^2/H_S^2-1}{L_N^2(\Omega_S)}}} \ge H_C \tag{4.64}$$

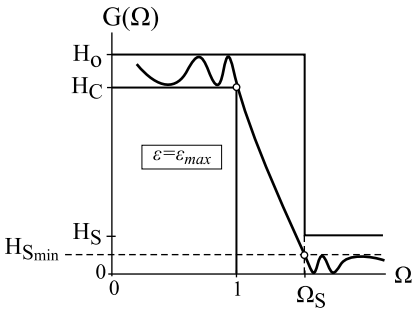

Fig. 4.12 Case A: $\varepsilon = \varepsilon_{\max}$ (stopband edge frequency gain optimization)

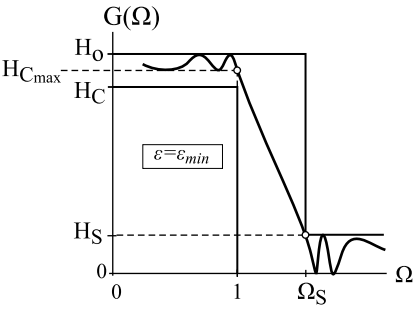

Fig. 4.13 Case B: $\varepsilon = \varepsilon_{\min}$ (passband optimization)

This means that when we are given the specifications $\{\Omega_S, \alpha_{\max}, \alpha_{\min}\}$, a better filter of the same order N can be designed with specifications $\{\Omega_S, \alpha_{\max 0} < \alpha_{\max}, \alpha_{\min}\}$ or, in terms of plain gain, $\{\Omega_S, H_o, H_{C\max} > H_C, H_S\}$. This filter is the *passband optimized* and is designed using $\varepsilon = \varepsilon_{\min}$ [8]. Figure 4.13 shows the gain of such a passband optimized design.

Case C. When $\{\alpha_{\max}, \alpha_{\min}\}$ and N are specified, then the minimum stopband edge frequency $\Omega_{S\min}$ can be calculated from (4.60) so as to make $L_N(\Omega_{S\min}) = 1/g$. This means that when we are given the specifications $\{\Omega_S, \alpha_{\max}, \alpha_{\min}\}$, a better filter of the same order N can be designed with specifications $\{\Omega_{S\min} < \Omega_S, \alpha_{\max}, \alpha_{\min}\}$ or equivalently, in terms of plain gain $\{\Omega_{S\min} < \Omega_S, H_o, H_C, H_S\}$. This filter is the *transition band optimized* [8]. Figure 4.14 shows the gain of such a transition band optimized design.

To determine $\Omega_{S\min}$, equation

$$L_N(\Omega_S) = 1/g \quad \Rightarrow \quad L_N(\Omega_S) = \sqrt{\frac{10^{\frac{\alpha_{\min}}{10}} - 1}{10^{\frac{\alpha_{\max}}{10}} - 1}} \tag{4.65}$$

must be solved for Ω_S. The root $\Omega_{S\min}$, if used in the order equation with the value of g calculated from the specified $\alpha_{\max}$ and $\alpha_{\min}$, gives integer $N_d = N$. In this case, $k = 1/\Omega_{S\min}$ can be calculated from (4.47) with

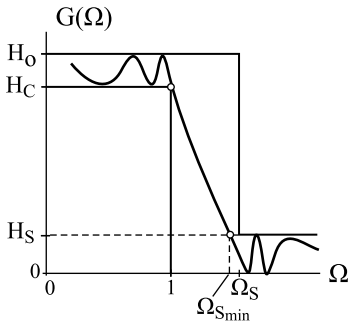

Fig. 4.14 Case C: Transition band optimization

integer N:

$$\frac{K(k)}{K(\sqrt{1-k^2})} \cdot \frac{K(\sqrt{1-g^2})}{K(g)} = N \tag{4.66}$$

To find $k = 1/\Omega_{S\min}$, (4.66) must be solved for $k = 1/\Omega_{S\min}$.

Finally, to calculate the minimum stopband edge frequency $\Omega_{S\min}$ from $\{N, \alpha_{\max}, \alpha_{\min}\}$, either (4.65) or (4.66) must be solved. This is not an easy task and (4.66) was only solved analytically in 2004 by Huber [9]:

$$\Omega_{S\min} = \frac{1}{\sqrt{1 - \frac{1}{L_N^2(\Omega_g)}}} \quad \text{where } \Omega_g = \frac{1}{\sqrt{1-g^2}} \tag{4.67}$$

If the filter is designed with specifications $\{\Omega_{S\min}, \alpha_{\max}, \alpha_{\min}\}$, then $\varepsilon_{\min} = \varepsilon_{\max}$ and the gain of the elliptic approximation will fully cover the specified passband and the stopband tolerances, with steeper transition band gain since the gain assumes the value H_S at $\Omega_{S\min} < \Omega_S$.

Example 4.3 Given $\{\Omega_S = 1.2020, H_o = 1, H_C = 0.988, H_S = 0.02\}$, we find $N = 6$. From (4.67) we find $\Omega_{S\min} = 1.13606967$, meaning that the transition band optimized elliptic filter can be designed with $\{\Omega_S = 1.13606967, H_o = 1, H_C = 0.988, H_S = 0.02\}$ from which we find $N = 6$ and $\varepsilon_{\min} = \varepsilon_{\max} = 0.15633$.

4.7.1 Stopband Optimization $\Omega_{S\max}$

One more optimization can be performed in the elliptic approximation. Let us consider that we have the stopband edge frequency optimized design with $\varepsilon = \varepsilon_{\max}$ of Case A (Fig. 4.12) where the stopband maxima and $G(\Omega_S)$ assume equal values $H_{S\min}$ (see (4.62)), lower than the specified H_S. This design is shown in Fig. 4.15a.

The frequency Ω_{Hs} at which $G(\Omega_{Hs}) = H_S$ satisfies the relation

$$G(\Omega_{Hs}) = \frac{H_o}{\sqrt{1 + \varepsilon_{\max}^2 R_N^2(\Omega_S, \Omega_{Hs})}} = H_S \quad \Rightarrow \quad R_N(\Omega_S, \Omega_{Hs}) = \frac{1}{g} \tag{4.68}$$

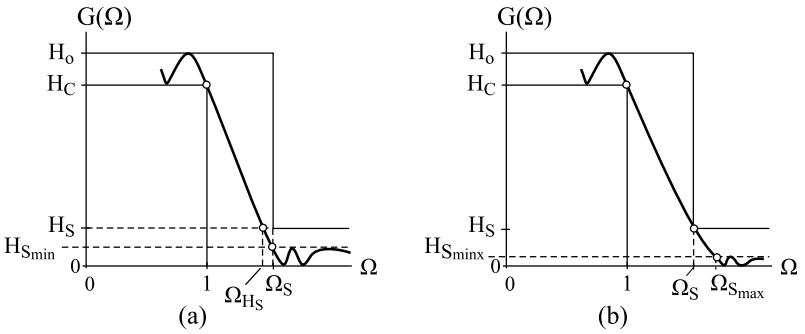

Fig. 4.15 (**a**) Stopband edge frequency optimized design. (**b**) Stopband optimized design

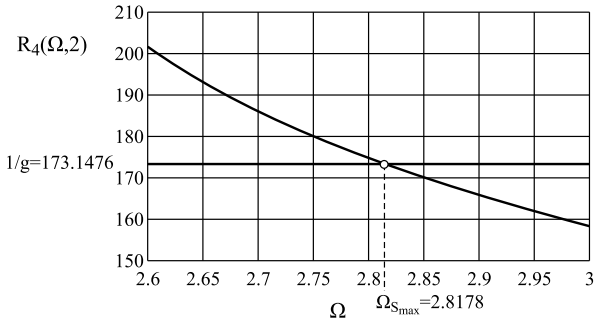

Fig. 4.16 Graphical calculation of the maximum stopband edge frequency

If we drag Ω_{Hs} to the right until the curve touches the point $\{\Omega_S, H_S\}$, frequency Ω_{Hs} becomes equal to Ω_S and the frequency at which the gain becomes equal to the stopband maxima moves to a frequency $\Omega_{S\max} > \Omega_S$. Moreover, the stopband maxima will decrease to the value

$$H_{S\min x} = \frac{H_o}{\sqrt{1+\varepsilon_{\max}^2 L_N^2(\Omega_{S\max})}} < H_{S\max} < H_S \tag{4.69}$$

This situation is shown in Fig. 4.15b.

In order to find $\Omega_{S\max}$, we set $\Omega_S = \Omega_{S\max}$ and $\Omega_{Hs} = \Omega_S$ in (4.68), which after some manipulation becomes

$$R_N(\Omega_{S\max}, \Omega_S) = \frac{1}{g} \tag{4.70}$$

This equation cannot be solved analytically for $\Omega_{S\max}$ and the use of mathematical software is inevitable. Figure 4.16 shows a way to calculate $\Omega_{S\max}$ graphically for $\Omega_S = 2$ and $H_o = 1 H_C = 0.86596432$ and $H_S = 0.01$ or $\alpha_{\max} = 1.25$ dB, $\alpha_{\min} = 40$ dB which require $N = 4$. It is found that parameter $g = 0.005775 \Rightarrow 1/g = 173.1476$. Curves $R_4(2, \Omega)$ and line $1/g$ intersect at the frequency $\Omega_{S\max} = 2.8178$.

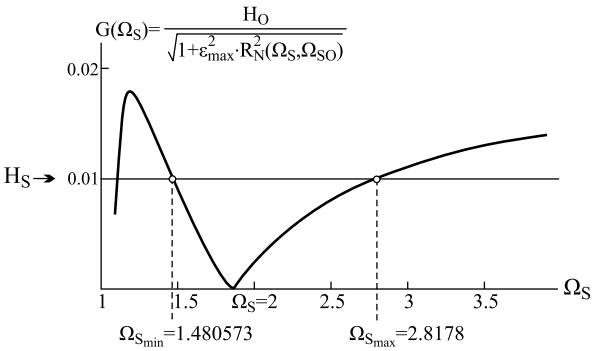

Fig. 4.17 Graphical determination of $\Omega_{S\min}$ and $\Omega_{S\max}$

Therefore, if absolute minimum stopband ripple is required, the filter can be designed using $\Omega_{S\max}$ instead of the specified Ω_S without change of the order. Elliptic filters designed with $\Omega_{S\max}$ are referred to as *stopband optimized* [8].

For a specific order N and stopband edge frequency Ω_{S0}, the gain at Ω_{S0} can be seen as a function of Ω_S, the parameter used in the definition of the ERF, i.e.

$$G(\Omega_S) = \frac{H_o}{\sqrt{1 + \varepsilon_{\max}^2 R_N^2(\Omega_S, \Omega_{S0})}}$$

The two boundary frequencies $\Omega_{S\min}$ and $\Omega_{S\max}$ can then be determined graphically as shown in Fig. 4.17. For this example, we have used the specifications $\Omega_{S0} = 2$, $H_o = 1 (\alpha_o = 0)$, $H_C = 0.86596432$ ($\alpha_{\max} = 1.25$ dB) and $H_S = 0.01$ ($\alpha_{\min} = 40$ dB), which require $N = 4$.

Example 4.4 Given the normalized lowpass specifications $\Omega_S = 2.0$ and

$$\{H_o = 1, H_C = 0.86596432, H_S = 0.01\} \quad \text{or} \quad \{\alpha_{\max} = 1.25 \text{ dB}, \alpha_{\min} = 40 \text{ dB}\}$$

from (4.47), expressed with AGMs in equation (4.49), we find $N_d = 3.2548 \Rightarrow N = 4$. From (4.37) $\Rightarrow L_N(\Omega_S) = L_4(2) = 773.9781$ and from (4.58), we find $\varepsilon_{\min} = 0.12919616$ and $\varepsilon_{\max} = 0.577513$. Equation (4.67) gives $\Omega_{S\min} = 1.480573$, and using the graphical method described above we find $\Omega_{S\max} = 2.8178$ (see Figs. 4.16 and 4.17).

For the four optimized designs we find:

1. Design with $\varepsilon = \varepsilon_{\max} = 0.577513 \Rightarrow H_{S\min} = 0.002237$ (53.0058 dB)
2. Design with $\varepsilon = \varepsilon_{\min} = 0.12919616 \Rightarrow H_{C\max} = 0.99175$ (0.0719 dB)
3. Design with $\Omega_S = \Omega_{S\min} = 1.480573 \Rightarrow L_4(1.480573) = 173.1476$
4. Design with $\Omega_S = \Omega_{S\max} = 2.8178 \Rightarrow L_4(2.8178) = 3532.783 \Rightarrow H_{S\min x} = 0.00049$ (66.1936 dB)

Figure 4.18 shows the passband and stopband details of the plain gain. The curves have been numbered in the same order as the above design results.

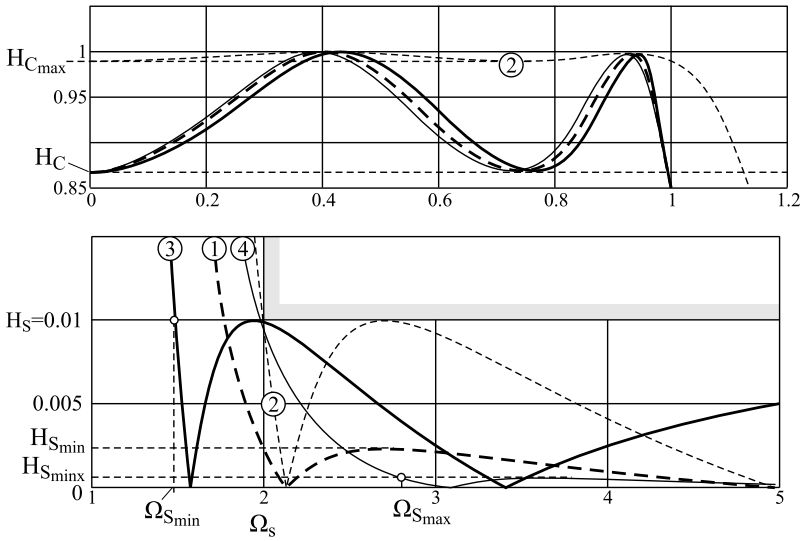

Fig. 4.18 Passband and stopband details of elliptic filter of Example 4.4 (curve numbers correspond to the numbering of the design results)

4.8 The Transfer Function

The elliptic rational function $R_N(\Omega_S, \Omega)$, as defined in (4.15), is a rational function. Therefore (4.14) defines a rational approximation according to (3.1) and (3.5) of Sect. 4.3 of the previous chapter, with:

$$F_R(\Omega) = R_N(\Omega_S, \Omega) = \frac{N_R(\omega)}{D_R(\omega)} \tag{4.71}$$

Polynomials $N_R(\Omega)$ and $D_R(\Omega)$ are given in (4.20) and (4.21) respectively:

$$N_R(\Omega) = A_N(\Omega_S)\Omega^\eta \prod_{m=1}^{\frac{N-\eta}{2}} (\Omega^2 - \Omega_{ZR}^2(m)) \quad \text{(odd or even)} \tag{4.72}$$

$$D_R(\Omega) = \prod_{m=1}^{\frac{N-\eta}{2}} \left(\Omega^2 - \frac{\Omega_S^2}{\Omega_{ZR}^2(m)}\right) \quad \text{(always even)} \tag{4.73}$$

where $\eta = \begin{cases} 0 \text{ for } N \text{ even} \\ 1 \text{ for } N \text{ odd} \end{cases}$ and $\Omega_{ZR}(m)$ the zeros of the elliptic rational function given in (4.16) and calculated from (4.34). Taking into account that

- Polynomial $N_R(\Omega)$ is of even or odd degree N and has $N - \eta$ non-zero roots $\Omega_{ZR}(m)$ and one zero root at $\Omega = 0$ when N is odd ($\eta = 1$),
- The coefficient of the highest order term of $N_R(\Omega)$ is $A_N(\Omega_S)$,
- Polynomial $D_R(\Omega)$ is of even degree $N - \eta$ and has $(N - \eta)$ roots $\Omega_S/\Omega_{ZR}(m)$,

• The coefficient of the highest order term of $D_R(\Omega)$ is 1,
then, according to (3.19), the corresponding transfer function will be

$$H(s) = C \cdot \frac{\prod_{m=1}^{\frac{N-\eta}{2}} (s^2 + \frac{\Omega_S^2}{\Omega_{ZR}^2(m)})}{\prod_{m=1}^{N} (s - p(m))} \tag{4.74}$$

where

$$C = \frac{H_o}{\sqrt{\varepsilon^2 A_N^2(\Omega_S) + 1 - \eta}} \tag{4.75}$$

The poles $p(m)$ of $H(s)$ are the left half s-plane roots of the even denominator polynomial of (3.8), repeated here and adapted for the needs of the elliptic approximation:

$$\begin{aligned} &D_R^2(\Omega)|_{\Omega^2=-s^2} + \varepsilon^2 N_R^2(\Omega)|_{\Omega^2=-s^2} \quad \text{or} \\ &\prod_{m=1}^{N-\eta} \left(s^2 + \frac{\Omega_S^2}{\Omega_{ZR}^2(m)} \right) + \varepsilon^2 A_N^2(\Omega_S)(-s^2)^\eta \prod_{m=1}^{N-\eta} (s^2 + \Omega_{ZR}^2(m)) \end{aligned} \tag{4.76}$$

The polynomial of (4.76) is of even degree $2N$ and therefore has N root pairs: N roots in the left half s-plane and their opposite N roots in the right half s-plane. If N is odd, then one of the root pairs is real of the form $\pm\Omega_R$. If the rest of the transfer function poles $p(m)$ are the $(N-\eta)/2$ conjugate pairs with $\sigma_H(m) \le 0$:

$$p(m) = \sigma_H(m) + j\Omega_H(m) \quad \text{and} \quad p^*(m) = \sigma_H(m) - j\Omega_H(m) \tag{4.77}$$

then the transfer function of (4.74) can be expressed as

$$H(s) = \frac{C \prod_{m=1}^{\frac{N-\eta}{2}} (s^2 + \frac{\Omega_S^2}{\Omega_{ZR}^2(m)})}{(s + \Omega_R)^\eta \prod_{m=1}^{\frac{N-\eta}{2}} (s - p(m))(s - p^*(m))} \tag{4.78}$$

or

$$H(s) = \frac{C \prod_{m=1}^{\frac{N-\eta}{2}} (s^2 + \frac{\Omega_S^2}{\Omega_{ZR}^2(m)})}{(s + \Omega_R)^\eta \prod_{m=1}^{\frac{(N-\eta)}{2}} (s^2 - 2\sigma_H(m)s + \sigma_H^2(m) + \Omega_H^2(m))} \tag{4.79}$$

Expressing the conjugate pole pairs $p(m) = \sigma_H(m) \pm j\Omega_H(m)$ in terms of their pole frequency and quality factor

$$\Omega_o(m) = \sqrt{\sigma_H^2(m) + \Omega_H^2(m)} \quad Q_o(m) = \frac{\Omega_o(m)}{2\,|\sigma_H(m)|} \tag{4.80}$$

the transfer function will be

$$H(s)=\frac{C\prod_{m=1}^{\frac{N-\eta}{2}}(s^2+\frac{\Omega_S^2}{\Omega_{ZR}^2(m)})}{(s+\Omega_R)^{\eta}\prod_{m=1}^{\frac{(N-\eta)}{2}}(s^2+\frac{\Omega_o(m)}{Q_o(m)}s+\Omega_o^2(m))} \tag{4.81}$$

As in all approximations, the calculation of the poles of $H(s)$ as the roots of a polynomial of the form of (4.76) of degree $2N$ is the most laborious task. For the elliptic approximation, for the calculation of $\Omega_o(m)$ and $Q_o(m)$ of the poles of the transfer function, the commonly used procedure has been adopted with serious modifications so as to make use of the already calculated parameters of the ERF $R_N(\Omega_S,\Omega)$. The details of the solution can be found in [1], where calculation is based on the fact that $1/L_N(\Omega_S)$ is very small. This is true since in practice the discrimination factor $L_N(\Omega_S)$ assumes very high values and in the end, the calculated values for the pole frequencies $\Omega_o(m)$ and the pole quality factors $Q_o(m)$ are very accurate.

Initially, the quantity

$$\Lambda=\frac{1}{2\pi N}\ln\left(\frac{\sqrt{\varepsilon^2+1}+1}{\sqrt{\varepsilon^2+1}-1}\right) \tag{4.82}$$

is calculated. If the maximum ripple factor $\varepsilon_{\max}$ of (4.58) is used, then:

$$\Lambda=\frac{1}{2\pi N}\ln\left(\frac{H_o+H_C}{H_o-H_C}\right)=\frac{1}{2\pi N}\ln\left(\frac{10^{\alpha_{\max}/20}+1}{10^{\alpha_{\max}/20}-1}\right)\quad\text{(only for }\varepsilon_{\max}\text{)} \tag{4.83}$$

The quantity Λ is then used for the calculation of another auxiliary parameter σ:

$$\sigma=\frac{\theta_{1h}(\Lambda,q(1/\Omega_S))}{\theta_{0h}(\Lambda,q(1/\Omega_S))} \tag{4.84}$$

Theta functions θ_{0h} and θ_{1h} are similar to the theta functions defined in (4.10) and (4.11) with the unique difference that they use hyperbolic sinh and cosh instead of their simple trigonometric counterparts:

$$\theta_{0h}(z,y)=1+2\sum_{m=1}^{m_{\max}=\infty}(-1)^m y^{m^2}\cosh[2m\pi z] \tag{4.85}$$

$$\theta_{1h}(z,y)=2y^{\frac{1}{4}}\sum_{m=0}^{m_{\max}=\infty}(-1)^m y^{m(m+1)}\sinh[(2m+1)\pi z] \tag{4.86}$$

Functions θ_{0h} and θ_{1h} also converge rapidly, even using 9 terms, i.e. $m_{\max}=9$.

Calculation of the parameter σ is slightly complicated since it requires the calculation of Nome $q(1/\Omega_S)$. This value, however, has been calculated during the determination of the order and can always be calculated from (4.6) or from the very accurate approximate formula (4.8).

Having parameter σ, the next equations give the poles in terms of their frequencies $\Omega_o(m)$ and quality factors $Q_o(m)$.

$$\Omega_o(m) = \frac{\Omega_S}{\Omega_{ZR}(m)} \sqrt{\frac{\sigma^2 + \frac{\Omega_{ZR}^2}{\Omega_S}}{\sigma^2 + \frac{\Omega_S}{\Omega_{ZR}^2}}} = \sqrt{\Omega_S \frac{\Omega_S \sigma^2 + \Omega_{ZR}^2(m)}{\Omega_S + \sigma^2 \Omega_{ZR}^2(m)}} \tag{4.87}$$

$$Q_o(m) = \frac{1}{2\sigma} \sqrt{\sigma^2 + \frac{\Omega_{ZR}^2(m)(\Omega_S + \sigma^2)(1 + \Omega_S \sigma^2)}{(\Omega_{ZR}^2(m) - \Omega_S^2)(\Omega_{ZR}^2(m) - 1)}} \tag{4.88}$$

or

$$Q_o(m) = \frac{\Omega_{ZR}(m)}{2\sigma} \sqrt{\frac{(\sigma^2 + \frac{\Omega_{ZR}^2}{\Omega_S})(\sigma^2 + \frac{\Omega_S}{\Omega_{ZR}^2})}{\Omega_S (1 - \frac{\Omega_{ZR}^2(m)}{\Omega_S^2})(1 - \Omega_{ZR}^2(m))}} \tag{4.89}$$

Index m in (4.87)–(4.89): $m = 1, 2, \ldots, \frac{N-\eta}{2}$

The poles of $H(s)$ expressed as complex numbers will be

$$p(m) = \sigma_H(m) \pm j\Omega_H(m) = -\frac{\Omega_o(m)}{2Q_o(m)} \pm j\Omega_o(m) \sqrt{1 - \frac{1}{4Q_o^2(m)}} \tag{4.90}$$

If N is odd, the real pole of $H(s)$ at $s_0 = -\Omega_R$ of (4.81) is given by

$$s_0 = -\Omega_R \quad \text{with } \Omega_R = \sigma\sqrt{\Omega_S} \tag{4.91}$$

It is clear that the determination of the transfer function using (4.87)–(4.89) requires only knowledge of parameter σ and the zeros Ω_{ZR} of the elliptic rational function $R_N(\Omega_S, \Omega)$. This is very important since the zeros Ω_{ZR} have already been calculated earlier in any design from (4.16) or (4.34).

Constant C of the transfer function can be calculated from (4.75), but in order to absorb any inaccuracies of the calculations of the poles, it is preferable to be calculated from an expression involving the poles. This expression can be derived by using (4.23)

$$G(0) = H(0) = H_o(1 + \varepsilon^2)^{\frac{\eta-1}{2}} \tag{4.92}$$

to finally find

$$C = \frac{H_o \sigma^\eta}{(1 + \varepsilon^2)^{\frac{1-\eta}{2}} \Omega_S^{\frac{2N-3\eta}{2}}} \prod_{m=1}^{\frac{N-\eta}{2}} [\Omega_{ZR}^2(m) \Omega_o^2(m)] \tag{4.93}$$

Example 4.5 Given the normalized lowpass specifications

$$\Omega_S = 1.8, \qquad H_o = 1, \qquad H_C = 0.988, \qquad H_S = 0.02$$

we find $N = 4$ and $\varepsilon_{\max} = 0.15632983$. $A_N(\Omega_S) = A_4(1.8) = 470.45040854$ is calculated from (4.17) and the roots $\Omega_{ZR}(m)$ from (4.34). For the calculated values, the elliptic rational function $R_4(1.8, \Omega)$ will be:

$$R_4(1.8, \Omega) = 470.45040854 \frac{(\Omega^2 - 0.93567074^2)(\Omega^2 - 0.41306747^2)}{(\Omega^2 - 1.92375364^2)(\Omega^2 - 4.35764165^2)}$$

Polynomial of (4.76), with $\eta = 0$, since $N = 4$ becomes

$$(\Omega^2 - 1.92375364^2)(\Omega^2 - 4.35764165^2) + 0.15632983^2 \cdot 470.45039716^2 \cdot (\Omega^2 - 0.93567074^2)(\Omega^2 - 0.41306747^2)$$

The roots of the above polynomial are calculated using a mathematical software package, and the left hand half s-plane roots are

$$-0.671556207 \pm j0.553890978 \quad \text{with } \Omega_{o1} = 0.870507297 \text{ and } Q_{o1} = 0.648126909$$

and

$$-0.202311475 \pm j1.111407969 \quad \text{with } \Omega_{o2} = 1.129671459 \text{ and } Q_{o2} = 2.791911247$$

From (4.75), we find $C = 0.01359578034$

If (4.87)–(4.89) are used for the calculation of the two conjugate pole pairs of $H(s)$, we find:

$-0.671\mathbf{5}70457 \pm j0.5538\mathbf{9}6944$ with $\Omega_{o1} = 0.87052\mathbf{2}09$ and $Q_{o1} = 0.64812\mathbf{4}17$

and

$-0.20231\mathbf{4}754 \pm j1.1114\mathbf{1}4375$ with $\Omega_{o2} = 1.12967\mathbf{8}35$ and $Q_{o2} = 2.791\mathbf{8}8325$

The values calculated from (4.87)–(4.89) are accurate up to the 5th or 6th decimal place. If these poles are used for the transfer function, constant C must be calculated from (4.93), which gives $C = 0.01359\mathbf{6}408$, a value that differs from the previous in the 6th decimal place.

Example 4.6 Design an elliptic filter to meet the following specifications:

$$\Omega_S = 1.7, \qquad H_o = 1, \qquad H_C = 0.99, \qquad H_S = 0.01$$

or equivalently

$$\Omega_S = 1.7, \qquad \alpha_o = 1, \qquad \alpha_{\max} = 0.087296 \text{ dB}, \qquad \alpha_{\min} = 40 \text{ dB}$$

Order Calculation

$$k = 1/\Omega_S = 1/1.7 = 0.58823529 \qquad g = \frac{\sqrt{H_o^2/H_C^2 - 1}}{\sqrt{H_o^2/H_S^2 - 1}}$$

$$\Rightarrow \quad g = \frac{\sqrt{1^2/0.99^2 - 1}}{\sqrt{1^2/0.01^2 - 1}} = 0.00142499$$

Using $k = 0.5882352$, $\sqrt{1-k^2} = 0.80868983$ and $g = 0.00142499$, $\sqrt{1-g^2} = 0.99999898$, the order can be calculated from (4.49). The AGMs can be calculated by a few iterations even by hand, as we did in Example 4.1.

$$M(1, 0.5882352) = 0.78048228 \qquad M(1, 0.80868983) = 0.90180659$$

$$M(1, 0.00142499) = 0.19783614 \qquad M(1, 0.99999898) = 0.99999949$$

$$\Rightarrow \quad N_d = \frac{0.99999949}{0.19783614} \cdot \frac{0.78048228}{0.90180659} = 4.374655$$

Therefore, the integer order will be taken $N = 5 \Rightarrow \eta = 1$.

Order N and Ω_S Dependent Parameters The ERF will have $(N - \eta)/2 = 2$ zeros calculated from (4.16), or preferably from (4.34), since we already have the necessary $M(1, k) = M(1, 0.5882352) = 0.78048228$ and $M(1, \sqrt{1-k^2}) = M(1, 0.80868983) = 0.90180659$:

$$\Omega_{ZR}(1) = 0.96003616 \qquad \Omega_{ZR}(2) = 0.62811501$$

$$\frac{\Omega_S}{\Omega_{ZR}(1)} = 1.77076664 \qquad \frac{\Omega_S}{\Omega_{ZR}(2)} = 2.70651072$$

From (4.17) or (4.35), we find

$$A_N(\Omega_S) = A_5(1.7) = 284.82104688$$

From (4.26) or (4.27) or (4.36) or (4.37) (preferably from the last since the necessary AGMs in the theta functions are already available):

$$L_N(\Omega_S) = L_5(1.7) = 2183.254839$$

The calculated quantities up to here determine the elliptic rational function and do not depend on the value of the ripple factor ε but only on Ω_S. The value of the ripple factor affects the transfer function calculated below for the two boundary values $\varepsilon_{\max}$ and $\varepsilon_{\min}$

A. Calculation of the Transfer Function with $\varepsilon = \varepsilon_{\max}$ (The Stopband Edge Frequency Gain Optimized Filter)

$$\varepsilon_{\max} = \sqrt{H_o^2/H_C^2 - 1} = \sqrt{1^2/0.99^2 - 1} = 0.14249228$$

From (4.62), the stopband plain gain maxima and $G(\Omega_S)$ will have the value

$$H_{S\min} = G(\Omega_S) = \frac{H_o}{\sqrt{1 + (H_o^2/H_C^2 - 1)L_N^2(\Omega_S)}}$$

$$\Rightarrow \quad H_{S\min} = \frac{1}{\sqrt{1 + (1^2/0.99^2 - 1)L_5^2(1.7)}} = 0.003214 < H_S = 0.01$$

or $H_{S\min} = G(1) = H_o/\sqrt{1+\varepsilon_{\max}^2} = 1/\sqrt{1 + 0.14249228^2} = 0.003214$. $H_{S\min}$ corresponds to $\alpha_{\min 0} = 49.85796 \geq \alpha_{\min} = 40$ dB.

From (4.82) $\Rightarrow \Lambda = 0.16849113$ and from (4.84) $\Rightarrow \sigma = 0.48788888$.

With these values, we find from (4.87)–(4.89) the frequencies and the quality factors of the $(N-\eta)/2 = 2$ pole pairs:

Pole Pair 1

$$\Omega_o(1) = 1.08384858 \qquad Q_o(1) = 4.164298$$

$$\Rightarrow \quad p(1) = -0.130135809 + j1.076007625$$

This pole pair contributes to the transfer function the term

$$s^2 + \frac{1.08384858}{4.164298}s + 1.08384858^2 = s^2 + 0.26027162s + 1.08384858^2$$

Pole Pair 2

$$\Omega_o(2) = 0.87025924 \qquad Q_o(2) = 0.99827726$$

$$\Rightarrow \quad p(2) = -0.43588053 + j0.753232571$$

This pole pair contributes to the transfer function the term

$$s^2 + \frac{0.87025924}{0.99827726}s + 0.87025924^2 = s^2 + 0.87176106s + 0.87025924^2$$

Since $N = 5$ is odd, a real pole will also exist (4.91):

$$s_0 = -\sigma\sqrt{\Omega_S} = -0.63612927$$

The constant C of the transfer function can now be calculated from (4.92) with $\varepsilon = \varepsilon_{\max} = 0.14249228$:

$$C = 24.63983088 \cdot 10^{-3}$$

Finally, from (4.81), the transfer function for $\varepsilon = \varepsilon_{\max} = 0.14249228$ will be:

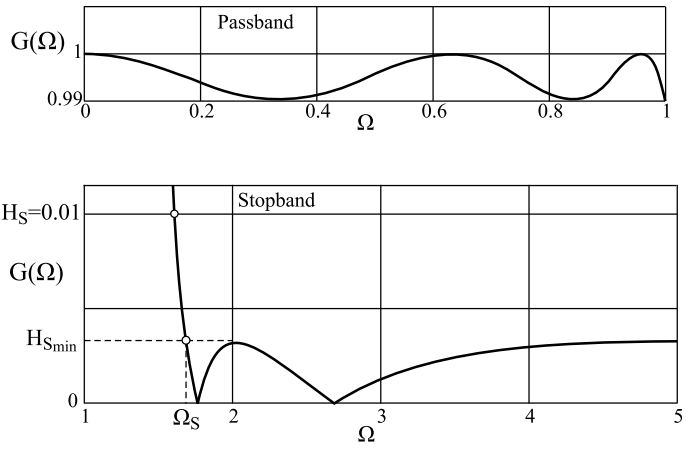

Fig. 4.19 Gain plot from transfer function $H_1(s)$ with $\varepsilon = \varepsilon_{\max}$

$$H_1(s) = \frac{24.639831 \cdot 10^{-3}(s^2 + 1.770767^2)(s^2 + 2.706511^2)}{(s + 0.636129)(s^2 + 0.260272s + 1.083849^2)(s^2 + 0.871766s + 0.870259^2)}$$

Figure 4.19 shows the gain of the stopband edge frequency optimized elliptic filter which meets the stopband specifications with $H_{S\min} < H_S$.

B. Calculation of the Transfer Function with $\varepsilon = \varepsilon_{\min}$ (The Passband Gain Optimized Filter)

$$\varepsilon_{\min} = \frac{\sqrt{H_o^2/H_S^2 - 1}}{L_N(\Omega_S)} = \frac{\sqrt{10^{\alpha_{\min}/10} - 1}}{L_N(\Omega_S)} = \frac{\sqrt{10^{40/10} - 1}}{L_N(\Omega_S)} = 0.04580088$$

From (4.64), the passband plain gain minima and $G(1)$ will have the value

$$H_{C\max} = G(1) = \frac{H_o}{\sqrt{1 + \frac{H_o^2/H_S^2 - 1}{L_N^2(\Omega_S)}}} = \frac{1}{\sqrt{1 + \frac{1^2/0.01^2 - 1}{2183.254839}}} = 0.99895279 > H_C$$

or $H_{C\max} = G(1) = H_o/\sqrt{1 + \varepsilon_{\min}^2} = 1/\sqrt{1 + 0.04580088^2} = 0.99895279$.

$H_{C\max}$ corresponds to $\alpha_{\max 0} = 0.0091 \le \alpha_{\max} = 0.087296$ dB.

From (4.82) $\Rightarrow \Lambda = 0.24045912$ and from (4.84) $\Rightarrow \sigma = 0.7627331$.

With these values, we find from (4.87)–(4.89) the frequencies and the quality factors of the $(N - \eta)/2 = 2$ pole pairs:

Pole Pair 1

$$\Omega_o(1) = 1.20520833 \qquad Q_o(1) = 3.45087706$$
$$\Rightarrow \quad p(1) = -0.174623481 + j1.192490565$$

This pole pair contributes to the transfer function the term

$$s^2 + \frac{1.20520833}{3.45087706}s + 1.20520833^2 = s^2 + 0.349247s + 1.20520833^2$$

Pole Pair 2

$$\Omega_o(2) = 1.10406059 \qquad Q_o(2) = 0.87134937$$
$$\Rightarrow \quad p(2) = -0.633534966 + j0.904203095$$

This pole pair contributes to the transfer function the term

$$s^2 + \frac{1.10406059}{0.87134937}s + 1.10406059^2 = s^2 + 1.267067s + 1.10406059^2$$

Since $N = 5$ is odd, a real pole also exists

$$s_0 = -\sigma\sqrt{\Omega_S} = -0.994482$$

The constant C of the transfer function is calculated from (4.92) with $\varepsilon = \varepsilon_{\min} = 0.04580088$:

$$C = 76.65931781 \cdot 10^{-3}$$

Finally, from (4.81), the transfer function for $\varepsilon = \varepsilon_{\min} = 0.04580088$ will be:

$$H_2(s) = \frac{76.65931781 \cdot 10^{-3}(s^2 + 1.770767^2)(s^2 + 2.706511^2)}{(s + 0.994482)(s^2 + 0.349247s + 1.205208^2)(s^2 + 1.267067s + 1.104061^2)}$$

Figure 4.20 shows the gain of the passband optimized elliptic filter which meets the passband specifications with $H_{C\max} > H_C$.

C. Calculation of the Transfer Function with $\Omega_{S\min}$ (The Transition Band Optimized Filter) From (4.67) and $g = 0.00142499$, we get

$$\Omega_g = \frac{1}{\sqrt{1 - g^2}} = \frac{1}{\sqrt{1 - 0.00142499^2}} = 1.0000010153$$

Using $N = 5$ and $k = 1/\Omega_g = 0.9999989847$ in (4.36) or (4.37), we find $L_5(0.9999989847) = 1.39767786$ and therefore (4.67) yields

$$\Omega_{S\min} = \frac{1}{\sqrt{1 - \frac{1}{L_N^2(\Omega_g)}}} = \frac{1}{\sqrt{1 - \frac{1}{1.39767786^2}}} = 1.4313504$$

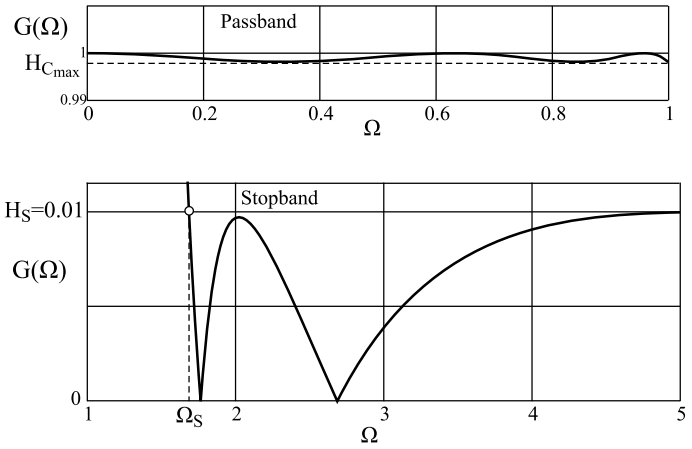

Fig. 4.20 Gain plot from transfer function $H_2(s)$ with $\varepsilon = \varepsilon_{\min}$

The filter must now be redesigned with the same magnitude specifications but with $\Omega_S = \Omega_{S\min} = 1.4313504$. Although it is not necessary to recalculate the order, if it is calculated it will be found that $N_d = 4.99999999$, practically $5 \Rightarrow N = 5$. The $(N - \eta)/2 = 2$ zeros of the ERF are calculated from (4.16) or (4.34). Since Ω_S is no longer 1.7, all quantities related to Ω_S must be recalculated. Finally, we find:

$$\Omega_{ZR}(1) = 0.96462678 \qquad \Omega_{ZR}(2) = 0.65076878$$

$$\frac{\Omega_S}{\Omega_{ZR}(1)} = 1.48383854 \qquad \frac{\Omega_S}{\Omega_{ZR}(2)} = 2.19947615$$

From (4.17) or (4.35), we find

$$A_N(\Omega_{S\min}) = A_5(1.4313504) = 115.11724131$$

From (4.26) or (4.27) or (4.36) or (4.37):

$$L_N(\Omega_{S\min}) = L_5(1.4313504) = 701.757313$$

When $\Omega_{S\min}$ is used, the boundary values of the ripple factor become equal, i.e. $\varepsilon_{\min} = \varepsilon_{\max} = \varepsilon = \sqrt{H_o^2/H_C^2 - 1} = \sqrt{1^2/0.99^2 - 1} = 0.14249228$. Moreover, $H_{S\min} = H_S$ and $H_{C\max} = H_C$, meaning that the passband and stopband tolerances are fully reached.

From (4.82) $\Rightarrow \Lambda = 0.16849113$ and from (4.84), $\sigma = 0.57504894$. With these values, we find from (4.87)–(4.89) the frequencies and the quality factors of the two pole pairs:

Pole Pair 1

$$\Omega_o(1) = 1.07491324 \qquad Q_o(1) = 4.87337$$
$$\Rightarrow \quad p(1) = -0.110284386 + j\,1.069240772$$

This pole pair contributes to the transfer function the term

$$s^2 + \frac{1.07491324}{4.87337}s + 1.07491324^2 = s^2 + 0.220569s + 1.07491324^2$$

Pole Pair 2

$$\Omega_o(2) = 0.90382277 \qquad Q_o(2) = 1.06634799$$
$$\Rightarrow \quad p(2) = -0.423793536 + j0.798307361$$

This pole pair contributes to the transfer function the term

$$s^2 + \frac{0.90382277}{1.06634799}s + 0.90382277^2 = s^2 + 0.847587s + 0.90382277^2$$

Since $N = 5$ is odd, a real pole also exists:

$$s_0 = -\sigma\sqrt{\Omega_S} = -0.687983$$

The constant C of the transfer function can now be calculated from (4.92) with $\varepsilon = 0.14249228$:

$$C = 60.96482924 \cdot 10^{-3}$$

Finally, from (4.81), the transfer function will be:

$$H_3(s) = \frac{60.96482924 \cdot 10^{-3}(s^2 + 1.48383854^2)(s^2 + 2.19947615^2)}{(s + 0.687983)(s^2 + 0.220569s + 1.074913^2)(s^2 + 0.847587s + 0.903823^2)}$$

Figure 4.21 shows the gain of the transition band optimized elliptic filter designed with $\Omega_{S\min} < \Omega_S$.

D. Calculation of the Transfer Function with $\Omega_{S\max}$ (The Stopband Optimized Filter) In order to calculate $\Omega_{S\max}$, (4.70) must be solved. In fact, the value Ω must be found for which

$$R_N(\Omega, \Omega_S) = \frac{1}{g}$$

This equation cannot be solved analytically for Ω, and the use of mathematical software is inevitable. Figure 4.22 shows the graphical solution, from which we find

$$\Omega_{S\max} = 1.856427$$

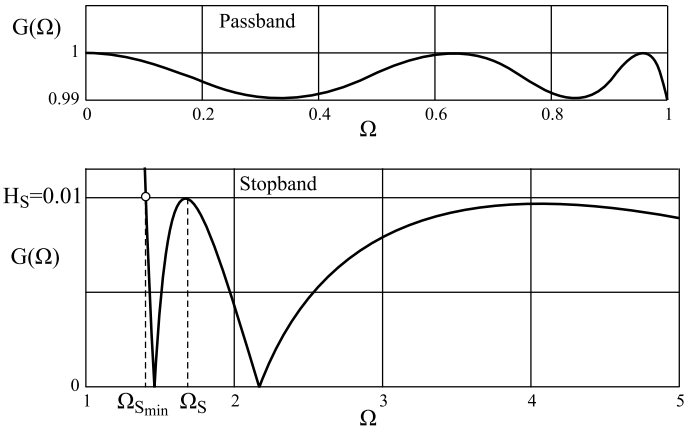

Fig. 4.21 Gain plot from transfer function $H_3(s)$ of the filter designed with $\Omega_{\min}$

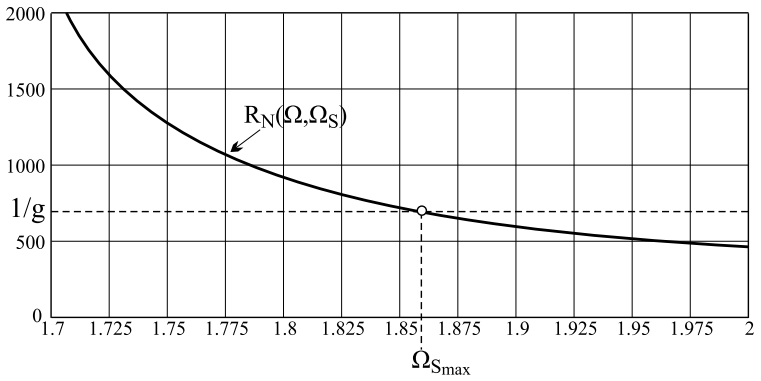

Fig. 4.22 Graphical calculation of $\Omega_{S\max}$

The filter must now be redesigned with the same magnitude specifications but with $\Omega_S = \Omega_{S\max} = 1.856427$. Although there is no need to recalculate the order, if it is calculated it will be found that $N_d = 4.131013642 \Rightarrow N = 5$. Since the purpose of this design is to minimize the stopband gain, $\varepsilon_{\max} = 0.142492$ must be used. The two zeros of the ERF are calculated as in the previous designs from (4.16) or (4.34) but with $\Omega_S = \Omega_{S\max} = 1.856427$. Since Ω_S is no longer equal to 1.7, all quantities related to Ω_S must be recalculated. Finally, we find:

$$\Omega_{ZR}(1) = 0.95840529 \qquad \Omega_{ZR}(2) = 0.62042454$$

$$\frac{\Omega_S}{\Omega_{ZR}(1)} = 1.93699578 \qquad \frac{\Omega_S}{\Omega_{ZR}(2)} = 2.99218824$$

From (4.17) or (4.35) we find

$$A_N(\Omega_{S\max}) = A_5(1.856427) = 436.83228444$$

From (4.26) or (4.27) or (4.36) or (4.37):

$$L_N(\Omega_{S\max}) = L_5(1.856427) = 3728.623175$$

From (4.82) $\Rightarrow \Lambda = 0.16849113$ and from (4.84) $\Rightarrow \sigma = 0.45473624$.

With these values, we find from (4.87)–(4.89) the frequencies and the quality factors of the two pole pairs:

Pole Pair 1

$$\Omega_o(1) = 1.08698361 \qquad Q_o(1) = 3.95583441$$
$$\Rightarrow \quad p(1) = -0.137389928 + j1.078265911$$

This pole pair contributes to the transfer function the term

$$s^2 + \frac{1.08698361}{3.95583441}s + 1.08698361^2 = s^2 + 0.27478s + 1.08698361^2$$

Pole Pair 2

$$\Omega_o(2) = 0.85860319 \qquad Q_o(2) = 0.97757845$$
$$\Rightarrow \quad p(2) = -0.439147974 + j0.737799764$$

This pole pair contributes to the transfer function the term

$$s^2 + \frac{0.85860319}{0.97757845}s + 0.85860319^2 = s^2 + 0.878296s + 0.85860319^2$$

Since $N = 5$ is odd, a real pole also exists:

$$s_0 = -\sigma\sqrt{\Omega_S} = -0.619582$$

The constant C of the transfer function can now be calculated from (4.92) with $\varepsilon = 0.14249228$:

$$C = 16.06550276 \cdot 10^{-3}$$

Finally, from (4.81), the transfer function for the stopband optimized filter will be:

$$H_4(s) = \frac{16.06550276 \cdot 10^{-3}(s^2 + 1.93699578^2)(s^2 + 2.99218824^2)}{(s + 0.619582)(s^2 + 0.27478s + 1.086984^2)(s^2 + 0.878296s + 0.8586032^2)}$$

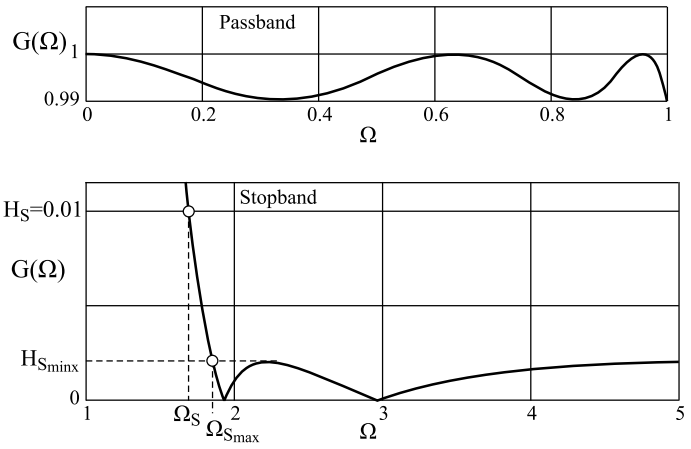

Fig. 4.23 Gain plot from transfer function $H_4(s)$ of the filter designed with $\Omega_{\min}$

Figure 4.23 shows the gain of the stopband optimized elliptic filter designed with $\Omega_{S\max} = 1.856427 > \Omega_S$ which meets the specifications with minimum stopband gain.

According to (4.81), the transfer functions of elliptic filters, i.e. filters designed with the elliptic approximation, have the general form:

$$H(s) = \frac{C(s^2+\Omega_{PR1}^2)(s^2+\Omega_{PR2}^2)\cdots(s^2+\Omega_{PRx}^2)}{(s+\Omega_R)^\eta(s^2+\frac{\Omega_{o1}}{Q_{o1}}s+\Omega_{o1}^2)(s^2+\frac{\Omega_{o2}}{Q_{o2}}s+\Omega_{o2}^2)\cdots(s^2+\frac{\Omega_{ox}}{Q_{ox}}s+\Omega_{ox}^2)} \tag{4.94}$$

where $\Omega_{PRi} = \frac{\Omega_S}{\Omega_{ZRi}}$ and $x = (N-\eta)/2$.

The resemblance of the elliptic transfer function of (4.94) to that of the inverse Chebyshev and inverse Pascal should be noted.

The transfer function of (4.94) can be realized by cascading a first order section to realize the real pole in the case of odd N, and $(N-\eta)/2$ second order notch sections as becomes clear from (4.95):

$$H(s) = \frac{C_0}{(s+\Omega_R)^\eta} \times \frac{C_1(s^2+\Omega_{PR1}^2)}{(s^2+\frac{\Omega_{o1}}{Q_{o1}}s+\Omega_{o1}^2)} \times \cdots \times \frac{C_x(s^2+\Omega_{PRx}^2)}{(s^2+\frac{\Omega_{ox}}{Q_{ox}}s+\Omega_{ox}^2)}$$

$$\text{with } C_0C_1C_2\cdots C_{(N-\eta)/2} = C,\ \Omega_{PRi} = \frac{\Omega_S}{\Omega_{ZRi}} \text{ and } x = (N-\eta)/2 \tag{4.95}$$

Filters designed using the elliptic approximation as presented in this chapter are referred to as "Case A" elliptic filters. The corresponding transfer functions are not suitable for ladder passive-LC realization when N is even, and require the employment of ideal transformers. This is due to the fact that when N is even, the gain for

$\Omega \to \infty$ is not zero but assumes the value $H_o/\sqrt{1+\varepsilon^2 L_N^2(\Omega_S)}$ (see (4.29)) while in passive LC ladder filters the gain for $\omega \to \infty$ is expected to be zero.

Using a special transformation which moves the higher transmission zero to infinity leads to "Case B" elliptic filters. Another transformation which maps the frequency of the lowest passband gain maximum to zero leads to "Case C" elliptic filters. The reason we do not deal with Case B and Case C elliptic filters is that they are not important in modern filter design and in addition, due to the transformations, they do not perform as well as the Case A elliptic filters. Given the specifications of a passive filter, if the order N is calculated to be even, it is preferable to design a filter of odd order $N+1$.

4.9 Elliptic Filter Design Aids

Although today everybody has access to a personal computer and mathematical software like MATLAB, Mathcad, Maple, Mathematica etc., that can perform the necessary calculations, elliptic filter design can be facilitated in the traditional way by using the available tables and nomographs.

4.9.1 The Order Nomograph

If the order equation (4.47) seems difficult, even in its AGM form of (4.49), the nomograph of Fig. 4.24 can be used. We first calculate $20\log(\frac{1}{g})$ where g is given in (4.48), repeated here for convenience:

$$g = \sqrt{\frac{(H_o/H_C)^2 - 1}{(H_o/H_S)^2 - 1}} = \sqrt{\frac{10^{\alpha_{\max}/10} - 1}{10^{\alpha_{\min}/10} - 1}} \tag{4.96}$$

Then we draw a horizontal line from the point of the vertical axis that corresponds to $HP = 20\log(\frac{1}{g})$. Finally, a vertical line is drawn from the point of the horizontal axis that corresponds to the specified Ω_S. The two lines intersect at a point which lies between two curves. The number of the upper curve is the integer order of the approximation. This is shown in Fig. 4.25, where for $HP = 46$ and $\Omega_S = 1.7$, the order is $N = 4$.

If for $\varepsilon = \varepsilon_{\max}$ we require the plain gain at $\Omega = \Omega_S$ to be less or equal to the specified H_S, i.e. $G(\Omega_S) \le H_S$, then we end up with the inequality (4.46), which yields the order inequality

$$R_N(\Omega_S, \Omega_S) \ge \frac{1}{g}$$

or

$$20\log(R_N(\Omega_S, \Omega_S)) \ge 20\log(1/g) \tag{4.97}$$

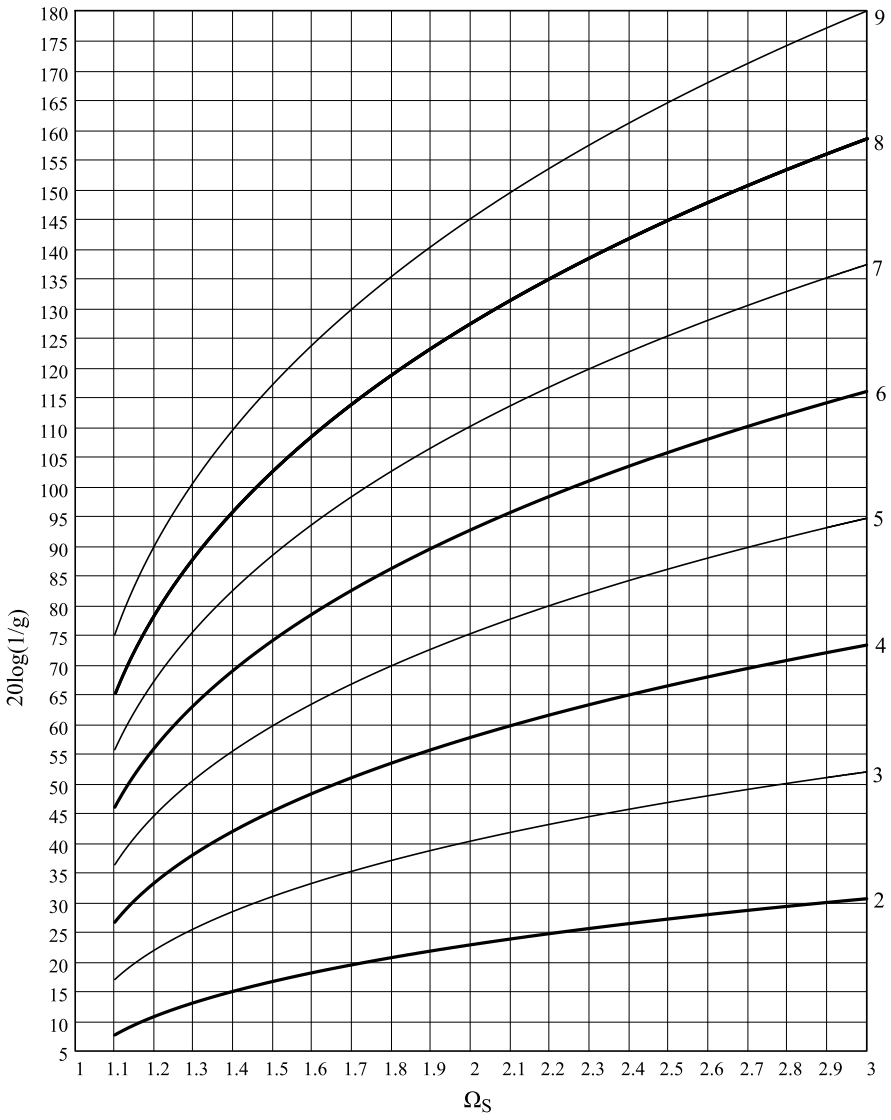

Fig. 4.24 Nomograph for the calculation of the order

It should be noted that $R_N(\Omega_S, \Omega_S)$ is the discrimination factor $L_N(\Omega_S)$ and is a positive quantity according to (4.26). The curves of the order nomograph are in fact the plots of $20\log(R_N(\Omega_S, \Omega_S))$ for various values of the order N. Using the nomograph in the described manner, we determine the minimum integer order N for which the order inequality (4.97) is valid. The determination of the order from the nomograph cannot be very accurate, especially if the point of intersection turns

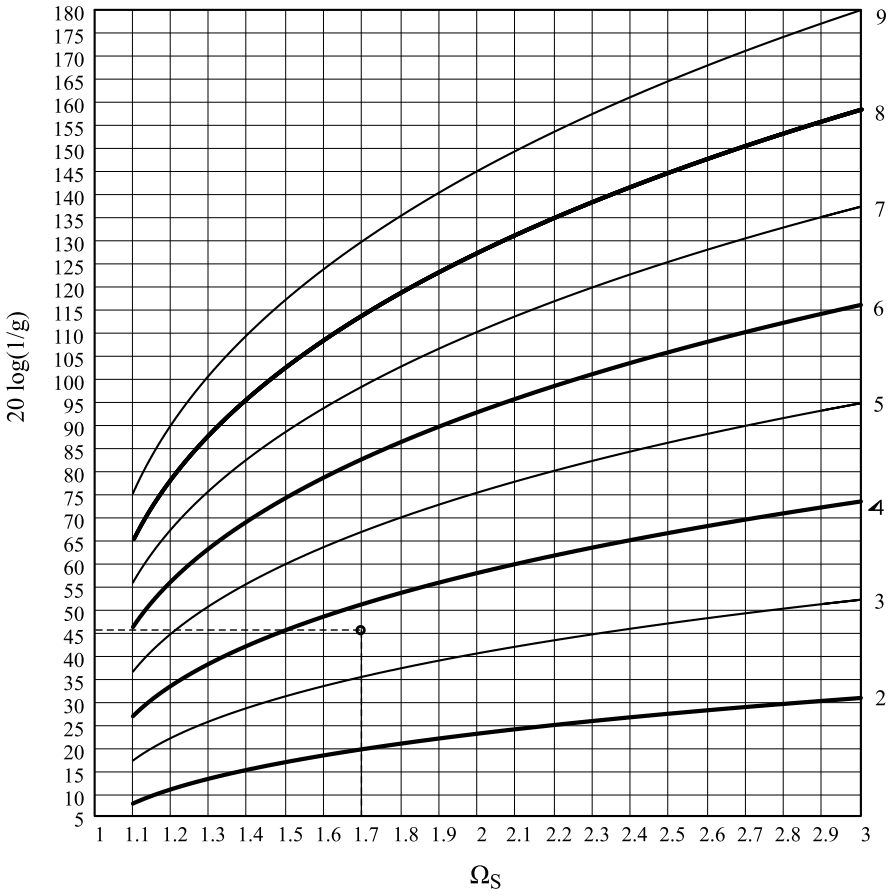

Fig. 4.25 Example order determination

out to be very close or on one of the curves. In such cases, the exact order equations (4.47) or (4.49) must be used.

4.9.2 Transfer Function Tables

For the calculation of the constant C and the poles and zeros of the transfer function, there exist some classical tables [6, 14, 18] but we are going to use the more recent tables by Kendall Su [15]. The transfer function of the elliptic filters is of the general form of (4.94)

$$H(s) = \frac{C(s^2 + \Omega_{PR1}^2)(s^2 + \Omega_{PR2}^2)\cdots(s^2 + \Omega_{PRx}^2)}{(s + \Omega_R)^\eta (s^2 + \frac{\Omega_{o1}}{Q_{o1}}s + \Omega_{o1}^2)(s^2 + \frac{\Omega_{o2}}{Q_{o2}}s + \Omega_{o2}^2)\cdots(s^2 + \frac{\Omega_{ox}}{Q_{ox}}s + \Omega_{ox}^2)} \tag{4.98}$$

Table 4.1 Sample table 2-39 from Kendal Su's Handbook [15]

Tables with prescribed α_p and ω_s Table 2.39 $\alpha_p = 0.10$ dB $\omega_s = 1.70$					
N	α_s (dB)	K	α_i	b_i	ω_{zi}^2
2	4.88830	5.69619469E–01	1.3729000	3.01194309	5.22711358
3	18.98094	5.20513860E–01	0.67543406	1.59592677	3.66684818
			1.19594792		
4	34.69117	1.84264323E–02	0.39179951	1.27738666	3.28939231
			1.36848169	0.79515703	16.56602649
5	50.45438	2.30046327E–02	0.25422395	1.16148462	3.13561449
			0.84839928	0.73710979	7.32520020
			0.61717997		
6	66.21900	4.88708695E–04	0.17787258	1.10628944	3.05698115
			0.57612247	0.76800575	5.22711358
			0.94241089	0.33100321	35.60087619
7	81.98366	8.54038790E–04	0.13127662	1.07554212	3.01113617
			0.41708885	0.80750873	4.37445896
			0.70934209	0.39686243	13.00292897
			0.42438390		
8	97.74831	1.29593847E–05	0.10080635	1.05658341	2.98199086
			0.31616420	0.84156978	3.93118859
			0.54440231	0.48258979	8.13602356
			0.71134209	0.18143017	62.26654812

where $\Omega_{PRi} = \frac{\Omega_S}{\Omega_{ZRi}}$.

In Kendal Su's Handbook, the transfer function is expressed as

$$H(s) = \frac{K(s^2 + \omega_{z1}^2)(s^2 + \omega_{z2}^2)\cdots(s^2 + \omega_{zx}^2)}{(s + \omega_R)^\eta (s^2 + a_1 s + b_1)(s^2 + a_2 s + b_2)\cdots(s^2 + a_x s + b_x)} \tag{4.99}$$

In both equations $x = (N - \eta)/2$. The tables give $\{K, \omega_{zi}^2, \omega_R, a_i \text{ and } b_i\}$. This set corresponds to our $\{C, \Omega_{PRi}^2 = \frac{\Omega_S^2}{\Omega_{ZRi}^2}, \Omega_R, \frac{\Omega_{oi}}{Q_{oi}} \text{ and } \Omega_{oi}^2\}$ respectively. Su's tables are organized into two groups:

- In the first group of tables, given α_p and ω_s (our $\alpha_{\max}$ and Ω_S respectively), the tables give the maximum α_s (our $\alpha_{\min}$) which can be achieved for $N = 2$ to $N = 12$. For each order N, the transfer function parameters a_i, b_i and ω_i^2 are also given. A typical table of this group is shown in Table 4.1 for $\alpha_p = 0.10$ dB and $\omega_s = 1.70$. This is one of the 105 tables which are included for various combinations of α_p and ω_s.

  Using this group of tables corresponds to designing the stopband edge frequency gain optimized elliptic filter using $\varepsilon = \varepsilon_{\max}$.

Table 4.2 Sample table 3-42 from Kendal Su's Handbook [15]

Tables with prescribed α_p and α_s Table 3.42 $\alpha_p = 0.10$ dB $\alpha_s = 30$ dB					
N	ω_s	K	α_i	b_i	ω_{zi}^2
2	7.23045	3.16227766E–02	2.33346454	3.32851327	104.05196647
3	2.45497	2.22798307E–01	0.83664197	1.65308497	7.86067376
			1.05944028		
4	1.53040	3.16227766E–02	0.35539508	1.26168579	2.64423304
			1.39232286	0.85455865	12.74657075
5	1.22578	1.50232690E–01	0.16092293	1.11689151	1.59155056
			0.77192757	0.89084304	3.16772431
			0.76123733		
6	1.10253	3.16227766E–02	0.07506946	1.05435825	1.24952295
			0.39199567	0.94123439	1.72748473
			1.19581536	0.62168813	8.93511422
7	1.04794	1.38567752E–01	0.03553071	1.02570941	1.11277511
			0.19230222	0.97079464	1.29898684
			0.72267315	0.74465198	2.67795534
			0.70446939		
8	1.02272	3.16227766E–02	0.01693576	1.01225239	1.05260350
			0.09312092	0.98581554	1.13563481
			0.38220226	0.87471132	1.59417410
			1.15243548	0.57698199	8.27632903

- In the second group of tables, for each of the 140 combinations of α_p and α_s and for $N = 3$ to $N = 12$, the minimum ω_s that can be used is given together with the parameters of the corresponding transfer function. A typical table of this group is shown in Table 4.2 for $\alpha_p = 0.10$ dB and $\alpha_s = 30$ dB. Designing a filter using these second group of Su's tables corresponds to designing the transition band optimized filter with $\Omega = \Omega_{S\,\min}$.

Example 4.7 Filter specifications:

$$\Omega_S = 1.7, \qquad \alpha_o = 0, \qquad \alpha_{\max} = 0.1 \text{ dB} \qquad (H_C = 0.988553),$$
$$\alpha_{\min} = 30 \text{ dB} \qquad (H_S = 0.0316228)$$

In Su's notation, $\alpha_p = \alpha_{\max}, \alpha_s = \alpha_S$ and $\omega_s = \Omega_S$. In Table 4.1, for $\alpha_p = 0.1$ dB, $\omega_s = 1.7$ we look for N that gives $\alpha_s > 30$ dB. For $N = 3$ the table gives $\alpha_s = 18.98094$ which is not enough, and only for $N = 4 \Rightarrow \alpha_s = 34.69117 > 30$ dB. Therefore, the order must be taken $N = 4$ and the transfer function will be

$$H_1(s) = \frac{0.0184264 \cdot (s^2 + 3.2893923)(s^2 + 16.56602649)}{(s^2 + 0.39179951s + 1.27738666)(s^2 + 1.36848169s + 0.79515703)}$$

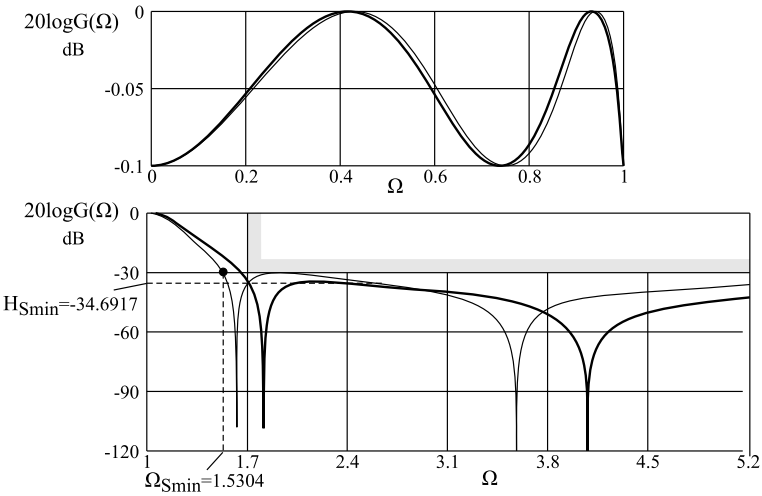

Fig. 4.26 Logarithmic gain plots from $H_1(s)$ and $H_2(s)$ of Example 4.7

This design corresponds to our design with $\varepsilon = \varepsilon_{\max}$.

The same order would be determined from Table 4.2, in which we observe that for $N = 4 \Rightarrow \omega_s = 1.53040 < 1.7$. Frequency $\omega_s = 1.53040$ is the minimum stopband edge frequency which can be used with specifications $N = 4$, $\alpha_p = 0.1$, $\alpha_s = 30$ dB. Using the parameters of this table, we find:

$$H_2(s) = \frac{0.0316227766 \cdot (s^2 + 2.64423304)(s^2 + 12.74657075)}{(s^2 + 0.35539508s + 1.26168579)(s^2 + 1.39232286s + 0.85455865)}$$

This transfer function corresponds to our design using $\Omega_{S\min}$, i.e. to the transition band optimized filter. Figure 4.26 shows the logarithmic gain plots of the two designs.

The use of filter tables is not always possible and depends on whether there exists a suitable table with the values given in the specifications. For example, the tables of the first group are given for

$$\alpha_p: \quad 0.01,\ 0.05,\ 0.1,\ 0.5,\ 1.0,\ 2.0,\ 3.0$$

and for each one of these seven α_p values for

$$\omega_s: \quad 1.02,\ 1.05,\ 1.10,\ 1.20,\ 1.30,\ 1.40,\ 1.50,\ 1.60,\ 1.70,\ 1.80,\ 1.90,\ 2.0,\ 2.5,\ 3.0,\ 4.0$$

If we are given $\alpha_p = 1.5$ and $\omega_s = 1.25$, there are no tables for these values and we have to deploy interpolation techniques [15] with doubtable accuracy. In such cases the tables are of little help and the use of the analysis and design procedure presented in this chapter is highly recommended.

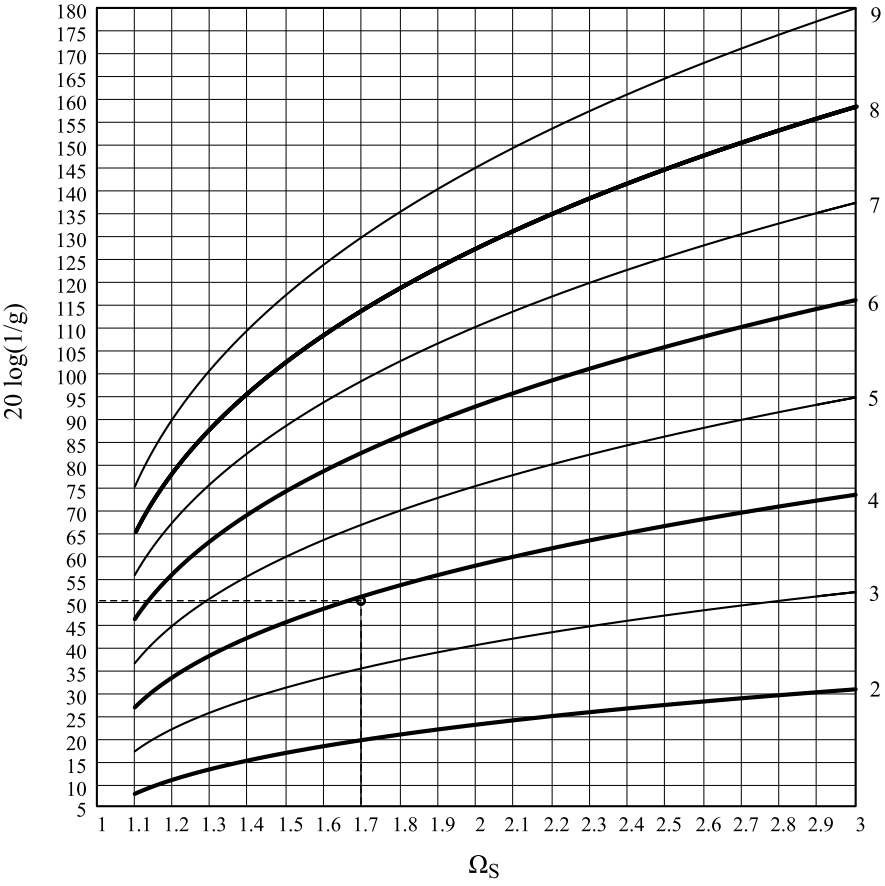

Fig. 4.27 Determination of the order of the elliptic filter

Consider a second example with $\omega_s = 1.7$, $\alpha_p = 0.15$ and $\alpha_s = 36$ dB. Since there are no tables for $\alpha_p = 0.15$, the most probable is to be tempted to use Su's Table 2.39 shown in Table 4.1 with $\alpha_p = 0.10$. From this table we find that only for $N = 5$ the stopband attenuation is higher than the specified $\alpha_s = 36$ dB and therefore $N = 5$ must be used. However, using the order equation (4.49) or even the order nomograph with $20\log(1/g) = 50.5418$ and $\Omega_S = 1.7$, we find $N = 4$ (see Fig. 4.27).

4.9.3 Computer Aided Elliptic Filter Design

MATLAB Signal Processing Toolbox offers all necessary functions to design elliptic filters. Function *ellipord()* can be used to calculate the order of the elliptic filter from the specifications and *ellip()* does the rest. The functions are well documented and can be used to calculate all elliptic filter parameters.

In addition, several specialized filter design programs also exist freely or commercially. Among them, *Filter Solutions* by Newherz Technologies offers a free version called *Filter Free* the functionality of which is limited to $N = 3$ but is worth using to investigate its potential.

It should be underlined here that the existence of such powerful computer programs does not mean that engineers should not be aware of the design details simply because computers can do the job. Engineers must know the underlying theory so as to be able to understand, modify, improve and optimize the filters produced by the computer. These advanced filter programs have been designed as tools for those who know, and not as substitutes for the missing knowledge.

4.10 Problems

4.1 Calculate the arithmetic-geometric mean $M(2.4,\ 5.2)$ using a scientific calculator.

4.2 Calculate the arithmetic-geometric mean $M(1.2,\ 2.6)$ using a scientific calculator and verify the property $0.5M(2.4,\ 5.2) = M(1.2,\ 2.6)$.

4.3 Calculate the Jacobi Nome $q(\frac{1}{\sqrt{2}})$ using (4.6). Then calculate the same quantity using the approximate formulae (4.8) and (4.9).

4.4 Repeat Example 4.2 with $\Omega_S = 1.4$.

4.5 Use (4.13) to derive (4.37) from (4.36).

4.6 Given $\alpha_{\max} = 0.2$ dB, $\alpha_{\min} = 32$ dB and $\Omega_S = 1.2$, determine the order N of the normalized elliptic lowpass filter from the nomograph of Fig. 4.24.

4.7 Given $\alpha_{\max} = 0.1$ dB, $\alpha_{\min} = 30$ dB and $\Omega_S = 2.5$, determine the order N of the normalized elliptic lowpass filter from the nomograph of Fig. 4.24 and from Su's sample tables.

4.8 Determine the transfer function of a filter with the specifications of Problem 4.7.

References[3]

1. Antoniou, A.: Digital Filters Analysis Design and Applications, 2nd edn. McGraw-Hill, New York (1993)
2. Borwein, J.M., Borwein, P.B.: Pi and the AGM. Canadian Mathematical Society Series of Monographs and Advanced Texts, vol. 4. Wiley, New York (1987)

[3] All references, whether or not cited within the text, are recommended for further reading.

3. Cauer, W.: Electric wave filters, US Patent 1.989.545 Filed 8 June 1928 in Germany. Filed 6 December 1930 in the USA, issued 29 January 1935 (1035)
4. Cauer, W.: Synthesis of Linear Communication Networks. McGraw-Hill, New York (1958), translated from the German "Theorie der Linearen Wechselstorm-Schaltungen", Akad. Verlags-gesellschaft, Becker und Erler, Leipzig, 1st edn., 1941
5. Chen, W.-K. (ed.): Passive, Active and Digital Filters. The Circuits and Filters Handbook, vol. V. CRC Press, Boca Raton (2009). Chapter 14 by Wasfy B. Mikhael
6. Christian, E., Eisenmann, E.: Filter Design Tables and Graph. Wiley, New York (1966)
7. Daniels, R.W.: Approximation Methods for Electronic Filter Design. McGraw-Hill, New York (1974)
8. Dimopoulos, H.G.: Optimal use of some classical approximations in filter design. IEEE Trans. Circuits Syst. II, Analog Digit. Signal Process. **54**(9), 780–784 (2007)
9. Huber, K.: On the design of Cauer filters. AEÜ, Int. J. Electron. Commun., **58**(3), 223–224 (2004)
10. Innes, R.T.A.: Jacobi's Nome (q) in Astronomical Tables and Formulae. Monthly Notices of the Royal Astronomical Society, p. 493, 05/1902, Bibliographic Code 1902MNRAS..62..493I, May 1902
11. Lutovac, M.D., Tosic, D.V., Evans, B.L.: Filter Design for Signal Processing using MATLAB and Mathematica. Prentice Hall, Upper Saddle River (2001)
12. Orchard, H.J., Willson, A.N.: Elliptic functions for filter design. IEEE Trans. Circuits Syst. I **44**(4), 273–287 (1997)
13. Paarmann, L.D.: Design and Analysis of Analog Filters—A Signal Processing Perspective—With MATLAB Examples. Kluwer Academic, Dordrecht (2001)
14. Saal, R.: Handbook of Filter Design. AEG-Telefunken
15. Su, K.L.: Handbook of Tables for Elliptic Function Filters. Kluwer, Dordrecht (1990)
16. Van Valkenburg, M.E.: Analog Filter Design. Oxford University Press, London (1982)
17. Williams, A., Taylor, F.: Electronic Filter Design Handbook. McGraw-Hill, New York (2006)
18. Zverev, A.I.: Handbook of Filter Synthesis. Wiley, New York (1967)

Frequency Transformations

5

All approximations presented in the previous chapters are used to approximate the ideal lowpass gain within certain tolerances determined with the lowpass filter specifications. In order to design other types of filters, e.g. highpass, the corresponding approximations should be presented. Instead of repeating all approximations for highpass, bandpass and band-reject (bandstop) filters, *frequency transformations* are used that transform a normalized lowpass filter into any other filter type. In other words, in order to design a highpass, bandpass or band-reject filter, it will be shown that we can first design an auxiliary normalized lowpass filter which can then be transformed to any other filter type.

5.1 The Lowpass to Highpass (LP-HP) Frequency Transformation

If the frequency transformation

$$s \quad \leftrightarrow \quad \frac{1}{s} \tag{5.1}$$

is applied to the transfer function $H_{LPn}(s)$ of a normalized lowpass filter, i.e. if s is replaced by $1/s$, then for the new transfer function, denoted by $H_{HPn}(s)$, we have:

$$H_{HPn}(s) = H_{LPn}\left(\frac{1}{s}\right)$$

The transformation $s \leftrightarrow \frac{1}{s}$ is called *lowpass to highpass transformation* and performs the following mapping:

1. Frequency Ω_x maps to $1/\Omega_x$ and if $|H_{LPn}(j\Omega_x)| = H_x$ then $|H_{HPn}(j1/\Omega_x)| = H_x$.
2. Frequency $\Omega = 1$ maps to $\Omega = 1$ and if $|H_{LPn}(j1)| = H_o$, then $|H_{HPn}(j1)| = H_o$.

H.G. Dimopoulos, *Analog Electronic Filters*, Analog Circuits and Signal Processing,
DOI 10.1007/978-94-007-2190-6_5, © Springer Science+Business Media B.V. 2012

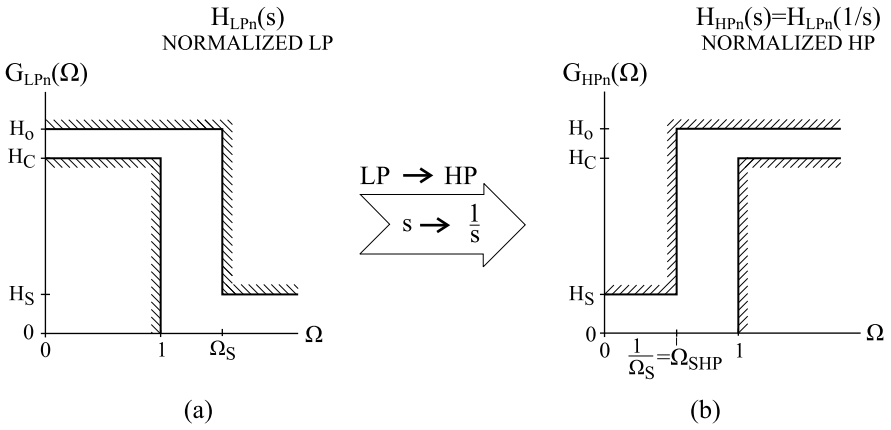

Fig. 5.1 LP-HP frequency transformation

3. Frequency $\Omega = 0$ maps to $\Omega = \infty$ and whatever occurs to $H_{LPn}(s)$ at $\Omega = 0$ occurs also to $H_{HPn}(s)$ at $\Omega = \infty$: If $|H_{LPn}(j0)| = H_o$, then $|H_{HPn}(j\infty)| = H_o$.
4. Frequency $\Omega = \infty$ maps to $\Omega = 0$ and whatever happens in $H_{LPn}(s)$ at $\Omega = \infty$, happens to $H_{HPn}(s)$ at $\Omega = 0 : |H_{HPn}(j0)| = |H_{LPn}(j\infty)|$.
5. Passband frequencies $0 < \Omega < 1$ of the lowpass map to $1 < \Omega < \infty$. Whatever happens to $H_{LPn}(s)$ in the passband will happen to $H_{HPn}(s)$ for frequencies $\Omega > 1$. This means that if the lowpass passband gain varies from H_o to H_C, then the gain $|H_{HPn}(j\Omega)|$ will vary from H_C to H_o for $\Omega > 1$.
6. Stopband frequencies $\Omega > 1$ of the lowpass map to $0 < \Omega < 1$, and the gain $|H_{HPn}(j\Omega)|$ remains below H_S for $0 < \Omega < 1$.

Based on the above mapping and referring to Fig. 5.1, it is clear that $H_{HPn}(s)$ is the transfer function of a normalized highpass filter with the same gain tolerances as the lowpass.

Therefore, in order to design a normalized ($\Omega_C = 1$) highpass filter with the specifications of Fig. 5.1b $\{H_o,\ H_C,\ H_S,\ \Omega_{SHP} < 1\}$, we can start with the design of an auxiliary normalized lowpass filter with specifications

$$\left\{H_o, H_C, H_S, \Omega_S = \frac{1}{\Omega_{SHP}} > 1\right\}$$

When the transfer function $H_{LPn}(s)$ of the so designed auxiliary normalized lowpass filter has been determined, the transfer function of the normalized highpass filter will be given by

$$H_{HPn}(s) = H_{LPn}\left(\frac{1}{s}\right)$$

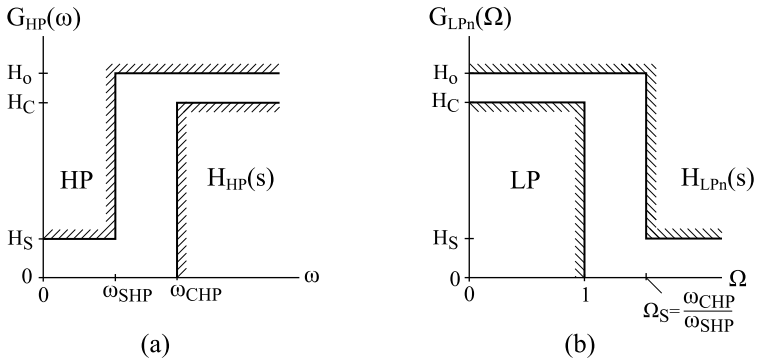

Fig. 5.2 (**a**) Highpass filter specifications. (**b**) Normalized specifications of the auxiliary lowpass filter

When the highpass frequency specifications ω_{CHP} and ω_{SHP} are not given in normalized form, as for example in Fig. 5.2a, scaled with ω_{CHP}:

$$\Omega_{CHP} = 1, \qquad \Omega_{SHP} = \frac{\omega_{SHP}}{\omega_{CHP}}$$

In this case, the normalized specifications of the auxiliary normalized lowpass filter will be as follows:

$$\Omega_C = 1, \qquad \Omega_S = \frac{1}{\Omega_{SHP}} = \frac{\omega_{CHP}}{\omega_{SHP}}$$

as shown in Fig. 5.2b.

The transfer function of the highpass filter with cut-off frequency ω_{CHP} and stopband edge frequency $\Omega_S \cdot \omega_{CHP}$ will be

$$H_{HP}(s) = H_{HPn}\left(\frac{s}{\omega_{CHP}}\right) = H_{LPn}\left(\frac{\omega_{CHP}}{s}\right)$$

5.1.1 The LP-HP Frequency Transformation at Transfer Function Level

As seen in the previous chapters, the general form of an all-pole lowpass transfer function obtained by a polynomial approximation like Butterworth, Chebyshev or Pascal of order N, is of the form:

$$H(s) = \frac{N_{TF}(s)}{D_{TF}(s)} = \frac{A}{(s+\Omega_R)^{\eta}(s^2 + \frac{\Omega_{o1}}{Q_{o1}}s + \Omega_{o1}^2)\cdots(s^2 + \frac{\Omega_{ox}}{Q_{ox}}s + \Omega_{ox}^2)} \tag{5.2}$$

In the above equations, Ω_{oi} and Q_{oi} are the frequencies and the quality factors of the complex conjugate pole pairs, and Ω_R the real pole when N is odd. For η, we have:

$$\eta = \begin{cases} 0 & \text{for } N \text{ even} \\ 1 & \text{for } N \text{ odd} \end{cases} \qquad x = (N - \eta)/2 \tag{5.3}$$

The general form of a lowpass transfer function with transmission zeros, obtained by a rational approximation like inverse Chebyshev, inverse Pascal or elliptic of order N, is

$$H(s) = \frac{N_{TF}(s)}{D_{TF}(s)} = \frac{A(s^2 + \Omega_{z1}^2) \cdots (s^2 + \Omega_{zx}^2)}{(s + \Omega_R)^\eta (s^2 + \frac{\Omega_{o1}}{Q_{o1} s} + \Omega_{o1}^2) \cdots (s^2 + \frac{\Omega_{ox}}{Q_{ox}} s + \Omega_{ox}^2)} \tag{5.4}$$

Transfer functions of (5.2) and (5.4) can be expressed as products of the following three terms:

$$\begin{aligned} H_1(s) &= \frac{1}{s + \Omega_R} \qquad H_2(s) = \frac{1}{s^2 + \frac{\Omega_o}{Q_o} s + \Omega_o^2} \\ H_3(s) &= \frac{s^2 + \Omega_z^2}{s^2 + \frac{\Omega_o}{Q_o} s + \Omega_o^2} \end{aligned} \tag{5.5}$$

The term $H_1(s)$ corresponds to the real pole, which exists when N is odd, and is the transfer function of a first order lowpass filter. $H_2(s)$ corresponds to a conjugate pole pair and is the transfer function of a second order lowpass filter. $H_3(s)$ appears only in rational approximations and is the transfer function of a second order band-reject filter.

When the LP-HP transformation is applied to these terms, we get the following transformed terms:

$$H_1(s) = \frac{1}{(s + \Omega_R)} \xrightarrow{s \to \frac{1}{s}} \frac{\frac{1}{\Omega_R} s}{s + \frac{1}{\Omega_R}} \tag{5.6}$$

This is a first order highpass function which can be realized by a simple RC circuit or any active-RC lossy integrator (see Chaps. 9 and 10).

$$H_2(s) = \frac{1}{(s^2 + \frac{\Omega_o}{Q_o} s + \Omega_o^2)} \xrightarrow{s \to \frac{1}{s}} \frac{\frac{1}{\Omega_o^2} s^2}{s^2 + \frac{1}{\Omega_o Q_o} s + \frac{1}{\Omega_o^2}} \tag{5.7}$$

This is a second order highpass transfer function which can be realized by a second order active-RC highpass circuit (see Chap. 10).

$$H_3(s) = \frac{s^2 + \Omega_z^2}{(s^2 + \frac{\Omega_o}{Q_o} s + \Omega_o^2)} \xrightarrow{s \to \frac{1}{s}} \frac{\frac{\Omega_z^2}{\Omega_o^2}(s^2 + \frac{1}{\Omega_z^2})}{s^2 + \frac{1}{\Omega_o Q_o} s + \frac{1}{\Omega_o^2}} \tag{5.8}$$

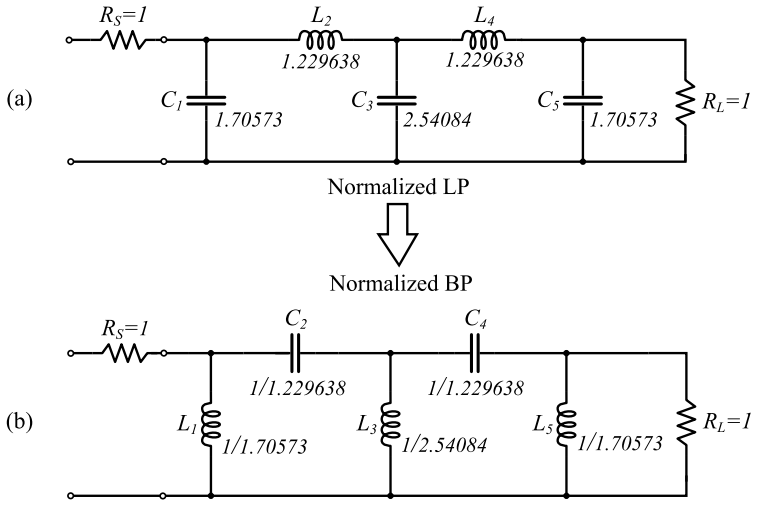

Fig. 5.3 Component level application of the LP-HP transformation to a normalized passive LP filter

This is a second order band-reject transfer function which can be realized by a second order active-RC band-reject (notch) circuit (see Chap. 10). It should be noted that the poles of the transformed terms of (5.7) and (5.8) preserve the quality factor Q_o of the poles of $H_2(s)$ and $H_3(s)$ respectively.

5.1.2 The LP-HP Frequency Transformation at Component Level

The LP-HP transformation of (5.1) can be applied at component level, i.e. to the impedance of each element as follows:

1. Resistor $R \xrightarrow{s\to\frac{1}{s}}$ Resistor R
2. Inductor $Z_{LP}(s) = sL \xrightarrow{s\to\frac{1}{s}} \frac{1}{s\frac{1}{L}} = Z_{HP}(s) =$ Capacitor with $C = \frac{1}{L}$
3. Capacitor $Z_{LP}(s) = \frac{1}{sC} \xrightarrow{s\to\frac{1}{s}} s\frac{1}{C} = Z_{HP}(s) =$ Inductor with $L = \frac{1}{C}$

The LP-HP transformation applied at component level to a normalized lowpass circuit simply transforms inductors to capacitors and capacitors to inductors with reciprocal element values. Figure 5.3 shows an example of such an application of the LP-HP transformation to a normalized passive lowpass filter at component level.

In inductorless circuits, like the active-RC circuits, the LP-HP transformation is implemented by replacing capacitors C with inductors $L = 1/C$. The filter becomes highpass but it is not inductorless any more. However, if we now apply impedance scaling with scaling factor s, all resistors R_i will acquire scaled impedance R/s, which is a capacitor of value $1/R$. Inductors will acquire scaled impedance $sL/s = L = 1/C$, which is a resistor with value $1/C$. Finally, the LP-

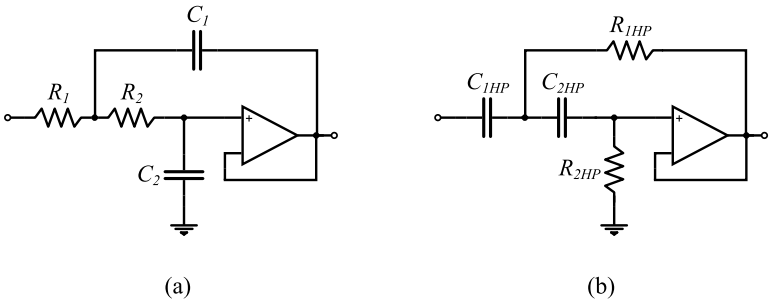

Fig. 5.4 Component level application of the LP-HP transformation to an active-RC lowpass filter

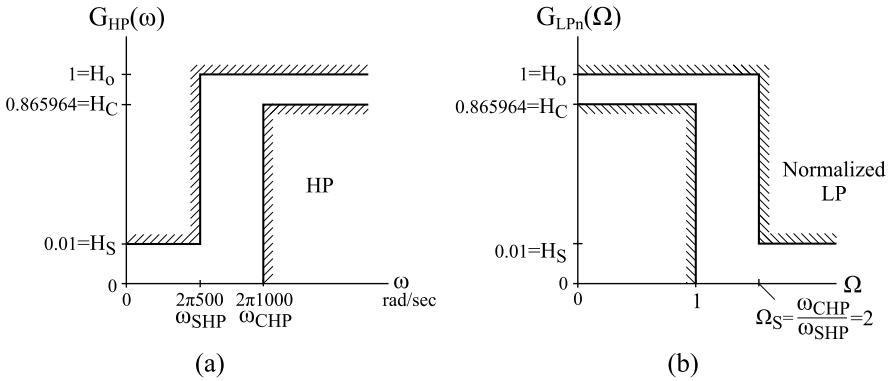

Fig. 5.5 (**a**) Highpass filter specifications. (**b**) Normalized specifications of the auxiliary lowpass filter

HP transformation is applied to normalized inductorless active-RC circuits by simply replacing resistors R_i with capacitors $C_i = 1/R_i$ and capacitors C_k with resistors $R_k = 1/C_k$ to obtain the normalized transformed circuit. This transformation of active-RC circuits is known as *RC-CR transformation* and transforms lowpass circuits to highpass and vice versa [4]. Figure 5.4 shows the application of the LP-HP transformation to a normalized active-RC lowpass filter to derive a normalized highpass filter with $C_{1HP} = 1/R_1$, $C_{2HP} = 1/R_2$, $R_{1HP} = 1/C_1$, $R_{2HP} = 1/C_2$.

Example 5.1 Determine the transfer function of a highpass filter with Pascal response from the specifications shown in Fig. 5.5a and plot the frequency response.

With $f_{SHP} = 500$ Hz and $f_{CHP} = 1000$ Hz, the highpass specifications are:

$$H_o = 1, \qquad \omega_{CHP} = 2\pi f_{CHP} \text{ rad/s}, \qquad \omega_{SHP} = 2\pi f_{SHP} \text{ rad/s},$$
$$H_C = 0.865964 \quad \text{and} \quad H_S = 0.01$$

or equivalently

$$\alpha_o = 0, \qquad \omega_{CHP} = 2\pi f_{CHP} \text{ rad/s}, \qquad \omega_{SHP} = 2\pi f_{SHP} \text{ rad/s}$$
$$\alpha_{\max} = 1.25 \text{ dB} \quad \text{and} \quad \alpha_{\min} = 40 \text{ dB}$$

In order to determine the transfer function of the highpass filter with the specifications of Fig. 5.5a, the transfer function $H_{LPn}(s)$ of a normalized lowpass filter with specifications

$$H_o = 1, \qquad \Omega_C = 1, \qquad \Omega_S = 2, \qquad H_C = 0.865964 \quad \text{and} \quad H_S = 0.01$$
$$(\alpha_o = 0,\ \Omega_S = 2,\ \alpha_{\max} = 1.25 \text{ dB and } \alpha_{\min} = 40 \text{ dB})$$

(see Fig. 5.5b) must be first designed. Then, the transfer function of the highpass filter which meets the normalized specifications can be determined as

$$H_{HPn}(s) = H_{LPn}\left(\frac{1}{s}\right)$$

and the transfer function which meets the specifications of Fig. 5.5a will be

$$H_{HP}(s) = H_{HPn}\left(\frac{s}{\omega_{CHP}}\right) = H_{LPn}\left(\frac{\omega_{CHP}}{s}\right)$$

Let us first determine $H_{LPn}(s)$ using Pascal approximation with $\lambda = \lambda_{\max}$.

From (2.88) of Chap. 2, we find $HP = 44.77$. Using this value, the order of the filter can be determined from the Pascal order nomograph of Fig. 2.43: $N = 5$. For the stopband edge optimized filter with $\lambda = \lambda_{\max} = 19.083796$ (from (2.86)), from Table 2.4 for $N = 5$, we get $P_{\max} = 0.03026194$ and $\Omega_D = 0.70639006$. From Tables 2.8 for $N = 5$ and $\alpha_{\max} = 1.25$, we get $C = 0.147125$, real pole -0.38346582 and two conjugate pole pairs:

$$-0.28603316 \pm j0.55842122 \quad \rightarrow \quad \Omega_1 = 0.62741472, \qquad Q_1 = 1.09675171$$
$$-0.09430025 \pm j0.98273254 \quad \rightarrow \quad \Omega_2 = 0.98724656, \qquad Q_2 = 5.23459125$$

Having C and the poles, the transfer function is determined from (2.90):

$$H_{LPn}(s) = \frac{0.147125}{(s + 0.38346582)(s^2 + \frac{\Omega_1}{Q_1}s + \Omega_1^2)(s^2 + \frac{\Omega_2}{Q_2}s + \Omega_2^2)}$$

and finally

$$H_{LPn}(s) = \frac{0.147125}{(s + 0.38346582)(s^2 + 0.5721s + 0.62742^2)(s^2 + 0.1886s + 0.987247^2)}$$

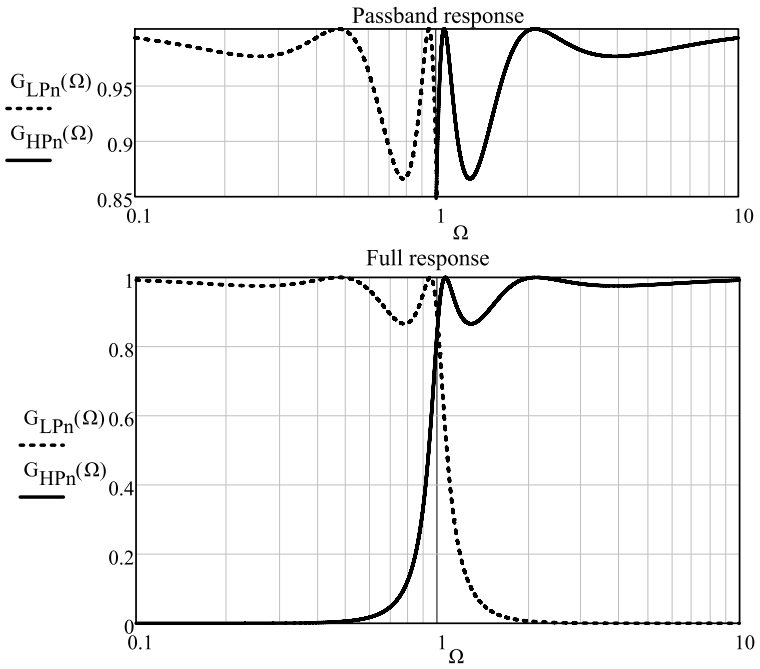

Fig. 5.6 Normalized gain plots of Example 5.1: Passband and full responses

Applying the LP-HP transformation to this function, i.e. replacing s with $\frac{1}{s}$, the transfer function $H_{HPn}(s)$ of the normalized highpass filter is obtained:

$$H_{HPn}(s) = \frac{s^5}{(s+2.607794)(s^2+1.453239s+2.540333)(s^2+0.193505s+1.026003)}$$

Figure 5.6 shows the gain plots from $H_{LPn}(s)$ and $H_{HPn}(s)$, the transfer functions of the auxiliary normalized lowpass (dashed curves) and the normalized highpass filters.

The transfer function of the highpass filter which satisfies the specifications of Fig. 5.5a will be

$$H_{HP}(s) = H_{HPn}\left(\frac{s}{\omega_{CHP}}\right)$$

Figure 5.7 shows the gain of the final filter. In fact, this is the plot of $G_{HP}(f) = |H_{HPn}(j\frac{f}{f_{CHP}})|$.

Example 5.2 Determine the transfer function of a highpass filter with Chebyshev response from the specifications of Fig. 5.8a.

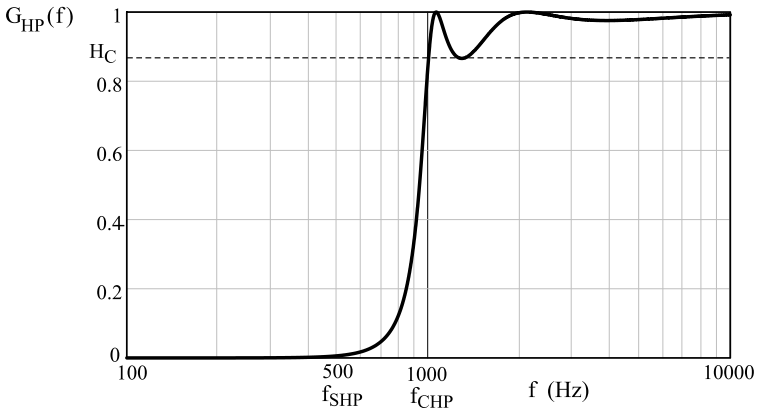

Fig. 5.7 Frequency response of the final filter of Example 5.1

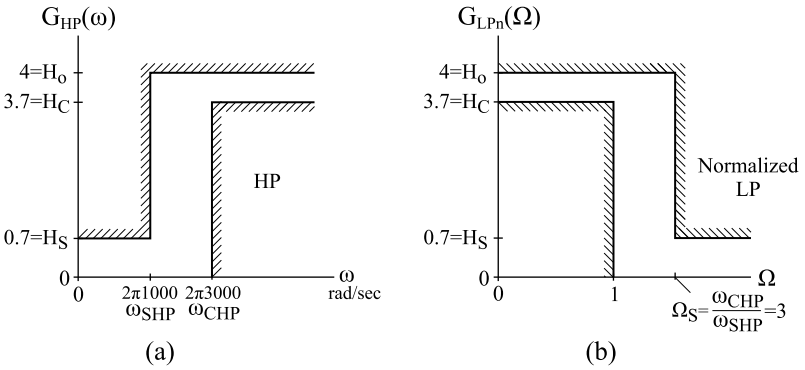

Fig. 5.8 (**a**) Highpass filter specifications. (**b**) Normalized specifications of the auxiliary lowpass filter

In order to design the highpass filter with the specifications of Fig. 5.8a, the corresponding transfer function must be determined. To do that, the transfer function $H_{LPn}(s)$ of a normalized lowpass with the specifications of Fig. 5.8b must first be determined. Then the transfer function of the highpass filter which meets the normalized specifications can be determined as

$$H_{HPn}(s) = H_{LPn}\left(\frac{1}{s}\right)$$

and the transfer function which meets the specifications of Fig. 5.8a will be

$$H_{HP}(s) = H_{LPn}\left(\frac{\omega_{CHP}}{s}\right)$$

Let us first determine $H_{LPn}(s)$ using Chebyshev approximation. The maximum value of the ripple factor will be

$$\epsilon = \epsilon_{\max} = \sqrt{\left(\frac{H_o}{H_C}\right)^2 - 1} = \sqrt{\left(\frac{4}{3.9}\right)^2 - 1} = 0.2279$$

and the decimal order

$$N_d = \frac{\cosh^{-1}\left(\sqrt{\frac{\frac{4^2}{0.7^2}-1}{\frac{4^2}{3.9^2}-1}}\right)}{\cosh^{-1}(3)} = 2.2119$$

Therefore, we must take $N = 3$, and finally the normalized lowpass transfer function will be (see (2.61)):

$$H_{LPn}(s) = \frac{H_o}{\epsilon c_3 \prod_{k=1}^{3}(s - s_k)} \quad \text{with } s_k = \sigma_k + j\Omega_k$$

$$\sigma_k = \sin\left(\frac{(2N + 2k - 1)\pi}{2N}\right) \sinh\left[\frac{1}{N}\sinh^{-1}\left(\frac{1}{\epsilon}\right)\right]$$

$$\Omega_k = \cos\left(\frac{(2N + 2k - 1)\pi}{2N}\right) \cosh\left[\frac{1}{N}\sinh^{-1}\left(\frac{1}{\epsilon}\right)\right] \quad \text{for } k = 1, \ldots, 3$$

Constant c_3 is the coefficient of the 3_{rd} order term of the Chebyshev polynomial and $c_3 = 2^{3-1} = 2^2 = 4$. The poles are found from the above equations:

$$-0.794339 \quad \text{and} \quad -0.397169 \pm j1.105997$$

in which case the transfer function will be:

$$H_{LPn}(s) = \frac{4.38784}{(s + 0.794339)(s^2 + 0.7943386s + 1.38097375)}$$

Applying the LP-HP transformation to this function, i.e. replacing s with $\frac{1}{s}$, the transfer function of the normalized highpass filter is obtained:

$$H_{HPn}(s) = \frac{4.38784}{(\frac{1}{s} + 0.794339)(\frac{1}{s^2} + 0.7943386\frac{1}{s} + 1.38097375)}$$

$$= \frac{\frac{1}{0.794339} \cdot \frac{4.38784}{1.38097375} s^3}{(s + \frac{1}{0.794339})(s^2 + s\frac{0.7943386}{1.38097375} + \frac{1}{1.38097375})}$$

and finally

$$H_{HPn}(s) = \frac{4s^3}{(s + 1.25891)(s^2 + 0.5752s + 0.8509563^2)} \tag{5.9}$$

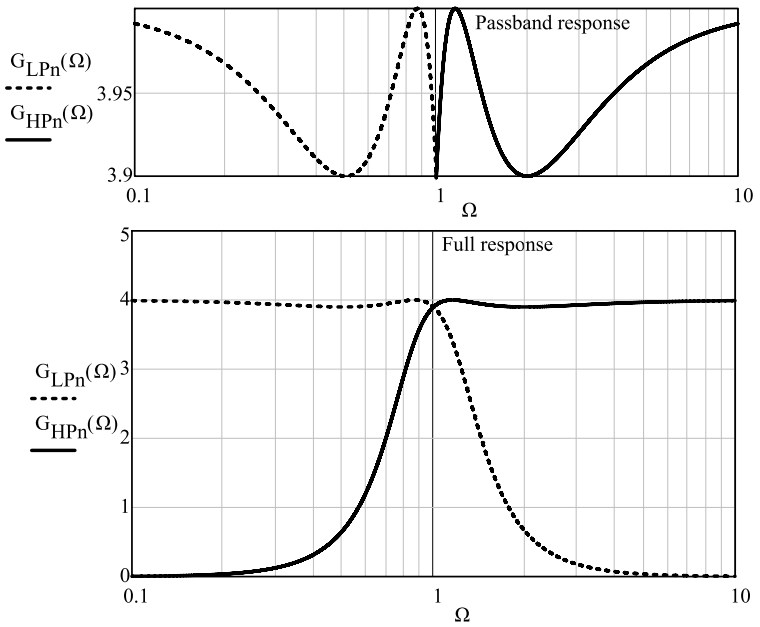

Fig. 5.9 Normalized gain plots of Example 5.2: Passband and full responses

Figure 5.9 shows the gain plots calculated from $H_{LPn}(s)$ (dashed curves) and $H_{HPn}(s)$. The transfer function of the highpass filter with the specifications of Fig. 5.8a will be:

$$H_{HP}(s) = H_{HPn}\left(\frac{s}{\omega_{CHP}}\right)$$

and the related gain will be given by

$$G_{HP}(f) = |H_{HP}(j2\pi f)| = \left|H_{HPn}\left(j\frac{2\pi f}{2\pi f_{CHP}}\right)\right| = \left|H_{HPn}\left(j\frac{f}{f_{CHP}}\right)\right|$$

Example 5.3 Design an active-RC highpass filter with the specifications of Fig. 5.8a.

The transfer function of the normalized Chebyshev highpass filter has been determined in the previous example (see (5.9)):

$$H_{HPn}(s) = \frac{4s^3}{(s+1.25891)(s^2+0.5752s+0.8509563^2)}$$

or

$$H_{HPn}(s) = \frac{A_1 s}{s+1.25891}\,\frac{A_2 s^2}{s^2+0.5752s+0.8509563^2}$$

with $A_1 A_2 = 4$.

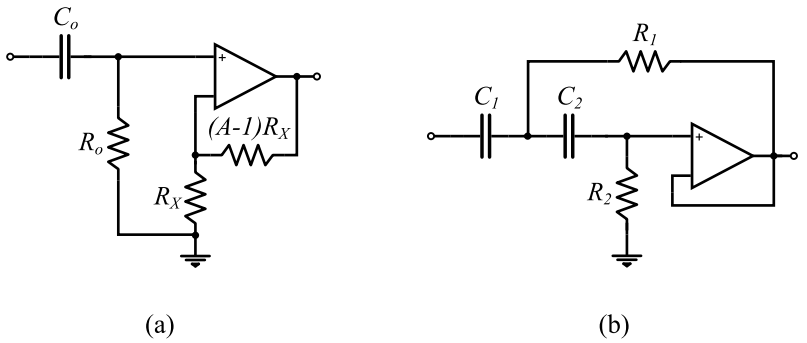

Fig. 5.10 (**a**) First order circuit. (**b**) Second order Sallen-Key highpass circuit

This factorized expression of the transfer function implies that the normalized highpass filter can be realized as a cascade connection of two sections:

$$H_1(s) = \frac{A_1 s}{s + 1.25891} \quad \text{and} \quad H_2(s) = \frac{A_2 s^2}{s^2 + 0.5752s + 0.8509563^2}$$

If from the realization of these two sections we get $A_1 A_2 = A_x \neq 4$, then a gain $A = 4/A_x$ should be introduced in the cascade.

The first term $H_1(s)$, which expresses the real pole, can be realized using a first order RC section, like the one shown in Fig. 5.10a.

The non-inverting voltage amplifier has voltage gain A and has been added in order to isolate the passive-RC section from the next sections and in addition to provide adjustability of the final gain. The transfer function of the circuit of Fig. 5.10a is

$$H_1(s) = \frac{s}{s + 1/R_o C_o} A$$

Any element values that satisfy $R_o C_o = \frac{1}{1.25891} = 0.79434$ can be chosen to realize the real pole. For this example, we select $R_o = 1$ and therefore $C_o = \frac{1}{1.25891} = 0.79434$. With these values, the transfer function of the first section will be

$$H_1(s) = \frac{s}{s + 0.79434} A$$

The term

$$H_2(s) = \frac{A_2 s^2}{s^2 + 0.5752s + 0.8509563^2}$$

is a second order highpass function with $\omega_o = 0.8509563$ and $Q = \frac{0.8509563}{0.5752} = 1.4794$, and as such can be realized by a Sallen-Key second order highpass circuit with $k = 1$. The circuit is shown in Fig. 5.10b and is presented analytically in

Chap. 10. The transfer function of this circuit with $C_1 = C_2 = C$ is given by:

$$H_2(s) = \frac{V_o(s)}{E(s)} = \frac{s^2}{s^2 + s(2/R_2C) + 1/R_1R_2C^2}$$

$$\text{with } \omega_o = \frac{1}{C\sqrt{R_1R_2}} \text{ and } Q = \frac{1}{2}\sqrt{\frac{R_2}{R_1}}$$

from which we find

$$R_1 = \frac{1}{2\omega_o QC} \quad \text{and} \quad R_2 = \frac{2Q}{\omega_o C}$$

At this point, any value can be selected for capacitor C, but we prefer to have $C = C_o = 0.79434$, i.e. the same capacitor value selected for the first section. Using the already calculated $\omega_o = 0.8509563$ and $Q = 1.4794$, we find from the above equation:

$$R_1 = 1/2QC = 0.5 \qquad R_2 = 2Q/(\omega_o C) = 4.3773 \qquad A_2 = 1$$

The transfer function of the cascade of the two sections with $A = 4$ will be:

$$H_o(s) = \frac{4s^3}{(s + 0.79434)(s^2 + 0.5752s + 0.8509563^2)} = H_{HPn}(s)$$

This circuit, as designed, is normalized and realizes the normalized transfer function $H_{HPn}(s)$. Frequency denormalization is achieved by dividing all capacitor values by ω_{CHP}. Moreover, since resistor values are very low, they can be multiplied by say R_n (Ohm) and, in order to keep the transfer function unchanged, capacitor values must be divided by the same factor. Finally, multiplying all resistor values by R_n and dividing all capacitor values by $R_n\omega_{CHP}$, the filter will satisfy the denormalized specifications of Fig. 5.8a. Choosing $R_n = 10^4$ Ohm, we get:

$$R_o \to 1 \cdot 10^4 \text{ Ohm} = 10 \text{ kOhm} \qquad C_o = C \to \frac{0.79434}{2\pi \cdot 3 \cdot 10^3 \cdot 10^4} = 4.2162 \text{ nF}$$

$$R_1 \to 0.5 \cdot 10^4 \text{ Ohm} = 5 \text{ kOhm} \qquad R_2 \to 4.3773 \cdot 10^4 \text{ Ohm} = 43773 \text{ Ohm}$$

The values of resistors $3R_x$ and R_x are not important as long as their ratio equals 3 in order to make the gain $A = 1 + \frac{3R_x}{R_x} = 4$. The usual order of the values of the resistors in active-RC circuits is 10^4 Ohm since low resistance values may demand high currents from the operational amplifier, a situation which is not desirable. Figure 5.11 shows the final denormalized highpass filter.

The order of connecting the sections in the cascade is mathematically not important and the circuit of Fig. 5.12 has exactly the same transfer function. However,

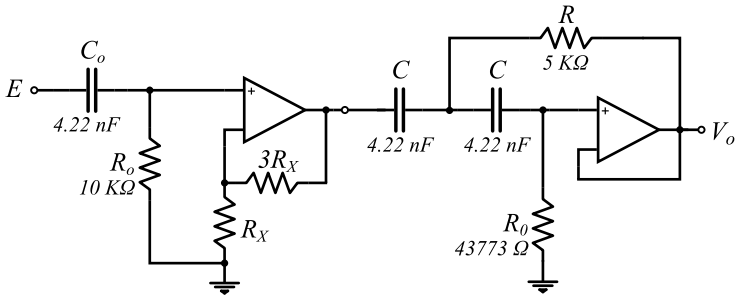

Fig. 5.11 Denormalized active highpass filter

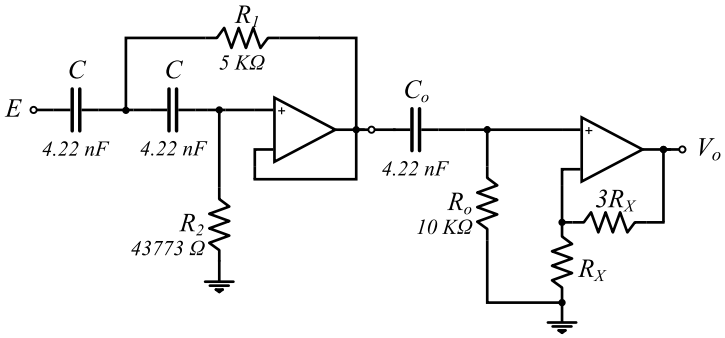

Fig. 5.12 Alternative connection

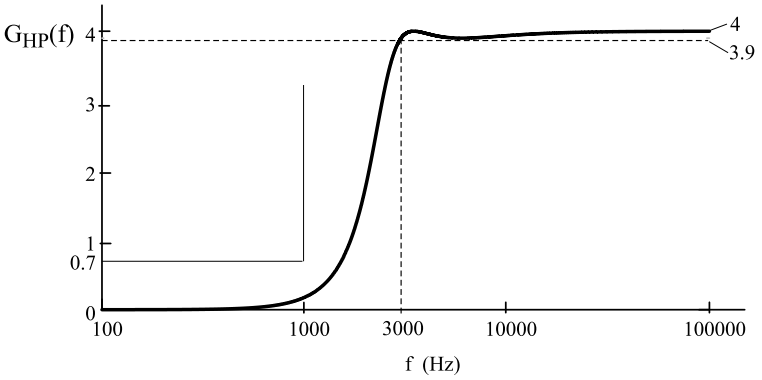

Fig. 5.13 Frequency response of the denormalized highpass filter

the common practice is to connect the sections in increasing Q order. Sections with high Q-values tend to be more sensitive and should be connected last.

Figure 5.13 shows the frequency response of the final denormalized highpass filter (simulation).

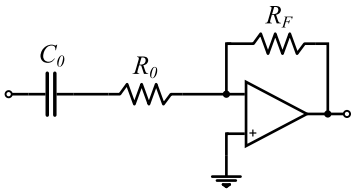

Fig. 5.14 Alternative first order section

The realization of the filter sections is left to the imagination, the experience and the knowledge of the designer. There are many circuits that realize the first and second order sections involved in such a cascade realization. As an example, the second order section can be realized by a multiple feedback highpass circuit (see Chap. 10) and the circuit shown in Fig. 5.14 can be used for the realization of the first order section since its transfer function is

$$H_1(s) = -\frac{sR_F/R_o}{s + \frac{1}{R_o C_o}}$$

Using this circuit, gain $A = \frac{R_F}{R_o}$ can be adjusted by R_F.

5.2 The Lowpass to Bandpass (LP-BP) Frequency Transformation

If the frequency transformation

$$s \quad \leftrightarrow \quad \frac{s^2 + \omega_o^2}{sBW} \tag{5.10}$$

is applied to the transfer function $H_{LPn}(s)$ of a normalized lowpass filter, i.e. if s is replaced by $\frac{s^2+\omega_o^2}{sBW}$, then for the new transfer function, denoted by $H_{BP}(s)$, we have:

$$H_{BP}(s) = H_{LPn}\left(\frac{s^2 + \omega_o^2}{sBW}\right) \tag{5.11}$$

The transformation defined in (5.10) is called *lowpass to bandpass* (LP-BP) transformation and, as will be seen, transforms a normalized lowpass filter into a bandpass filter with center frequency ω_o and passband bandwidth BW.

The LP-BP transformation, when expressed in terms of real frequencies, reveals the mapping of the lowpass real frequencies Ω to the bandpass frequencies ω:

$$j\Omega_x \quad \leftrightarrow \quad \frac{-\omega^2 + \omega_o^2}{j\omega \cdot BW} \quad \Rightarrow \quad \Omega_x \quad \leftrightarrow \quad \frac{\omega^2 - \omega_o^2}{\omega \cdot BW} \tag{5.12}$$

The transformation equation, derived directly from (5.10):

$$\omega^2 - \omega\, \Omega_x BW - \omega_o^2 = 0$$

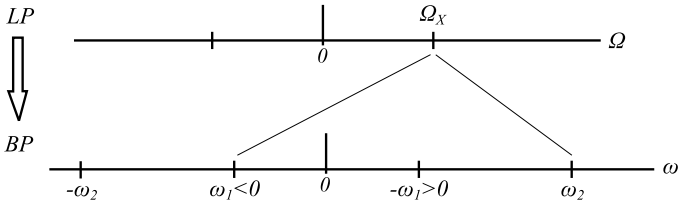

Fig. 5.15 The LP-BP transformation of positive frequencies

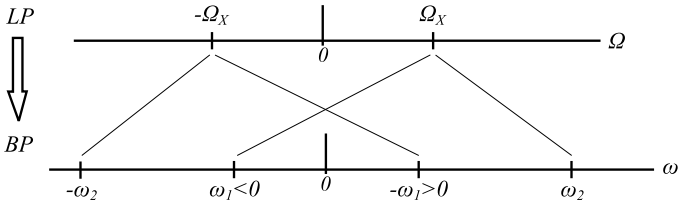

Fig. 5.16 The LP-BP transformation of positive and negative frequencies

gives two roots:

$$\begin{aligned}\omega_1 &= +\frac{BW}{2}\Omega_x - \sqrt{\frac{BW^2}{4}\Omega_x^2 + \omega_o^2} < 0 \quad \text{and} \\ \omega_2 &= +\frac{BW}{2}\Omega_x + \sqrt{\frac{BW^2}{4}\Omega_x^2 + \omega_o^2} > 0\end{aligned} \tag{5.13}$$

This means that the LP-BP transformation maps a normalized frequency Ω_x of the lowpass to two frequencies:

$$\omega_1 < 0 \quad \text{and} \quad \omega_2 > 0$$

as shown in Fig. 5.15.

Negative frequencies $-\Omega_x$ of the lowpass also map to two bandpass frequencies

$$\begin{aligned}-\omega_1 &= -\frac{BW}{2}\Omega_x + \sqrt{\frac{BW^2}{4}\Omega_x^2 + \omega_o^2} > 0 \quad \text{and} \\ -\omega_2 &= -\frac{BW}{2}\Omega_x - \sqrt{\frac{BW^2}{4}\Omega_x^2 + \omega_o^2} < 0\end{aligned} \tag{5.14}$$

as shown in Fig. 5.16

From (5.13), it is clear that for the characteristic values of Ω we have:

1. $\Omega_x = 0$ maps to $\pm\omega_o$
2. $\Omega_x = \infty$ maps to $\omega = 0$ and $\omega = \infty$

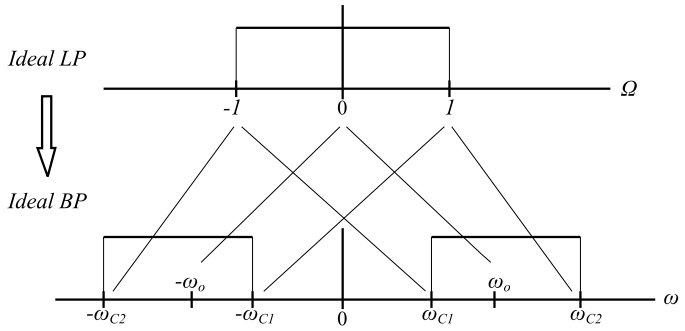

Fig. 5.17 LP-BP transformation of the gain of an ideal lowpass filter

3. Frequency $\Omega_x = 1$ maps to

$$\omega_{C2} = +\frac{BW}{2} + \sqrt{\frac{BW^2}{4} + \omega_o^2} \quad \text{and} \quad -\omega_{C1} = +\frac{BW}{2} - \sqrt{\frac{BW^2}{4} + \omega_o^2} < 0 \tag{5.15}$$

4. Frequency $\Omega_x = -1$ maps to

$$\omega_{C1} = -\frac{BW}{2} + \sqrt{\frac{BW^2}{4} + \omega_o^2} > 0 \quad \text{and} \quad -\omega_{C2} = -\frac{BW}{2} - \sqrt{\frac{BW^2}{4} + \omega_o^2} < 0 \tag{5.16}$$

Figure 5.17 shows the LP-BP transformation of the gain of an ideal normalized lowpass filter.

5. Frequency Ω_S maps to

$$\begin{aligned} \omega_{S2} &= +\frac{BW}{2}\Omega_S + \sqrt{\frac{BW^2}{4}\Omega_S^2 + \omega_o^2} \quad \text{and} \\ -\omega_{S1} &= +\frac{BW}{2}\Omega_S - \sqrt{\frac{BW^2}{4}\Omega_S^2 + \omega_o^2} < 0 \end{aligned} \tag{5.17}$$

6. Frequency $-\Omega_S$ maps to

$$\begin{aligned} \omega_{S1} &= -\frac{BW}{2}\Omega_S + \sqrt{\frac{BW^2}{4}\Omega_S^2 + \omega_o^2} > 0 \quad \text{and} \\ -\omega_{S2} &= -\frac{BW}{2}\Omega_S - \sqrt{\frac{BW^2}{4}\Omega_S^2 + \omega_o^2} < 0 \end{aligned} \tag{5.18}$$

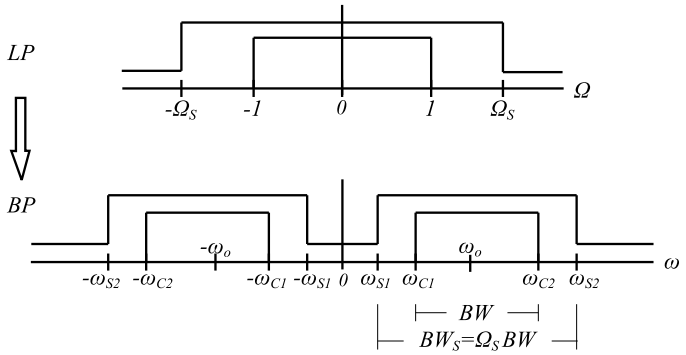

Fig. 5.18 LP-BP transformation of the specifications of a real lowpass filter

From (5.15) to (5.18), it can be found that

$$\begin{aligned} &\omega_{C1}\omega_{C2} = \omega_{S1}\omega_{S2} = \omega_o^2 \\ &\omega_{C2} - \omega_{C1} = BW \quad \text{and} \quad \omega_{S2} - \omega_{S1} = BW_S = \Omega_S BW \end{aligned} \tag{5.19}$$

It should be noted that ω_o is the geometric and not the arithmetic mean of both passband and stopband edge frequencies, i.e. ω_o is not $\frac{1}{2}(\omega_{C1} + \omega_{C2})$.

The complete LP-BP transformation of the box constraints of a practical normalized lowpass filter is shown in Fig. 5.18. It should be noticed that due to the characteristics of the transformation, the maximum gains in the two stopbands of the bandpass filter are equal to the maximum stopband gain of the lowpass specifications.

Based on the above mapping, and referring to Fig. 5.19, it is clear that $H_{BP}(s)$ of (5.11) is the transfer function of a bandpass filter with the same gain tolerances as the lowpass.

Therefore, in order to design a bandpass filter with the specifications of Fig. 5.20a

$$\{H_o,\ H_C,\ H_S,\ \omega_o,\ BW,\ BW_S\}$$

or in terms of logarithmic gain

$$\{\alpha_o,\ \alpha_{\max},\ \alpha_{\min},\ BW,\ BW_S\}$$

we can first design a normalized lowpass filter with the specifications of Fig. 5.20b

$$\left\{H_o,\ H_C,\ H_S,\ \Omega_S = \frac{BW_S}{BW} > 1\right\} \quad (\Omega_C = 1)$$

or in terms of logarithmic gain

$$\left\{\alpha_o,\ \alpha_{\max},\ \alpha_{\min},\ \Omega_S = \frac{BW_S}{BW} > 1\right\} \quad (\Omega_C = 1)$$

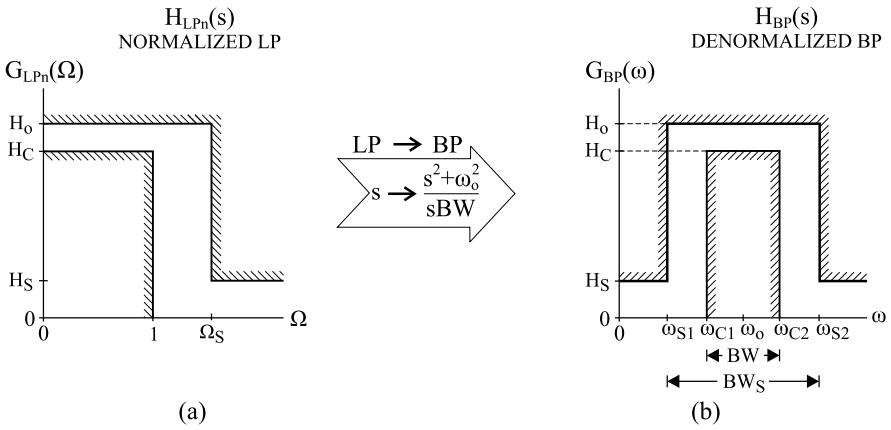

Fig. 5.19 The effect of the LP-BP transformation on the specifications of a normalized lowpass filter

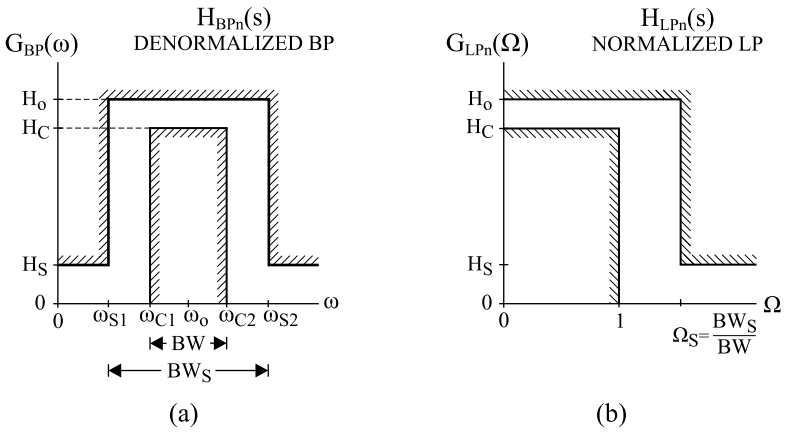

Fig. 5.20 (**a**) BP specifications. (**b**) Normalized specifications of the auxiliary LP filter

If the transfer function of the so designed normalized lowpass filter is $H_{LPn}(s)$, the transfer function of the denormalized bandpass filter will be

$$H_{BP}(s) = H_{LPn}\left(\frac{s^2+\omega_o^2}{sBW}\right)$$

As mentioned above, due to the characteristics of the transformation, the two stopbands of the bandpass filter are symmetric with maximum gain equal to the maximum stopband gain of the lowpass specifications. This means that if a bandpass filter with non-symmetric stopband gains is specified, the strictest specifications should be considered.

5.2.1 The LP-BP Frequency Transformation at Transfer Function Level

We have seen that the normalized lowpass transfer functions of (5.2) and (5.4) can be expressed as products of the following three terms:

$$H_1(s) = \frac{1}{s+\Omega_R} \qquad H_2(s) = \frac{1}{s^2 + \frac{\Omega_q}{Q_q}s + \Omega_q^2} \qquad H_3(s) = \frac{s^2+\Omega_z^2}{s^2 + \frac{\Omega_q}{Q_q}s + \Omega_q^2} \tag{5.20}$$

The result of applying the LP-BP transformation to these terms is presented below.

5.2.1.1 Transformation of First Order Terms $\frac{1}{s+\Omega_R}$

$$\frac{1}{s+\Omega_R} \xrightarrow{s\to\frac{s^2+\omega_o^2}{sBW}} \frac{sBW}{s^2 + s\frac{\omega_o}{Q_R} + \omega_o^2} \quad \text{where } Q_R = \frac{\omega_o}{\Omega_R BW} \tag{5.21}$$

This is a second order bandpass function which can be realized by a second order active-RC bandpass circuit like Sallen-Key, Deliyiannis etc. (see Chap. 10).

5.2.1.2 Transformation of Second Order Terms $\frac{1}{s^2+\frac{\Omega_q}{Q_q}s+\Omega_q^2}$

$$\frac{1}{(s^2 + \frac{\Omega_q}{Q_q}s + \Omega_q^2)} \xrightarrow{LP\to BP} \frac{sBW}{(s^2 + s\frac{\omega_1}{Q} + \omega_1^2)} \times \frac{sBW}{(s^2 + s\frac{\omega_2}{Q} + \omega_2^2)} \tag{5.22}$$

This is a product of two second order bandpass transfer functions which can be realized by two second order active-RC bandpass circuits (see Chap. 10).

Parameters ω_1, ω_2 and the common Q have been determined as follows:

$$Q = \frac{1}{2c}\sqrt{2b + 2\sqrt{b^2 - 4\alpha^2 c^2}} \quad \text{and} \tag{5.23}$$

$$\omega_2 = \frac{BW}{2}\left(cQ + \sqrt{\omega_q^2 - \frac{\alpha^2}{Q^2}}\right), \qquad \omega_1 = \frac{\omega_o^2}{\omega_2} \quad \Rightarrow \quad \omega_1\omega_2 = \omega_o^2 \tag{5.24}$$

where

$$\alpha = \frac{\omega_o}{BW} \qquad b = \omega_q^2 + 4\alpha^2 \qquad c = \frac{\omega_q}{Q_q} \tag{5.25}$$

Finally, the transformation maps the lowpass pole pair $\{\Omega_q, Q_q\}$ to two pole pairs $\{\omega_1, Q\}$ and $\{\omega_2, Q\}$ with common Q and pole frequencies given by (5.23) and (5.24). The common Q of the new poles $\{\omega_1, Q\}$ and $\{\omega_2, Q\}$ might be much

higher than Q_q of the lowpass, since it depends on $a = \frac{\omega_o}{BW}$, which assumes very high values in narrowband filters.

5.2.1.3 Transformation of Second Order Terms $\frac{s^2+\Omega_z^2}{s^2+\frac{\Omega_q}{Q_q}s+\Omega_q^2}$

Terms of the form $(s^2 + \Omega_z^2)/(s^2 + s\Omega_q/Q_q + \Omega_q^2)$ appear in the transfer function of normalized lowpass filters designed with rational approximations (see Chap. 3), e.g. inverse Chebyshev, inverse Pascal or elliptic, and they are transformed as follows:

$$\frac{s^2+\Omega_z^2}{s^2+\frac{\Omega_q}{Q_q}s+\Omega_q^2} \xrightarrow{LP\to BP} \frac{(s^2+\omega_{1Z}^2)(s^2+\omega_{2Z}^2)}{(s^2+\frac{\omega_1}{Q}s+\omega_1^2)(s^2+\frac{\omega_2}{Q}s+\omega_2^2)} \tag{5.26}$$

Q and frequencies ω_1 and ω_2 of the denominator are calculated from (5.23) and (5.24) and the transmission zeros are given by

$$\omega_{1Z} = \frac{BW}{2}\sqrt{4\left(\frac{\omega_o}{BW}\right)^2 + 2\Omega_z^2 - 2\Omega_z\sqrt{4\left(\frac{\omega_o}{BW}\right)^2 + \Omega_z^2}} \tag{5.27}$$

$$\omega_{2Z} = \frac{BW}{2}\sqrt{4\left(\frac{\omega_o}{BW}\right)^2 + 2\Omega_z^2 + 2\Omega_z\sqrt{4\left(\frac{\omega_o}{BW}\right)^2 + \Omega_z^2}} \tag{5.28}$$

$$\omega_{1Z}\omega_{2Z} = \omega_o^2 \tag{5.29}$$

Example 5.4 In order to design an elliptic bandpass filter with specifications $\{\alpha_o = 0, \alpha_{\max} = 1.25$ dB, $\alpha_{\min} = 30$ dB$\}$ and $\{f_o = 5000$ Hz, $BW = 2\pi 2000$ rad/s, $BW_S = 2\pi 3400$ rad/s$\}$, we must first design a normalized elliptic lowpass filter with specifications $\{\alpha_o = 0,\ \alpha_{\max} = 1.25$ dB, $\alpha_{\min} = 30$ dB, $\Omega_S = 3400/2000 = 1.7\}$. Following the design procedure of Chap. 4, we find $N = 3$ and:

$$H_{LPn}(s) = 137.5982 \cdot 10^{-3}\frac{(s^2+3.667)}{(s+0.514)(s^2+0.3764s+0.9816)} \tag{5.30}$$

Applying the LP-BP transformation to the first and second order terms as described above, we end up with the transfer function of the denormalized bandpass filter:

$$H_{BP}(s) = \frac{1729.1s(s^2+466.966\cdot 10^6)(s^2+2086.0\cdot 10^6)}{(s^2+6459.1s+\omega_o^2)(s^2+1913.4s+\omega_1^2)(s^2+2817.7s+\omega_2^2)} \tag{5.31}$$

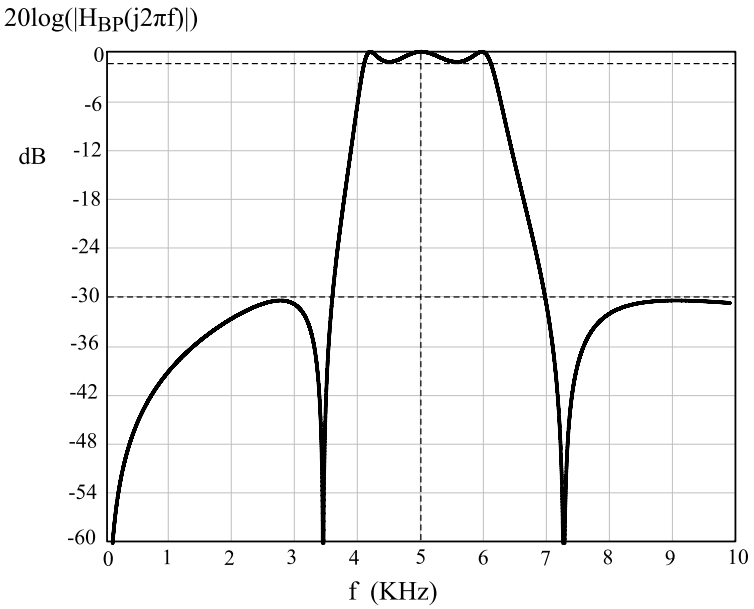

Fig. 5.21 Logarithmic gain of the bandpass filter of Example 5.4

where $\omega_o^2 = 986.96 \cdot 10^6$, $\omega_1^2 = 670.22 \cdot 10^6$ and $\omega_2^2 = 1453.4 \cdot 10^6$. Figure 5.21 shows the plot of the logarithmic gain $20 \log |H_{BP}(j2\pi f)|$.

5.2.2 The LP-BP Frequency Transformation at Component Level

The LP-BP transformation of (5.10) can be applied at component level, i.e. to the impedance of each element, as follows:

1. Resistor $R \overset{LP \to BP}{\longrightarrow}$ Resistor R
2. Inductor with $Z_{LP}(s) = sL \overset{LP \to BP}{\longrightarrow} Z_{BP}(s) = \frac{L}{BW} s + \frac{1}{s \frac{BW}{\omega_o^2 L}} =$ inductor with $L_{BP} = \frac{L}{BW}$ in series with capacitor with $C_{BP} = \frac{BW}{\omega_o^2 L}$
3. Capacitor with $Y_{LP}(s) = sC \overset{LP \to BP}{\longrightarrow} Y_{BP}(s) = s \frac{C}{BW} + \frac{1}{s \frac{BW}{\omega_o^2 C}} =$ capacitor with $C_{BP} = \frac{C}{BW}$ in parallel with inductor with $L_{BP} = \frac{BW}{\omega_o^2 C}$

The LP-BP transformation applied at component level to a normalized lowpass circuit, simply transforms inductors to series resonant circuits and capacitors to parallel resonant circuits. Figure 5.22 shows an example of the application of the LP-BP transformation to a normalized passive lowpass filter.

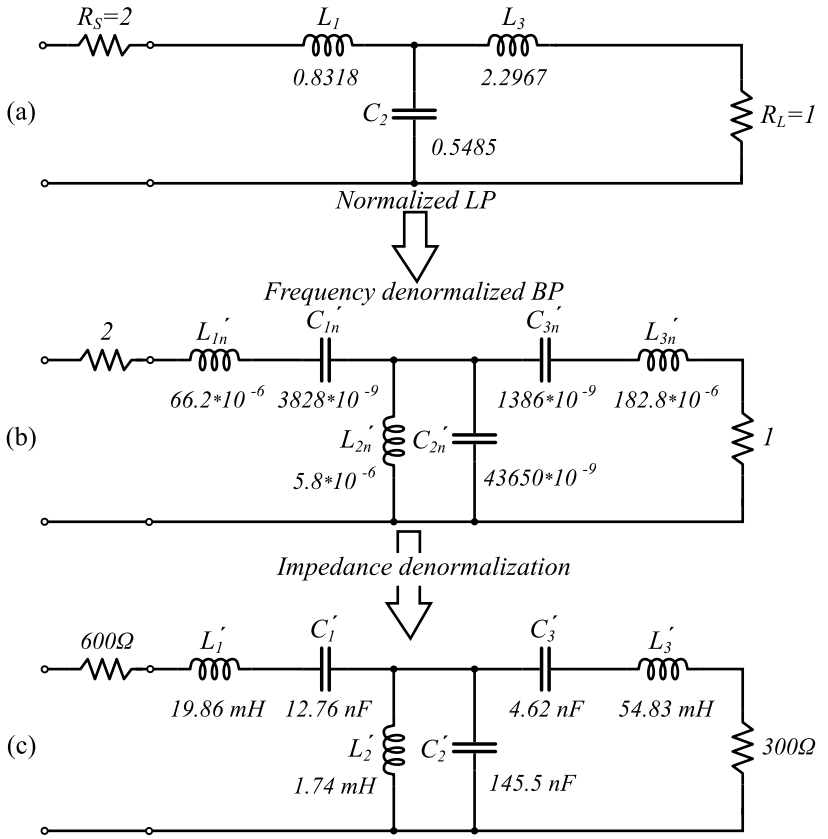

Fig. 5.22 Application of the LP-BP transformation to a passive lowpass filter at component level

The component values of the bandpass obtained by the LP-BP transformation, are still impedance scaled since the transformation performs only frequency denormalization. Therefore, impedance denormalization is required to bring the resistor values to the desirable level.

Example 5.5 The circuit of Fig. 5.22a is a passive normalized lowpass filter. If the LP-BP transformation is applied with $\omega_o = 2\pi\,10955.4$ rad/s and $BW = 2\pi\,2000$ rad/s, the bandpass filter of Fig. 5.22b is derived with normalized resistors. Impedance scaling can now be applied to bring the load to the desirable level, e.g. 300 Ohm. It is reminded that this is done by multiplying all resistor and inductor values by 300 Ohm and dividing all capacitor values by 300 Ohm, as has been done in Fig. 5.22c.

In inductorless circuits, like active-RC circuits, the LP-BP transformation could be implemented by replacing capacitors C with parallel resonant circuits but the circuit would not be inductorless any more. For this reason, the transformation is

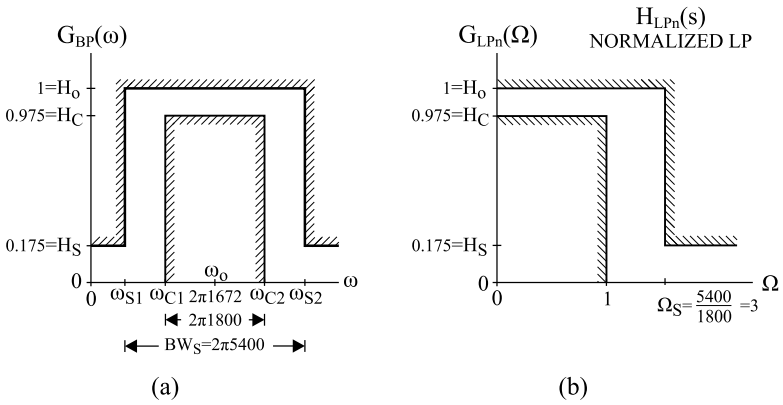

Fig. 5.23 (**a**) BP specifications. (**b**) Normalized specifications of the auxiliary LP filter

not used to directly transform active-RC lowpass filters to bandpass, as was the case with the LP-HP transformation.

Example 5.6 Design an active-RC bandpass filter with Chebyshev response from the gain specifications shown in Fig. 5.23a.

From Fig. 5.23a we have:

$$\omega_o = 2\pi\,1672 \text{ rad/s}, \qquad BW = 2\pi\,1800 \text{ rad/s} \quad \text{and} \quad BW_S = 2\pi\,5400 \text{ rad/s}$$

Although not necessary, the edge frequencies can be calculated from $\omega_{C1}\omega_{C2} = \omega_{S1}\omega_{S2} = \omega_o^2$, $\omega_{C2} - \omega_{C1} = BW$ and $\omega_{S2} - \omega_{S1} = BW_S$.

The auxiliary normalized lowpass filter will have the specifications shown in Fig. 5.23b. From the Chebyshev order equation (2.46), we find $N = 3$. The transfer function of the normalized lowpass is determined for the stopband edge frequency gain optimized filter with $\epsilon = \epsilon_{\max}$ (see Sect. 2.3.4):

$$H_{LPn}(s) = 1.09696\frac{1}{s + 0.794339}\,\frac{1}{s^2 + 0.7943386s + 1.38097375} \tag{5.32}$$

According to (5.21), the first order term with $\Omega_R = 0.794339$ is transformed into

$$\frac{sBW}{s^2 + s\frac{\omega_o}{Q_R} + \omega_o^2} \quad \text{with } \omega_o = 2\pi\,1672 \text{ and } Q_R = \frac{\omega_o}{\Omega_R BW} = 1.16939$$

The second order term with $\Omega_q = \sqrt{1.38097375} = 1.1751438$ and $Q_q = 1.1751438/0.7943386 = 1.4794047$ is transformed according to (5.22) into

$$\frac{sBW}{(s^2 + s\frac{\omega_1}{Q} + \omega_1^2)}\,\frac{sBW}{(s^2 + s\frac{\omega_2}{Q} + \omega_2^2)}$$

From (5.23) to (5.25), we find $\omega_1 = 5919.92$, $\omega_2 = 18643$ and $Q = 2.73415$.

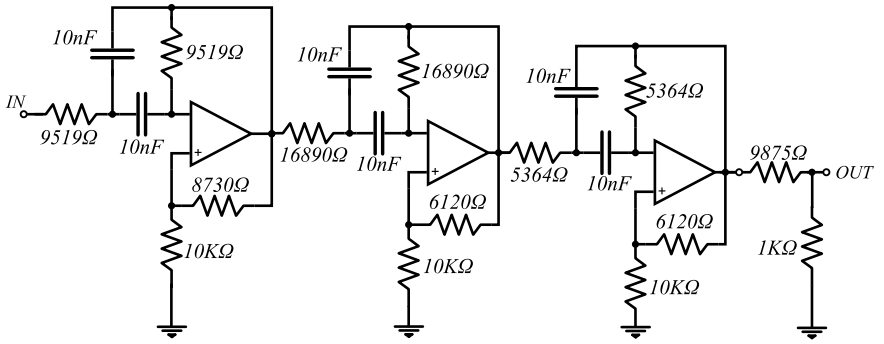

Fig. 5.24 The denormalized active BP filter

Finally, the transfer function of the bandpass filter will be

$$1.09696 \cdot BW^3 \cdot \frac{s}{(s^2 + s\frac{\omega_o}{Q_R} + \omega_o^2)} \cdot \frac{s}{(s^2 + s\frac{\omega_1}{Q} + \omega_1^2)} \frac{s}{(s^2 + s\frac{\omega_2}{Q} + \omega_2^2)}$$

with

$$\omega_o = 2\pi 1672 \qquad Q_R = 1.16939 \qquad \omega_1 = 5919.92$$
$$\omega_2 = 18643 \qquad Q = 2.73415$$

The three bandpass sections can now be realized using any bandpass second order circuit. If the Deliyannis biquad is used (see Chap. 10), the final bandpass filter will be that of Fig. 5.24. The final resistive attenuator has been added to adjust the frequency independent gain of the numerator. The filter was simulated and Fig. 5.25 shows the plain gain plot.

5.3 The Lowpass to Band-Reject (LP-BR) Frequency Transformation

If the frequency transformation

$$s \quad \leftrightarrow \quad \frac{sBW}{s^2 + \omega_o^2} \tag{5.33}$$

is applied to the transfer function $H_{LPn}(s)$ of a normalized lowpass filter, i.e. if s is replaced by $\frac{sBW}{s^2+\omega_o^2}$, then for the new transfer function, denoted by $H_{BR}(s)$, we have:

$$H_{BR}(s) = H_{LPn}\left(\frac{sBW}{s^2 + \omega_o^2}\right) \tag{5.34}$$

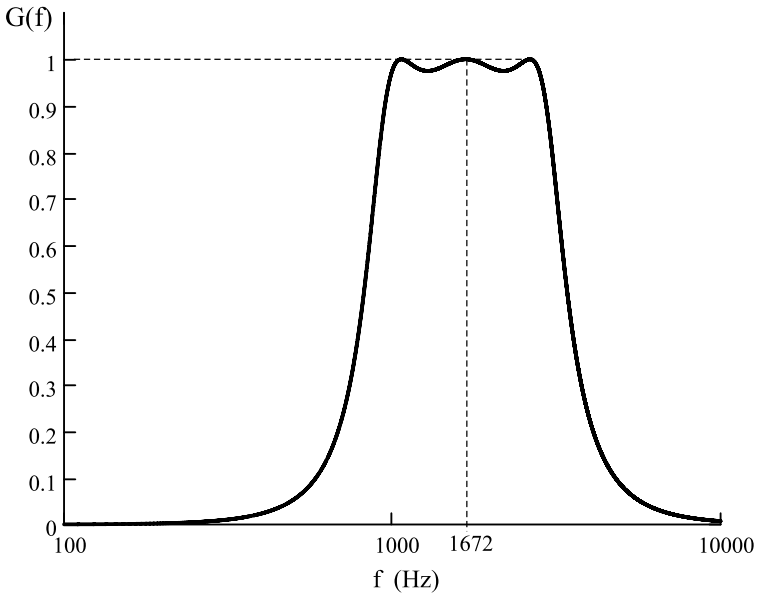

Fig. 5.25 Gain plot of the bandpass filter (simulation)

The frequency transformation defined in (5.33) is called *lowpass to band-reject* (LP-BR) transformation and as will be seen, transforms a normalized lowpass filter into a band-reject filter with center frequency ω_o and passband bandwidth BW.

The LP-BR transformation, when expressed in terms of real frequencies, reveals the mapping of the lowpass real frequencies Ω to the band-reject frequencies ω:

$$j\Omega_x \quad \leftrightarrow \quad j\frac{\omega \cdot BW}{-\omega^2+\omega_o^2} \quad \Rightarrow \quad \Omega_x \quad \leftrightarrow \quad \frac{\omega \cdot BW}{\omega_o^2-\omega^2} \tag{5.35}$$

The transformation equation

$$\omega^2\Omega_x + \omega BW - \omega_o^2\Omega_x = 0$$

derived directly from (5.35), gives two roots:

$$\begin{aligned} \omega_1 &= \frac{BW}{2\Omega_x}\left(-1+\sqrt{1+4\frac{\omega_o^2}{BW^2}\Omega_x^2}\right) > 0 \quad \text{and} \\ \omega_2 &= \frac{BW}{2\Omega_x}\left(-1-\sqrt{1+4\frac{\omega_o^2}{BW^2}\Omega_x^2}\right) < 0 \end{aligned} \tag{5.36}$$

This means that the LP-BR transformation maps a normalized frequency Ω_x of the lowpass to two frequencies:

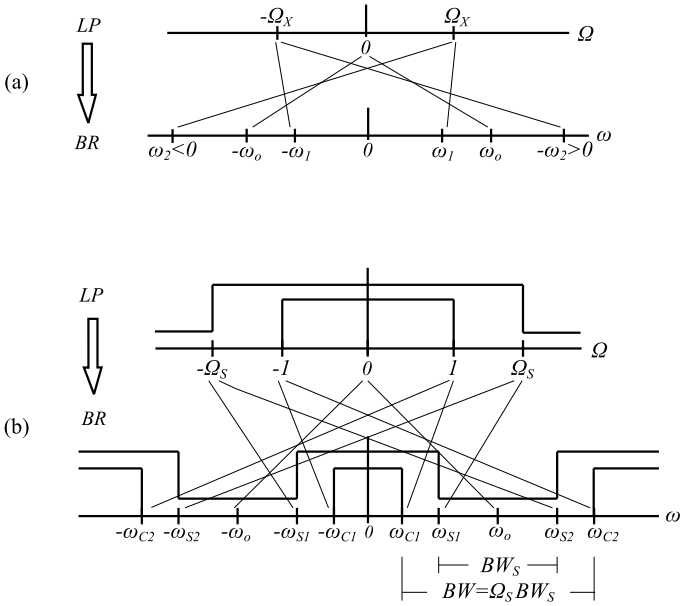

Fig. 5.26 The LP-BR mapping (**a**) of a single frequency, (**b**) of the LP specifications

$$\omega_1 > 0 \quad \text{and} \quad \omega_2 < 0$$

as shown in Fig. 5.26a.

Negative frequencies $-\Omega_x$ of the lowpass, also map to two band-reject frequencies

$$\begin{aligned} -\omega_1 &= -\frac{BW}{2\Omega_x}\left(-1+\sqrt{1+4\frac{\omega_o^2}{BW^2}\Omega_x^2}\right) < 0 \quad \text{and} \\ -\omega_2 &= \frac{BW}{2\Omega_x}\left(+1+\sqrt{1+4\frac{\omega_o^2}{BW^2}\Omega_x^2}\right) > 0 \end{aligned} \tag{5.37}$$

as shown in Fig. 5.26a.

From (5.36) it is clear that for the characteristic values of Ω we have:

1. $\Omega_x = \infty$ maps to $\pm\omega_o$
2. $\Omega_x = 0$ maps to 0 and ∞
3. Frequency $\Omega_x = 1$ maps to

$$\begin{aligned} \omega_{C1} &= \frac{BW}{2}\left(-1+\sqrt{1+4\frac{\omega_o^2}{BW^2}}\right) > 0 \quad \text{and} \\ -\omega_{C2} &= -\frac{BW}{2}\left(1+\sqrt{1+4\frac{\omega_o^2}{BW^2}}\right) < 0 \end{aligned} \tag{5.38}$$

4. Frequency $\Omega_x = -1$ maps to

$$\begin{aligned} -\omega_{C1} &= -\frac{BW}{2}\left(-1+\sqrt{1+4\frac{\omega_o^2}{BW^2}}\right) < 0 \quad \text{and} \\ \omega_{C2} &= \frac{BW}{2\Omega_x}\left(1+\sqrt{1+4\frac{\omega_o^2}{BW^2}}\right) > 0 \end{aligned} \tag{5.39}$$

5. Frequency Ω_S maps to

$$\begin{aligned} \omega_{S1} &= \frac{BW}{2\Omega_S}\left(-1+\sqrt{1+4\frac{\omega_o^2}{BW^2}\Omega_S^2}\right) > 0 \quad \text{and} \\ \omega_{S2} &= \frac{BW}{2\Omega_S}\left(-1-\sqrt{1+4\frac{\omega_o^2}{BW^2}\Omega_S^2}\right) < 0 \end{aligned} \tag{5.40}$$

6. Frequency $-\Omega_S$ maps to

$$\begin{aligned} -\omega_{S1} &= -\frac{BW}{2\Omega_S}\left(-1+\sqrt{1+4\frac{\omega_o^2}{BW^2}\Omega_S^2}\right) < 0 \quad \text{and} \\ -\omega_{S2} &= \frac{BW}{2\Omega_S}\left(+1+\sqrt{1+4\frac{\omega_o^2}{BW^2}\Omega_S^2}\right) > 0 \end{aligned} \tag{5.41}$$

From (5.38) to (5.41), it can be found that

$$\begin{aligned} &\omega_{C1}\omega_{C2} = \omega_{S1}\omega_{S2} = \omega_o^2 \\ &\omega_{S2} - \omega_{S1} = BW_S \quad \text{and} \quad \omega_{C2} - \omega_{C1} = BW = BW_S \cdot \Omega_S \end{aligned} \tag{5.42}$$

As in the bandpass case, center frequency ω_o is the geometric and not the arithmetic mean of both passband and stopband edge frequencies. It should be underlined that although in the band-reject filter the band of interest is BW_S, the LP-BR transformation uses the bandwidth $BW = \omega_{C2} - \omega_{C1} = BW_S$.

The complete LP-BR transformation of the box constraints of a practical normalized lowpass filter is shown in Fig. 5.26b. The part of interest is shown better in Fig. 5.27. It should be noted again that due to the characteristics of the transformation, the gains in the two passbands of the band-reject filter are equal to the gain of the lowpass in the passband.

Based on the above mapping and referring to Fig. 5.27, it is clear that $H_{BR}(s)$ of (5.34) is the transfer function of a band-reject filter with the same gain tolerances as the lowpass.

Therefore, in order to design a band-reject filter with the specifications of Fig. 5.28a

$$\{H_o, H_C, H_S, \omega_o, BW, BW_S < BW\}$$

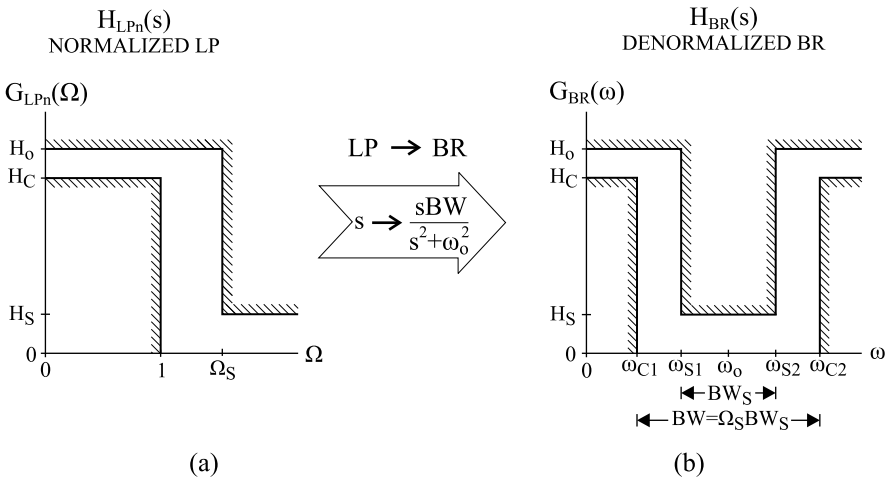

Fig. 5.27 (**a**) Normalized LP specifications. (**b**) Denormalized BR specifications

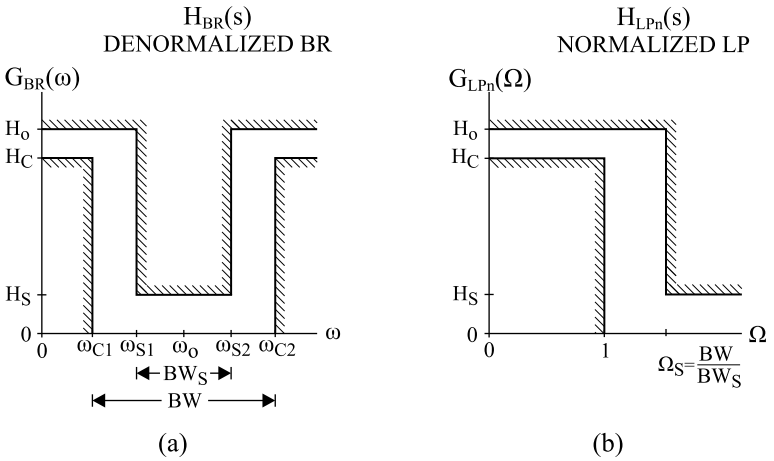

Fig. 5.28 (**a**) BR specifications. (**b**) Specifications of the auxiliary normalized LP filter

or in terms of logarithmic gain

$$\{\alpha_o, \alpha_{\max}, \alpha_{\min}, BW, BW_S < BW\}$$

we can first design an auxiliary normalized lowpass filter with the specifications of Fig. 5.28b

$$\left\{H_o, H_C, H_S, \Omega_S = \frac{BW}{BW_S} > 1\right\} \quad (\Omega_C = 1)$$

or in terms of logarithmic gain

$$\left\{\alpha_o, \alpha_{\max}, \alpha_{\min}, \Omega_S = \frac{BW}{BW_S} > 1\right\} \quad (\Omega_C = 1)$$

and if the transfer function of the so designed normalized lowpass filter is $H_{LPn}(s)$, the transfer function of the frequency denormalized band-reject filter will be

$$H_{BR}(s) = H_{LPn}\left(\frac{sBW}{s^2 + \omega_o^2}\right)$$

As mentioned above, due to the characteristics of the transformation, the two passbands of the band-reject filter are symmetric with gain equal to the gain of the lowpass passband. This means that if a band-reject filter with non-symmetric passband gains is specified, the strictest specifications should be considered.

5.3.1 The LP-BR Frequency Transformation at Transfer Function Level

As seen, normalized lowpass transfer functions can be expressed as products of the following three terms, repeated here for convenience:

$$\frac{1}{s + \Omega_R} \qquad \frac{1}{s^2 + \frac{\Omega_q}{Q_q}s + \Omega_q^2} \qquad \frac{s^2 + \Omega_z^2}{s^2 + \frac{\Omega_q}{Q_q}s + \Omega_q^2}$$

The result of applying the LP-BR transformation to these terms is presented below.

5.3.1.1 Transformation of First Order Terms $\frac{1}{s+\Omega_R}$

$$\frac{1}{(s + \Omega_R)} \quad \overset{s \to \frac{sBW}{s^2+\omega_o^2}}{\longrightarrow} \quad \frac{\frac{1}{\Omega_R}(s^2 + \omega_o^2)}{s^2 + s\frac{\omega_o}{Q_R} + \omega_o^2} \quad \text{where } Q_R = \frac{\omega_o \Omega_R}{BW} \tag{5.43}$$

This is a second order band-reject function which can be realized by a second order active-RC notch circuit like Tow-Thomas, CGIC, etc. (see Chap. 10).

5.3.1.2 Transformation of Second Order Terms $\frac{1}{s^2+\frac{\Omega_q}{Q_q}s+\Omega_q^2}$

$$\frac{1}{(s^2 + \frac{\Omega_q}{Q_q}s + \Omega_q^2)} \quad \overset{LP \to BR}{\longrightarrow} \quad \frac{1}{\Omega_q^2}\frac{s^2 + \omega_o^2}{(s^2 + s\frac{\omega_1}{Q} + \omega_1^2)} \times \frac{s^2 + \omega_o^2}{(s^2 + s\frac{\omega_2}{Q} + \omega_2^2)} \tag{5.44}$$

This is a product of two second order band-reject transfer functions which can be realized by two second order active-RC band-reject circuits (see Chap. 10).

Parameters ω_1, ω_2 and the common Q, are calculated as follows:

$$Q = Q_q \sqrt{\frac{1}{2} + 2a^2\Omega_q^2 + \sqrt{\frac{1}{4} + 2a^2\Omega_q^2 + 4a^4\Omega_q^4 - a^2\frac{\Omega_q^2}{Q_q^2}}} \quad \text{and} \tag{5.45}$$

$$\omega_2 = \frac{BW}{2Q}\left(\sqrt{\frac{Q^2}{\Omega_q^2} - a^2} + \sqrt{\frac{Q^2}{\Omega_q^2} - a^2 + 4a^2Q^2}\right) \qquad \omega_1 = \frac{\omega_o^2}{\omega_2}$$

$$\text{where } \alpha = \frac{\omega_o}{BW} \tag{5.46}$$

Finally, the transformation maps the lowpass pole pair $\{\Omega_q, Q_q\}$ to two pole pairs $\{\omega_1, Q\}$ and $\{\omega_2, Q\}$ with common Q and pole frequencies given by (5.45) and (5.46). The common Q of the band-reject poles $\{\omega_1, Q\}$ and $\{\omega_2, Q\}$ might be much higher than Q_q of the lowpass, since it depends on $a = \frac{\omega_o}{BW}$, which assumes very high values in narrowband filters.

5.3.1.3 Transformation of Second Order Terms $\frac{s^2+\Omega_z^2}{s^2+\frac{\Omega_q}{Q_q}s+\Omega_q^2}$

The terms of the form $(s^2 + \Omega_z^2)/(s^2 + s\Omega_q/Q_q + \Omega_q^2)$ that appear in the transfer function of normalized lowpass filters designed with rational approximations (see Chap. 3), are transformed as follows:

$$\frac{s^2 + \Omega_z^2}{s^2 + \frac{\Omega_q}{Q_q}s + \Omega_q^2} \xrightarrow{LP\to BR} \frac{\frac{\Omega_z^2}{\Omega_q^2}(s^2 + \omega_{1Z}^2)(s^2 + \omega_{2Z}^2)}{(s^2 + \frac{\omega_1}{Q}s + \omega_1^2)(s^2 + \frac{\omega_2}{Q}s + \omega_2^2)} \tag{5.47}$$

Q and frequencies ω_1 and ω_2 of the denominator are calculated from (5.45) and (5.46) and the transmission zeros ω_{1Z} and ω_{2Z} are given by

$$\omega_{1Z} = \sqrt{b_c - \sqrt{b_c^2 - \omega_o^4}} \quad \omega_{2Z} = \sqrt{b_c + \sqrt{b_c^2 - \omega_o^4}}$$

$$\text{where } b_c = \frac{BW^2 + 2\omega_o^2\Omega_z^2}{2\Omega_z^2} \tag{5.48}$$

Example 5.7 In order to design an elliptic band-reject filter with specifications $\{\alpha_o = 0, \alpha_{\max} = 1.25 \text{ dB}, \alpha_{\min} = 30 \text{ dB}\}$ and $\{f_o = 5000 \text{ Hz}, BW_S = 2\pi 4000 \text{ rad/s}, BW = 2\pi 6800 \text{ rad/s}\}$, we must first design a normalized elliptic lowpass filter with specifications $\{\alpha_o = 0, \alpha_{\max} = 1.25 \text{ dB}, \alpha_{\min} = 30 \text{ dB}, \Omega_S = 6800/4000 = 1.7\}$. Following the design procedure of Chap. 4, we find that the order is $N = 3$ and the transfer function:

$$H_{LPn}(s) = 137.5982 \cdot 10^{-3} \frac{(s^2 + 3.667)}{(s + 0.514)(s^2 + 0.3764s + 0.9816)} \tag{5.49}$$

Applying the LP-BR transformation to the first and second order terms as described above, we end up with the transfer function of the frequency denormalized band-

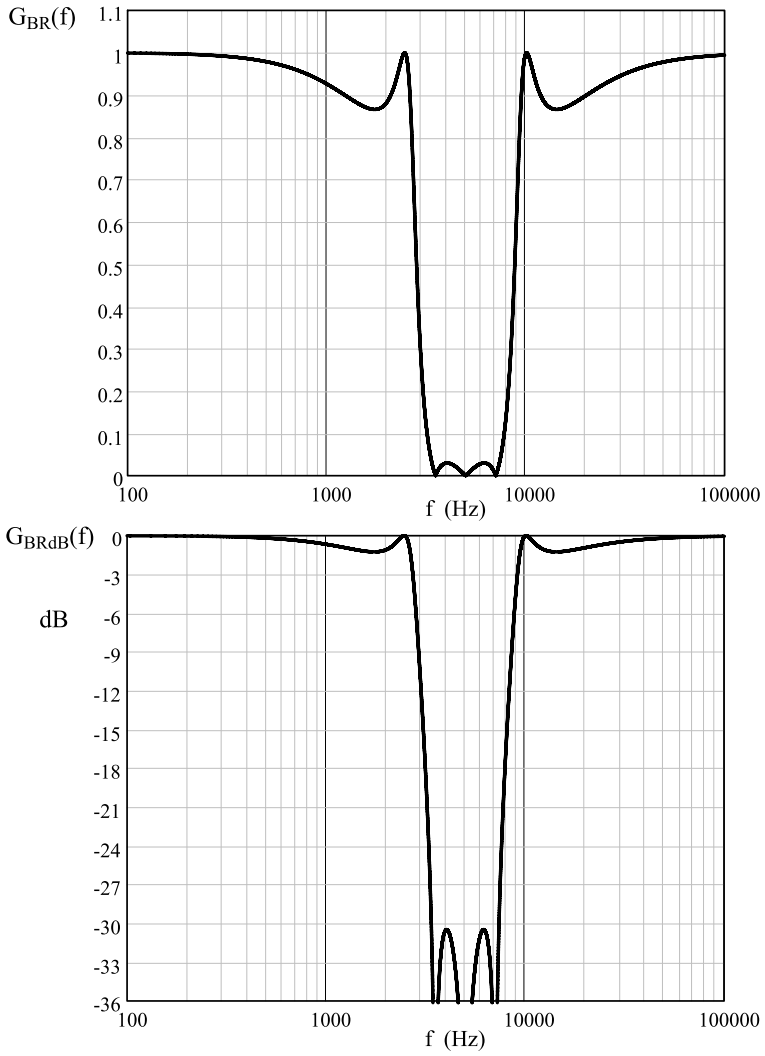

Fig. 5.29 Gain plots of Example 5.7

reject filter:

$$H_{BR}(s) = \frac{(s^2 + 986.96 \cdot 10^6)(s^2 + 492 \cdot 10^6)(s^2 + 1980 \cdot 10^6)}{(s^2 + 83124s + \omega_o^2)(s^2 + 3596s + \omega_1^2)(s^2 + 12784s + \omega_2^2)} \tag{5.50}$$

where $\omega_o^2 = 986.96 \cdot 10^6$, $\omega_1^2 = 277.59 \cdot 10^6$ and $\omega_2^2 = 3509.2 \cdot 10^6$. Figure 5.29 shows the plain gain $|H_{BR}(j2\pi f)|$ and the logarithmic gain $20\log|H_{BR}(j2\pi f)|$ of the band-reject filter.

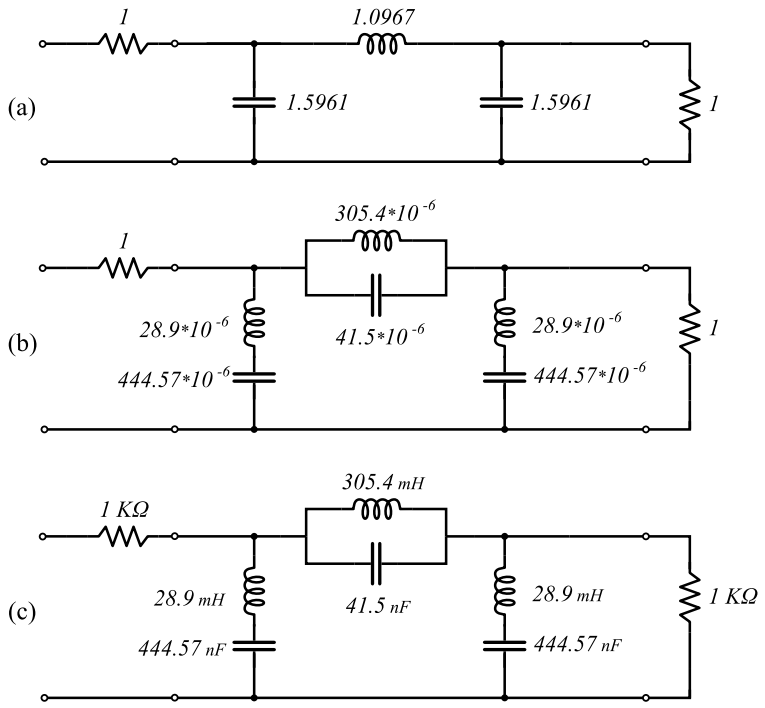

Fig. 5.30 LP-BR transformation of a passive lowpass filter

5.3.2 The LP-BR Frequency Transformation at Component Level

The LP-BR transformation of (5.33) can be applied at component level as follows:

1. Resistor $R \overset{LP\to BR}{\longrightarrow}$ Resistor R
2. Inductor $Y_{LP}(s) = \frac{1}{sL} \overset{LP\to BR}{\longrightarrow} Y_{BR}(s) = s\frac{1}{L\cdot BW} + \frac{1}{s\frac{L\cdot BW}{\omega_o^2}} =$ Capacitor with $C_{BR} = \frac{1}{L\cdot BW}$ in parallel with inductor with $L_{BR} = \frac{L\cdot BW}{\omega_o^2}$
3. Capacitor with $Z_{LP}(s) = sC \overset{LP\to BR}{\longrightarrow} Z_{BR}(s) = s\frac{1}{C\cdot BW} + \frac{1}{s\frac{C\cdot BW}{\omega_o^2}} =$ Inductor with $L_{BR} = \frac{1}{C\cdot BW}$ in series with capacitor with $C_{BR} = \frac{C\cdot BW}{\omega_o^2}$

When the LP-BR transformation is applied at component level to a normalized lowpass circuit, it simply transforms inductors to parallel resonant circuits and capacitors to series resonant circuits. Figure 5.30 shows an example of such an application of the LP-BR transformation to a normalized passive lowpass filter.

The component values of the bandpass obtained by the LP-BP transformation are still impedance scaled since the transformation performs only frequency denormalization. Therefore, impedance denormalization is required to bring the resistor values to the desirable level.

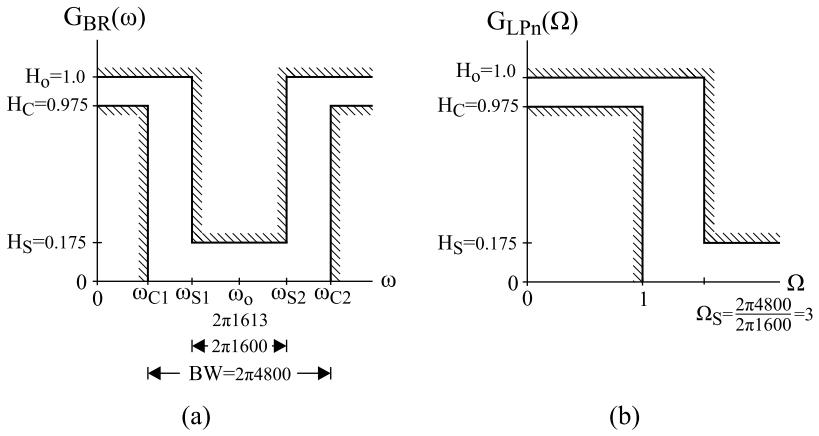

Fig. 5.31 (**a**) BR specifications. (**b**) Specifications of the auxiliary normalized LP filter

Example 5.8 The circuit of Fig. 5.30a is a 3rd order passive normalized lowpass filter. If the LP-BR transformation is applied with $\omega_o = 2\pi 1414.2$ rad/s and $BW = 2\pi 3500$ rad/s, the bandpass filter of Fig. 5.30b is derived with normalized resistors. Impedance scaling can now be applied to bring the load to the desirable level, e.g. 1000 Ohm. This is achieved by multiplying all resistor and inductor values by 1000 Ohm and dividing all capacitor values by 1000 Ohm, as has been done in Fig. 5.30c.

Example 5.9 In this example, a Chebyshev band-reject filter with the specifications of Fig. 5.31a will be designed.

From Fig. 5.31a, we have:

$$\omega_o = 2\pi 1613 \text{ rad/s} \qquad BW = 2\pi 4800 \text{ rad/s} \quad \text{and} \quad BW_S = 2\pi 1600 \text{ rad/s}.$$

Although not necessary, the edge frequencies can be determined from $\omega_{C1}\omega_{C2} = \omega_{S1}\omega_{S2}\omega_o^2$, $\omega_{C2} - \omega_{C1} = BW$ and $\omega_{S2} - \omega_{S1} = BW_S$.

The specifications of the auxiliary normalized lowpass are shown in Fig. 5.31b. From the Chebyshev design equations (see Chap. 2 Sect. 2.3), we find $N = 3$, and for the stopband edge frequency gain optimized filter with $\epsilon = \epsilon_{\max}$, the transfer function of the auxiliary normalized lowpass can be determined:

$$H_{LPn}(s) = 1.09696 \frac{1}{s + 0.794339} \frac{1}{s^2 + 0.7943386s + 1.38097375}$$

According to (5.43), the term $1/(s + 0.794339)$ with $\Omega_R = 0.794339$ and $Q_R = \omega_o \Omega_R / BW = 0.266931$ is transformed into

$$H_1(s) = \frac{\frac{1}{\Omega_R}(s^2 + \omega_o^2)}{s^2 + s\frac{\omega_o}{Q_R} + \omega_o^2} \quad \text{where } Q_R = \frac{\omega_o \Omega_R}{BW}$$

This can be realized by a 2nd order notch circuit.

According to (5.44), the term $1/(s^2 + 0.7943386s + 1.38097375)$ with $\Omega_q = 1.1751483$ and $Q_q = 1.4794047$ is transformed to

$$H_2(s) = \frac{1}{\Omega_q^2} \frac{s^2 + \omega_o^2}{(s^2 + s\frac{\omega_1}{Q} + \omega_1^2)} \times \frac{s^2 + \omega_o^2}{(s^2 + s\frac{\omega_2}{Q} + \omega_2^2)}$$

with $Q = 1.85879$ from (5.45), $\omega_1 = 3584$ and $\omega_2 = 28660$ from (5.46). This term can be realized by two 2nd order BR circuits, one notch-LP and one notch-HP. Finally, the transfer function of the band-reject filter will be

$$H_{BR}(s) = 1.09696 \cdot H_1(s) \cdot H_2(s) \tag{5.51}$$

It is clear that for the active-RC realization of the transfer function, 3 2nd order band-reject circuits are needed. If the modified CGIC biquad is used (see Chap. 10), which realizes all three notch types, the final circuit will be that of Fig. 5.32. A voltage amplifier with gain $K = 7.8125$ has been added after the last section in order to make the product of the frequency independent numerator constants of the cascaded sections equal to $\frac{1.09696}{\Omega_R \Omega_q^2}$, which is expected from (5.51). The frequency response of the band-reject filter is shown in Fig. 5.33 (simulation).

5.4 Problems

5.1 Figure 5.34 shows an elliptic lowpass filter designed with cutoff frequency $f_C = 2$ KHz, passband ripple $\alpha_{\max} = 0.5$ dB and $\alpha_{\min} = 30$ dB. Transform it into a passive highpass filter with the same resistive terminations, $\alpha_{\max}$ and $\alpha_{\min}$ and cutoff frequency $f_{CHP} = 5.0$ kHz.

5.2 Repeat problem 5.1 using the same tolerances $\alpha_{\max}$ and $\alpha_{\min}$ but the highpass filter will have $R_L = 1.0$ kOhm, $R_S = 500$ Ohm and cutoff frequency $f_{CHP} = 6.0$ kHz.

5.3 Determine the voltage transfer functions $H_a(s)$ of the normalized second order lowpass filter of Fig. 5.35a and $H_b(s)$ of the normalized second order highpass filter of Fig. 5.35b. Show that for the element values shown in the highpass filter, $H_b(s) = H_a(1/s)$.

5.4 Find the transfer function of a bandpass filter with the specifications of Example 5.6 but with double center frequency $f_o = 2 \cdot 1672 = 3344$ Hz. Did the values of the quality factors of the poles increase or decrease.

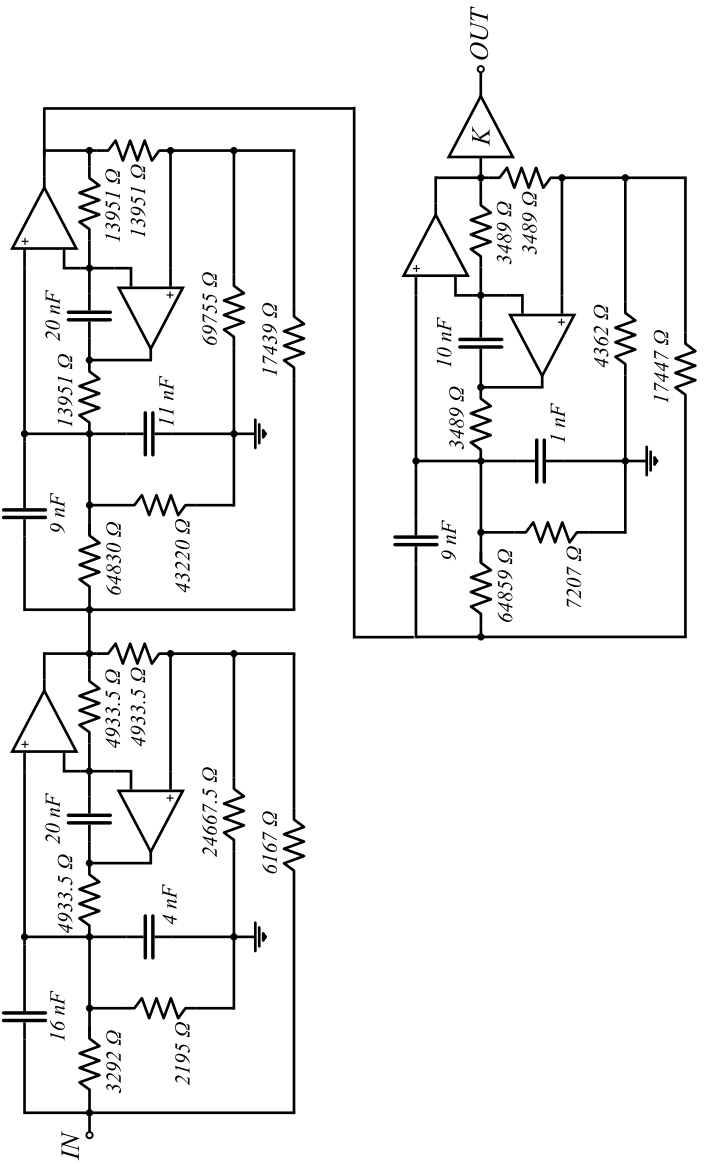

Fig. 5.32 The denormalized active BR filter

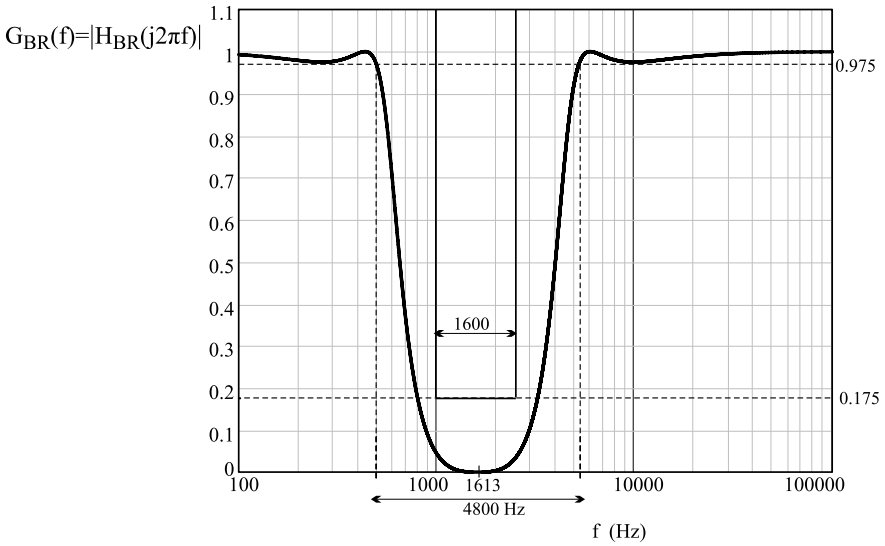

Fig. 5.33 The frequency response of the active BR filter (simulation)

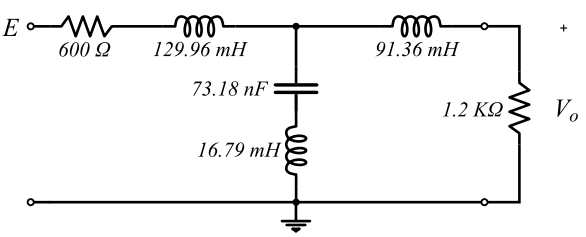

Fig. 5.34 Circuit for Problem 5.1

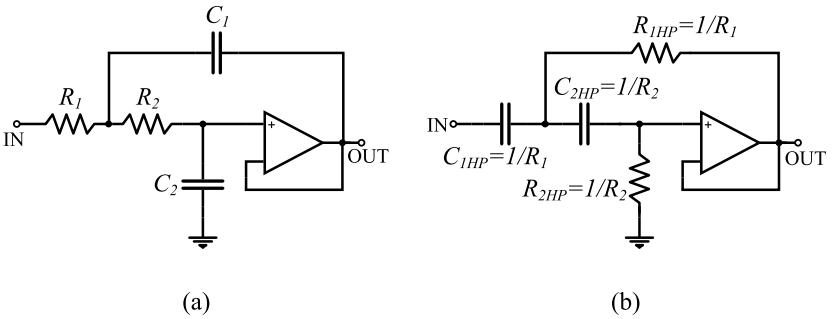

Fig. 5.35 Circuits for Problem 5.3

5.5 Find the transfer function of a bandpass filter with the specifications of Example 5.6 but with half bandwidths $BW = 2\pi 900$ and $BW_S = 2\pi 2700$ rad/s. Did the values of the quality factors of the poles increase or decrease.

5.6 Design an active-RC bandpass filter from the transfer function of (5.31) of Example 5.4

$$H_{BP}(s) = \frac{1729.1(s^2 + 466.966 \cdot 10^6)(s^2 + 2086.0 \cdot 10^6)}{(s^2 + 6459.1s + \omega_o^2)(s^2 + 1913.4s + \omega_1^2)(s^2 + 2817.7s + \omega_2^2)}$$

using the modified CGIC biquad of Fig. 10.47 of Chap. 10 and verify your results by simulating the filter in Pspice.

5.7 Repeat problem 5.8 using the generalized CGIC biquad of Sect. 10.7.2.4 of Chap. 10. Verify your results by simulating the filter in Pspice.

5.8 Design an active-RC band-reject filter from the transfer function of (5.50) of Example 5.7

$$H_{BR}(s) = \frac{(s^2 + 986.96 \cdot 10^6)(s^2 + 492 \cdot 10^6)(s^2 + 1980 \cdot 10^6)}{(s^2 + 83124s + \omega_o^2)(s^2 + 3596s + \omega_1^2)(s^2 + 12784s + \omega_2^2)}$$

using the modified CGIC biquad of Fig. 10.47 of Chap. 10. Verify your results by simulating the filter in Pspice.

5.9 Repeat problem 5.10 using the generalized CGIC biquad of Sect. 10.7.2.4 of Chap. 10. Verify your results by simulating the filter in Pspice.

5.10 Using a mathematical software package, verify that the magnitude response of the transfer function given by (5.50) is that shown in Fig. 5.29.

5.11 Determine the transfer function of a normalized Chebyshev highpass filter with the following specifications:

$$\Omega_{SHP} = 0.27 \qquad \alpha_o = 0 \qquad \alpha_{\max} = 1 \text{ dB} \qquad \alpha_{\min} = 22 \text{ dB}$$

5.12 Determine the transfer function of a normalized Chebyshev bandpass filter with center frequency $\Omega_o = 1$ and the following specifications:

$$\alpha_o = 0 \qquad \alpha_{\max} = 1 \text{ dB} \qquad \alpha_{\min} = 22 \text{ dB} \qquad BW = 0.5 \qquad BW_S = 2$$

5.13 Determine the transfer function of a normalized Chebyshev band-reject filter with center frequency $\Omega_o = 1$ and the following specifications:

$$\alpha_o = 0 \qquad \alpha_{\max} = 1 \text{ dB} \qquad \alpha_{\min} = 22 \text{ dB} \qquad BW = 2 \qquad BW_S = 0.5$$

References[1]

1. Chen, W.-K.: Passive, Active and Digital Filters. The Circuits and Filters Handbook, vol. V. CRC Press, Boca Raton (2009). Chapter 14 by Wasfy B. Mikhael
2. Chirlian, P.M.: Signals and Filters. Springer, Berlin (1994)
3. Daniels, R.W.: Approximation Methods for Electronic Filter Design. McGraw-Hill, New York (1974)
4. Mitra, S.K.: A network transformation for Active RC Networks. Proc. IEEE **55**, 2021–2022 (1967)
5. Paarmann, L.D.: Design and Analysis of Analog Filters—A Signal Processing Perspective—With MATLAB Examples. Kluwer Academic, Dordrecht (2001)
6. Schaumann, R., Van Valkenburg, M.E.: Design of Analog Filters. Oxford University Press, London (2001)
7. Van Valkenburg, M.E.: Analog Filter Design. Oxford University Press, London (1982)
8. Williams, A., Taylor, F.: Electronic Filter Design Handbook. McGraw-Hill, New York (2006)

[1] All references, whether or not cited within the text, are recommended for further reading.

Passive Filters: Basic Theory and Concepts

6

Passive filters are implemented using passive elements, mainly inductors, capacitors and resistors. They are still used, and will continue to be used, in modern systems when other technologies cannot be used or are too expensive to be employed. On the other hand, the simulation of passive-LC filters offers a powerful design tool in many cases such as active-RC filters, switched capacitor filters, Log domain, MOS-C, OTA-C or $g_m - C$ filters, and even digital filters. This is the main reason why passive-LC filter design is essential for the design of filters in any other technology.

Passive filter theory and design has been a subject of advanced research for many decades and as a result, modern design is completely different from the "theory of wave filters" of Wagner and Campbell, presented in 1915, and from Zobel's complicated *mirror image theory* which, after all, could not produce high precision filters.

Today, passive filters are designed using the insertion parameters (also known as effective parameters) which lead to the so-called precise design method developed with contributions from great circuit theorists like Norton, Bennett, Cauer, Guillemin, Darlington, Belevitch and Piloty. The method assumes that a passive-LC circuit, the filter, is inserted between the source and the load, introducing a frequency dependent insertion loss. The subject of passive filter design is the determination of the parameters of the inserted passive-LC circuit so as to satisfy certain gain or attenuation specifications.

The precise filter design method is presented in this chapter not only from its theoretical point of view but also in terms for its usefulness for the electronics engineer, who will be able to design passive filters from given specifications using systematic and well structured knowledge.

It should be made clear from the beginning that passive filter design differs from active filter design, mainly in the following aspects:

i. In passive filters there are additional specifications for the source and the load, the characteristics of which are involved in the design and play a very significant role.
ii. Cascading passive sections is not as easy as it sounds. Due to loading, the transfer functions of the passive sections cannot simply be multiplied to obtain the transfer function of the cascade.

H.G. Dimopoulos, *Analog Electronic Filters*, Analog Circuits and Signal Processing,
DOI 10.1007/978-94-007-2190-6_6, © Springer Science+Business Media B.V. 2012

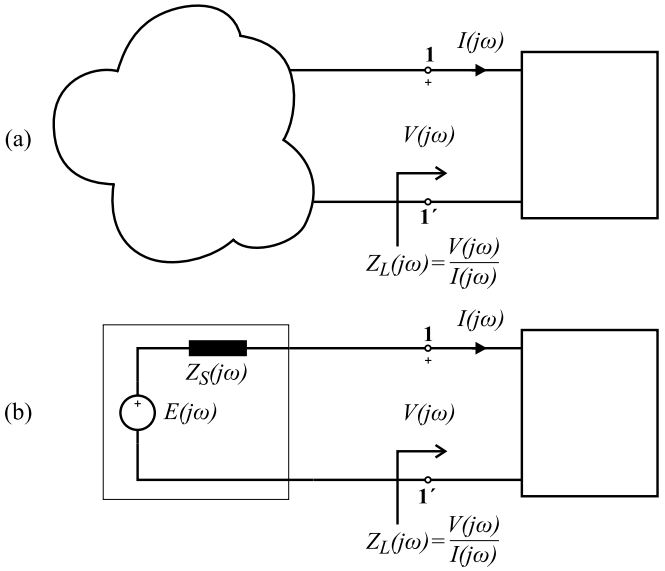

Fig. 6.1 A two-terminal circuit connected (**a**) to the preceding sections (**b**) to the equivalent voltage source

iii. Filter operation is based on the precious power of the input signal, which must be handled with respect. In active filters, power amplification is possible and the designer does not necessarily worry about effective input signal power handling.

6.1 Power and Maximum Power Transfer

A *two-terminal* or *one-port* circuit with input driving-point impedance $Z_L(j\omega)$ is connected to the preceding sections at its two terminals 1-1′ as shown in Fig. 6.1a. The preceding sections, no matter how complicated, can be represented by the Thevenin equivalent ideal voltage source $E(j\omega)$ and series impedance $Z_S(j\omega)$ as shown in Fig. 6.1b. Impedance $Z_L(j\omega)$ is the *load* and the *complex power* at terminals 1-1′ is defined as:

$$S(j\omega) = \frac{1}{2}V(j\omega)I^*(j\omega) = \frac{1}{2}|I(j\omega)|^2 Z_L(j\omega) = \frac{1}{2}|V(j\omega)|^2 Y_L^*(j\omega) \qquad (6.1)$$

(In the above expression $X^*(j\omega)$ denotes the conjugate of $X(j\omega)$.)

It should be underlined that the coefficient $\frac{1}{2}$ in (6.1) does not appear when RMS voltage and current values are used.

Complex power $S(j\omega)$, as a complex function, has a real and an imaginary part:

$$S(j\omega) = \mathrm{Re}[S(j\omega)] + j\,\mathrm{Im}[S(j\omega)] = P_\mu(\omega) + jQ(\omega) \qquad (6.2)$$

The real part $P_\mu(\omega)$ defines the *average* or *real* power and the imaginary part the *reactive power* $Q(\omega)$, which is not really dissipated. The magnitude of complex power $|S(j\omega)|$ is referred to as the *apparent power*.

The part of interest is the average power $P_\mu(\omega)$ since it is dissipated and raises the temperature of the circuit. Both real and imaginary parts of the complex power are functions of the frequency. In classical electrical engineering, where the frequency is constant $\omega = 2\pi 50$ or $\omega = 2\pi 60$ rad/s, the two parts of the power are denoted simply as P_μ and Q, but in electronics and communications, where frequency is the main variable, we prefer to make the dependency of power on frequency clear, using $P_\mu(\omega)$ and $Q(\omega)$.

Returning to Fig. 6.1, where the sinusoidal source $E(j\omega)$ is connected directly to the load with impedance $Z_L(j\omega)$, we have

$$\begin{aligned} Z_L(j\omega) &= \frac{V(j\omega)}{I(j\omega)} = R_L(\omega) + jX_L(\omega) = Z_L(\omega)e^{j\phi(\omega)} \\ &\text{where } Z_L(\omega) = |Z_L(j\omega)| = \sqrt{R_L(\omega)^2 + X_L(\omega)^2} \text{ and } \phi(\omega) = \sphericalangle Z_L(j\omega) \end{aligned} \tag{6.3}$$

Angle $\phi_L(\omega)$ is of course the phase difference between voltage $V(j\omega)$ and current $I(j\omega)$. The term $\cos(\phi(\omega))$ is referred to as *power factor*.

Due to the internal impedance of the source, the load does not receive at terminals 1-1′ voltage $E(j\omega)$ but $V(j\omega) = Ve^{j(\omega t+\theta)}$ and therefore for the current $I(j\omega)$ we have

$$\begin{aligned} I(j\omega) &= \frac{V(j\omega)}{Z_L(j\omega)} = \frac{V(\omega)e^{j(\omega t+\theta)}}{Z_L(\omega)e^{j\phi(\omega)}} = \frac{V(\omega)}{Z_L(\omega)}e^{j(\omega t+\theta-\phi(\omega))} \\ \Rightarrow \quad I^*(j\omega) &= \frac{V(\omega)}{Z_L(\omega)}e^{-j(\omega t+\theta-\phi(\omega))} \end{aligned} \tag{6.4}$$

The complex power at terminals 1-1′ will be

$$\begin{aligned} S(j\omega) &= \frac{1}{2}V(j\omega)I^*(j\omega) = \frac{1}{2}(V(\omega)e^{j(\omega t+\theta)})\left(\frac{V(\omega)}{Z_L(\omega)}e^{-j(\omega t+\theta-\phi(\omega))}\right) \\ &= \frac{1}{2}\frac{V(\omega)^2}{Z_L(\omega)}e^{j\phi(\omega)} = \frac{1}{2}\frac{V(\omega)^2}{Z_L(\omega)}\cos[\phi(\omega)] + j\frac{1}{2}\frac{V(\omega)^2}{Z_L(\omega)}\sin[\phi(\omega)] \end{aligned} \tag{6.5}$$

with the following apparent definitions of the average and reactive power

$$\begin{aligned} P_\mu(\omega) &= \frac{1}{2}\frac{V(\omega)^2}{Z_L(\omega)}\cos[\phi(\omega)] = \frac{1}{2}\frac{V(\omega)^2}{Z_L(\omega)^2}\mathrm{Re}[Z_L(j\omega)] \\ Q(\omega) &= \frac{1}{2}\frac{V(\omega)^2}{Z_L(\omega)}\sin[\phi(\omega)] = \frac{1}{2}\frac{V(\omega)^2}{Z_L(\omega)^2}\mathrm{Im}[Z_L(j\omega)] \end{aligned} \tag{6.6}$$

If

$$I(\omega) = |I(j\omega)| = \frac{|V(j\omega)|}{|Z_L(j\omega)|} \quad \Rightarrow \quad I(\omega) = \frac{V(\omega)}{Z_L(\omega)} \tag{6.7}$$

is used for the magnitude of the current, (6.6) for the average and reactive power become:

$$P_\mu(\omega) = \frac{1}{2} V(\omega) I(\omega) \cos[\phi(\omega)] \qquad Q(\omega) = \frac{1}{2} V(\omega) I(\omega) \sin[\phi(\omega)] \tag{6.8}$$

It should be noted that if RMS values are used for the voltage and the current, then

$$P_\mu = V_{RMS} I_{RMS} \cos\phi(\omega) \qquad Q = V_{RMS} I_{RMS} \sin\phi(\omega)$$

When a voltage source $E(j\omega)$ with internal impedance $Z_S(j\omega)$ is connected to a load $Z_L(j\omega)$ as in Fig. 6.2, the current will be

$$I(j\omega) = \frac{E(j\omega)}{Z_S(j\omega) + Z_L(j\omega)} \tag{6.9}$$

and the voltage at the terminals of the load will be given by:

$$V(j\omega) = \frac{Z_L(j\omega)}{Z_S(j\omega) + Z_L(j\omega)} E(j\omega) \tag{6.10}$$

Expressing $Z_S(j\omega)$ and $Z_L(j\omega)$ in terms of their magnitude and argument as well as in terms of their real and imaginary parts, we get

$$\begin{aligned} Z_L(j\omega) &= Z_L(\omega) e^{j\phi(\omega)} = R_L(\omega) + jX_L(\omega) \quad \text{and} \\ Z_S(j\omega) &= Z_S(\omega) e^{j\phi_S(\omega)} = R_S(\omega) + jX_S(\omega) \end{aligned} \tag{6.11}$$

where

$$\begin{aligned} Z_L(\omega) &= |Z_L(j\omega)| = \sqrt{R_L^2(\omega) + X_L^2(\omega)} \\ Z_S(\omega) &= |Z_S(j\omega)| = \sqrt{R_S^2(\omega) + X_S^2(\omega)} \\ R_L(\omega) &= Z_L(\omega)\cos\phi(\omega) \qquad R_S(\omega) = Z_S(\omega)\cos\phi_S(\omega) \\ \phi(\omega) &= \sphericalangle Z_L(j\omega) \quad \text{and} \quad \phi_S(\omega) = \sphericalangle Z_S(j\omega) \end{aligned} \tag{6.12}$$

Since $\cos[\phi(\omega)] = \frac{R_L(\omega)}{Z_L(\omega)}$ and in view of (6.7), the average power will be:

$$P_\mu(\omega) = \frac{1}{2} V(\omega) I(\omega) \cos[\phi(\omega)] = \frac{1}{2} \frac{V(\omega)^2 R_L(\omega)}{Z_L^2(\omega)} \tag{6.13}$$

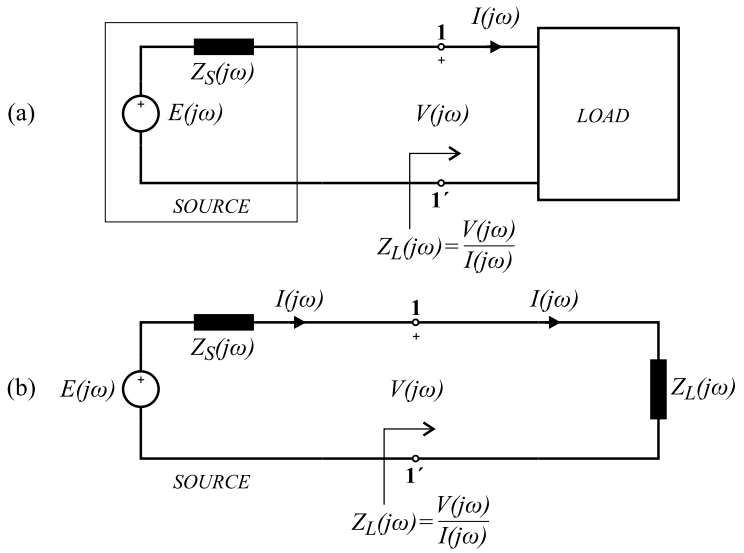

Fig. 6.2 Direct connection of a load to a voltage source

Using (6.10) and (6.11) in (6.13), the average power can be finally expressed as:

$$P_\mu(\omega) = \frac{1}{2}\frac{R_L(\omega)E^2}{|R_S(\omega)+R_L(\omega)+j(X_L(\omega)+X_S(\omega))|^2}$$

$$\Rightarrow \quad P_\mu(\omega) = \frac{1}{2}\frac{R_L(\omega)E^2}{(R_L(\omega)+R_S(\omega))^2+(X_L(\omega)+X_S(\omega))^2} \tag{6.14}$$

where $E = |E(j\omega)|$.

An important question that arises is whether the average power at the terminals 1-1′ of the load can be maximized under certain load conditions. Equation (6.14) must therefore be investigated to find the values of $R_L(\omega)$ and $X_L(\omega)$, if any, for which $P_\mu(\omega)$ assumes its maximum value. This maximum value will be the maximum power the source can deliver.

From (6.14) it is clear that when $X_L(\omega) = -X_S(\omega)$, the denominator is minimized since the non-negative term $[X_L(\omega) + X_S(\omega)]^2$ becomes zero. Under this condition, the average power is given by:

$$P_\mu(\omega) = \frac{1}{2}\frac{R_L(\omega)E^2}{[R_L(\omega)+R_S(\omega)]^2} \tag{6.15}$$

and the value of $R_L(\omega)$ for which the average power is maximized can be determined by finding the roots of the derivative of $P_\mu(\omega)$:

$$\frac{d}{dR_L(\omega)}P_\mu(\omega) = \frac{E^2}{2}\cdot\frac{R_S(\omega)-R_L(\omega)}{[R_S(\omega)+R_L(\omega)]^3} \tag{6.16}$$

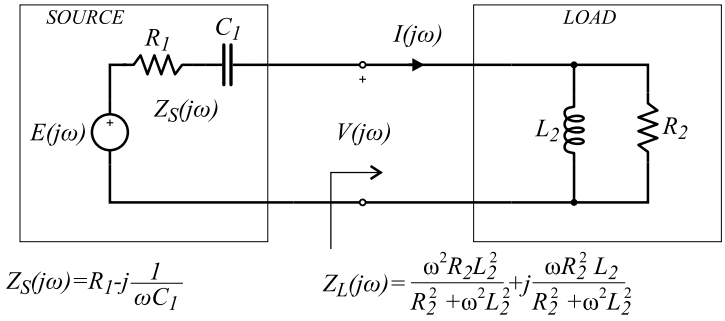

Fig. 6.3 Connection of a load to a voltage source

For $R_L(\omega) = R_S(\omega)$, the derivative becomes zero and $P_\mu(\omega)$ assumes its maximum value:

$$P_{\max} = \frac{E^2}{8R_S(\omega)} = \frac{E_{RMS}^2}{4R_S(\omega)} \tag{6.17}$$

This is the maximum average power which can be delivered by a source with internal impedance $Z_S(j\omega) = R_S(\omega) + jX_S(\omega)$. The maximum power is delivered only to a "matched" load under maximum power transfer conditions, i.e. when the source "sees" a load $Z_L(j\omega) = R_L(\omega) + jX_L(\omega) = R_S(\omega) - jX_S(\omega) = Z_S^*(j\omega)$, equal to the conjugate of its impedance. The condition

$$Z_L(j\omega) = Z_S^*(j\omega)$$
$$\text{i.e. } \mathrm{Re}[Z_L(j\omega)] = \mathrm{Re}[Z_S(j\omega)] \text{ and } \mathrm{Im}[Z_L(j\omega)] = -\mathrm{Im}[Z_S(j\omega)] \tag{6.18}$$

under which the load receives the maximum power that can be delivered by the source is referred to as *maximum power transfer condition*. Equation (6.18) is also referred to as the *maximum power transfer theorem*, discovered by the Prussian engineer and physicist Moritz Hermann (Boris Semyonovich) von Jacobi around 1840 (not to be confused with his contemporary mathematician Carl Gustav Jacob Jacobi). The practice of designing the input impedance of an electrical load or the output impedance of its corresponding signal source in order to maximize the power transfer and minimize reflections from the load is referred to as *reflectionless impedance matching*, or simply *impedance matching*.

It should be noted that $R_L(\omega)$, $X_L(\omega)$, $R_S(\omega)$ and $X_S(\omega)$ are in general functions of frequency, as for example in Fig. 6.3. From the same figure, it is also clear that the real part of an impedance may depend on the capacitor and inductor values and not only on the values of the resistors.

The maximum power transfer condition $Z_L(j\omega) = Z_S^*(j\omega)$ cannot be valid for all frequencies unless the circuit is purely resistive.

Example 6.1 In the circuit of Fig. 6.3, the load matches the source when

$$Z_L(j\omega) = Z_S^*(j\omega) \quad \Leftrightarrow \quad \frac{\omega^2 R_2 L_2^2}{R_2^2 + \omega^2 L_2^2} = R_1 \quad \text{and} \quad \frac{\omega R_2^2 L_2}{R_2^2 + \omega^2 L_2^2} = \frac{1}{\omega C_1}$$

From the first condition, we can get the frequency ω_o at which the real parts of the source and load impedances become equal:

$$\omega_o^2 = \frac{R_2^2}{L_2(R_2^2 C_1 - L_2)} \tag{6.19}$$

From the second condition and for $\omega = \omega_o$, we get the relationship of the element values in order to have equal imaginary parts at $\omega = \omega_o$ and therefore maximum power transfer:

$$L_2 = R_1 R_2 C_1 \tag{6.20}$$

For maximum power transfer to occur at ω_o of (6.19), component values must satisfy (6.20), in which case the maximum power transfer frequency will be given by:

$$\omega_o = \sqrt{\frac{1}{R_1 C_1^2 (R_2 - R_1)}} \quad \text{with } R_2 > R_1 \tag{6.21}$$

If all component values are given, then it must be examined whether they satisfy (6.20). If they do, the frequency of the maximum power transfer will be ω_o of (6.21), provided that $R_2 > R_1$. If two of the component values are given, e.g. R_1 and C_1, the other two can be determined so as to have the maximum power transfer at a prescribed frequency ω_o. For $R_1 = 1$ kOhm and $R_2 = 2$ kOhm, L_2 and C_1 can be calculated at say $f_o = 10$ kHz ($\omega_o = 2\pi f_o$):

$$L_2 = 2 \cdot 10^6 C_1 \qquad \omega_o = 2\pi \cdot 10^4 = \sqrt{\frac{1}{10^3 \cdot C_1^2 \cdot 10^3}}$$

$$\Rightarrow \quad C_1 = 11.26 \text{ nF} \qquad L_2 = 22.52 \text{ mH}$$

Example 6.2 In the circuit of Fig. 6.4, the voltage source with purely resistive internal resistance R_S is connected to the RLC load.

(a) Find the frequency of the maximum power transfer and any necessary relationship between the element values.

(a) Determine L and C in order to have maximum power transfer at a given frequency.

The impedance of the load is

$$Z_L(j\omega) = \frac{R_L}{1 + \omega^2 R_L^2 C^2} + j\omega \frac{L - R_L^2 C(1 - \omega^2 LC)}{1 + \omega^2 R_L^2 C^2}$$

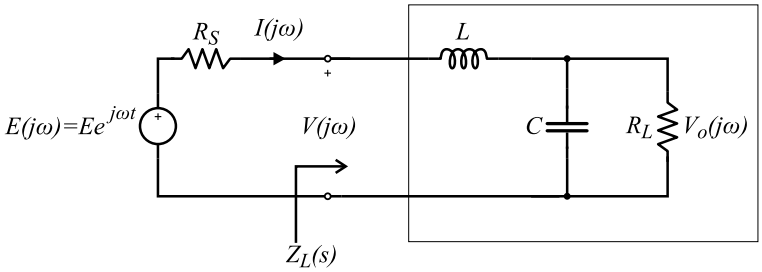

Fig. 6.4 A RLC circuit connected to a voltage source

In order to have maximum power transfer:

$$Z_L(j\omega) = R_S \quad \Leftrightarrow \quad R_S = \frac{R_L}{1+\omega_o^2 R_L^2 C^2} \quad \text{and} \quad \frac{L - R_L^2 C(1-\omega_o^2 LC)}{1+\omega_o^2 R_L^2 C^2} = 0$$

(a) From the maximum power transfer conditions, we find

$$\omega_o^2 = \frac{R_L - R_S}{R_S R_L^2 C^2} \quad \text{and} \quad \omega_o^2 = \frac{1}{LC} - \frac{1}{R_L^2 C^2} \tag{6.22}$$

and therefore

$$L = R_S R_L C \quad \text{and} \quad \omega_o = \sqrt{\frac{R_S(R_L - R_S)}{L^2}} = \sqrt{\frac{R_S(R_L - R_S)}{R_S^2 R_L^2 C^2}} \tag{6.23}$$

The above relationship $L = R_S R_L C$ between the component values is determined from (6.22) by equating the right hand sides of the two expressions for ω_o. From (6.23) it becomes clear that if $R_L < R_S$ there is no real maximum power transfer frequency.

(b) From (6.23) we find

$$L = \frac{1}{\omega_o}\sqrt{R_S(R_L - R_S)} \quad \text{and} \quad C = \frac{L}{R_S R_L} \tag{6.24}$$

which requires $R_L \geq R_S$.

In order to verify our results, it will be shown that in this particular circuit with the determined values of the elements, the average power at frequency ω_o equals the maximum power

$$P_{\max} = \frac{E^2}{8R_S}$$

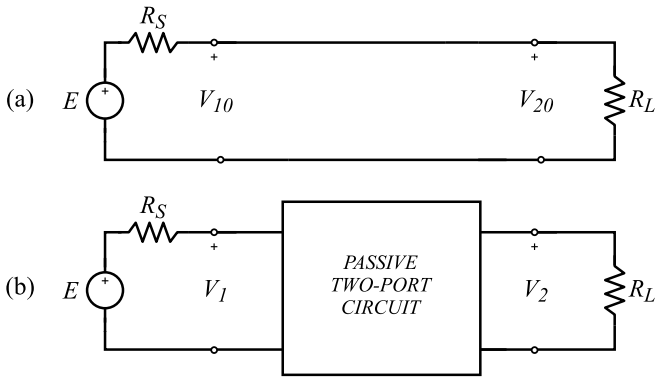

Fig. 6.5 Connection of a resistive load to a voltage source (**a**) directly (**b**) through a passive two-port

which can be delivered by the source. The average power at the load is according to (6.6)

$$P_\mu(\omega) = \frac{1}{2}\frac{|V(j\omega)|^2}{|Z_L(j\omega)|^2}\,\mathrm{Re}[Z_L(j\omega)]$$

with

$$V(j\omega) = \frac{Z_L(j\omega)}{R_S + Z_L(j\omega)}E(j\omega)$$

For $\omega = \omega_o$ and $L = R_S R_L C$ we have:

$$Z_L(j\omega_o) = R_S \quad \text{and} \quad V(j\omega_o) = \frac{R_S}{R_S + Z_L(j\omega_o)}E(j\omega_o) = \frac{1}{2}E(j\omega_o)$$

and finally

$$P_\mu(\omega_o) = \frac{1}{2}\frac{|V(j\omega_o)|^2}{|Z_L(j\omega_o)|^2}\,\mathrm{Re}[Z_L(j\omega_o)] = \frac{E^2}{8R_S} = P_{MAX}$$

At $\omega = \omega_o$ the maximum power P_{MAX} enters the load and is dissipated on resistor R_L since L and C are lossless elements that do not dissipate any power.

6.2 Insertion (Transmission or Effective) Parameters

Figure 6.5a shows a voltage source with internal resistance R_S connected directly to a resistive load R_L. The voltage of the load, the output voltage, is

$$V_{20}(j\omega) = \frac{R_L}{R_S + R_L}E(j\omega)$$

The maximum power that can be delivered by the source is:

$$P_{MAX} = \frac{|E(j\omega)|^2}{8R_S}$$

and the average power dissipated at the load is given by

$$P_{20} = \frac{|V_{20}(j\omega)|^2}{2R_L} = \frac{R_L^2|E(j\omega)|^2}{2R_L(R_S+R_L)^2} = \frac{4R_SR_L}{(R_S+R_L)^2}P_{MAX}$$

$$\Rightarrow \quad \frac{P_{MAX}}{P_{20}} = \frac{(R_S+R_L)^2}{4R_SR_L} \geq 1 \tag{6.25}$$

It is clear that the average power P_{20} which reaches the load is a frequency independent fraction of the maximum available power of the source. If we wish to control the power which is dissipated on the load at various frequencies, e.g. a high portion of P_{MAX} to reach the load at low frequencies and a high portion at high frequencies, an appropriate two-port circuit may be inserted between source and load, as shown in Fig. 6.5b. In order to achieve selectivity, the inserted circuit must include elements with frequency dependent behavior, i.e. inductors and capacitors. In fact, in the rest of this book, LC two-port networks are inserted between source and load to perform the filtering operation and the term "passive filter" refers to doubly resistively terminated LC two-ports. In this case, the average power $P_2(\omega)$ at the load will depend on frequency and will be given by

$$P_2(\omega) = \frac{|V_2(j\omega)|^2}{2R_L} = \frac{|V_2(j\omega)|^2 P_{MAX}}{2R_L P_{MAX}} = \frac{|V_2(j\omega)|^2 4R_S}{|E(j\omega)|^2 R_L}P_{MAX} \tag{6.26}$$

from which we get

$$\frac{P_{MAX}}{P_2(\omega)} = \frac{|E(j\omega)|^2}{|V_2(j\omega)|^2}\cdot\frac{R_L}{4R_S} = \left[\frac{1}{2}\sqrt{\frac{R_L}{R_S}}\left|\frac{E(j\omega)}{V_2(j\omega)}\right|\right]^2 \geq 1 \tag{6.27}$$

From this expression, we can observe that

(a) Since the ratio $P_{MAX}/P_2(\omega) \geq 1$, the voltage gain

$$G(\omega) = \frac{|V_2(j\omega)|}{|E(j\omega)|}$$

cannot exceed the value

$$\frac{1}{2}\sqrt{\frac{R_L}{R_S}}$$

which is defined by the resistive terminations. Moreover, this maximum value of the gain is achieved only under maximum power transfer conditions, i.e. when $P_{MAX}/P_2(\omega) = 1$.

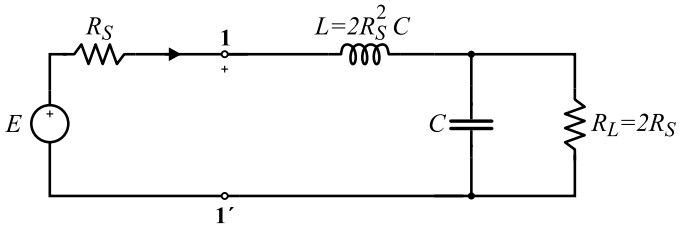

Fig. 6.6 Connection of a resistive load to a voltage source through a passive LC circuit

(b) The insertion of a passive-LC circuit permits at some frequencies $P_2(\omega)$ to be greater than P_{20}, the average power before the insertion of the LC circuit. This may happen because after the insertion of the lossless LC circuit, there may exist some frequencies at which the source matches the input impedance of the inserted LC circuit terminated by R_L, in which case the maximum power will be transferred to R_L.

As an example, in Fig. 6.6, the average power dissipated on $R_L = 2R_S$ when connected directly to the voltage source $\{E, R_S\}$ is $P_{20} = \frac{E^2}{9R_S}$. With the LC circuit inserted, at 1-1′ impedance matching occurs at $\omega_o = \frac{1}{2R_SC}$ and the power reaching the load R_L will be

$$P_2(\omega_o) = P_{\max} = \frac{E^2}{8R_S} > P_{20}$$

6.2.1 The Effective Attenuation

Referring to Fig. 6.5b and taking into account (6.27), effective attenuation is defined as

$$A(\omega) = 10\log\left(\frac{P_{MAX}}{P_2(\omega)}\right) = 20\log\left(\frac{1}{2}\sqrt{\frac{R_L}{R_S}}\frac{|E(j\omega)|}{|V_2(j\omega)|}\right) \text{ (dB)} \tag{6.28}$$

where $P_2(\omega)$ is the average power of the load R_L and P_{MAX} the maximum power of the source.

Effective attenuation $A(\omega)$ cannot assume negative values since $P_{MAX} \geq P_2(\omega)$. Moreover, $A(\omega)$ becomes zero by definition when $P_2(\omega) = P_{MAX}$, i.e. at the frequencies, if any, at which the source resistance matches the input impedance of the load, which is the inserted lossless LC circuit terminated by R_L.

In the case of the direct connection of R_L to the source (Fig. 6.5a), the average power of R_L has been found (see (6.25)):

$$P_{20} = \frac{4R_SR_L}{(R_S+R_L)^2}P_{MAX} \quad \Rightarrow \quad \frac{P_{MAX}}{P_{20}} = \frac{(R_S+R_L)^2}{4R_SR_L}$$

The corresponding attenuation in this direct connection is determined from (6.28)

$$A_o = 10\log\left(\frac{P_{MAX}}{P_{20}}\right) = 20\log\left(\frac{R_S + R_L}{2\sqrt{R_L R_S}}\right) \tag{6.29}$$

Equation (6.28) can be written as

$$\begin{aligned} A(\omega) &= 10\log\left(\frac{P_{MAX}}{P_2(\omega)}\right) = 20\log\left(\frac{1}{2}\sqrt{\frac{R_L}{R_S}}\frac{|E(j\omega)|}{|V_{20}(j\omega)|}\right) \\ &= 20\log\left(\frac{R_S + R_L}{2\sqrt{R_L R_S}} \cdot \frac{R_L}{R_S + R_L}\frac{|E(j\omega)|}{|V_{20}(j\omega)|}\right) \end{aligned} \tag{6.30}$$

and finally the attenuation is given by:

$$A(\omega) = 20\log\left(\frac{R_S + R_L}{2\sqrt{R_L R_S}}\right) + 20\log\left(\frac{R_L}{R_S + R_L}\frac{|E(j\omega)|}{|V_2(j\omega)|}\right) = A_o + A_{ins}(\omega) \tag{6.31}$$

It becomes clear that attenuation $A(\omega)$ is expressed as the sum of two terms:

(i) $A_o = 20\log(\frac{R_S+R_L}{2\sqrt{R_L R_S}})$ which depends only on the terminations and not on frequency

(ii) $A_{ins}(\omega) = 20\log(\frac{R_L}{R_S+R_L}\frac{|E(j\omega)|}{|V_2(j\omega)|})$ which is introduced by the inserted two-port:

$$A(\omega) = A_o + A_{ins}(\omega)$$

$$\text{with } A_o = 20\log\left(\frac{R_S + R_L}{2\sqrt{R_L R_S}}\right) \tag{6.32}$$

$$\begin{aligned} \text{and } A_{ins}(\omega) &= 20\log\left(\frac{R_L}{R_S + R_L}\frac{|E(j\omega)|}{|V_2(j\omega)|}\right) \\ &= 20\log\left(\frac{|V_{20}(j\omega)|}{|V_2(j\omega)|}\right) \end{aligned} \tag{6.33}$$

The attenuation $A_{ins}(\omega)$ due to the insertion of the two-port is referred to as the *insertion loss*. Insertion loss can assume zero, positive and even negative values and as a result $A(\omega)$ can take values lower or higher than A_o.

Defining the transmission or transducer function

$$T(s) = \frac{1}{2}\sqrt{\frac{R_L}{R_S}}\frac{E(s)}{V_2(s)} \tag{6.34}$$

the attenuation can be expressed as:

$$A(\omega) = 20\log(|T(j\omega)|) = 10\log\left(\frac{P_{MAX}}{P_2(\omega)}\right) = 20\log\left(\frac{1}{2}\sqrt{\frac{R_L}{R_S}}\frac{|E(j\omega)|}{|V_2(j\omega)|}\right) \tag{6.35}$$

All quantities refer to Figs. 6.5b or 6.7.

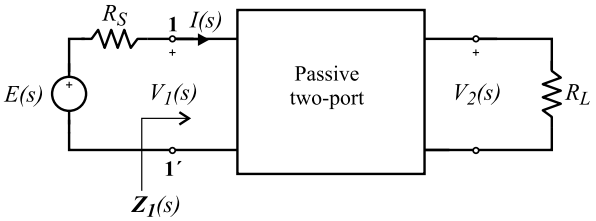

Fig. 6.7 The doubly resistively terminated two-port network

Transmission function $T(s)$ is the inverse of the transfer function $H(s) = \frac{V_2(s)}{E(s)}$, multiplied by the frequency independent factor $\frac{1}{2}\sqrt{\frac{R_L}{R_S}}$

$$T(s) = \frac{1}{2}\sqrt{\frac{R_L}{R_S}}\frac{E(s)}{V_2(s)} = \frac{1}{2}\sqrt{\frac{R_L}{R_S}}\frac{1}{H(s)} \tag{6.36}$$

6.2.2 The Reflected Power and the Reflection Coefficient

Referring to Fig. 6.7, where a passive two-port has been inserted between the voltage source $\{E, R_S\}$ and the load R_L, the source sees as its load the input impedance $Z_1(j\omega)$ of the resistively terminated passive two-port.

The average power at the input terminals 1-1′ of the terminated two-port is, according to (6.13):

$$P_{2Z}(\omega) = \frac{1}{2}|V_1(j\omega)||I(j\omega)|\cos\phi_1(\omega) \quad \text{with } \phi_1(\omega) = \sphericalangle Z_1(j\omega)$$

which gives

$$P_{2Z}(\omega) = \frac{1}{2}\left|\frac{Z_1(j\omega)E(j\omega)}{Z_1(j\omega)+R_S}\right| \cdot \left|\frac{E(j\omega)}{Z_1(j\omega)+R_S}\right| \cdot \cos[\phi_1(\omega)] \tag{6.37}$$

The load $Z_1(j\omega)$, as a complex quantity, can be expressed in terms of its real and imaginary part as:

$$Z_1(j\omega) = R_1(\omega) + jX_1(\omega) \quad \text{where } R_1(\omega) = |Z_1(j\omega)|\cos[\phi_1(\omega)]$$

It should be remembered that $R_1(\omega)$, $X_1(\omega)$ and $\phi_1(\omega)$ are all real functions of ω. Setting

$$Z_1(j\omega) = R_1(\omega) + jX_1(\omega)$$

in (6.37), we find that the average power at the terminals 1-1′ of the terminated two-port is

$$P_{2Z}(\omega) = \frac{1}{2}\frac{R_1(\omega)E^2}{|R_1(\omega)+R_S+jX_1(\omega)|^2} = \frac{1}{2}\frac{R_1(\omega)E^2}{(R_1(\omega)+R_S)^2+X_1^2(\omega)} \tag{6.38}$$

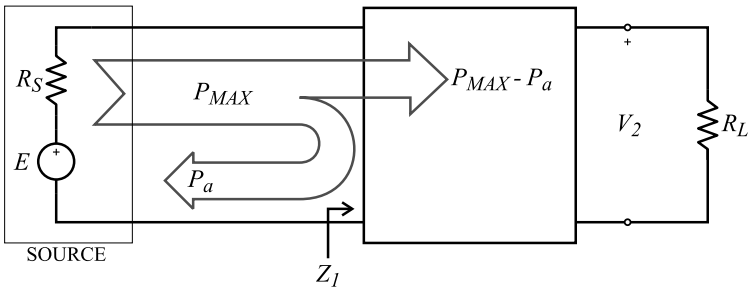

Fig. 6.8 Power flow in a doubly terminated passive two-port

where $E = |E(j\omega)|$. The maximum power that the source can deliver under matching conditions

$$R_1(\omega) = R_S \quad \text{and} \quad X_1(\omega) = 0$$

is $P_{MAX} = \frac{E^2}{8R_S}$ (see (6.17)) and $P_{2Z}(\omega)$ cannot exceed this value.

At frequencies where no maximum power transfer occurs, the power flow can be modeled as in Fig. 6.8, where $P_{2Z}(\omega) = P_{MAX} - P_a(\omega)$ enters the two-port and the rest $P_a(\omega) = P_{MAX} - P_{2Z}(\omega)$ is reflected back to the source. $P_a(\omega)$ is referred to as the *reflected power* and, taking into account (6.38), can be evaluated as follows:

$$\begin{aligned} P_a(\omega) = P_{MAX} - P_{2Z}(\omega) &= \frac{E^2}{8R_S} - \frac{1}{2}\frac{R_1(\omega)E^2}{(R_1(\omega)+R_S)^2 + X_1^2(\omega)} \\ &= \frac{E^2}{8R_S}\left(1 - \frac{4R_S R_1(\omega)}{(R_1(\omega)+R_S)^2 + X_1^2(\omega)}\right) \\ &= P_{MAX}\left(\frac{(R_S - R_1(\omega))^2 + X_1^2(\omega)}{(R_1(\omega)+R_S)^2 + X_1^2(\omega)}\right) \\ \Rightarrow \quad P_a(\omega) &= P_{MAX}\left|\frac{R_S - Z_1(j\omega)}{R_S + Z_1(j\omega)}\right|^2 = P_{MAX}|\rho(j\omega)|^2 \end{aligned} \tag{6.39}$$

The factor $|\rho(j\omega)|^2$ determines the portion of the maximum power that is reflected and is defined as:

$$|\rho(j\omega)|^2 = \frac{P_a(\omega)}{P_{MAX}} = \left|\frac{R_S - Z_1(j\omega)}{R_S + Z_1(j\omega)}\right|^2 \tag{6.40}$$

The function $\rho(s)$ which has

$$|\rho(s)|^2_{s=j\omega} = \left|\frac{R_S - Z_1(j\omega)}{R_S + Z_1(j\omega)}\right|^2$$

is:

$$\rho(s) = \pm \frac{R_S - Z_1(s)}{R_S + Z_1(s)} \tag{6.41}$$

and defines the *reflection coefficient function*, or simply the *reflection coefficient* of the interconnection. The dependency of $\rho(s)$ on the frequency gives the circuit the desired selectivity since it can assume low values at certain frequency bands (the passbands) and high values at others (the stopbands).

6.2.3 The Transmission Function $T(s)$ and the Characteristic Function $K(s)$

The two-port circuit inserted between source $\{E, R_S\}$ and the load R_L, is a lossless circuit, i.e. a circuit with lossless elements L and C. Coupled elements with mutual inductances M can also be used, but in general they are avoided. This kind of LCM circuits do not dissipate any power and transfer all power P_{2Z} to the resistive load R_L. The dissipated at R_L average power is

$$P_2(\omega) = \frac{1}{2} \frac{{V_2}^2}{R_L}$$

where V_2 is the amplitude of the voltage: $V_2 = |V_2(j\omega)|$. For the transmission function defined in (6.34) as

$$T(s) = \frac{1}{2} \sqrt{\frac{R_L}{R_s}} \frac{E(s)}{V_2(s)}$$

it can easily be shown that

$$|T(j\omega)|^2 = \frac{P_{MAX}}{P_2(\omega)} = \frac{P_2(\omega) + P_a(\omega)}{P_2(\omega)} = 1 + \frac{P_a(\omega)}{P_2(\omega)} \tag{6.42}$$

In passive circuits, the quantity $\frac{P_a(\omega)}{P_2(\omega)}$ is non-negative at all frequencies and therefore $|T(j\omega)|^2$ can be expressed as

$$|T(j\omega)|^2 = 1 + |K(j\omega)|^2 \tag{6.43}$$

$$|K(j\omega)|^2 = \frac{P_a(\omega)}{P_2(\omega)} = \frac{P_a(\omega)}{P_{MAX}} \frac{P_{MAX}}{P_2(\omega)} = |\rho(j\omega)|^2 \cdot |T(j\omega)|^2 \tag{6.44}$$

Function $K(s)$ is referred to as *characteristic function* of the doubly terminated two-port and expresses the ratio of reflected to dissipated power. From (6.44) we also have

$$K(s) = \rho(s) T(s) \tag{6.45}$$

and

$$T(s)T(-s) = 1 + K(s)K(-s) \tag{6.46}$$

6.2.4 Relationship Between $\rho(s)$ and $T(s)$ or $H(s)$

From (6.42), we have

$$|T(j\omega)|^2 = \frac{P_{MAX}}{P_2(\omega)} = \frac{P_{MAX}}{P_{MAX} - P_a(\omega)} = \frac{1}{1 - \frac{P_a(\omega)}{P_{MAX}}} = \frac{1}{1 - |\rho(j\omega)|^2} \tag{6.47}$$

from which we get

$$|T(j\omega)|^2 = \frac{1}{1 - |\rho(j\omega)|^2} \quad \Rightarrow \quad |\rho(j\omega)|^2 = 1 - \frac{1}{|T(j\omega)|^2} \tag{6.48}$$

and finally the Feldtkellers's equation

$$\rho(s)\rho(-s) = 1 - \frac{1}{T(s)T(-s)} = 1 - \frac{4R_S}{R_L} H(s)H(-s) \tag{6.49}$$

Functions $T(s)$, $H(s)$, $\rho(s)$ and $K(s)$ are rational functions of s and they share some polynomials as follows:

$$\begin{aligned} T(s) &= \frac{e(s)}{p(s)} \qquad & H(s) &= \left(\frac{1}{2}\sqrt{\frac{R_L}{R_S}}\right)\frac{p(s)}{e(s)} \\ K(s) &= \frac{f(s)}{p(s)} \qquad & \rho(s) &= \frac{f(s)}{e(s)} \end{aligned} \tag{6.50}$$

It is worth noting that at the roots of $p(s)$, i.e. the poles of $T(s)$ and $K(s)$, the output voltage is zero and no power is transferred to the load, making the reflected power equal to P_{MAX}. These poles are in fact, according to (6.50), the zeros of the transfer function $H(s)$ and are referred to as *attenuation poles*, *loss poles*, or *transmission zeros* of the filter circuit. The roots of $f(s)$, i.e. the zeros of the reflection coefficient function, correspond to frequencies at which maximum power transfer occurs and are referred to as *reflection zeros* or *zero attenuation frequencies*. It is finally noted that from all three polynomials, only $e(s)$ is a Hurwitz polynomial (i.e. its roots cannot lie in the right half s-plane) and that there are no restrictions as to the location of the roots of the other polynomials.

Example 6.3 The voltage transfer function of the normalized filter of Fig. 6.9 is:

$$H(s) = \frac{V_2(s)}{E(s)} = \frac{1}{s^2 + 2s + 2}$$

From the definition of $T(s)$, we have:

$$T(s) = \frac{1}{2}\sqrt{\frac{R_L}{R_s}}\frac{E(s)}{V_2(s)} = \frac{1}{2}(s^2 + 2s + 2)$$

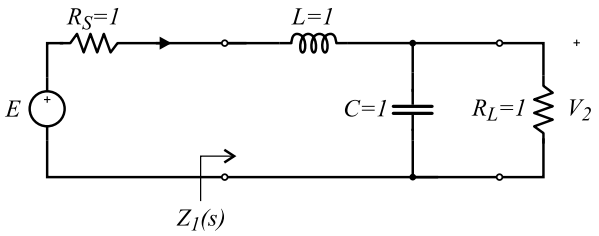

Fig. 6.9 Circuit of Example 6.3

The characteristic function $K(s)$ is evaluated from (6.43)

$$|T(j\omega)|^2 = 1 + |K(j\omega)|^2$$

using the identity

$$|X(j\omega)|^2_{\omega^2=-s^2} = X(s)X(-s)$$

to find

$$\begin{aligned} T(s)T(-s) &= 1 + K(s)K(-s) \\ \Rightarrow \quad K(s)K(-s) &= T(s)T(-s) - 1 \\ \Rightarrow \quad K(s)K(-s) &= \frac{1}{4}(s^2+2s+2)(s^2-2s+2) - 1 = \cdots = \frac{1}{4}s^4 \\ \Rightarrow \quad K(s) &= \pm\frac{1}{2}s^2 \end{aligned}$$

Equation (6.46) is used for the determination of the reflection coefficient function to find

$$\rho(s) = \frac{K(s)}{T(s)} = \frac{\pm s^2}{s^2+2s+2}$$

In order to determine $\rho(s)$ using (6.41) with the negative sign, $Z_1(s)$ is needed and can be easily evaluated directly from the circuit:

$$Z_1(s) = \frac{s^2+s+1}{s+1} \quad \Rightarrow \quad \rho(s) = \frac{s^2}{s^2+2s+2}$$

Using (6.41) with the positive sign we find

$$\rho(s) = \frac{-s^2}{s^2+2s+2}$$

If (6.49) had been used from the beginning, we would have arrived at the same result:

$$\rho(s) = \frac{\pm s^2}{s^2+2s+2}$$

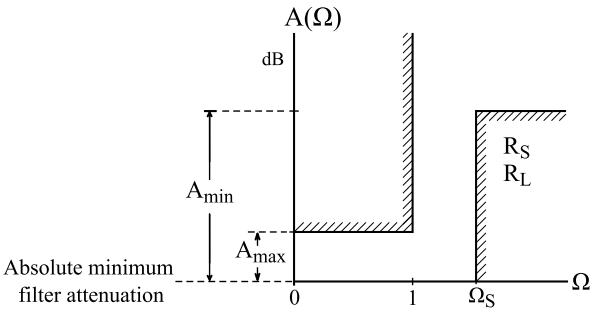

Fig. 6.10 Passive lowpass filter attenuation specifications

The magnitude of $T(s)$ for $s = j\omega$ is:

$$|T(j\omega)| = \left|\frac{1}{2}(2-\omega^2) + j\omega\right| = \sqrt{\frac{(2-\omega^2)^2}{4} + \omega^2} = \sqrt{1 + \frac{\omega^4}{4}}$$

and

$$A(\omega) = 20\log(|T(j\omega)|) = 20\log\sqrt{1 + (\omega^4/4)}\ \text{dB}$$

6.3 The Passive Filters Design Procedure

In passive filter design, the magnitude specifications are given in terms of the effective attenuation defined in (6.28). A typical normalized specifications diagram is shown in Fig. 6.10 where $A_{\max}$ and $A_{\min}$ (in dB) are always positive. $A_{\max}$ specifies the maximum allowed tolerance of the attenuation in the passband. $A_{\min}$ specifies the minimum allowed attenuation in the stopband, measured from the absolute minimum passband attenuation. Both $A_{\max}$ and $A_{\min}$ are relative to the minimum attenuation realized by the filter. This minimum attenuation can be A_o, the frequency independent part of the attenuation of (6.29):

$$A_o = 20\log\left(\frac{R_S + R_L}{2\sqrt{R_L R_S}}\right)$$

However, there are cases where the insertion loss assumes negative values decreasing the minimum attenuation of the filter. Such cases will be presented in the next chapter. Therefore, when the two positive quantities $A_{\max}$ and $A_{\min}$ are specified, they might be interpreted in the two ways shown in Figs. 6.11a and b.

To design a normalized passive lowpass filter from given specifications, first of all, an attenuation function $A(\Omega)$ must be found, which satisfies the specifications and whose plot does not enter the shaded areas of Fig. 6.11. This is the approximation procedure which is completely analogous to the approximations presented in Chaps. 2–4. As has been underlined there, not all gain or attenuation functions are suitable for filter design and some of them may have a plot fitting the specifications diagram but they cannot be realized by passive filters. Fortunately, all known

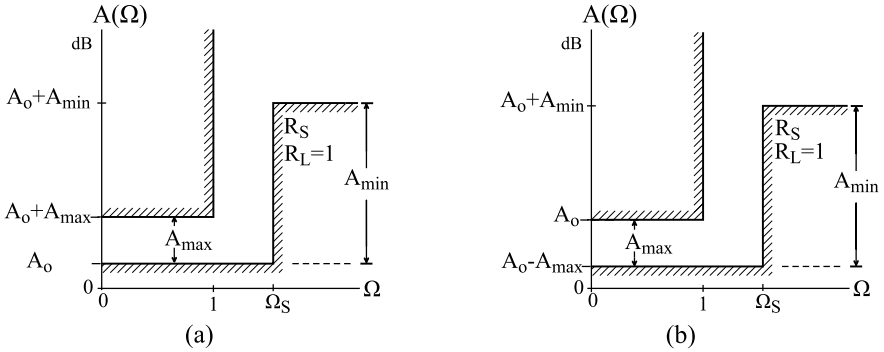

Fig. 6.11 Alternative interpretation of attenuation specifications

approximations (Butterworth, Chebyshev, Pascal, elliptic, Bessel etc.) lead to attenuation and transfer functions which can be realized by passive filters. In the next chapter, these approximations are presented adapted to passive filter design.

When $A(\Omega)$ has been determined from the approximation, the related function $|H(j\Omega)|$ is also determined, and for $H(s)$ we have:

$$H(s)H(-s) = |H(j\Omega)|^2_{\Omega^2=-s^2}$$

In passive filter design, the isolation of the transfer function $H(s)$ is not required since the reflection coefficient can be determined from (6.49) and $H(s)H(-s)$. The input impedance $Z_1(s)$ of the two-port terminated with R_L can then be determined from (6.41). Finally, $Z_1(s)$ can be synthesized using one of the classical RLCM driving-point impedance synthesis methods of Chap. 12.

The verification of the synthesis result is usually done by simulating the circuit using an appropriate computer program like Pspice. Figure 6.12 shows the work flow diagram of the passive filter design procedure.

6.4 Determination of $Z_1(s)$ of a Lowpass Filter

Referring to Fig. 6.7, the source sees as its load the input impedance $Z_1(j\omega)$ of the terminated with R_L filter two-port. At zero frequency ($s = 0$), where inductors become short circuits and capacitors open circuits, the input impedance $Z_1(s)$ of an LC two-port terminated by R_L can assume one of the following values:

$$Z_1(0) = 0 \quad \text{or} \quad Z_1(0) = \infty \quad \text{or} \quad Z_1(0) = R_L$$

If $Z_1(0) = 0$ or $Z_1(0) = \infty$, then no power is transferred to R_L and the attenuation $A(0) = 10\log(P_{\max}/P_2) \to \infty$. This is not expected in lowpass filters, where in the passband the attenuation must be very low. Therefore, in lowpass filters the expected LC two-port can only have a structure which, when terminated by R_L, presents input

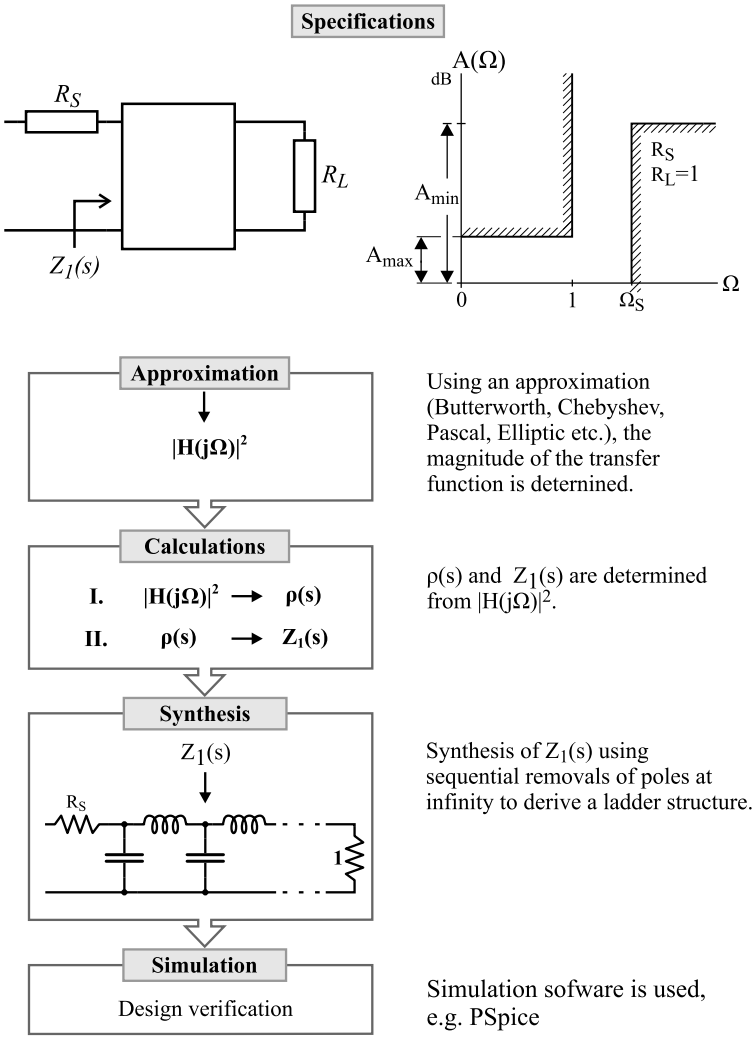

Fig. 6.12 Passive filter design work flow diagram

impedance $Z_1(0) = R_L$, i.e. the two-port becomes transparent at zero frequency and attenuation $A(0)$ is given by

$$A(0) = 20\log\left(\frac{R_S + R_L}{2\sqrt{R_L R_S}}\right) = A_o \tag{6.51}$$

At very high frequencies ($s \rightarrow \infty$), where inductors become open circuits and capacitors short circuits, the input impedance $Z_1(s)$ of an LC two-port terminated

by R_L can again assume one of the following values:

$$Z_1(\infty) = 0 \quad \text{or} \quad Z_1(\infty) = \infty \quad \text{or} \quad Z_1(\infty) = R_L$$

If $Z_1(\infty) = R_L$, then the attenuation $A(\infty) = 10\log(\frac{R_S+R_L}{2\sqrt{R_S R_L}}) = A_o$. This is not expected in lowpass filters where attenuation must be very high at very high frequencies. If $Z_1(\infty) = 0$ or $Z_1(\infty) = \infty$ then no power is transferred to R_L and the attenuation $A(\infty) = 10\log(P_{\max}/P_2) \to \infty$. This is expected in lowpass filters and therefore the LC two-port can only have a structure which, when terminated by R_L, presents $Z_1(\infty) = \infty$ or $Z_1(\infty) = 0$. Summarizing for the resistively terminated LC lowpass two-port, we expect

$$A(0) = 20\log\left(\frac{R_S + R_L}{2\sqrt{R_L R_S}}\right) = A_o \quad \text{and} \quad A(\infty) = \infty \tag{6.52}$$

The above relationships (6.52) imply that at zero frequency, the attenuation of all passive LC lowpass filters is A_o and that there are always attenuation poles at infinity. Therefore, the attenuation function of all lowpass approximation must satisfy (6.52) as a minimum realizability requirement.

6.4.1 Determination of $Z_1(s)$ via $\rho(s)$

In filter design, the approximation initially gives $|H(j\Omega)|$, from which $H(s)H(-s)$ can be determined from $H(s)H(-s) = |H(j\Omega)|^2_{\Omega^2=-s^2}$.

The reflection coefficient function $\rho(s)$ can then be determined from $H(s)H(-s)$ and Feldtkeller's equation (6.49):

$$\rho(s)\rho(-s) = 1 - \frac{4R_S}{R_L}H(s)H(-s) = 1 - \frac{1}{T(s)T(-s)}$$

When one or more expressions for $\rho(s)$ are available, then $Z_1(s)$ can be determined from (6.41):

$$\rho(s) = \pm\frac{R_S - Z_1(s)}{R_S + Z_1(s)}$$

as follows:

$$\text{When } \rho(s) = +\frac{R_S - Z_1(s)}{R_S + Z_1(s)} \text{ is used} \quad \Rightarrow \quad Z_{1a}(s) = R_S\frac{1-\rho(s)}{1+\rho(s)} \tag{6.53}$$

$$\text{When } \rho(s) = -\frac{R_S - Z_1(s)}{R_S + Z_1(s)} \text{ is used} \quad \Rightarrow \quad Z_{1b}(s) = R_S\frac{1+\rho(s)}{1-\rho(s)} \tag{6.54}$$

For each expression of $\rho(s)$, the above equations (6.53)–(6.54) yield two expressions for the input impedance: $Z_{1a}(s)$ and $Z_{1b}(s)$ related by

$$Z_{1a}(s) \cdot Z_{1b}(s) = R_S^2 \tag{6.55}$$

From these two expressions, $Z_{1a}(s)$ and $Z_{1b}(s)$, only one is useful, namely the one having $Z_1(0) = R_L = 1$. The other, when synthesized, leads to an LC two-port terminated by $R_S^2 \neq 1$.

It can be shown that when $\rho(s)$ is determined using any of the known approximations, the corresponding impedances $Z_{1a}(s)$ and $Z_{1b}(s)$ of (6.53)–(6.54) are positive real (PR) rational function of s (see Chap. 11) and can therefore be synthesized as passive RLCM one-port circuits, using the RLCM driving point impedance synthesis methods presented in Chap. 12. In fact, all known approximations have been designed so as to lead to realizable positive real $Z_1(s)$ functions which are usually synthesized using the method of sequential removal of poles at infinity to derive a ladder filter circuit structure.

It is clear that in $Z_{1a}(s)$ of (6.53), the degree of the denominator polynomial is higher than the degree of the numerator polynomial and therefore $Y_{1a}(s) = Z_{1a}^{-1}(s)$ has a pole at infinity, which is removed first in the synthesis phase, as a shunt capacitor. When the input driving-point impedance of the terminated two-port is determined by $Z_{1b}(s)$ of (6.54), it has a pole at infinity, which is removed first in the synthesis phase, as a series inductor. Therefore, using (6.53) or (6.54) determines whether the first arm of the filter will be a shunt capacitor or a series inductor.

Example 6.4 For a normalized passive filter with equal terminations $R_S = R_L = 1$, we found from the approximation procedure that $|H(j\Omega)| = \frac{1}{\sqrt{\Omega^4+4}}$ and therefore

$$H(s)H(-s) = |H(j\Omega)|^2_{\Omega^2=-s^2} = \frac{1}{s^4+4}$$

From (6.49), we get

$$\rho(s)\rho(-s) = 1 - \frac{4R_S}{R_L}H(s)H(-s) = 1 - \frac{4}{s^4+4}$$
$$= \frac{s^4}{s^4+1} = \frac{s^4}{(s^2+2s+2)(s^2-2s+2)}$$

from which, allocating the left half s-plane roots of the denominator to $\rho(s)$ we get:

$$\rho(s) = \frac{s^2}{s^2+2s+2} \quad \text{and} \quad \rho(-s) = \frac{s^2}{s^2-2s+2}$$

From (6.53) and (6.54), we get

$$Z_{1a}(s) = \frac{s+1}{s^2+s+1} \quad \text{or} \quad Z_{1b}(s) = \frac{s^2+s+1}{s+1}$$

Both expressions can be used since $Z_{1a}(0) = R_L = 1$ and $Z_{1b}(0) = R_L = 1$. It is clear that for $Z_{1b}(s)$ we have

$$Z_{1b}(s) = \frac{s^2+s+1}{s+1} = s + \frac{1}{s+1}$$

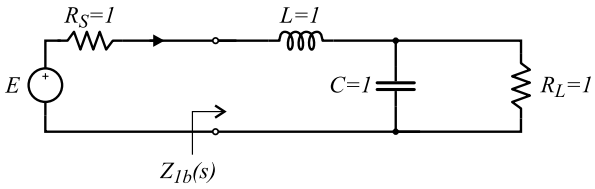

Fig. 6.13 Impedance synthesis

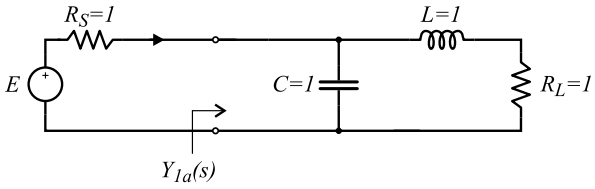

Fig. 6.14 Admittance synthesis

and therefore, the circuit is that of Fig. 6.13 (see Chap. 12).

For the synthesis of $Z_{1a}(s)$, we start from $Y_{1a}(s) = Z_{1a}^{-1}(s)$, which has a pole at infinity:

$$Y_{1a}(s) = \frac{1}{Z_{1a}(s)} = \frac{s^2 + s + 1}{s + 1} = s + \frac{1}{s + 1}$$

Synthesis of $Y_{1a}(s)$ gives the circuit of Fig. 6.14.

The filters of Figs. 6.13 and 6.14 have the same transfer function and the specified gain function $|H(j\Omega)| = \frac{1}{\sqrt{\Omega^4+4}}$.

6.4.2 Determination of $Z_1(s)$ via $ABCD$ Two-Port Parameters

This method for determining $Z_1(s)$ via the ABCD two-port parameters can be used as an alternative way to determine $Z_1(s)$. Before we present the method, some equations from the two-port network theory will be repeated.

Referring to Fig. 6.15, when a two-port is described with its $ABCD$ parameters, the voltage transfer function of the doubly terminated two-port is given by

$$H(s) = \frac{V_2(s)}{E(s)} = \frac{R_L}{AR_L + B + CR_SR_L + DR_S} \tag{6.56}$$

and therefore:

$$T(s) = \frac{AR_L + B + CR_SR_L + DR_S}{2\sqrt{R_SR_L}} \tag{6.57}$$

All two-port parameters are functions of s. For the input driving-point impedance $Z_1(s)$, we have:

$$Z_1(s) = \frac{V_1(s)}{I_1(s)} = \frac{AR_L + B}{CR_L + D} \tag{6.58}$$

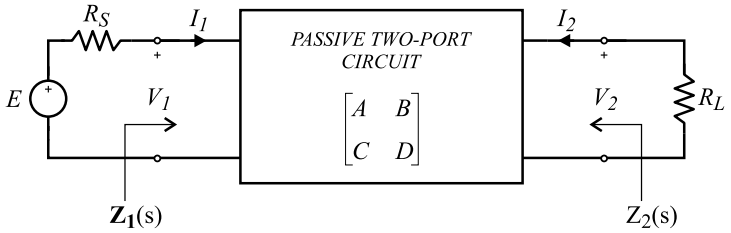

Fig. 6.15 Doubly resistively terminated passive two-port described by its ABCD parameters

When $|H(j\omega)|^2$ has been found from the approximation procedure, we obtain:

$$H(s)H(-s) = |H(j\omega)|^2_{\omega^2=-s^2} \quad \Rightarrow \quad T(s)T(-s) = \frac{R_L}{4R_S}\frac{1}{|H(j\omega)|^2_{\omega^2=-s^2}}$$

$T(s)$ and $H(s)$ can be separated from $T(s)T(-s)$ and $H(s)H(-s)$ respectively. The parameters $ABCD$ of the inserted lossless LCM two-port can then be determined based on the fact that in LCM circuits, parameters A and D are even functions and B and C odd functions of s. From (6.57), we get

$$T(s) = \frac{(AR_L + DR_S) + (B + CR_SR_L)}{2\sqrt{R_SR_L}} \tag{6.59}$$

The even and odd parts of $T(s)$ are given by

$$T_e = \frac{AR_L + DR_S}{2\sqrt{R_SR_L}} \quad \text{(even)} \qquad T_o = \frac{B + CR_SR_L}{2\sqrt{R_SR_L}} \quad \text{(odd)} \tag{6.60}$$

Using (6.46) in conjunction to (6.41) with the positive sign, it can be found that

$$\begin{aligned} K(s) = \rho(s)T(s) &= \frac{R_S - Z_1(s)}{R_S + Z_1(s)}T(s) \\ &= \frac{R_S - \frac{AR_L+B}{CR_L+D}}{R_S + \frac{AR_L+B}{CR_L+D}}\frac{AR_L + DR_S + B + CR_SR_L}{2\sqrt{R_SR_L}} \end{aligned}$$

which after some manipulation yields

$$K(s) = \mp\frac{(AR_L - DR_S) + (B - CR_SR_L)}{2\sqrt{R_SR_L}}$$

The even and odd parts of $K(s)$ are clearly defined from the above expression:

$$K_e = \pm\frac{AR_L - DR_S}{2\sqrt{R_SR_L}} \quad \text{(even)} \qquad K_o = \pm\frac{B - CR_SR_L}{2\sqrt{R_SR_L}} \quad \text{(odd)} \tag{6.61}$$

The four equations, two from (6.60) and two from (6.61), can be solved for the chain parameters to find:

$$\begin{bmatrix} A & B \\ C & D \end{bmatrix} = \frac{1}{\sqrt{R_S R_L}} \begin{bmatrix} (T_e + K_e)R_S & (T_o + K_o)R_S R_L \\ (T_o - K_o) & (T_e - K_e)R_L \end{bmatrix} \tag{6.62}$$

or

$$\begin{bmatrix} A & B \\ C & D \end{bmatrix} = \frac{1}{\sqrt{R_S R_L}} \begin{bmatrix} (T_e - K_e)R_S & (T_o - K_o)R_S R_L \\ (T_o + K_o) & (T_e + K_e)R_L \end{bmatrix} \tag{6.63}$$

Having ABCD parameters, $Z_1(s)$ can be now determined from (6.58):

$$Z_1(s) = \frac{AR_L + B}{CR_L + D} \tag{6.64}$$

Example 6.5 For an equally terminated with $R_L = R_S = 1$ passive normalized lowpass filter, the approximation gave the gain function $|H(j\Omega)| = \frac{1}{\sqrt{\Omega^4+4}}$. Therefore

$$H(s)H(-s) = |H(j\Omega)|^2_{\Omega^2=-s^2} = \frac{1}{s^4+4}$$

and

$$T(s)T(-s) = \frac{R_L}{4R_S}\frac{1}{H(s)H(-s)} = \frac{s^4+4}{4} = \left(\frac{s^2+2s+2}{2}\right)\left(\frac{s^2-2s+2}{2}\right)$$

$$\Rightarrow \quad T(s) = \frac{s^2+2s+2}{2} \text{ and } T(-s) = \frac{s^2-2s+2}{2}$$

$K(s)$ is evaluated from (6.46)

$$K(s)K(-s) = T(s)T(-s) - 1 = \frac{s^4+1}{4} - 1 = \frac{s^4}{4} \quad \Rightarrow \quad K(s) = \frac{1}{2}s^2$$

Using (6.62)–(6.63) with

$$T_e = \frac{1}{2}(s^2+2) \qquad T_o = s \qquad K_e = \frac{1}{2}s^2 \qquad K_o = 0$$

we find

$$\begin{bmatrix} A & B \\ C & D \end{bmatrix} = \begin{bmatrix} s^2+1 & s \\ s & 1 \end{bmatrix} \quad \text{or} \quad \begin{bmatrix} A & B \\ C & D \end{bmatrix} = \begin{bmatrix} 1 & s \\ s & s^2+1 \end{bmatrix}$$

From (6.58), we finally find:

$$Z_{1a}(s) = \frac{(s^2+1)+s}{s+1} = \frac{s^2+s+1}{s+1} = s + \frac{1}{s+1}$$

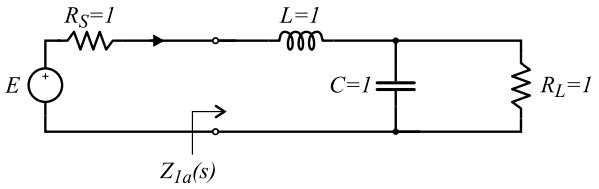

Fig. 6.16 Impedance synthesis

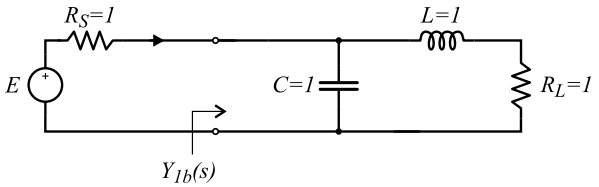

Fig. 6.17 Admittance synthesis

or

$$Z_{1b}(s) = \frac{1+s}{s^2+s+1} = \frac{1}{s+\frac{1}{s+1}}$$

$Z_{1a}(s)$ can be realized as shown in Fig. 6.16. $Y_{1b} = \frac{1}{Z_{1b}(s)}$ can be realized as shown in Fig. 6.17.

Example 6.6 For a 3rd order passive normalized lowpass filter with $R_L = 1$, the approximation gave the square of the gain function:

$$|H(j\omega)|^2 = \frac{1}{(R_S+1)^2(1+\omega^6)}$$

and therefore

$$|T(j\omega)|^2 = \frac{(R_S+1)^2}{4R_S}(1+\omega^6) \tag{6.65}$$

In order to determine $Z_1(s)$, $\rho(s)$ must be first calculated. This will be done using the two presented methods.

Determination via $\rho(s)$

From (6.48) we find:

$$|\rho(j\omega)|^2 = 1 - \frac{1}{|T(j\omega)|^2} = \frac{(\frac{R_S-1}{R_S+1})^2+\omega^6}{1+\omega^6} = \frac{k^6+\omega^6}{1+\omega^6} \tag{6.66}$$

$$\text{where } k^3 = \pm\frac{1-R_S}{1+R_S} \text{ i.e. } k_+^3 = \frac{1-R_S}{1+R_S} \text{ or } k_-^3 = \frac{R_S-1}{R_S+1} \tag{6.67}$$

The two values of k^3 emerge from the term $(R_S-1)^2$, which appears in the above calculations. In order to determine $\rho(s)$, we use:

$$\rho(s)\rho(-s) = |\rho(j\omega)|^2_{\omega^2=-s^2} = \frac{k^6 - s^6}{1 - s^6}$$
$$= \frac{(s+k)(s-k)(s^2+ks+k^2)(s^2-ks+k^2)}{(s+1)(s-1)(s^2+s+1)(s^2-s+1)}$$

Since the denominator polynomial of the reflection coefficient is a Hurwitz polynomial and no restrictions exist for the numerator polynomial, the following expressions can be obtained for $\rho(s)$:

$$\rho_1(s) = \frac{(s+k)(s^2-ks+k^2)}{(s+1)(s^2+s+1)} = \frac{s^3+k^3}{s^3+2s^2+2s+1}$$
$$\rho_2(s) = \frac{(s+k)(s^2+ks+k^2)}{(s+1)(s^2+s+1)} = \frac{s^3+2ks^2+2k^2s+k^3}{s^3+2s^2+2s+1}$$
$$\rho_3(s) = \frac{(s-k)(s^2-ks+k^2)}{(s+1)(s^2+s+1)} = \frac{s^3-k^3}{s^3+2s^2+2s+1}$$
$$\rho_4(s) = \frac{(s-k)(s^2+ks+k^2)}{(s+1)(s^2+s+1)} = \frac{s^3-2ks^2+2k^2s-k^3}{s^3+2s^2+2s+1}$$

Using (6.54) for the determination of $Z_1(s)$ from the above four expressions of $\rho(s)$, we get:

$$\rho_1(s) \quad \Rightarrow \quad Z_{1B}(s) = \frac{2s^3+2s^2+2s+1+k^3}{2s^2+2s+1-k^3} R_S \tag{6.68}$$

$$\rho_2(s) \quad \Rightarrow \quad Z_{1D}(s) = \frac{2s^3+2(1+k)s^2+2(1+k^2)s+1+k^3}{2(1-k)s^2+2(1-k^2)s+1-k^3} R_S \tag{6.69}$$

$$\rho_3(s) \quad \Rightarrow \quad Z_{1X}(s) = \frac{2s^3+2s^2+2s+1-k^3}{2s^2+2s+1+k^3} R_S \tag{6.70}$$

$$\rho_4(s) \quad \Rightarrow \quad Z_{1Y}(s) = \frac{2s^3+2(1-k)s^2+2(1+k^2)s+1-k^3}{2(1+k)s^2+2(1-k^2)s+1+k^3} R_S \tag{6.71}$$

Impedances $Z_{1B}(s)$ and $Z_{1D}(s)$ satisfy the realizability condition $Z_1(0) = R_L = 1$ for $k^3 = k_+^3 = \frac{1-R_S}{1+R_S}$. Impedances $Z_{1X}(s)$ and $Z_{1Y}(s)$ give $Z_1(0) = R_L = 1$ for $k^3 = k_-^3 = -k_+^3$, in which case they become equal to $Z_{1B}(s)$ and $Z_{1D}(s)$ respectively. Therefore, only $Z_{1B}(s)$ and $Z_{1D}(s)$ of (6.68) and (6.69) will lead to different circuits.

If we use (6.53) for the evaluation of $Z_1(s)$ from the above four expressions for $\rho(s)$, we get:

$$\rho_1(s) \quad \Rightarrow \quad Z_{1A}(s) = \frac{2s^2+2s+1-k^3}{2s^3+2s^2+2s+1+k^3} R_S \tag{6.72}$$

$$\rho_2(s) \quad \Rightarrow \quad Z_{1C}(s) = \frac{2(1-k)s^2+2(1-k^2)s+1-k^3}{2s^3+2(1+k)s^2+2(1+k^2)s+1+k^3} R_S \tag{6.73}$$

$$\rho_3(s) \quad \Rightarrow \quad Z_{1X}(s) = \frac{2s^2 + 2s + 1 + k^3}{2s^3 + 2s^2 + 2s + 1 - k^3} R_S \tag{6.74}$$

$$\rho_4(s) \quad \Rightarrow \quad Z_{1Y}(s) = \frac{2(1+k)s^2 + 2(1-k^2)s + 1 + k^3}{2s^3 + 2(1-k)s^2 + 2(1+k^2)s + 1 - k^3} R_S \tag{6.75}$$

Impedances $Z_{1A}(s)$ and $Z_{1C}(s)$ satisfy the realizability condition $Z_1(0) = R_L = 1$ for $k^3 = k_-^3 = \frac{R_S - 1}{1 + R_S}$. Impedances $Z_{1X}(s)$ and $Z_{1Y}(s)$ give $Z_1(0) = R_L = 1$ for $k^3 = k_+^3 = -k_-^3$, in which case they become equal to $Z_{1A}(s)$ and $Z_{1C}(s)$ respectively. Therefore, only $Z_{1A}(s)$ and $Z_{1C}(s)$ of (6.72) and (6.73) will lead to different circuits.

Determination via $ABCD$ Two-Port Parameters

$$T(s)T(-s) = |T(j\omega)|^2_{\omega^2 = -s^2} = \frac{(R_S+1)^2}{4R_S}(1+\omega^6)\bigg|_{\omega^2=-s^2} = \frac{(R_S+1)^2}{4R_S}(1-s^6)$$

From this equation, and taking into account that the numerator of $T(s)$ is a Hurwitz polynomial, we allocate the left hand s-half plane roots to $T(s)$:

$$T(s) = \frac{R_S+1}{2\sqrt{R_S}}(s+1)(s^2+s+1) = \frac{R_S+1}{2\sqrt{R_S}}(s^3+2s^2+2s+1)$$

The even and odd part of $T(s)$ are given below:

$$T_e(s) = \frac{R_S+1}{2\sqrt{R_S}}(2s^2+1) \qquad T_o(s) = \frac{R_S+1}{2\sqrt{R_S}}(s^3+2s)$$

We now need the characteristic function $K(s)$ which can be determined from (6.43):

$$|K(j\omega)|^2 = |T(j\omega)|^2 - 1 = \frac{(R_S+1)^2}{4R_S}\left[\omega^6 + \left(\frac{R_S-1}{R_S+1}\right)^2\right]$$

$$= \frac{(R_S+1)^2}{4R_S}(\omega^6 + k^6)$$

with

$$k^3 = \frac{R_S-1}{R_S+1} \quad \text{or} \quad k^3 = \frac{1-R_S}{R_S+1}$$

Now we can write

$$K(s)K(-s) = |K(j\omega)|^2_{\omega^2=-s^2} = \frac{(R_S+1)^2}{4R_S}(k^6 - s^6)$$

$$\Rightarrow \quad K(s)K(-s) = \frac{(R_S+1)^2}{4R_S}(s+k)(s^2+ks+k^2)(s-k)(s^2-ks+k^2)$$

From the last equation, and taking into account that there are no restrictions for the root location of the numerator polynomial of $K(s)$, we find

$$K_1(s) = \frac{R_S+1}{2\sqrt{R_S}}(s+k)(s^2-ks+k^2) = \frac{R_S+1}{2\sqrt{R_S}}(s^3+k^3)$$

or

$$K_2(s) = \frac{R_S+1}{2\sqrt{R_S}}(s+k)(s^2+ks+k^2) = \frac{R_S+1}{2\sqrt{R_S}}(s^3+2ks^2+2k^2s+k^3)$$

The even and odd parts of $K_1(s)$ will be:

$$K_{e1}(s) = \frac{R_S+1}{2\sqrt{R_S}}k^3 \qquad K_{o1}(s) = \frac{R_S+1}{2\sqrt{R_S}}s^3$$

The even and odd parts of $K_2(s)$ will be:

$$K_{e2}(s) = \frac{R_S+1}{2\sqrt{R_S}}(2ks^2+k^3) \qquad K_{o2}(s) = \frac{R_S+1}{2\sqrt{R_S}}(s^3+2k^2s)$$

We can now use (6.62)–(6.63), which gives $ABCD$ in terms of the even and odd parts of $T(s)$ and $K(s)$.

For $K_1(s)$, (6.62) gives:

$$\begin{bmatrix} A & B \\ C & D \end{bmatrix} = \frac{1}{\sqrt{R_S R_L}} \begin{bmatrix} (T_e+K_e)R_S & (T_o+K_o)R_S R_L \\ (T_o-K_o) & (T_e-K_e)R_L \end{bmatrix}$$

$$A = \frac{R_S+1}{2}(2s^2+1-k^3),\ B = \frac{R_S+1}{2}2s$$

$$C = \frac{R_S+1}{2R_S}(2s^3+2s),\ D = \frac{R_S+1}{2R_S}(2s^2+1+k^3)$$

From (6.63), using again $K_1(s)$, we get:

$$\begin{bmatrix} A & B \\ C & D \end{bmatrix} = \frac{1}{\sqrt{R_S R_L}} \begin{bmatrix} (T_e-K_e)R_S & (T_o-K_o)R_S R_L \\ (T_o+K_o) & (T_e+K_e)R_L \end{bmatrix}$$

$$A = \frac{R_S+1}{2}(2s^2+1+k^3),\ B = \frac{R_S+1}{2}(2s^3+2s)$$

$$C = \frac{R_S+1}{2R_S}2s,\ D = \frac{R_S+1}{2R_S}(2s^2+1-k^3)$$

For $R_L = 1$, we finally find from (6.58):

$$Z_{1A}(s) = \frac{AR_L+B}{CR_L+D} = \frac{2s^2+2s+1-k^3}{2s^3+2s^2+2s+1+k^3}R_S$$

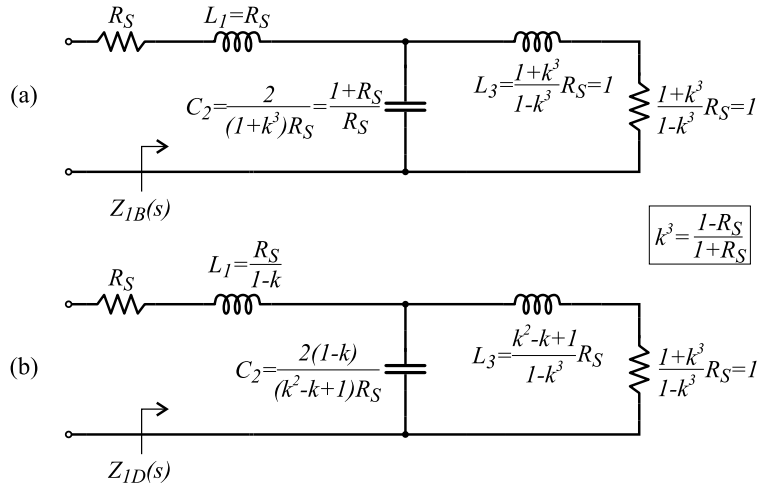

Fig. 6.18 Synthesis of two alternative expressions of the driving-point impedance

From the second set of $ABCD$ parameters, we get:

$$Z_{1B}(s) = \frac{AR_L + B}{CR_L + D} = R_S \frac{2s^3 + 2s^2 + 2s + 1 + k^3}{2s^2 + 2s + 1 - k^3}$$

For $K_2(s)$, we find in a similar manner:

$$Z_{1C}(s) = \frac{2s^2(1-k) + 2s(1-k^2) + 1 - k^3}{2s^3 + 2s^2(1+k) + 2s(1+k^2) + 1 + k^3} R_S$$

$$Z_{1D}(s) = \frac{2s^3 + 2s^2(1+k) + 2s(1+k^2) + 1 + k^3}{2s^2(1-k) + 2s(1-k^2) + 1 - k^3} R_S$$

LCM Synthesis

Using the two alternative methods for the determination of $Z_1(s)$, we found the same four expressions $Z_{1A}(s)$, $Z_{1B}(s)$, $Z_{1C}(s)$ and $Z_{1D}(s)$, which can be synthesized using the RLCM driving-point function synthesis methods of Chap. 12. Synthesis of $Z_{1B}(s)$ and $Z_{1D}(s)$ using sequential removals of poles at infinity leads to the circuits of Fig. 6.18.

Synthesis of $Z_{1A}(s)$ and $Z_{1C}(s)$ using sequential removals of poles at infinity starting from $Y_{1A}(s)$ and $Y_{1C}(s)$ yields the circuits of Fig. 6.19.

Figures 6.20 and 6.21 show the circuits of Figs. 6.18 and 6.19 for $R_S = 0.5$ and $R_S = 2$ respectively. All eight circuits have the specified

$$|H(j\omega)|^2 = \frac{1}{(R_S + 1)^2(1 + \omega^6)}$$

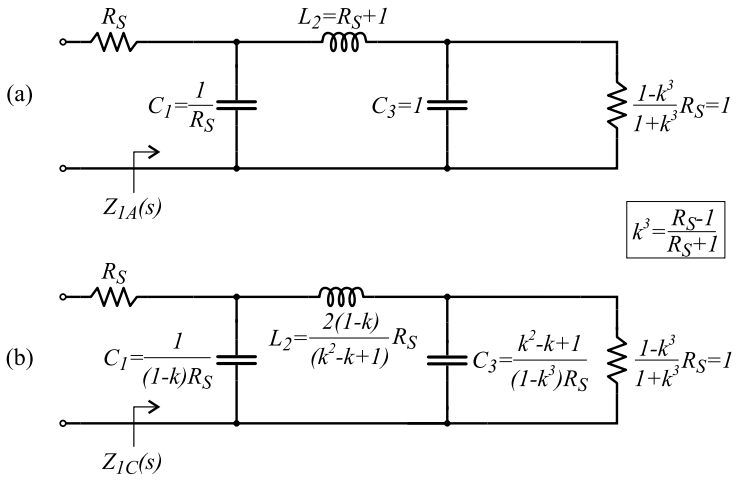

Fig. 6.19 Synthesis of two alternative expressions of the driving-point impedance

6.5 Problems

6.1 In the circuit of Fig. 6.22 the source with internal resistance R_1 sees as its load the rest of the circuit. Show that maximum power transfer may occur if $R_2 > R_1$ and $L_2 = R_1 R_2 C_1$ and determine the maximum power transfer frequency ω_o.

6.2 Use the results of problem 6.1 with $R_1 = 1$ kOhm and $R_2 = 2$ kOhm to determine C_1 and L_2 so that maximum power transfer occurs at $f_o = 10$ kHz.

6.3 Determine the transfer function $H(s)$, the characteristic function $K(s)$ and the reflection coefficient function $\rho(s)$ of the circuit of Fig. 6.23.

6.4 For a normalized lowpass passive filter with $R_L = 1$ and $R_S = 0.5$ we found:

$$H(s)H(-s) = \frac{4.10936}{s^8 + 9.24607}$$

Determine the function $\rho(s)\rho(-s)$.

6.5 For a normalized lowpass passive filter we found that $\rho(s)\rho(-s)$ is given by:

$$\frac{(s^2 + 1.85s + 1.01)(s^2 - 1.85s + 1.01)(s^2 + 0.77s + 1.01)(s^2 - 0.77s + 1.01)}{(s^2 + 2.44s + 1.74)(s^2 - 2.44s + 1.74)(s^2 + 1.01s + 1.74)(s^2 - 1.01s + 1.74)}$$

Determine all permitted expressions of $\rho(s)$.

6.6 For a normalized lowpass passive filter with equal terminations we found:

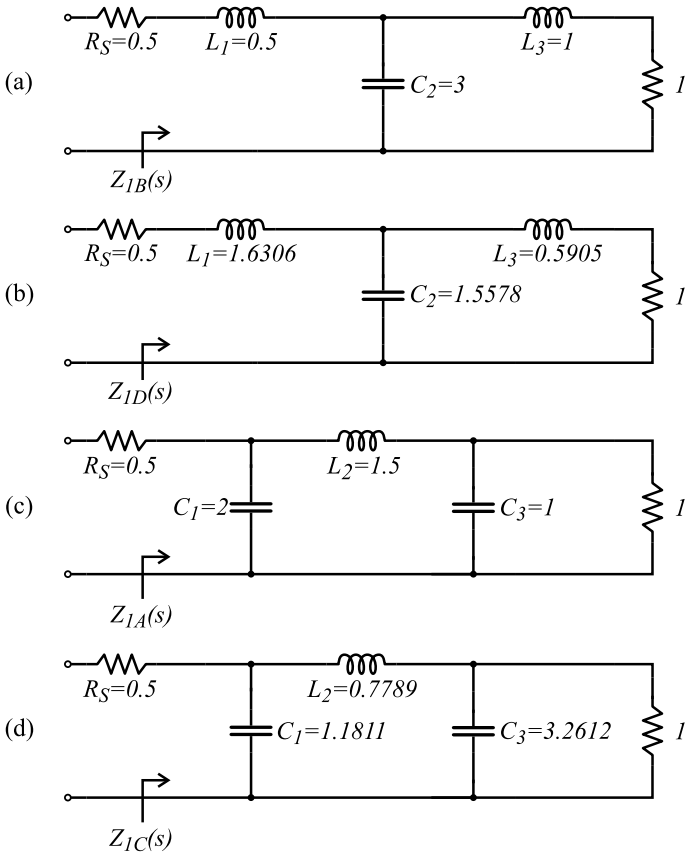

Fig. 6.20 Synthesis of the four alternative expressions of the driving-point impedance

$$\rho(s)\rho(-s) = \frac{-s^6}{(s+1)(1-s)(s^2+s+1)(s^2-s+1)}$$

Determine all permitted expressions of $\rho(s)$ and $Z_1(s)$.

6.7 For the normalized lowpass filter of Fig. 6.24, we have found that

$$|T(j\omega)|^2 = T(s)T(-s)|_{s^2=-\omega^2} = 1.125(1+\omega^6)$$

Determine the values of L_1, C_2 and L_3.

6.8 For the normalized lowpass filter of Fig. 6.25, we have found that

$$|T(j\omega)|^2 = T(s)T(-s)|_{s^2=-\omega^2} = 1.125(1+\omega^6)$$

Determine the values of C_1, L_2, C_3.

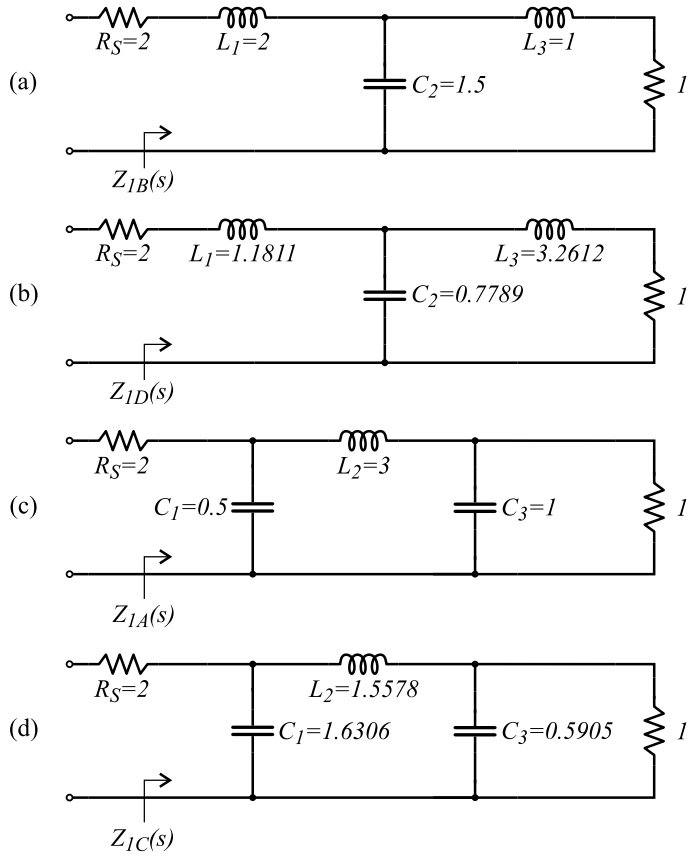

Fig. 6.21 Synthesis of the four alternative expressions of the driving-point impedance

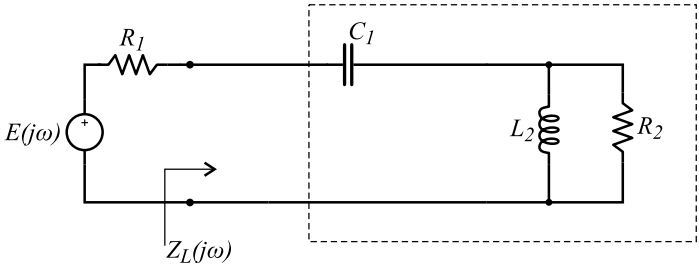

Fig. 6.22 Circuit for Problem 6.1

6.9 For a normalized lowpass passive filter with $R_L = 1$ and $R_S = 2$, the square of the magnitude response is given by $|H(j\Omega)|^2 = \frac{1}{\Omega^4+9}$. Determine the two possible expressions for the reflection coefficient $\rho(s)$ and all four expressions for $Z_1(s)$. Synthesize the two of them which have $Z_1(0) = 1$.

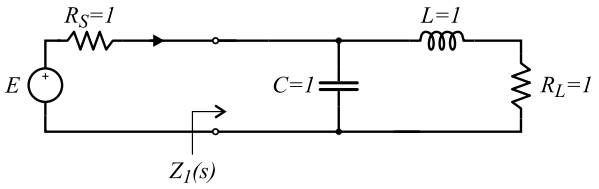

Fig. 6.23 Circuit for Problem 6.3

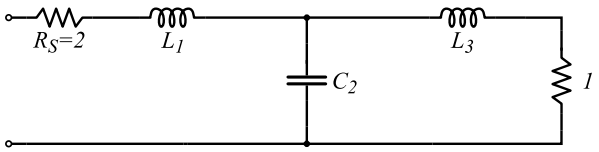

Fig. 6.24 Circuit for Problem 6.7

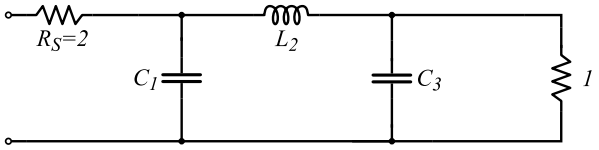

Fig. 6.25 Circuit for Problem 6.8

6.10 For a normalized lowpass passive filter with $R_L = 1$ and $R_S = 0.5$, the square of the magnitude response is given by $|H(j\Omega)|^2 = \frac{1}{\Omega^4+9}$. Determine the two possible expressions for the reflection coefficient $\rho(s)$ and all four expressions for $Z_1(s)$. Synthesize the two of them, which have $Z_1(0) = 1$.

6.11 Verify that the filters of Fig. 6.20 have

$$|H(j\omega)|^2 = \frac{1}{1.5^2(1+\omega^6)}$$

6.12 Verify that the filters of Fig. 6.21 have

$$|H(j\omega)|^2 = \frac{1}{9(1+\omega^6)}$$

6.13 Synthesize a ladder RLC one-port with input impedance:

$$Z_1(s) = \frac{s^4 + 0.68443542s^3 + 1.24599439s^2 + 0.52444123s + 0.19199176}{0.76631472s^3 + 0.52449295s^2 + 0.64815469s + 0.19199176}$$

6.14 Synthesize a ladder RLC one-port with the following input impedance:

$$Z_1(s) = \frac{6.0s^5 + 4.760661s^4 + 8.937805s^3 + 4.800773s^2 + 2.665519s + 0.551719}{3.506885s^4 + 2.782506s^3 + 3.977509s^2 + 1.816958s + 0.551719}$$

References[1]

1. Chen, W.-K. (ed.): The Circuits and Filters Handbook. Passive, Active and Digital Filters, vol. V. CRC Press, Boca Raton (2009)
2. Daniels, R.W.: Approximation Methods for Electronic Filter Design. McGraw-Hill, New York (1974)
3. Paarmann, L.D.: Design and Analysis of Analog Filters—A Signal Processing Perspective—With MATLAB Examples. Kluwer Academic, Dordrecht (2001)
4. Schaumann, R., Van Valkenburg, M.E.: Design of Analog Filters. Oxford University Press, London (2001)
5. Sedra, A.S., Brackett, P.O.: Filter Theory and Design: Active and Passive. Pitman, London (1978)
6. Temes, G.C., LaPatra, J.W.: Introduction to Circuit Synthesis and Design. McGraw-Hill, New York (1977)
7. van Roermund, A.H.M., Casier, H., Steyaert, M. (eds.): Analog Circuit Design, Smart Data Converters, Filters on Chip, Multimode Transmitters. Springer, Berlin (2010)
8. Van Valkenburg, M.E.: Analog Filter Design. Oxford University Press, London (1982)
9. Wanhammar, L.: Analog Filters Using MATLAB. Springer, Berlin (2009)
10. Williams, A., Taylor, F.: Electronic Filter Design Handbook. McGraw-Hill, New York (2006)

[1] All references, whether or not cited within the text, are recommended for further reading.

Synthesis and Design of Passive Filters

7

7.1 Preliminaries

Passive filters are LC two-port networks that are inserted between a signal source and a load. The signal source represents all preceding sections of the system and is usually modeled by a voltage source with internal resistance R_S. The load is represented by a resistor R_L, which in fact is the input resistance of the load circuit. The LC two-port filter with its source and load terminations is shown in Fig. 7.1 and is referred to as the doubly resistively terminated lossless two-port or simply the filter.

Referring to Fig. 7.1, the voltage transfer function $H(s) = \frac{V_2(s)}{E(s)}$ can be expressed in terms of the transmission or $ABCD$ parameters of the inserted lossless two-port as follows:

$$H(s) = \frac{V_2(s)}{E(s)} = \frac{R_L}{AR_L + B + CR_SR_L + DR_S} \tag{7.1}$$

Although parameters $ABCD$ depend only on the LC two-port itself, it is clear that the transfer function of the filter depends also on the termination resistances R_S and R_L. Therefore, for the determination of the transfer function of a passive filter, the terminating resistances R_S and R_L must be given with the filter specifications. As mentioned in Chap. 6, this is the main difference in passive filter design as compared to active filter design, where, due to the existence of simple isolation methods (e.g. buffers), the source and load resistances are of no importance.

Passive filters are designed from the specifications

$$\{\omega_C, \omega_S, R_S, R_L, A_{\max}, A_{\min}\}$$

In order to minimize the number of design parameters, these specifications are normalized for unity load ($R_{Ln} = 1$) and unity cutoff frequency ($\Omega_C = 1$).

When the normalized filter has been designed from the normalized specifications, the normalized element values (denoted with subscript n) can then be denormalized for the desired load resistance level R_L and the desired cutoff frequency ω_C. This

H.G. Dimopoulos, *Analog Electronic Filters*, Analog Circuits and Signal Processing,
DOI 10.1007/978-94-007-2190-6_7, © Springer Science+Business Media B.V. 2012

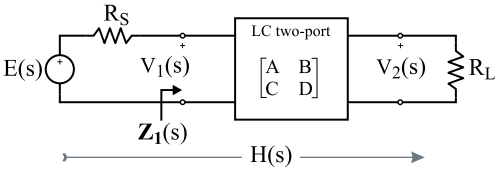

Fig. 7.1 Doubly resistively terminated passive two-port

can be done according to (1.29) of Sect. 1.6.3 (Chap. 1):

$$\omega = \omega_C \Omega \qquad R = R_n R_L \qquad L = \frac{R_L L_n}{\omega_C} \qquad C = \frac{1}{\omega_C R_L} C_n$$

Passive filter magnitude specifications can be given in terms of plain or logarithmic gain. However, traditionally they are given in terms of effective attenuation, as defined in Sect. 6.2.1 of the previous chapter (6.28):

$$A(\omega) = 10 \log\left(\frac{P_{MAX}}{P_2(\omega)}\right) = 20 \log\left(\frac{1}{2}\sqrt{\frac{R_L}{R_S}}\frac{|E(j\omega)|}{|V_2(j\omega)|}\right) \text{ (dB)} \tag{7.2}$$

where $P_2(\omega)$ is the average power of the load R_L and P_{MAX} the maximum power the source can deliver under maximum power transfer conditions (see Sect. 6.1, (6.17)). A detailed analysis of the specifications of passive lowpass filters is given in Sect. 6.3.

In the rest of this chapter we are going to deploy the classical and useful approximations, presented in Chaps. 2–4, in the design of normalized doubly resistively terminated passive LC lowpass filters. All approximations, no matter how simple or complicated they are, lead to the determination of a gain function $G(\Omega) = |H(j\Omega)|$ which meets the specifications. From $|H(j\Omega)|$, the corresponding transfer function $H(s)$ can then be precisely determined, although this is not necessary in passive filter design, where synthesis is based on the input impedance $Z_1(s)$ of Fig. 7.1, for the determination of which, $H(s)$ is not required. When $Z_1(s)$ has been determined, it can then be synthesized, using the RLCM synthesis methods.

For the determination of $Z_1(s)$, only the gain function of the approximation $G(\Omega) = |H(j\Omega)|$ is required since, according to (6.53)–(6.54), $Z_1(s)$ depends on the reflection coefficient function $\rho(s)$ (repeated here for convenience)

$$Z_{1a}(s) = R_S \frac{1 - \rho(s)}{1 + \rho(s)} \tag{7.3}$$

$$Z_{1b}(s) = R_S \frac{1 + \rho(s)}{1 - \rho(s)} \tag{7.4}$$

and $\rho(s)$ can be determined from Feldtkeller's equation (6.49):

$$\rho(s)\rho(-s) = 1 - \frac{4R_S}{R_L} H(s)H(-s) = 1 - \frac{4R_S}{R_L} |H(j\Omega)|^2_{\Omega^2 = -s^2} \tag{7.5}$$

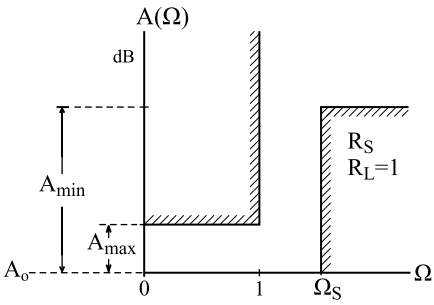

Fig. 7.2 Normalized lowpass filter attenuation specifications

The reflection coefficient function $\rho(s)$ can be isolated from $\rho(s)\rho(-s)$ of (7.5), taking into account that

i. $\rho(s)$ and $\rho(-s)$ have opposite poles and opposite zeros
ii. the poles of $\rho(s)$ lie in the left half s-plane, i.e. the denominator polynomial of $\rho(s)$ is strictly Hurwitz.

Since there are no restrictions for the location of the zeros of $\rho(s)$, the above procedure leads to more than one function $\rho(s)$ and therefore (7.3)–(7.4) can give more than one function for $Z_1(s)$, which, when synthesized, yield more than one filter circuit. More on the determination of $Z_1(s)$ from $\rho(s)$ can be found in Sect. 6.4.1.

Finally, it should be stated that our attention will be focused on passive lowpass filters since other types (highpass, bandpass and band-reject), can be derived from lowpass filters, using the corresponding frequency transformations presented in Chap. 5.

7.2 The Butterworth Approximation in Passive Filter Design

Figure 7.2 shows the normalized lowpass filter specifications

$$\{A_{\max}, A_{\min}, \Omega_S, R_S, R_L = 1, \Omega_C = 1\}$$

and we are looking for a minimum order gain function $G(\Omega) = |H(j\Omega)|$ for which

$$A(\Omega) = 20\log\left(\frac{1}{2}\sqrt{\frac{R_L}{R_S}}\frac{|E(j\Omega)|}{|V_2(j\Omega)|}\right) = 20\log\left(\frac{1}{2}\sqrt{\frac{R_L}{R_S}}\frac{1}{|H(j\Omega)|}\right) \tag{7.6}$$

satisfies these specifications.

The Butterworth approximation has already been presented in Sect. 2.2 of Chap. 2 in terms of plain gain. In this section, the approximation is presented in terms of effective attenuation, as it is actually used in passive filter design.

The Butterworth attenuation is defined as

$$A(\Omega) = A_o + 20\log\left(\sqrt{1+\beta^2\Omega^{2N}}\right) \quad \text{where } A_o = 20\log\left(\frac{R_S+R_L}{2\sqrt{R_S R_L}}\right) \tag{7.7}$$

$$\Rightarrow \quad A(\Omega) = 20\log\left(\frac{R_S + R_L}{2\sqrt{R_S R_L}}\sqrt{1+\beta^2\Omega^{2N}}\right) \quad (R_L = 1) \tag{7.8}$$

As has been shown in Sect. 2.2 (2.15), the value of the design parameter β can be selected from the range:

$$\frac{10^{\frac{A_{\min}}{10}} - 1}{\Omega_S^N} = \beta_{\min} \le \beta \le \beta_{\max} = \sqrt{10^{\frac{A_{\max}}{10}} - 1} \tag{7.9}$$

For any value of the design parameter β within this range, a Butterworth filter can be designed the attenuation of which will satisfy the specifications in a distinctly different manner. Details can be found in Sect. 2.2.1 of Chap. 2.

The integer order N of the approximation is defined as the minimum integer value which satisfies:

$$N \ge N_d = \frac{\log(\frac{10^{\frac{A_{\min}}{10}}-1}{\beta_{\max}^2})}{2\log\Omega_S} = \frac{\log(\frac{10^{\frac{A_{\min}}{10}}-1}{10^{\frac{A_{\max}}{10}}-1})}{2\log\Omega_S} \tag{7.10}$$

N_d is referred to as the decimal order of the approximation. The proof is similar to that given in Sect. 2.2.

As we have seen in Sect. 2.2.2, the characteristic frequency Ω_{3dB} at which the gain drops by 3 dB from H_o to $H_o/\sqrt{2}$ is given by:

$$\Omega_{3dB} = \beta^{-\frac{1}{N}} \tag{7.11}$$

It is clear that the attenuation at Ω_{3dB} will be 3 dB higher than the lowest passband attenuation A_o at $\Omega = 0$.

The squared magnitude $|H(j\Omega)|^2$ can be determined from (7.6) and (7.7):

$$|H(j\Omega)|^2 = \left|\frac{V_2(j\Omega)}{E(j\Omega)}\right|^2 = \frac{R_L^2/(R_S+R_L)^2}{1+\beta^2\Omega^{2N}} \tag{7.12}$$

According to Sect. 2.2.3, the logarithmic gain in the stopband decreases at a rate of $6N$ dB/octave and therefore the attenuation increases at the same rate, the cutoff rate.

The voltage transfer function of the normalized lowpass Butterworth filter ($\Omega_C = 1$, $R_L = 1$) can be determined as in Chap. 2 (Sect. 2.2.4):

$$H(s) = \frac{\frac{R_L}{\beta(R_S+R_L)}}{\prod_{k=1}^{N}(s - s_k)} \tag{7.13}$$

where

$$s_k = \beta^{-\frac{1}{N}} e^{j(\frac{2k+N-1}{2N}\pi)} \quad \text{for } k = 1, 2, \ldots, N$$

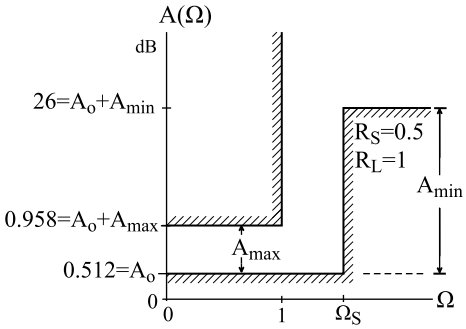

Fig. 7.3 Normalized lowpass filter attenuation specifications of Example 7.1

Example 7.1

(a) Find and plot the minimum order Butterworth effective attenuation function $A(\Omega)$ which satisfies the normalized specifications:

$$\{A_{\max} = 0.446 \text{ dB},\ A_{\min} = 25.4880 \text{ dB},\ R_S = 0.5,\ \Omega_S = 3\}$$

(b) Find and plot the minimum order Butterworth effective attenuation function $A(\Omega)$ to satisfy the specifications

$$\begin{aligned} A_{\max} &= 0.446 \text{ dB} & A_{\min} &= 25.4880 \text{ dB} \\ R_S &= 300 \text{ Ohm} & R_L &= 600 \text{ Ohm} \\ f_C &= 3 \text{ kHz} & f_S &= 9 \text{ kHz} \end{aligned}$$

A_o is determined by the termination resistors R_S and R_L and its value is determined using (7.7):

$$A_o = 20\log\left(\frac{R_S + R_L}{2\sqrt{R_S R_L}}\right) = 20\log\left(\frac{0.5 + 1.0}{2\sqrt{0.5 \cdot 1.0}}\right) = 0.512 \text{ dB}$$

The normalized specifications are shown in Fig. 7.3.

(a) For the determination of Butterworth attenuation $A(\Omega)$ of (7.7), only the order N and the parameter β are required. N can be determined from (7.10)

$$N \geq N_d = \frac{\log\left(\frac{10^{\frac{A_{\min}}{10}} - 1}{10^{\frac{A_{\max}}{10}} - 1}\right)}{2\log\Omega_S} = \frac{\log\left(\frac{10^{\frac{25.4880}{10}} - 1}{10^{\frac{0.446}{10}} - 1}\right)}{2\log 3} = 3.682 \quad \Rightarrow \quad N = 4$$

The value of the design parameter β can now be selected from the range given in (7.9). Let us select $\beta = \beta_{\max}$ for this example:

$$\beta = \beta_{\max} = \sqrt{10^{\frac{A_{\max}}{10}} - 1} = \sqrt{10^{0.0446} - 1} = 0.328867 \quad \Rightarrow \quad \beta^2 = 0.108154$$

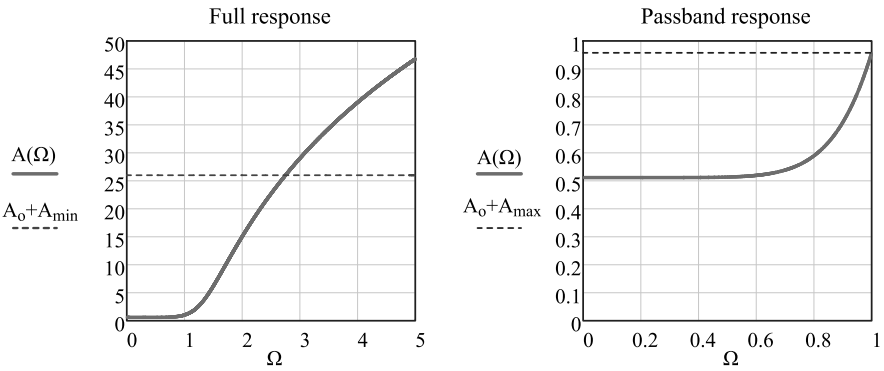

Fig. 7.4 Full and passband attenuation response

For $N = 4$ and $\beta = 0.328867$, (7.7) yields

$$A(\Omega) = 20\log\left(\frac{1.0 + 0.5}{2\sqrt{1.0 \cdot 0.5}}\sqrt{1 + 0.108154\Omega^8}\right)$$

$$\Rightarrow \quad A(\Omega) = 20\log\left(1.06066\sqrt{1 + 0.108154\Omega^8}\right)$$

From the above attenuation function, we get

$$A(0) = 0.511525 \qquad A(1) = 0.957525 \qquad A(3) = 29.027755$$

from which it is verified that

$$A(1) - A(0) = 0.446 \text{ dB} = A_{\max}$$

$$A(3) - A(0) = 28.51623 > A_{\min} = 25.4880 \text{ dB}$$

Figure 7.4 shows the attenuation plots of the normalized filter.

(b) We note that in this case $R_S = 0.5R_L$ as in the normalized case and therefore the coefficient $\frac{R_S + R_L}{2\sqrt{R_S R_L}}$ of $A(\Omega)$ does not change value. Moreover, since $f_S/f_C = 3$ as in the normalized case, the attenuation function will be

$$A_C(\omega) = A\left(\frac{\omega}{\omega_C}\right)$$

or

$$A_C(f) = A\left(\frac{f}{f_C}\right) = 20\log\left(1.06066\sqrt{1 + 0.108154\left(\frac{f}{3000}\right)^8}\right)$$

Figure 7.5 shows the plot of $A_C(f)$.

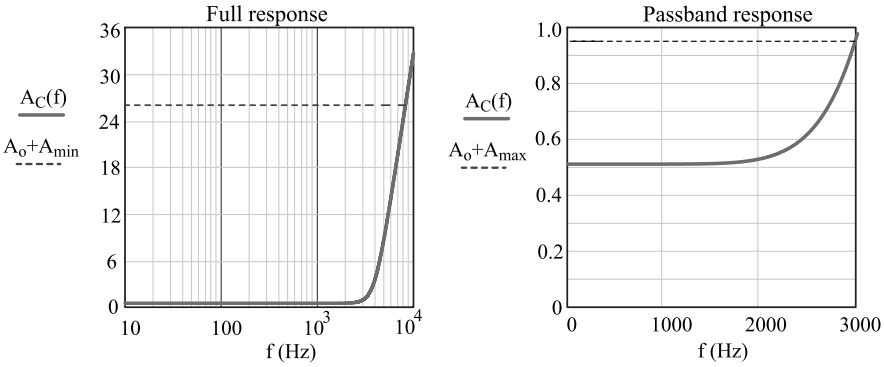

Fig. 7.5 Full and passband attenuation response

In order to determine the reflection coefficient function $\rho(s)$, the product $H(s)H(-s)$ is required. Function $H(s)H(-s)$ can be determined directly from the approximation since

$$H(s)H(-s) = |H(j\Omega)|^2_{\Omega^2=-s^2} = \frac{R_L^2}{(R_S+R_L)^2} \times \frac{1}{[1+\beta^2\Omega^{2N}]_{\Omega^2=-s^2}}$$

$$\Rightarrow \quad H(s)H(-s) = \frac{R_L^2/(R_S+R_L)^2}{1+\beta^2(-s^2)^N} \tag{7.14}$$

Function $\rho(s)\rho(-s)$ can now be determined from (7.5):

$$\rho(s)\rho(-s) = 1 - \frac{4R_S}{R_L}|H(j\Omega)|^2_{\Omega^2=-s^2} = \frac{1+\beta^2(-s^2)^N - \frac{4R_SR_L}{(R_S+R_L)^2}}{1+\beta^2(-s^2)^N} \tag{7.15}$$

Since the denominator of $\rho(s)$ is a Hurwitz polynomial, it can be separated using the procedure presented in Sect. 11.6 of Chap. 11. This procedure may yield several expressions for $\rho(s)$ and each can be used with (7.3) or (7.4) to determine a driving-point input impedance function $Z_1(s)$ of Fig. 7.1. Input impedance $Z_1(s)$ can finally be synthesized as an RLCM two-port circuit using sequential removals of poles at infinity.

Example 7.2 Given the normalized specifications of Example 7.1, determine the following:
(a) $H(s)H(-s)$
(b) $\rho(s)\rho(-s)$
(c) $\rho(s)$ and
(d) $Z_1(s)$.
Use $\beta = \beta_{max}$

Fig. 7.6 Poles of $\rho(s)\rho(-s)$

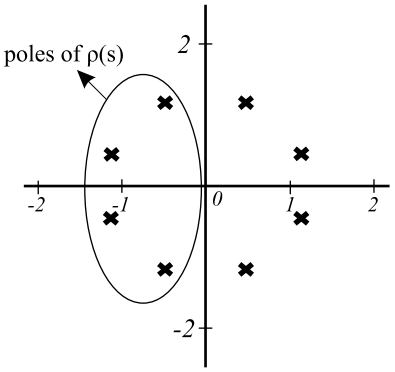

(a) For the determination of $H(s)H(-s)$, (7.14) will be used with $N = 4$, $R_S = 0.5$, $R_L = 1$ and $\beta = 0.328867$ to get

$$H(s)H(-s) = \frac{R_L^2/(R_S + R_L)^2}{1 + \beta^2(-s^2)^N} = \frac{0.444444}{1 + 0.108154s^8} = \frac{4.1093662}{s^8 + 9.246075}$$

(b) $\rho(s)\rho(-s)$ can then be determined from (7.15)

$$\rho(s)\rho(-s) = 1 - \frac{4R_S}{R_L}H(s)H(-s) = 1 - 2\frac{4.1093662}{s^8 + 9.246075} = \frac{s^8 + 0.888889}{s^8 + 9.246075}$$

It is clear that $\rho(s)\rho(-s)$ could have been determined directly from (7.15) without first finding $H(s)H(-s)$.

(c) The eight poles (roots of the denominator) of $\rho(s)\rho(-s)$ are calculated by solving the binomial equation $s^8 + 9.246075 = 0$ for s to find:

$$\begin{aligned}
&-1.2200009 + j0.5053409 \qquad -1.2200009 - j0.5053409\\
&-0.5053409 + j1.2200009 \qquad -0.5053409 - j1.2200009\\
&+1.2200009 + j0.5053409 \qquad +1.2200009 - j0.5053409\\
&+0.5053409 + j1.2200009 \qquad +0.5053409 - j1.2200009
\end{aligned}$$

These poles lie on a circle of radius $\beta^{-\frac{1}{N}}$ and are schematically shown in Fig. 7.6.

Since the denominator of $\rho(s)$ is a Hurwitz polynomial, only the left half s-plane poles can be allocated to $\rho(s)$ and the rest, the right half s-plane poles, to $\rho(-s)$. Therefore, the poles of $\rho(s)$ are

$$\begin{aligned}
&-1.2200009 + j0.5053409 \qquad -1.2200009 - j0.5053409\\
&-0.5053409 + j1.2200009 \qquad -0.5053409 - j1.2200009
\end{aligned}$$

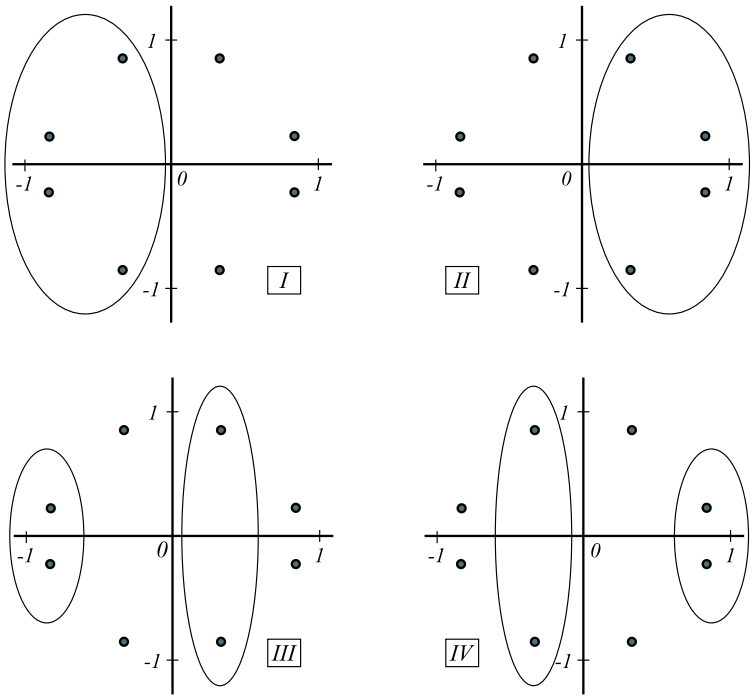

Fig. 7.7 Possible sets of zeros of $\rho(s)$

The eight zeros of $\rho(s)\rho(-s)$ can be determined by solving the binomial equation $s^8 + 0.888889$ for s to find:

$$\begin{array}{ll} -0.927002 + j0.383976 & -0.927002 - j0.383976 \\ -0.383976 + j0.927002 & -0.383976 - j0.927002 \\ +0.927002 + j0.383976 & +0.927002 - j0.383976 \\ +0.383976 + j0.927002 & +0.383976 - j0.927002 \end{array}$$

Since there are no restrictions as to the location of the zeros of $\rho(s)$, and $\rho(s)$ and $\rho(-s)$ have opposite roots, we can have the four sets of $\rho(s)$ zeros, shown in Fig. 7.7. Each of the four selections leads to a different expression for the $\rho(s)$ function.

Selecting the zeros of $\rho(s)$ to be that of set I of Fig. 7.7, i.e.

$$\begin{array}{ll} -0.927002 + j0.383976 & -0.927002 - j0.383976 \\ -0.383976 + j0.927002 & -0.383976 - j0.927002 \end{array}$$

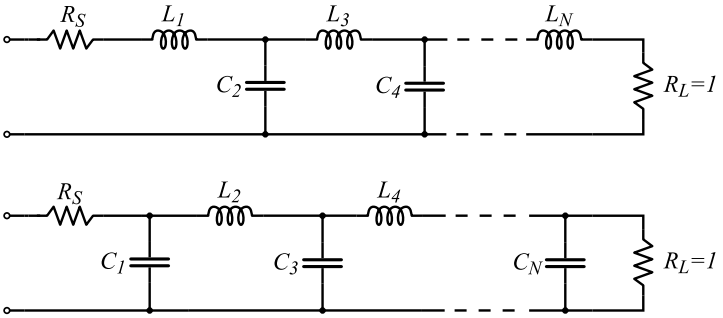

Fig. 7.8 Typical ladder filter structures

after some manipulations we find

$$\rho_I(s) = \frac{s^4 + 2.6219527s^3 + 3.43731798s^2 + 2.6396957963s + 1.0135800}{s^4 + 3.4506838s^3 + 5.95360948s^2 + 6.0172053177s + 3.040740}$$

Selecting set IV of zeros, i.e.

$$-0.383976 + j0.927002 \qquad -0.383976 - j0.927002$$
$$+0.927002 + j0.383976 \qquad +0.927002 - j0.383976$$

we find

$$\rho_{IV}(s) = \frac{s^4 - 1.08604838s^3 + 0.58975054s^2 - 1.09339781s + 1.0135800}{s^4 + 3.4506838s^3 + 5.95360948s^2 + 6.0172053177s + 3.040740}$$

For sets II and III, two more functions $\rho(s)$ can be determined.

(d) Using (7.4) with set of $\rho(s)$ zeros I, we find:

$$Z_{1I}(s) = \frac{s^4 + 3.036318s^3 + 4.6954637s^2 + 4.328450557s + 2.02716014}{0.82873114s^3 + 2.5162915s^2 + 3.3775095s + 2.02716014} \tag{7.16}$$

According to Sect. 6.4.1, the input driving point impedance $Z_1(s)$ of the terminated with R_L two-port, as determined from (7.3) or (7.4), is a positive real function (see Chap. 11) of order N and therefore it can be synthesized as a ladder circuit using sequential removals of poles at infinity. Moreover, in all-pole approximations of order N, the so-derived ladder circuit is *canonical* in the sense that it contains N lossless elements, with inductors in the series and capacitors in the shunt arms of the ladder, as shown in Fig. 7.8. As for the type of the first arm, it will be a series inductor when (7.3) is used. When (7.4) is used, the first arm of the ladder will be a shunt capacitor. As an example, when Z_{1I} of (7.16) is synthesized using sequential removals of poles at infinity, it leads to the filter shown in Fig. 7.9.

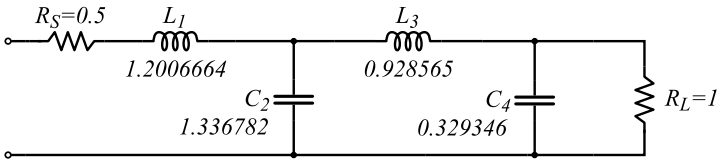

Fig. 7.9 Filter derived from $Z_{1I}(s)$ of (7.16) using ladder synthesis

The synthesis of passive lowpass Butterworth filters, i.e. passive lowpass filters with maximally flat Butterworth magnitude response, will be demonstrated with two detailed examples.

Example 7.3 Design a 3rd order prototype passive lowpass Butterworth filter with equal terminations $R_S = R_L = 1$.

Prototype filters have $A_{\max} = 3$ dB $\Rightarrow$ $\beta_{\max} = 1$. This maximum value of β will be used, i.e. $\beta = \beta_{\max} = 1$. Function $\rho(s)\rho(-s)$ is determined from (7.15):

$$\rho(s)\rho(-s) = 1 - \frac{4R_S}{R_L}|H(j\Omega)|^2_{\Omega^2=-s^2} = \frac{1+\beta^2(-s^2)^3 - \frac{4R_SR_L}{(R_S+R_L)^2}}{1+\beta^2(-s^2)^3}$$

$$\Rightarrow \quad \rho(s)\rho(-s) = \frac{-s^6}{1-s^6} = \frac{-s^6}{(1+s)(1-s)(s^2+s+1)(s^2-s+1)}$$

The poles of $\rho(s)\rho(-s)$ are:

$$s = \pm 1, \qquad s = -\frac{1}{2} \pm j\frac{\sqrt{3}}{2} \quad \text{and} \quad s = \frac{1}{2} \pm j\frac{\sqrt{3}}{2}$$

Since the reflection coefficient function $\rho(s)$ must have all its poles in the left half s-plane, we get:

$$\rho(s) = \frac{s^3}{(s+1)(s^2+s+1)} = \frac{s^3}{s^3+2s^2+2s+1}$$

with poles $s = -1$ and $s = -\frac{1}{2} \pm j\frac{\sqrt{3}}{2}$.

Input impedance $Z_1(s)$ can be determined from any of (7.3) or (7.4)

$$Z_{1A}(s) = R_S\frac{1-\rho(s)}{1+\rho(s)} \quad \text{or} \quad Z_{1B}(s) = R_S\frac{1+\rho(s)}{1-\rho(s)}$$

to find

$$Z_{1A}(s) = \frac{2s^2+2s+1}{2s^3+2s^2+2s+1} \quad \text{or} \quad Z_{1B}(s) = \frac{2s^3+2s^2+2s+1}{2s^2+2s+1}$$

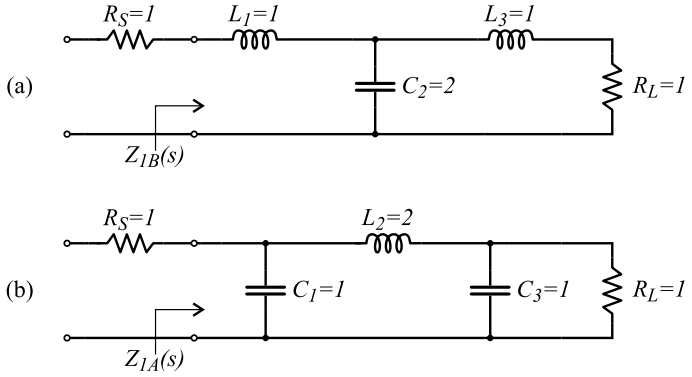

Fig. 7.10 Filter synthesized (**a**) from Z_{1B} (**b**) from $Y_{1A}(s) = Z_{1A}^{-1}(s)$

Z_{1B} has a pole at infinity since the degree of the numerator polynomial is higher than the degree of the denominator polynomial. This is also true for

$$Y_{1A}(s) = \frac{1}{Z_{1A}(s)} = \frac{2s^3 + 2s^2 + 2s + 1}{2s^2 + 2s + 1}$$

and therefore synthesis can start by removing this pole at infinity.

Removing the pole at infinity from $Z_{1B}(s)$ as a series inductor with $L_1 = 1$, the remaining impedance $Z_{2B} = Z_{1B} - s = \frac{s+1}{2s^2+2s+1}$ has no pole at infinity. However $Y_{2B} = \frac{2s^2+2s+1}{s+1}$ has as pole at infinity which can be removed as a shunt capacitor $C_2 = 2$ and the remaining admittance will be $Y_{3B} = Y_{2B} - 2s = \frac{1}{s+1} \Rightarrow Z_{3B} = s+1$. This is a series arm inductor with $L_3 = 1$ in series with a resistor with $R_L = 1$. The final circuit is shown in Fig. 7.10a.

Removing the pole at infinity from $Y_{1A}(s)$ as a shunt inductor with $C_1 = 1$, the remaining impedance $Y_{2A} = Y_{1A} - s = \frac{s+1}{2s^2+2s+1}$ has no pole at infinity. However $Z_{2A} = \frac{2s^2+2s+1}{s+1}$ has a pole at infinity which can be removed as a series inductor with $L_2 = 2$ and the remaining impedance will be $Z_{3A} = Z_{2A} - 2s = \frac{1}{s+1} \Rightarrow Y_{3A} = s+1$. This is a shunt arm capacitor with $C_3 = 1$ in parallel with a resistor with $R_L = 1$. The final circuit is shown in Fig. 7.10b.

Prototype filters have $A(1) = 3$ dB and if a different value is required, e.g. $A(1) = 0.5$, all inductor and capacitor values must be divided by

$$\Omega_{3dB} = \beta^{-\frac{1}{N}} = \frac{1}{(10^{\frac{0.5}{10}} - 1)^{\frac{1}{2N}}} = \frac{1}{(10^{\frac{0.5}{10}} - 1)^{\frac{1}{2\cdot 3}}} = \frac{1}{0.122018^{\frac{1}{6}}} = 1.41992$$

If $A(1) = 0.5$ dB is required for the filter of Fig. 7.10b, the lossless element values must be changed to $C_{1a} = C_{3a} = 1/1.41992$ and $L_{2a} = 2/1.41992$.

In order to denormalize the filter for $R_L = R_S = 1$ kOhm and $\omega_C = 2\pi \times 5000$ rad/s, the element values must be denormalized according to (1.29):

$$R_S = R_L = 1 \text{ kOhm} \qquad C_1 = C_3 = \frac{C_{1a}}{2\pi \cdot 5000 \cdot 1000} = 22.43 \text{ nF}$$

$$L_2 = \frac{1000 \cdot L_{2a}}{2\pi \cdot 5000} = 44.86 \text{ mH}$$

Example 7.4 Design a passive lowpass filter with Butterworth response with the following specifications:

$$R_S = 600 \text{ Ohm} \qquad R_L = 1200 \text{ Ohm} \qquad A_{\max} = 0.35 \text{ dB} \qquad A_{\min} = 30 \text{ dB}$$

$$f_C = 2.0 \text{ kHz} \qquad f_S = 6.5 \text{ kHz}$$

It is evident that $\omega_C = 2\pi 2000$ and $\omega_S = 2\pi 6500$ rad/s and that the normalized specifications will be

$$R_S = 0.5 \qquad R_L = 1 \qquad A_{\max} = 0.35 \text{ dB} \qquad A_{\min} = 30 \text{ dB}$$

$$\Omega_C = 1.0 \qquad \Omega_S = 3.25$$

The normalized filter will be designed initially. Equation (7.10) gives the decimal order

$$N_d = \frac{\log(\frac{10^{30/10}-1}{10^{0.35/10}-1})}{2\log(3.25)} = 3.98$$

and therefore $N = 4$.

The design parameter β can be taken equal to its maximum value $\beta = \beta_{\max} = \sqrt{10^{0.35/10} - 1} = 0.289701$ and from (7.15) we get

$$\rho(s)\rho(-s) = \frac{1 + \beta^2(-s^2)^N - 4R_S R_L/(R_S + R_L)^2}{1 + \beta^2(-s^2)^N} = \frac{s^8 + 1.323903}{s^8 + 11.915129}$$

Since the denominator polynomial of $\rho(s)\rho(-s)$ is a binomial of order 8, it has 8 poles grouped in four conjugate pole pairs, each of which corresponds to a second order denominator term as shown below:

	Poles of $\rho(s)\rho(-s)$	Denominator term
Poles $\rho(s)$	$-1.259296 + j0.521617$ $-1.259296 - j0.521617$	$s^2 + 2.518591s + 1.857910$
	$-0.521617 + j1.259296$ $-0.521617 - j1.259296$	$s^2 + 1.043235s + 1.857910$
Poles $\rho(-s)$	$+1.259296 - j0.521617$ $+1.259296 + j0.521617$	$s^2 - 2.518591s + 1.857910$
	$+0.521617 - j1.259296$ $+0.521617 + j1.259296$	$s^2 - 1.043235s + 1.857910$

The left hand half s-plane poles of $\rho(s)\rho(-s)$ are allocated to $\rho(s)$.

The 8 zeros of $\rho(s)\rho(-s)$ are also grouped in 4 conjugate zero pairs as shown below.

	Zeros of $\rho(s)\rho(-s)$	Numerator term
I	$-0.956858 + j0.396343$ $-0.956858 - j0.396343$	$s^2 + 1.913716s + 1.072665$
II	$-0.396343 + j0.956858$ $-0.396343 - j0.956858$	$s^2 + 0.792687s + 1.072665$
$-I$	$+0.956858 - j0.396343$ $+0.956858 + j0.396343$	$s^2 - 1.913716s + 1.072665$
$-II$	$+0.396343 - j0.956858$ $+0.396343 + j0.956858$	$s^2 - 0.792687s + 1.072665$

Since there are no restrictions as to the location of the zeros of the reflection coefficient function, the following combinations of zeros can be allocated to $\rho(s)$:

$$\{I, II\} \qquad \{-I, -II\} \qquad \{II, -I\} \qquad \{I, -II\}$$

each leading to a different function $\rho(s)$:

$$\rho_1(s) = \frac{(s^2 + 0.79268690s + 1.07266485)(s^2 + 1.91371547s + 1.07266485)}{(s^2 + 1.04323460s + 1.85791004)(s^2 + 2.51859120s + 1.85791004)}$$

$$\rho_2(s) = \frac{(s^2 - 0.79268690s + 1.07266485)(s^2 - 1.91371547s + 1.07266485)}{(s^2 + 1.04323460s + 1.85791004)(s^2 + 2.51859120s + 1.85791004)}$$

$$\rho_3(s) = \frac{(s^2 + 0.79268690s + 1.07266485)(s^2 - 1.91371547s + 1.07266485)}{(s^2 + 1.04323460s + 1.85791004)(s^2 + 2.51859120s + 1.85791004)}$$

$$\rho_4(s) = \frac{(s^2 - 0.79268690s + 1.07266485)(s^2 + 1.91371547s + 1.07266485)}{(s^2 + 1.04323460s + 1.85791004)(s^2 + 2.51859120s + 1.85791004)}$$

For the determination of $Z_1(s)$, (7.4)

$$Z_{1b}(s) = R_S \frac{1 + \rho(s)}{1 - \rho(s)}$$

will be used to lead to four different expressions, one for each expression of $\rho(s)$:

$$Z_{11b}(s) = \frac{s^4 + 3.134119s^3 + 5.002818s^2 + 4.760324s + 2.30123}{0.855414s^3 + 2.680969s^2 + 3.714461s + 2.30123}$$

$$Z_{12b}(s) = \frac{s^4 + 0.427707s^3 + 5.002818s^2 + 1.857231s + 2.30123}{6.268238s^3 + 2.680969s^2 + 9.520648s + 2.30123}$$

$$Z_{13b}(s) = \frac{s^4 + 1.220397s^3 + 3.485829s^2 + 2.707527s + 2.30123}{4.682858s^3 + 5.714946s^2 + 7.820055s + 2.30123}$$

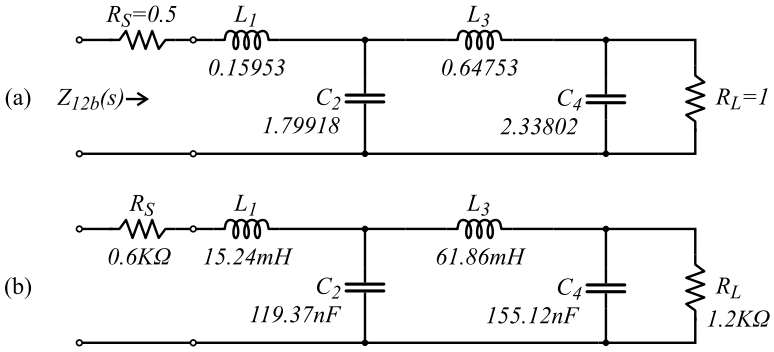

Fig. 7.11 Filter of Example 7.4 synthesized from $Z_{12b}(s)$: (**a**) Normalized. (**b**) Denormalized

$$Z_{14b}(s) = \frac{s^4 + 2.341429s^3 + 3.485829s^2 + 3.910027s + 2.30123}{2.440794s^3 + 5.714946s^2 + 5.415055s + 2.30123}$$

It should be noted that since (7.4) was used, all four expressions $Z_{1kb}(s)$ have a pole at infinity. Moreover, for all above input impedances $Z_{1kb}(s)$ we have $Z_{1kb}(0) = R_L = 1$. This is expected since at zero frequency (DC) the LC two-port inserted between R_S and R_L becomes transparent and the input impedance is equal to the load resistance $R_L = 1$. If (7.3) had been used, all expressions of $Z_{1ka}(s)$ would have $Z_{1ka}(0) = R_S^2 = 0.25 \neq R_L = 1$.

Selecting one of the above impedances, e.g. $Z_{12b}(s)$, it can be synthesized by sequential removal of poles at infinity to yield the normalized filter of Fig. 7.11a. Denormalizing for $R_L = 1.2$ kOhm and $\omega_C = 2\pi 2000$ rad/s, we get:

$$R_S = 0.5 \cdot 1200 = 0.6 \text{ kOhm} \qquad R_L = 1.0 \cdot 1200 = 1.2 \text{ kOhm}$$

$$L_1 = \frac{0.15953 \cdot 1200}{2 \cdot \pi \cdot 2000} = 15.24 \text{ mH} \qquad C_2 = \frac{1.79918}{2 \cdot \pi \cdot 2000 \cdot 1200} = 119.37\text{nF}$$

$$L_3 = \frac{0.64753 \cdot 1200}{2 \cdot \pi \cdot 2000} = 61.86 \text{ mH} \qquad C_4 = \frac{2.33802}{2 \cdot \pi \cdot 2000 \cdot 1200} = 155.12 \text{ nF}$$

The denormalized filter is shown in Fig. 7.11b. The plot of the attenuation response is shown in Fig. 7.12

The synthesis of the input driving-point function reveals the filter structure and the element values. In Butterworth normalized lowpass filter design and only in the special case of equal terminations $R_S = R_L$, it can be shown that the values T_k of the N normalized lossless elements are given by

$$T_k = 2\beta^{\frac{1}{N}} \sin\left(\frac{2k-1}{2N}\pi\right) \quad k = 1, 2, \ldots, N \tag{7.17}$$

There is no similar simple formula for the case of unequal terminations, where the element values can be determined using one of the following methods:

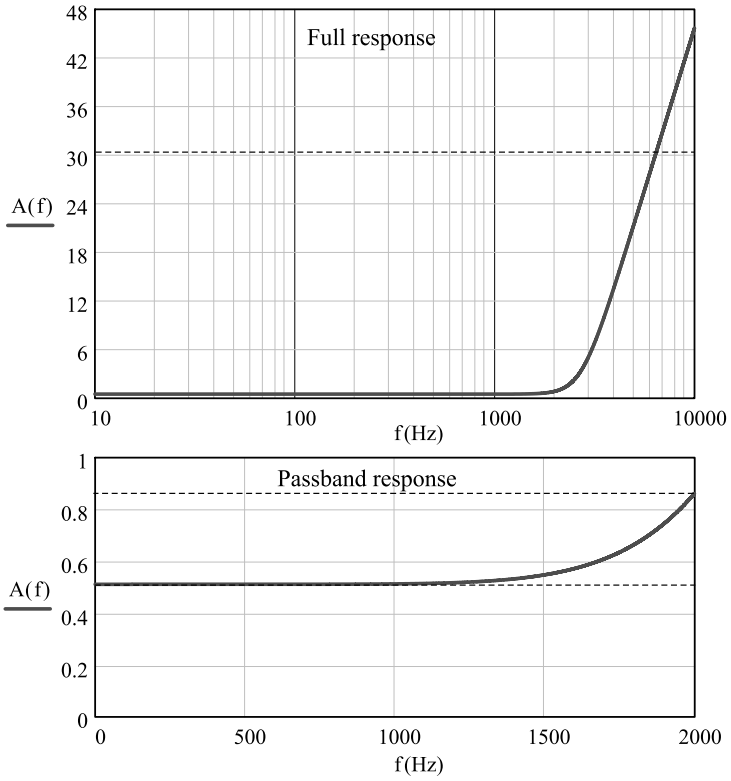

Fig. 7.12 Attenuation response of the filter of Example 7.4

1. By synthesis, as has been presented in this section, i.e. by determining $\rho(s)$ and then $Z_1(s)$, which is finally synthesized as an RLC one-port circuit.
2. By analysis of the ladder structure which is known once the order N has been determined from the specifications (N lossless elements with inductors in the series arms and capacitors in the shunt arms). When the transfer function has been determined by analysis, it can be made equal to the corresponding Butterworth attenuation function of (7.7) and solve the system of equations which emerges from coefficient matching. This method is practical for low order filters and will be demonstrated in the next section.
3. By using Butterworth filter design tables and nomographs.

7.2.1 Butterworth Filter Design by Analysis

The order N of a lowpass Butterworth filter and the design parameter β can be determined directly from the specifications. An alternative method to find the values of the circuit elements and avoid synthesis is to use the conclusions of synthesis, i.e. that the filter is an LC ladder with N reactive arms, with inductors in the series and

capacitors in the shunt arms. The first arm may be a series or a shunt arm and the LC ladder is terminated by the load resistor $R_L = 1$.

The transfer function $H(s)$ of the circuit can then be determined using any analysis method and therefore, the effective attenuation will be

$$A_{circ}(\Omega) = 20\log\left(\frac{1}{2}\sqrt{\frac{R_L}{R_S}}\frac{1}{|H(j\Omega)|}\right) \tag{7.18}$$

which is a function of Ω and the coefficients depend on the values of the reactive elements. On the other hand, the Butterworth attenuation from (7.8) is

$$A(\Omega) = 20\log\left(\frac{R_S + R_L}{2\sqrt{R_S R_L}}\sqrt{1 + \beta^2\Omega^{2N}}\right) \quad (R_L = 1)$$

and the two expressions must be made identical, i.e.

$$\frac{R_L}{4R_S}\frac{1}{|H(j\Omega)|^2} \equiv \frac{(R_S + R_L)^2}{4R_S R_L}(1 + \beta^2\Omega^{2N}) \tag{7.19}$$

This can be done by matching the coefficients of the two polynomials which yields N equations. The method is demonstrated by two detailed examples.

Example 7.5 Design a passive lowpass filter with Butterworth response with the following specifications:

$$R_S = R_L = 600 \text{ Ohm} \qquad A_{\max} = 3 \text{ dB} \qquad \omega_C = 2\pi 5000 \text{ rad/s}$$
$$A_{\min} = 20 \text{ dB} \qquad \omega_S = 2\pi 16000 \text{ rad/s}$$

The normalized specifications are

$$R_S = R_L = 1 \qquad A_{\max} = 3 \text{ dB} \qquad \Omega_C = 1 \qquad A_{\min} = 20 \text{ dB} \qquad \Omega_S = 3.2$$

and the order is determined from (7.10): $N = 2$.

Parameter β is taken equal to $\beta_{\max} = 1$. Therefore, since we have $R_S = R_L$ the filter will be either the one shown in Fig. 7.13a starting with a series inductor or the one shown in Fig. 7.13b starting with a shunt capacitor.

Analyzing the filter of Fig. 7.13b, we find $H(s)$ and

$$|H(j\Omega)|^2 = \frac{1}{C_1^2 L_2^2\Omega^4 + ((C_1 + L_2)^2 - 4C_1L_2)\Omega^2 + 4}$$

and therefore (7.19) yields

$$\frac{1}{4}(C_1^2L_2^2\Omega^4 + ((C_1 + L_2)^2 - 4C_1L_2)\Omega^2 + 4) \equiv (1 + \beta^2\Omega^4)$$
$$\Rightarrow \quad \frac{1}{4}C_1^2L_2^2\Omega^4 + \frac{1}{4}(C_1 - L_2)^2\Omega^2 + 1 \equiv \Omega^4 + 1$$

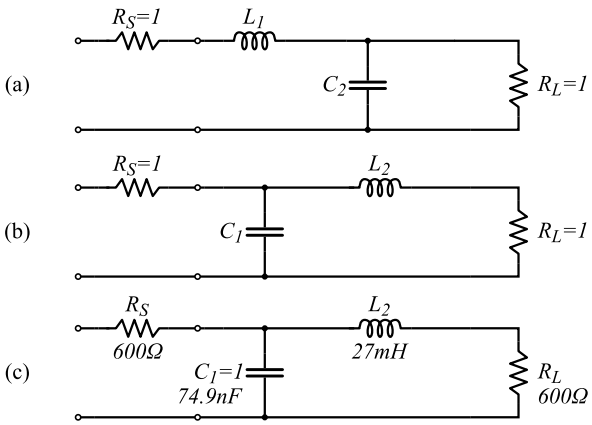

Fig. 7.13 Filter of Example 7.5: (**a**) Normalized starting with L. (**b**) Normalized starting with C. (**c**) Denormalized

In order for the left hand side polynomial to be identical to that of the right side, the following conditions must hold:

$$C_1 = L_2 \quad \text{and} \quad \frac{1}{4}C_1^2 L_2^2 = 1 \quad \Rightarrow \quad C_1 = L_2 = \sqrt{2}$$

Figure 7.13c shows the denormalized filter with

$$R_S = R_L = 1 \cdot 600 \text{ Ohm} \qquad L = \frac{600\sqrt{2}}{2\pi 5000} = 27 \text{ mH}$$

$$C = \frac{\sqrt{2}}{2\pi \cdot 5000 \cdot 600} = 74.9 \text{ nF}$$

and Fig. 7.14 the frequency response of both normalized and denormalized filters.

Example 7.6 Design a passive lowpass filter with Butterworth response with the following specifications:

$$R_S = R_L = 1.0 \text{ kOhm} \qquad A_{\max} = 0.5 \text{ dB} \qquad \omega_C = 2\pi 5000 \text{ rad/s}$$

$$A_{\min} = 25 \text{ dB} \qquad \omega_S = 2\pi 20000 \text{ rad/s}$$

The normalized specifications are

$$R_S = R_L = 1 \qquad A_{\max} = 0.5 \text{ dB} \qquad \Omega_C = 1 \qquad A_{\min} = 25 \text{ dB} \qquad \Omega_S = 4.0$$

and the order is determined from (7.10): $N = 3$. Parameter β is taken equal to $\beta_{\max} = 0.349311$. Therefore, the filter will be either the one shown in Fig. 7.15a starting with a series inductor or the one shown in Fig. 7.15b starting with a shunt capacitor.

Analyzing the filter of Fig. 7.15b, we find $H(s)$ and

$$|H(j\Omega)|^2 = \frac{1}{K_6\Omega^6 + K_4\Omega^4 + K_2\Omega^2 + 4}$$

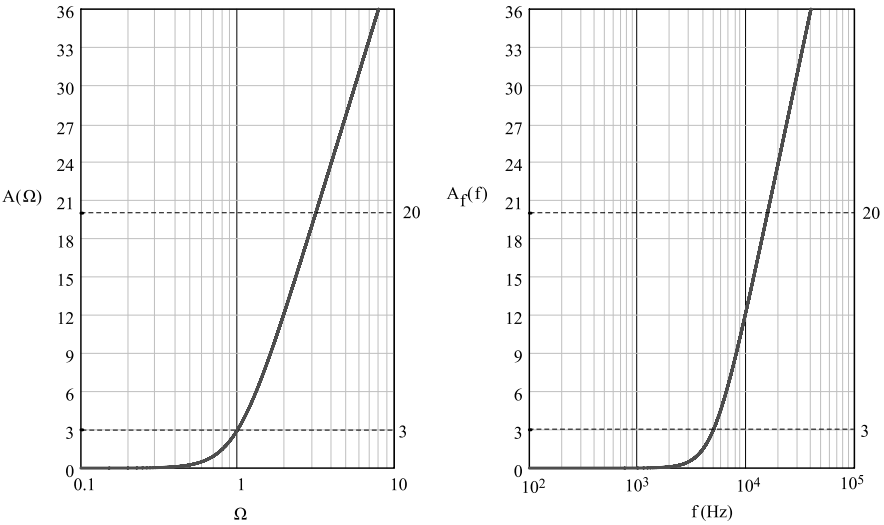

Fig. 7.14 Attenuation response of the filter of Example 7.5

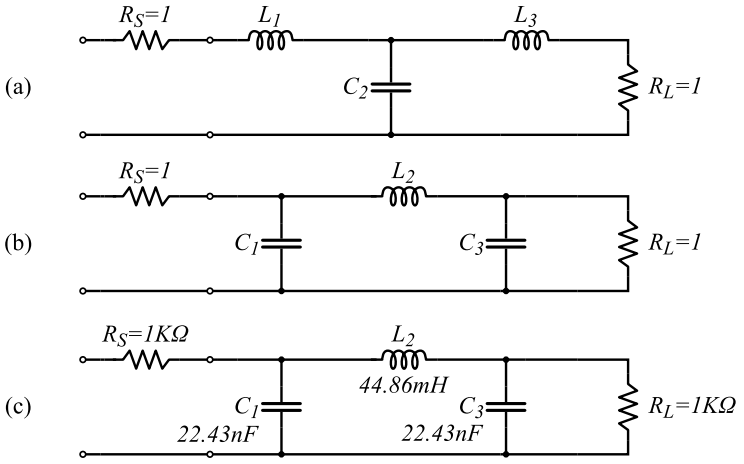

Fig. 7.15 Filter of Example 7.6: (**a**) Normalized starting with L. (**b**) Normalized starting with C. (**c**) Denormalized

where

$$K_6 = C_1^2 L_2^2 C_3^2$$

$$K_4 = L_2[L_2(C_1 + C_3)^2 - 2C_1C_3(C_1 + L_2 + C_3)] \quad \text{and}$$

$$K_2 = (C_1 + C_3 - L_2)^2$$

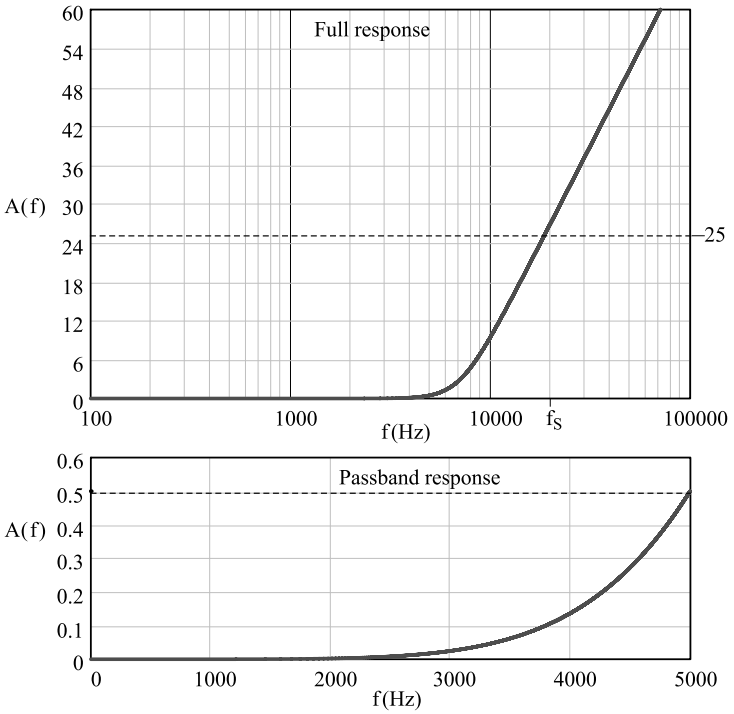

Fig. 7.16 Attenuation response of the filter of Example 7.6

and therefore (7.19) yields

$$\frac{1}{4}(K_6\Omega^6 + K_4\Omega^4 + K_2\Omega^2 + 4) \equiv (\beta^2\Omega^6 + 1)$$

In order for the left hand side polynomial to be identical to that of the right side, the following conditions must be met

$$C_1L_2C_3 = 2\beta \qquad L_2(C_1 + C_3)^2 = 2C_1C_3(C_1 + L_2 + C_3) \qquad C_1 - L_2 + C_3 = 0$$

Solving this system of equations for C_1, L_2 and C_3 we get

$$C_1 = C_3 = 0.7042674 \quad \text{and} \quad L_2 = 1.4085348$$

Figure 7.15c shows the denormalized filter with

$$R_S = R_L = 1 \cdot 1000 = 1.0 \text{ kOhm} \qquad L = \frac{1000 \cdot 1.4085348}{2\pi \cdot 5000} = 44.86 \text{ mH}$$

$$C_1 = C_3 = \frac{0.7042674}{2\pi \cdot 5000 \cdot 1000} = 74.9 \text{ nF}$$

and Fig. 7.16 the frequency response of the denormalized filter.

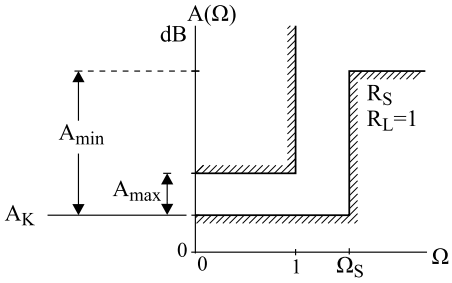

Fig. 7.17 Attenuation specifications of passive lowpass filters

It is evident that, as the order N increases, the analysis of the ladder circuit and the solution of the corresponding system of equations becomes more laborious than the determination of $Z_1(s)$ and its synthesis.

7.3 The Chebyshev Approximation in Passive Filter Design

Given the normalized specifications

$$\{A_{\max},\ A_{\min},\ \Omega_S,\ R_S\} \quad (\Omega_C = 1 \text{ and } R_L = 1)$$

of a passive lowpass filter, we are looking for an effective attenuation function $A(\Omega)$, the plot of which does not enter the shaded area of Fig. 7.17, where A_K is the minimum attenuation that is achieved by the filter. Attenuation $A(\Omega)$ is related to the magnitude of the transfer function of the filter to be designed by:

$$A(\Omega) = 20\log\left(\frac{1}{2}\sqrt{\frac{R_L}{R_S}}\frac{1}{|H(j\Omega)|}\right)$$

It must be remembered that our final goal is to determine the input driving-point impedance $Z_1(s)$ of Fig. 7.1 from the reflection coefficient expression $\rho(s)\rho(-s)$, which is directly related to the magnitude of the transfer function via (7.5):

$$\rho(s)\rho(-s) = 1 - \frac{4R_S}{R_L}|H(j\Omega)|^2_{\Omega^2=-s^2}$$

In passive filter design, the Chebyshev approximation is defined as

$$A(\Omega) = A_K + 20\log\left(\sqrt{1+\varepsilon^2 C_N^2(\Omega)}\right) \tag{7.20}$$

where
- ε is the ripple factor, a design parameter which depends on the specifications
- $C_N(\Omega)$ is the Chebyshev polynomial of order N:

$$C_N(\Omega) = \cos(N\cos^{-1}\Omega) \quad \text{or} \quad C_N(\Omega) = \cosh(N\cosh^{-1}\Omega)$$

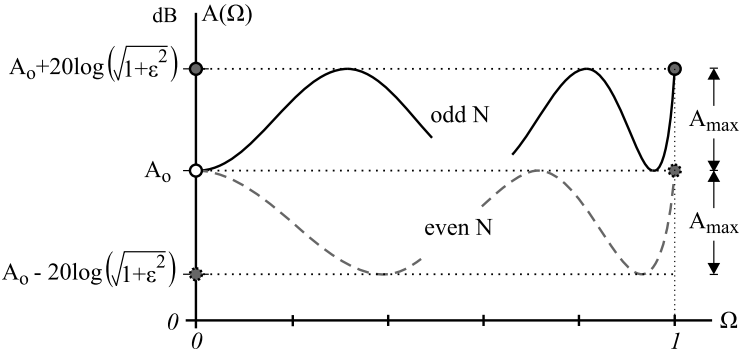

Fig. 7.18 Odd and even order passband ripple

– A_K, the minimum passband attenuation, is given by:

$$A_K = \begin{cases} A_o & \text{for } N \text{ odd} \\ A_o - 20\log\sqrt{1+\varepsilon^2} & \text{for } N \text{ even} \end{cases} \tag{7.21}$$

– A_o is the attenuation before the filter is inserted between source and load (see (6.29)) and is given by

$$A_o = 20\log\left(\frac{R_S + R_L}{2\sqrt{R_L R_S}}\right)$$

From the properties of the Chebyshev polynomial, we have

$$C_N^2(0) = \begin{cases} 0 & \text{for } N \text{ odd} \\ 1 & \text{for } N \text{ even} \end{cases} \quad \text{and} \quad C_N^2(1) = 1 \quad \text{for even and odd } N$$

and therefore:

$$A(0) = A_o \quad \text{for all } N \quad \text{and} \quad A(1) = \begin{cases} A_o & \text{for } N \text{ even} \\ A_o + 20\log\sqrt{1+\varepsilon^2} & \text{for } N \text{ odd} \end{cases}$$

Since for $0 \le \Omega \le 1$ the Chebyshev polynomial $C_N(\Omega)$ assumes values between 0 and 1, attenuation $A(\Omega)$ assumes values from A_o to $A_o + \sqrt{1+\varepsilon^2}$ when N is odd. When N is even, the Chebyshev attenuation varies from A_o to $A_o - \sqrt{1+\varepsilon^2}$ in the same frequency range $0 \le \Omega \le 1$. Figure 7.18 shows the plot of $A(\Omega)$ in the passband for an even and an odd N. It should be noted that at $\Omega = 0$ there exists an extremum and that there are exactly N attenuation extrema in the passband.

Due to the ability of the Chebyshev attenuation to assume values lower than A_o when N is even, plain gain specifications are related to effective parameters specifications as follows:

$$H_C = H_o \cdot 10^{-\frac{A_{\max}}{20}} \qquad H_S = H_o \cdot 10^{-\frac{A_{\min}}{20}}$$

$$\text{where } H_o = \begin{cases} \frac{R_L}{R_S+R_L} & \text{for } N \text{ odd} \\ \frac{R_L}{R_S+R_L} 10^{\frac{A_{\max}}{20}} & \text{for } N \text{ even} \end{cases} \tag{7.22}$$

From the above analysis, and in view of Fig. 7.18, it becomes evident that the term $20\log\sqrt{1+\varepsilon^2}$ can be at most equal to $A_{\max}$ and therefore the maximum value of the ripple factor ε is given by:

$$\varepsilon \leq \sqrt{10^{\frac{A_{\max}}{10}} - 1} = \varepsilon_{\max} \tag{7.23}$$

Combining (7.23) and (7.22), we also get

$$\varepsilon_{\max} = \sqrt{10^{\frac{A_{\max}}{10}} - 1} = \sqrt{\frac{H_o^2}{H_C^2} - 1}$$

which is the value determined in Sect. 2.3.2 of Chap. 2.

The Chebyshev attenuation function $A(\Omega)$ is monotonically increasing for $\Omega > 1$ and therefore the stopband specifications are met if

$$A(\Omega_S) \geq A_K + A_{\min} \quad \Longleftrightarrow \quad 20\log\sqrt{1+\varepsilon^2 C_N^2(\Omega_S)} \geq A_{\min}$$

from which we find for the integer order N of the approximation:

$$N \geq N_d = \frac{\cosh^{-1}\left(\sqrt{\frac{10^{\frac{A_{\min}}{10}}-1}{10^{\frac{A_{\max}}{10}}-1}}\right)}{\cosh^{-1}\Omega_S} \tag{7.24}$$

As should be expected, this is the same value found in Sect. 2.3.2 of Chap. 2. Integer order N is of course selected to be the lowest integer which satisfies $N \geq N_d$. As has been explained in Sect. 2.3.2, this leaves room for optimization and defines the lower boundary of the design parameter ε, which can be selected from the range

$$\frac{\sqrt{10^{\frac{A_{\min}}{10}} - 1}}{C_N(\Omega_s)} = \varepsilon_{\min} \leq \varepsilon \leq \varepsilon_{\max} = \sqrt{10^{\frac{A_{\max}}{10}} - 1} \tag{7.25}$$

For any value of the ripple factor ε within this range, a Chebyshev filter can be designed, the attenuation of which will satisfy the specifications in a slightly different manner. The details can be found in Sect. 2.3.2 of Chap. 2.

In order for the filter circuit to have Chebyshev attenuation, its corresponding attenuation function must be made equal to the attenuation of the Chebyshev approximation, i.e.

$$A(\Omega) = 20\log\left(\frac{1}{2}\sqrt{\frac{R_L}{R_S}}\frac{1}{|H(j\Omega)|}\right) = A_K + 20\log\left(\sqrt{1+\varepsilon^2 C_N^2(\Omega)}\right) \tag{7.26}$$

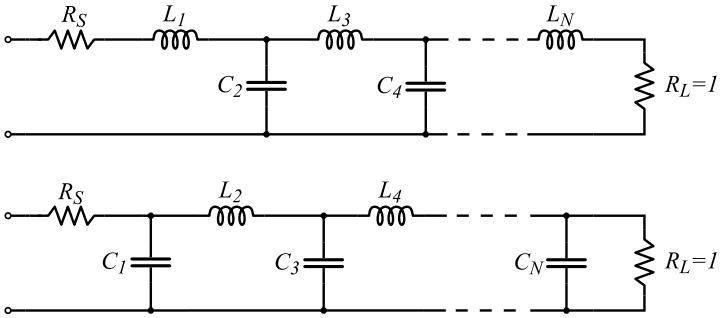

Fig. 7.19 Doubly resistively terminated LC ladder filters

from which we get

$$|H(j\Omega)|^2 = \frac{H_{Cho}^2}{(1+\varepsilon^2 C_n^2(\Omega))}$$

$$\text{where } H_{Cho} = \frac{10^{-\frac{A_K}{20}}}{2}\sqrt{\frac{R_L}{R_S}} = \begin{cases} \frac{R_L}{R_S+R_L} & \text{when } N \text{ is odd} \\ \frac{R_L}{R_S+R_L}\sqrt{1+\varepsilon^2} & \text{when } N \text{ is even} \end{cases} \tag{7.27}$$

This expression of $|H(j\Omega)|$ can be used in (7.5) to determine the necessary function $\rho(s)\rho(-s)$:

$$\rho(s)\rho(-s) = 1 - \frac{4R_S}{R_L}|H(j\Omega)|^2_{\Omega^2=-s^2} = 1 - \frac{\frac{4R_S}{R_L}H_{Cho}^2}{1+\varepsilon^2[C_N^2(\Omega)]_{\Omega^2=-s^2}} \tag{7.28}$$

The transfer function $H(s)$ can also be determined from $H(s)H(-s) = |H(j\Omega)|^2_{\Omega^2=-s^2}$, as has been done in Sect. 2.3.2 of Chap. 2, to find

$$H(s) = \frac{H_{Cho}}{\varepsilon \cdot 2^{N-1} \cdot \prod_{k=1}^{N}(s-s_k)}$$

$$\text{where } s_k = \sigma_k + j\Omega_k \text{ for } k = 1, 2, \ldots, N \tag{7.29}$$

$$\sigma_k = \sin\left(\frac{(2N+2k-1)\pi}{2N}\right)\sinh\left[\frac{1}{N}\sinh^{-1}\left(\frac{1}{\varepsilon}\right)\right]$$

$$\Omega_k = \cos\left(\frac{(2N+2k-1)\pi}{2N}\right)\cosh\left[\frac{1}{N}\sinh^{-1}\left(\frac{1}{\varepsilon}\right)\right] \tag{7.30}$$

The Chebyshev transfer function is an all-pole function, similar to the Butterworth transfer function. The only difference is that the Butterworth poles lie on a circle and the Chebyshev poles on an ellipse. Therefore, it should not be a surprise that when the input driving-point impedance $Z_1(s)$ is determined from $\rho(s)\rho(-s)$ and synthesized, the resulting filter will have the ladder structure shown in Fig. 7.19.

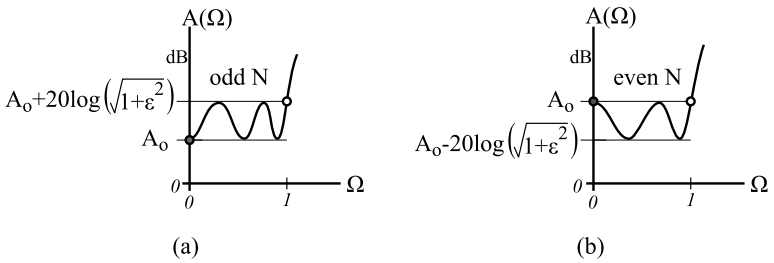

Fig. 7.20 Typical Chebyshev attenuation plots: (**a**) $N =$ odd. (**b**) $N =$ even

It is evident that due to this circuit topology, at $\Omega = 0$ (DC) the plain gain is $\frac{R_L}{R_S+R_L}$ since the reactive part of the circuit becomes transparent for odd and even N and therefore, the corresponding effective attenuation at $\Omega = 0$ is given by:

$$A(0) = 20\log\left(\frac{R_S + R_L}{2\sqrt{R_S R_L}}\right) = A_o$$

Figure 7.20 shows the Chebyshev attenuation plot for an odd and an even order, namely for $N = 5$ and $N = 4$.

The cutoff rate of the passive Chebyshev filters is $6N$ dB/octave and the 3-dB frequency is given by

$$\Omega_{3dB} = \cosh\left(\frac{1}{N}\cosh^{-1}\left(\frac{1}{\varepsilon}\right)\right) \tag{7.31}$$

7.3.1 Even Order Passive Chebyshev Filters

Effective attenuation $A(\Omega)$, as defined in (7.2), assumes by definition only non–negative values since the average power P_2 dissipated on the load cannot exceed the maximum power $P_{\max}$ delivered by the source.

In odd order Chebyshev filters, where the attenuation is always above the non-negative value A_o (see Fig. 7.20a), there are no restrictions on the ripple tolerance $A_{\max}$ as opposed to even order Chebyshev filters, where some complications exist. When, for example, equal terminations $R_S = R_L$ are specified, then $A_o = 0$ and an even order Chebyshev filter cannot exist since its passband attenuation would be below $A_o = 0$, i.e. negative. This is better understood by reference to Fig. 7.20b or Fig. 7.18 with $A_o = 0$. The conclusion is that it is not possible to design an even order passive Chebyshev filter with equal terminations. In case equal terminations are specified and order N is determined to be even, it should be increased to the next odd order $N + 1$. Alternatively, instead of increasing the order, the modified Chebyshev filter can be designed using the modified Chebyshev approximation of the next Sect. 7.3.2.

When unequal terminations $R_S \neq R_L$ are specified, i.e. $A_o > 0$, and the order N is determined to be even, then, referring to Fig. 7.18 or Fig. 7.20b, it is clear that if the specified $A_{\max} \leq A_o$ then the filter can be directly designed with the determined even order N. If the filter must have exactly the specified passband ripple $A_{\max}$, this imposes a constraint on the value of R_S derived from $A_{\max} \leq A_o$ ($R_L = 1$ has been used):

$$A_{\max} \leq 20\log\left(\frac{R_S+1}{2\sqrt{R_S}}\right) \quad \Leftrightarrow \quad R_S^2 - 2\left(2\cdot 10^{\frac{A_{\max}}{10}} - 1\right)R_S + 1 \geq 0 \tag{7.32}$$

This is only possible if $R_S \geq R_{S2}$ or $R_S \leq R_{S1}$ where R_{S1} and R_{S1} are the roots of $R_S^2 - 2(2\cdot 10^{\frac{A_{\max}}{10}} - 1)R_S + 1 = 0$:

$$\begin{aligned} R_{S1} &= 2\cdot 10^{\frac{A_{\max}}{10}} - 1 - 2\sqrt{10^{\frac{A_{\max}}{10}}(10^{\frac{A_{\max}}{10}} - 1)} = R_{S2}^{-1} \\ R_{S2} &= 2\cdot 10^{\frac{A_{\max}}{10}} - 1 + 2\sqrt{10^{\frac{A_{\max}}{10}}(10^{\frac{A_{\max}}{10}} - 1)} = R_{S1}^{-1} \end{aligned} \tag{7.33}$$

It is clear that for $R_{S1} < R_S < R_{S2}$ we have $A_o < A_{\max}$.

Equation (7.32) implies that for each value of R_S there is a maximum ripple value $20\log(\frac{R_S+R_L}{2\sqrt{R_S R_L}})$, which can be realized by an even order passive Chebyshev filter and for each ripple value $A_{\max}$ there is a range $R_{S1} < R_S < R_{S2}$ for which it cannot be realized. Attenuation A_o has been plotted as a function of R_S in Fig. 7.21. From Fig. 7.21a, we can see that the ripple $A_{\max} = 0.5$ dB can only be achieved when $R_S \geq R_{S2} = 1.9841$ or $R_S \leq R_{S1} = 0.504$, as determined from (7.33). This is the reason why in Chebyshev filter tables [12] with ripple 0.5 dB, the R_S value starts from 1.9841 for all even orders. If $A_{\max} = 1$ is specified, then the filter can be directly designed only if $R_S \geq R_{S2} = 2.6597$ or $R_S \leq R_{S1} = 0.3760$, as determined from (7.33). This is shown in Fig. 7.21b, and in this case, if $R_S = 0.5$ is specified, the passive filter with ripple exactly $A_{\max} = 1$ dB cannot be directly designed with any even order N.

However, when for the specified R_S we have $R_{S1} < R_S < R_{S2}$, the filter can still be directly designed with lower ripple $A_o = 20\log(\frac{R_S+1}{2\sqrt{R_S}})$, determined by R_S, provided that the specified $A_{\min}$ is lower than the maximum $A_{\min}$ which can be satisfied by a filter of order N and $\{R_S, R_L = 1, \Omega_S\}$. This value can be determined from the order equation (7.24) by setting $A_{\max} = A_o$ to find:

$$A_{Smx} = 10\log\left(\frac{(R_S-1)^2}{4R_S}C^2(N,\Omega_S) + 1\right) \tag{7.34}$$

When $A_{\min} < A_{Smx}$, the filter can be designed with ripple $A_o \leq A_{\max}$ using

$$\varepsilon_o = \sqrt{10^{A_o/10} - 1} = \frac{|R_S - R_L|}{2\sqrt{R_S R_L}} \tag{7.35}$$

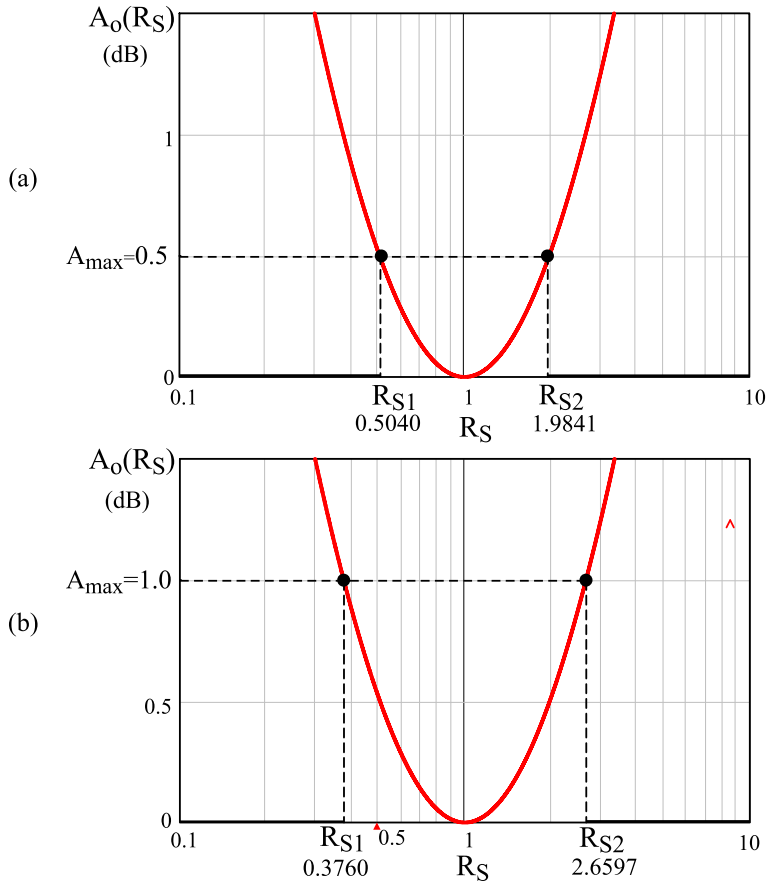

Fig. 7.21 A_o as a function of the normalized input termination R

or lower using any value from the range

$$\varepsilon_{\min} = \frac{\sqrt{10^{A_{\min}/10} - 1}}{C(N, \Omega_S)} \leq \varepsilon \leq \frac{|R_S - R_L|}{2\sqrt{R_S R_L}} = \varepsilon_o \tag{7.36}$$

provided that $\varepsilon_{\min} \leq \varepsilon_o$. Any value of ε from the above range leads to ripple less than the initially specified and the resulting filter meets stricter passband specifications. More specifically, selecting the value ε_o, the ripple will be from A_o to zero, and selecting $\varepsilon_{\min}$, the ripple will be even smaller, namely from A_o to $A_o - 20\log\sqrt{1+\varepsilon_{\min}^2}$. In both cases, the stopband specifications are met.

Example 7.7 Given the normalized specifications ($\Omega_C = 1$ and $R_L = 1$)

$$\{A_{\max} = 1,\ A_{\min} = 30,\ \Omega_S = 2.2,\ R_S = 0.5\}$$

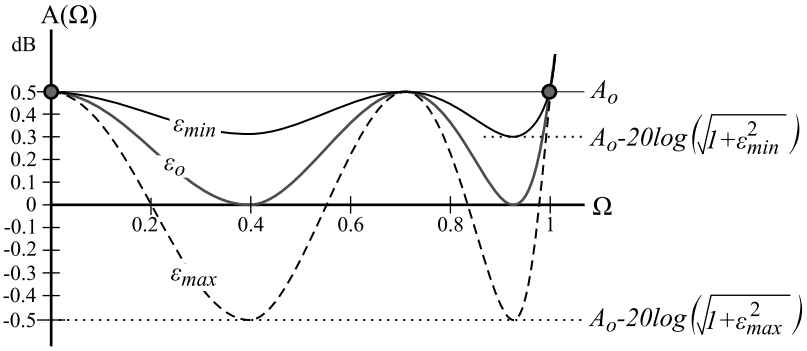

Fig. 7.22 The passband attenuation for the two boundary permitted values of the ripple factor

the order is found $N = 4$ and

$$A_o = 20\log\left(\frac{R_S + R_L}{2\sqrt{R_S R_L}}\right) = 20\log\left(\frac{0.5+1}{2\sqrt{0.5\cdot 1}}\right) = 0.511525 < A_{\max} = 1$$

If we want the passband ripple to be exactly the specified $A_{\max} = 1$ dB, then since $A_{\max} > A_o$, the even order $N = 4$ must be increased to $N = 5$. Alternatively, the modified Chebyshev filter (see next section) must be designed with $N = 4$. However, since

$$A_{Smx} = 10\log\left(\frac{(R_S - R_L)^2}{4R_S R_L}C_N^2(\Omega_S) + 1\right) = 10\log\left(\frac{(0.5-1)^2}{2}C_4^2(2.2) + 1\right)$$

$$= 34.4727$$

$$\Rightarrow \quad A_{\min} = 30 < A_{Smx} = 34.4727$$

these designs can be avoided if we accept lower passband ripple, i.e. stricter specifications, using

$$0.211157 = \varepsilon_{\min} \le \varepsilon \le \varepsilon_o = 0.353553$$

Figure 7.22 shows the passband attenuation for the two boundary permitted values of the ripple factor and for the obviously not permitted value $\varepsilon_{\max} = 0.508847$.

Example 7.8 Given the normalized specifications ($\Omega_C = 1$ and $R_L = 1$)

$$\{A_{\max} = 1,\ A_{\min} = 36,\ \Omega_S = 2.2,\ R_S = 0.5\}$$

the order is found again $N = 4$ and

$$A_o = 20\log\left(\frac{R_S + R_L}{2\sqrt{R_S R_L}}\right) = 20\log\left(\frac{0.5+1}{2\sqrt{0.5\cdot 1}}\right) = 0.511525 < A_{\max} = 1$$

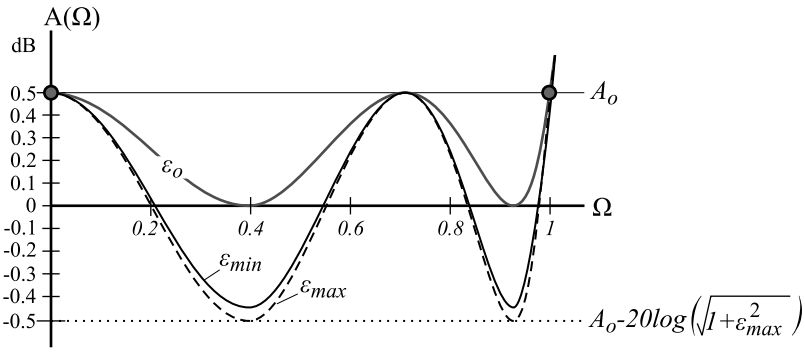

Fig. 7.23 Passband response for some characteristic values of the ripple factor

If we want the passband ripple to be exactly the specified $A_{\max} = 1$ dB, then since $A_{\max} > A_o$ the even order $N = 4$ must be increased to $N = 5$. Alternatively, the modified Chebyshev filter can be designed with $N = 4$.

For the stopband specifications $A_{\min} = 36$ dB of this example,

$$A_{Smx} = 10\log\left(\frac{(R_S - R_L)^2}{4R_S R_L}C_N^2(\Omega_S) + 1\right) = 10\log\left(\frac{(0.5-1)^2}{2}C_4^2(2.2) + 1\right)$$

$$\Rightarrow \quad A_{Smx} = 34.4727 < A_{\min} = 36 \text{ dB}$$

and the filter cannot be directly designed with lower passband ripple. This becomes obvious if we determine the boundary values of the ripple factor

$$\varepsilon_{\min} = 0.421471 \qquad \varepsilon_o = 0.353553$$

where $\varepsilon_{\min} > \varepsilon_o$. Figure 7.23 shows the passband attenuation of the filter with $N = 4$ for the characteristic values of ε. It is clear that for $\varepsilon = \varepsilon_{\min} = 0.421471$ and $\varepsilon = \varepsilon_{\max} = 0.508847$ the attenuation assumes negative values for certain frequencies and, therefore, these values of ε cannot be used. For $\varepsilon = \varepsilon_o$, the passband specifications are met but the stopband specifications are violated. As a consequence, the filter cannot satisfy the specifications with $N = 4$. In this case, the order must be increased to $N = 5$ or the modified Chebyshev filter must be designed according to the next section.

7.3.2 The Modified Chebyshev Approximation

As we have seen, the value $C_N(0) = C(N, 0)$ of the odd order Chebyshev polynomials $C_N(\Omega) = C(N, \Omega)$ at $\Omega = 0$ is equal to zero. When N is even, $C(N, 0) = \pm 1$ and this causes the design issue addressed in the previous section in even order passive filters with Chebyshev response. A solution to the problem is to modify the Chebyshev polynomial [9] in such a way as to have zero value at zero frequency

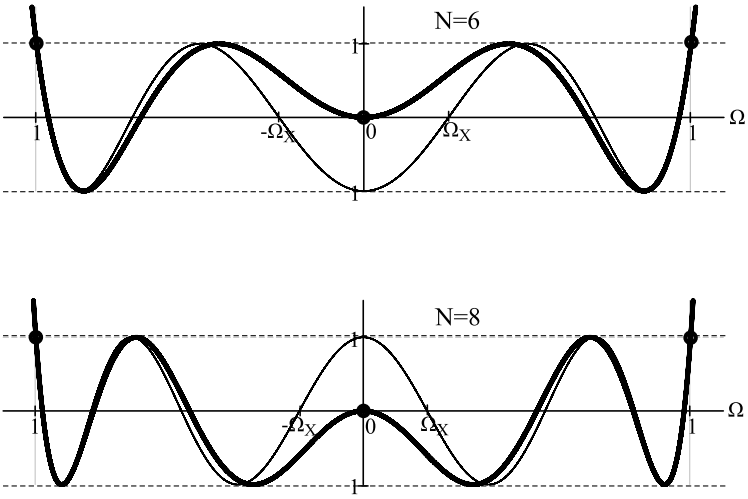

Fig. 7.24 The Chebyshev (*thin line*) and modified Chebyshev (*thick line*) polynomials for $N = 6$ and $N = 8$

while retaining the value 1 at $\Omega = 1$. Such a modification can be accomplished by replacing Ω with

$$\Omega_V = \sqrt{\Omega^2(1 - \Omega_x^2) + \Omega_x^2} \tag{7.37}$$

where Ω_x is the lowest root of $C(N, \Omega)$ given by

$$\Omega_x = \pm \cos\left(\frac{N-1}{2N}\pi\right) \tag{7.38}$$

This transformation moves the lower roots $\pm\Omega_x$ of the even order Chebyshev polynomial to zero. The modified Chebyshev polynomial is expressed as

$$C_m(N, \Omega) = C(N, \Omega_V) \tag{7.39}$$

with a double root at $\Omega = 0$, $(N-2)/2$ positive roots and $(N-2)/2$ negative roots. Two indicative plots of the modified Chebyshev polynomials are shown in Fig. 7.24 for $N = 6$ and $N = 8$.

The modified Chebyshev approximation is defined as

$$A(\Omega) = A_o + 20\log\sqrt{1 + \varepsilon^2 C_m^2(N, \Omega)} \tag{7.40}$$

and a typical attenuation plot is shown in Fig. 7.25 for $N = 6$. It should be noted that the attenuation curve has $N - 1$ passband extrema, one less than the extrema of the non-modified Chebyshev attenuation.

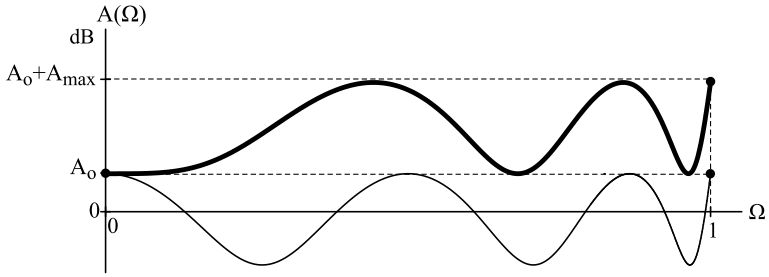

Fig. 7.25 The Chebyshev (*thin line*) and modified Chebyshev (*thick line*) attenuation plot for $N = 6$

The modified Chebyshev approximation can be used whenever an even order passive Chebyshev filter cannot be directly designed because the specified ripple $A_{\max}$ exceeds the value A_o imposed by the terminations. However, it can be shown that this is only possible if

$$g \geq \frac{1}{C_m(N, \Omega_S)} \quad \text{where } g = \sqrt{\frac{10^{\frac{A_{\max}}{10}} - 1}{10^{\frac{A_{\min}}{10}} - 1}} \tag{7.41}$$

This constraint, which is reported for the first time, is in fact the order inequality of the modified Chebyshev approximation and will be demonstrated in the next example.

Example 7.9 Given the normalized specifications of Example 7.7

$$\{A_{\max} = 1,\ A_{\min} = 30,\ \Omega_S = 2.2,\ R_S = 0.5\}$$

the order has been found $N = 4$ and

$$A_o = 0.511525 < A_{\max} = 1 \qquad \varepsilon_{\max} = \sqrt{10^{0.1 \cdot A_{\max}} - 1} = 0.508847$$

Moreover, the conclusion reached is that the filter can be designed with lower passband ripple satisfying stricter specifications. However, if the passband ripple must be exactly $A_{\max} = 1$ dB, either the even order $N = 4$ must be increased to $N = 5$ or the modified Chebyshev filter must be designed with $N = 4$ and $\varepsilon = \varepsilon_{\max} = 0.508847$ provided that condition (7.41) holds:

$$g = \sqrt{\frac{10^{\frac{A_{\max}}{10}} - 1}{10^{\frac{A_{\min}}{10}} - 1}} = \sqrt{\frac{10^{\frac{1.0}{10}} - 1}{10^{\frac{30}{10}} - 1}} = 0.016099$$

$$\Omega_x = \pm \cos\left(\frac{N-1}{2N}\pi\right) = 0.38268343$$

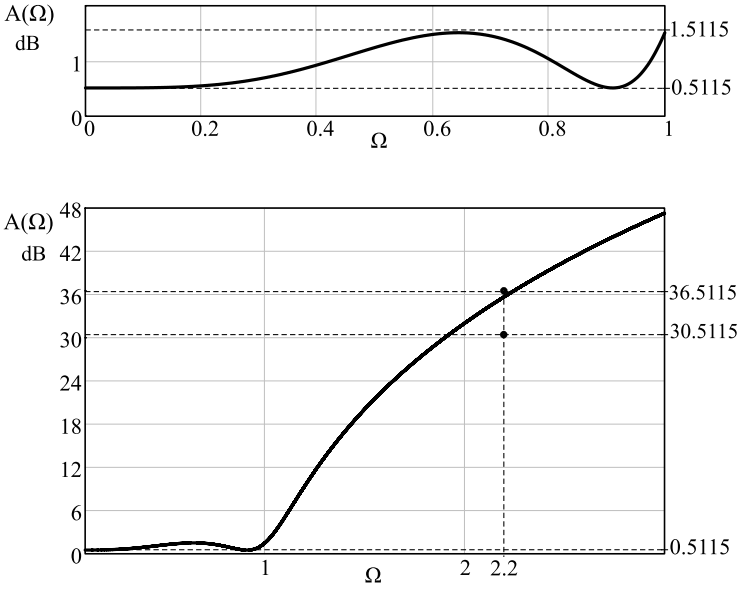

Fig. 7.26 Attenuation plots of Example 7.9

$$C_m(4, 2.2) = C(4, \sqrt{2.2^2(1 - 0.38268343^2) + 0.38268343^2} = 113.16481517$$

$$\Rightarrow \quad \frac{1}{C_m(4, 2.2)} = 0.00883667 < g = 0.016099$$

Since condition (7.41) holds, the modified Chebyshev attenuation will not violate the stopband specifications. The attenuation in this case will be

$$A(\Omega) = A_o + 20 \log \sqrt{1 + \varepsilon^2 C_m^2(N, \Omega)}$$

which varies from A_o to $A_o + A_{\max}$ as shown in Fig. 7.26. The attenuation at $\Omega_S = 2.2$ will be 35.2073 dB above $A_o = 0.5115$.

If $A_{\min} = 36$ dB had been specified, as in Example 7.8, then

$$g = \sqrt{\frac{10^{\frac{A_{\max}}{10}} - 1}{10^{\frac{A_{\min}}{10}} - 1}} = \sqrt{\frac{10^{\frac{1.0}{10}} - 1}{10^{\frac{36}{10}} - 1}} = 0.0080657$$

and $\frac{1}{C_m(4,2.2)} = 0.00883667 > g = 0.0080657$ which violates condition (7.41) and the modified Chebyshev attenuation cannot meet the stopband specifications. Indeed, in this case the attenuation at $\Omega_S = 2.2$ will be again 35.2073 dB above $A_o = 0.5115$, violating the specifications which require $A_{\min} = 36$ dB above $A_o = 0.5115$ and finally the only way to design a Chebyshev filter with the given specifications and $A_{\min} = 36$ dB is to increase the order to $N = 5$.

7.3.3 The Synthesis of Passive Chebyshev Filters

The goal of filter design is to determine the filter circuit structure and the values of all circuit elements. This can be done in various ways, the most general of which is synthesis. Given the normalized lowpass specifications, the order N of the Chebyshev approximation and the filter can be determined from (7.24), taking into account Sect. 7.3.1 if N turns out to be even. The value of the ripple factor ε can, in general, be selected from (7.25), although special attention must be paid when N is even.

Having N and ε, the reflection coefficient related function $\rho(s)\rho(-s)$ can be determined from (7.28):

$$\rho(s)\rho(-s) = 1 - \frac{4R_S}{R_L}|H(j\Omega)|^2_{\Omega^2=-s^2} = 1 - \frac{\frac{4R_S}{R_L}H^2_{Cho}}{1+\varepsilon^2[C^2_N(\Omega)]_{\Omega^2=-s^2}} \tag{7.42}$$

from which $\rho(s)$ can be separated, taking into account that $\rho(s)$ and $\rho(-s)$ have opposite poles and zeros and the poles of $\rho(s)$ are located in the left half s-plane. For each expression of $\rho(s)$, the input driving-point impedance of the terminated with $R_L = 1$ reactive two-port can be determined from (7.3) or (7.4), repeated here for convenience:

$$Z_{1a}(s) = R_S\frac{1-\rho(s)}{1+\rho(s)} \tag{7.43}$$

or

$$Z_{1b}(s) = R_S\frac{1+\rho(s)}{1-\rho(s)} \tag{7.44}$$

$Z_1(s)$ can finally be synthesized using sequential removals of poles at infinity to obtain a resistively terminated ladder LC circuit. The above outlined synthesis procedure is identical to the procedure used in Butterworth filter synthesis and will be demonstrated by several examples.

Example 7.10 Design a 2nd order normalized lowpass Chebyshev filter with

$$R_S = 0.5 \qquad R_L = 1 \qquad A_{\max} = 0.5\ \text{dB}$$

Attenuation A_o is initially calculated:

$$A_o = 20\log\left(\frac{R_S+R_L}{2\sqrt{R_SR_L}}\right) = 20\log\left(\frac{0.5+1}{2\sqrt{0.5\cdot 1}}\right) = 0.511525$$

Since the order $N = 2$ is even but $A_{\max} = 0.5 < A_o = 0.511525$, the value of the ripple factor ε can be selected from $\varepsilon_{\min} \le \varepsilon \le \varepsilon_{\max}$. We select $\varepsilon = \varepsilon_{\max}$:

$$\varepsilon^2 = \varepsilon^2_{\max} = 10^{\frac{0.5}{10}} - 1 = 0.12201845$$

From (7.29), we get

$$H_{Cho} = \frac{R_L}{R_S+R_L}\sqrt{1+\varepsilon^2} = \frac{1}{0.5+1}\sqrt{1+0.12201845} = 0.70616915$$

and since

$$C_2^2(\Omega) = (2\Omega^2 - 1)^2 = 4\Omega^4 - 4\Omega^2 + 1$$

we find

$$\begin{aligned}\rho(s)\rho(-s) &= 1 - \frac{\frac{4R_S}{R_L}H_{Cho}^2}{1 + \varepsilon^2[C_2^2(\Omega)]_{\Omega^2=-s^2}} \\ &= 1 - \frac{0.99734974}{1 + 0.12201845[4s^4 + 4s^2 + 1]} \\ \Rightarrow \quad \rho(s)\rho(-s) &= \frac{s^4 + s^2 + 0.25543}{s^4 + s^2 + 2.29887}\end{aligned}$$

The zeros of $\rho(s)\rho(-s)$ are

$$-0.051966 \pm j0.709014 \quad \text{and} \quad +0.051966 \pm j0.709014$$

and the poles

$$-0.712812 \pm j1.004042 \quad \text{and} \quad +0.712812 \pm j1.004042$$

Therefore, since the poles of $\rho(s)$ must be in the left half s-plane, poles $-0.712812 \pm j1.004042$ will be allocated to its denominator polynomial $D_\rho(s)$:

$$\begin{aligned}D_\rho(s) &= (s + 0.712812 - j1.004042)(s + 0.712812 + j1.004042) \\ \Rightarrow \quad D_\rho(s) &= s^2 + 1.425624s + 1.516201285\end{aligned}$$

Zeros $-0.051966 \pm j0.709014$ or $+0.051966 \pm j0.709014$ can be allocated to the numerator N_ρ of $\rho(s)$. Allocating the left half s-plane zeros to N_ρ, we get

$$\begin{aligned}N_\rho(s) &= (s + 0.051966 - j0.709014)(s + 0.051966 + j0.709014) \\ &= s^2 + 0.10393s + 0.50540\end{aligned}$$

and finally

$$\rho(s) = \frac{N_\rho(s)}{D_\rho(s)} = \frac{s^2 + 0.103931s + 0.50540126}{s^2 + 1.425624s + 1.516201285}$$

From (7.43) and (7.44) we find

$$Z_{1a}(s) = R_S\frac{1 - \rho(s)}{1 + \rho(s)} = \frac{2.6434s + 2.0216}{8s^2 + 6.1182s + 8.0864}$$

and

$$Z_{1b}(s) = R_S\frac{1 + \rho(s)}{1 - \rho(s)} = \frac{s^2 + 0.76481s + 1.0108}{1.32176s + 1.0108}$$

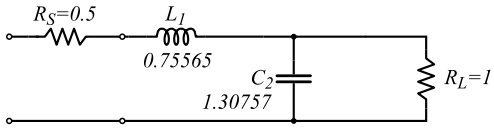

Fig. 7.27 Second order Chebyshev filter of Example 7.10

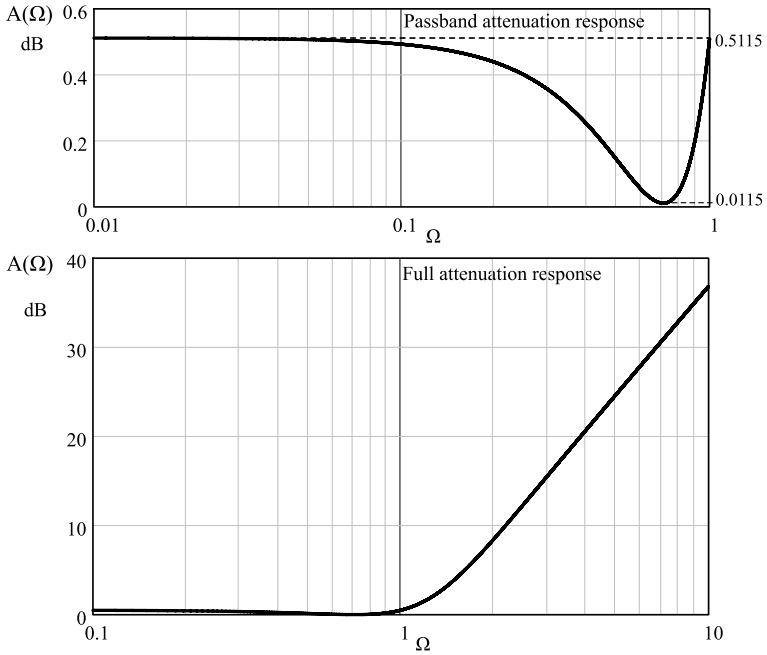

Fig. 7.28 Attenuation plots of the second order Chebyshev filter of Example 7.10

$Z_{1a}(s)$ has $Z_{1a}(0) = R_S^2 = 0.25$ and cannot be used. Synthesis of $Z_{1b}(s)$ (with $Z_{1b}(0) = R_L = 1$) yields the filter shown in Fig. 7.27, the attenuation plots of which are shown in Fig. 7.28

If the right half s-plane zeros of $\rho(s)\rho(-s)$ are allocated to $\rho(s)$, then:

$$\rho(s) = \frac{s^2 - 0.103931s + 0.50540126}{s^2 + 1.425624s + 1.516201285}$$

For this expression of $\rho(s)$, (7.43) and (7.44) give:

$$Z_{1a}(s) = \frac{0.3824s + 0.2527}{s^2 + 0.6608s + 1.0108} \qquad Z_{1b}(s) = \frac{s^2 + 0.6608s + 1.0108}{1.5296s + 1.0108}$$

Again, since $Z_{1b}(0) = R_L = 1$, synthesis of $Z_{1b}(s)$ is possible and leads to a ladder similar to that of Fig. 7.27 but with different element values.

Example 7.11 Design a normalized 3rd order lowpass Chebyshev filter with

$$R_L = 1.0 \qquad R_S = 2 \qquad A_{\max} = 0.5 \text{ dB}$$

Attenuation A_o is initially calculated:

$$A_o = 20\log\left(\frac{R_S + R_L}{2\sqrt{R_S R_L}}\right) = 20\log\left(\frac{2+1}{2\sqrt{2\cdot 1}}\right) = 0.511525 \text{ dB}$$

We will use $\varepsilon = \varepsilon_{\max}$, which is found to be $\varepsilon_{\max} = 0.349311 \Rightarrow \varepsilon^2 = 0.12201845$. For

$$H_{Cho} = \frac{R_L}{R_S + R_L} = \frac{1}{2+1} = 0.33333$$

and

$$C_3^2(\Omega) = (4\Omega^3 - 3\Omega)^2 = 16\Omega^6 - 24\Omega^4 + 9\Omega^2$$
$$\Rightarrow \quad [C_3^2(\Omega)]_{\Omega^2 - s^2} = -16s^6 - 24s^4 - 9s^2$$

we find from (7.42):

$$\rho(s)\rho(-s) = 1 - \frac{\frac{4R_S}{R_L}H_{Cho}^2}{1 + \varepsilon^2[C_n^2(\Omega)]_{\Omega^2 = -s^2}} = \frac{s^6 + 1.5s^4 + 0.5625s^2 - 0.056913}{s^6 + 1.5s^4 + 0.5625s^2 - 0.51222}$$

The zeros of $\rho(s)\rho(-s)$ are:

$$\pm 0.286670 \qquad -0.143340 \pm j0.90090 \qquad +0.143340 \pm j0.90090$$

The poles of $\rho(s)\rho(-s)$ are:

$$\pm 0.626457 \qquad -0.313228 \pm j1.02193 \qquad +0.313228 \pm j1.02193$$

The left half s-plane poles must be allocated to the denominator polynomial $D_\rho(s)$ of $\rho(s)$, which becomes:

$$D_\rho(s) = (s + 0.626457)(s + 0.313228 - j1.02193)(s + 0.313228 + j1.02193)$$
$$\Rightarrow \quad D_\rho(s) = (s + 0.626457)(s^2 + 0.626457s + 1.14245)$$

There are four possible combinations of zeros that can be allocated to $\rho(s)$. In this example, we allocate -0.28667 and $+0.14334 \pm j0.9009$ to the numerator polynomial $N_\rho(s)$ of $\rho(s)$ to obtain:

$$N_\rho(s) = (s + 0.28667)(s - 0.14334 - j0.9009)(s - 0.14334 + j0.9009)$$
$$\Rightarrow \quad N_\rho(s) = (s + 0.28667)(s^2 - 0.28667s + 0.83218)$$
$$= s^3 + 0.75s + 0.238565$$

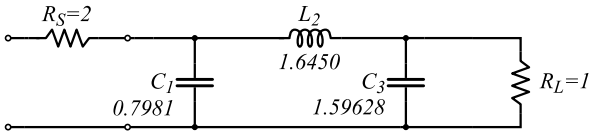

Fig. 7.29 The normalized lowpass with $N = 3$

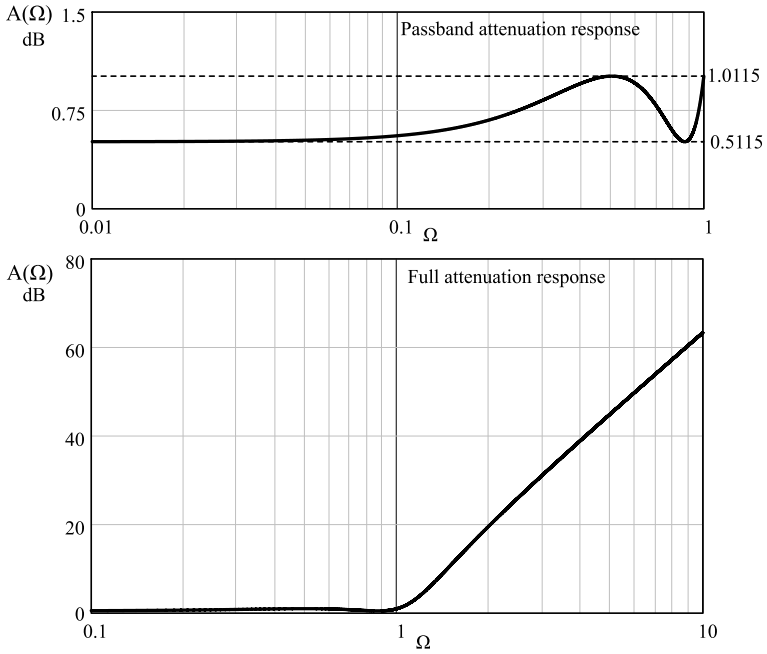

Fig. 7.30 Passband and full attenuation response of filter with $N = 3$

Finally, for this choice of numerator zeros we get:

$$\rho(s) = \frac{N_\rho(s)}{D_\rho(s)} = \frac{s^3 + 0.75s + 0.23856}{s^3 + 1.2529s^2 + 1.53489s + 0.71569}$$

From (7.43)–(7.44), we find

$$Z_{1a}(s) = R_S \frac{1 - \rho(s)}{1 + \rho(s)} = \frac{1.2529s^2 + 0.7849s + 0.47713}{s^3 + 0.62646s^2 + 1.14245s + 0.47713}$$

$$Z_{1b}(s) = R_S \frac{1 + \rho(s)}{1 - \rho(s)} = \frac{s^3 + 0.62646s^2 + 1.14245s + 0.47713}{0.3132s^2 + 0.1962s + 0.1193}$$

$Z_{1b}(s)$ is not useful since $Z_{1b}(0) = R_S^2 = 4$. The input admittance $Y_{1a}(s) = 1/Z_{1a}(s)$ with $Y_{1a}(0) = 1$ and a pole at infinity can be synthesized by sequential removals of such poles to derive the filter shown in Fig. 7.29. The attenuation plots of the filter are shown in Fig. 7.30.

Example 7.12 Design a passive lowpass filter with Chebyshev response from the following specifications

$$R_S = 600 \text{ Ohm} \qquad R_L = 1.5 \text{ kOhm} \qquad A_{\max} = 0.5 \text{ dB} \qquad A_{\min} = 36 \text{ dB}$$
$$f_C = 2.0 \text{ kHz} \qquad f_S = 4.6 \text{ kHz}$$

From the specifications, it is evident that

$$\omega_C = 2\pi 2000 \text{ rad/s} \qquad \omega_S = 2\pi 4600 \text{ rad/s}$$

The specifications of the normalized filter are $A_{\max} = 0.5$ dB, $A_{\min} = 36$ dB and

$$R_S = 0.4 \qquad R_L = 1 \qquad \Omega_C = 1 \qquad \Omega_S = 2.3$$

The decimal order $N_d = 3.9927$ is determined from (7.24) and the integer order is taken $N = 4$. According to Sect. 7.3.1, the realizability of the even order Chebyshev filter with unequal terminations depends initially on the relation of the specified $A_{\max}$ and A_o.

$$A_o = 20\log\left(\frac{R_S + R_L}{2\sqrt{R_S R_L}}\right) = 20\log\left(\frac{1.5+1}{2\sqrt{1.5 \cdot 1}}\right) = 0.88136 \text{ dB}$$

Since $A_{\max} = 0.5 < A_o = 0.88136$, the filter can be realized with $N = 4$ and the value of the ripple factor ε can be selected from the range $\varepsilon_{\min} \le \varepsilon \le \varepsilon_{\max}$. We select $\varepsilon = \varepsilon_{\max}$ and we find $\varepsilon_{\max} = \sqrt{10^{0.5/10} - 1} = 0.34931$ and $\varepsilon_{\max}^2 = 0.12201845$.

From (7.27), we find

$$H_{Cho} = \frac{R_L}{R_S + R_L}\sqrt{1+\varepsilon^2} = \frac{1}{0.4+1}\sqrt{1+0.12201845} = 0.75661$$

and for $C_4^2(\Omega)$, we have:

$$C_4^2(\Omega) = (8\Omega^4 - 8\Omega^2 + 1)^2 = 64\Omega^8 - 128\Omega^6 + 80\Omega^4 - 16\Omega^2 + 1$$
$$\Rightarrow \quad [C_4^2(\Omega)]_{\Omega^2 = -s^2} = 64s^8 + 128s^6 + 80s^4 + 16s^2 + 1$$

Equation (7.28) gives:

$$\rho(s)\rho(-s) = 1 - \frac{\frac{4R_S}{R_L} H_{Cho}^2}{1 + \varepsilon^2 [C_4^2(\Omega)]_{\Omega^2 = -s^2}} = \frac{s^8 + 2s^6 + 1.25s^4 + 0.25s^2 + 0.02639}{s^8 + 2s^6 + 1.25s^4 + 0.25s^2 + 0.14368}$$

The poles and zeros of $\rho(s)\rho(-s)$ are given below:

Poles of $\rho(s)\rho(-s)$	Zeros of $\rho(s)\rho(-s)$
$-0.42334 - j0.42095$	$-0.17564 - j0.38954$
$-0.42334 + j0.42095$	$-0.17564 + j0.38954$
$-0.17535 - j1.01625$	$-0.07275 - j0.94043$
$-0.17535 + j1.01625$	$-0.07275 + j0.94043$
$+0.17535 - j1.01625$	$+0.07275 - j0.94043$
$+0.17535 + j1.01625$	$+0.07275 + j0.94043$
$+0.42334 - j0.42095$	$+0.17564 - j0.38954$
$+0.42334 + j0.42095$	$+0.17564 + j0.38954$

Left half s-plane poles are allocated to $\rho(s)$ and their opposites, located in the right half s-plane, to $\rho(-s)$. After some manipulations, the corresponding denominator polynomial $D_\rho(s)$ of $\rho(s)$ is found:

$$D_\rho(s) = s^4 + 1.19738s^3 + 1.716858s^2 + 1.025449s + 0.379052217$$

For the zeros of $\rho(s)$, there are four possible choices:

$$\begin{aligned}
\text{I:} \quad & -0.17564 \pm j0.38954 \qquad -0.07275 \pm j0.94043 \\
\text{II:} \quad & +0.17564 \pm j0.38954 \qquad +0.07275 \pm j0.94043 \\
\text{III:} \quad & +0.17564 \pm j0.38954 \qquad -0.07275 \pm j0.94043 \\
\text{IV:} \quad & -0.17564 \pm j0.38954 \qquad +0.07275 \pm j0.94043
\end{aligned}$$

Using choice II, i.e. allocating the right half s-plane zeros to $\rho(s)$, the numerator polynomial $N_\rho(s)$ of $\rho(s)$ becomes

$$N_\rho(s) = s^4 - 0.49678s^3 + 1.12340321s^2 - 0.339101s + 0.16245126$$

and therefore, for this choice of numerator zeros:

$$\rho(s) = \frac{N_\rho(s)}{D_\rho(s)} = \frac{s^4 - 0.49678s^3 + 1.12340321s^2 - 0.339101s + 0.16245126}{s^4 + 1.19738s^3 + 1.716858s^2 + 1.025449s + 0.379052217}$$

The input impedance $Z_1(s)$ can now be determined from (7.4)

$$Z_{1b}(s) = R_S \frac{1 + \rho(s)}{1 - \rho(s)}$$

to get

$$Z_1(s) = \frac{0.8s^4 + 0.28024s^3 + 1.1361045s^2 + 0.2745391445s + 0.21660139}{1.69416s^3 + 0.5934548s^2 + 1.36455023s + 0.21660139}$$

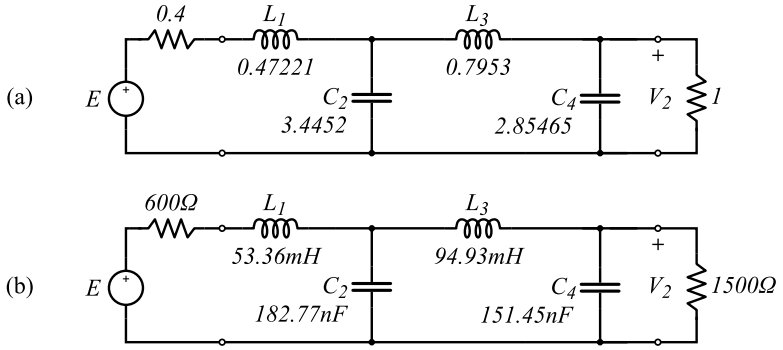

Fig. 7.31 Zeros combination II: (**a**) Normalized. (**b**) Denormalized

Since $Z_1(s)$ has pole at infinity, it can be removed as a series inductor $L_1 = \frac{0.8}{1.69416} = 0.4722104$, leaving the remaining impedance

$$Z_2(s) = Z_1(s) - sL_1 = \frac{0.49174965s^2 + 0.1722579s + 0.2166}{1.69416s^3 + 0.5934548s^2 + 1.36455s + 0.2166}$$

Admittance $Y_2(s) = 1/Z_2(s)$ will be used in order to continue removing poles at infinity:

$$Y_2(s) = \frac{1.69416s^3 + 0.5934548s^2 + 1.36455s + 0.2166}{0.49174965s^2 + 0.1722579s + 0.2166}$$

Removing a shunt capacitor $C_2 = \frac{1.69416}{0.49174965} = 3.4452$, the remaining admittance is

$$Y_3(s) = Y_2(s) - sC_2 = \frac{0.618322s + 0.2166}{0.4917496546s^2 + 0.1722579s + 0.2166}$$

and therefore:

$$Z_3(s) = \frac{0.4917496546s^2 + 0.1722579s + 0.2166}{0.618322s + 0.2166}$$

From $Z_3(s)$, a series inductor $L_3 = \frac{0.4917496546}{0.618322} = 0.7953$ can be removed to leave

$$Z_4(s) = Z_3(s) - sL_3 = \frac{0.2166}{0.618322s + 0.2166}$$

$$\Rightarrow \quad Y_4(s) = \frac{0.618322s + 0.2166}{0.2166} = 2.85465s + 1$$

This represents a shunt capacitor $C_4 = 2.85465$ in parallel with a resistor $R_L = 1$. The final normalized circuit is shown in Fig. 7.31a.

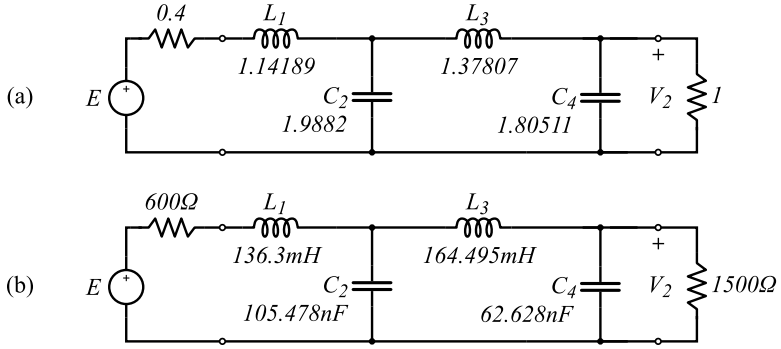

Fig. 7.32 Zeros combination I: (**a**) Normalized. (**b**) Denormalized

The normalized element values can now be denormalized using $\omega_C = 2\pi$ 2000 rad/s and $R_L = 1500$ Ohm to finally get the circuit shown in Fig. 7.31b with

$$L_1 = 56.36 \text{ mH} \qquad C_2 = 182.77 \text{ nF} \qquad L_3 = 94.93 \text{ mH} \qquad C_4 = 151.45 \text{ nF}$$

If choice I had been preferred for the zeros of $\rho(s)$, i.e. if the left half s-plane zeros had been allocated to $\rho(s)$, the resulting normalized filter would have been that of Fig. 7.32a with

$$L_1 = 1.14189 \qquad C_2 = 1.9882 \qquad L_3 = 1.37807 \qquad C_4 = 1.80511$$

The denormalized filter with

$$L_1 = 136.3 \text{ mH} \qquad C_2 = 105.48 \text{ nF} \qquad L_3 = 164.5 \text{ mH} \qquad C_4 = 62.63 \text{ nF}$$

is shown in Fig. 7.32b. Both denormalized filters will have the same attenuation shown in Fig. 7.33.

The Chebyshev approximation, as an all-pole approximation, leads to passive ladder structures with inductors in the series an capacitors in the shunt arms. The synthesis procedure reveals the values of the passive elements. However, in the equal terminations case, the values T_k of the elements can be calculated from the following recursive formulas:

$$\begin{aligned} T_k &= \frac{a_k a_{k-1}}{b_k T_{k-1}} \quad \text{with } T_0 = \gamma \text{ and } k = 1, 2, \ldots, N \\ a_k &= \sin\left(\frac{(2k-1)\pi}{2N}\right) \text{ with } a_0 = 1 \\ b_k &= \gamma^2 + \sin^2(k\pi/N) \text{ with } b_0 = 2 \\ \gamma &= \sinh\left[\frac{1}{2N} \ln\left(\frac{10^{A_{\max}/20}+1}{10^{A_{\min}/20}+1}\right)\right] \end{aligned} \tag{7.45}$$

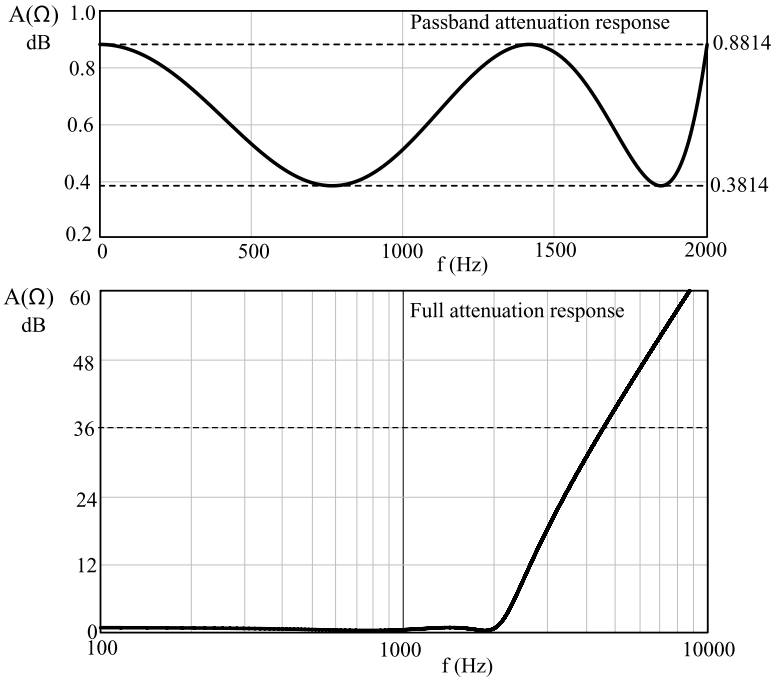

Fig. 7.33 Attenuation plot of the denormalized filter

7.3.3.1 Determination of the Element Values by Analysis

The order N of a lowpass Chebyshev filter and the ripple factor ε can be determined directly from the specifications. For low order filters, the synthesis procedure can be avoided by exploiting its conclusions, i.e. that the normalized filter will be a ladder with N lossless elements, inductors in the series and capacitors in the shunt arms, terminated by $R_L = 1$.

Therefore, after determining the order, we know the structure of the filter circuit, and its voltage transfer function and attenuation function can be determined by analysis. By equating the so determined attenuation function with the corresponding Chebyshev attenuation function, the element values can be determined by solving the system of equations which emerges from coefficient matching. This method has been presented in Sect. 7.2.1 for the Butterworth case and will be demonstrated in the Chebyshev case by an example.

Example 7.13 Design a passive lowpass filter with Chebyshev response from the following specifications:

$$R_S = R_L = 1.5\ \text{kOhm} \qquad A_{\max} = 0.5\ \text{dB} \qquad A_{\min} = 25\ \text{dB}$$

$$f_C = 1.0\ \text{kHz} \qquad f_S = 4.0\ \text{kHz}$$

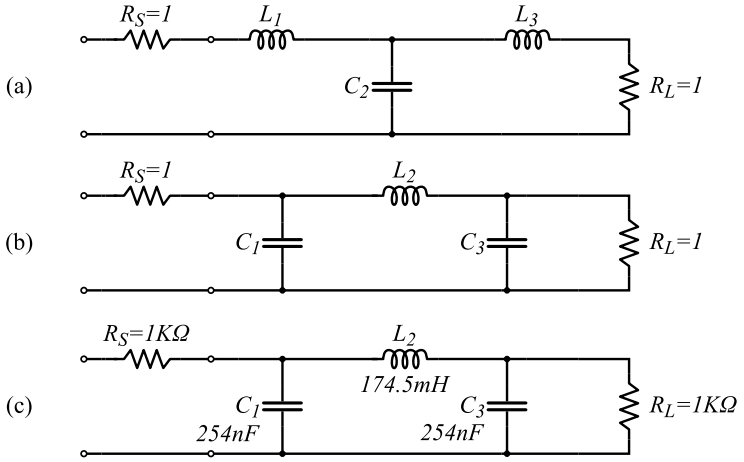

Fig. 7.34 (**a**) Normalized. (**b**) Normalized. (**c**) Denormalized

From the specifications, it is evident that

$$\omega_C = 2\pi\,1000 \text{ rad/s} \qquad \omega_S = 2\pi\,4000 \text{ rad/s}$$

The specifications of the normalized filter are $A_{\max} = 0.5$ dB, $A_{\min} = 25$ dB and

$$R_S = R_L = 1 \qquad \Omega_C = 1 \qquad \Omega_S = 4$$

The decimal order $N_d = 2.2397$ is determined from (7.24) and the integer order is taken $N = 3$. Therefore, the normalized filter will be that of Fig. 7.34a or b. The transfer function of the filter of Fig. 7.34b can be determined by analysis:

$$H_{Circ}(s) = \frac{V_2(s)}{E(s)} = \frac{1}{C_1L_2C_3s^3 + L_2(C_1+C_3)s^2 + (C_1+L_2+C_3)s + 2} \quad \Rightarrow$$

$$|H_{Circ}(j\Omega)|^2 = \frac{1}{[2 - L_2(C_1+C_3)\Omega^2]^2 + \Omega^2[C_1+L_2+C_3 - C_1L_2C_3\Omega^2]^2}$$

$$= \frac{1}{C_1^2L_2^2C_3^2\Omega^6 + L_2[L_2(C_1+C_3)^2 - 2C_1C_3(C_1+L_2+C_3)]\Omega^4 + (C_1+C_3-L_2)^2\Omega^2 + 4}$$

From (7.27), with $N = 3$ we find

$$H_{Cho} = \frac{R_L}{R_S + R_L} = \frac{1}{1+1} = 0.5$$

and since

$$C_3^2(\Omega) = (4\Omega^3 - 3\Omega)^2 = 16\Omega^6 - 24\Omega^4 + 9\Omega^2$$

we find

$$|H(j\Omega)|^2 = \frac{H_{Cho}^2}{1+\varepsilon^2 C_n^2(\Omega)}$$
$$= \frac{1}{4+4\varepsilon^2(16\Omega^6-24\Omega^4+9\Omega^2)} = \frac{1}{64\varepsilon^2\Omega^6-96\varepsilon^2\Omega^4+36\varepsilon^2\Omega^2+4}$$

In order to have

$$|H_{Circ}(j\Omega)|^2 \equiv |H(j\Omega)|^2$$

the coefficients of the two denominator polynomials must be equal, and therefore:

$$C_1L_2C_3 = 8\varepsilon \qquad L_2^2(C_1+C_3)^2 - 2C_1L_2C_3(C_1+L_2+C_3) = -96\varepsilon^2$$
$$C_1+C_3-L_2 = 6\varepsilon$$

The ripple factor ε can be selected from the range $\varepsilon_{\min} \le \varepsilon \le \varepsilon_{\max}$. If we select $\varepsilon = \varepsilon_{\max} = 0.34931$, solving the above system of equations, we get the element values of the normalized filter:

$$C_1 = C_3 = 1.5962 \quad \text{and} \quad L_2 = 1.0967$$

The element values are finally denormalized for $\omega_C = 2\pi 1000$ rad/s and $R_L =$ 1.0 kOhm to find:

$$C_1 = C_3 = 254 \text{ nF} \quad \text{and} \quad L_2 = 174.5 \text{ mH}$$

The final denormalized filter is shown in Fig. 7.34c.

7.4 The Pascal Approximation in Passive Filter Design

Given the normalized specifications

$$\{A_{\max},\ A_{\min},\ \Omega_S,\ R_S\} \quad (\Omega_C = 1 \text{ and } R_L = 1)$$

of a passive lowpass filter we are looking for an effective attenuation function $A(\Omega)$, the plot of which does not enter the shaded area of Fig. 7.35, where A_K is the minimum attenuation that is achieved by the filter. $A(\Omega)$ is related to the magnitude of the voltage transfer function $H(s)$ of the filter to be designed by the following relationship:

$$A(\Omega) = 20\log\left(\frac{1}{2}\sqrt{\frac{R_L}{R_S}}\frac{1}{|H(j\Omega)|}\right)$$

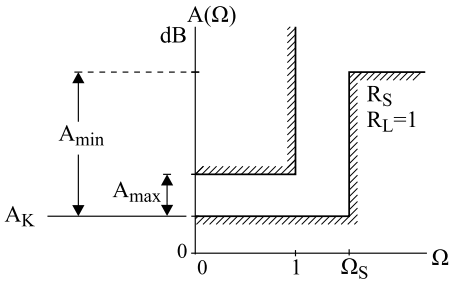

Fig. 7.35 Attenuation specifications of passive lowpass filters

As with all other approximations, our final goal is to determine the input driving-point impedance $Z_1(s)$ of Fig. 7.1 from the reflection coefficient expression $\rho(s)\rho(-s)$, which is directly related to the magnitude of the transfer function $H(s)$ via (7.5), i.e.:

$$\rho(s)\rho(-s) = 1 - \frac{4R_S}{R_L}|H(j\Omega)|^2_{\Omega^2=-s^2}$$

The effective attenuation function of the Pascal approximation is defined as

$$A(\Omega) = A_K + 20\log\left(\sqrt{1+\lambda^2 P_D^2(N,\Omega)}\right) \tag{7.46}$$

where

- N is the integer order of the approximation.
- λ is the ripple factor, a design parameter which depends on the specifications and has been thoroughly examined in Sect. 2.4.1. Its boundary values have been given in (2.86).
- $P_D(N,\Omega)$ is the filter-appropriate Pascal polynomial of order N, as defined in (2.69) and (2.71) of Sect. 2.4 in Chap. 2.
- A_K is the minimum passband attenuation given by

$$A_K = \begin{cases} A_o & \text{for } N \text{ odd} \\ A_o - \delta A & \text{for } N \text{ even} \end{cases} \tag{7.47}$$

The quantity

$$\delta A = 20\log\sqrt{1+\lambda^2 P_D^2(N,0)} \tag{7.48}$$

is zero when N is odd, since $P_D^2(N,0) = 0$, and assumes a very low value when N is even, since $P_D^2(N,0)$ is very low. In passive filter design using the Pascal approximation, the value $P_D(N,0)$ of the filter-appropriate polynomial $P_D(\Omega)$ at $\Omega = 0$ is crucial and is given by (2.75). It is also tabulated in Table 2.6. The absolute value $|P_D(N,0)|$ is very small as compared to $|P_{\max}|$.

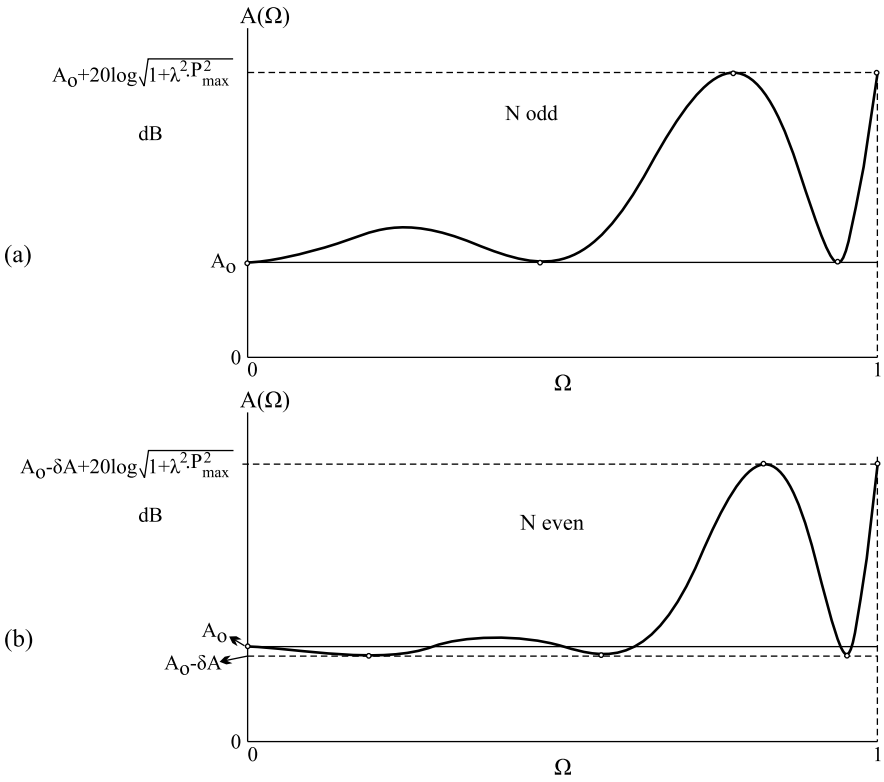

Fig. 7.36 Pascal passband attenuation ripple (**a**) odd N (**b**) even N

– A_o is the attenuation before the filter is inserted between source and load (see (6.29)) and is given by

$$A_o = 20\log\left(\frac{R_S + R_L}{2\sqrt{R_L R_S}}\right)$$

The Pascal passband attenuation, as defined in (7.46), varies as follows:
– From A_o to $A_o + 20\log\sqrt{1+\lambda^2 P_{\max}^2}$ when N is odd. This is shown in Fig. 7.36a.
– From $A_o - \delta A$ to $A_o - \delta A + 20\log\sqrt{1+\lambda^2 P_{\max}^2}$ when N is even. This is shown in Fig. 7.36b.

It should be remembered that the quantity $P_{\max}$ depends only on the order N and can be taken from Table 2.4 of Sect. 2.4.

Due to the ability of the Pascal attenuation function to assume values lower than A_o when N is even, plain gain specifications are related to effective parameters specifications in a similar way to the Chebyshev case as follows:

$$H_C = H_o \cdot 10^{-\frac{A_{\max}}{20}} \qquad H_S = H_o \cdot 10^{-\frac{A_{\min}}{20}}$$

$$\text{where } H_o = \begin{cases} \frac{R_L}{R_S+R_L} & \text{for } N \text{ odd} \\ \frac{R_L}{R_S+R_L} 10^{\frac{\delta A}{20}} & \text{for } N \text{ even} \end{cases} \tag{7.49}$$

From the above analysis, and in view of Fig. 7.36, it becomes evident that $20\log\sqrt{1+\lambda^2 P_{\max}^2}$ can be at most equal to $A_{\max}$, from which the maximum value of the ripple factor λ is derived:

$$20\log\sqrt{1+\lambda^2 P_{\max}^2} \le A_{\max} \quad \Leftrightarrow \quad \lambda \le \frac{\sqrt{10^{\frac{A_{\max}}{10}}-1}}{|P_{\max}|} = \lambda_{\max} \tag{7.50}$$

This maximum value of the ripple factor has been also found in Sect. 2.4.1.

The Pascal attenuation function $A(\Omega)$ is monotonically increasing for $\Omega > 1$ and therefore the stopband specifications are met if

$$A(\Omega_S) \ge A_K + A_{\min} \quad \Longleftrightarrow \quad 20\log\sqrt{1+\lambda^2 P_D^2(N,\Omega_S)} \ge A_{\min}$$

from which, setting $\lambda = \lambda_{\max}$, we get the order inequality:

$$\left|\frac{P_D(N,1)}{P_D(N,\Omega_S)}\right| = \left|\frac{P_{\max}}{P_D(N,\Omega_S)}\right| \le g = \sqrt{\frac{10^{\frac{A_{\max}}{10}}-1}{10^{\frac{A_{\min}}{10}}-1}} \ll 1 \tag{7.51}$$

This is the same inequality found in Sect. 2.4.2 and, as explained there, cannot be analytically solved for N, and the order is determined from the nomograph of Fig. 2.43. The usage of the nomograph has also been presented in Sect. 2.4.2. Having the order N, the lower boundary value of the ripple factor can be determined and finally λ can be selected from the range of (2.86), repeated here for convenience:

$$\frac{\sqrt{10^{\frac{A_{\min}}{10}}-1}}{|P_D(N,\Omega_S)|} = \lambda_{\min} \le \lambda \le \lambda_{\max} = \frac{\sqrt{10^{\frac{A_{\max}}{10}}-1}}{|P_{\max}|} \tag{7.52}$$

The value of $|P_{\max}| = |P_D(N,1)|$ depends only on N and can be taken from Table 2.4 of Sect. 2.4.

For any value of the ripple factor λ within this range, a Pascal filter can be designed, the attenuation of which will satisfy the specifications in a different manner. For $\lambda = \lambda_{\max}$, the passband attenuation fully covers the specified passband tolerance $A_{\max}$ and $A(\Omega_S)$ is better (higher) than the specified. For $\lambda = \lambda_{\min}$, $A(\Omega_S)$ satisfies the specified lower stopband attenuation in an exact manner, while the passband attenuation ripple is lower than the specified. Details can be found in Sect. 2.4.1 of Chap. 2.

In order for the filter to have Pascal attenuation, its corresponding circuit function must be made equal to the attenuation of the Pascal approximation i.e.:

$$A(\Omega) = 20\log\left(\frac{1}{2}\sqrt{\frac{R_L}{R_S}}\frac{1}{|H(j\Omega)|}\right) = A_K + 20\log\left(\sqrt{1+\lambda^2 P_D^2(N,\Omega)}\right) \tag{7.53}$$

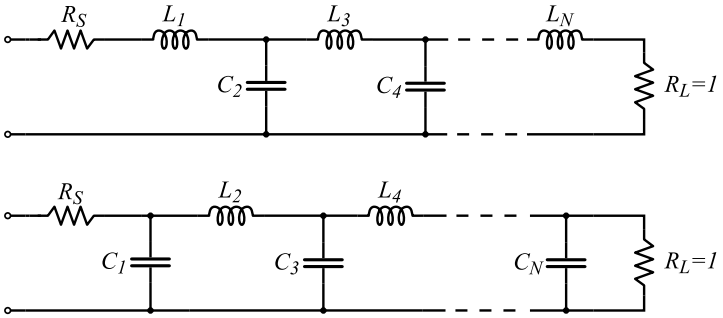

Fig. 7.37 Doubly resistively terminated LC ladder filters

From (7.53), we get

$$|H(j\Omega)|^2 = \frac{H_{Po}^2}{(1+\lambda^2 P_D^2(N,\Omega))}$$

$$\text{where } H_{Po}^2 = \left(\frac{R_L}{R_S+R_L}\right)^2 (1+\lambda^2 P_D^2(N,0))$$

$$= \left(\frac{R_L}{R_S+R_L}\right)^2 10^{\frac{\delta A}{10}} \tag{7.54}$$

It should be remembered that when N is odd, $P_D(N,0)=0$ and $\delta A = 0$. The above expression of $|H(j\Omega)|^2$ can be used in Feldtkeller's equation (7.5) to determine the necessary function $\rho(s)\rho(-s)$:

$$\rho(s)\rho(-s) = 1 - \frac{4R_S}{R_L}|H(j\Omega)|^2_{\Omega^2=-s^2} = 1 - \frac{\frac{4R_S}{R_L}H_{Po}^2}{1+\lambda^2[P_D^2(N,\Omega)]_{\Omega^2=-s^2}} \tag{7.55}$$

The transfer function $H(s)$ can be determined from

$$H(s)H(-s) = |H(j\Omega)|^2_{\Omega^2=-s^2}$$

as has been done in Sect. 2.4.3. The Pascal transfer function is an all-pole function, as in the Butterworth and Chebyshev cases, and therefore it is not surprising that when the input driving-point impedance $Z_1(s)$ is determined from $\rho(s)$ and properly synthesized, the resulting filter will have a ladder structure terminated by R_L as shown in Fig. 7.37.

It is evident that due to this circuit topology, the plain gain at $\Omega = 0$ (DC) is $\frac{R_L}{R_S+R_L}$, since the reactive part of the circuit becomes transparent for odd and even N and therefore the corresponding effective attenuation at $\Omega = 0$ is given by

$$A(0) = 20\log\left(\frac{R_S+R_L}{2\sqrt{R_S R_L}}\right) = A_o$$

which is in accordance with Fig. 7.36.

Example 7.14 Design a passive lowpass filter with Pascal response from the following normalized specifications:

$$A_{\max} = 1.25 \text{ dB} \qquad A_{\min} = 36 \text{ dB} \qquad R_S = 0.6 \qquad R_L = 1$$
$$\Omega_C = 1 \qquad \Omega_S = 2.0$$

We first calculate

$$HP = 20\log\left(\frac{1}{g}\right) = 20\log\sqrt{\frac{10^{\frac{A_{\min}}{10}} - 1}{10^{\frac{A_{\max}}{10}} - 1}} = 40.7677 \quad \text{(see (2.88))}$$

The order is then determined from the order nomograph of Fig. 2.43 with $HP = 40.7677$ and $\Omega_S = 2$. We find $N = 5$.

For $N = 5$, polynomial $P_D(5, \Omega)$ is given in Table 2.7

$$P_D(5, \Omega) = -0.356162\Omega^5 + 0.396539\Omega^3 - 0.070639s$$
$$\Rightarrow \quad P_D^2(5, \Omega)|_{\Omega^2 = -s^2} = 0.126851s^{10} + 0.282464s^8 + 0.2075610s^6 + 0.0560222s^4 + 0.004999s^2$$

From (7.55)

$$\rho(s)\rho(-s) = 1 - \frac{4R_S}{R_L}|H(j\Omega)|^2_{\Omega^2=-s^2} = 1 - \frac{4R_S}{R_L}\frac{H_{Po}^2}{1 + \lambda^2 P_D^2(4, \Omega)|^2_{\Omega^2=-s^2}}$$

Using $\lambda = \lambda_{\max} = 19.083814$ from (7.52), we find

$$\rho(s)\rho(-s) = \frac{46.19825s^{10} + 102.87121s^8 + 75.59206s^6 + 20.40285s^4 + 1.81727s^2 - 0.0625}{46.19825s^{10} + 102.87121s^8 + 75.59206s^6 + 20.40285s^4 + 1.81727s^2 - 1}$$

The poles and zeros of $\rho(s)\rho(-s)$ are determined using a mathematical software package and are given below:

Poles of $\rho(s)\rho(-s)$	Zeros of $\rho(s)\rho(-s)$
-0.383466	-0.161329
$-0.286033 + j0.558421$	$-0.110689 - j0.491241$
$-0.286033 - j0.558421$	$-0.110689 + j0.491241$
$-0.094300 + j0.982732$	$-0.030024 - j0.947743$
$-0.094300 - j0.982732$	$-0.030024 + j0.947743$
$+0.094300 + j0.982732$	$+0.030024 + j0.947743$
$+0.094300 - j0.982732$	$+0.030024 - j0.947743$
$+0.286033 + j0.558421$	$+0.110689 + j0.491241$
$+0.286033 - j0.558421$	$+0.110689 - j0.491241$
$+0.383466$	$+0.161329$

Left half s-plane poles are allocated to $\rho(s)$ and their opposite, located in the right half s-plane, to $\rho(-s)$. The corresponding denominator polynomial $D_\rho(s)$ of $\rho(s)$ is determined as

$$D_\rho(s) = s^5 + 1.144132s^4 + 1.767885s^3 + 1.1978797s^2 + 0.625949s + 0.147125$$

For the zeros of $\rho(s)$, there are eight possible choices. Allocating, for example, the left half s-plane zeros to $\rho(s)$, the numerator polynomial $N_\rho(s)$ of $\rho(s)$ becomes

$$N_\rho(s) = s^5 + 0.442755s^4 + 1.211383s^3 + 0.402378s^2 + 0.262557s + 0.036781$$

and therefore, for this choice of zeros, we have:

$$\begin{aligned}\rho(s) &= \frac{N_\rho(s)}{D_\rho(s)} \\ &= \frac{s^5 + 0.442755s^4 + 1.211383s^3 + 0.402378s^2 + 0.262557s + 0.036781}{s^5 + 1.144132s^4 + 1.767885s^3 + 1.1978797s^2 + 0.625949s + 0.147125}\end{aligned}$$

The input impedance $Z_1(s)$ can be determined from (7.3) or (7.4). The first gives $Z_{1a}(s)$ with $Z_{1a}(0) = R_S^2 = 0.36$, which is not useful. In this case, either (7.4) must be used to determine $Z_{1b}(s)$, or it can be determined from $Z_{1a}(s)Z_{1b}(s) = R_S^2 = 0.36$. In any case, we find:

$$\begin{aligned}&Z_{1b}(s) \\ &= \frac{6.0s^5 + 4.760661s^4 + 8.937805s^3 + 4.800773s^2 + 2.665519s + 0.551719}{3.506885s^4 + 2.782506s^3 + 3.977509s^2 + 1.816958s + 0.551719}\end{aligned}$$

$Z_1(s) = Z_{1b}(s)$ has a pole at infinity and it can be removed as a series inductor $L_1 = 6.0/3.506885 = 1.710920$, leaving the remaining impedance $Z_2(s) = Z_1(s) - sL_1$. The synthesis continues by removing the pole at infinity of $Y_2(s)$ as a

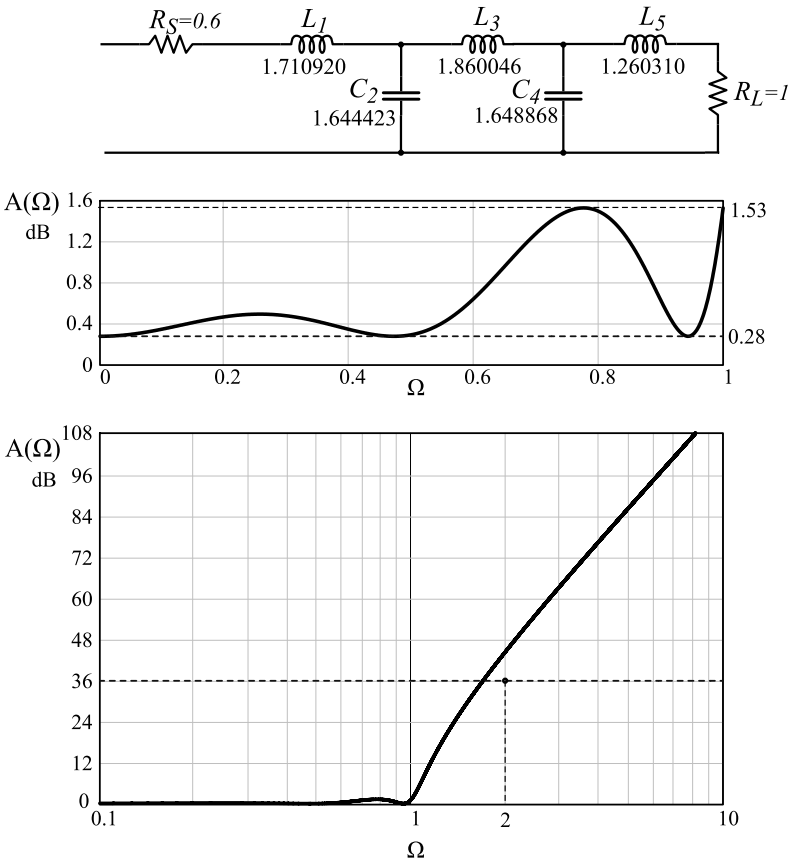

Fig. 7.38 Circuit and attenuation plots of Example 7.14

shunt capacitor $C_2 = 1.644423$ and so on. The final normalized circuit is shown in Fig. 7.38, together with the attenuation plots.

7.4.1 Even Order Passive Pascal Filters

As in the Chebyshev case, the specified normalized terminations R_S and $R_L = 1$ determine the effective attenuation A_o of the passive filter at zero frequency according to (6.29):

$$A_o = 20\log\left(\frac{R_S + R_L}{2\sqrt{R_L R_S}}\right) \tag{7.56}$$

Effective attenuation $A(\Omega)$ assumes by definition only non-negative values. In odd order Pascal filters, where due to (7.46)–(7.47) the attenuation is always above the non-negative value A_o, there are no restrictions on the value of the specified pass-

band ripple $A_{\max}$. In even order Pascal filters, the passband attenuation varies from $A_o - \delta A$ to $A_o - \delta A + A_{\max}$, where from (7.48) we have:

$$\delta A = 20\log\sqrt{1+\lambda_{\max}^2 P_D^2(N,0)} = 20\log\sqrt{1+(10^{0.1A_{\max}}-1)\frac{P_D^2(N,0)}{P_{\max}^2(N)}} \quad (7.57)$$

For the passband attenuation to be non-negative, δA can be at most equal to A_o. Since A_o depends only on the terminations, for each value of R_S there is a maximum ripple which can be realized by an even order passive Pascal filter, and for each ripple value $A_{\max}$ there is a range $R_{S1} < R_S < R_{S2}$ for which it cannot be realized. This range is determined by finding the roots R_{S1} and R_{S2} of the equation

$$\delta A = A_o \quad \Leftrightarrow \quad \sqrt{1+(10^{\frac{A_{\max}}{10}}-1)\frac{P_D^2(N,0)}{P_{\max}^2}} = \frac{R_S+1}{2\sqrt{R_S}}$$

$$R_{S1,2} = 1 + 2\frac{P_D^2(N,0)}{P_{\max}^2(N)}\left(10^{\frac{A_{\max}}{10}}-1\right) \quad (7.58)$$

$$\mp 2\left|\frac{P_D(N,0)}{P_{\max}(N)}\right|\sqrt{\left(10^{\frac{A_{\max}}{10}}-1\right)\left[1+\frac{P_D^2(N,0)}{P_{\max}^2(N)}\left(10^{\frac{A_{\max}}{10}}-1\right)\right]}$$

The maximum ripple $A_{\max o}$ that can be realized by an even order N passive Pascal filter is a function of R_S and can be determined by a setting $\delta A = A_o$ to find:

$$A_{\max o}(R_S) = 20\log\sqrt{1+\frac{(R_S-1)^2 P_{\max}^2(N)}{4R_S P_D^2(N,0)}} \quad (7.59)$$

In Fig. 7.39, $A_{\max o}$ has been plotted as a function of R_S. From Fig. 7.39a, it is clear that ripple $A_{\max} = 0.5$ dB can only be achieved when $R_S \geq R_{S2} = 1.1563$ or $R_S \leq R_{S1} = 0.8649$, determined from (7.58). If $A_{\max} = 1$ is specified, then the filter is realizable only if $R_S \geq R_{S2} = 1.2353$ or $R_S \leq R_{S1} = 0.8095$ determined from (7.58). This is shown in Fig. 7.39b, and in this case, if $R_S = 0.5$ is specified, the Pascal passive filter with ripple exactly $A_{\max} = 0.5$ dB can be directly designed, as opposed to the Chebyshev case (see Fig. 7.21).

It can be shown that even when for the specified R_S we have $R_{S1} < R_S < R_{S2}$ (or equivalently $A_{\max} > A_{\max o}(R_S)$), the filter can still be directly designed with lower ripple $A_{\max o}$ given by (7.59), provided that the specified $A_{\min}$ is lower than the maximum stopband specification A_{Smx}, which can be satisfied by a Pascal filter

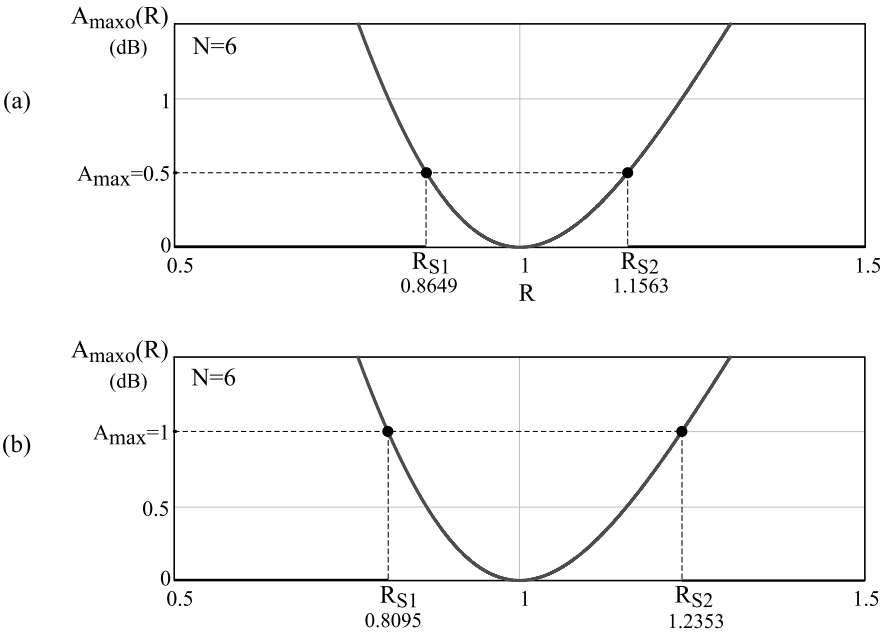

Fig. 7.39 $A_{\max o}$ as a function of the input termination R

of order N and $\{R_S, R_L = 1, \Omega_S\}$. The value of A_{Smx} can be determined from the order inequality (7.51) with $A_{\max} = A_{\max o}$:

$$\left|\frac{P_{\max}}{P_D(N,\Omega_S)}\right| = \sqrt{\frac{10^{\frac{A_{\max o}}{10}} - 1}{10^{\frac{A_{Smx}}{10}} - 1}}$$

$$\Leftrightarrow \quad A_{Smx} = 10\log\left(\frac{(R_S-1)^2}{4R_S}\frac{P_D^2(N,\Omega_S)}{P_D^2(N,0)} + 1\right) \tag{7.60}$$

Finally, the even order N passive Pascal filter cannot be directly designed with the specified ripple $A_{\max}$ in the following two cases:

i. $R_S = R_L \Leftrightarrow A_o = 0$

ii. $R_S \neq R_L \Leftrightarrow A_o > 0$ and

$$\delta A > A_o \quad \Leftrightarrow \quad R_{S1} < R_S < R_{S2}$$

$$\Leftrightarrow \quad A_{\max} > 10\log\sqrt{\frac{(R_S-R_L)^2}{4R_SR_L}\frac{P_{\max}^2}{P_D^2(N,0)} + 1}$$

The filter can, however, be directly designed even if $R_{S1} < R_S < R_{S2}$, with lower ripple given by

$$10\log\sqrt{\frac{(R_S-R_L)^2}{4R_SR_L}\frac{P_{\max}^2}{P_D^2(N,0)}+1} < A_{\max}$$

provided that for the specified $A_{\min}$ and Ω_S:

$$A_{\min} > 10\log\left(\frac{(R_S-R_L)^2}{4R_SR_L}\frac{P_D^2(N,\Omega_S)}{P_D^2(N,0)}+1\right) \tag{7.61}$$

Example 7.15 Given the normalized specifications

$$\{\Omega_C=1,\ R_L=1,\ A_{\max}=1,\ A_{\min}=30,\ \Omega_S=2.2,\ R_S=0.5\}$$

of Example 7.7, the order is determined from the nomograph of Fig. 2.43 using $HP(1.0,30)=35.86$ and $\Omega_S=2.2$: $N=4\rightarrow P_D(4,0)=0.0234375$ (taken from Table 2.6) and $P_{\max}=-0.04166667$ from Table 2.4. Now δA can be calculated from (7.57):

$$\delta A = 20\log\sqrt{1+\lambda_{\max}^2P_D^2(N,0)} = 0.341974$$

$$A_o = 20\log\left(\frac{R_S+R_L}{2\sqrt{R_SR_L}}\right) = 20\log\left(\frac{0.5+1}{2\sqrt{0.5\cdot 1}}\right) = 0.511525 > \delta A = 0.341974$$

and therefore the filter can be directly designed for any value of λ in the range $5.635663=\lambda_{\min}\le\lambda\le\lambda_{\max}=12.212331$ given in (7.52). If $\lambda=\lambda_{\max}=12.212331$ is used, the input impedance $Z_1(s)$ is found to be:

$$Z_1(s)=\frac{s^4+0.68443542s^3+1.24599439s^2+0.52444123s+0.19199176}{0.76631472s^3+0.52449295s^2+0.64815469s+0.19199176}$$

with pole at infinity. $Z_1(s)$ can be synthesized using sequential removals of poles at infinity to yield the passive Pascal filter of Fig. 7.40a, which is shown with the corresponding attenuation plots. It should be noted that this filter could not be directly designed with Chebyshev response and ripple exactly $A_{\max}=1$ dB (see Example 7.7).

Example 7.16 Given the same normalized ($\Omega_C=1$ and $R_L=1$) specifications of Examples 7.7 and 7.15 but with $A_{\min}=36$, i.e.

$$\{A_{\max}=1,\ A_{\min}=36,\ \Omega_S=2.2,\ R_S=0.5\}$$

the order is found again $N=4$ from the nomograph ($HP(1.0,36)=41.87$) and nothing changes for the quantities calculated in Example 7.15:

$P_D(4,0)=0.0234375$ $\quad P_{\max}=-0.04166667$ $\quad \delta A=0.341974$ and

$A_o=0.511525>\delta A=0.341974$

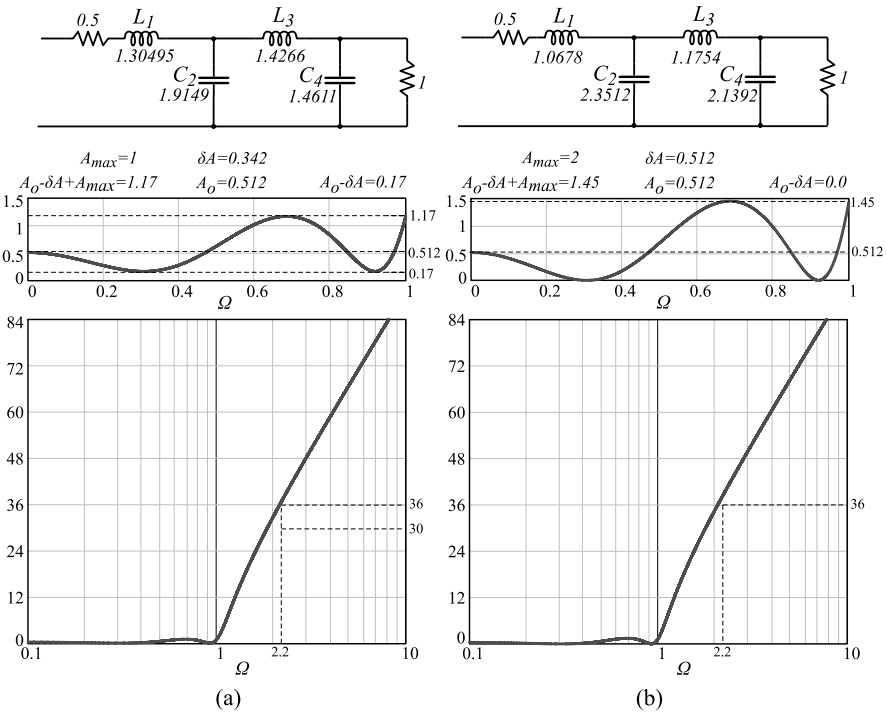

Fig. 7.40 Pascal passive filter and attenuation plots. (**a**) Examples 7.15 and 7.16. (**b**) Example 7.17

Therefore, the filter can still be designed for any value of λ in the range $11.248839 = \lambda_{\min} \leq \lambda \leq \lambda_{\max} = 12.212331$. Selecting $\lambda = \lambda_{\max}$, the passive Pascal filter will be that of Example 7.15, shown in Fig. 7.40a with the corresponding attenuation plots. It should be emphasized that the specifications of this example with $A_{\max} = 1$ and $A_{\min} = 36$ dB cannot be met by a passive Chebyshev filter with $N = 4$ (refer to Example 7.8) and either the order must be increased to $N = 5$ or the modified Chebyshev filter must be designed.

Example 7.17 Given the normalized specifications ($\Omega_C = 1$ and $R_L = 1$)

$$\{A_{\max} = 2,\ A_{\min} = 36,\ \Omega_S = 2.2,\ R_S = 0.5\}$$

the order of the Pascal approximation is found again $N = 4$ (from the nomograph with $HP(2.0, 36) = 38.3$). In this case, we find $A_o = 0.511525$ and $\delta A = 0.73742 > A_o$.

The condition $\delta A > A_o$ is equivalent to having the value of the specified $R_S = 0.5$ between $R_{S1} = 2.306744$ and $R_{S2} = 0.433511$, as determined from (7.58), which is true, and therefore the passive Pascal filter cannot be directly designed with $A_{\max} = 2$. The maximum ripple which can be realized with $R_S = 0.5$ is $A_{\max o}$

given by (7.59):

$$A_{\max o} = 10\log\left(\frac{(0.5-1)^2 0.041667^2}{4\ddot{0}.5 \cdot 0.023438^2} + 1\right) = 1.445934 \text{ dB}$$

and the design of the filter depends on whether $A_{\min} = 36 \leq A_{Smx}$. From (7.60), we find $A_{Smx} = 38.5482 > A_{\min} = 36$ and therefore the filter can be designed with ripple

$$A_{\max o} = 1.445934 \Rightarrow \lambda_{\max} = \frac{1}{|P_{\max}|}\sqrt{10^{\frac{1.445934}{10}} - 1} = 15.084943$$

The input impedance $Z_1(s)$ is found to be:

$$Z_1(s) = \frac{s^4 + 0.46826645s^3 + 1.15785038s^2 + 0.35565916s + 0.15840908}{0.9365329s^3 + 0.43812045s^2 + 0.71131833s + 0.15840908}$$

Synthesis of $Z_1(s)$ by sequential removals of poles at infinity leads to the filter of Fig. 7.40b which also shows the corresponding attenuation curves.

As we have seen, in both Chebyshev and Pascal passive filter design, when $R_S = R_L$ ($A_o = 0$), no even order N passive filter can be directly designed and either N must be increased to the next odd order $N+1$ or the modified filter must be designed. When $R_S \neq R_L$ ($A_o > 0$), then the even order filter cannot be directly designed with the specified ripple $A_{\max}$ as follows:

A. In Chebyshev approximation when

$$A_{\max} > A_o = 20\log\left(\frac{R_S + R_L}{2\sqrt{R_S R_L}}\right) \quad \Leftrightarrow \quad R_{S1} < R_S < R_{S2}$$

B. In Pascal approximation

$$\begin{aligned} \delta A > A_o \quad &\Leftrightarrow \quad R_{S1} < R_S < R_{S2} \\ &\Leftrightarrow \quad A_{\max} > 10\log\sqrt{\frac{(R_S - R_L)^2}{4R_S R_L}\frac{P_{\max}^2}{P_D^2(N,0)} + 1} \end{aligned} \tag{7.62}$$

In Fig. 7.41, the dotted curves are the plots of the order independent R_{S1} and R_{S2} of (7.33) as functions of the ripple $A_{\max}$ in the Chebyshev case. For each value of $A_{\max}$, the dotted curves specify the range of the non-permitted values of R_S. If, for example, $A_{\max} = 0.5$, then the filter cannot be directly designed with $R_S = 1.2$ since $0.5040 < R_S < 1.9841$. The width of the range of non-permitted R_S values is for all orders 1.4801.

The solid curves in Fig. 7.41 are the corresponding Pascal plots of the order dependent R_{S1} and R_{S2} of (7.58) as functions of the ripple $A_{\max}$ for $N = 6$ and $N = 8$. The solid curves specify the range of the non permitted values of R_S for each value of $A_{\max}$. If, for example, $A_{\max} = 0.5$ and $N = 6$, then the filter can be

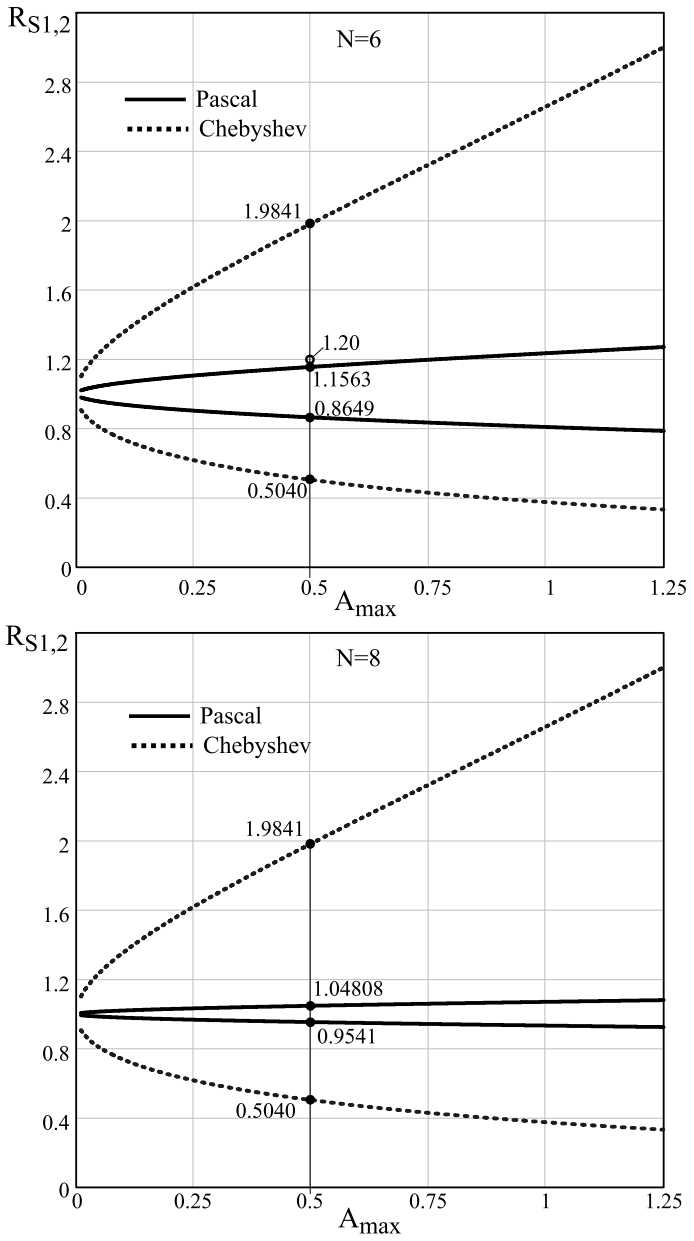

Fig. 7.41 Comparison of Chebyshev and Pascal conditions for direct design

directly designed with $R_S = 1.2$ since the value 1.2 is outside the range $0.8649 < R_S < 1.1563$ of width 0.2914, which is less than 20% of the corresponding width of the Chebyshev case. For $N = 8$, the range of the non-permitted values of R_S is

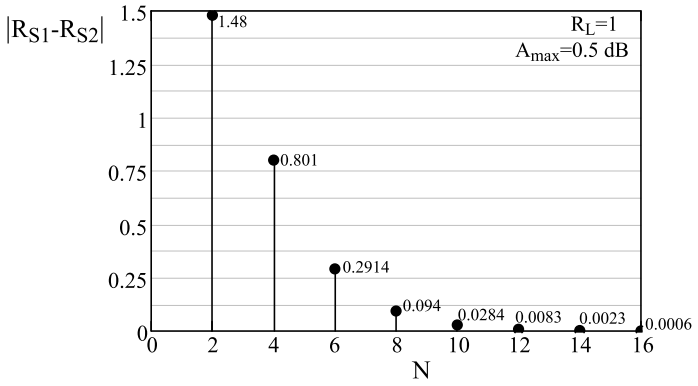

Fig. 7.42 Passive Pascal filters: Width of non-permitted values of R_S as a function of the order N

$0.9541 < R_S < 1.04808$ of width 0.094, which is 6.35% of the corresponding width of the Chebyshev case. The width $\Delta R = |R_{S1} - R_{S2}|$ is a monotonically decreasing function of N and for $A_{\max} = 0.5$ dB and $N = 16$ is $\Delta R = 0.0006$, i.e. 0.04% of the Chebyshev case. Fig. 7.42 shows ΔR as a function of N and for $A_{\min} = 0.5$. The plot does not change much for other values of $A_{\max}$.

It is evident that passive even order Pascal filter design is less restricted as far as the even order issue is concerned and therefore, in this respect, Pascal filters are superior to their Chebyshev counterparts. In fact, there are specifications which can be met by a directly designed Pascal filter of even order N which cannot be met by a directly designed Chebyshev filter of the same order.

As we have seen, if the value of R_S is in the non-permitted range, even order Chebyshev filters can be directly designed with ripple A_o, lower than the specified $A_{\max}$, provided that for the rest of the specifications, $A_{\min}$ and Ω_S, we have $A_{\min} \leq A_{Smx}$ of (7.34):

$$A_{Smx} = 10 \log \left(\frac{(R_S - 1)^2}{4R_S} C^2(N, \Omega_S) + 1 \right)$$

The corresponding condition to design the even order Pascal filter with lower ripple $A_{\max o}$ of (7.59) is given in (7.60):

$$A_{Smx} = 10 \log \left(\frac{(R_S - 1)^2}{4R_S} \frac{P_D^2(N, \Omega_S)}{P_D^2(N, 0)} + 1 \right)$$

The two relationships for A_{Smx} for the two cases are similar, with the only difference being that instead of $C^2(N, \Omega_S)$ of the Chebyshev case, in the Pascal case we have $M_P^2(N, \Omega_S) = \frac{P_D^2(N,\Omega_S)}{P_D^2(N,0)} > C^2(N, \Omega_S)$. The ratio $\frac{M_P^2(N,\Omega_S)}{C^2(N,\Omega_S)}$ is plotted in Fig. 7.43 for $N = 4 - 8$. Since this ratio is always much higher than unity, especially for high orders, A_{Smx} is higher in the Pascal case and condition $A_{\min} \leq A_{Smx}$ is less restricting. This is one more advantage of even order Pascal filters over even order Chebyshev filters.

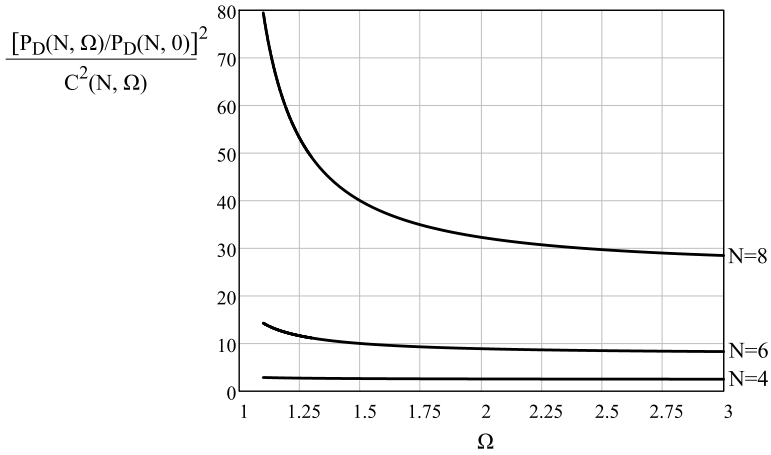

Fig. 7.43 Ratio $\frac{M_P^2(N,\Omega_S)}{C^2(N,\Omega_S)} = \frac{P_D^2(N,\Omega_S)/P_D^2(N,0)}{C^2(N,\Omega_S)}$

Example 7.18 Given the normalized specifications ($R_L = 1$, $\Omega_C = 1$)

$$R_S = 1.2 \qquad A_{\max} = 0.5 \text{ dB} \qquad A_{\min} = 48 \text{ dB} \qquad \Omega_S = 2$$

in the Pascal case, we find from the nomograph with $HP(0.5, 48) = 57.14$, $N = 6$. From the Chebyshev order equation we also find $N = 6$. However, since $A_{\max} = 0.5 > A_o = 0.0360$ the filter cannot be directly designed with the Chebyshev approximation. This is also clear from Fig. 7.41 since $R_S = 1.2$ is in the non-permitted range. From the same figure, we see that in the Pascal case, the value $R_S = 1.2$ is in the permitted range and therefore the filter can be directly designed using the Pascal approximation. This could also have been ascertained by checking if $\delta A \leq A_o = 0.0360$. From (7.57) with $\lambda = \lambda_{\max} = 14.88112$, we find $\delta A = 0.022869$ and therefore $\delta A = 0.022869 \leq A_o = 0.0360$ and the filter can be directly designed. Indeed, following the synthesis procedure we find one expression for the input admittance:

$$Y_1(s) = \frac{s^6 + 0.961687s^5 + 1.993448s^4 + 1.364118s^3 + 1.026960s^2 + 0.382167s + 0.0836313}{0.843297s^5 + 0.810985s^4 + 1.293164s^3 + 0.777314s^2 + 0.394837s + 0.0836313}$$

$Y_1(s)$ has a pole at infinity which can be removed as a shunt capacitor $C_1 = 1/0.843297 = 1.185822$. Continuing the synthesis with the inverse of the remaining admittance, we find the second element, which is a series inductor $L_2 = 1.833322$ and so on until we find all six elements. The filter with its attenuation curves is shown in Fig. 7.44.

The Chebyshev approximation leads to equiripple passband attenuation and to the lowest order, as compared to all other all-pole approximations. The Pascal all-pole approximation leads to passband attenuation with increasing ripple. The order,

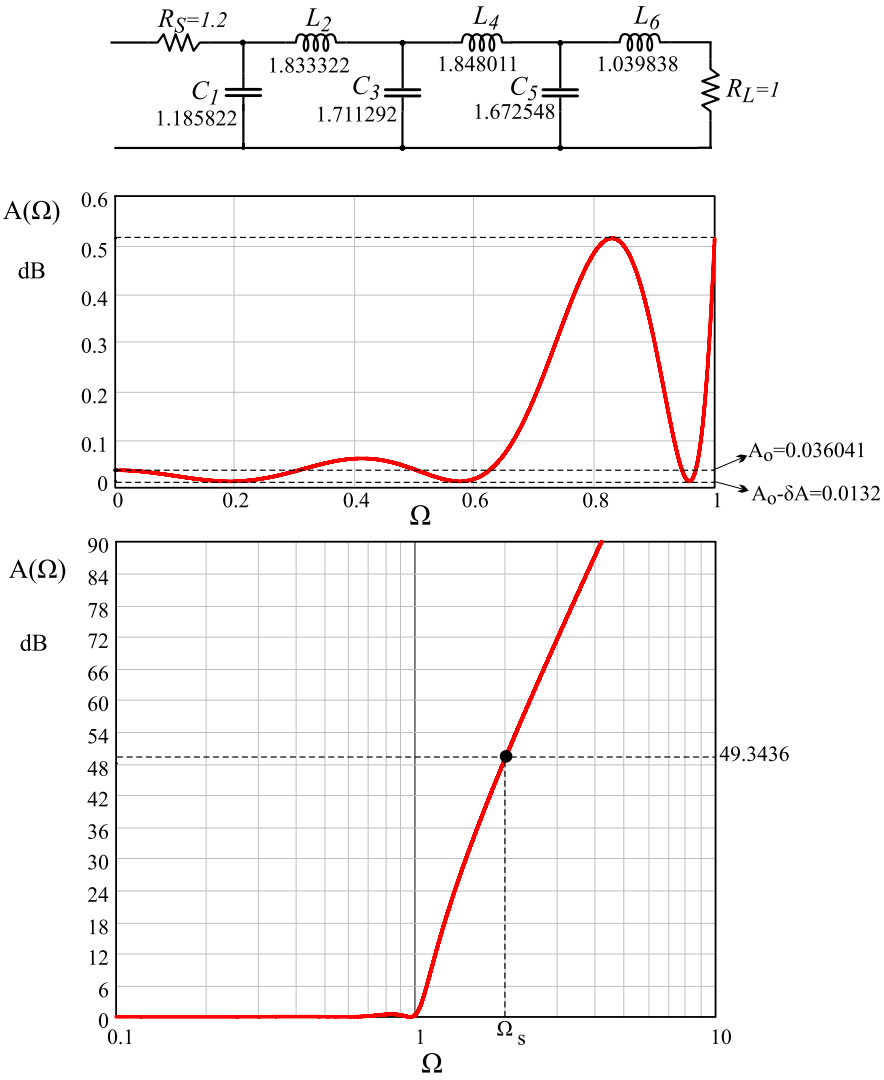

Fig. 7.44 6th order Pascal filter of Example 6: $R_S = 1.2$, $A_{\max} = 0.5$

as determined from the specifications, is in most cases equal to that of the Chebyshev approximation determined from the same specifications [5].

Both Pascal and Chebyshev approximations present similar difficulties in the design of even order passive filters and the exact conditions under which even order passive filters cannot be directly designed have been set for both approximations. Namely, even order passive Chebyshev filters cannot be directly designed if $A_{\max} > A_o$, a condition which corresponds to a wide range of non-permitted values of R_S according to (7.33). Two indicative plots are shown with the dotted curves in

Fig. 7.41. The width of this range is the same for all even orders and is an increasing function of the specified $A_{\max}$. The term direct design has been used to imply that the even order passive filter can be synthesized using the straightforward methods without recourse to the modified filter or the increase of the order to the next odd order.

The conditions under which passive even order Pascal filters cannot be directly designed have also been set and found less restricting as compared to the corresponding conditions of the Chebyshev case. Even order passive Pascal filters cannot be directly designed if $\delta A > A_o$, which corresponds to a range of non-permitted values of R_S according to (7.58). Two indicative plots are shown with the solid curves in Fig. 7.41. The width of the non-permitted values of R_S in the Pascal case is much lower than the corresponding range in the Chebyshev case due to the fact that according to (7.57), $\delta A(A_{\max}) < A_{\max}$. Moreover, for a given $A_{\max}$, this width decreases as the even order increases, in contrast to the Chebyshev case where it is order independent.

As a result, there are specifications which can be directly satisfied by even order passive Pascal filters but cannot be met by directly designed even order passive Chebyshev filters of the same or higher even order. This superiority of Pascal filters in the design of even order passive filters has been shown theoretically and has been demonstrated by several design examples.

7.4.2 The Modified Pascal Approximation

As we have seen, the value $P_D(N, 0)$ of odd order Pascal polynomials $P_D(N, \Omega)$ at $\Omega = 0$ is equal to zero. When N is even, $P_D(N, 0) \neq 0$ and this causes the design issue addressed in the previous section. A solution to the problem is to modify the Pascal polynomial $P_D(N, \Omega)$ in such a way as to have zero value at zero frequency while retaining the value $P_{\max}$ at $\Omega = 1$. Such a modification, which is analogous to the modification of the Chebyshev polynomial of Sect. 7.3.2, can be accomplished by replacing Ω with

$$\Omega_V = \sqrt{\Omega^2(1 - \Omega_x^2) + \Omega_x^2} \tag{7.63}$$

where Ω_x is the lowest root of $P_D(N, \Omega)$ given by

$$\Omega_x = \pm \frac{1}{\Omega_D} \left(\frac{1}{N+1} \right) \tag{7.64}$$

This transformation moves the lower roots $\pm\Omega_x$ of the even order Pascal polynomial to zero. The modified Pascal polynomial is expressed as

$$P_{Dm}(N, \Omega) = P_D(N, \Omega_V) \tag{7.65}$$

with a double root at $\Omega = 0$, $(N-2)/2$ positive roots and $(N-2)/2$ negative roots. Two indicative plots of the modified Pascal polynomials are shown in Fig. 7.45 for $N = 6$ and $N = 8$.

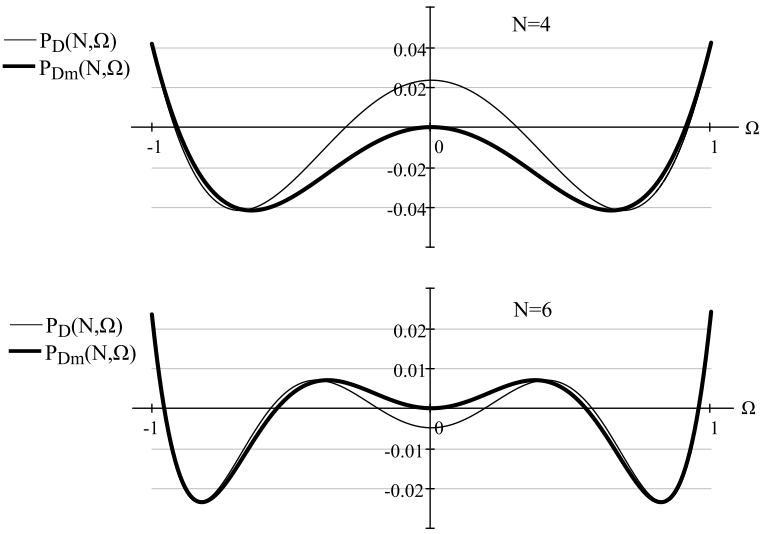

Fig. 7.45 The Pascal (*thin line*) and modified Pascal (*thick line*) polynomials for $N = 4$ and $N = 6$

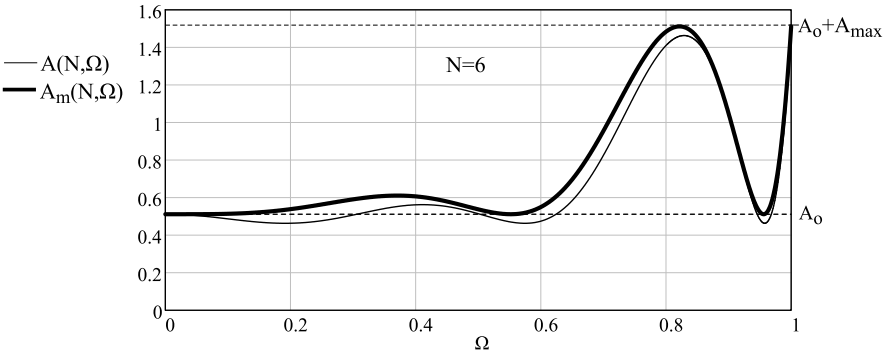

Fig. 7.46 The Pascal (*thin line*) and the modified Pascal (*thick line*) attenuation plot for $N = 6$

The modified Pascal approximation is defined as

$$A_m(\Omega) = A_o + 20\log\sqrt{1 + \lambda^2 P_{Dm}^2(N, \Omega)} \tag{7.66}$$

and a typical attenuation plot is shown in Fig. 7.46 for $N = 6$. It should be noted that, as in the case of the modified Chebyshev approximation, the attenuation curve has $N - 1$ passband extrema, one less than the extrema of the non-modified Pascal attenuation.

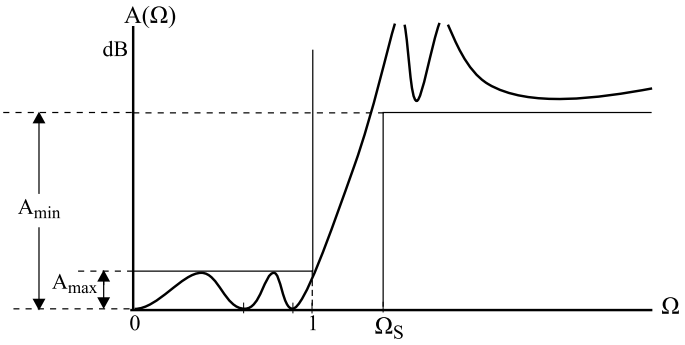

Fig. 7.47 Typical elliptic filter attenuation plot ($N = 5$)

The modified Pascal approximation can be used whenever an even order passive Pascal filter cannot be directly designed, i.e. when $A_o = 0$ ($R_S = R_L$) or $\delta A > A_o$. However, it can be shown that this is only possible if

$$g \geq \frac{P_{\max}}{P_{Dm}(N, \Omega_S)} \quad \text{where } g = \sqrt{\frac{10^{\frac{A_{\max}}{10}} - 1}{10^{\frac{A_{\min}}{10}} - 1}} \tag{7.67}$$

in order to ensure that the stopband specifications are met.

7.5 The Elliptic Approximation in Passive Filter Design

The elliptic or Cauer approximation is a rational approximation and has been thoroughly presented in its general form in Chap. 4. Its main feature is that it has equiripple passband and stopband magnitude response, as shown in Fig. 7.47. In this section, elliptic approximation will be presented as used in the design of normalized passive lowpass filters from the normalized specifications:

$$\{R_L = 1,\ R_S,\ \Omega_C = 1,\ \Omega_S,\ A_{\max},\ A_{\min}\}$$

For the purpose of designing passive elliptic filters, the attenuation of the elliptic approximation is defined as follows:

$$\left.\begin{aligned} A(\Omega) &= A_K + 20\log\left(\sqrt{1+\varepsilon^2 R_N^2(\Omega_S, \Omega)}\right) \\ A_K &= A_o - (1-\eta)20\log\sqrt{1+\varepsilon^2} = \begin{cases} A_o & \text{for } N \text{ odd} \\ A_o - 20\log\sqrt{1+\varepsilon^2} & \text{for } N \text{ even} \end{cases} \\ A_o &= 20\log\left(\frac{R_S + R_L}{2\sqrt{R_L R_S}}\right) \quad \eta = \begin{cases} 0 & \text{for } N \text{ even} \\ 1 & \text{for } N \text{ odd} \end{cases} \end{aligned}\right\} \tag{7.68}$$

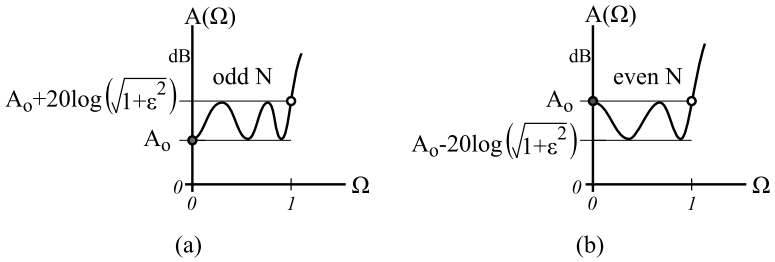

Fig. 7.48 Typical elliptic attenuation plots: (**a**) $N =$ odd. (**b**) $N =$ even

Parameter ε is the ripple factor and $\Omega_S > 1$ is the specified stopband edge frequency. Function $R_N(\Omega_S, \Omega)$ is the elliptic rational function (ERF, or Chebyshev rational function) of order N as defined in (4.15)–(4.17):

$$R_N(\Omega_S, \Omega) = A_N(\Omega_S)\Omega^\eta \prod_{m=1}^{\frac{N-\eta}{2}} \left(\frac{\Omega^2 - \Omega_{ZR}^2(m)}{\Omega^2 - \frac{\Omega_S^2}{\Omega_{ZR}^2(m)}} \right) \tag{7.69}$$

$$\Omega_{ZR}(m) = \mathrm{sn}\left[\left(\frac{2m-1}{N} + 1 \right) K(k), k \right] < 1 \quad \left(k = \frac{1}{\Omega_S} < 1 \right) \tag{7.70}$$

$$A_N(\Omega_S) = \prod_{m=1}^{\frac{N-\eta}{2}} \left(\frac{1 - \frac{\Omega_S^2}{\Omega_{ZR}^2(m)}}{1 - \Omega_{ZR}^2(m)} \right) \quad \text{so that } R_N(\Omega_S, 1) = 1 \tag{7.71}$$

From the properties of the ERF presented in Sect. 4.4, we have that $R_N^2(\Omega_S, \Omega)$ varies between 0 and 1 when $0 \le \Omega \le 1$ and

$$R_N(\Omega_S, 1) = 1 \quad \text{for all } N, \text{ even and odd} \qquad R_N(\Omega_S, 0) = \begin{cases} \pm 1 & \text{for even } N \\ 0 & \text{for odd } N \end{cases}$$

and therefore from (7.68) $\Rightarrow A(0) = A_o = 20\log(\frac{R_S + R_L}{2\sqrt{R_S R_L}})$ for all N. The passband attenuation $A(\Omega)$ varies

$$\text{from } A_o \text{ to } A_o + 20\log\sqrt{1+\varepsilon^2} \quad \text{when } N \text{ is odd}$$
$$\text{from } A_o \text{ to } A_o - 20\log\sqrt{1+\varepsilon^2} \quad \text{when } N \text{ is even}$$

as shown in Fig. 7.48.

The plain gain specifications shown in Fig. 7.49b are related to the effective attenuation specifications as follows:

$$H_C = H_o \cdot 10^{-\frac{A_{\max}}{20}} \qquad H_S = H_o \cdot 10^{-\frac{A_{\min}}{20}} \quad \text{with } H_o = \frac{R_L}{R_S + R_L} 10^{\frac{A_{\max}}{20}(1-\eta)}$$

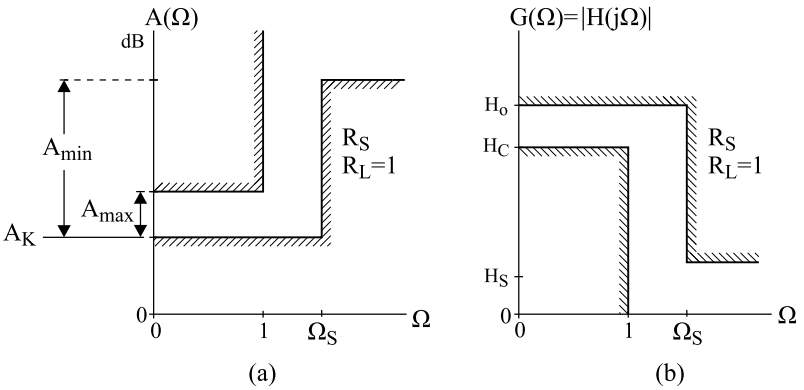

Fig. 7.49 (**a**) Effective attenuation specifications. (**b**) Plain gain specifications

Setting $A(\Omega)$ from (7.68) equal to the circuit attenuation, we get:

$$A(\Omega) = A_K + 20\log\Big(\sqrt{1+\varepsilon^2 R_N^2(\Omega_S,\Omega)}\Big) = 20\log\Big(\frac{1}{2}\sqrt{\frac{R_L}{R_S}}\frac{1}{|H(j\Omega)|}\Big)$$

$$\Rightarrow \quad |H(j\Omega)|^2 = \frac{(\frac{R_L}{R_S+R_L})^2(1+\varepsilon^2)^{1-\eta}}{1+\varepsilon^2 R_N^2(\Omega_S,\Omega)} \tag{7.72}$$

The reflection coefficient related function $\rho(s)\rho(-s)$ can be determined from Feldtkeller's equation (6.49):

$$\rho(s)\rho(-s) = 1 - \frac{4R_S}{R_L}|H(j\Omega)|^2_{\Omega^2=-s^2} = 1 - \frac{\frac{4R_S R_L}{(R_S+R_L)^2}(1+\varepsilon^2)^{1-\eta}}{1+\varepsilon^2 R_N^2(\Omega_S,\Omega)|_{\Omega^2=-s^2}} \tag{7.73}$$

Function $\rho(s)$ can then be isolated, taking into account that $\rho(s)$ and $\rho(-s)$ have opposite poles and opposite zeros and that the poles of $\rho(s)$ lie in the left half s-plane. Since there are no restrictions for the location of the zeros of $\rho(s)$, the above procedure leads to more than one function $\rho(s)$ and therefore (7.3)–(7.4) can give more than one function for $Z_1(s)$, which, when synthesized, yield more than one filter circuits.

The integer order N of the elliptic approximation is the rounded up decimal order N_d given by (4.47):

$$N_d = \frac{K(k)}{K(\sqrt{1-k^2})} \cdot \frac{K(\sqrt{1-g^2})}{K(g)} \tag{7.74}$$

where

$$k = \frac{1}{\Omega_S} < 1 \quad \text{and} \quad g = \sqrt{\frac{10^{A_{\max}/10}-1}{10^{A_{\min}/10}-1}} \tag{7.75}$$

$K(x)$ is the complete elliptic integral presented in Chap. 4, where the range of the permitted values of the ripple factor ε has also been given (see (4.58)):

$$\frac{\sqrt{10^{\frac{A_{\min}}{10}}-1}}{L_N(\Omega_S)} = \varepsilon_{\min} \le \varepsilon \le \varepsilon_{\max} = \sqrt{10^{\frac{A_{\max}}{10}}-1} \tag{7.76}$$

$L_N(\Omega_S)$ is the discrimination factor

$$L_N(\Omega_S) = R_N(\Omega_S, \Omega_S) \tag{7.77}$$

7.5.1 Odd Order Elliptic Passive Filters

When order N is odd, the passband attenuation plot is above A_o and $A(\infty) = \infty$. As a result, odd order elliptic filters do not present any design complications when following the synthesis procedure used in other approximations, i.e. determination of $\rho(s)$ from (7.73) and of $Z_1(s)$ from (7.3) or (7.4):

$$Z_{1a}(s) = R_S \frac{1-\rho(s)}{1+\rho(s)} \tag{7.78}$$

$$Z_{1b}(s) = R_S \frac{1+\rho(s)}{1-\rho(s)} \tag{7.79}$$

$Z_{1b}(s)$ has a pole at infinity which is removed as a series inductor resulting in a ladder starting with a series inductor. $Y_{1a}(s)$ has a pole at infinity which is removed as a shunt capacitor resulting in a ladder starting with a shunt capacitor. This is shown in Figs. 7.50 and 7.51. However, due to the transfer function zeros (attenuation poles), the synthesis of $Z_{1b}(s)$ or $Y_{1a}(s)$ cannot be accomplished solely by sequential removals of poles at infinity as in the case of all-pole approximations. In the elliptic case, minimum positive real functions emerge which require a Brune cycle (see Chap. 11), each producing a resonant LC circuit as shown in Figs. 7.50 and 7.51.

Example 7.19 Design an elliptic lowpass filter from the following normalized ($\Omega_C = 1$, $R_L = 1$) specifications:

$$\{A_{\max} = 0.5 \text{ dB},\ A_{\min} = 30 \text{ dB},\ \Omega_S = 2,\ R_S = 0.5\}$$

The decimal order N_d is determined from (7.74), where the complete elliptic integral can be calculated using the AGM according to Chap. 4:

$$N_d = 2.93184 \quad \Rightarrow \quad N = 3$$

The elliptic rational function for $N = 3$ and $\Omega_S = 2$ is determined from (7.69)–(7.71):

$$R_N(\Omega_S, \Omega) = R_3(2, \Omega) = -18.558954 \frac{\Omega(\Omega^2 - 0.88103084^2)}{\Omega^2 - 2.27006809^2}$$

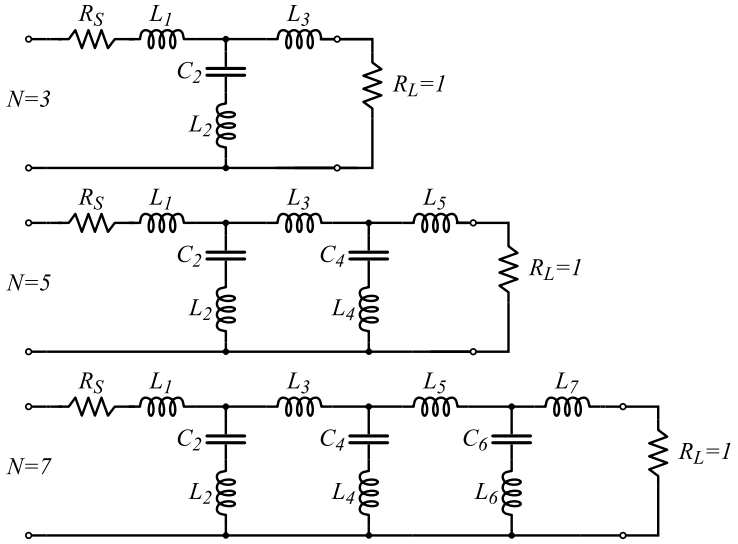

Fig. 7.50 Typical odd order elliptic filters

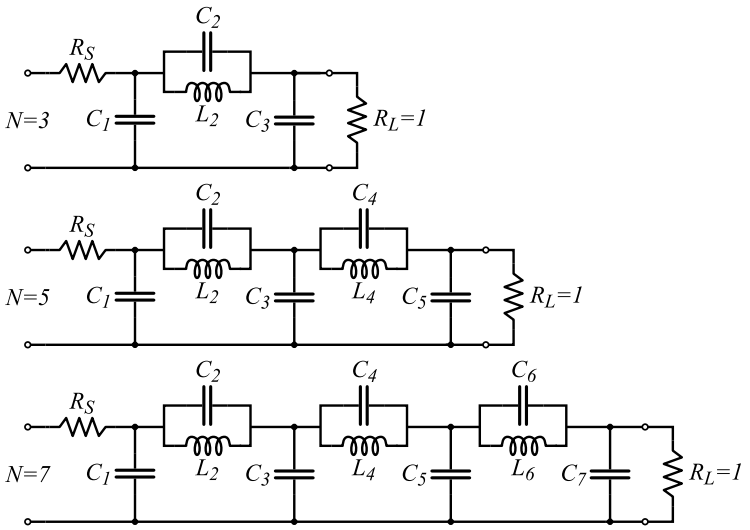

Fig. 7.51 Typical odd order elliptic filters

Using $\varepsilon = \varepsilon_{\max} = 0.349311$ from (7.76), (7.72) yields

$$|H(j\Omega)|^2 = \frac{(\frac{R_L}{R_S+R_L})^2(1+\varepsilon^2)^{1-\eta}}{1+\varepsilon^2 R_N^2(\Omega_S,\Omega)} = \frac{4/9}{1+\varepsilon^2 R_3^2(2,\Omega)}$$

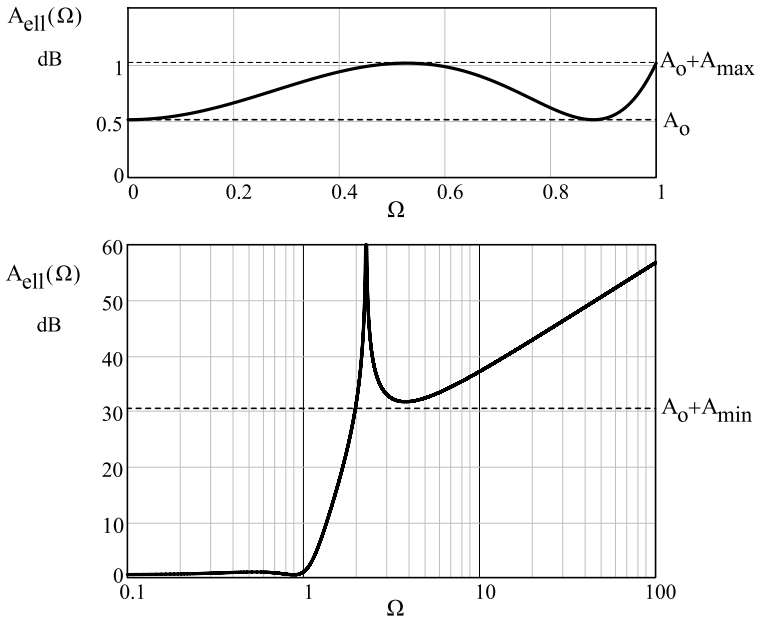

Fig. 7.52 Passband and full attenuation response

$$\Rightarrow \quad |H(j\Omega)|^2 = \frac{4\Omega^4 - 41.225673\Omega^2 + 106.2222575}{378.246575\Omega^6 - 578.201588\Omega^4 + 135.139676\Omega^2 + 239.000079}$$

Before we continue with synthesis, the correctness of $|H(j\Omega)|^2$ will be checked by plotting the attenuation

$$A_{ell}(\Omega) = 20\log\left(\frac{1}{2}\sqrt{\frac{R_L}{R_S}}\frac{1}{|H(j\Omega)|}\right)$$

The corresponding plots are shown in Fig. 7.52 and are exactly as expected.

Therefore, the synthesis procedure may start by determining $\rho(s)\rho(-s)$ from (7.73):

$$\rho(s)\rho(-s) = \frac{s^6 + 1.5497858s^4 + 0.5752507s^2 - 0.070237}{s^6 + 1.5286265s^4 + 0.3571746s^2 - 0.6321330}$$

The poles and zeros of $\rho(s)\rho(-s)$ are calculated using a mathematical software package and are given below:

Zeros of $\rho(s)\rho(-s)$	Poles of $\rho(s)\rho(-s)$
-0.309561329561	-0.69221756
$-0.1290663427 + j0.91622327589$	$-0.268965786 - j1.037419121$
$-0.1290663427 - j0.91622327589$	$-0.268965786 + j1.037419121$
$+0.1290663427 + j0.91622327589$	$+0.268965786 + j1.037419121$
$+0.1290663427 - j0.91622327589$	$+0.268965786 - j1.037419121$
$+0.309561329561$	$+0.69221756$

Left half s-plane poles are allocated to $\rho(s)$ and their opposites, located in the right half s-plane, to $\rho(-s)$. The corresponding denominator polynomial $D_\rho(s)$ of $\rho(s)$ will be:

$$D_\rho(s) = s^3 + 1.23014913s^2 + 1.52094671s + 0.795067956$$

For the zeros of $\rho(s)$, there are six possible choices and we select one, the left half s-plane zeros. For this particular choice, the numerator polynomial $N_\rho(s)$ of $\rho(s)$ is:

$$N_\rho(s) = s^3 + 0.56769403s^2 + 0.936031114s + 0.265022655$$

For this choice of zeros, we get:

$$\rho(s) = \frac{s^3 + 0.56769403s^2 + 0.936031114s + 0.265022655}{s^3 + 1.23014913s^2 + 1.52094671s + 0.795067956}$$

The input impedance $Z_1(s)$ can be determined from (7.4)

$$Z_{1b}(s) = R_S \frac{1 + \rho(s)}{1 - \rho(s)}$$

to get:

$$Z_1(s) = \frac{s^3 + 0.898921582s^2 + 1.22848891s + 0.53004530}{0.662455099s^2 + 0.584915592s + 0.53004530}$$

$Z_1(s)$ has a pole at infinity and it can be removed as a series inductor $L_1 = 1.0/0.662455099 = 1.50953627$ leaving the remaining impedance $Z_2(s)$

$$Z_2(s) = Z_1(s) - sL_1 = \frac{0.01597028s^2 + 0.42836630s + 0.5300453}{0.662455099s^2 + 0.584915592s + 0.5300453}$$

as shown in Fig. 7.53.

$Z_2(s)$ does not have any poles or zeros on the $j\omega$-axis and it is minimum positive real requiring a Brune cycle in order to continue the synthesis. It can be found that the real part $\mathrm{Re}[Z_2(j\Omega)]$ becomes zero at $\Omega_1 = 2.270068$ and $X_1 = \mathrm{Im}[Z_2(j\Omega_1)] = -0.33721$. According to Brune's method, a negative series inductor

$$L_{11} = \frac{X_1}{\Omega_1} = -0.148546$$

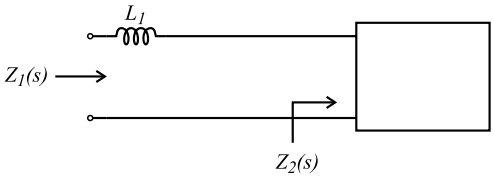

Fig. 7.53 Removal of impedance pole at infinity

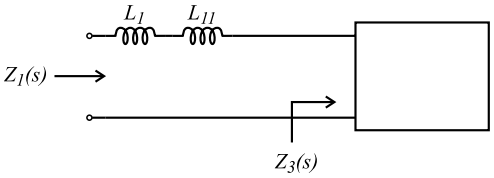

Fig. 7.54 Removal of a negative inductor

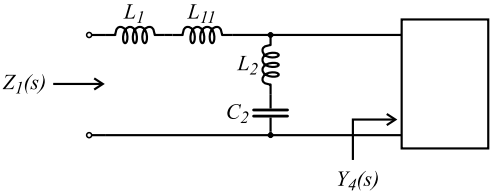

Fig. 7.55 Removal of a shunt arm series LC circuit

can be removed from $Z_2(s)$, in which case the remaining impedance will be

$$Z_3(s) = Z_2(s) - (-0.148546s) = \frac{s^3 + 1.0452423s^2 + 5.1532086s + 5.3863546}{6.73191147s^2 + 5.943950s + 5.3863546}$$

Figure 7.54 shows the result of this synthesis stage.

The admittance

$$Y_3(s) = Z_3^{-1}(s) = \frac{6.73191147s^2 + 5.943950s + 5.3863546}{s^3 + 1.0452423s^2 + 5.1532086s + 5.3863546}$$

has a real pole at $s = -1.04524277658$ and an imaginary conjugate pole pair $\pm j\Omega_2$ with $\Omega_2 = 2.270068$. This imaginary pole pair can be removed as a shunt arm series resonant circuit as shown in Fig. 7.55 with

$$L_2 = \frac{1}{2k_2} \qquad C_2 = \frac{2k_2}{\Omega_2} \quad \text{where } k_2 = 2.843334 \text{ and } \Omega_2 = 2.270068$$
$$\Rightarrow \quad L_2 = 0.17585 \qquad C_2 = 1.10352$$

(k_2 is the residue of $Y_3(s)$ at pole $j\Omega_2$, see Chap. 12). The remaining admittance $Y_4(s)$ after removing the imaginary conjugate pole pair will be

$$Y_4(s) = \frac{1}{0.9567156s + 1} \quad \Rightarrow \quad Z_4(s) = 0.9567156s + 1$$

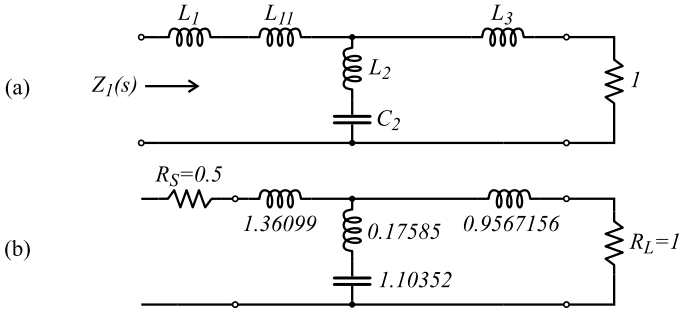

Fig. 7.56 Elliptic filter: (**a**) normalized, (**b**) denormalized

which is an inductor $L_3 = 0.9567156$ in series with $R_L = 1$ as shown in Fig. 7.56a. The final elliptic filter is shown in Fig. 7.56b, where $L_1 = 1.50953627$ and $L_{11} = -0.148546$ have been combined in one positive inductor $L = 1.50953627 - 0.148546 = 1.36099$.

Analyzing the final filter circuit, we find

$$H(s) = \frac{0.1028573(s^2 + 2.270068^2)}{(s + 0.6922175)(s^2 + 0.5379315s + 1.14858102)}$$

and the corresponding attenuation plots are found to be identical to those of Fig. 7.52.

7.5.2 Even Order Elliptic Passive Filters

The order of the passive elliptic filter depends on the specifications and is determined from the order inequality (7.74). When it is even, we have two problems:

1. According to (4.29), when N is even

$$\lim_{\Omega \to \infty} R_N(\Omega_S, \Omega) = L_N(\Omega_S) = R_N(\Omega_S, \Omega_S)$$

   which is a finite value. Therefore, the attenuation function $A(\Omega)$ as defined in (7.68) will not have a pole at infinity as required by (6.52) of Sect. 6.4, and as a consequence $A(\Omega)$ cannot be realized by a doubly resistively terminated LC two-port without coupled elements (transformers). This problem can be overcome by modifying the elliptic rational function by moving its higher pole to infinity. This modification leads to a family of modified elliptic filters referred to as type-B elliptic filters. Figure 7.57 shows an indicative plot of the attenuation of a type-B elliptic filter with $N = 4$.
2. When N is even, the passband attenuation plot is below A_o and therefore there is a maximum value of ripple $A_{\max}$ which can be realized by a normalized doubly resistively terminated LC two-port with specified R_S and $R_L = 1$. This maximum

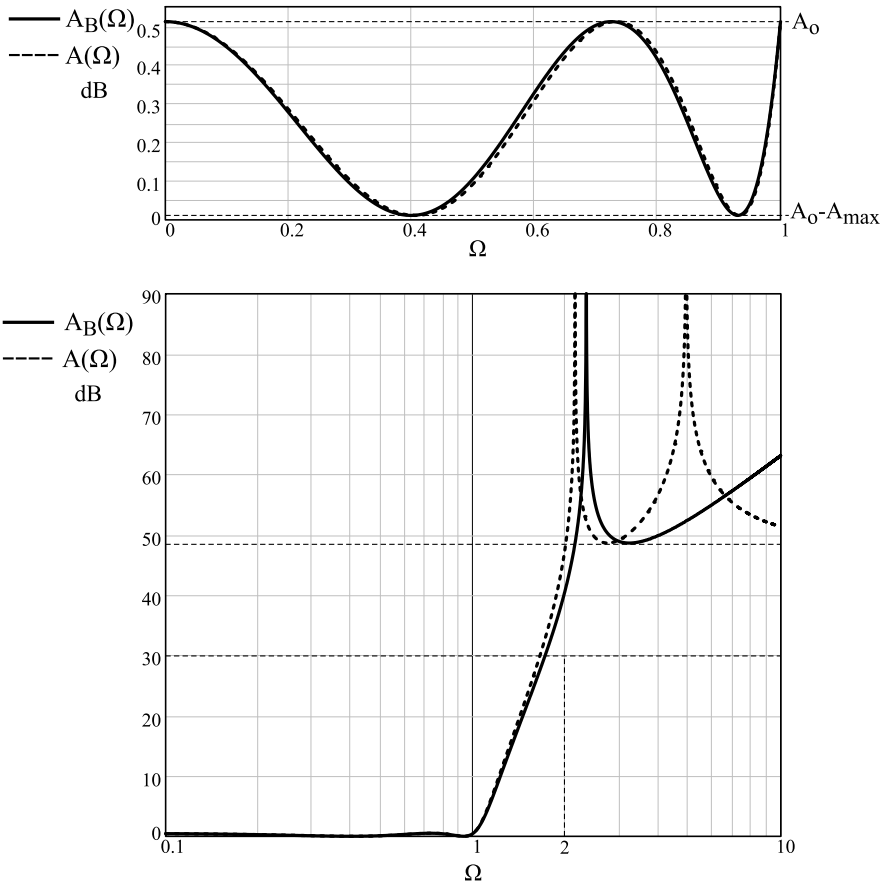

Fig. 7.57 Attenuation of elliptic filters ($N = 4$): Type-A (*dashed*), Type-B (*thick*)

ripple is of course A_o. On the other hand, a specified ripple $A_{\max}$ can only be realized if

$$A_{\max} \le 20\log\left(\frac{R_S+1}{2\sqrt{R_S}}\right) \quad \Leftrightarrow \quad R_S^2 - 2\left(2\cdot 10^{\frac{A_{\max}}{10}} - 1\right)R_S + 1 \ge 0 \tag{7.80}$$

Condition (7.80) holds only if $R_S \ge R_{S2}$ or $R_S \le R_{S1}$, where R_{S1} and R_{S1} are the roots of $R_S^2 - 2(2\cdot 10^{\frac{A_{\max}}{10}} - 1)R_S + 1 = 0$:

$$\begin{aligned} R_{S1} &= 2\cdot 10^{\frac{A_{\max}}{10}} - 1 - 2\sqrt{10^{\frac{A_{\max}}{10}}\left(10^{\frac{A_{\max}}{10}} - 1\right)} = R_{S2}^{-1} \\ R_{S2} &= 2\cdot 10^{\frac{A_{\max}}{10}} - 1 + 2\sqrt{10^{\frac{A_{\max}}{10}}\left(10^{\frac{A_{\max}}{10}} - 1\right)} = R_{S1}^{-1} \end{aligned} \tag{7.81}$$

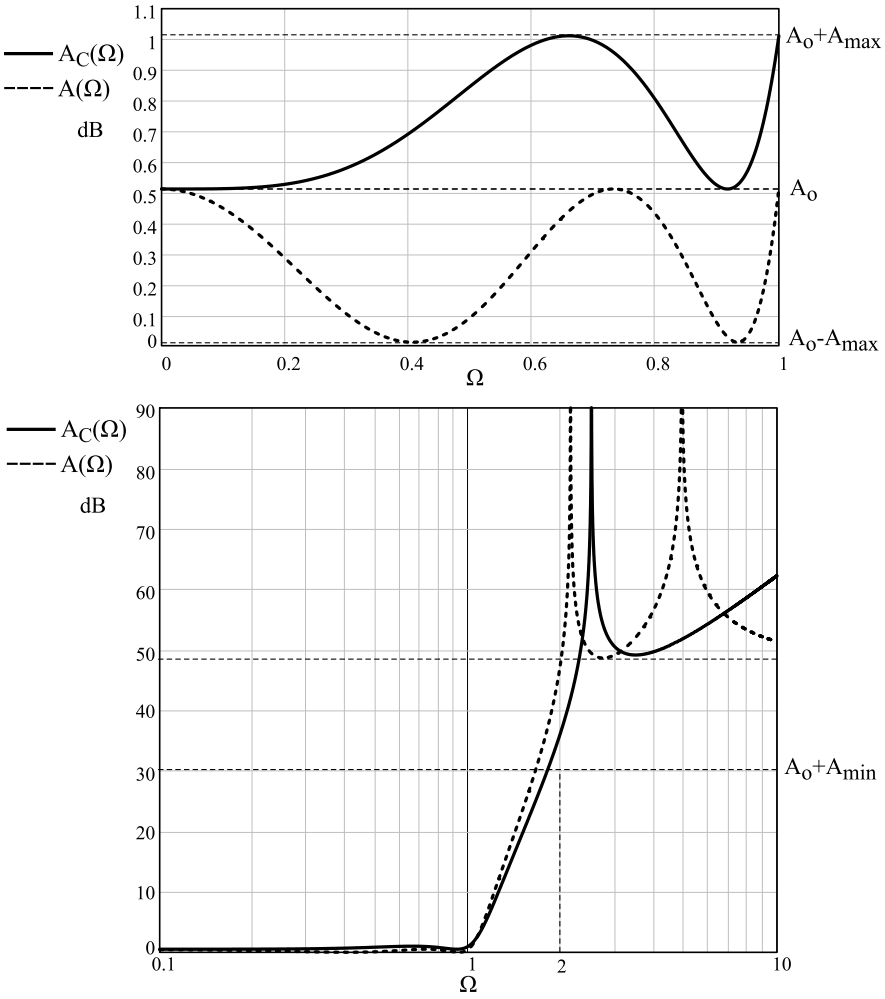

Fig. 7.58 Attenuation of elliptic filters ($N = 4$): Type-A (*dashed*), Type-C (*thick*)

When ripple $A_{\max}$ is given, R_{S1} and R_{S2} define the range of the non-permitted values of R_S as in the even order Chebyshev case, namely (7.32)–(7.33). This limitation can be overcome by modifying the elliptic rational function, moving its lower root to zero as we did in the modified Chebyshev case. This modification, when applied to the already modified ERF in order to have attenuation pole at infinity, leads to a family of modified elliptic filters referred to as type-C elliptic filters. The passband attenuation of type-C elliptic filters is above A_o, as in the odd order case, and has $N - 1$ extrema. Figure 7.58 shows an indicative plot of the attenuation of a type-C elliptic filter with $N = 4$.

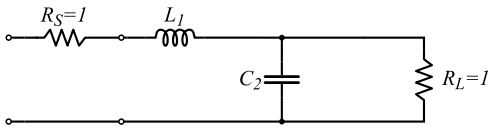

Fig. 7.59 Circuit for Problems 7.7 and 7.8

7.6 Problems

7.1 In Example 7.2, (7.4) was used with $\rho_I(s)$ to determine $Z_{1I}(s)$ of (7.16) with $Z_{1I}(0) = R_L = 1$. Verify that, if (7.3) had been used instead, for the resulting input impedance $Z_1(s)$, we would have $Z_1(0) \neq R_L = 1$.

7.2 In Example 7.2, determine the input impedance using $\rho_{IV}(s)$ (set IV of the zeros of $\rho(s)\rho(-s)$).

7.3 In Example 7.2, determine the reflection coefficient $\rho(s)$ and the corresponding input impedance $Z_{II}(s)$ using set II of the zeros of $\rho(s)\rho(-s)$ of Fig. 7.7.

7.4 In Example 7.2, determine the reflection coefficient $\rho(s)$ and the corresponding input impedance $Z_{III}(s)$ using set III of the zeros of $\rho(s)\rho(-s)$ of Fig. 7.7.

7.5 Design a 2nd order prototype passive lowpass Butterworth filter with equal terminations $R_S = R_L = 1$.

7.6 Verify that all four expressions $Z_{1kb}(s)$ of Example 7.4 are correct. Why are we using (7.4) and not (7.3) to determine the input impedance?

7.7 Determine the element values of the normalized Butterworth lowpass filter of Fig. 7.59 by analysis, so as to have $A(1) = 2$ dB.

7.8 Determine the element values of the normalized Chebyshev lowpass filter of Fig. 7.59 by analysis, so as to have passband ripple $A_{\max} = 2$ dB.

7.9 Determine the element values of the normalized Butterworth lowpass filter of Fig. 7.60 by analysis, so as to have $A(1) = 2$ dB.

7.10 Determine the element values of the normalized Chebyshev lowpass filter of Fig. 7.60 by analysis, so as to have passband ripple $A_{\max} = 2$ dB.

7.11 Explain why the normalized lowpass specifications ($\Omega_C = 1$ and $R_L = 1$)

$$\{A_{\max} = 1 \text{ dB},\ A_{\min} = 30 \text{ dB},\ \Omega_S = 2.2,\ R_S = 0.5\}$$

cannot be met by a passive Chebyshev filter with $N = 4$.

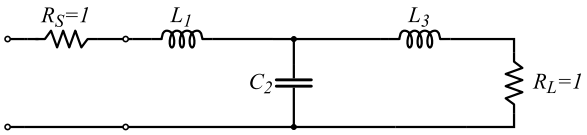

Fig. 7.60 Circuit for Problems 7.9 and 7.10

7.12 Explain why the normalized lowpass specifications ($\Omega_C = 1$ and $R_L = 1$)

$$\{A_{\max} = 0.511525 \text{ dB},\ A_{\min} = 36 \text{ dB},\ \Omega_S = 2.2,\ R_S = 0.5\}$$

cannot be met by a passive Chebyshev filter with $N = 4$.

7.13 Design the Chebyshev filter of Example 7.12 using choices III and IV for the zeros of $\rho(s)$.

7.14 Synthesize $Z_{1b}(s) = \frac{s^2+0.6608s+1.0108}{1.5296s+1.0108}$ of Example 7.10.

7.15 Design the Pascal filter of Example 7.14 allocating the right half s-plane zeros of $\rho(s)\rho(-s)$ to $\rho(s)$.

References[1]

1. Chen, W.-K. (ed.): Passive, Active and Digital Filters. The Circuits and Filters Handbook, vol. V. CRC Press, Boca Raton (2009)
2. Chirlian, P.M.: Signals and Filters. Springer, Berlin (1994)
3. Christian, E., Eisenmann, E.: Filter Design Tables and Graphs. Wiley, New York (1966)
4. Daniels, R.W.: Approximation Methods for Electronic Filter Design. McGraw-Hill, New York (1974)
5. Dimopoulos, H.G., Sarri, E.: The modified pascal polynomial approximation and filter design method. Int. J. Circuit Theory Appl. (2010). doi:10.1002/cta.711
6. Lutovac, M.D., Tosic, D.V., Evans, B.L.: Filter Design for Signal Processing using MATLAB and Mathematica. Prentice Hall, Upper Saddle River (2001)
7. Paarmann, L.D.: Design and Analysis of Analog Filters—A Signal Processing Perspective—With MATLAB Examples. Kluwer Academic, Dordrecht (2001)
8. Schaumann, R., Van Valkenburg, M.E.: Design of Analog Filters. Oxford University Press, London (2001)
9. Sedra, A., Bracket, P.O.: Filter Theory and Design: Active and Passive. Pitman, London (1978)
10. Van Valkenburg, M.E.: Analog Filter Design. Oxford University Press, London (1982)
11. Williams, A., Taylor, F.: Electronic Filter Design Handbook. McGraw-Hill, New York (2006)
12. Zverev, A.I.: Handbook of Filter Synthesis. Wiley, New York (1967)

[1] All references, whether or not cited within the text, are recommended for further reading.

Active Simulation of Passive Ladder Filters 8

There are two general and systematic methods for the design of active filters. The first is based on the determination of the corresponding transfer function $H(s)$ using one of the known approximations. Then, the transfer function is seen as a product of first and second order terms, each related to a real pole or to a conjugate pole pair of $H(s)$. These first and second order terms are then realized by simple active circuits, which are finally cascaded to yield the final filter structure. Some examples of this simple method have been given in previous chapters (Examples 2.4, 2.9, 5.3, 5.6 and 5.9). Active filters designed using this simple straightforward method, the cascade approach, are usually more sensitive than active filters designed by simulating passive ladder filters.

The simulation of passive, doubly resistively terminated LC ladder filters (Fig. 8.1) is the second major method of designing active filters. In fact, a passive filter is initially designed to meet the specifications, which is then simulated using various methods, as will be explained in the next sections.

Active filters derived from passive LC circuits by some form of simulation technique maintain some desirable properties of the passive original. For example, the sensitivity, of passive filters within the passband is extremely low since it appears to be proportional to the reflection coefficient ρ, which assumes very low values within the passband. This low passband sensitivity property is inherited by the simulated circuit.

H.J. Orchard proved [7] that in doubly resistively terminated ladder LC filters, the first order differential gain sensitivity with respect to inductors and capacitors is very low in the passband and zero at the frequencies of maximum power transfer, where the effective attenuation and the reflection coefficient become zero. Since the passband attenuation is a smooth continuous function, the corresponding sensitivity at frequencies between these maximum power transfer frequencies remains low.

Doubly resistively terminated LC ladder filters with maximum power transfer frequencies, referred to as *well-designed doubly terminated LC ladder filters*, can be used as a design vehicle for active filters. Such passive filters, when simulated using active circuits, lead to active filters that maintain the low sensitivity property of the original passive circuits.

H.G. Dimopoulos, *Analog Electronic Filters*, Analog Circuits and Signal Processing,
DOI 10.1007/978-94-007-2190-6_8, © Springer Science+Business Media B.V. 2012

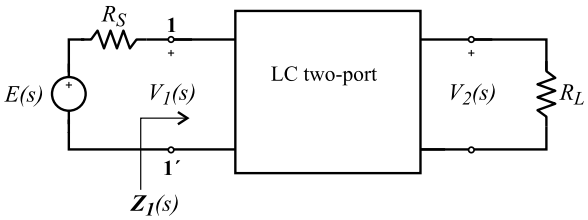

Fig. 8.1 The doubly resistively terminated passive two-port

For the active simulation of doubly resistively terminated LC ladder filters, three methods are used:

1. The direct simulation method, where inductors are replaced by simulated inductors, i.e. active inductorless circuits with inductive behavior.
2. The frequency dependent impedance scaling of the passive RLC ladder, which leads to inductorless circuits, as will be seen in Sect. 8.2.
3. The structural simulation method, which, although it appears in many distinct forms (Wave Active Filters, Leap-frog, Signal Flow Graph etc.), these can all be seen as special cases of the more general Linear Transformation Active (LTA) method [5], as will be seen in Sect. 8.3. With proper selection of the linear transformation matrices, the LTA approach can lead to circuit structures suitable for op amp realizations but also for realizations employing any other active device (OTAs, CCIIs etc.).

8.1 Inductance Simulation

The most straightforward method of transforming a passive ladder filter into an active inductorless circuit is to replace all its inductors by active circuits with inductive behavior, referred to as the *simulated inductors*. Simulated inductors are one-port circuits, the input driving-point impedance of which is of the form $Z_{IN}(s) = sL$. Although there are many circuits that behave like inductors, the most popular are the Riordan's and the Antoniou's circuits, which have been used for several decades.

8.1.1 Riordan's Simulated Inductor

Analyzing the Riordan's circuit of Fig. 8.2, we find that its input driving-point impedance $Z_{IN}(s)$ is given by:

$$Z_{IN}(s) = \frac{E(s)}{I(s)} = \frac{Z_1(s)Z_3(s)Z_5(s)}{Z_2(s)Z_4(s)} \tag{8.1}$$

It is clear that if Z_2 is a capacitor with impedance $Z_2(s) = \frac{1}{sC_2}$ and all the other impedances $Z_i(s)$ are resistors R_i, as in Fig. 8.3, the input impedance becomes

$$Z_{IN}(s) = s\frac{R_1R_3R_5C_2}{R_4} \tag{8.2}$$

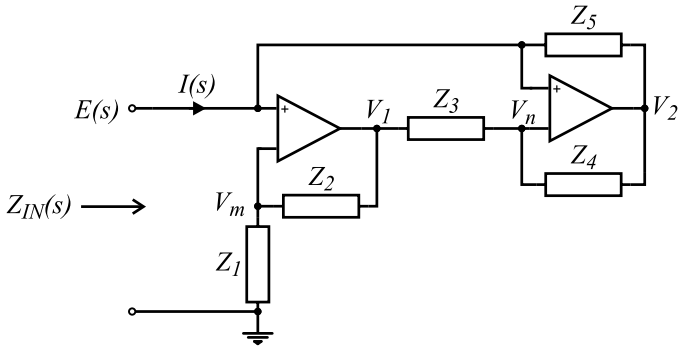

Fig. 8.2 Riordan's general impedance converter

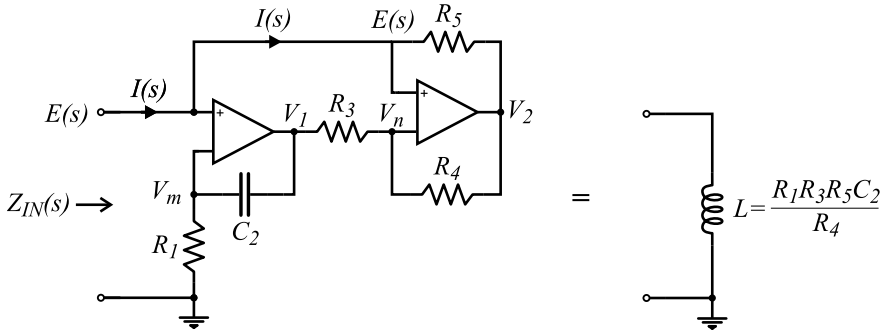

Fig. 8.3 Riordan's simulated inductor

which represents an inductor with inductance given by

$$L = \frac{R_1 R_3 R_5 C_2}{R_4} \tag{8.3}$$

Since one of the terminals of the input port of Riordan's circuit is ground, it realizes grounded simulated inductors. The floating simulated inductors will be presented in Sect. 8.1.3. Finally, it should be noted that if Z_4 is a capacitor with $Z_4(s) = \frac{1}{sC_4}$ and all the other impedances $Z_i(s)$ are resistors R_i, the circuit realizes a grounded simulated inductor with

$$L = \frac{R_1 R_3 R_5 C_4}{R_2}$$

Example 8.1 Figure 8.4 shows a passive Chebyshev highpass filter of order $N = 3$, designed to meet the following specifications:

$$f_C = 10\,\text{kHz} \qquad f_S = 333.33\,\text{kHz} \qquad A_{\max} = 0.5\,\text{dB} \qquad A_{\min} = 30\,\text{dB}$$

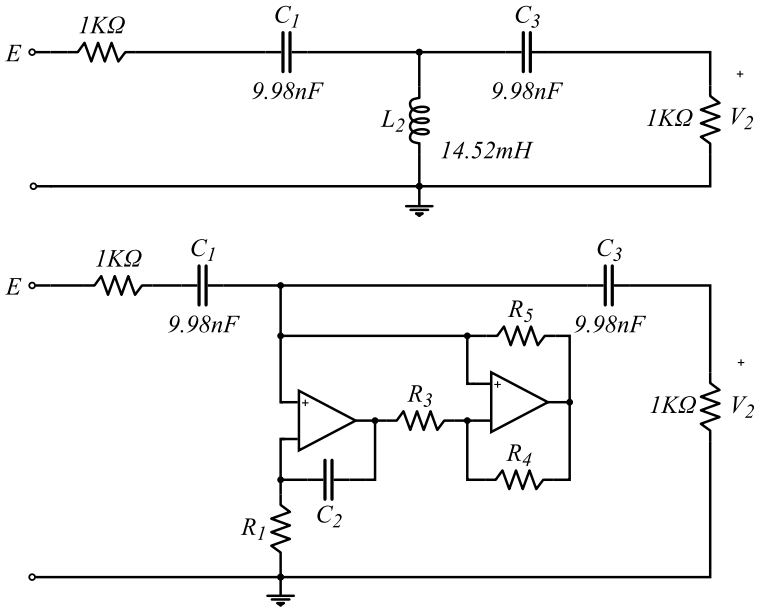

Fig. 8.4 Highpass filter of Example 8.1

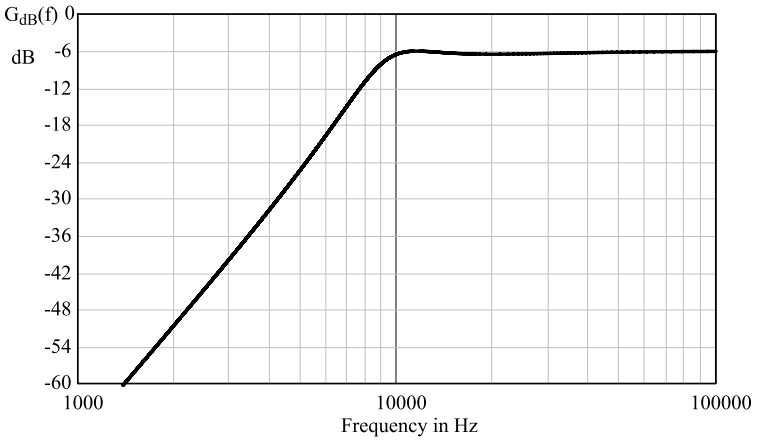

Fig. 8.5 Logarithmic gain plot of active filter of Example 8.1

The grounded inductor of the passive filter is replaced by a Riordan's simulated inductor with $C_2 = 9.98$ nF. If we let $R_3 = R_4 = R_5 = R$, then the value of R_1 can be calculated from $R_1 = \frac{L_2}{RC_2}$. For $R = 1000$ Ohm, $C_2 = 9.98$ nF and $L_2 = 14.52$ mH, we get $R_1 = 1455$ Ohm. The logarithmic gain plots of the passive and the active circuits are identical, as expected, and they are shown in Fig. 8.5.

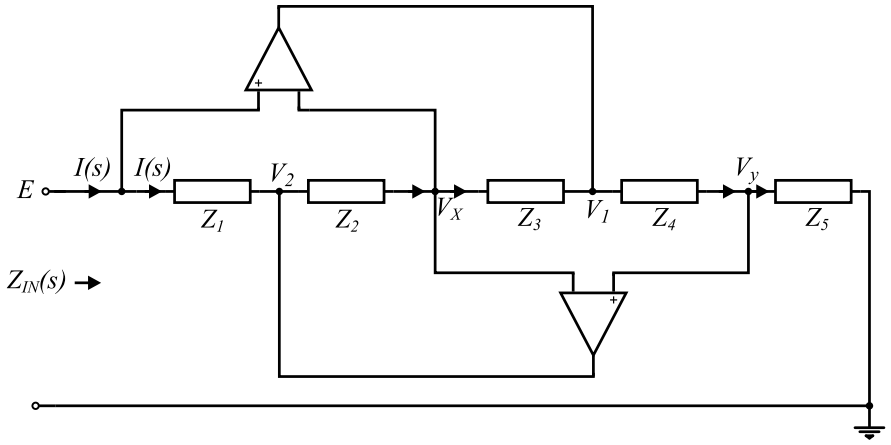

Fig. 8.6 Antoniou's general circuit

8.1.2 Antoniou's Simulated Inductor

The input driving-point impedance of the circuit of Fig. 8.6, proposed by A. Antoniou, is given by:

$$Z_{IN}(s) = \frac{E(s)}{I(s)} = \frac{Z_1(s)Z_3(s)Z_5(s)}{Z_2(s)Z_4(s)} \tag{8.4}$$

The circuit is a general impedance converter (GIC), which, when Z_2 represents a capacitor and all the other impedances Z_i represent resistors R_i, as Fig. 8.7, gives

$$Z_{IN}(s) = s\frac{R_1R_3R_5C_2}{R_4} \tag{8.5}$$

which is the impedance of an inductor with inductance

$$L = \frac{R_1R_3R_5C_2}{R_4} \tag{8.6}$$

It is clear that when Z_4 represents a capacitor and all the other impedances Z_i represent resistors R_i, the input impedance of the circuit will be that of an inductor

$$L = \frac{R_1R_3R_5C_4}{R_2}$$

Since one of the terminals of the input port of Antoniou's circuit is ground, it realizes grounded simulated inductors. The floating simulated inductors will be presented in the next section.

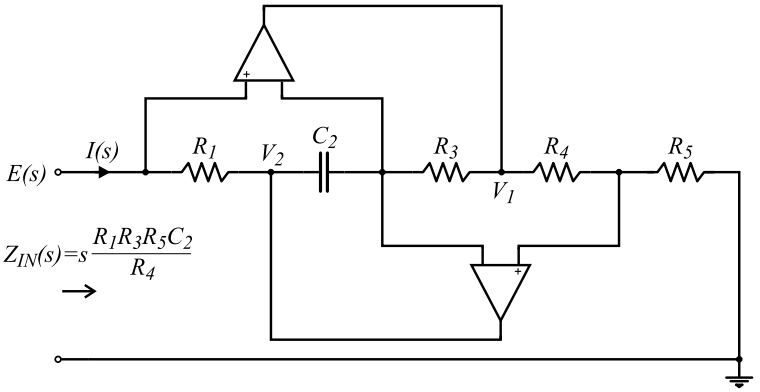

Fig. 8.7 Antoniou's simulated inductor

8.1.3 Floating Simulated Inductors

It has already been noted that both the Riordan's and the Antoniou's simulated inductors are grounded and therefore neither of these circuits can be directly used to simulate a floating inductor. Floating inductors are simulated using two identical grounded simulated inductor circuits connected back-to-back. Figure 8.8 shows two Antoniou's simulated inductors connected back-to-back and it will be shown that currents $I_1(s)$ and $I_2(s)$ are equal and in addition, the current-voltage relationship is given by:

$$I_1(s) = I_2(s) = \frac{1}{sL}(E_1(s) - E_2(s)) \tag{8.7}$$

In order to simplify the analysis, we consider ideal op amps with infinite input impedances and open loop gains. In this case, the inverting and non-inverting inputs of each op amp will have equal voltages, as shown in Fig. 8.8. Writing KCL for nodes a, b, c and d, we get:

$$\text{From node a:} \quad (V_2 - E_1)sC_2 = \frac{E_1 - V_1}{R_3}$$

$$\text{From node b:} \quad \frac{V_1 - E_1}{R_4} = \frac{E_1 - E_2}{2R_5}$$

$$\text{From node c:} \quad (E_2 - V_4)sC_2 = \frac{V_3 - E_2}{R_3}$$

$$\text{From node d:} \quad \frac{E_2 - V_3}{R_4} = \frac{E_1 - E_2}{2R_5}$$

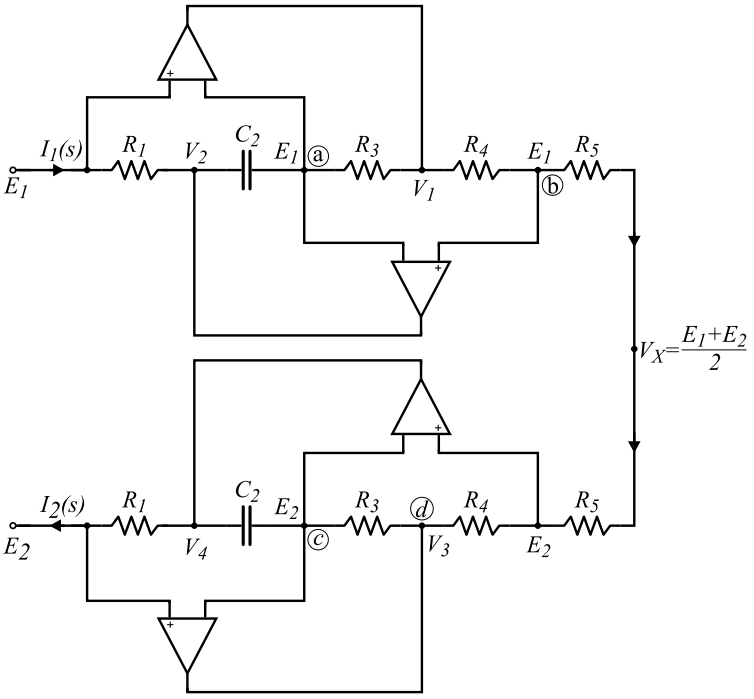

Fig. 8.8 Floating inductor using back-to-back connection of two Antoniou's simulated inductors

From the above four equations we find:

$$V_2(s) = \frac{(2sC_2R_3R_5 - R_4)E_1 + R_4E_2}{2sC_2R_3R_5}$$

$$V_4(s) = \frac{R_4E_1 + (2sC_2R_3R_5 - R_4)E_2}{2sC_2R_3R_5}$$

For the currents I_1 and I_2, we find that they are equal:

$$I_1 = \frac{E_1 - V_2}{R_1} = \frac{R_4}{2sC_2R_1R_3R_5}(E_1 - E_2)$$

$$I_2 = \frac{V_4 - E_2}{R_1} = \frac{R_4}{2sC_2R_1R_3R_5}(E_1 - E_2)$$

Therefore, the impedance of the floating element will be given by:

$$Z_{IN}(s) = \frac{E_1(s) - E_2(s)}{I_1(s)} = s\left(\frac{2R_1R_3R_5C_2}{R_4}\right)$$

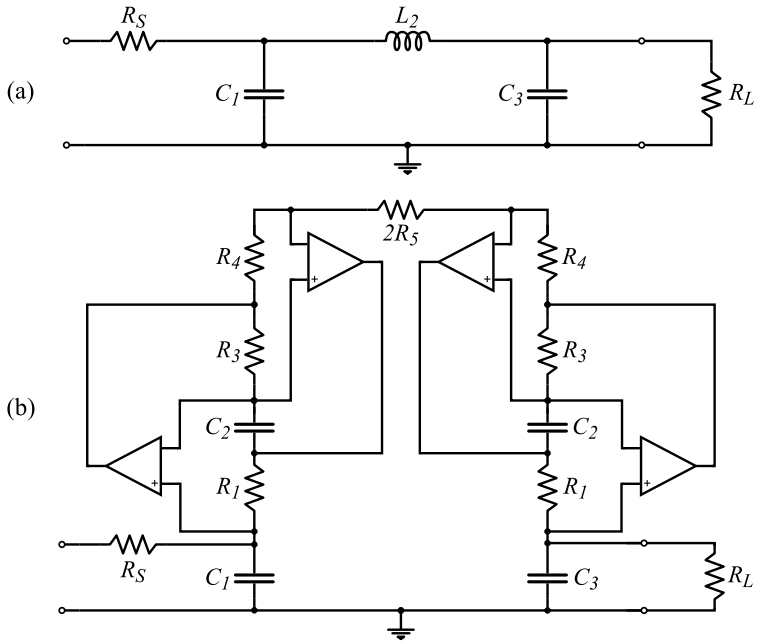

Fig. 8.9 The active-RC simulation of a third order passive lowpass filter

It is clear that the circuit simulates a floating inductor with inductance

$$L = 2\frac{R_1 R_3 R_5}{R_4} C_2 \tag{8.8}$$

It can be shown in a similar manner that the back-to-back connection of two identical Riordan's simulated inductors gives a floating inductor.

Example 8.2 Figure 8.9a shows a passive lowpass filter with

$$R_S = R_L = 1 \text{ kOhm} \qquad C_1 = C_3 = 31.1847 \text{ nF} \qquad L_2 = 63.6942 \text{ mH}$$

In Fig. 8.9b, the inductor L_2 has been replaced by a simulated floating inductor obtained as a back-to-back connection of two identical Antoniou's circuits with all resistors equal to $R = 1$ kOhm. The value of the two equal capacitors is calculated from (8.8): $C_2 = \frac{L_2}{2R^2} = 31.847$ nF.

Figure 8.10 shows the logarithmic gain of the passive and the active filters of Fig. 8.9.

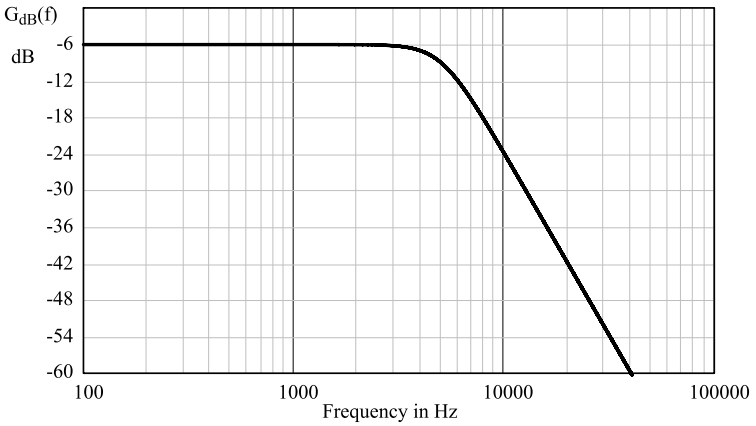

Fig. 8.10 The logarithmic gain plot of the simulated filter

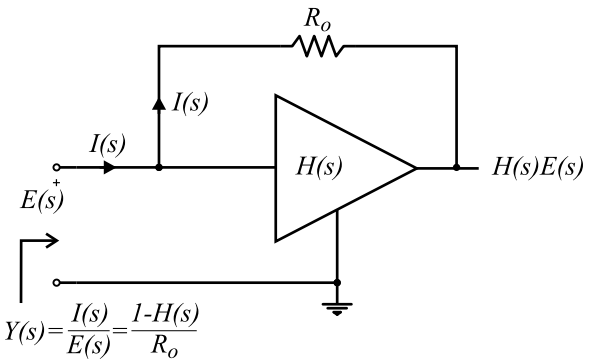

Fig. 8.11 A general circuit for the simulation of grounded inductors

8.1.4 A General Approach

Figure 8.11 shows a circuit with voltage transfer function $H(s)$. The output voltage is fed back to the input via a resistor R_o. Considering infinite input resistance and zero output resistance of the circuit, the input admittance of the device will be:

$$Y(s) = \frac{I(s)}{E(s)} = \frac{1 - H(s)}{R_o} \tag{8.9}$$

For

$$H(s) = 1 - \frac{1}{sT_d} \tag{8.10}$$

the input admittance of (8.9) becomes

$$Y(s) = \frac{1}{sT_d R_o} \tag{8.11}$$

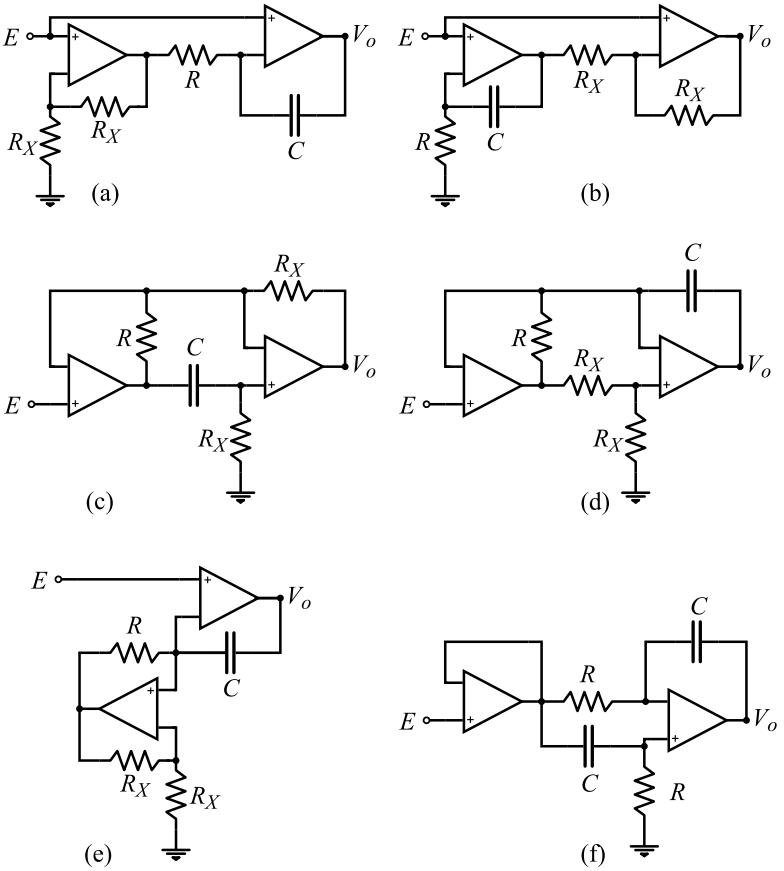

Fig. 8.12 Simulated inductors

which is the admittance of an inductor $L = T_d R_o$.

Figure 8.12 shows six circuits with voltage transfer function of the form $H(s) = 1 - \frac{1}{sT_d}$ where $T_d = RC$. All six circuits have infinite input and zero output resistance and therefore they can be used in the device of Fig. 8.11 to produce grounded simulated inductors.

When the circuits of Fig. 8.12a and b are used in the device of Fig. 8.11, the two Riordan's simulated inductors are obtained, as shown in Fig. 8.13. Similarly, the circuits of Fig. 8.12c and d lead to the Antoniou's simulated inductors, as shown in Fig. 8.14.

Using the circuit of Fig. 8.12e in the device of Fig. 8.11, a new grounded simulated inductor is derived, shown in Fig. 8.15. The new circuit is based on a negative resistor which appears between node a and ground.

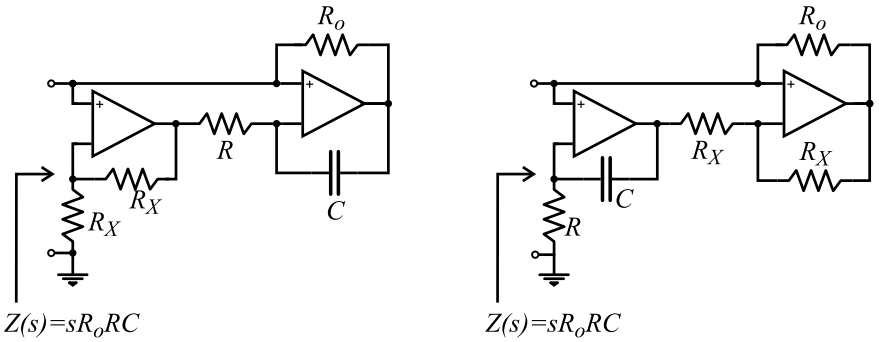

Fig. 8.13 Riordan's simulated inductors

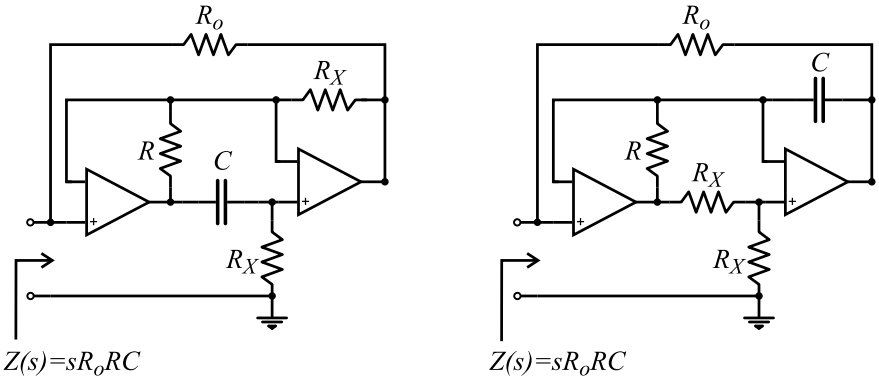

Fig. 8.14 Antoniou's simulated inductors

8.1.5 A Single Op Amp Simulated Inductor

Considering the op amp in the circuit of Fig. 8.16 to be ideal, the voltages of its inverting and non-inverting inputs become equal to $V_x = \frac{\lambda}{\lambda+1}E$. The current $I(s)$ entering the circuit is the sum of the currents of the three resistors R, R_o and kR_o:

$$I(s) = \frac{E-V_x}{R} + \frac{E-V_o}{R_o} + \frac{E-V_x}{kR_o} = \frac{E}{(\lambda+1)R} + \frac{E}{k(\lambda+1)R_o} + \frac{E-V_o}{R_o} \quad (8.12)$$

For the currents of the common node of the two capacitors, we have:

$$\frac{E-V_x}{kR_o} + (V_o - V_x)sC = s\mu C V_x \Rightarrow V_o = \frac{\lambda(\mu+1)}{\lambda+1}E - \frac{1}{sk(\lambda+1)R_o^2C} \quad (8.13)$$

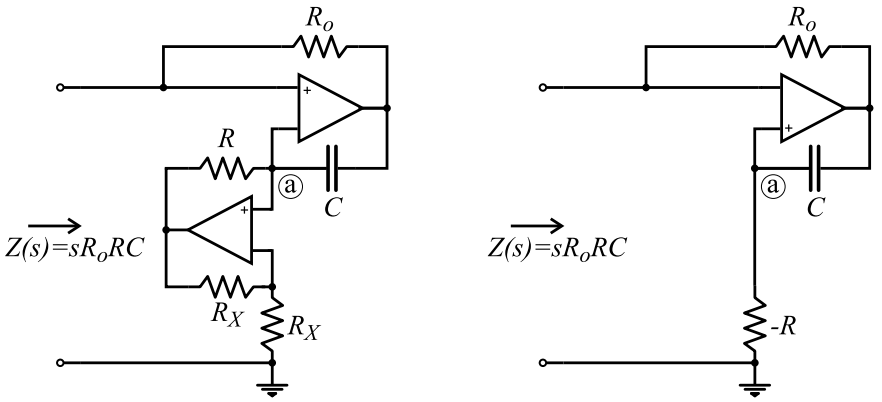

Fig. 8.15 Simulated inductors

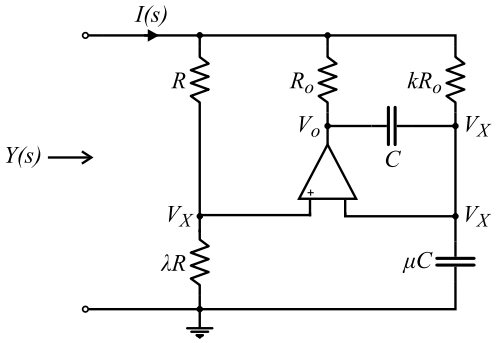

Fig. 8.16 Single operational amplifier simulated inductor

Combining (8.13) and (8.12) we find:

$$Y_{IN}(s) = \frac{E}{I(s)} = \frac{1}{\lambda+1}\left[\frac{1}{R} + \frac{1}{kR_o} + \frac{1-\lambda\mu}{R_o}\right] + \frac{1}{sk(\lambda+1)R_o^2C} \tag{8.14}$$

$Y_{IN}(s)$ represents a grounded resistor R_p in parallel with a grounded inductor L with:

$$\frac{1}{R_p} = \frac{1}{\lambda+1}\left[\frac{1}{R} + \frac{1}{kR_o} + \frac{1-\lambda\mu}{R_o}\right] \quad \text{and} \quad L = k(\lambda+1)R_o^2C \tag{8.15}$$

It is clear that for

$$\lambda\mu = 1 + \frac{R_o}{R} + \frac{1}{k} \quad \Rightarrow \quad \mu = \frac{k(1+\frac{R_o}{R})+1}{k\lambda} \tag{8.16}$$

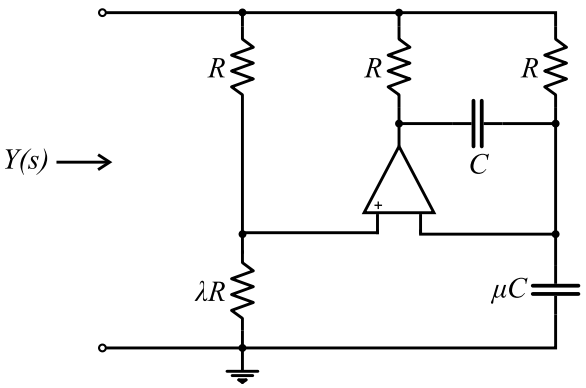

Fig. 8.17 The equal resistors single operational amplifier simulated inductor

we have $1/R_p = 0$ and the input admittance becomes

$$Y_{IN}(s) = \frac{1}{sk(\lambda+1)R_o^2C} \tag{8.17}$$

which is purely inductive. Since one terminal of the input port is ground, the circuit with its parameters satisfying (8.16) simulates a grounded inductor with $L = k(\lambda + 1)R_o^2C$.

It should be noted that the value of the simulated inductance $L = k(\lambda + 1)R_o^2C$ of (8.15) does not depend either on R or on μ. This means that the values of the parameters k, λ, R_o and C can be selected so as to give the desired value of L according to (8.17) and then R and μ can be used to make the parasitic conductance $1/R_p$ of (8.15) equal to zero.

Let us now consider that $R_o = R$ and $k = 1$. This equal resistance circuit is shown in Fig. 8.17.

To design the circuit so that it simulates a grounded inductor with given L:

1. λ and μ are selected so that $\lambda\mu = 3$.
2. The value of either R or C, is selected at will.
3. If R is selected, then from $L = (\lambda + 1)R^2C \Rightarrow C = \frac{L}{(\lambda+1)R^2}$.
   If C is selected, then from $L = (\lambda + 1)R^2C \Rightarrow R = \sqrt{\frac{L}{(\lambda+1)C}}$.

Example 8.3 In order to simulate a grounded inductor with $L = 16.506$ mH using the circuit of Fig. 8.17:

1. We select $\lambda = 3$ and $\mu = 1$ so that $\lambda\mu = 3$.
2. We select $C = 1$ nF.
3. From $L = (\lambda + 1)R^2C \Rightarrow R = \sqrt{\frac{L}{(\lambda+1)C}} = 2031$ Ohm.

In order to simulate a grounded inductor with $L = 22.566$ mH using the circuit of Fig. 8.17:

1. We select $\lambda = 3$ and $\mu = 1$ so that $\lambda\mu = 3$.
2. We select $C = 1$ nF.
3. From $L = (\lambda + 1)R^2C \Rightarrow R = \sqrt{\frac{L}{(\lambda+1)C}} = 2375$ Ohm.

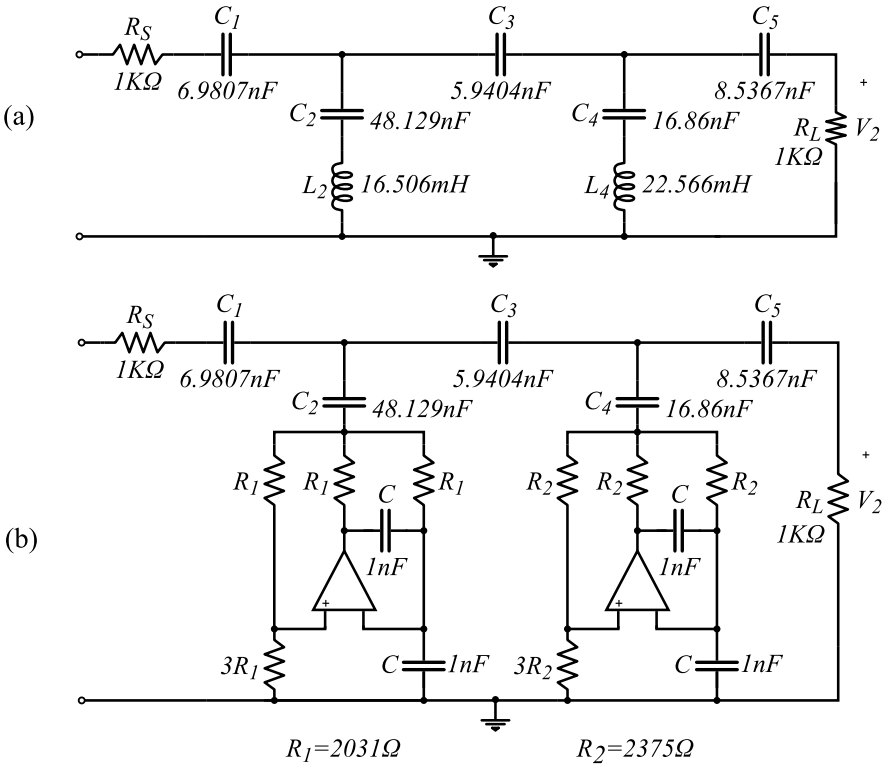

Fig. 8.18 The simulation of an elliptic highpass filter using the single op amp simulated inductor

Example 8.4 The grounded inductors of the passive elliptic highpass filter of Fig. 8.18a have been replaced by single amplifier simulated inductors. The resulting filter is shown in Fig. 8.18b and the necessary parameters have been calculated in Example 8.3. Simulation of the two circuits of Fig. 8.18 shows that their frequency responses are identical.

In order to simulate a floating inductor using the single op amp simulated inductor, two identical circuits must be connected back-to-back, as shown in Fig. 8.19.

For the back-to-back connection of Fig. 8.19, it can be shown that $I_1(s) = I_2(s)$ and that the input admittance is given by:

$$Y_{IN}(s) = \frac{1}{\lambda+1}\left[\frac{1}{R} + \frac{1}{kR_o} + \frac{1-\lambda\mu}{R_o}\right] + \frac{1}{2sk(\lambda+1)R_o^2C} \tag{8.18}$$

Setting

$$\lambda\mu = 1 + \frac{R_o}{R} + \frac{1}{k} \quad \Rightarrow \quad \mu = \frac{k(1+\frac{R_o}{R})+1}{k\lambda} \tag{8.19}$$

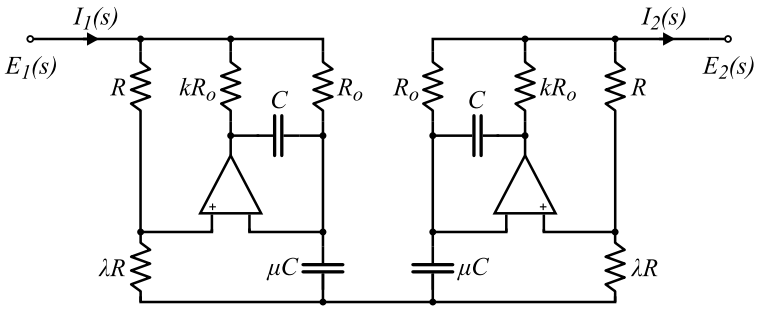

Fig. 8.19 Floating simulated inductor

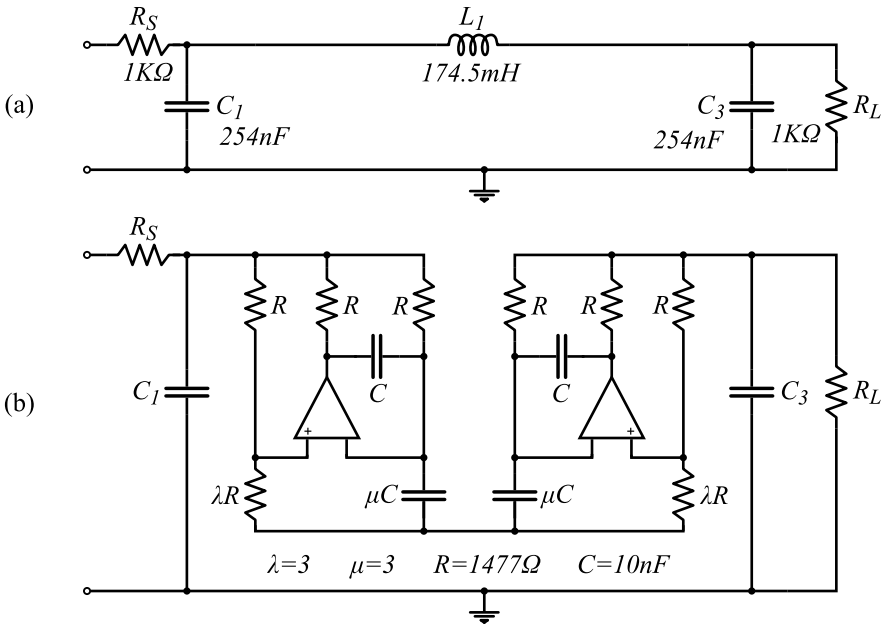

Fig. 8.20 Simulation of a 3rd order lowpass filter

the first term of (8.18) becomes zero and the circuit simulates a floating inductor with:

$$L = 2k(\lambda + 1)R_o^2 C \tag{8.20}$$

Example 8.5 Figure 8.20a shows a Chebyshev lowpass filter of order $N = 3$. The floating inductor is replaced by the simulated floating inductor of Fig. 8.19 and the filter is shown in Fig. 8.20b.

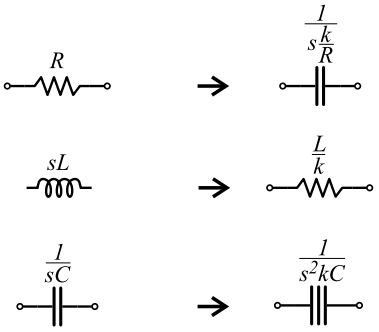

Fig. 8.21 Elements table for the frequency dependent impedance scaling

8.2 Frequency Dependent Impedance Scaling

L.T. Bruton introduced the concept of frequency dependent impedance scaling, in which all arm impedances of a doubly resistively terminated LC ladder filter are divided (scaled) by a factor of the form sk. If constant k has dimensions of time (s), the factor sk is dimensionless. Such a frequency dependent impedance scaling transforms the elements of the filter without affecting the voltage transfer function. More specifically:

1. The impedance of a resistor R becomes $\frac{R}{sk}$, which represents a capacitor with $C = k/R$.
2. The impedance $Z_L(s) = sL$ of an inductor becomes L/k, which represents an inductor $R = \frac{L}{k}$.
3. The impedance $Z_C(s) = 1/sC$ of a capacitor becomes $Z_S = \frac{1}{s^2kC}$, which represents a new element, referred to as *supercapacitor* or *frequency dependent negative resistor* (FDNR), since $Z_S(j\omega) = -\frac{1}{\omega^2 kC}$.

Figure 8.21 shows the frequency dependent impedance scaling table and the symbol of the new element, the FDNR.

There are several ways to realize a frequency dependent negative resistor. The most common is to employ Antoniou's GIC circuit of Fig. 8.6, repeated in Fig. 8.22a. The input impedance of this circuit is given by (8.4):

$$Z_{IN}(s) = \frac{Z_1(s)Z_3(s)Z_5(s)}{Z_2(s)Z_4(s)} \tag{8.21}$$

When two of the numerator impedances (e.g. Z_1 and Z_3) represent capacitors and all the other impedances Z_i represent resistors R_i, as in Fig. 8.22b, we have:

$$Z_{IN}(s) = \frac{1}{s^2 D} \quad \text{with } D = \frac{R_2 R_4 C_1 C_3}{R_5}$$

Riordan's circuit can also be used in a similar manner, as shown in Fig. 8.23. The input impedance of the circuit is again

$$Z_{IN}(s) = \frac{Z_1(s)Z_3(s)Z_5(s)}{Z_2(s)Z_4(s)}$$

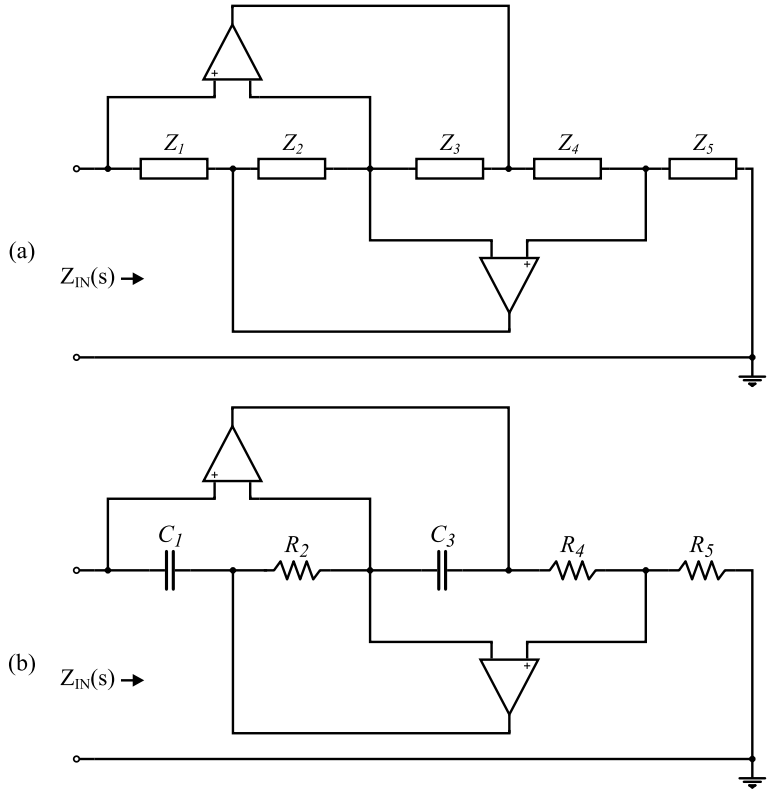

Fig. 8.22 (**a**) Antoniou's GIC. (**b**) A FDNR realization using Antoniou's GIC

In the circuit of Fig. 8.23b, the numerator impedances Z_3 and Z_5 represent capacitors and all the other resistors and therefore:

$$Z_{IN}(s) = \frac{1}{s^2 D} \quad \text{with } D = \frac{R_2 R_4 C_3 C_5}{R_1}$$

A single op amp FDNR realization is shown in Fig. 8.24. The input impedance of this circuit is given by:

$$Y(s) = \left[\frac{C_o + C + (1 - \lambda\mu)C_1}{\lambda + 1}\right] s + \frac{C_o C_1 R}{\lambda + 1} s^2 \tag{8.22}$$

Circuit parameters can be selected so that the bracketed term becomes zero and therefore the circuit realizes an FDNR circuit with:

$$D = \frac{C_o C_1 R}{\lambda + 1}$$

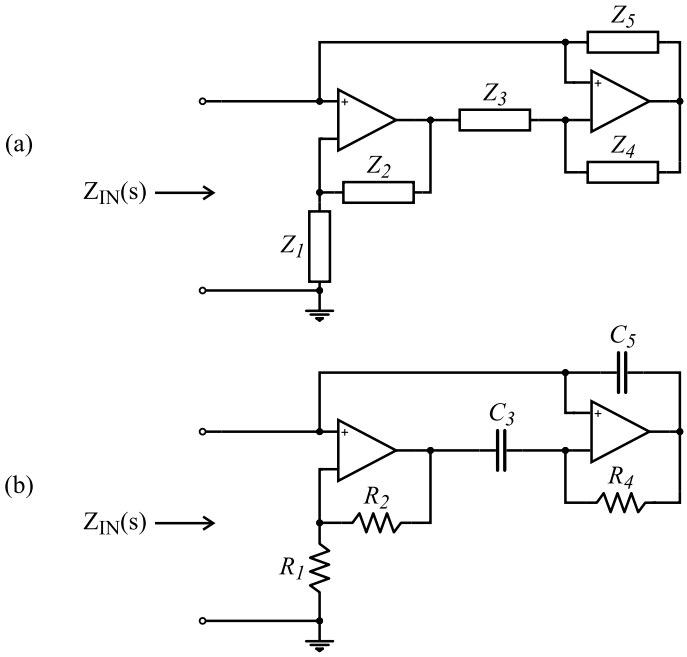

Fig. 8.23 (**a**) Riordan's GIC. (**b**) A FDNR realization using Riordan's GIC

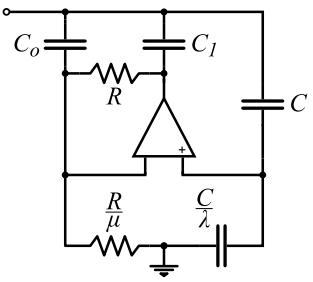

Fig. 8.24 Single op amp FDNR realization

If, for example, we select $C_o = C_1 = C$, $\lambda = 1$ and $\mu = 3$, then

$$Y(s) = \frac{C^2 R}{2} s^2 \quad \Rightarrow \quad D = \frac{C^2 R}{2}$$

All FDNR circuits presented in this section are grounded circuits, i.e. one of their terminals is grounded. Floating FDNRs can be realized by connecting two identical grounded simulated FDNRs back-to-back, as we have done in order to simulate floating inductors.

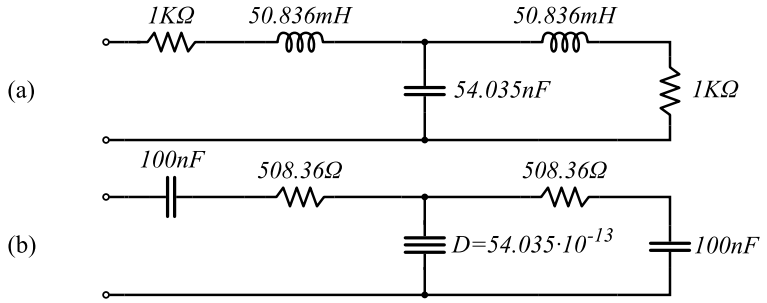

Fig. 8.25 The simulation of a third order passive lowpass filter

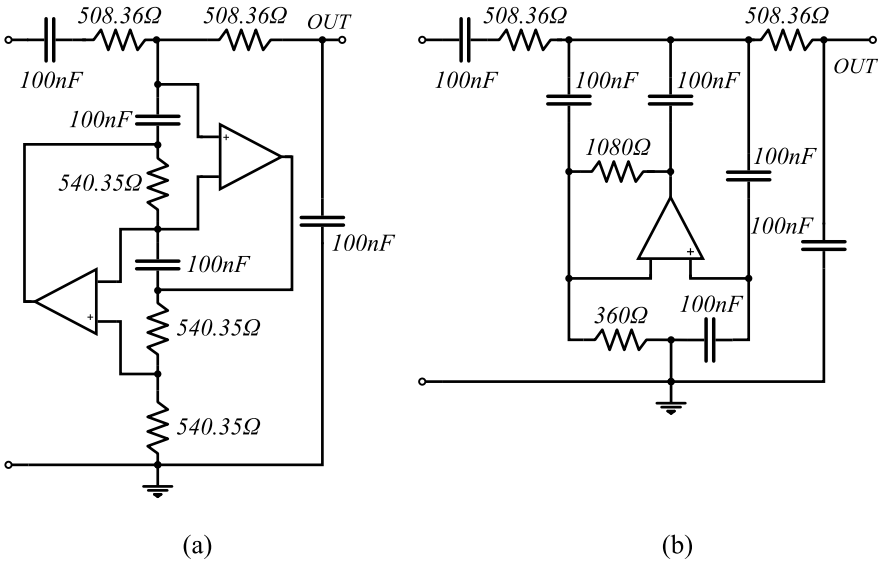

Fig. 8.26 Final circuits of Example 8.6

Example 8.6 Figure 8.25a shows a third order passive lowpass filter. If all impedances are divided by ks with $k = 10^{-4}$ s, then the scaled circuit is shown in Fig. 8.25b. The FDNR with $D = 54.0350 \cdot 10^{-13}$ can be realized using Antoniou's GIC circuit or the single op amp circuit. Figure 8.26 shows the final inductorless active filter with these two alternative FDNR realizations.

8.3 Linear Transformation Active Filters

The third method to simulate a passive ladder filter is based on the simulation of its structural and operational characteristics and although it appears in many distinct forms (Wave Active Filters, Leap-frog, Signal Flow Graph etc.), they can all be seen

as special cases of the more general Linear Transformation Active (LTA) method [2, 5], which will be presented in this section. It should be noted that with proper selection of the linear transformation matrices, the LTA approach can lead to circuit structures suitable for voltage-mode op amp realizations as well as for realizations employing any other active device (OTAs, CCIIs etc.).

The two-port circuit of Fig. 8.27a is described by its transmission (or ABCD) parameters as follows:

$$\begin{bmatrix} V_1 \\ I_1 \end{bmatrix} = \begin{bmatrix} A & B \\ C & D \end{bmatrix} \begin{bmatrix} V_2 \\ -I_2 \end{bmatrix} \tag{8.23}$$

Equation (8.23) can also be written as follows

$$\begin{bmatrix} V_1 \\ I_1 \end{bmatrix} = \begin{bmatrix} A & -B \\ C & -D \end{bmatrix} \begin{bmatrix} V_2 \\ I_2 \end{bmatrix} \tag{8.24}$$

where the negative sign of $-I_2$ has been absorbed by parameters B and D. The new matrix

$$T' = \begin{bmatrix} A & -B \\ C & -D \end{bmatrix}$$

is referred to as the *modified transmission matrix* of the two-port circuit and will be used in this section instead of the original transmission matrix T. The modified transmission matrix of a series ladder arm with impedance $Z(s)$ is:

$$T' = \begin{bmatrix} 1 & -Z(s) \\ 0 & -1 \end{bmatrix}$$

The modified transmission matrix of a shunt ladder arm with admittance $Y(s)$ is:

$$T' = \begin{bmatrix} 1 & 0 \\ Y(s) & -1 \end{bmatrix}$$

The LTA method is based on the linear transformation of the input and output vectors

$$\begin{bmatrix} V_1 \\ I_1 \end{bmatrix} \quad \text{and} \quad \begin{bmatrix} V_2 \\ I_2 \end{bmatrix}$$

as follows:

$$\begin{bmatrix} x_1 \\ y_1 \end{bmatrix} = \begin{bmatrix} \alpha_1 & \beta_1 \\ \gamma_1 & \delta_1 \end{bmatrix} \begin{bmatrix} V_1 \\ I_1 \end{bmatrix} \quad \text{and} \quad \begin{bmatrix} x_2 \\ y_2 \end{bmatrix} = \begin{bmatrix} \alpha_2 & \beta_2 \\ \gamma_2 & \delta_2 \end{bmatrix} \begin{bmatrix} V_2 \\ I_2 \end{bmatrix} \tag{8.25}$$

Matrices

$$Q_1 = \begin{bmatrix} \alpha_1 & \beta_1 \\ \gamma_1 & \delta_1 \end{bmatrix} \quad \text{and} \quad Q_2 = \begin{bmatrix} \alpha_2 & \beta_2 \\ \gamma_2 & \delta_2 \end{bmatrix}$$

are referred to as left and right linear transformation matrices respectively.

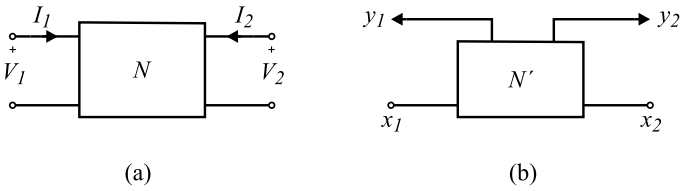

Fig. 8.27 (**a**) Two-port circuit. (**b**) Linearly transformed structure

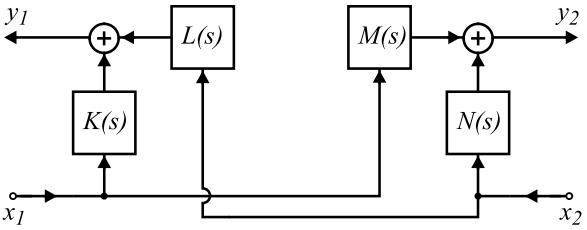

Fig. 8.28 Block diagram of the linearly transformed structure

If, in the transformation matrices, elements α_i and γ_i are dimensionless and β_i and δ_i represent resistances, then the transformed quantities x_i and y_i will represent voltages. If x_1 and x_2 are taken as the voltage inputs of the transformed circuit, y_1 and y_2 will be the outputs of the linearly transformed circuit, which can be represented as in Fig. 8.27b.

Combining (8.24) and (8.25), we find:

$$\begin{bmatrix} x_1 \\ y_1 \end{bmatrix} = \begin{bmatrix} \alpha_1 & \beta_1 \\ \gamma_1 & \delta_1 \end{bmatrix} \begin{bmatrix} A & -B \\ C & -D \end{bmatrix} \begin{bmatrix} \alpha_2 & \beta_2 \\ \gamma_2 & \delta_2 \end{bmatrix}^{-1} \begin{bmatrix} x_2 \\ y_2 \end{bmatrix} \tag{8.26}$$

From the above equation, the outputs y_i can be expressed in terms of the inputs x_i:

$$\begin{bmatrix} y_1 \\ y_2 \end{bmatrix} = \begin{bmatrix} K(s) & L(s) \\ M(s) & N(s) \end{bmatrix} \begin{bmatrix} x_1 \\ y_2 \end{bmatrix} \tag{8.27}$$

This input-output relationship can be realized as shown in Fig. 8.28. It should be noted that the linearly transformed structure of Figs. 8.28 or 8.27b does not simulate the original two-port. It is simply a linearly transformed version of the original two-port under the linear transformation defined by the transformation matrices.

Example 8.7 The simple series arm inductor of Fig. 8.29a with modified transmission matrix

$$T' = \begin{bmatrix} A & -B \\ C & -D \end{bmatrix} = \begin{bmatrix} 1 & -sL \\ 0 & -1 \end{bmatrix}$$

will be linearly transformed using

$$Q_1 = \begin{bmatrix} \alpha_1 & \beta_1 \\ \gamma_1 & \delta_1 \end{bmatrix} = \begin{bmatrix} 1 & R_o \\ 0 & R_o \end{bmatrix} \quad \text{and} \quad Q_2 = \begin{bmatrix} \alpha_2 & \beta_2 \\ \gamma_2 & \delta_2 \end{bmatrix} = \begin{bmatrix} -1 & 0 \\ 0 & -R_o \end{bmatrix}$$

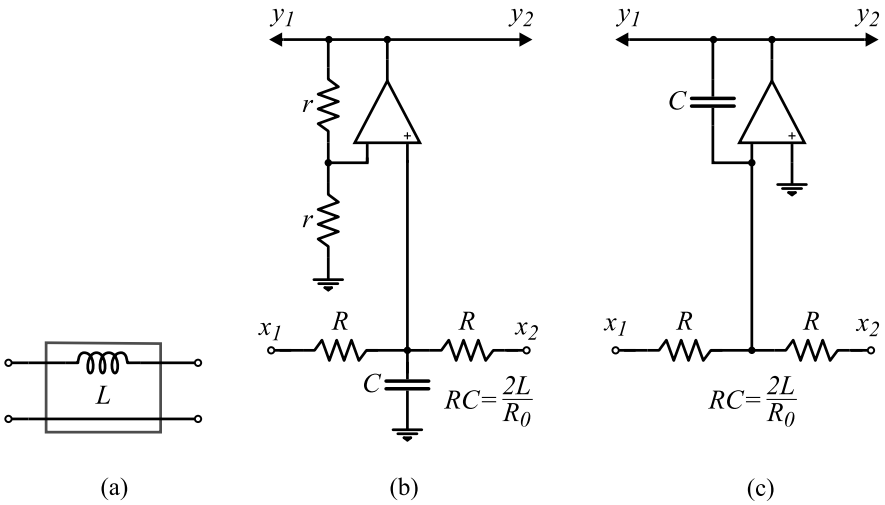

Fig. 8.29 A series arm inductor and two linearly transformed circuits

If R_o represents resistance, then all transformed variables will represent voltages. After some manipulations, (8.26) yields:

$$y_1 = y_2 \quad \text{and} \quad y_2 = \frac{1}{1 + s\frac{L}{R_o}} x_1 + \frac{1}{1 + s\frac{L}{R_o}} x_2 \tag{8.28}$$

Since x_1, x_2, y_1 and y_2 are voltages, the linearly transformed circuit described by the above relationships can be realized as shown in Fig. 8.29b.

If we use the transformation matrices

$$Q_1 = \begin{bmatrix} \alpha_1 & \beta_1 \\ \gamma_1 & \delta_1 \end{bmatrix} = \begin{bmatrix} 1 & 0 \\ 0 & -R_o \end{bmatrix} \quad \text{and} \quad Q_2 = \begin{bmatrix} \alpha_2 & \beta_2 \\ \gamma_2 & \delta_2 \end{bmatrix} = \begin{bmatrix} -1 & 0 \\ 0 & -R_o \end{bmatrix}$$

equation (8.26) gives

$$y_1 = y_2 \quad \text{and} \quad y_2 = -\frac{1}{s\frac{L}{R_o}} x_1 - \frac{1}{s\frac{L}{R_o}} x_2 \tag{8.29}$$

which can be realized as shown in Fig. 8.29c using a summing inverting Miller integrator.

It should be remembered that the linearly transformed structures of Fig. 8.29b and c do not simulate the original floating inductor of Fig. 8.29a. They are simply transformed versions of the original two-port under the linear transformation as it is defined each time by the transformation matrices Q_1 and Q_2.

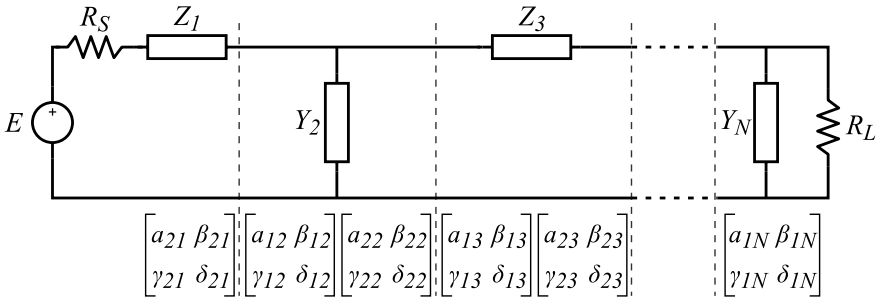
R_S
Z_1
Z_3
E
Y_2
Y_N
R_L
$\begin{bmatrix} a_{21} & \beta_{21} \\ \gamma_{21} & \delta_{21} \end{bmatrix}$
$\begin{bmatrix} a_{12} & \beta_{12} \\ \gamma_{12} & \delta_{12} \end{bmatrix}$
$\begin{bmatrix} a_{22} & \beta_{22} \\ \gamma_{22} & \delta_{22} \end{bmatrix}$
$\begin{bmatrix} a_{13} & \beta_{13} \\ \gamma_{13} & \delta_{13} \end{bmatrix}$
$\begin{bmatrix} a_{23} & \beta_{23} \\ \gamma_{23} & \delta_{23} \end{bmatrix}$
$\begin{bmatrix} a_{1N} & \beta_{1N} \\ \gamma_{1N} & \delta_{1N} \end{bmatrix}$

Fig. 8.30 Application of the LTA method

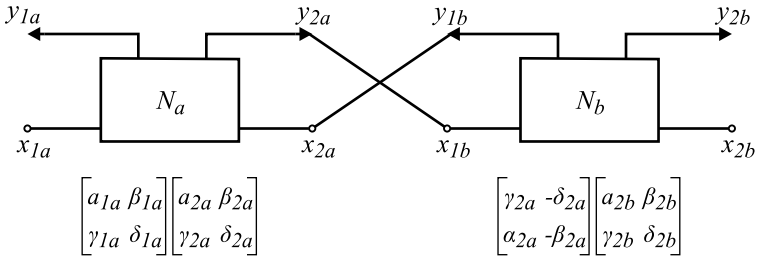

Fig. 8.31 The cross-cascade connection

8.3.1 Connection of Linearly Transformed Two-Ports

To design a linearly transformed filter from a passive ladder filter, the ladder is seen as a cascade of elementary two-ports, series and shunt arms, as shown in Fig. 8.30. Each elementary two-port is linearly transformed and the transformed circuits are properly connected to form the linearly transformed filter. The interconnection of the linear transformed arms of the ladder depends on the transformation matrices which have been used to transform the adjacent arms of the passive ladder. In order for the connection of two linearly transformed circuits to be as simple as possible, namely the cross-cascade shown in Fig. 8.31, the left transformation matrix of the second section (subscripts $1b$) must be related to the right transformation matrix Q_{2a} of the preceding section (subscripts $2a$) as follows:

$$\begin{bmatrix} \alpha_{1b} & \beta_{1b} \\ \gamma_{1b} & \delta_{1b} \end{bmatrix} = \begin{bmatrix} \gamma_{2a} & -\delta_{2a} \\ \alpha_{2a} & -\beta_{2a} \end{bmatrix} \tag{8.30}$$

Equation (8.30) implies that in order to have the cross-cascade connection, the left matrix Q_{1b} of a section must be derived from the right matrix Q_{2a} of the preceding section by simply interchanging its rows and changing the sign of the second column. The right matrix Q_{2b} of the second section can be freely selected and it will determine the left matrix of the next section, in view of the cross-cascade connection constraint of (8.30).

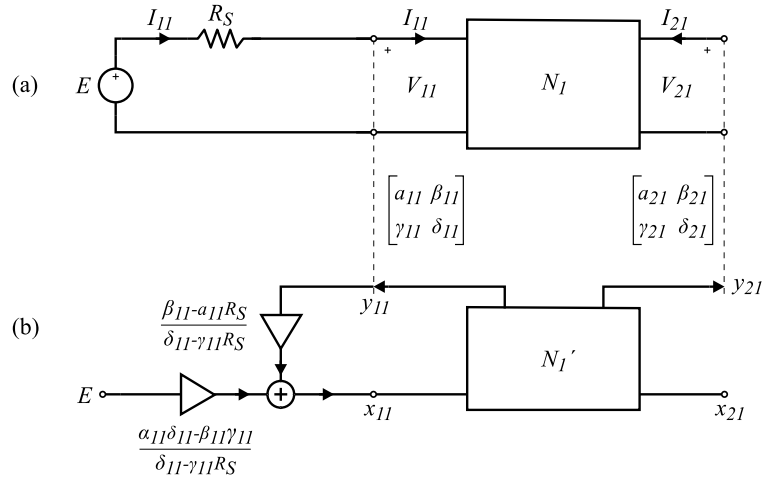

Fig. 8.32 The input termination

As an example, if the following transformation matrices are used for a section

$$Q_{1a} = \begin{bmatrix} \alpha_{1a} & \beta_{1a} \\ \gamma_{1a} & \delta_{1a} \end{bmatrix} = \begin{bmatrix} 1 & 0 \\ 0 & -R_o \end{bmatrix} \quad \text{and} \quad Q_{2a} = \begin{bmatrix} \alpha_{2a} & \beta_{2a} \\ \gamma_{2a} & \delta_{2a} \end{bmatrix} = \begin{bmatrix} -1 & 0 \\ 0 & -R_o \end{bmatrix}$$

then, in order for the transformed sections to be cross-cascaded, the left transformation matrix Q_{1b} of the next section must be:

$$Q_{1b} = \begin{bmatrix} \alpha_{1b} & \beta_{1b} \\ \gamma_{1b} & \delta_{1b} \end{bmatrix} = \begin{bmatrix} \gamma_{2a} & -\delta_{2a} \\ \alpha_{2a} & -\beta_{2a} \end{bmatrix} = \begin{bmatrix} 0 & R_o \\ -1 & 0 \end{bmatrix}$$

8.3.2 Input Termination

The first reactive arm N_1 of the doubly terminated lossless ladder filter of Fig. 8.32 is terminated by the source resistor R_S. Let N_1 be transformed using the transformation matrices

$$Q_{11} = \begin{bmatrix} \alpha_{11} & \beta_{11} \\ \gamma_{11} & \delta_{11} \end{bmatrix} Q_{21} = \begin{bmatrix} \alpha_{21} & \beta_{21} \\ \gamma_{21} & \delta_{21} \end{bmatrix}$$

as shown in Fig. 8.32. From (8.26), we have

$$\begin{bmatrix} x_{11} \\ y_{11} \end{bmatrix} = \begin{bmatrix} \alpha_{11} & \beta_{11} \\ \gamma_{11} & \delta_{11} \end{bmatrix} T_1 \begin{bmatrix} \alpha_{21} & \beta_{21} \\ \gamma_{21} & \delta_{21} \end{bmatrix}^{-1} \begin{bmatrix} x_{21} \\ y_{21} \end{bmatrix} \tag{8.31}$$

where T_1 is the modified transmission matrix of the first reactive arm and for the resistive input termination, we have $V_{11} = E - I_{11}R_S$ or

$$\begin{bmatrix} 1 & R_S \end{bmatrix} \begin{bmatrix} V_{11} \\ I_{11} \end{bmatrix} = E$$

When this equation is combined with the left transformed variable vector of arm N_1

$$\begin{bmatrix} x_{11} \\ y_{11} \end{bmatrix} = \begin{bmatrix} \alpha_{11} & \beta_{11} \\ \gamma_{11} & \delta_{11} \end{bmatrix} \begin{bmatrix} V_{11} \\ I_{11} \end{bmatrix}$$

we obtain the relationship:

$$\begin{bmatrix} 1 & R_S \end{bmatrix} \begin{bmatrix} \alpha_{11} & \beta_{11} \\ \gamma_{11} & \delta_{11} \end{bmatrix}^{-1} \begin{bmatrix} x_{11} \\ y_{11} \end{bmatrix} = E \tag{8.32}$$

Equation (8.32) describes the linearly transformed input termination and can be used to express the input x_{11} in terms of the other variables:

$$x_{11} = \frac{\alpha_{11}\delta_{11} - \beta_{11}\gamma_{11}}{\delta_{11} - \gamma_{11}R_S} E + \frac{\beta_{11} - \alpha_{11}R_S}{\delta_{11} - \gamma_{11}R_S} y_{11} \tag{8.33}$$

The implementation of this relationship is illustrated in Fig. 8.32b, from which it can be seen that the corresponding LT structure of the first reactive arm of the ladder, when taken in conjunction with the source resistance, is in fact a two-input-one-output system with one of the two inputs being equal to the source voltage E. The description of this two-input-one-output LT structure, which corresponds to the first reactive arm of the ladder and the source resistance, can be derived from (8.31) and (8.32) by eliminating the left linearly transformed vector $[x_{11}\ y_{11}]^T$, to get:

$$\begin{bmatrix} 1 & R_S T_1 \end{bmatrix} \begin{bmatrix} \alpha_{21} & \beta_{21} \\ \gamma_{21} & \delta_{21} \end{bmatrix} \begin{bmatrix} x_{21} \\ y_{21} \end{bmatrix} = E \tag{8.34}$$

It is worth observing that this relationship depends only on the right transformation matrix of the first reactive arm N_1. The explicit forms of (8.34) are given below when N_1 is taken to be a series arm with impedance $Z_1(s)$ or a shunt arm with admittance $Y_1(s)$:

$$\text{Series arm:} \quad y_{21} = \frac{\delta_{21} + \gamma_{21}(Z_1 + R_S)}{\beta_{21} + \alpha_{21}(Z_1 + R_S)} x_{21} - \frac{\alpha_{21}\delta_{21} - \beta_{21}\gamma_{21}}{\beta_{21} + \alpha_{21}(Z_1 + R_S)} E \tag{8.35}$$

$$\text{Shunt arm:} \quad y_{21} = \frac{\gamma_{21}R_S + \delta_{21}(Y_1R_S + 1)}{\alpha_{21}R_S + \beta_{21}(Y_1R_S + +1)} x_{21} - \frac{\alpha_{21}\delta_{21} - \beta_{21}\gamma_{21}}{\alpha_{21}R_S + \beta_{21}(Y_1R_S + 1)} E \tag{8.36}$$

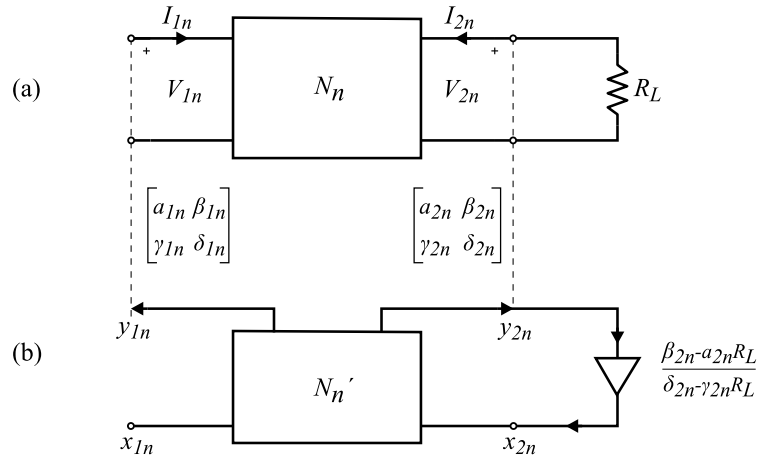

Fig. 8.33 The input termination

8.3.3 Output Termination

The last reactive arm N_n of the ladder filter is shown in Fig. 8.33a together with the resistive termination, which represents the load of the filter. On applying the linear transformation to N_n with transformation matrices

$$Q_{1n} = \begin{bmatrix} \alpha_{1n} & \beta_{1n} \\ \gamma_{1n} & \delta_{1n} \end{bmatrix} \qquad Q_{2n} = \begin{bmatrix} \alpha_{2n} & \beta_{2n} \\ \gamma_{2n} & \delta_{2n} \end{bmatrix}$$

the linearly transformed structure will be derived from (8.26):

$$\begin{bmatrix} x_{1n} \\ y_{1n} \end{bmatrix} = \begin{bmatrix} \alpha_{1n} & \beta_{1n} \\ \gamma_{1n} & \delta_{1n} \end{bmatrix} T_n \begin{bmatrix} \alpha_{2n} & \beta_{2n} \\ \gamma_{2n} & \delta_{2n} \end{bmatrix}^{-1} \begin{bmatrix} x_{2n} \\ y_{2n} \end{bmatrix} \tag{8.37}$$

However, since

$$V_{2n} = -R_L I_{2n} \quad \text{or} \quad \begin{bmatrix} 1 & -R_L \end{bmatrix} \begin{bmatrix} V_{2n} \\ I_{2n} \end{bmatrix} = 0$$

and moreover,

$$\begin{bmatrix} V_{2n} \\ I_{2n} \end{bmatrix} = \begin{bmatrix} \alpha_{2n} & \beta_{2n} \\ \gamma_{2n} & \delta_{2n} \end{bmatrix}^{-1} \begin{bmatrix} x_{2n} \\ y_{2n} \end{bmatrix}$$

the following relationship between y_{2n} and x_{2n} can be derived:

$$\begin{bmatrix} 1 & -R_L \end{bmatrix} \begin{bmatrix} \alpha_{2n} & \beta_{2n} \\ \gamma_{2n} & \delta_{2n} \end{bmatrix}^{-1} \begin{bmatrix} x_{2n} \\ y_{2n} \end{bmatrix} = 0 \tag{8.38}$$

In fact, (8.38) represents the LT resistive termination of the filter and it shows the relationship between x_{2n} and y_{2n}, which can be written explicitly as:

$$x_{2n} = \frac{\beta_{2n} - \alpha_{2n} R_L}{\delta_{2n} - \gamma_{2n} R_L} y_{2n} \tag{8.39}$$

The above relationship is illustrated in Fig. 8.33b, where y_{2n} is considered to be the output of the LTA filter. If y_{2n} is expressed in terms of the output voltage V_{2n} of the original ladder filter, it can be shown that

$$y_{2n} = \left(\gamma_{2n} - \frac{\delta_{2n}}{R_L}\right) V_{2n} \tag{8.40}$$

It should be noted that if y_{2n} is to be taken to represent the output voltage V_{2n}, then the factor $\gamma_{2n} - \delta_{2n}/R_L$ must be frequency independent and ideally equal to unity.

The LT structure for the last reactive ladder arm N_n in conjunction with the resistive termination (Fig. 8.33b) can be considered as a single-input-single-output circuit in a manner similar to the input termination case. The description of this circuit can be derived from (8.37) and (8.38):

$$\begin{bmatrix} 1 & -R_L \end{bmatrix} T_n^{-1} \begin{bmatrix} \alpha_{1n} & \beta_{1n} \\ \gamma_{1n} & \delta_{1n} \end{bmatrix}^{-1} \begin{bmatrix} x_{1n} \\ y_{1n} \end{bmatrix} = 0 \tag{8.41}$$

It should be noted that this equation involves only the left transformation matrix. The explicit forms of (8.41) are given below when N_n is taken to be a series arm with impedance $Z_n = Z_n(s)$ or a shunt arm with admittance $Y_n = Y_n(s)$:

$$\text{Series arm } Z_n: \quad y_{1n} = \frac{\delta_{1n} + \gamma_{1n}(Z_n + R_L)}{\beta_{1n} + \alpha_{1n}(Z_n + R_L)} x_{1n} \tag{8.42}$$

$$\text{Shunt arm } Y_n: \quad y_{1n} = \frac{\gamma_{1n} R_L + \delta_{1n}(Y_n R_L + 1)}{\alpha_{1n} R_L + \beta_{1n}(Y_n R_L + 1)} x_{1n} \tag{8.43}$$

However, if this single-input-single-output model for the terminated last reactive ladder arm is employed, the y_{2n} output which is directly associated with the output V_{2n} of the original ladder filter is no longer available explicitly. In such a case, the output node of the LTA filter must be located from (8.37), which can be written as

$$\begin{bmatrix} x_{1n} \\ y_{1n} \end{bmatrix} = \begin{bmatrix} \alpha_{1n} & \beta_{1n} \\ \gamma_{1n} & \delta_{1n} \end{bmatrix} T_n \begin{bmatrix} 1 \\ -\frac{1}{R_L} \end{bmatrix} V_{2n} \tag{8.44}$$

When N_n is a series arm with

$$T_n = \begin{bmatrix} 1 & -Z_n \\ 0 & -1 \end{bmatrix}$$

then (8.44) gives:

$$x_{1n} = [\alpha_{1n}(1 + Z_n G_L) + \beta_{1n} G_L] V_{2n} \tag{8.45}$$

$$y_{1n} = [\gamma_{1n}(1 + Z_n G_L) + \delta_{1n} G_L] V_{2n} \tag{8.46}$$

In order for one of x_{1n} or y_{1n} to be suitable as a direct output, either α_{1n} or γ_{1n} must be equal to zero.

– If we want y_{1n} to be the output, then we must set $\gamma_{1n} = 0$, in which case

$$V_{2n} = y_{1n} \frac{R_L}{\delta_{1n}} \quad \text{(series last arm and } \gamma_{1n} = 0)$$

– If we want x_{1n} to be the output, then we must set $\alpha_{1n} = 0$, in which case

$$V_{2n} = x_{1n} \frac{R_L}{\beta_{1n}} \quad \text{(series last arm and } \alpha_{1n} = 0)$$

When N_n is a shunt arm with

$$T_n = \begin{bmatrix} 1 & 0 \\ Y_n & -1 \end{bmatrix}$$

then (8.44) gives:

$$x_{1n} = [\alpha_{1n} + \beta_{1n}(Y_n + G_L)] V_{2n} \tag{8.47}$$

$$y_{1n} = [\gamma_{1n} + \delta_{1n}(Y_n + G_L)] V_{2n} \tag{8.48}$$

Similarly, in order for one of x_{1n} or y_{1n} to be suitable as a direct output, either β_{1n} or δ_{1n} must be equal to zero.

– If we want y_{1n} to be the output, then we must set $\delta_{1n} = 0$, in which case

$$V_{2n} = y_{1n} \frac{1}{\gamma_{1n}} \quad \text{(shunt last arm and } \delta_{1n} = 0)$$

– If we want x_{1n} to be the output, then we must set $\beta_{1n} = 0$, in which case

$$V_{2n} = x_{1n} \frac{1}{\alpha_{1n}} \quad \text{(shunt last arm and } \beta_{1n} = 0)$$

It is, therefore, essential that there must exist a proper zero entry in the left transformation matrix of the last reactive arm, in order that the single-input-single-output model be used effectively without the need for extra passive and active components to generate an output node other than the already available x_{1n} and y_{1n}.

Example 8.8 In order to simulate the passive lowpass filter of Fig. 8.34 using the LTA method, we select the transformation matrix:

$$Q_{21} = \begin{bmatrix} \alpha_{21} & \beta_{21} \\ \gamma_{21} & \delta_{21} \end{bmatrix} = \begin{bmatrix} 0 & -R \\ 1 & -R \end{bmatrix}$$

for the first shunt arm $Y_1(s) = sC_1$ and the input termination.

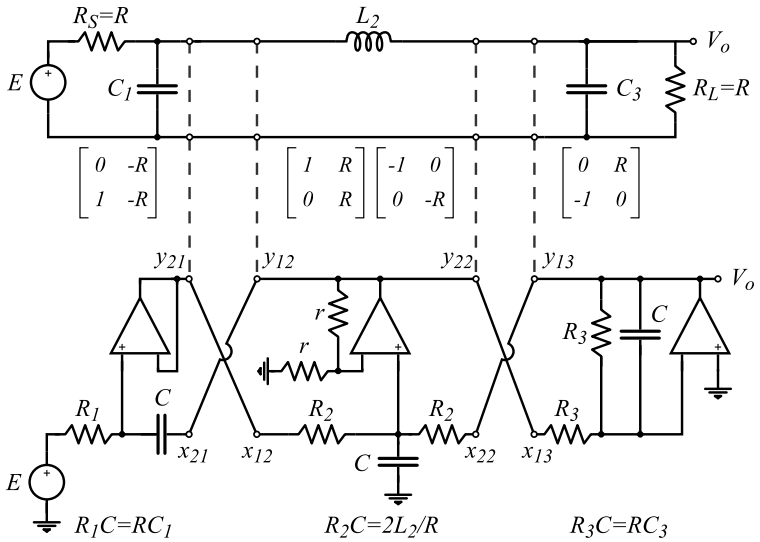

Fig. 8.34 The application of the method to a third order lowpass circuit

Equation (8.36) gives:

$$y_{21} = \frac{sRC_1}{sRC_1+1}x_{21} + \frac{1}{sRC_1+1}E \tag{8.49}$$

One way to implement the two-input-one-output circuit described by (8.49) is shown in Fig. 8.34. The circuit uses a series RC circuit and a buffer.

The left transformation matrix of the next arm, the series arm inductor L_2, is determined by the cross-cascade connection constraint:

$$Q_{12} = \begin{bmatrix} \alpha_{12} & \beta_{12} \\ \gamma_{12} & \delta_{12} \end{bmatrix} = \begin{bmatrix} \gamma_{21} & -\delta_{21} \\ \alpha_{21} & -\beta_{21} \end{bmatrix} = \begin{bmatrix} 1 & R \\ 0 & R \end{bmatrix}$$

For the right transformation matrix of the same arm, we may chose

$$Q_{22} = \begin{bmatrix} \alpha_{22} & \beta_{22} \\ \gamma_{22} & \delta_{22} \end{bmatrix} = \begin{bmatrix} -1 & 0 \\ 0 & -R \end{bmatrix}$$

For the above Q_{12} and Q_{22} and the modified transmission matrix of the series ladder arm

$$T_2 = \begin{bmatrix} A & -B \\ C & -D \end{bmatrix} = \begin{bmatrix} 1 & -sL_2 \\ 0 & -1 \end{bmatrix}$$

equation (8.26) yields:

$$y_{12} = y_{22} \quad \text{and} \quad y_{22} = \frac{1}{1+s\frac{L_2}{R}}x_{12} + \frac{1}{1+s\frac{L_2}{R}}x_{22}$$

A possible implementation of this linearly transformed circuit is shown in Fig. 8.34.

The left transformation matrix of the third arm, the shunt capacitor C_3, is determined from the cross-cascade connection constraint as follows:

$$Q_{13} = \begin{bmatrix} \alpha_{13} & \beta_{13} \\ \gamma_{13} & \delta_{13} \end{bmatrix} = \begin{bmatrix} \gamma_{22} & -\delta_{22} \\ \alpha_{22} & -\beta_{22} \end{bmatrix} = \begin{bmatrix} 0 & R \\ -1 & 0 \end{bmatrix}$$

When this left transformation matrix is used to linearly transform shunt capacitor C_3 together with the load termination, (8.43) gives:

$$y_{13} = -\frac{1}{sRC_3 + 1} x_{13}$$

Since $\delta_{13} = 0$, direct output can be taken from y_{13} as has been explained.

8.3.4 Wave Active Filters

Wave Active Filters, as presented in [3] and independently in [10] under the name *Scattering Parameter Active Filters*, can be derived as a special case of the LTA method using the same transformation matrices for all the series and the shunt arms of the ladder, namely:

$$Q_1 = \begin{bmatrix} \alpha_1 & \beta_1 \\ \gamma_1 & \delta_1 \end{bmatrix} = \begin{bmatrix} 1 & R \\ 1 & -R \end{bmatrix} \quad \text{and} \quad Q_2 = \begin{bmatrix} \alpha_2 & \beta_2 \\ \gamma_2 & \delta_2 \end{bmatrix} = Q_1 = \begin{bmatrix} 1 & R \\ 1 & -R \end{bmatrix}$$

Under this linear transformation, for the series arms with impedance $Z(s)$, we get:

$$y_1 = \frac{Z(s)}{Z(s) + 2R} x_1 + \frac{2R}{Z(s) + 2R} x_2 \qquad y_2 = \frac{2R}{Z(s) + 2R} x_1 + \frac{Z(s)}{Z(s) + 2R} x_2 \tag{8.50}$$

For the shunt arms with admittance $Y(s)$, we get:

$$y_1 = -\frac{RY(s)}{RY(s) + 2} x_1 + \frac{2}{RY(s) + 2} x_2 \qquad y_2 = \frac{2}{RY(s) + 2} x_1 - \frac{RY(s)}{RY + 2} x_2 \tag{8.51}$$

The Wave Active Filter terminology stems from the fact that under this specific transformation set, the transformed variables x_i and y_i can be identified with the incident and reflected voltage waves at the corresponding ports. The voltage transfer ratios, which multiply x_1 and x_2 in (8.50) and (8.51), are equal to the elements of the scattering matrix of the corresponding ladder arms, thereby justifying the name Scattering Parameter Active Filters.

As far as the input termination is concerned, for the Wave Active Filters case, (8.34) yields

$$x_{11} = \frac{2R}{R + R_S} E$$

which becomes $x_{11} = E$ for $R = R_S$. This implies that the x_{11} input of the LT structure corresponding to the first reactive ladder arm N_1 represents the actual input of the Wave Active Filter.

The output termination of the Wave Active Filters can be found from (8.39) as follows:

$$x_{2n} = \frac{R_L - R}{R_L + R} y_{2n}$$

This implies that for $R = R_L$, the input x_{2n} must be grounded, in which case from (8.40) we find $y_{2n} = 2V_{2n}$. Therefore, the output y_{2n} of the Wave Active filter structure represents the output of the original ladder filter with a gain of 2. The single-input-single-output model for the last reactive arm, when transformed in conjunction with the load R_L, cannot be used due to the absence of a proper zero entry in the left transformation matrix, which is required for the existence of a convenient output node.

8.3.5 Leap-Frog Filters

The well-known *leap-frog* or *active ladder* synthesis [6] emerges from the general LTA procedure by considering the transformation matrices to be as follows:

For the series ladder arms:

$$Q_1 = \begin{bmatrix} \alpha_1 & \beta_1 \\ \gamma_1 & \delta_1 \end{bmatrix} = \begin{bmatrix} \alpha & 0 \\ 0 & \delta \end{bmatrix} \quad \text{and} \quad Q_2 = \begin{bmatrix} \alpha_2 & \beta_2 \\ \gamma_2 & \delta_2 \end{bmatrix} = \begin{bmatrix} -\alpha & 0 \\ 0 & \delta \end{bmatrix}$$

For the shunt ladder arms:

$$Q_1 = \begin{bmatrix} \alpha_1 & \beta_1 \\ \gamma_1 & \delta_1 \end{bmatrix} = \begin{bmatrix} 0 & -\delta \\ -\alpha & 0 \end{bmatrix} \quad \text{and} \quad Q_2 = \begin{bmatrix} \alpha_2 & \beta_2 \\ \gamma_2 & \delta_2 \end{bmatrix} = \begin{bmatrix} 0 & -\delta \\ \alpha & 0 \end{bmatrix}$$

Parameter α is a real dimensionless number and δ represents resistance. It should be noted that the transformation matrices are chosen so that the cross-cascade connection constraint is satisfied. The original leap-frog synthesis can be derived using $\alpha = 1$ and $\delta = R_S$.

Such a scheme for the LT structure of the series arm $Z(s)$ yields the following relationships:

$$y_1 = -y_2 \quad y_2 = -\frac{\delta}{\alpha Z(s)}(x_1 + x_2) \tag{8.52}$$

For the shunt arm $Y(s)$ we get:

$$y_1 = -y_2 \quad y_2 = -\frac{\alpha}{\delta Y(s)}(x_1 + x_2) \tag{8.53}$$

The two-input-one-output model can be employed for the input termination. Moreover, due to the zero entries of the left transformation matrix, the single-input-single-output model can be used for the last reactive arm when taken in conjunction with the resistive load.

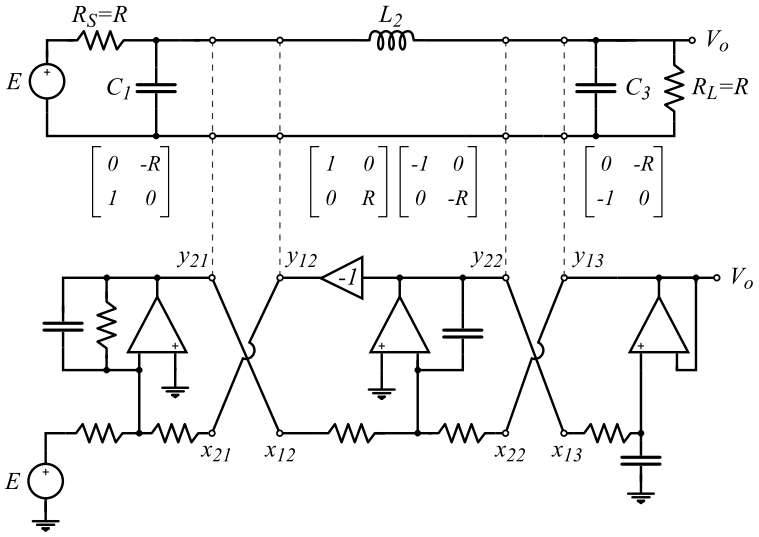

Fig. 8.35 The derivation of the leapfrog filter

Example 8.9 The third order passive ladder filter of Fig. 8.35 will be linearly transformed using the leap-frog transformation matrices. For the first shunt arm, the capacitor C_1 with the input termination, the right transformation matrix will be

$$Q_{21} = \begin{bmatrix} \alpha_{21} & \beta_{21} \\ \gamma_{21} & \delta_{21} \end{bmatrix} = \begin{bmatrix} 0 & -R \\ 1 & 0 \end{bmatrix}$$

From (8.36) we get

$$y_{21} = -\frac{1}{sRC_1 + 1} x_{21} + \frac{1}{sRC_1 + 1} E$$

which can be realized as shown in Fig. 8.35. For the exact implementation, input E should have been inverted but this is not necessary since it would only affect the phase.

Next ladder arm, inductor L_2, will be transformed using the following leap-frog transformation matrices:

$$\begin{bmatrix} 1 & 0 \\ 0 & R \end{bmatrix} \begin{bmatrix} -1 & 0 \\ 0 & R \end{bmatrix}$$

which will give the LT structure described by:

$$y_{12} = -y_{22} \quad y_{22} = -\frac{1}{\frac{L_2}{R} s} x_{12} - \frac{1}{\frac{L_2}{R} s} x_{22}$$

Output y_{22} can be implemented using a summing inverting Miller integrator. Output $y_{12} = -y_{22}$ can be taken from y_{22} using a voltage amplifier with gain equal to -1, as shown in Fig. 8.35. Finally, the last shunt arm, capacitor C_3, will be transformed together with the load using

$$Q_{13} = \begin{bmatrix} 0 & -R \\ -1 & 0 \end{bmatrix}$$

to give

$$y_{13} = \frac{1}{sRC_3 + 1} x_{13} \quad \text{and} \quad y_{13} = -V_o$$

This can be implemented as shown in Fig. 8.35. The output of the filter will be $V_o = -y_{13}$. The minus sign affects only the phase and it is not necessary to use a voltage amplifier with gain equal to -1.

8.4 Problems

8.1 Prove that the input driving-point impedance $Z_{IN}(s)$ of the Riordan's circuit of Fig. 8.2 is given by (8.1).

8.2 Prove that the input driving-point impedance $Z_{IN}(s)$ of the Antoniou's circuit of Fig. 8.6 is given by (8.4).

8.3 Prove that the back-to-back connection of two identical Riordan's simulated inductors is a floating inductor.

8.4 Prove that the voltage transfer function of all six circuits of Fig. 8.12 is

$$H(s) = 1 - \frac{1}{sRC}$$

8.5 Prove that the input admittance of the circuit of Fig. 8.36 is given by

$$Y(s) = \frac{1 - \lambda\mu}{(\lambda + 1)R_o} + \frac{1}{sk(\lambda + 1)R_o^2 C}$$

and make it simulate a grounded inductor with $L = 10$ mH.

8.6 Determine the input admittance of the circuit of Fig. 8.37 and set the conditions under which it realizes a simulated grounded inductor.

8.7 Use Pspice to verify that the gain responses of the two filters of Fig. 8.18 are practically identical.

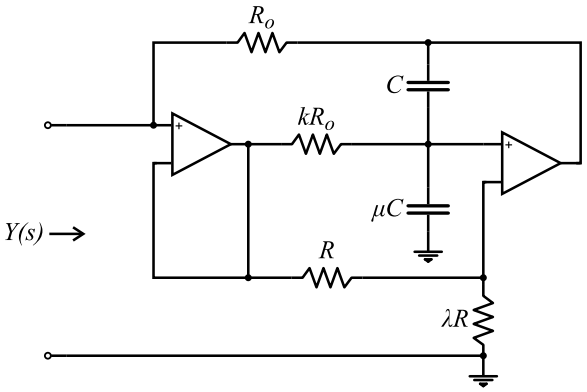

Fig. 8.36 Circuit for Problem 8.5

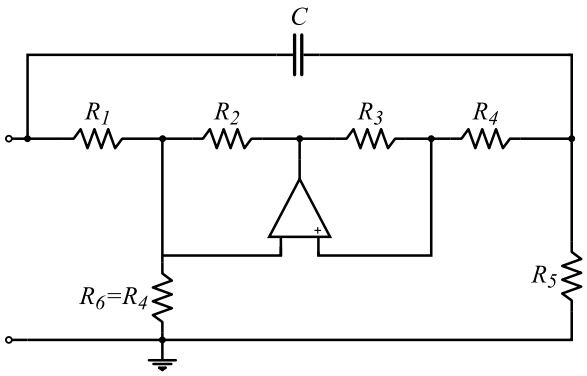

Fig. 8.37 The Orchard-Wilson simulated inductor

8.8 Use Pspice to verify that the gain responses of the two filters of Fig. 8.20 are practically identical.

8.9 Figure 8.38a shows a passive elliptic lowpass filter. In Fig. 8.38b, the floating inductor has been replaced by the simulated floating inductor of Fig. 8.19. Calculate all element values and parameters so that the two filters have identical frequency responses.

8.10 Show that the circuit of Fig. 8.39a has the same admittance as the circuit of Fig. 8.39b with:

$$C_1 = \frac{\lambda}{\lambda+1}C_o \qquad L_1 = (\lambda+1)R_oR_1C \qquad R_x = \frac{\lambda+1}{\frac{1}{R_1} - \frac{\lambda\mu-1}{R_o}}$$

(This means that the circuit of Fig. 8.39a simulates a grounded parallel RLC circuit.)

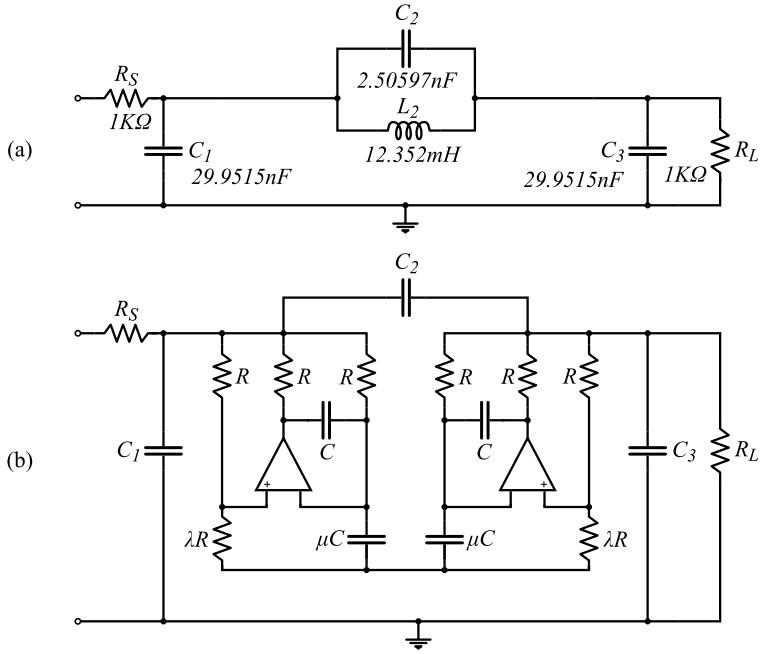

Fig. 8.38 Circuit for Problem 8.9

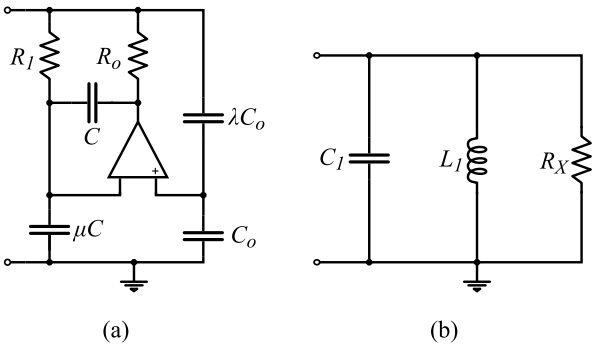

Fig. 8.39 Circuit for Problem 8.10

8.11 Show that the circuit of Fig. 8.40a has the same admittance as the circuit of Fig. 8.40b with:

$$C_1 = \frac{\lambda}{2(\lambda+1)}C_o \qquad L_1 = 2(\lambda+1)R_oR_1C \qquad R_x = \frac{2(\lambda+1)}{\frac{1}{R_1} - \frac{\lambda\mu-1}{R_o}}$$

(This means that the circuit of Fig. 8.40a simulates a floating parallel RLC circuit.)

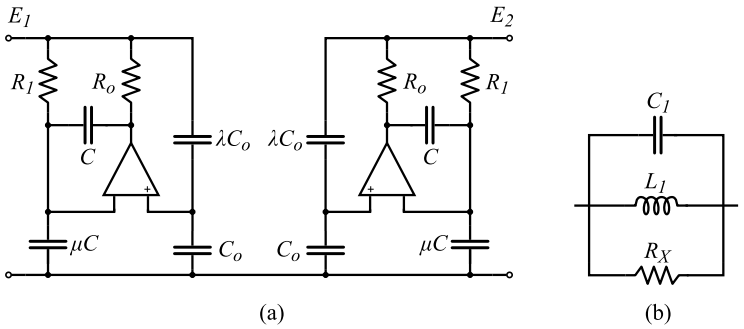

Fig. 8.40 Circuit for Problem 8.11

Fig. 8.41 Circuit for Problem 8.15

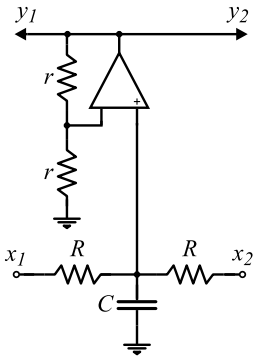

8.12 For the back-to-back connection of Fig. 8.19, show that $I_1(s) = I_2(s)$ and that the input admittance is given by (8.18):

$$Y_{IN}(s) = \frac{1}{\lambda+1}\left[\frac{1}{R} + \frac{1}{kR_o} + \frac{1-\lambda\mu}{R_o}\right] + \frac{1}{2sk(\lambda+1)R_o^2C}$$

8.13 Show that the driving-point admittance of the circuit of Fig. 8.24 is given by (8.22):

$$Y(s) = \left[\frac{C_o + C + (1-\lambda\mu)C_1}{\lambda+1}\right]s + \frac{C_oC_1R}{\lambda+1}s^2$$

8.14 Prove (8.28) and (8.29) of Example 8.7

8.15 Prove that in the circuit Fig. 8.41 we have

$$y_1 = y_2 = \frac{1}{1+s\frac{RC}{2}}x_1 + \frac{1}{1+s\frac{RC}{2}}x_2$$

Quantities x_i and y_i represent voltages.

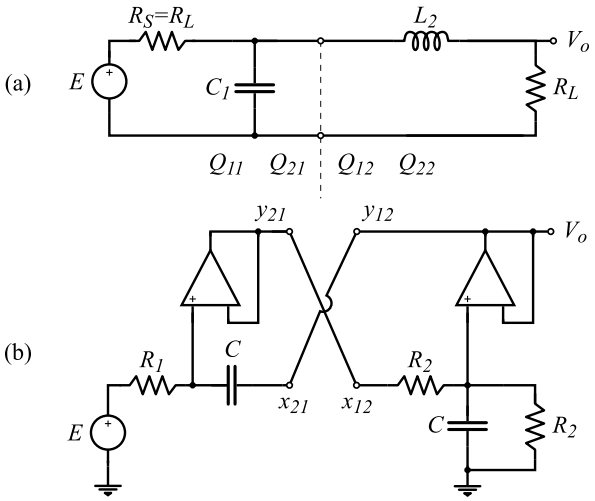

Fig. 8.42 Circuit for Problem 8.16

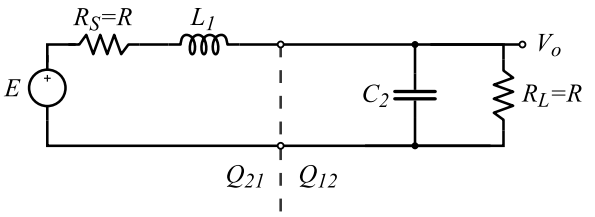

Fig. 8.43 Circuit for Problems 8.17 and 8.18

8.16 Prove that if the passive filter of Fig. 8.42a is linearly transformed using

$$Q_{21} = \begin{bmatrix} 0 & -R_S \\ 1 & -R_S \end{bmatrix} \quad \text{and} \quad Q_{12} = \begin{bmatrix} 1 & R_S \\ 0 & R_S \end{bmatrix}$$

the LTA filter can be implemented as shown in Fig. 8.42b. Determine all element values.

8.17 Use

$$Q_{21} = \begin{bmatrix} 1 & R \\ 0 & R \end{bmatrix} \quad \text{and} \quad Q_{12} = \begin{bmatrix} 0 & -R \\ 1 & -R \end{bmatrix}$$

to linearly transform the passive circuit of Fig. 8.43.

8.18 Use

$$Q_{21} = \begin{bmatrix} 1 & 0 \\ 1 & -R \end{bmatrix} \quad \text{and} \quad Q_{12} = \begin{bmatrix} 1 & R \\ 1 & 0 \end{bmatrix}$$

to linearly transform the passive circuit of Fig. 8.43.

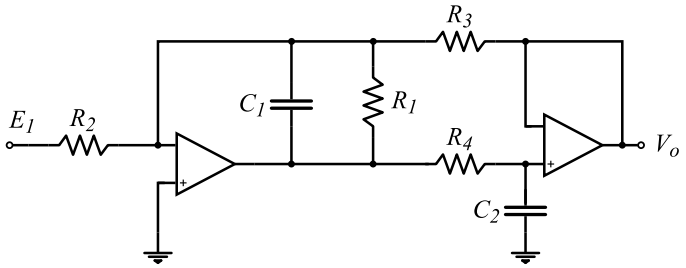

Fig. 8.44 Circuit for Problem 8.19

8.19 Use

$$Q_{21} = \begin{bmatrix} 1 & 0 \\ 0 & -R \end{bmatrix} \quad \text{and} \quad Q_{12} = \begin{bmatrix} 0 & R \\ 1 & 0 \end{bmatrix}$$

to linearly transform the passive circuit of Fig. 8.43. Determine the element values of the circuit shown in Fig. 8.44 so that it implements the corresponding LTA filter.

References[1]

1. Chirlian, P.M.: Signals and Filters. Springer, Berlin (1994)
2. Constantinides, A.G., Dimopoulos, H.G.: Active RC filters derivable from LC ladder filters via linear transformations. IEE J. Electron. Circuits Syst. **1**(1), 17–21 (1976)
3. Constantinides, A.G., Haritantis, G.: Wave active filters. Electron. Lett. **11**, 254–256 (1975)
4. Deliyannis, T., Sun, Y., Fidler, J.K.: Continuous-Time Active Filter Design. CRC Press, Boca Raton (1999)
5. Dimopoulos, H.G., Constantinides, A.G.: Linear transformation active filters. IEEE Trans. Circuits Syst. **CAS-25**(10) (1978)
6. Girling, F.E.J., Good, E.F.: Active filters 12. The leap-frog or active ladder synthesis. Wirel. World **76**, 341–345 (1970)
7. Orchard, H.J.: Inductorless filters. Electron. Lett. **2**, 224 (1966)
8. Paarmann, L.D.: Design and Analysis of Analog Filters—A Signal Processing Perspective—With MATLAB Examples. Kluwer Academic, Dordrecht (2001)
9. Williams, A., Taylor, F.: Electronic Filter Design Handbook. McGraw-Hill, New York (2006)
10. Wupper, H., Meerkoetter, K.: New active filter synthesis based on scattering parameters. In: IEEE Symposium on Circuits and Systems, pp. 254–257 (1975)

[1] All references, whether or not cited within the text, are recommended for further reading.

Operational Amplifiers

9

9.1 Introduction

The importance of the operational amplifier (OA or op amp) as a very powerful component in the arsenal of electronic circuits has been recognized since the '40s. At that time, they were implemented using electronic tubes. Twenty or so years later, advances in semiconductor and integrated circuits technology made possible the manufacture of low cost monolithic operational amplifiers. This provided a phenomenal impetus to the profound and wide-ranging applications of such components.

In 1952, the first operational amplifier was made commonly available to the public. It was the K2-W, designed by George A. Philbrick of G.A. Philbrick Researches Inc. Tubes were replaced by transistors in the K2-W only in 1962. At the same time, Burr Brown Corporation developed a transistor operational amplifier. In 1963, Robert Widlar designed the first monolithic operational amplifier, the μA702, which, in spite of its inherent design weaknesses, was sold by Fairchild Semiconductors at the price of 300 dollars, mainly for military and aerospace applications. Two years later in 1965, Fairchild introduced its own μA709, designed again by Widlar. The new chip had significantly improved features as compared to its predecessor and was initially sold for "only" 70 dollars, though soon its price fell to 5 dollars. In 1970, the price of operational amplifiers had already fallen to under 2 dollars per unit.

Widlar had in the meanwhile left Fairchild for a new company, National Semiconductors, where he designed the LM101, a chip which needed an external compensation capacitor. A little later, the LH101, the first operational amplifier with internal compensation, was introduced, followed by the LM107. Fairchild responded in May 1968 by introducing the μA748 with external compensation and the μA741, designed by Dave Fullagar, with internal compensation. In 1974, National introduced the LM324, the first single supply chip, and Raytheon Semiconductor the RC4558, the first monolithic dual operational amplifier.

H.G. Dimopoulos, *Analog Electronic Filters*, Analog Circuits and Signal Processing,
DOI 10.1007/978-94-007-2190-6_9, © Springer Science+Business Media B.V. 2012

In 1975, RCA introduced the CA3130, the first FET operational amplifier, and National replied with J-FET technology offering the LF355. The same technology was used by Texas Instruments to introduce a quad chip in 1976, the TL084. This was just the start of significant developments.

Many of the chips mentioned in this short historical review, based mainly on [4] are still available on the market with improved characteristics due to improved technology. New operational amplifiers have also appeared with much better specifications as compared to the old chips. The price of high-specifications commercial op amps is today under half a dollar, and at only marginally above this price, one can obtain chips with outstanding characteristics.

All these operational amplifiers handle voltages to produce voltages and are characterized as *voltage-mode* or *voltage feedback* op amps. In the early '80s, Comlinear, a company bought later by National Semiconductors, introduced *current-mode* or *current feedback* operational amplifiers. These amplifiers handle currents instead of voltages and, as will be seen later, they have wider bandwidth.

Filter designers took advantage of the constantly improving characteristics of op amps and from the early '70s designed active filters, creating a new engineering area which is still at the cutting edge of electrical engineering research. Using operational amplifiers and similar operational devices like operational transconductance amplifiers (OTA) implemented in MOS/CMOS technology, high-frequency low-power consumption filters can be easily integrated, serving the needs for such circuits, especially in mobile communications systems.

9.2 Operational Amplifier Models

Operational amplifiers are the fundamental building blocks of active filters, and for this reason a thorough understanding of their operation, limitations and usage is absolutely necessary for anyone who studies or designs filters. The subject will be presented mainly at device level, avoiding wherever possible the details of their internal circuits. Most books on electronics deal with the circuits that implement operational amplifiers.

As already mentioned, operational amplifiers can be categorized into two major categories: voltage-mode and current-mode. The mostly commonly used operational amplifiers are voltage-mode devices designed with voltage signals in mind, in contrast to current-mode amplifiers, which are designed for current handling. This situation may, of course, change as the bandwidth advantage of the current-mode type is deployed in a wide range of products.

9.2.1 Voltage-Mode Operational Amplifiers

Figure 9.1a shows the symbol of the ideal voltage-mode operational amplifier. Although real OAs chips provide more terminals (pins), e.g. for DC biasing, external compensation etc., in this symbol only the operational signal terminals are shown.

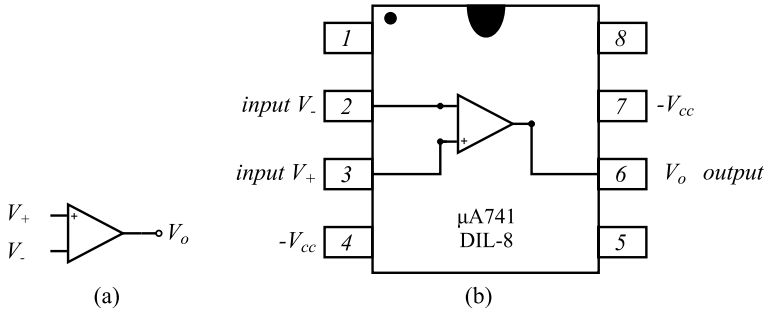

Fig. 9.1 (**a**) Operational amplifier circuit symbol. (**b**) The μA741

Operational amplifiers have two input terminals, the inverting and the non-inverting, denoted by "−" and "+" respectively. In the linear range of the performance of the device, the output voltage is proportional to the voltage difference of the two inputs:

$$v_o(t) = A(v_+(t) - v_-(t)) \quad \text{or} \quad V_o(s) = A(V_+(s) - V_-(s)) \tag{9.1}$$

The factor A is frequency independent in ideal operational amplifiers and is referred to as *open-loop gain*. Its value is theoretically infinite although in real OAs it is frequency dependent, with very high values only at low frequencies, as we will see later.

The electronic circuit of a real operational amplifier uses transistors, resistors and capacitors. A typical example of an op amp circuit is that of Fig. 9.2. The simplified version of this circuit, shown in Fig. 9.3 [6], is used to better understand the way the op amp works.

Circuits of Fig. 9.2 and of Fig. 9.3 are structured in three discrete functional sections. Modern CMOS and biCMOS operational amplifiers have similar functional structure. Referring to Fig. 9.3, the first section, consisting of transistors $Q_1 - Q_4$, ensures very high input resistance and functions as a differential amplifier, distributing the bias current I_A to I_1 and I_2 in a proportion depending on the voltage difference of the inputs. When this difference is very low, then

$$i_1(t) - i_2(t) = g_m(v_+(t) - v_-(t)) \quad \text{or} \quad I_1(s) - I_2(s) = g_m(V_+(s) - V_-(s))$$

Transistors Q_3 and Q_4 force currents I_3 and I_4 to be equal, resulting in:

$$i_{o1}(t) = -g_m(v_+(t) - v_-(t)) \quad \text{or} \quad I_{o1}(s) = -g_m(V_+(s) - V_-(s))$$

This high input impedance section is in fact a transconductance which creates a current that is proportional to the voltage difference of the two inputs.

The next section is a Darlington pair of transistors Q_5-Q_6 with high gain $-A_b$ and a compensation capacitor C which creates a pole at $\omega_a = \frac{1}{RA_bC}$. The resistance R is the equivalent resistance between the input of this section and ground.

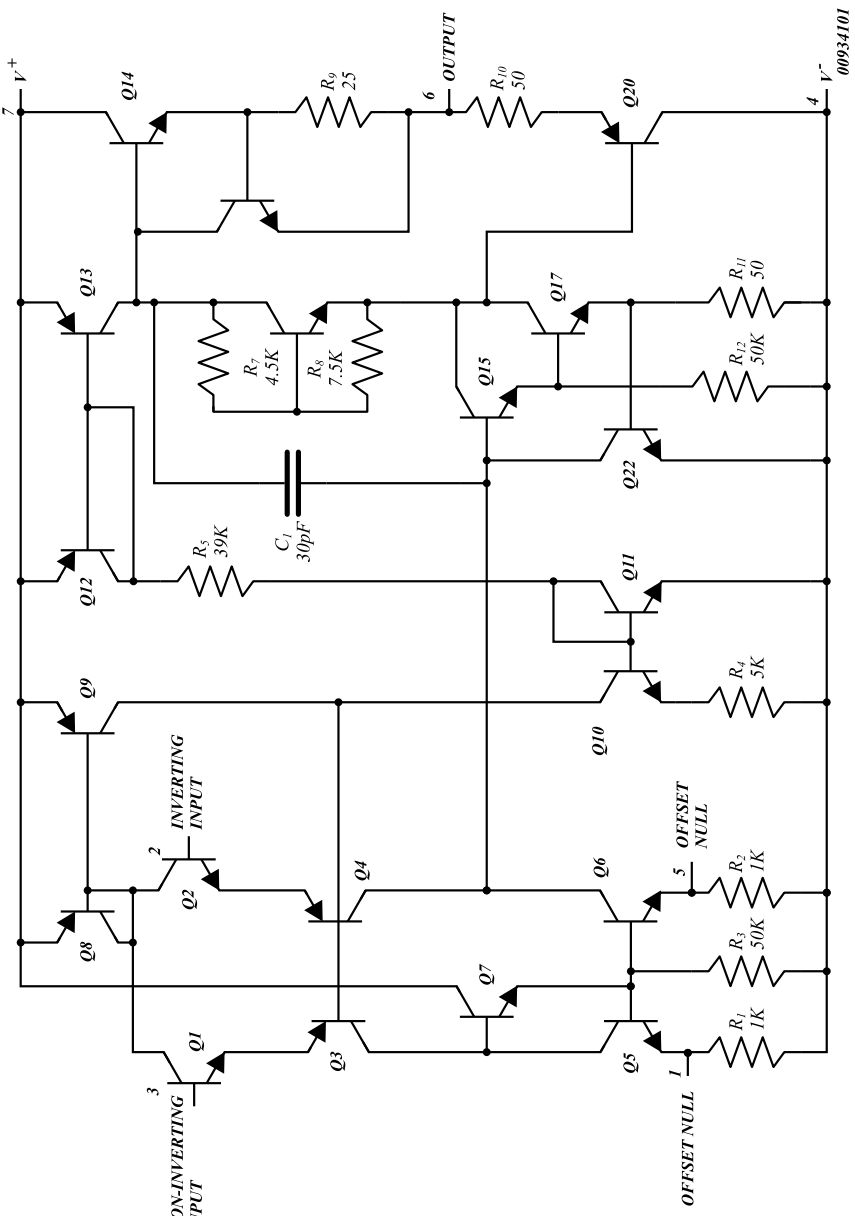

Fig. 9.2 The electronic circuit of LM741 (National Semiconductors)

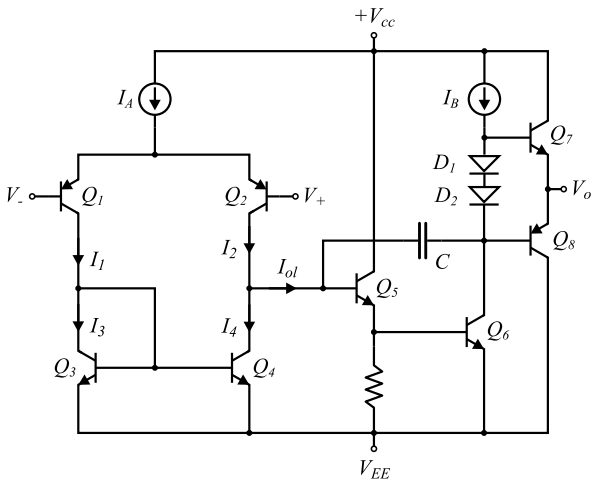

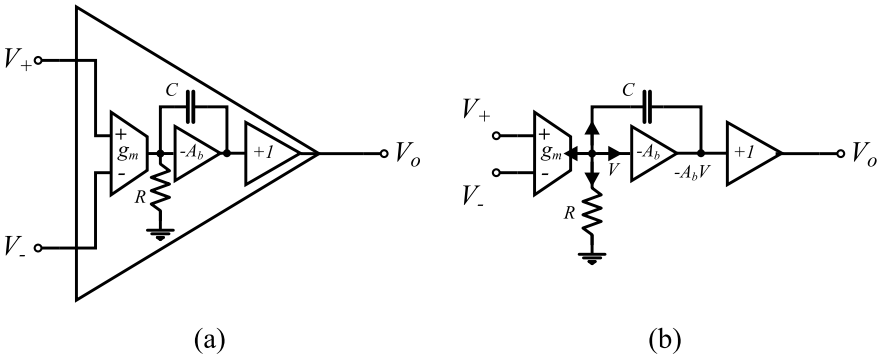

Fig. 9.3 Simplified circuit of a monolithic op amp

Fig. 9.4 Functional diagram of the operational amplifier

The third section consists of transistors Q_7-Q_8 in a push-pull connection that provides unity voltage gain but very high current gain, making this section a power amplifier. It should be noted that this section has very low output resistance and therefore behaves like an ideal voltage source.

Keeping in mind the above analysis, the operational amplifier can be represented with the functional diagram of Fig. 9.4. Capacitor C is the compensation capacitor, which creates, as mentioned, a pole at $\omega_a = \frac{1}{RA_bC}$ and serious problems no matter whether is internal or external.

Writing the KCL for the first node with voltage V (Fig. 9.4) we have:

$$g_m(V_+ - V_-) + \frac{V}{R} + (V + A_bV)sC = 0 \tag{9.2}$$

Since $V_o = -A_b V$, (9.2) yields:

$$V_o = \frac{g_m}{\frac{1}{RA_b} + sC(1 + \frac{1}{A_b})}(V_+ - V_-) \tag{9.3}$$

In the operational amplifier circuit, $A_b \gg 1$ and therefore equation (9.3) can be written as

$$V_o = \frac{g_m}{\frac{1}{RA_b} + sC}(V_+ - V_-) = \frac{g_m/C}{\frac{1}{RCA_b} + s}(V_+ - V_-) \tag{9.4}$$

and finally, the voltage transfer function of the voltage-mode operational amplifier is given by:

$$\boxed{A(s) = \frac{V_o}{(V_+ - V_-)} = \frac{g_m/C}{s + \frac{1}{RCA_b}}} \tag{9.5}$$

In the case of the ideal op amp, where A_b tends to infinity and (9.5) gives:

$$A(s) = \frac{g_m R A_b}{sRCA_b + 1} \approx \frac{g_m}{sC} \tag{9.6}$$

If in addition we consider that for the ideal op amp $C \to 0$, (9.6) yields:

$$A(s) = \lim_{C \to 0}\left(\frac{g_m}{sC}\right) = A \quad \text{where } A \to \infty \tag{9.7}$$

Finally, for the ideal operational amplifier we have:

$$\boxed{V_o = A(V_+ - V_-) \quad \text{with } A \to \infty} \tag{9.8}$$

Equation (9.8) is the model of the ideal operational amplifier, in which it is assumed that the open-loop gain is not only infinite but also frequency independent. No matter how simple this model appears, it can be used without hesitation for the analysis of real circuits with operational amplifiers embedded in them and having feedback paths, at least for the estimation of their performance.

The ideal voltage-mode operational amplifier can be represented by the equivalent circuit model of Fig. 9.5.

This model clearly shows the external characteristics of the voltage-mode operational amplifier. The input resistance R_{IN} is very high in order to ensure near zero input currents. The output resistance, appearing as the internal resistance R_{OUT} of the voltage controlled voltage source, is very low, ensuring that the output voltage does not depend in any substantial way on the current drawn from the output terminal.

Another more realistic model of the voltage-mode op amp is given by (9.5), repeated here

$$A(s) = \frac{V_o}{(V_+ - V_-)} = \frac{g_m/C}{s + \frac{1}{RCA_b}} \tag{9.9}$$

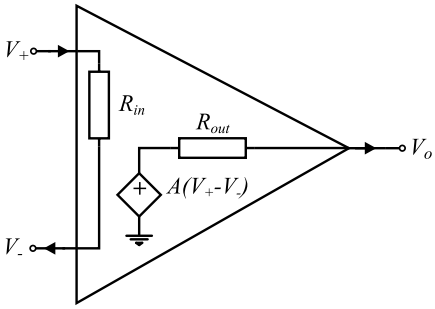

Fig. 9.5 Circuit model of the voltage-mode operational amplifier

This equation constitutes the *one-pole model* for obvious reasons. The pole is of course $s_a = -\frac{1}{RCA_b}$.

Defining the pole frequency and the DC open-loop gain respectively as

$$\boxed{\omega_a = \frac{1}{RCA_b} \quad \text{and} \quad A_{dc} = A(0) = g_m R A_b} \tag{9.10}$$

equation (9.9) of the one-pole model becomes:

$$\boxed{A(s) = \frac{\omega_a A_{dc}}{s + \omega_a}} \tag{9.11}$$

Comparing (9.9) and (9.11), we get

$$\frac{g_m}{C} = \omega_a A_{dc} \tag{9.12}$$

The product $\omega_a A_{dc} = \omega_t$ is defined as the gain-bandwidth product (GBP) of the operational amplifier and is one of its most important characteristics.

$$\boxed{GBP = \omega_t = \omega_a A_{dc} = \frac{g_m}{C}} \tag{9.13}$$

The one-pole model equation (9.11) can be rewritten in terms of the gain-bandwidth product as follows:

$$\boxed{A(s) = \frac{\omega_t}{s + \omega_a}} \tag{9.14}$$

The open-loop gain at the pole frequency $\omega_a = \frac{1}{RCA_b}$ is

$$A(j\omega_a) = \frac{\omega_a}{j\omega_a + \omega_a} A_{dc} = \frac{1}{1+j} A_{dc} \quad \longrightarrow \quad |A(j\omega_a)| = \frac{\sqrt{2}}{2} A_{dc} \tag{9.15}$$

This means that at the pole frequency ω_a the logarithmic open-loop gain falls by 3 dB from the level at DC. The frequency ω_a defines the *open-loop bandwidth* of the voltage-mode operational amplifier.

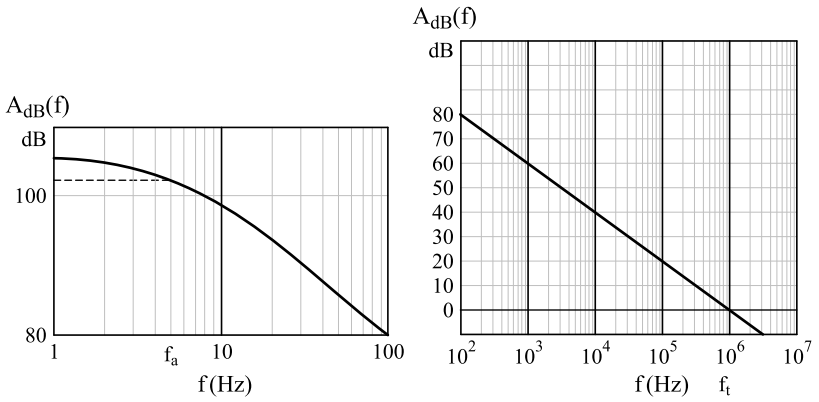

Fig. 9.6 Open-loop gain plots

The open-loop gain of the op amp at the frequency ω_t of the GBP is

$$|A(j\omega_t)| = \frac{\omega_t}{\sqrt{\omega_t^2 + \omega_a^2}} = \frac{1}{\sqrt{1 + \frac{\omega_a^2}{\omega_t^2}}} = \frac{1}{\sqrt{1 + \frac{1}{A_{dc}^2}}} \approx 1 \tag{9.16}$$

The quantity A_{dc}^2 is extremely high, of the order of 10^{10}, even for low quality operational amplifiers. This means that the logarithmic gain of the op amp at $\omega = \omega_t$ is zero. Gain-bandwidth product is a measure of the useful frequency bandwidth of an operational amplifier. The higher the GBP, the higher the frequency up to which the operational amplifier behaves usefully.

It should be remembered that $A(s)$ is the open-loop voltage transfer function of the operational amplifier. The typical specifications of the popular μA741 are: $R = 10^5$ Ohm, $A_b = 10^4$, $C = 30$ nF and $g_m = 200$ µSiemens. For these values, A_{dc}, ω_a and ω_t can be calculated: $A_{dc} = 200,000$, $\omega_a = 2\pi \cdot 5.3$ rad/s and $\omega_t = 2\pi \cdot 1.06 \cdot 10^6$ rad/s. Figure 9.6 shows the corresponding open-loop gain as a function of frequency.

Equation (9.14) can be rewritten as

$$A(s) = \frac{\omega_t}{s + \omega_a} = \frac{1}{\frac{s}{\omega_t} + \frac{\omega_a}{\omega_t}} \tag{9.17}$$

Since $\omega_t \gg \omega_a$, the ratio $\frac{\omega_a}{\omega_t} \to 0$ and the above equation (9.17) can be simplified to

$$\boxed{A(s) = \frac{\omega_t}{s}} \tag{9.18}$$

Equation (9.18) defines the *integrator model* of the voltage-mode operational amplifier, which is also used extensively due to its simplicity.

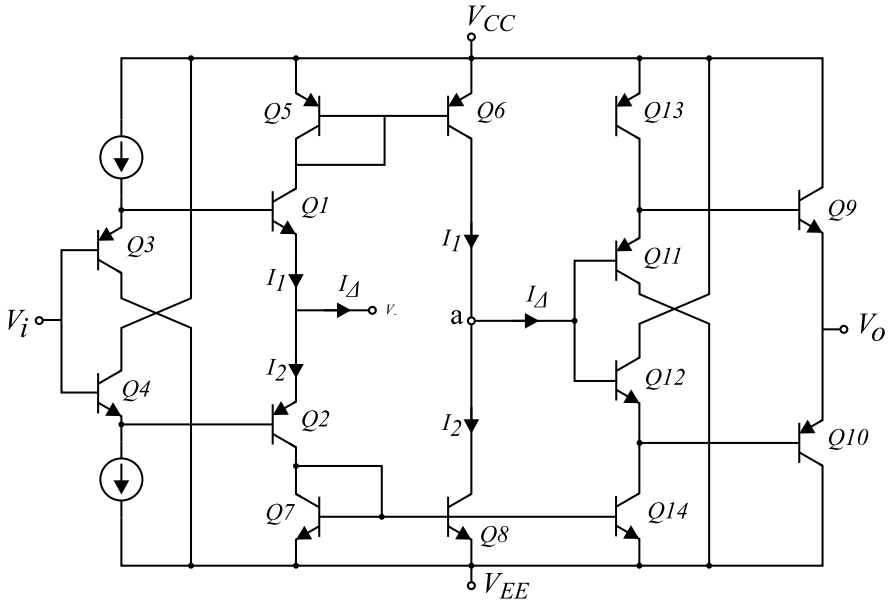

Fig. 9.7 Simplified circuit of current-mode operational amplifier

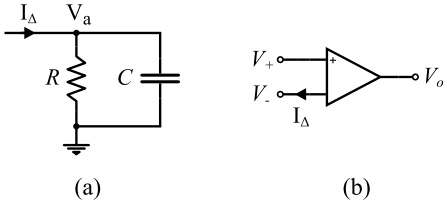

Fig. 9.8 The symbol of the current-mode operational amplifier

9.2.2 Current-Mode Operational Amplifiers

Current-mode operational amplifiers are based on "current logic" instead of voltage logic. Figure 9.7 shows a simplified electronic circuit that implements a current-mode op amp. Again, three sections can be discerned.

The first section ($Q_1 - Q_4$) tries, by adjusting the current of the inverting input $I_\Delta = I_1 - I_2$, to make the voltages V_+ and V_- of the two inputs equal. The circuit, provides very low input resistances, in contrast to the voltage-mode op amp, where input resistances are very high.

The second section ($Q_5 - Q_8$) creates "mirror images" of currents I_1 and I_2 and their difference $I_\Delta = I_1 - I_2$ in node a. The circuitry of $Q_5 - Q_6$ and that of $Q_7 - Q_8$ are called *current mirrors* because they create the mirror images of currents I_1 and I_2. The difference $I_\Delta = I_1 - I_2$ is fed to the input of the next section, the resistance and capacitance of which are R and C respectively, as in Fig. 9.8a.

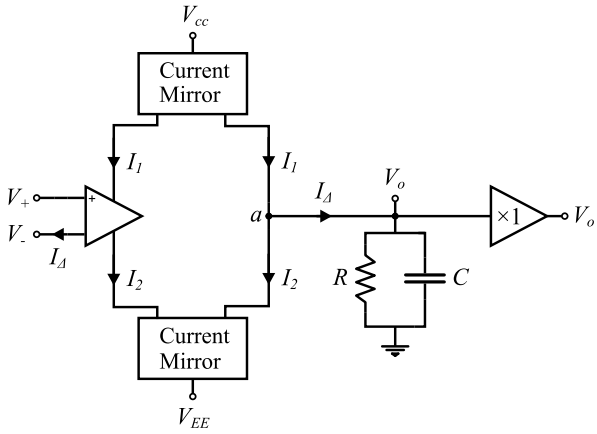

Fig. 9.9 Functional diagram of the current-mode op amp

As a result, the nodal voltage V_a is given by:

$$V_\alpha(s) = \frac{R}{sRC+1} I_\Delta(s) = \frac{1/C}{s+\frac{1}{RC}} I_\Delta(s)$$

The third section simply isolates the voltage of node a and forwards it with gain 1 to the output of the current-mode op amp with very low output resistance. Therefore,

$$\boxed{V_o(s) = V_\alpha(s) = \frac{R}{sRC+1} I_\Delta(s) = \frac{1/C}{s+\frac{1}{RC}} I_\Delta(s)} \tag{9.19}$$

The symbol of the current-mode operational amplifier is shown in Fig. 9.8b. The three sections described above are shown better in Fig. 9.9.

Equation (9.19) is the model of the current-mode op amp and the quantity

$$\boxed{Z_o(s) = \frac{V_o(s)}{I_\Delta(s)} = \frac{R}{sRC+1} = \frac{1/C}{s+\frac{1}{RC}}} \tag{9.20}$$

is called open-loop *transimpedance* of the current-mode op amp.

The DC transimpedance is $Z_{dc} = Z_o(0) = R$ and $Z_o(s)$ has a pole for $s_p = -\frac{1}{RC}$. At the frequency

$$\omega_a = \frac{1}{RC} \qquad \left(f_a = \frac{1}{2\pi RC}\right) \tag{9.21}$$

the magnitude of the transimpedance falls by 3 dB from Z_{dc}. Typical values of real life current-mode op amps, like Comlinear's CLC401, are $R = 710$ kOhm and $f_a = \omega_a/2\pi = 350$ kHz. These values used in (9.21) give $C = 0.64$ pF.

In current-mode operational amplifiers, the calculation of the open-loop voltage transfer function is meaningless. Voltage transfer functions can however be calculated when the amplifier is in a circuit with feedback. Let us, for example, study the

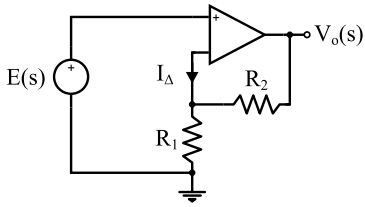

Fig. 9.10 Non-inverting voltage amplifier

circuit of Fig. 9.10, which is the typical non-inverting voltage amplifier with one current-mode op amp. The input signal is applied to the low input resistance non-inverting input and a fraction of the output is fed back to the inverting input through resistors R_1 and R_2.

The internal circuit of the current-mode op amp determines the current I_Δ so that the voltages of the inverting and non-inverting inputs are equal. This means that $V_- = E$ and from Kirchhoff's current law we get:

$$I_\Delta(s) = \frac{E(s)}{R_1} + \frac{E(s) - V_o(s)}{R_2} \tag{9.22}$$

From (9.19), we have

$$V_o(s) = Z_o(s) I_\Delta(s) \quad \Rightarrow \quad I_\Delta(s) = \frac{V_o(s)}{Z_o(s)}$$

where $Z_o(s)$ is the transimpedance $Z_o(s) = \frac{1/C}{s+\frac{1}{RC}}$ of the op amp according to (9.20). Combining these equations, we find the voltage transfer function of the device:

$$H(s) = \frac{V_o(s)}{E(s)} = \left(1 + \frac{R_2}{R_1}\right) \frac{1}{1 + \frac{R_2}{Z_o(s)}} \tag{9.23}$$

Transimpedance Z_o is very high at least up to the pole frequency $f_a = \omega_a/2\pi = 1/2\pi RC$ from which it starts falling. Typical value for f_a exceeds 300 kHz, and therefore the magnitude of the transimpedance remains high for much higher frequencies. R_2 is usually at such a level as to keep the ratio $\frac{R_2}{Z_o(s)}$ very low in (9.23). Setting $Z_o(s) = \frac{1/C}{s+\frac{1}{RC}}$ in (9.23), the transfer function becomes:

$$H(s) = k \frac{\frac{1}{R_2 C}}{s + \frac{R+R_2}{RR_2C}} \quad \text{with } k = 1 + \frac{R_2}{R_1} \tag{9.24}$$

The characteristics of such a transfer function are:

$$\begin{aligned} G_{dc} &= |H(j0)| = \frac{kR}{R+R_2} = \frac{1+(R_2/R_1)}{1+(R_2/R)} \quad \text{and} \\ \omega_{3dB} &= \frac{R+R_2}{RR_2C} = \frac{1+\frac{R_2}{R}}{R_2C} \end{aligned} \tag{9.25}$$

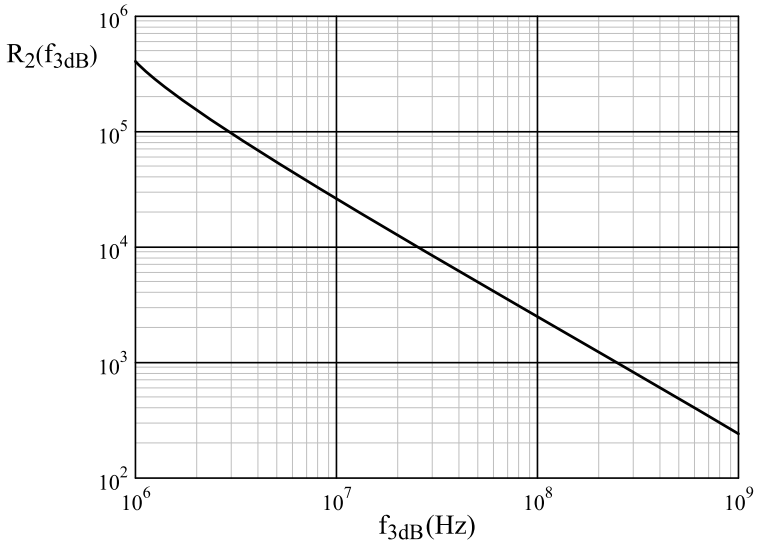

Fig. 9.11 Plot of the resistance as a function of bandwidth

It is very interesting to observe that the bandwidth ω_{3dB} of the device, the frequency at which the gain becomes $\frac{\sqrt{2}}{2}G_{dc}$, depends strongly on the value of R_2. This means that R_2 can be calculated from the desirable bandwidth ω_{3dB}, and the gain $k = 1 + \frac{R_2}{R_1}$ can be adjusted independently using R_1.

Example 9.1 The non-inverting voltage amplifier of Fig. 9.10 will be designed to implement voltage gain $k_o = 4$ using an integrated current-mode operational amplifier with $R = 710$ kOhm and $f_a = 350$ kHz $\rightarrow C = 0.64$ pF.

From (9.25) we have

$$G_{dc} = k_o = \frac{1 + (R_2/R_1)}{1 + (R_2/R)} \quad \Rightarrow \quad R_1 = \frac{R_2}{k_o(1 + (R_2/R)) - 1} \tag{9.26}$$

This means that we can select any value for R_2 and calculate the value of R_1 in order to have DC and low frequency gain equal to $k_o = 4$. The value of R_2 can be calculated from (9.25) and the desired bandwidth ω_{3dB}:

$$\omega_{3dB} = \frac{R + R_2}{RR_2C} = \frac{1 + \frac{R_2}{R}}{R_2C} \quad \Rightarrow \quad R_2 = \frac{1}{2\pi \cdot f_{3dB} \cdot C - \frac{1}{R}} \tag{9.27}$$

Figure 9.11 shows the plot of the value of R_2 as a function of bandwidth f_{3dB}, from which it is obvious that high values of R_2 correspond to low bandwidth values.

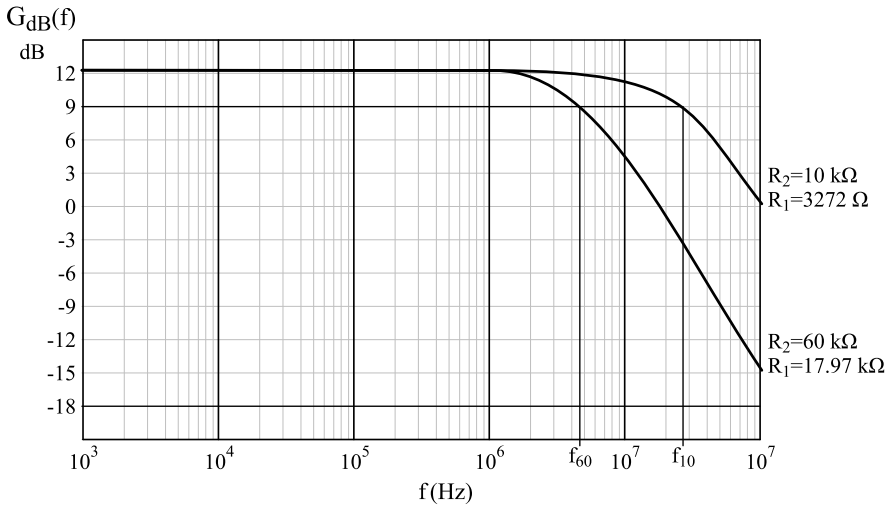

Fig. 9.12 Gain plot for two resistance values

For example:

$$R_2 = 60 \text{ kOhm}$$

$$\Rightarrow \quad f_{3dB} = \frac{1 + (R_2/R)}{2\pi \cdot R_2 C} = \frac{1 + (60 \cdot 10^3 / 710 \cdot 10^3)}{2\pi \cdot 60 \cdot 10^3 \cdot 0.64 \cdot 10^{-12}} \approx 4.5 \text{ MHz}$$

$$R_2 = 10 \text{ kOhm}$$

$$\Rightarrow \quad f_{3dB} = \frac{1 + (R_2/R)}{2\pi \cdot R_2 C} = \frac{1 + (10 \cdot 10^3 / 710 \cdot 10^3)}{2\pi \cdot 10 \cdot 10^3 \cdot 0.64 \cdot 10^{-12}} \approx 25 \text{ MHz}$$

From (9.26) with $k_o = 4$ and $R = 710$ kOhm, we find that:

$$R_1 = \begin{cases} 17.97 \text{ kOhm} & \text{for } R_2 = 60 \text{ kOhm} \\ 3.27 \text{ kOhm} & \text{for } R_2 = 10 \text{ kOhm} \end{cases}$$

Figure 9.12 shows the logarithmic gain of the circuit for the two values of R_2 as a function of frequency in order to highlight both its dependence on R_2 and the fact that the gain is reduced at a rate of 6 dB/octave after f_{3dB}.

Current-mode operational amplifiers, apart from their poor characteristics with respect to input offset voltage and input bias current, have some advantages over their voltage-mode counterparts, mainly as far as their high frequency operation is concerned.

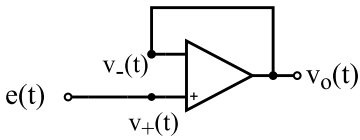

Fig. 9.13 The voltage follower or buffer

9.3 Basic Operational Amplifier Circuits

Some basic circuits with operational amplifiers will be presented in this section not only for their usefulness, but also as paradigms of analysis of circuits involving operational amplifiers.

9.3.1 Voltage Follower or Buffer

The simple circuit of Fig. 9.13 is a voltage-mode operational amplifier in which the output is fed back to the inverting input.

For the analysis of the circuit, we use $V_+(s) = E(s)$ and $V_-(s) = V_o(s)$ in (9.5), the basic equation of the ideal voltage-mode operational amplifier, to get

$$V_o(s) = A(s)(E(s) - V_o(s)) \quad \Rightarrow \quad V_o(s) = \frac{1}{1 + \frac{1}{A(s)}} E(s) \tag{9.28}$$

and therefore

$$H(s) = \frac{V_o(s)}{E(s)} = \frac{1}{1 + \frac{1}{A(s)}} \tag{9.29}$$

If the operational amplifier is ideal, then $A(s) = A \to \infty$ and (9.29) yields

$$H(s) = 1 \quad \Rightarrow \quad V_o(s) = E(s) \quad \text{and} \quad v_o(t) = e(t)$$

This justifies the name of voltage follower since output voltage follows the input voltage. Although the input-output voltage relationship is very simple, a voltage follower, when inserted between two sections, isolates them in that the second section does not draw any current from the first. The commonly used name "buffer" is due to this isolation property of the voltage follower.

If the operational amplifier used in the voltage follower circuit is not ideal, then according to the one-pole model (9.14), $A(s) = \frac{\omega_t}{s+\omega_a}$ and the transfer function of (9.29) becomes:

$$H(s) = \frac{V_o(s)}{E(s)} = \frac{1}{1 + \frac{1}{A(s)}} = \frac{\omega_t}{s + \omega_a + \omega_t}$$

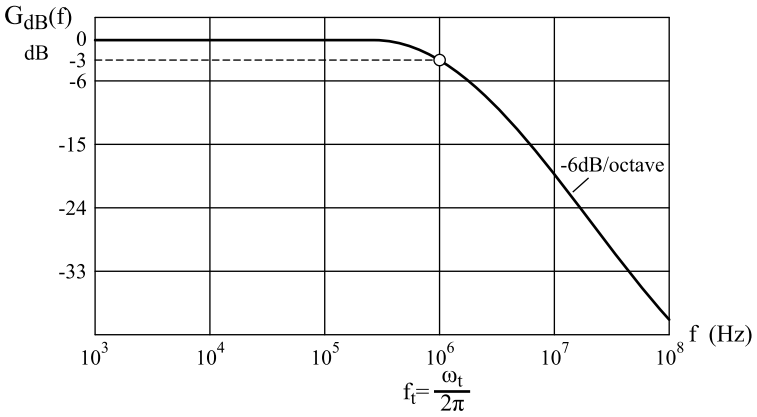

Fig. 9.14 Logarithmic gain of a voltage follower using the μA741

The gain of the voltage follower, the magnitude of $H(j\omega)$, is no longer frequency independent since

$$G(\omega) = |H(j\omega)| = \frac{\omega_t}{|j\omega + \omega_a + \omega_t|} = \omega_t \sqrt{\frac{1}{\omega^2 + (\omega_t + \omega_a)^2}} \tag{9.30}$$

and

$$G_{dB}(\omega) = 20\log(G(\omega)) \text{ dB}$$

For $\omega = 0$, the DC gain is $G_{dc} = G(0) = \frac{1}{1+\frac{\omega_a}{\omega_t}} \approx 1$ since $\omega_t \gg \omega_a$ (typical values are $f_a = 5$ Hz and $f_t = 1$ MHz). The frequency ω_{3dB} at which the gain becomes $\frac{\sqrt{2}}{2} G_{dc}$ can be calculated as follows:

$$G(\omega_{3dB}) = \frac{\sqrt{2}}{2} G_{dc} = \frac{\sqrt{2}}{2} \frac{\omega_t}{\omega_t + \omega_a} \quad \Rightarrow \quad \omega_{3dB} = \omega_t + \omega_a$$

For frequencies above this value, the logarithmic gain of the device $20\log(G(\omega))$ reduces at a rate of 6 dB/octave. Figure 9.14 shows the dependence of the logarithmic gain of the voltage follower on frequency. The useful bandwidth of the device depends on the affordable gain tolerance. If, for example, gain tolerance is 3 dB down from G_{dc}, then the useful bandwidth is $f_t = \frac{\omega_t}{2\pi}$. If the allowed tolerance is lower, e.g. 1 dB, the useful bandwidth is much lower.

9.3.2 Inverting Amplifier Circuits

In order to calculate the output of the inverting voltage amplifier of Fig. 9.15, we can start from the basic equation (9.5) of the voltage-mode operational amplifier $V_o(s) = A(s)(V_+(s) - V_-(s))$, which becomes $V_o(s) = -A(s)V_-(s)$ since $V_+ = 0$

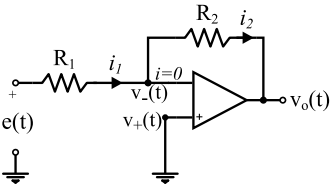

Fig. 9.15 The inverting voltage amplifier

(grounded). At the node of the inverting input, currents i_1 and i_2 are equal since the current drawn by the operational amplifier is zero or negligible even in real op amp chips. Equating the two currents we have:

$$\frac{E(s) - V_-(s)}{R_1} = \frac{V_-(s) - V_o(s)}{R_2}$$

Taking into account that $V_o(s) = -A(s)V_-(s)$, the above equation can be solved for V_o:

$$V_o(s) = -E(s)\frac{R_2}{R_1} \cdot \frac{A(s)}{A(s) + \frac{R_2}{R_1} + 1} = -\frac{(\beta - 1)}{1 + \frac{\beta}{A(s)}} E(s) \tag{9.31}$$

where $\beta = 1 + \frac{R_2}{R_1} > 1$.

If the operational amplifier is ideal with infinite open-loop gain A, then (9.31) gives

$$V_o(s) = -\frac{R_2}{R_1} E(s) \quad \text{or} \quad v_o(t) = -\frac{R_2}{R_1} e(t) \tag{9.32}$$

The usefulness of such a circuit is obvious, especially when the ratio of the two resistors R_2/R_1 can take any value. Moreover, it should be noticed that due to the negative sign, there is a phase difference of 180° between input-output. Finally, it is noteworthy that the voltage of the inverting input of the operational amplifier, given by

$$V_-(s) = -\frac{V_o(s)}{A(s)} = \frac{\beta - 1}{A(s) + \beta} E(s)$$

tends to zero due to the fact that in the ideal operational amplifier, the open-loop gain $A(s) = A \to \infty$. The operational amplifier succeeds in making the voltages of its inputs equal, a fact that can be considered as a basic function of its operation in the linear region.

Let us now consider that the operational amplifier used in the inverting voltage amplifier circuit is not ideal, i.e. its open-loop gain is frequency dependent given by the one-pole model (9.14), $A(s) = \frac{\omega_t}{s + \omega_a}$. Combining this with (9.31), we get:

$$H(s) = \frac{V_o(s)}{E(s)} = -\frac{R_2}{R_1} \cdot \frac{\frac{\omega_t}{\beta}}{s + \frac{\omega_t}{\beta} + \omega_a} = \frac{(1 - \beta)\frac{\omega_t}{\beta}}{s + \frac{\omega_t}{\beta} + \omega_a} \quad \text{where } \beta = 1 + \frac{R_2}{R_1} > 1 \tag{9.33}$$

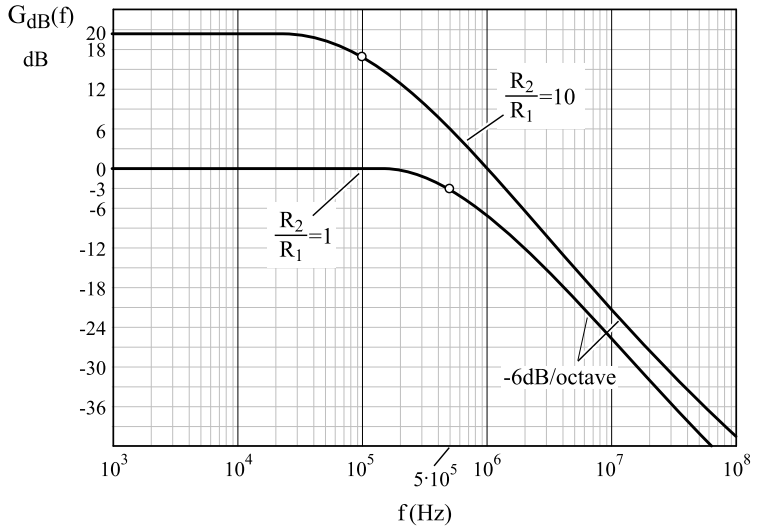

Fig. 9.16 Gain plots for two values of the resistance ratio

If G_{dc} is the DC gain at $s = 0$, then the frequency at which the gain falls by 3 dB and subsequently at a rate 6 dB/octave is the frequency of the pole:

$$\omega_{3dB} = \frac{\omega_t}{\beta} + \omega_a \quad \text{or} \quad f_{3dB} = \frac{f_t}{\beta} + f_a \tag{9.34}$$

The bandwidth of the device is ω_{3dB} and depends on $\beta = 1 + (R_2/R_1)$ in such a way that the useful bandwidth of the device decreases as the ratio R_2/R_1 increases.

Figure 9.16 shows this clearly and is drawn for an inverting voltage amplifier which uses a typical operational amplifier like μA741. For $R_2/R_1 = 1$, we have $f_{3dB} = 0.5$ MHz whilst for $R_2/R_1 = 10$ the 3 dB frequency is 0.1 MHz. In both cases, gain is decreasing at a rate of 6 dB/octave after f_{3dB}. The DC gain G_{dc} of the device can be calculated from (9.33) for $s = 0$:

$$G_{dc} = |H(s)|_{s=j0} = \frac{\beta - 1}{1 + \beta \frac{\omega_a}{\omega_t}} \tag{9.35}$$

Evidently, the DC gain depends on β and the characteristics of the operational amplifier. Using (9.35) in (9.34), we get an expression of the device bandwidth as a function of the op amp's characteristics:

$$\omega_{3dB} = \frac{\omega_t}{\beta} + \omega_a = \omega_t \frac{1 - G_{dc}\frac{\omega_a}{\omega_t}}{1 + G_{dc}} + \omega_a \tag{9.36}$$

Example 9.2 (Design of an Inverting Voltage Amplifier) The inverting voltage amplifier will be designed using a monolithic μA741 operational amplifier with $f_t = 1$ MHz and $f_a = 5.3$ Hz. The DC gain of the amplifier will be $G_{dc} = 4$, i.e. logarithmic gain $20\log(4) = 12$ dB.

From (9.35), we get

$$\beta = \frac{1 + G_{dc}}{1 - G_{dc}(\omega_a/\omega_t)} \quad \Rightarrow \quad \frac{R_2}{R_1} = \beta - 1 = G_{dc}\frac{1 + (\omega_a/\omega_t)}{1 - G_{dc}(\omega_a/\omega_t)} \tag{9.37}$$

For $G_{dc} = 4$, $\omega_a = 2\pi 5.3$ and $\omega_t = 2\pi 10^6$, the above equation (9.37) gives:

$$\beta = \frac{1+4}{1 - 4\frac{2\pi \cdot 5.3}{2\pi \cdot 10^6}} = 5.000106 \quad \Rightarrow \quad \frac{R_2}{R_1} = \beta - 1 = 4.000106$$

Any resistors R_1 and R_2 with ratio $R_2/R_1 = 4.000106$ can be used to ensure $G_{dc} = 4$. Resistor values of the order of 10 kOhm are usually preferred in active-RC circuit design. Very low resistor values can cause high currents that are not desirable. Very high resistor values tend to create very low currents comparable to the inevitable electronic noise. A decent choice in our example would be $R_1 = 10$ kOhm and $R_2 = 40$ kOhm.

The frequency ω_{3dB} at which the gain falls by 3 dB, i.e from 4 to $4 \cdot \frac{\sqrt{2}}{2} = 2.8284$ is given by (9.36):

$$f_{3dB} = \frac{\omega_{3dB}}{2\pi} = \frac{\omega_t}{2\pi}\frac{1 - G_{dc}\frac{\omega_a}{\omega_t}}{G_{dc} + 1} + \frac{\omega_a}{2\pi} \approx 2.0 \cdot 10^5 \text{ Hz} \tag{9.38}$$

The bandwidth of the inverting voltage amplifier cannot be adjusted since it depends only on the characteristics of the operational amplifier. If higher bandwidth is required, an operational amplifier with higher ω_t can be used. Figure 9.17 shows the logarithmic gain of the inverting voltage amplifier with $G_{dc} = 4$.

9.3.2.1 General Inverting Amplifier

On generalizing the analysis of the circuit of the inverting voltage amplifier with an ideal operational amplifier, we find that the voltage transfer function of the general inverting amplifier circuit of Fig. 9.18 is given by:

$$H(s) = \frac{V_o(s)}{E(s)} = -\frac{Z_2(s)}{Z_1(s)} \tag{9.39}$$

It is obvious that impedances $Z_1(s)$ and $Z_2(s)$ determine the form of the transfer function.

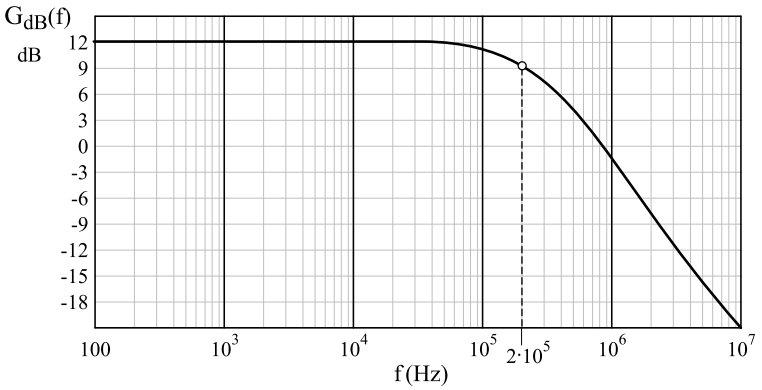

Fig. 9.17 Gain plot of the inverting voltage amplifier

Fig. 9.18 General inverting voltage amplifier

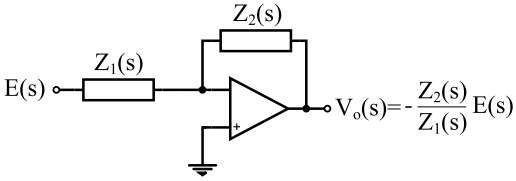

Fig. 9.19 The summation property of the inverting voltage amplifier

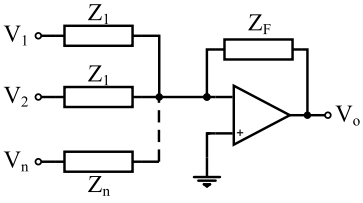

The inverting input of the operational amplifier of the voltage amplifier has the summation property, as shown in Fig. 9.19. The output of this circuit with more than one voltage inputs can be found:

$$V_o(s) = -\frac{Z_F}{Z_1}V_1(s) - \frac{Z_F}{Z_2}V_2(s) - \cdots - \frac{Z_F}{Z_n}V_n(s) \tag{9.40}$$

9.3.2.2 The Inverting Integrator (Miller)

The inverting integrator of Fig. 9.20, known as the Miller integrator, belongs to the inverting voltage amplifier family. In order to analyse this circuit, we assume initially that the op amp's inputs exhibit very high input resistance. Under this assumption, the current entering the operational amplifier is negligible, resulting in the current of R_1 being equal to that of the capacitor C_2. This is expressed in the

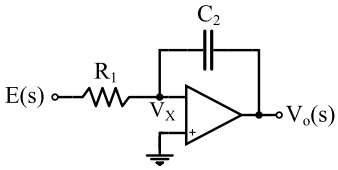

Fig. 9.20 The Miller inverting integrator

following equation:

$$\frac{E(s) - V_x(s)}{R_1} = (V_x(s) - V_o(s))sC_2 \tag{9.41}$$

where V_x is the voltage of the inverting input. Combining (9.41) with the model $V_o(s) = A(s)(V_+ - V_-)$ with $V_+ = 0$, we find

$$V_o(s) = -\frac{1}{(1 + \frac{1}{A(s)})sR_1C_2 + \frac{1}{A(s)}}E(s) \tag{9.42}$$

For ideal operational amplifier with constant $A(s) = A \to \infty$, this equation gives:

$$V_o(s) = -\frac{1}{sR_1C_2}E(s) \quad \text{or} \quad v_o(t) = -\frac{1}{R_1C_2}\int_0^t e(t)dt \tag{9.43}$$

The voltage transfer function of the Miller integrator with an ideal op amp will be

$$H(s) = \frac{V_o(s)}{E(s)} = -\frac{1}{sR_1C_2} \tag{9.44}$$

and the gain will be given by

$$G(\omega) = |H(j\omega)| = \frac{1}{\omega R_1C} \tag{9.45}$$

The plain and the logarithmic gain of a typical Miller integrator is shown in Fig. 9.21. The integrator's behavior when the operational amplifier is not ideal will be studied in Sect. 9.4. Nevertheless, in Sect. 9.4 there is a design example (Fig. 9.40) of an ideal inverting integrator, the gain plot of which is compared to the gain of the circuit when the real op amp characteristics are taken into account.

9.3.2.3 The Lossy Integrator

The voltage transfer function of the circuit of Fig. 9.22a is:

$$H(s) = \frac{V_o(s)}{E(s)} = \frac{1}{sR_1C_1 + 1} \tag{9.46}$$

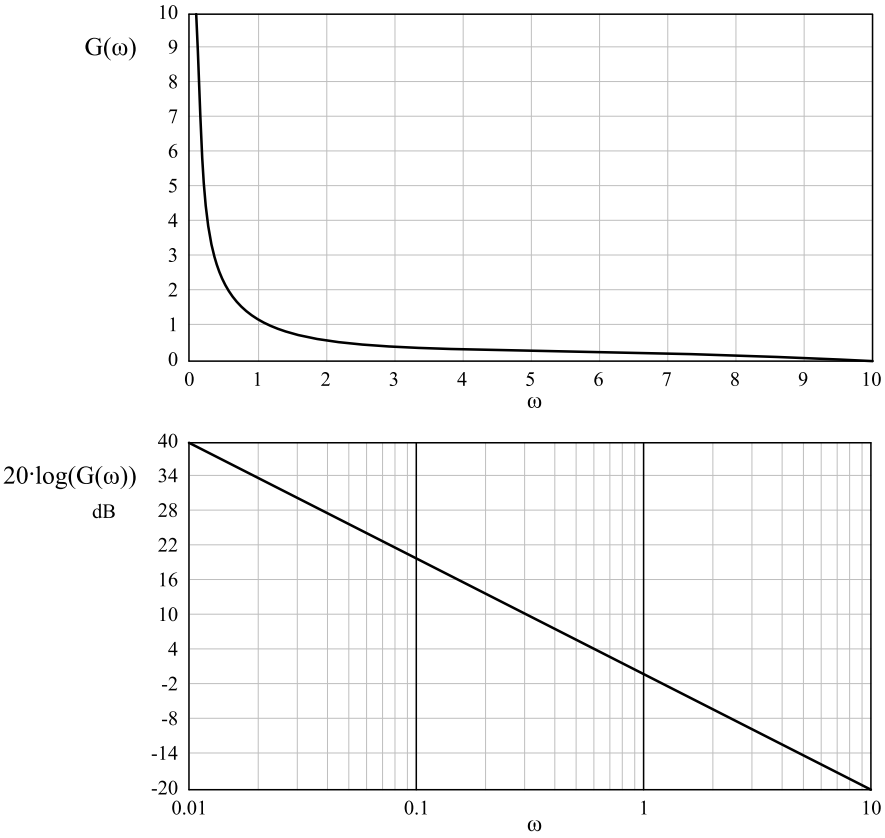

Fig. 9.21 Gain plots of a Miller integrator employing an ideal op amp

but changes if its output is connected to a circuit with finite input impedance. For example if a load R is connected to the output, as shown in Fig. 9.22b, the transfer function becomes:

$$H_b(s) = \frac{V_o(s)}{E(s)} = \frac{1}{sR_1C_1 + 1 + \frac{R_1}{R}} \tag{9.47}$$

A voltage follower can be connected to the output of the circuit of Fig. 9.22a to ensure that the transfer function will not change, as shown in the circuit of Fig. 9.22c.

The circuit of Fig. 9.23 has a voltage transfer function

$$H(s) = \frac{V_o(s)}{E(s)} = -\frac{1}{sR_1C_1 + \frac{R_1}{R}}$$

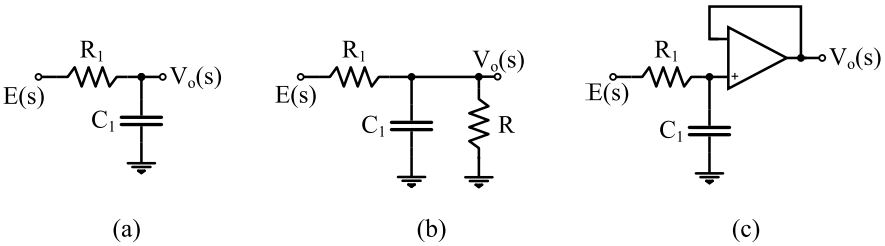

Fig. 9.22 Lossy integrators

Fig. 9.23 Inverting lossy integrator

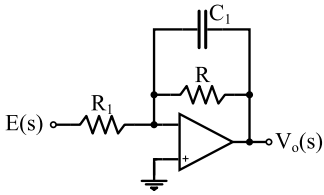

Fig. 9.24 Inverting differentiator

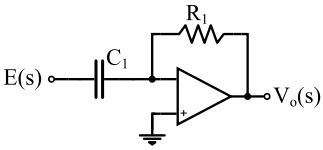

similar to that of the circuit of Fig. 9.22c but with a minus sign (phase inversion) and the capability to adjust the pole frequency using R. This resistor can be considered as the loss resistance of the capacitor C_1. When this loss resistor $R \to \infty$ (zero loss), the circuit becomes a Miller integrator. If R has a finite value, this introduces the term R_1/R into the transfer function.

Since this term R_1/R appears due to the loss resistance R it is referred to as "losses" of the integrator and circuits with a transfer function of the form $\frac{1}{s\tau+\psi}$, like those of Figs. 9.22c and 9.23, are referred to as *lossy integrators*. ψ denotes the loss of the lossy integrator. We shall return to lossy integrators in Sect. 9.4.

9.3.2.4 The Inverting Differentiator

A simple circuit that differentiates the voltage input signal, a differentiator, can be obtained from the general inverting amplifier circuit of Fig. 9.18 setting $Z_1(s) = 1/sC_1$ and $Z_2(s) = R_2$, as we have done in Fig. 9.24. For the inverting differentiator, we have:

$$V_o(s) = -sR_2C_1E(s) \quad \text{or} \quad v_o(t) = -R_2C_1\frac{d}{dt}e(t) \tag{9.48}$$

The voltage transfer function of the inverting differentiator is:

$$\frac{V_o(s)}{E(s)} = -sR_2C_1 \tag{9.49}$$

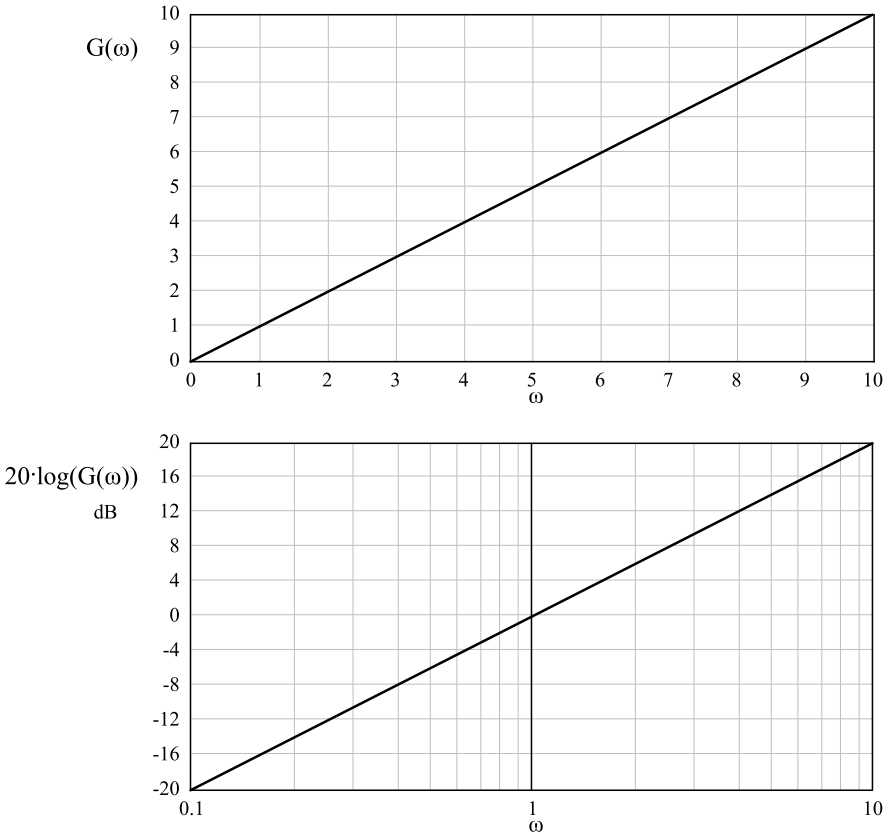

Fig. 9.25 Inverting differentiator

and its gain function

$$G(\omega) = |H(j\omega)| = \omega RC \tag{9.50}$$

Figure 9.25 shows the plain and the logarithmic gain plots of a typical inverting differentiator. It should be noted that the device amplifies high frequency noise and for this reason its use is normally avoided in filter design.

9.3.2.5 The Subtractor

The circuit of Fig. 9.26 can be obtained from that of the inverting voltage amplifier if, instead of grounding the non-inverting input, we apply a second input voltage through a voltage divider r_A/r_B so that the voltage of the non-inverting input becomes:

$$V_+(s) = \frac{r_A}{r_A + r_B} V_2(s) \tag{9.51}$$

Fig. 9.26 Subtractor

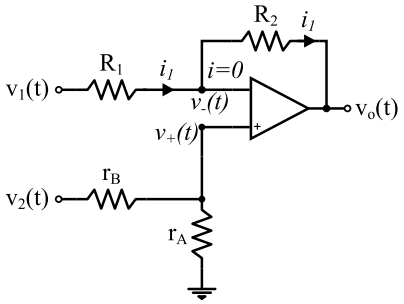

The output voltage is easily calculated as:

$$V_o(s) = \left(1 + \frac{R_2}{R_1}\right) \frac{r_A}{r_A + r_B} V_2(s) - \frac{R_2}{R_1} V_1(s) \tag{9.52}$$

It is clear that for $r_A = r_B$ and $R_1 = R_2$, the output voltage is $V_2 - V_1$

9.3.2.6 First Order Circuits Based on the Inverting Voltage Amplifier

First order circuits with a voltage transfer function

$$H(s) = \frac{s + z}{s + p} \tag{9.53}$$

are very important in designing active filters. The zero at $-z$ of this first order transfer function is real, since if it were complex, its conjugate $-z^*$ would also be a root of the numerator and the function would be of order 2. For the same reason, the pole at $-p$ is also real and $p > 0$ to ensure stability.

Based on the general circuit of the inverting voltage amplifier of Fig. 9.18, useful circuits with first order voltage transfer functions can be produced, some of which are summarized in Table 9.1.

9.3.2.7 A First Order Allpass Filter

The voltage transfer function of circuit of Fig. 9.27, based also on the general inverting voltage amplifier, is found to be:

$$H(s) = \frac{Z_2(s) - Z_1(s)}{Z_2(s) + Z_1(s)}$$

Setting $Z_1(s) = 1/sC$ (capacitor) and $Z_2(s) = R$ (resistor), the transfer function becomes:

$$H(s) = \frac{s - \frac{1}{RC}}{s + \frac{1}{RC}}$$

A first order transfer function of this form has a frequency independent gain $G(\omega) = |H(j\omega)| = 1$, while the phase response depends on frequency. The circuit realizes a first order allpass filter and can be used for phase (delay) compensation. The gain and phase characteristics of such a circuit are shown in Fig. 9.28.

Table 9.1 Circuits based on the inverting voltage amplifier

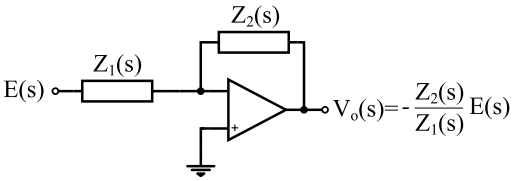

$Z_1(s)$	$Z_2(s)$	$H(s)$
	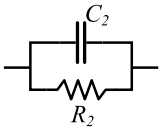	$-\dfrac{\frac{1}{R_1C_2}}{s+\frac{1}{R_2C_2}}$
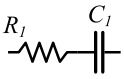		$-\dfrac{s\frac{R_2}{R_1}}{s+1/R_1C_1}$
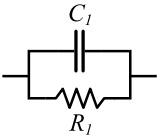	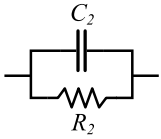	$-\dfrac{C_1}{C_2}\dfrac{s+\frac{1}{R_1C_1}}{s+\frac{1}{R_2C_2}}$
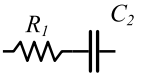		$-\dfrac{R_2}{R_1}\dfrac{s+\frac{1}{R_2C_2}}{s+\frac{1}{R_1C_1}}$

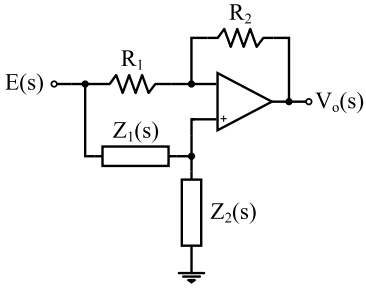

Fig. 9.27 A first order allpass filter

9.3.3 Circuits with Non-inverting Voltage Amplifier

In the circuit of the voltage follower of Fig. 9.29a, the full feedback of the output voltage to the inverting input has been replaced by a partial feedback of the output voltage to the inverting input through a voltage divider $R_A - R_B$. This is shown in the circuit of Fig. 9.29b. Assuming that the inverting input of the op amp draws zero

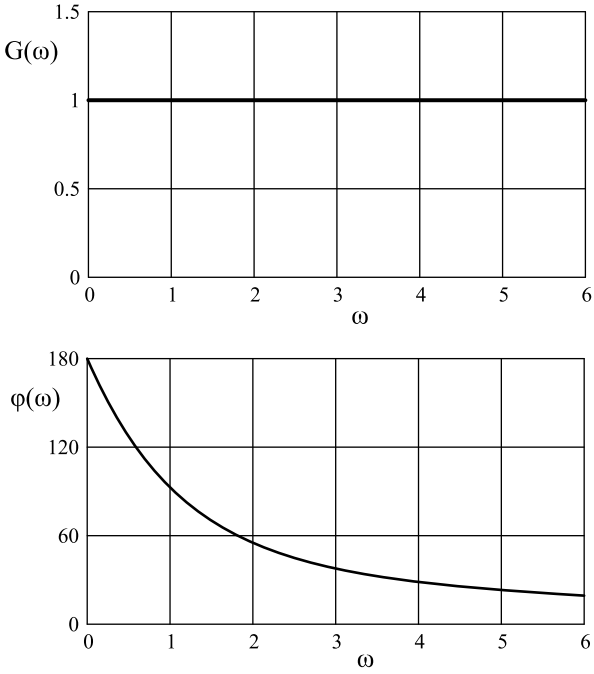

Fig. 9.28 Gain and phase plots of the first order allpass filter

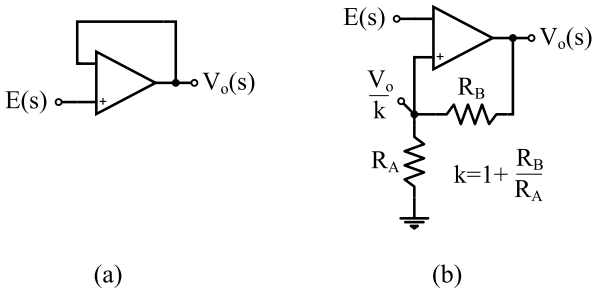

Fig. 9.29 (**a**) The voltage follower. (**b**) The non-inverting voltage amplifier

or negligible current, its voltage becomes:

$$V_-(s) = \frac{R_A}{R_A + R_B} V_o(s) = \frac{V_o(s)}{k} \quad \text{with } k = 1 + \frac{R_B}{R_A} > 1 \tag{9.54}$$

From the one-pole model of the voltage-mode operational amplifier,

$$V_o(s) = A(s)(V_+(s) - V_-(s)) \quad \text{with } A(s) = \frac{\omega_t}{s + \omega_a} \tag{9.55}$$

we find:

$$V_o(s) = \frac{k}{\frac{k}{A(s)} + 1} E(s) \quad \text{and} \quad H(s) = \frac{V_o(s)}{E(s)} = \frac{k}{\frac{k}{A(s)} + 1} \tag{9.56}$$

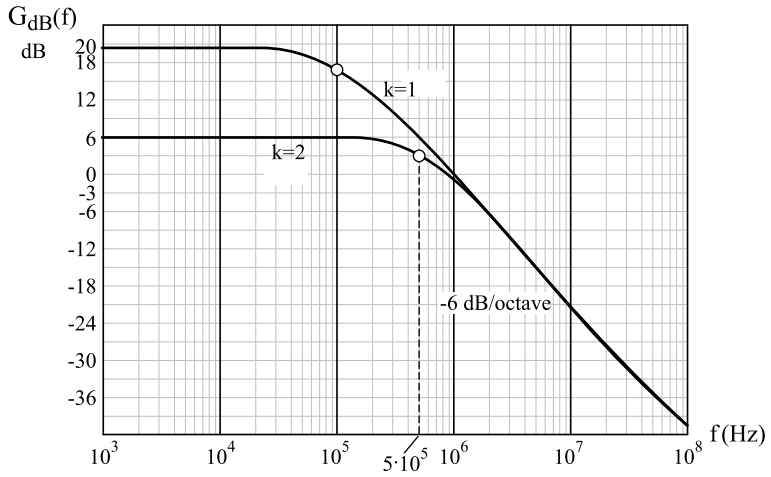

Fig. 9.30 Gain plots for two values of k

If the operational amplifier is ideal where $A(s) = A \to \infty$, equation (9.56) gives:

$$V_o(s) = kE(s) = \left(1 + \frac{R_B}{R_A}\right)E(s) \quad \text{and} \quad H(s) = \frac{V_o(s)}{E(s)} = k = 1 + \frac{R_B}{R_A} \tag{9.57}$$

The circuit in this case is a non-inverting voltage amplifier with constant gain $k = 1 + \frac{R_B}{R_A} > 1$.

In the case of non-ideal operational amplifier, the open-loop gain function is $A(s) = \frac{\omega_t}{s+\omega_a}$ and the transfer function of (9.56) becomes

$$H(s) = \frac{V_o(s)}{E(s)} = \frac{\omega_t}{s + \frac{\omega_t}{k} + \omega_a} \tag{9.58}$$

For dc ($\omega = 0$) we have

$$G_{dc} = |H(j0)| = \frac{k\omega_t}{\omega_t + k\omega_a} \tag{9.59}$$

The frequency at which this gain becomes $\frac{1}{\sqrt{2}}G_{dc}$, that is to say at which it falls by 3 dB from the DC level, corresponds to the pole frequency of the transfer function, i.e.

$$\omega_{3dB} = \frac{\omega_t}{k} + \omega_a \tag{9.60}$$

It can be seen that the useful bandwidth of the non-inverting voltage amplifier is inversely proportional to k and decreases as the ratio R_B/R_A increases. Figure 9.30 shows the logarithmic gain plots of $20\log|H(j\omega)|$ of the device for $R_B/R_A = 1 (k = 2)$ and $R_B/R_A = 10 (k = 11)$.

For the design of a non-inverting voltage amplifier, the value of the DC gain G_{dc} is usually given, and k and the ratio R_B/R_A must be calculated from the characteristics of the operational amplifier. From (9.59), we have:

$$G_{dc} = |H(j0)| = \frac{k\omega_t}{\omega_t + k\omega_a} \quad \Rightarrow \quad k = 1 + \frac{R_B}{R_A} = G_{dc}\frac{1}{1 - G_{dc}\frac{\omega_a}{\omega_t}} \tag{9.61}$$

The bandwidth of the device will be

$$\omega_{3dB} = \frac{\omega_t}{k} + \omega_a = \omega_t \frac{1 - G_{dc}\frac{\omega_a}{\omega_t}}{G_{dc}} + \omega_a \tag{9.62}$$

This equation shows the dependence of the device bandwidth on the DC gain.

Example 9.3 Design a non-inverting voltage amplifier with $G_{dc} = 4$ (logarithmic gain 12 dB) using the voltage-mode operational amplifier μA741 with $GBP = 1.0$ MHz ($\omega_t = 2\pi \cdot 10^6$ rad/s) and $f_a = 5.3$ Hz ($\omega_a = 2\pi \cdot 5.3$ rad/s).

From $k = 1 + \frac{R_B}{R_A}$ and (9.59), we have

$$G_{dc} = \frac{(1 + \frac{R_B}{R_A})\omega_t}{\omega_t + (1 + \frac{R_B}{R_A})\omega_a} \quad \Rightarrow \quad R_A = R_B \frac{1 - G_{dc}(\omega_a/\omega_t)}{G_{dc} - 1 + G_{dc}(\omega_a/\omega_t)}$$

We can therefore take any value for R_B and calculate the value of R_A from the above equation, ensuring a low frequency gain $G_{dc} = 4$. Gain decreases as frequency increases, and in this circuit we cannot adjust the 3 dB frequency, i.e. the frequency at which the gain becomes $\frac{1}{\sqrt{2}}G_{dc}$, since it depends on k and the OA's characteristics, according to (9.60).

$$\omega_{3dB} = \frac{\omega_t}{k} + \omega_a = \omega_t \frac{1 - G_{dc}\frac{\omega_a}{\omega_t}}{G_{dc}} + \omega_a$$

For our example, with G_{dc}, $\omega_t = 2\pi \cdot 10^6$ rad/s and $\omega_a = 2\pi \cdot 5.3$ rad/s,

$$f_{3dB} = \frac{\omega_{3dB}}{2\pi} = \frac{\omega_t}{2\pi}\frac{1 - G_{dc}(\omega_a/\omega_t)}{G_{dc}} + \frac{\omega_a}{2\pi} = 2.5 \cdot 10^5 \text{ Hz} = 0.25 \text{ MHz}$$

Figure 9.31 shows the logarithmic gain of the non-inverting voltage amplifier of this example.

9.3.3.1 The Linear Negative Resistor

Circuits with operational amplifiers are not only used for voltage transfer functions design but also for other functions, e.g. the driving-point input impedance design. The circuit of Fig. 9.32, for example, presents a very interesting input impedance function $Z_{in}(s) = \frac{E(s)}{I(s)}$. The operational amplifier is used as a voltage amplifier with gain 2, i.e. $V_o(s) = 2E(s)$. Therefore, for the input current we have:

$$I(s) = \frac{E(s) - V_o(s)}{R_o} = \frac{E(s) - 2E(s)}{R_o} = -\frac{E(s)}{R_o} \quad \Rightarrow \quad Z_{IN}(s) = \frac{E(s)}{I(s)} = -R_o$$

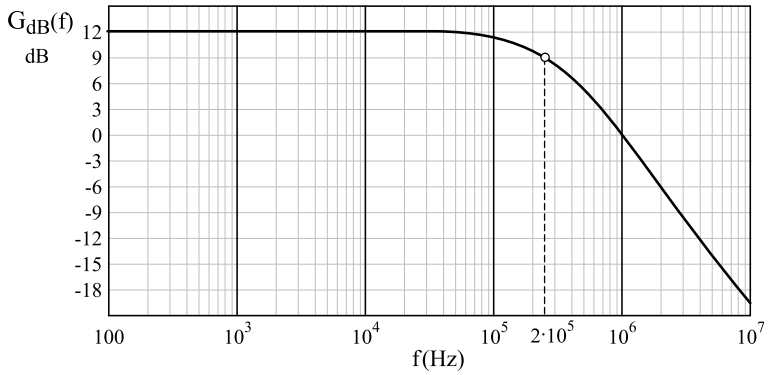

Fig. 9.31 Logarithmic gain plot of the non-inverting voltage amplifier

Fig. 9.32 The linear negative resistor

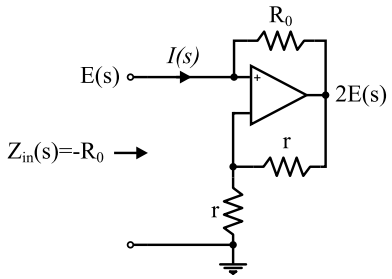

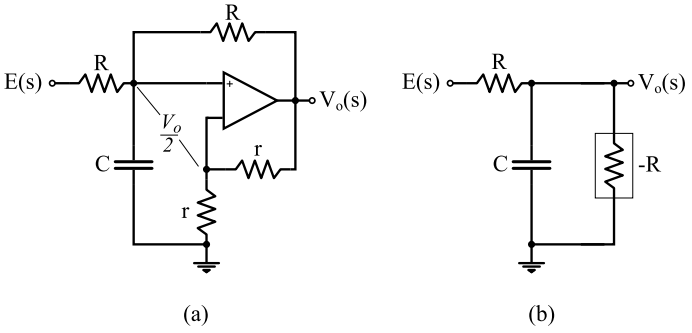

Fig. 9.33 The Deboo Integrator

This means that the circuit implements a grounded negative linear resistor. A negative resistor does not consume power like its positive counterpart, but produces signal power (this signal power is essentially derived from the power supply).

Example 9.4 (A non-inverting integrator) The circuit of Fig. 9.33 is a simple RC circuit with a negative resistor $-R$ connected in parallel to the capacitor.

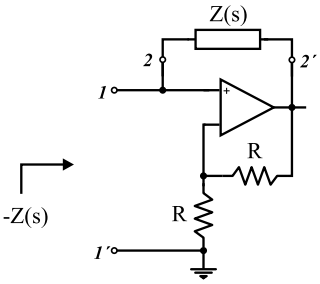

Fig. 9.34 Negative impedance converter (NIC)

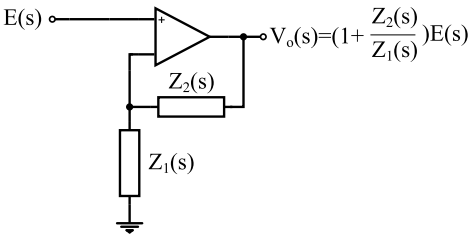

Fig. 9.35 General non-inverting voltage amplifier

Analysing the equivalent circuit shown in the same Fig. 9.33, we notice that the current of the input resistor $\frac{E(s)-V_o(s)}{R}$ equals the capacitor current $sCV_o(s)$ plus the current of the negative resistor $\frac{V_o(s)}{-R}$:

$$\frac{E(s)-V_o(s)}{R} = sCV_o + \frac{V_o(s)}{-R} \quad \Rightarrow \quad E(s) = \frac{sRC}{2}V_o(s)$$

$$\Rightarrow \quad H(s) = \frac{V_o(s)}{E(s)} = \frac{1}{s\frac{1}{2}RC}$$

The above circuit is a non-inverting voltage integrator, known as *Deboo integrator*, with integration constant equal to $\frac{1}{2}RC$. The Deboo integrator with a non-ideal operational amplifier will be studied in Sect. 9.4.

Figure 9.34 shows a circuit similar to that of the negative resistor (9.32) where the feedback resistor R_o has been replaced by impedance $Z(s)$. It can easily be found that the input impedance at terminals 1-1′ is $-Z(s)$.

Circuits that perform this impedance sign inversion are referred to as *negative impedance converters* (NIC). In our case, we have a grounded NIC since terminal 1′ is grounded. Using the circuit with a capacitor C_o connected at terminals 2-2′, we can have a negative grounded capacitor $-C_o$ at terminals 1-1′.

9.3.3.2 First Order Active Non-inverting Circuits

The general non-inverting voltage amplifier of Fig. 9.35 with voltage transfer function

$$H(s) = \frac{V_o(s)}{E(s)} = 1 + \frac{Z_2(s)}{Z_1(s)}$$

Table 9.2 Circuits based on the non-inverting voltage amplifier

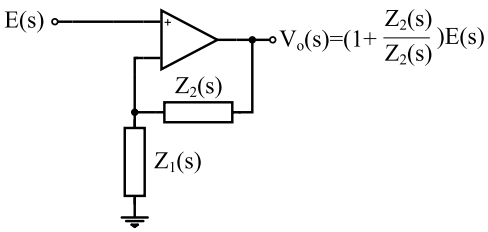

$Z_1(s)$	$Z_2(s)$	H(s)
	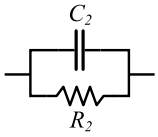	$\frac{s+\frac{1}{R_1C_2}+\frac{1}{R_2C_2}}{s+\frac{1}{R_2C_2}}$
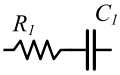		$(1+\frac{R_2}{R_2})\frac{s+\frac{1}{C_1(R_1+R_2)}}{s+\frac{1}{R_1C_1}}$
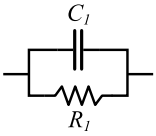	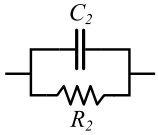	$(1+\frac{C_1}{C_2})\frac{s+\frac{1}{C_1+C_2}(\frac{1}{R_1}+\frac{1}{R_2})}{s+\frac{1}{R_2C_2}}$
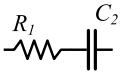	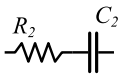	$\frac{R_2}{R_1}\frac{s+\frac{1}{R_2C_2}}{s+\frac{1}{R_1C_1}}$

can produce a series of useful first order non-inverting active-RC circuits by connecting various RC combinations at $Z_1(s)$ and $Z_2(s)$, as shown in Table 9.2.

9.3.3.3 First Order Passive Circuits

First order transfer functions can also be taken from passive circuits with one reactive element. Figure 9.36 shows some passive circuits with first order transfer functions.

For example, the input impedance and the transfer function of the circuit of Fig. 9.36a is given by:

$$Z(s) = \frac{V_{in}(s)}{I_{in}} = R_1 + \frac{R_2}{sR_2C + 1} = \frac{s + \frac{R_1+R_2}{R_1R_2C}}{s + \frac{1}{R_2C}}$$

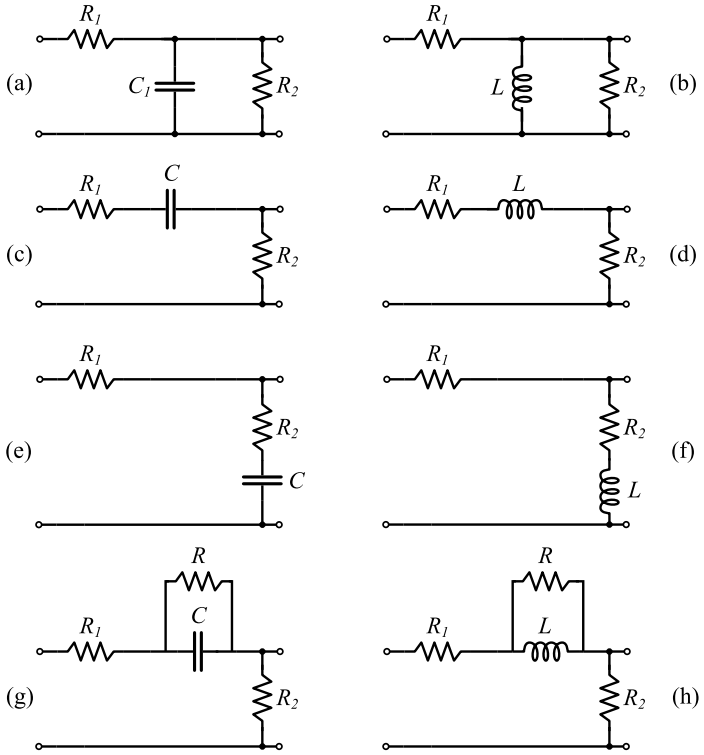

Fig. 9.36 Some 1st order passive circuits

$$H(s) = \frac{V_{out}(s)}{V_{in}} = \frac{\frac{1}{R_1 C}}{s + \frac{R_1 + R_2}{R_1 R_2 C}}$$

with real poles and zeroes.

Passive circuits of Fig. 9.36 cannot be used in cascade connections since their transfer function will be altered due to interstage loading. This can be overcome by adding a voltage follower (buffer) to their output.

The circuits (a) and (b) of Fig. 9.37 have transfer functions

$$H_a(s) = \frac{V_o(s)}{E(s)} = \frac{\frac{1}{RC}}{s + \frac{1}{RC}} \quad \text{and} \quad H_b(s) = \frac{V_o(s)}{E(s)} = \frac{s}{s + \frac{1}{RC}}$$

and the buffers ensure that they remain unchanged when connected to the next section.

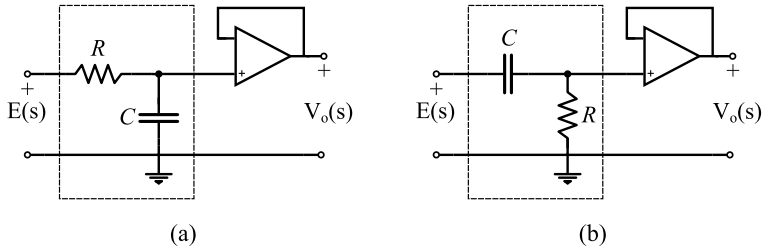

Fig. 9.37 Two first order RC circuits

Fig. 9.38 The capacitor with the parallel loss resistor

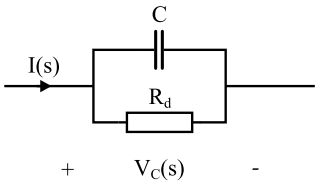

9.4 Integrators Revisited

Integrators are used extensively in active filter design and for this reason they are further studied in this section.

In the frequency domain, the ideal operation of integration is expressed by $\frac{1}{s\tau}$, where τ is the *integration constant*. Such an integration can be seen as an operation carried out by an ideal capacitor on a current $I(s)$ to produce a voltage $V_c(s)$ expressed as: $V_c(s) = \frac{1}{sC} I(s)$. When the capacitor is "lossy", its losses are represented as in Fig. 9.38, as a parallel resistor R_d.

In this case, the operation performed on the current to produce the voltage is

$$V_c(s) = \frac{1}{sC + \frac{1}{R_d}} I(s) \quad \text{or} \quad V_c(j\omega) = \frac{1}{j\omega + \frac{1}{R_d}} I(j\omega) \tag{9.63}$$

The quantity $1/R_d$ which is added to sC (or to $j\omega C$) in the denominator expresses the losses.

The transfer function of the voltage integrator is $\frac{1}{s\tau}$ and that of the lossy integrator $\frac{1}{s\tau+\psi}$ or $H(j\omega) = \frac{1}{j\omega\tau+\psi}$, where the integration constant τ has time dimensions and ψ, the losses, is a dimensionless quantity. The *integrator!quality factor* of the integrator can be defined as

$$Q = \frac{\omega\tau}{\psi} \tag{9.64}$$

By the term "voltage integrator", we mean circuits with voltage transfer function of the form

$$H(s) = \frac{V_{out}}{V_{in}(s)} = \frac{1}{s\tau + \psi} = \frac{1}{s\tau + \frac{\omega\tau}{Q}} \tag{9.65}$$

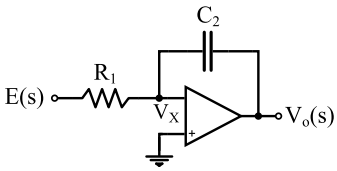

Fig. 9.39 The Miller inverting integrator

with $Q \to \infty$ or equivalently $\psi \to 0$. The performance evaluation of voltage integrators can be based on the evaluation of the losses ψ or of the quality factor Q. For a pure integrator with transfer function $\frac{1}{s\tau}$ the losses ψ must be zero or the quality factor Q must be ∞. We will see that these conditions cannot be fulfilled by real integrators, in which case any comparison must be based on the value of the quality factor. An integrator with higher value of Q is better than an integrator with lower value of Q. We will also see that the quality factor deteriorates as the integrator is used in higher frequencies.

9.4.1 Inverting Integrators

It was shown in Sect. 9.3.2.2 that the voltage transfer function of the Miller inverting integrator of Fig. 9.39 with an ideal operational amplifier is

$$H(s) = -\frac{1}{sR_1C_2} \tag{9.66}$$

If a non-ideal operational amplifier with a frequency dependent open-loop gain $A(s)$ is used, the transfer function becomes:

$$H(s) = \frac{V_o(s)}{E(s)} = \frac{1}{(1+\frac{1}{A(s)})sR_1C_2 + \frac{1}{A(s)}} \tag{9.67}$$

Using the integrator model $A(s) = \frac{\omega_t}{s}$ of (9.18) for the open-loop gain $A(s)$, (9.67) yields:

$$H(s) = -\frac{\omega_t}{s^2R_1C_2 + s(\omega_tR_1C_2 + 1)} = -\frac{1}{sC_2(s\frac{R_1}{\omega_t} + R_1 + \frac{1}{\omega_tC_2})} \tag{9.68}$$

For $s = j\omega$ we have:

$$H(j\omega) = -\frac{1}{j\omega(R_1C_2 + \frac{1}{\omega_t}) - \frac{\omega^2R_1C_2}{\omega_t}} \tag{9.69}$$

from which the integration constant and the losses can be recognized as

$$\tau = R_1C_2 + \frac{1}{\omega_t} \quad \text{and} \quad \psi = -\frac{\omega^2R_1C_2}{\omega_t} = -\frac{\omega R_1C_2}{|A(j\omega)|} \tag{9.70}$$

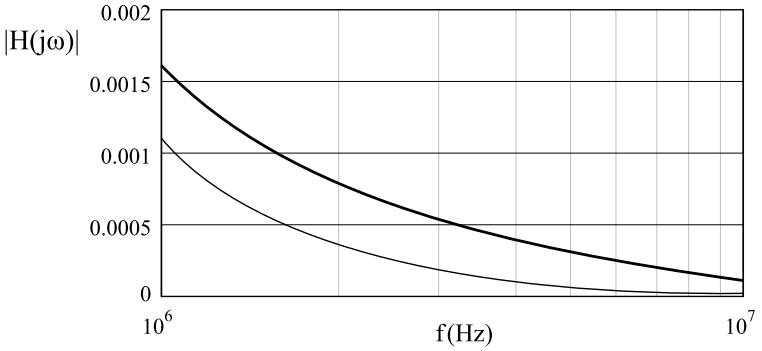

Fig. 9.40 High frequency magnitude response of a Miller integrator with ideal op amp (*thick curve*) and real op amp (*thin curve*)

Fig. 9.41 Improving the Miller integrator

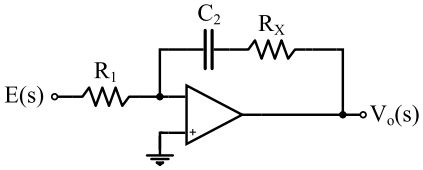

The quality factor for this circuit is

$$Q = \frac{\omega_t}{\psi} = -\frac{\omega_t + \frac{1}{R_1 C_2}}{\omega} = -|A(j\omega)| - \frac{1}{\omega R_1 C_2} \approx -|A(j\omega)| \tag{9.71}$$

Equation (9.68) shows that there is a severe deviation from the desirable integration transfer function $\frac{1}{j\omega R_1 C_2}$. As an example, in Fig. 9.40 the thin curve is the plot of the high frequency magnitude response of a Miller integrator calculated from (9.70) with $R_1 = 10$ kOhm, $C_2 = 10$ nF and a real op amp with $\omega_t = 2\pi 10^6$. The thick curve represents the magnitude response when the op amp is ideal.

Equation (9.68) implies a simple method to improve the circuit by decreasing the losses. This is achieved when the feedback capacitor with impedance $1/sC_2$ is replaced by a series $R_x - C_2$ circuit with impedance

$$R_x + \frac{1}{sC_2} = \frac{R_x C_2 (s + \frac{1}{R_x C_2})}{sC_2} \tag{9.72}$$

as shown in Fig. 9.41.

The voltage transfer function of the circuit (9.68) becomes

$$H(s) = -\frac{R_x C_2 (s + \frac{1}{R_x C_2})}{sC_2 (s\frac{R_1}{\omega_t} + R_1 + \frac{1}{\omega_t C_2})} = -\frac{R_x \omega_t C_2 (s + \frac{1}{R_x C_2})}{sR_1 C_2 (s + \omega_t + \frac{1}{R_1 C_2})} \tag{9.73}$$

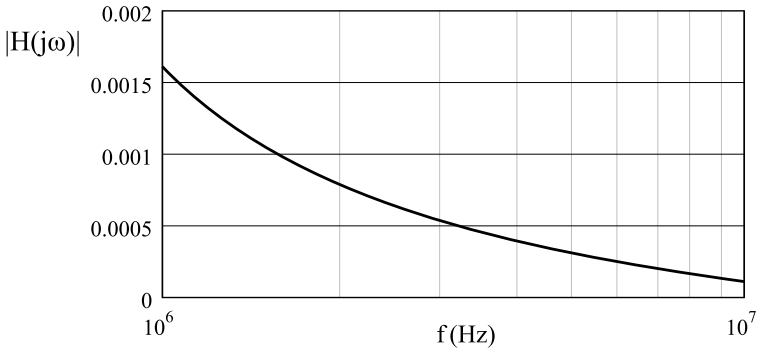

Fig. 9.42 High frequency magnitude response of an improved Miller integrator

In order to have pole-zero cancellation of the bracketed terms:

$$\frac{1}{R_x C_2} = \omega_t + \frac{1}{R_1 C_2} \quad \Rightarrow \quad R_x = \frac{R_1}{1 + \omega_t R_1 C_2} \tag{9.74}$$

Using this value for R_x in (9.73) we find that the transfer function of the improved inverting integrator is

$$H(s) = -\frac{1}{s R_1 C_2 (\frac{1+\omega_t R_1 C_2}{\omega_t R_1 C_2})} \tag{9.75}$$

This is the transfer function of a pure integrator without losses with integration constant slightly higher than $R_1 C_2$

$$\tau = R_1 C_2 \left(\frac{1 + \omega_t R_1 C_2}{\omega_t R_1 C_2} \right) = R_1 C_2 \left(1 + \frac{1}{\omega_t R_1 C_2} \right) \tag{9.76}$$

In practice, to design the improved inverting integrator of Fig. 9.41 given the integration constant τ, the value of the capacitor C_2 can be chosen arbitrarily and then, using (9.76), the value of R_1 can be calculated:

$$R_1 = \frac{\tau - 1/\omega_t}{C_2} \tag{9.77}$$

R_x can finally be calculated from (9.74).

Example 9.5 Given $\tau = 10^{-4}$, $C_2 = 10$ nF and $\omega_t = 2\pi 10^6$ rad/s, from (9.77) we get $R_1 = 9984$ Ohm and from (9.74), $R_x = 15.89$ Ohm. Figure 9.42 shows the plots of the magnitude response of the Miller integrator with $R_1 = 10$ kOhm, $C_2 = 10$ nF and ideal op amp and with real op amp ($\omega_t = 2\pi 10^6$) rad/s, $R_1 = 9984$ Ohm, $C_2 = 10$ nF in series with $R_x = 15.89$. The two curves coincide as expected.

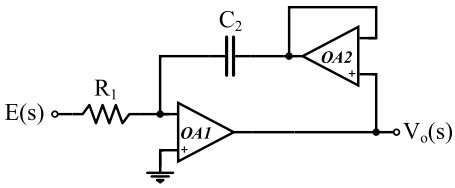

Fig. 9.43 Alternative improved inverting integrator

It was shown above that the characteristics of the non-ideal operational amplifier can be taken into account to create a more complicated model of the Miller integrator. The method of compensation of the non-infinite open-loop gain of the OA was based on calculations using the gain-bandwidth product ω_t of the real OA which is not constant for all chips of the same family, e.g. μA741, and must be measured for each individual chip. This is not very practical for discrete components implementations but if the circuit is to be integrated and produced in one process, it might be useful.

An alternative inverting integrator circuit is shown in Fig. 9.43, where a voltage follower has been added in the feedback path of the Miller integrator. This is done in order to introduce a real zero in the transfer function to cancel the real pole which appears due to the finite ω_t of the operational amplifier according to (9.68).

Assuming ideal operational amplifiers, the transfer function of the circuit can be found to be identical to that of the Miller integrator:

$$H(s) = -\frac{1}{sR_1C_2}$$

However, assuming real operational amplifiers with gain-bandwidth products ω_{t1} and ω_{t2}, the circuit based on the integrator model for the open-loop gain yields the following expression for the losses:

$$\psi = \frac{\omega^2 R_1 C_2}{\omega_{t2}(1 - \frac{\omega^2}{\omega_{t2}^2} - \frac{\omega_{t2}}{\omega_{t1}})} = \frac{\omega R_1 C_2}{|A_2(j\omega)|}\left(1 - \frac{1}{|A_2(j\omega)|^2} - \frac{\omega_{t2}}{\omega_{t1}}\right) \tag{9.78}$$

In the case of identical OAs with $A_1(s) = A_2(s) \Rightarrow \omega_{t1} = \omega_{t2}$, (9.78) gives for the losses and the quality factor:

$$\psi = -\frac{\omega R_1 C_2}{|A(j\omega)|^3} \quad \text{and} \quad Q = |A(j\omega)|^3 \tag{9.79}$$

This is a significant improvement since losses decrease as the cube of the open-loop gain and Q depends on the cube of the open-loop gain as compared to (9.70) and (9.71) of the original Miller integrator, for which we have $\psi = -\frac{\omega R_1 C_2}{|A(j\omega)|}$ and $Q \approx -|A(j\omega)|$.

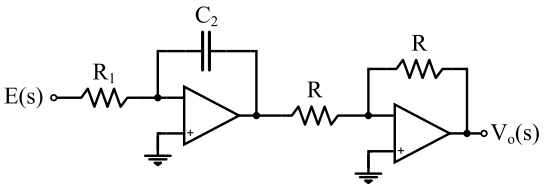

Fig. 9.44 A non-inverting integrator

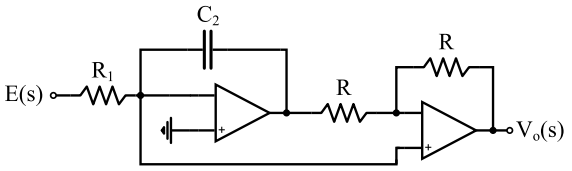

Fig. 9.45 Alternative non-inverting integrator

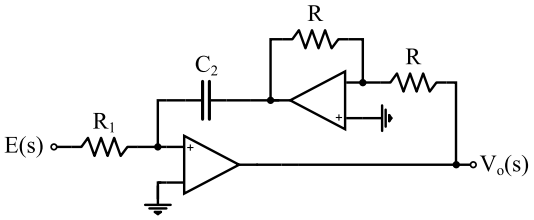

Fig. 9.46 Another alternative non-inverting integrator

9.4.2 Non-inverting Integrators

The simplest way to design a non-inverting integrator is to add an inverting voltage amplifier at its output, as shown in Fig. 9.44.

Assuming ideal OAs, the transfer function of the circuit will be $H(s) = \frac{1}{R_1 C_2}$. Introducing the integrator model for the open-loop gain of the two op amps has the effect that the quality factor of this non-inverting integrator is lower than its inverting counterpart, the Miller integrator. A small improvement can be achieved by connecting the non-inverting terminal of the second op amp to the virtual ground of the inverting terminal of the first op amp, as we have done in Fig. 9.45, although the quality factor still remains lower than that of the original Miller integrator.

Another variation is to add the inversion amplifier in the feedback path, as we have done in the circuit of Fig. 9.46, where in addition the terminals of the first op amp have been inverted for stability reasons.

For the ideal case with two ideal OAs, the transfer function will be $H(s) = \frac{1}{R_1 C_2}$. With two non-ideal OAs, the transfer function will be:

$$H(s) = \frac{1}{sR_1C_2\left(\frac{1}{1+\frac{2}{A(s)}}\right) + \frac{sR_1C_2+1}{A(s)}} \tag{9.80}$$

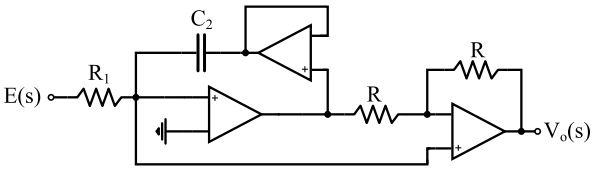

Fig. 9.47 A non-inverting integrator with 3 op amps

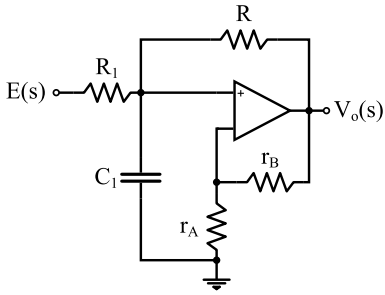

Fig. 9.48 The Deboo non-inverting integrator

If we now expand the term $\frac{1}{1+\frac{2}{A(s)}}$ in a Taylor series, we have:

$$H(s) = \frac{1}{sR_1C_2(1 - \frac{2}{A(s)} + \frac{4}{A(s)^2} - \frac{8}{A(s)^3} + \frac{16}{A(s)^4} \cdots) + \frac{sR_1C_2+1}{A(s)}}$$

On setting $A(s) = \frac{\omega_t}{s}$ (integrator model), we can determine $H(j\omega)$:

$$H(j\omega) = \frac{1}{j\omega R_1C_2 + \frac{\omega^2 R_1C_2}{\omega_t} + \frac{1}{\omega_t}} \tag{9.81}$$

The losses ψ in this case are found to be:

$$\psi \approx \frac{\omega^2 R_1C_2}{\omega_t} = \frac{\omega R_1C_2}{|A(j\omega)|} > 0 \tag{9.82}$$

In other words, losses are comparable to that of the Miller integrator.

By adding one more op amp to the circuit of Fig. 9.43, as shown in Fig. 9.47, it can be proved that $\psi = -\frac{\omega R_1C_2}{|A(j\omega)|^3}$, which is a significant improvement at the cost of one additional op amp.

The non-inverting Deboo integrator presented in Example 9.4 (Fig. 9.33), is shown in its general form in Fig. 9.48.

Assuming ideal op amp, the voltage transfer function of this circuit is:

$$H(s) = \frac{1 + \frac{r_B}{r_A}}{sR_1C_1 + 1 - \frac{R_1}{R} \cdot \frac{r_B}{r_A}} \tag{9.83}$$

Setting $\frac{R_1}{R} \cdot \frac{r_B}{r_A} - 1$, the circuit becomes a non-inverting integrator. In the case where the op amp is not ideal and its open-loop gain is $A(s) = \frac{\omega_t}{s}$, we can find that

$$H(s) = \frac{k}{s(R_1C_1 - \frac{R+R_1}{\omega_t R}) - 1 + \frac{kR_1}{R} - \frac{R_1}{R} - \omega^2 \frac{kR_1C_1}{\omega_t}} \quad \text{where } k = 1 + \frac{r_B}{r_A} \tag{9.84}$$

Setting $\frac{R_1}{R} \cdot \frac{r_B}{r_A} - 1$ to minimize losses, (9.84) gives:

$$H(s) = \frac{1}{s(\frac{R_1^2C_1}{R_1+R} - \frac{R_1}{\omega_t R}) - \omega^2 \frac{R_1C_1}{\omega_t}} \tag{9.85}$$

with

$$\tau = \frac{R_1^2C_1}{R_1+R} - \frac{R_1}{\omega_t R} \approx \frac{R_1^2}{R_1+R}C_1 \quad \text{and} \quad \psi = -\omega^2 \frac{R_1C_1}{\omega_t} = -\frac{\omega R_1C_1}{|A(j\omega)|} \tag{9.86}$$

The losses ψ are equal to that of the Miller integrator and the quality factor $Q = \frac{R_1}{R}|A(j\omega)|$ is also comparable to that of the Miller integrator given in (9.71).

9.5 Operational Amplifier Imperfections

It has been seen that real operational amplifiers do not behave in the same way as the ideal models. This is parallel to the deviation of the behavior of real inductors, resistors and capacitors from the ideal circuit elements. These deviations from the ideal behavior usually become more evident as the frequency of operation increases. High frequencies in general present problems for electronic circuits since the imperfections of both active and passive circuits become evident and at times dominant. However, this does not prevent filter designers from designing high precision filters.

Although the deviations from the ideal and desirable models are very often under control, they present a real problem in operational amplifiers at high frequencies. In this section we present some of the problems of real operational amplifiers at an encyclopaedic level. Detailed examination can be found in textbooks on electronics as well as in specialized books on operational amplifiers.

9.5.1 The Frequency Dependent Finite Open-Loop Gain

In ideal voltage-mode operational amplifiers, the open-loop gain is infinite and frequency independent. In real OAs, the gain is finite and frequency dependent according to the one-pole model of (9.14) or its simplified integrator model of (9.18). These models are sufficient for many applications of active circuits at high frequencies.

9.5.2 Other Imperfections

In a circuit of a typical operational amplifier such as the one in Fig. 9.2, the differential input stage performs the pre-amplification of the input signal and ensures high input resistance, approximately 2 MOhm (infinite in the ideal op amp). The two input terminals of the op amp in a bipolar transistor realization are connected to the bases of two transistors and a bias current is required. This implies that the input current cannot be zero as we assume when we analyse circuits with op amps. In fact, DC currents of the order of approximately 100 nA are required for the operation of the op amp and must be provided by feedback paths. Before the signal reaches the output, it is compensated by an RC circuit for stability reasons. The capacitor is of the order of 30 pF. Some op amp chips require an external compensating capacitor and provide the necessary pins for this. The μA741 operational amplifier was the first with internal compensation, but also provides external compensation pins. Finally, the output stage provides the low output resistance, zero in the ideal op amp but typically of the order of 100 Ohms in real operational amplifier chips.

A very important characteristic of the operational amplifiers is the *slew rate*, measured in V/μs and with typical values below 1 V/μs. The slew rate specifies the maximum rate at which the signals can change. A slew rate of 0.5 V/μs means that signals with voltage changes of up to 0.5 V in 1 second can be handled. A sinusoidal signal with amplitude A V changes from $-A$ to A in half a period i.e. $2A$ V in $T/2$. If the slew rate of the op amp is r V/μs, the minimum period of the signal will be $\frac{4A}{r}$ μs and the maximum frequency which can be handled by the op amp $\frac{r}{4A}$ MHz. For $A = 1$ and $r = 0.5$ V/μs, this maximum frequency will be 125 kHz and if $A = 2$, the maximum frequency will be 62.5 kHz. It is clear that an operational amplifier with specified slew rate handles better low voltage and low frequency signals. With low voltage signals, the maximum frequency handled without problems by an op amp can be increased to values higher than the limit set by the gain-bandwidth product. However, voltages cannot be made very low due to problems related to noise.

The output swing capability of an op amp is determined by its supply voltages V_{CC}-V_{EE}. Operational amplifiers cannot give at their output voltages higher than V_{CC} or lower than V_{EE}. The exact output swing depends on the type of the op amp. For bipolar op amps like μA741, the output voltage can swing from $V_{OH} = V_{CC} - 2$ V to $V_{OL} = V_{EE} + 2$ V. This means that if we use a μA741 op amp with supply voltages $+15$ and -15 V in a non-inverting voltage amplifier circuit with gain 7 and apply a 3 V input, the output cannot be $3 \cdot 7 = 21$ V but will be clipped to $V_{OH} = V_{CC} - 2 = 15 - 2 = 13$ V. In CMOS op amps we can get even "rail-to-rail" swing, i.e. from $V_{OH} = V_{CC}$ to $V_{OL} = V_{EE}$. This bounded output swing imposes limits on the input signals of high gain circuits and as we have seen, low voltages extend the frequency limit set by the slew rate. It should be repeated that extremely low voltages are affected more by the op amp's noise, which might be of the order of 10 μV.

In ideal op amps, if both input terminals are connected to ground, the output voltage will be zero. However, this is not true for real op amps, where we observe a non-zero voltage at the output as if there were a voltage difference between the

inputs. This apparent input voltage difference is referred to as *input offset voltage*. If, for example, in an op amp with open-loop gain $A = 10^4$ the output voltage is 5 V when both input terminals are grounded, then effectively it means that the input voltage difference, that is to say the input offset voltage, is $5/10^4$ V $= 0.5$ mV. Input offset voltage can be easily compensated for using a resistor of suitable value which depends on the input bias current under the operating specifications of the op amp.

An imperfection of real op amps which, however, does not significantly affect the operation of active filters, is described through the parameter known as the *Common-Mode Rejection Ratio*, CMRR, measured in dB. This op amp performance parameter is defined as follows. When the same signal source is connected to both inputs of the op amp, a zero output is expected. This is true for the ideal, but not for the real op amps, where there will be an output signal allowing for the definition of the *Common-Mode Gain* or *CMG* as the ratio of the output to the input. CMRR is then defined as:

$$CMRR = 20 \log \frac{G_{dc}}{CMG} \text{ dB}$$

where G_{dc} is the open-loop gain for $f = 0$.

The op amp imperfections depend strongly on temperature and therefore it is not possible to be completely compensated under all possible operating conditions.

9.5.3 Linear and Non-linear Operation

The open-loop operation of the op amp depends on the input voltage difference, which according to its value determines the linear or non-linear mode of operation. Figure 9.49 is a plot of the output voltage of the op amp as a function of the input voltage difference $V_+ - V_-$. The region where the linear relationship $V_o = A \cdot (V_+ - V_-)$ is valid is very narrow, namely from $\frac{V_{OL}}{A}$ to $\frac{V_{OH}}{A}$. Outside this region, the op amp saturates and provides constant output voltage, operating in a non-linear way. We saw that V_{OL} and V_{OH} depend on the op amp but in general are very near V_{EE} and V_{CC} respectively. Evidently, for linear operation the voltage difference $V_+ - V_-$ of the two inputs must me very low and this is ensured by the op amp itself when it operates in feedback mode, i.e. when the output is somehow fed back to any of the inputs.

Some applications are based on the non-linear operation of the op amp. The *comparator* of Fig. 9.50 is one of them, which gives constant positive output when the input is positive of any value and constant negative output when the input assumes any negative value. In the comparator, output changes only when input changes sign.

The circuit of Fig. 9.51a is the same as that of Fig. 9.50 but a reference voltage source has been connected to the inverting input of the op amp. In this circuit the op amp falls in positive saturation with $V_o = V_{OH}$ when input voltage applied to the non-inverting input is $V_+ > E$. When the input voltage is less than E, the output becomes $V_o = V_{OL}$. The operation of the circuit is shown in Fig. 9.51b.

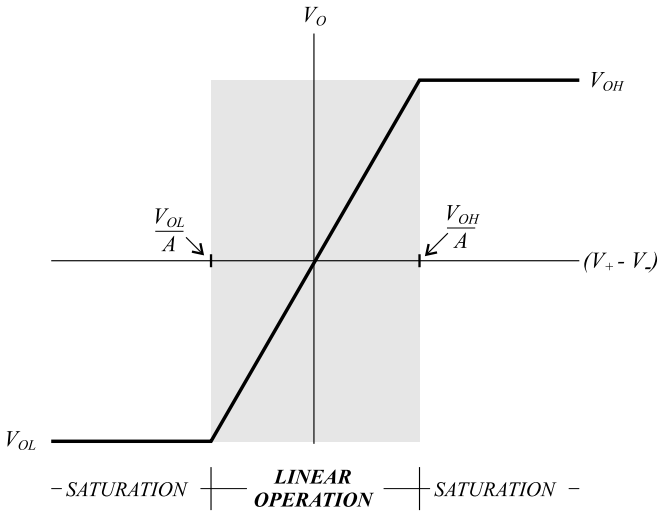

Fig. 9.49 Output voltage as a function of the difference of the input voltages

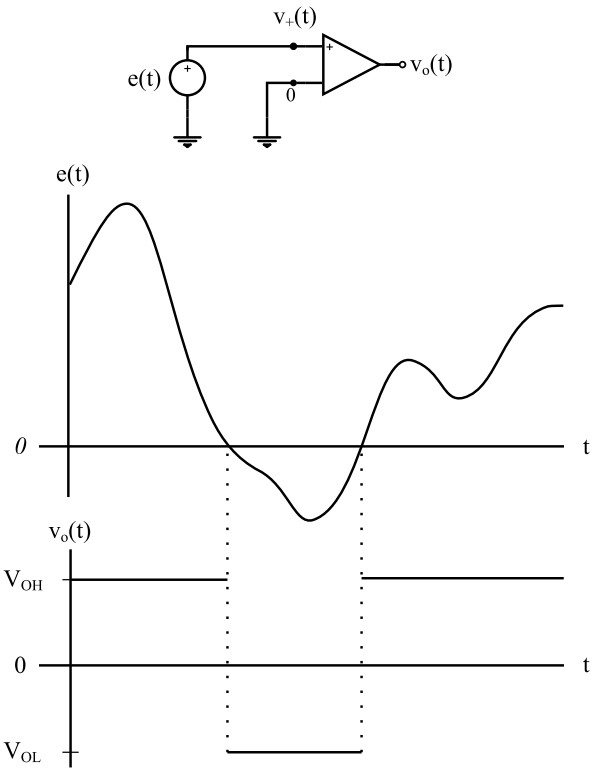

Fig. 9.50 The basic comparator

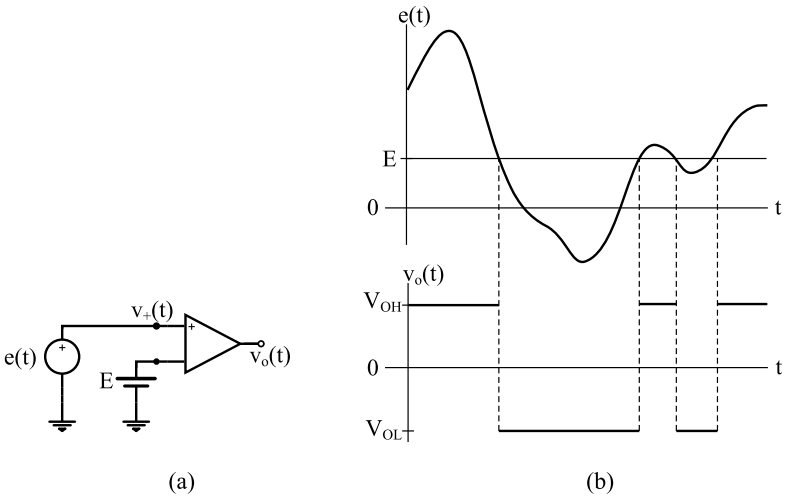

Fig. 9.51 The comparator

9.6 Problems

9.1 Repeat Example 9.1 with $k_o = 10$.

9.2 Repeat Example 9.2 with DC gain $G_{dc} = 2$ and $G_{dc} = 8$ and compare the corresponding f_{3dB}.

9.3 Show that the voltage transfer function of the general inverting amplifier circuit of Fig. 9.18 is given by (9.39):

$$H(s) = \frac{V_o(s)}{E(s)} = -\frac{Z_2(s)}{Z_1(s)}$$

9.4 Show that the output of the circuit of Fig. 9.19 is given by (9.40):

$$V_o(s) = -\frac{Z_F}{Z_1}V_1(s) - \frac{Z_F}{Z_2}V_2(s) - \cdots - \frac{Z_F}{Z_n}V_n(s)$$

9.5 Show that the output of the subtractor circuit of Fig. 9.26 is given by (9.52):

$$V_o(s) = \left(1 + \frac{R_2}{R_1}\right)\frac{r_A}{r_A + r_B}V_2(s) - \frac{R_2}{R_1}V_1(s)$$

9.6 Show that the voltage transfer function of the circuit of Fig. 9.27 is given by:

$$H(s) = \frac{Z_2(s) - Z_1(s)}{Z_2(s) + Z_1(s)}$$

9.7 Verify the first order voltage transfer functions given in Table 9.1.

9.8 Verify the first order voltage transfer functions given in Table 9.2.

9.9 Show that the transfer function of the circuit of Fig. 9.36a is given by:

$$H(s) = \frac{V_{out}(s)}{V_{in}} = \frac{\frac{1}{R_1 C}}{s + \frac{R_1 + R_2}{R_1 R_2 C}}$$

9.10 Determine the voltage transfer function of the passive circuits shown in Fig. 9.36g and h.

9.11 Verify (9.78) and (9.79) for the inverting integrator of Fig. 9.43.

9.12 Show that for the 3 op amp integrator of Fig. 9.47 we have

$$\psi = -\frac{\omega R_1 C_2}{|A(j\omega)|^3}$$

References[1]

1. Deliyannis, T., Sun, Y., Fidler, J.K.: Continuous-Time Active Filter Design. CRC Press, Boca Raton (1999)
2. Franco, S.: Design with Operational Amplifiers and Analog Integrated Circuits. McGraw-Hill, New York (1998)
3. Graeme, J.G., Tobey, G.E., Huelsman, L.P.: Operational Amplifiers. McGraw-Hill, New York (1971)
4. Jung, W.: Op Amp Applications Handbook. Analog Devices Series. Newnes, London (2004)
5. Schaumann, R., Van Valkenburg, M.E.: Design of Analog Filters. Oxford University Press, London (2001)
6. Solomon, J.E.: The monolithic operational amplifier: a tutorial study. IEEE J. Solid-State Circuits **SC-9**, 314–332 (1974)

[1] All references, whether or not cited within the text, are recommended for further reading.

Second Order Functions and Circuits 10

10.1 Introduction

All network functions of linear time invariant lumped circuits are rational functions of s, i.e. quotients of polynomials of s. The maximum degree of s appearing in a network function is the order of the circuit. The most general form of a second order rational function of s is the biquadratic form:

$$F(s) = \frac{A_z s^2 + B_z s + C_z}{A_p s^2 + B_p s + C_p} = K \frac{(s - z_1)(s - z_2)}{(s - p_1)(s - p_2)}$$

where z_i are the zeros and p_i the poles of the function $F(s)$. $K = \frac{A_z}{A_p}$ is a frequency independent constant, i.e. it does not depend on s. Circuits which realize a biquadratic function are referred to as *biquads* even if one of the numerator or denominator polynomials is not complete, e.g.

$$F_1(s) = \frac{k}{s^2 + as + b} \qquad F_2(s) = \frac{ks}{s^2 + as + b} \qquad F_3(s) = \frac{s^2 + 1}{s^2 + as + b} \quad (10.1)$$

Strictly speaking, in line with complex variable theory, a rational function of s has as many zeros as poles. If a rational function of s has constant numerator, it has only poles and no zeros (i.e. all its zeros are located at infinity), it is referred to as *all-pole*. $F_1(s)$ of (10.1), for example, is a second order all-pole function.

The general second order biquadratic function can be written as follows:

$$F(s) = \frac{A_z s^2 + B_z s + C_z}{A_p s^2 + B_p s + C_p} = K \frac{(s - z_1)(s - z_2)}{(s - p_1)(s - p_2)} = K \frac{s^2 + \frac{\omega_{oz}}{Q_z} s + \omega_{oz}^2}{s^2 + \frac{\omega_{op}}{Q_p} s + \omega_{op}^2} \quad (10.2)$$

where Q_z and Q_p are the *quality factors* of the zeros and poles respectively and $K = A_z/A_p$. Frequencies ω_{op} and ω_{oz} are the *natural frequencies* of the system described by $F(s)$, or simply the frequencies of its poles and zeros respectively. The

H.G. Dimopoulos, *Analog Electronic Filters*, Analog Circuits and Signal Processing,
DOI 10.1007/978-94-007-2190-6_10, © Springer Science+Business Media B.V. 2012

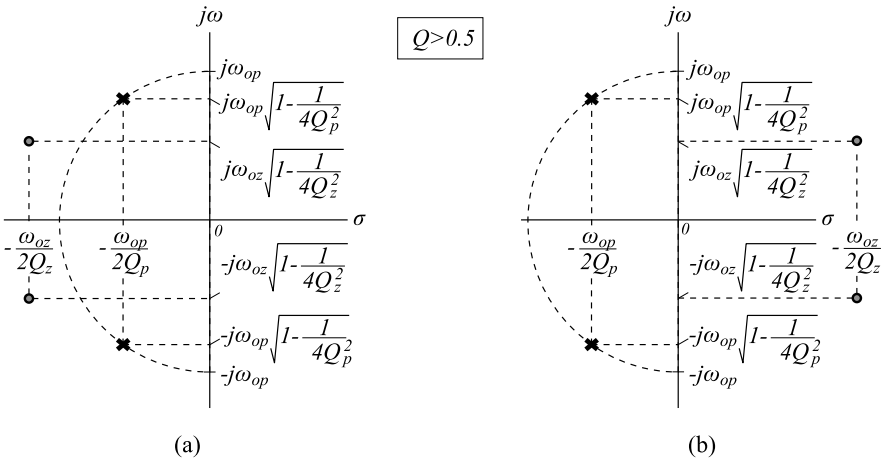

Fig. 10.1 Poles-zeros plot

quality factors and the frequencies of the poles and the zeros are expressed in terms of the polynomial coefficients as:

$$\omega_{oz} = \sqrt{\frac{C_z}{A_z}} \qquad Q_z = \frac{\omega_{oz}}{\frac{B_z}{A_z}} \qquad \omega_{op} = \sqrt{\frac{C_p}{A_p}} \qquad Q_p = \frac{\omega_{op}}{\frac{B_p}{A_p}} \tag{10.3}$$

Poles and zeros are in general complex. Real poles or zeros simply have zero imaginary part. The poles for example of $F(s)$ are given by

$$s_{1,2} = -\frac{B_p}{2A_p} \pm \sqrt{\frac{B_p^2}{4A_p^2} - \frac{C_p}{A_p}} = \omega_{op}\left(-\frac{1}{2Q_p} \pm \sqrt{\left(\frac{1}{2Q_p}\right)^2 - 1}\right) \tag{10.4}$$

and it can be seen that if $Q_p > 0.5$ the poles are complex. A similar expression gives the zeros of a rational biquadratic function. Figures 10.1a and b show the poles-zeros plot of $F(s)$ when both $Q_z > 0.5$ and $Q_p > 0.5$.

The poles of stable linear circuits are always located in the left half s-plane. Zeros can, however, be located in the right half s-plane. Thus, transfer functions can have zeros with positive real parts, as opposed to driving-point functions which must have all their poles and zeros in the left half s-plane or on the $j\omega$-axis. The situation shown in Fig. 10.1b can occur if $F(s)$ is a transfer function but not when it is a driving-point function.

The distance of the poles from the $j\omega$-axis depends on the quality factor Q_p, namely it is $\frac{\omega_{op}}{2Q_p}$. Thus, the higher the Q, the nearer to the $j\omega$-axis are the poles, thereby drastically affecting the behavior of the circuit. High selectivity is achieved with high Q values. In effect, circuits with inherently low pole-Q exhibit low selectivity.

We now consider an example to illustrate the points made above.

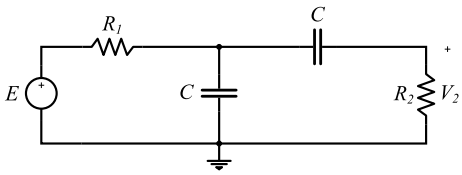

Fig. 10.2 A low Q passive RC circuit

Example 10.1 As an example consider the circuit of Fig. 10.2 with voltage transfer function:

$$H(s) = \frac{V_2(s)}{E(s)} = \frac{\frac{1}{R_1 C} s}{s^2 + s(\frac{1}{R_1 C} + \frac{2}{R_2 C}) + \frac{1}{R_1 R_2 C^2}}$$

Transfer function $H(s)$ has a zero $s = 0$ and two real poles with:

$$\omega_{op} = \frac{1}{C\sqrt{R_1 R_2}} \qquad Q_p = \sqrt{\frac{R_1 R_2}{2R_1 + R_2}}$$

The usefulness of this circuit as a highly selective filter is very limited since it can be shown that $Q_p \leq \frac{1}{2\sqrt{2}} = 0.3535$. In general, passive RC circuits have low Q in contrast to their passive RLC and active-RC counterparts, which can be made to have very high Q values.

In filter design, it is highly desirable to have circuits with easily adjustable Q and pole frequencies. An additional and desirable feature in a practical circuit is the facility to adjust Q independently from the pole frequency. In the low-Q passive RC circuit of Fig. 10.2, pole frequency can be adjusted by the capacitor C without affecting the value of Q, which depends only on the values of the resistors.

10.2 Second Order Functions

A second order rational function of the form

$$H(s) = \frac{N(s)}{D(s)} = \frac{N(s)}{s^2 + as + b} \tag{10.5}$$

is classified as *lowpass (LP)*, *highpass (HP)*, *bandpass (BP)*, *band-reject (BR)* or *all-pass (AP)* according to its zeros, i.e. according to the form and the roots of $N(s)$.

10.2.1 Second Order Lowpass (LP) Transfer Functions

The second order lowpass function is an all-pole rational function of the form

$$\boxed{H_{LP}(s) = \frac{A}{s^2 + \frac{\omega_o}{Q} s + \omega_o^2}} \tag{10.6}$$

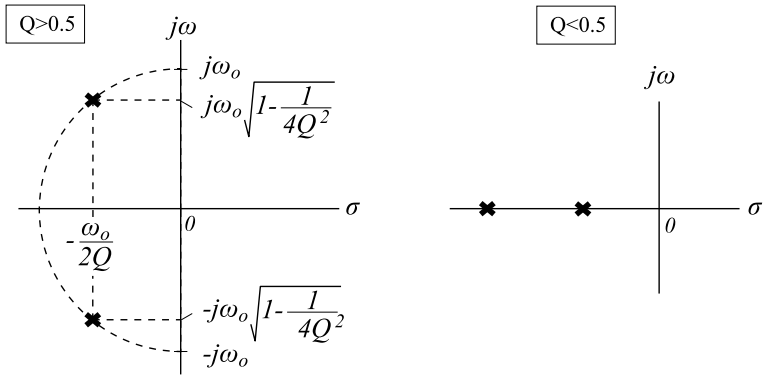

Fig. 10.3 Poles-zeros diagram

The corresponding poles-zeros diagram is shown in Fig. 10.3. The magnitude response of this transfer function, i.e. the gain function $G(\omega)$, is given by:

$$G(\omega) = |H(j\omega)| = \frac{A}{\sqrt{\omega^4 - 2\omega^2\omega_o^2(1 - \frac{1}{2Q^2}) + \omega_o^4}} \tag{10.7}$$

The gain $G(0)$ at zero frequency $\omega = 0$ is given by

$$G_o = G(0) = \frac{A}{\omega_o^2}$$

whilst at very high frequencies $\omega \to \infty$, we have:

$$G_\infty = G(\infty) = 0$$

The plot of $G(\omega)$ is shown in Fig. 10.4 for various values of Q.

The derivative of $G(\omega)$ of (10.7) assumes zero value at:

$$\omega_{MAX} = \omega_o\sqrt{1 - \frac{1}{2Q^2}} \tag{10.8}$$

Clearly for this real frequency to exist, $1 - \frac{1}{2Q^2} \geq 0 \Rightarrow Q \geq \frac{\sqrt{2}}{2} \geq 0.707$. Under this condition, $G(\omega)$ has a maximum value G_{MAX} for $\omega = \omega_{MAX}$:

$$G_{MAX} = \frac{G_o Q}{\sqrt{1 - \frac{1}{4Q^2}}} = \frac{AQ}{\omega_o^2\sqrt{1 - \frac{1}{4Q^2}}} \tag{10.9}$$

Figure 10.5 shows the ratios $\frac{\omega_{MAX}}{\omega_o}$, taken from (10.8), and $\frac{G_{MAX}}{QG_o}$, taken from (10.9), as functions of Q. It is evident that for high Q values:

$$\omega_{MAX} = \omega_o \quad \text{and} \quad G_{MAX} = G_o Q = \frac{AQ}{\omega_o^2} \tag{10.10}$$

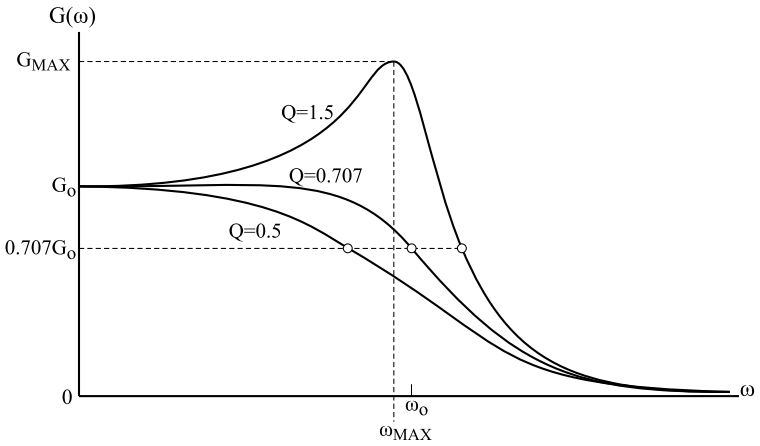

Fig. 10.4 Magnitude frequency response of second order LP function

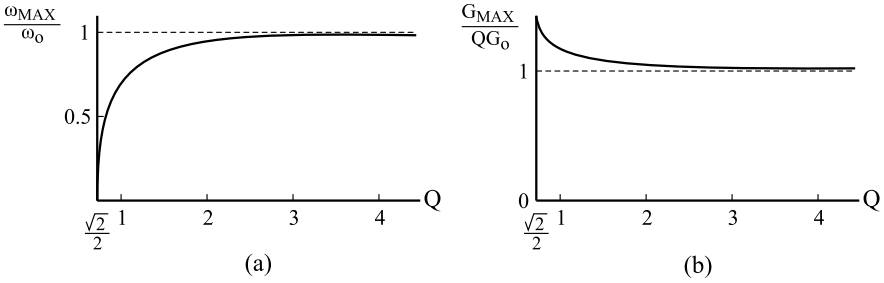

Fig. 10.5 Some characteristics as functions of Q

From Fig. 10.5, it can be inferred that the relationships of (10.10) are valid for $Q > 4$ but would lead to high inaccuracy if used for $Q < 2$.

There exists a frequency ω_C at which the gain becomes $G(\omega_C) = \frac{1}{\sqrt{2}} G_o$. Essentially at this frequency, the LP gain falls off by 3 dB from its value $G(0) = G_o$ at zero frequency and is referred to as the *prototype cutoff frequency*. ω_C can be calculated from (10.7):

$$\omega_C = \omega_o \sqrt{\left(1 - \frac{1}{2Q^2}\right) + \sqrt{\left(1 - \frac{1}{2Q^2}\right)^2 + 1}} \tag{10.11}$$

Figure 10.6 shows the relationship between ω_C and ω_o as a function of the quality factor Q. It is clear that for high Q values we have

$$\omega_C = \omega_o \sqrt{1 + \sqrt{2}} \approx 1.554 \omega_o$$

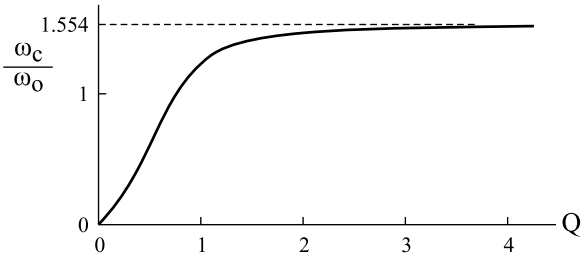

Fig. 10.6 The relationship of cutoff and pole frequency as a function of Q

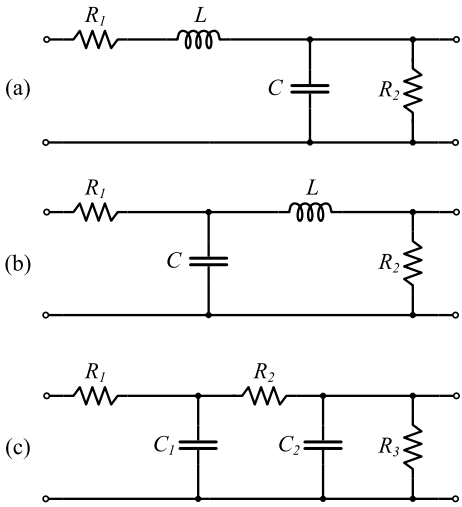

Fig. 10.7 Passive second order LP circuits

Passive RLC circuits with second order LP transfer functions have at least two lossless elements (inductors and capacitors). The circuits shown in Fig. 10.7 are typical examples of passive second order LP circuits.

Example 10.2 Show that the circuit of Fig. 10.7a is a lowpass filter and design it so that it has pole frequency $\omega_o = 2\pi 5000$ rad/s and $Q = 1$. Plot the magnitude frequency response for these values for frequencies 100 Hz to 10 kHz.

Apply a voltage source $E(s)$ at the input of the circuit and consider the voltage $V_2(s)$ across R_2 as output. The voltage transfer function can be calculated:

$$H(s) = \frac{V_2(s)}{E(s)} = \frac{\frac{1}{LC}}{s^2 + s(\frac{R_1}{L} + \frac{1}{R_2 C}) + \frac{R_1+R_2}{LCR_2}}$$

Since the numerator does not depend on s, this transfer function is a second order LP function with

$$\omega_o = \sqrt{\frac{R_1 + R_2}{LCR_2}} \qquad Q = \frac{\omega_o}{\frac{R_1}{L} + \frac{1}{CR_2}} = \sqrt{\frac{\frac{R_1+R_2}{LCR_2}}{\frac{R_1}{L} + \frac{1}{CR_2}}} \tag{10.12}$$

To design the filter so as to have $\omega_o = 2\pi 5000$ rad/s and $Q = 1$, the four unknown values of R_1, R_2, L and C must be calculated from the two design equations of (10.12). Considering $R_2 = R$ and $R_1 = kR$, (10.12) yield:

$$\omega_o = \sqrt{\frac{k+1}{LC}} \qquad Q = \frac{\omega_o}{\frac{kR}{L} + \frac{1}{CR}}$$

$$\Rightarrow \quad LC = \frac{k+1}{\omega_o^2} \qquad \frac{kR}{L} + \frac{1}{CR} = \frac{\omega_o}{Q}$$

$$\Rightarrow \quad L = \frac{k+1}{C\omega_o^2} \qquad \frac{kR\omega_o^2}{k+1}C^2 - \frac{\omega_o}{Q}C + \frac{1}{R} = 0$$

$$\Rightarrow \quad L = \frac{k+1}{C\omega_o^2} \quad C = \frac{k+1}{2kRQ\omega_o}\left[1 \pm \sqrt{1 - \frac{4kQ^2}{k+1}}\right]$$

For the capacitor C to assume real values,

$$4Q^2 \leq \frac{k+1}{k} \quad \Rightarrow \quad k \leq \frac{1}{4Q^2 - 1} \tag{10.13}$$

This allows the designer to select the value of k and in our case, in order to simplify calculations, we choose

$$\frac{k+1}{k} = 4Q^2 \quad \Rightarrow \quad k = \frac{1}{4Q^2 - 1}$$

in which case

$$C = \frac{k+1}{2kRQ\omega_o} = \frac{2Q}{R\omega_o} \quad \text{and} \quad L = \frac{k+1}{C\omega_o^2} = \frac{4Q^2}{(4Q^2 - 1)C\omega_o^2} \tag{10.14}$$

From (10.14), for an arbitrary choice of $R = 1000$ Ohm and for the given $\omega_o = 2\pi 5000$ rad/s and $Q = 1$, we finally get:

$$C = 63.6620 \text{ nF} \qquad L = 21.22 \text{ mH} \qquad k = \frac{1}{3}$$

$$R_2 = R = 1000 \text{ Ohm} \qquad R_1 = kR = 333.33 \text{ Ohm}$$

The magnitude frequency response of the circuit for these values is shown in Fig. 10.8.

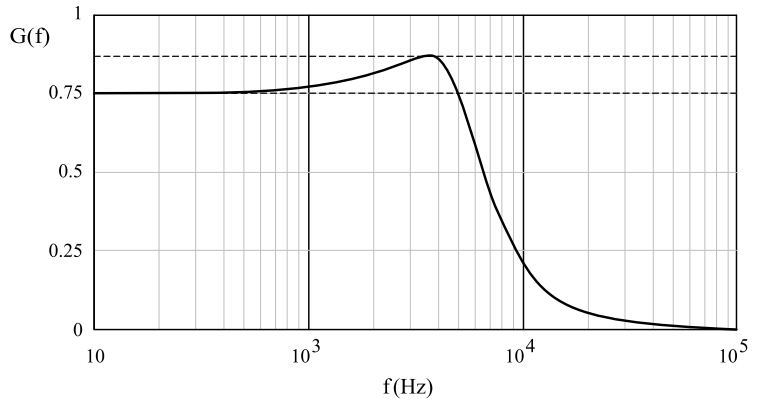

Fig. 10.8 Frequency response of Example 10.2

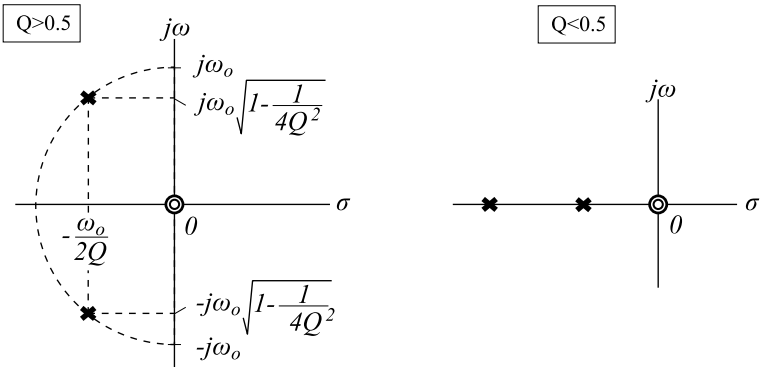

Fig. 10.9 Poles-zeros diagram of the HP second order function

10.2.2 Second Order Highpass (HP) Transfer Functions

The second order highpass function has the general form:

$$\boxed{H_{HP}(s) = \frac{As^2}{s^2 + s\frac{\omega_o}{Q} + \omega_o^2}} \tag{10.15}$$

The only difference from the lowpass function is that in the highpass case the numerator is s^2 giving a double zero at $s = 0$. The value of Q determines whether the HP function has two real poles or a complex conjugate pair of poles, as in the case of the LP function. Figure 10.9 shows the pole-zero diagram for these two cases, namely for $Q > 0.5$ and for $Q \leq 0.5$.

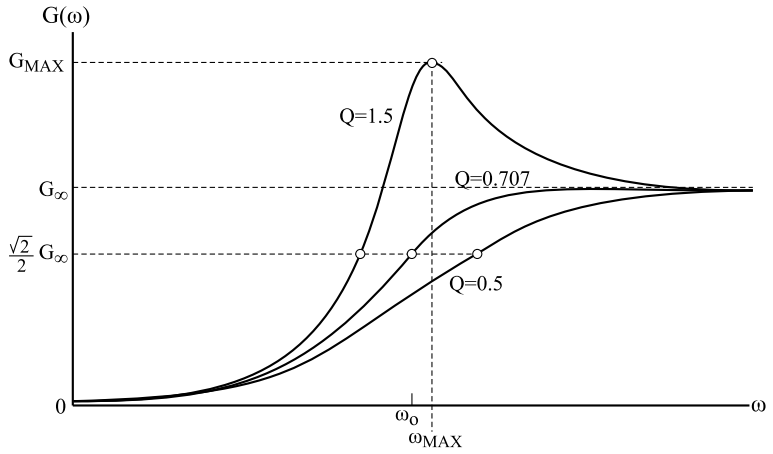

Fig. 10.10 Magnitude frequency response of the second order HP function

The magnitude of the second order HP function of (10.15) is:

$$G(\omega) = |H(j\omega)| = \frac{A\omega^2}{\sqrt{\omega^4 - 2\omega^2\omega_o^2(1 - \frac{1}{2Q^2}) + \omega_o^4}} \tag{10.16}$$

For $\omega = 0$, we have $G_o = G(0) = 0$, and for very high frequencies, i.e. when $\omega \to \infty$, we have $G_\infty = G(\infty) = A$.

The plot of the magnitude frequency response $G(\omega) = |H(j\omega)|$ is shown in Fig. 10.10 for several characteristic values of Q.

It can be easily shown that, as in the case of the LP function, if $Q > \frac{1}{\sqrt{2}}$, a maximum value G_{MAX} exists at frequency ω_{MAX}:

$$\omega_{MAX} = \omega_o \sqrt{\frac{1}{1 - \frac{1}{2Q^2}}} \tag{10.17}$$

The value of the maximum G_{MAX} at ω_{MAX} is given by

$$G_{MAX} = \frac{G_\infty Q}{\sqrt{1 - \frac{1}{4Q^2}}} = \frac{AQ}{\sqrt{1 - \frac{1}{4Q^2}}} \tag{10.18}$$

Obviously, for high Q-values we have $\omega_{MAX} = \omega_o$ and $G_{MAX} = G_\infty Q = AQ$.

The prototype cutoff frequency, the frequency at which the gain becomes $\frac{1}{\sqrt{2}} G_\infty = 0.707 G_\infty$, and the logarithmic gain drops by 3 dB from $20\log(G_\infty)$, is given by:

$$\omega_C = \omega_o \sqrt{\frac{1}{2Q^2} - 1 + \sqrt{\left(1 - \frac{1}{2Q^2}\right)^2 + 1}} \tag{10.19}$$

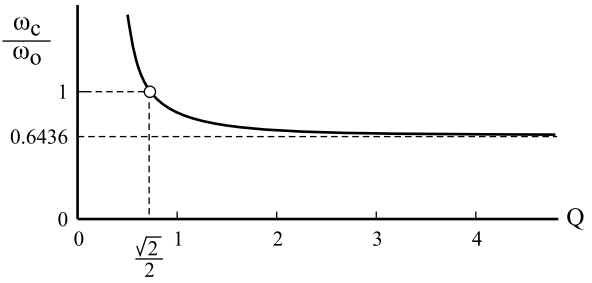

Fig. 10.11 The relationship of cutoff and pole frequency as a function of Q

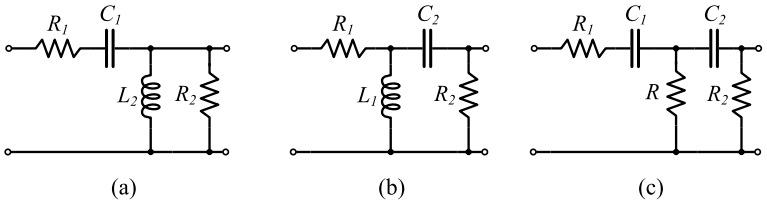

Fig. 10.12 Second order HP passive circuits

For high Q-values, (10.19) gives $\omega_C = \omega_o\sqrt{\sqrt{2}-1} = 0.6436\omega_o$. Figure 10.11 shows the ratio $\frac{\omega_C}{\omega_o}$ as a function of Q.

Passive circuits that realize a second order HP function have at least two lossless elements. Some typical circuits are shown in Fig. 10.12 and it would be a good exercise to determine their transfer functions.

It should be noticed that the LP function

$$H_{LP}(s) = \frac{A}{s^2 + s(\omega_o/Q) + \omega_o^2}$$

can be transformed into an HP function if s is replaced by $\frac{\omega_o^2}{s}$. Indeed, making this replacement in the LP function we get:

$$H(s) = \frac{\frac{A}{\omega_o^2}s^2}{s^2 + s(\omega_o/Q) + \omega_o^2}$$

which is a second order HP function with the same pole frequency and Q as the prototype lowpass case from which it was derived. Such frequency transformations will be presented in detail in Chap. 5

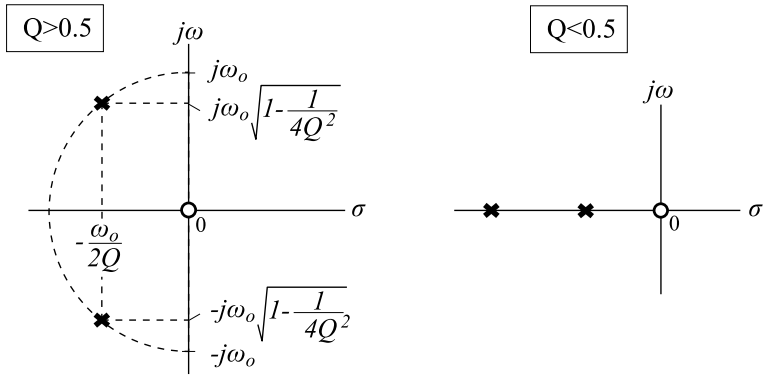

Fig. 10.13 Pole-zero diagram of 2nd order BP function

10.2.3 Second Order Bandpass (BP) Transfer Functions

The second order bandpass function is of the general form:

$$\boxed{H_{BP}(s) = \frac{As}{s^2 + s\frac{\omega_o}{Q} + \omega_o^2}} \tag{10.20}$$

The corresponding pole-zero diagram is shown in Fig. 10.13. The BP function differs from the LP function in that its numerator is s, i.e. it has a zero for $s = 0$. The two poles can be real ($Q \leq 0.5$) or form a complex conjugate pair ($Q > 0.5$). The magnitude frequency response will in this case be

$$G(\omega) = |H(j\omega)| = \frac{A\omega}{\sqrt{\omega^4 - 2\omega^2\omega_o^2(1 - \frac{1}{2Q^2}) + \omega_o^4}} \tag{10.21}$$

It is apparent that $G(0) = G(\infty) = 0$, and the gain plot is shown in Fig. 10.14 for some characteristic values of Q.

In the BP case, there is always a maximum at frequency $\omega_{MAX} = \omega_o$, and its value G_{MAX} can be determined from (10.20) by setting $\omega = \omega_o$:

$$G_{MAX} = G(\omega_o) = \frac{AQ}{\omega_o} \tag{10.22}$$

The frequencies ω_1 and ω_2 at which the gain $G(\omega) = |H(j\omega)| = \frac{1}{\sqrt{2}}G_{MAX}$, i.e. the logarithmic gain decreases by 3 dB from its maximum value $20\log(G_{MAX})$, are found to be:

$$\omega_1 = \frac{\omega_o}{2Q}\left[-1 + \sqrt{1 + 4Q^2}\right] \qquad \omega_2 = \frac{\omega_o}{2Q}\left[1 + \sqrt{1 + 4Q^2}\right] \tag{10.23}$$

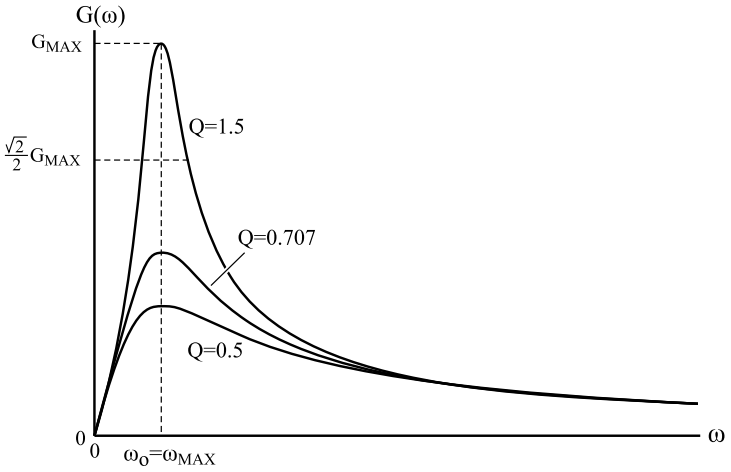

Fig. 10.14 Gain plot of 2nd order BP function

Fig. 10.15 Passive 2nd order BP circuits

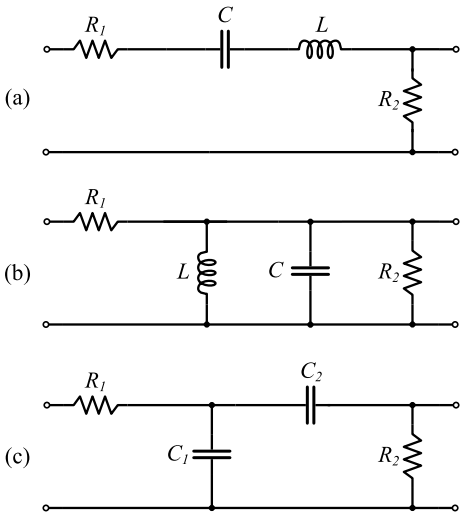

Frequencies ω_1 and ω_2 are called passband edge frequencies and define the passband bandwidth BW:

$$BW = \omega_2 - \omega_1 = \frac{\omega_o}{Q} \quad \text{with } \omega_1\omega_2 = \omega_o^2 \tag{10.24}$$

Figure 10.15 shows some passive circuits with 2nd order BP transfer functions.

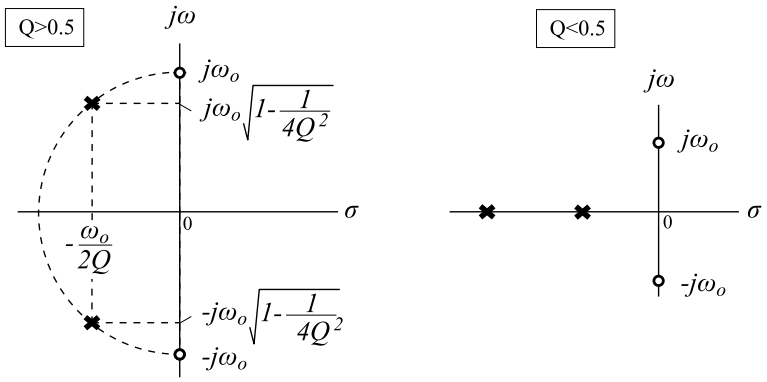

Fig. 10.16 Pole-zeros diagram of the 2nd order band-reject function

10.2.4 Second Order Band-Reject (BR) Transfer Functions

The 2nd order *band-reject* or *bandstop* or *band-elimination* function is of the general form:

$$H_{BR}(s) = \frac{A(s^2 + \omega_o^2)}{s^2 + s\frac{\omega_o}{Q} + \omega_o^2} \tag{10.25}$$

The characteristic of the BR function is that it has an imaginary conjugate pair of zeros $\pm j\omega_o$ on the $j\omega$-axis. As in the LP, HP and BP cases, the two poles can be real or a complex conjugate pair, as shown in Fig. 10.16.

The magnitude frequency response $G(\omega) = |H(j\omega)|$ is given by

$$G(\omega) = |H(j\omega)| = \frac{A|\omega_o^2 - \omega^2|}{\sqrt{\omega^4 - 2\omega^2\omega_o^2(1 - \frac{1}{2Q^2}) + \omega_o^4}} \tag{10.26}$$

The gain at $\omega = 0$ and $\omega = \infty$ can be determined from (10.26) and is $G(0) = G(\infty) = A$. The gain plot of the 2nd order BR function is shown in Fig. 10.17 for various values of Q.

In the BR case, there is always a transmission zero, i.e. a frequency at which the gain becomes zero at $\omega = \omega_o$. In addition, it should be observed that since the transmission zero frequency and the pole frequency are equal, the property $G(0) = G(\infty) = A$ is valid. In this case, the frequencies ω_1 and ω_2 at which the gain becomes $\frac{1}{\sqrt{2}}A$ are given by:

$$\begin{aligned} \omega_1 &= \frac{\omega_o}{2Q}\left[-1 + \sqrt{1 + 4Q^2}\right] \\ \omega_2 &= \frac{\omega_o}{2Q}\left[1 + \sqrt{1 + 4Q^2}\right] \end{aligned} \tag{10.27}$$

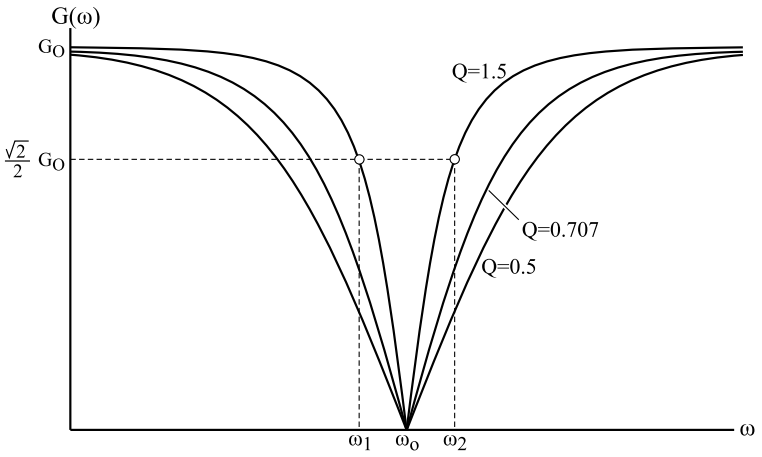

Fig. 10.17 Gain plot of the 2nd order band-reject function

The bandwidth BW of the BR function is defined as

$$BW = \omega_2 - \omega_1 = \frac{\omega_o}{Q} \quad \text{with } \omega_1\omega_2 = \omega_o^2 \tag{10.28}$$

When the zeros of the function occur at the pole frequencies ω_o, the BR function is referred to as *notch*. If the zeros are $\pm j\omega_z$ with $\omega_z \neq \omega_o$, then the BR function takes the general form:

$$H_{BR}(s) = \frac{A(s^2 + \omega_z^2)}{s^2 + s\frac{\omega_o}{Q} + \omega_o^2} \tag{10.29}$$

If $\omega_z > \omega_o$, the band-reject function is referred to as *lowpass-notch* due to the gain plot, which is of the form of Fig. 10.18a. In this case, $G(0) = A\frac{\omega_z^2}{\omega_o^2} > A$ and $G(\infty) = A$. If $\omega_z < \omega_o$, the BR function is referred to as *highpass-notch* due to the gain plot, which is of the form of Fig. 10.18b. In this case, $G(0) = A\frac{\omega_z^2}{\omega_o^2} < A$ and $G(\infty) = A$

Typical passive circuits which realize 2nd order band-reject functions are shown in Fig. 10.19.

10.2.5 Second Order Allpass (AP) Transfer Functions

The 2nd order allpass function has the general form

$$\boxed{H_{AP}(s) = \frac{s^2 - s\frac{\omega_o}{Q} + \omega_o^2}{s^2 + s\frac{\omega_o}{Q} + \omega_o^2}} \tag{10.30}$$

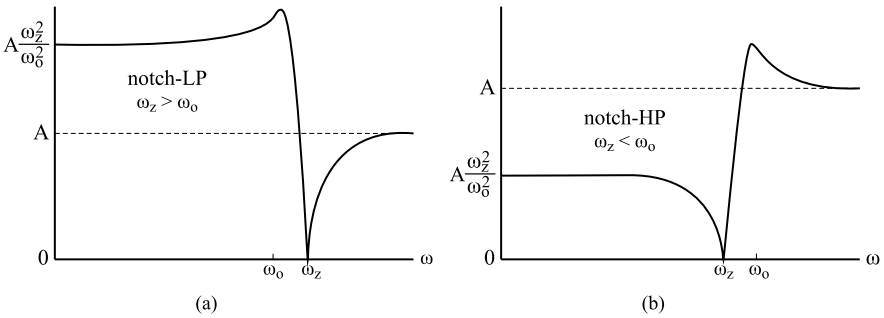

Fig. 10.18 (**a**) Notch-LP and (**b**) notch-HP gain

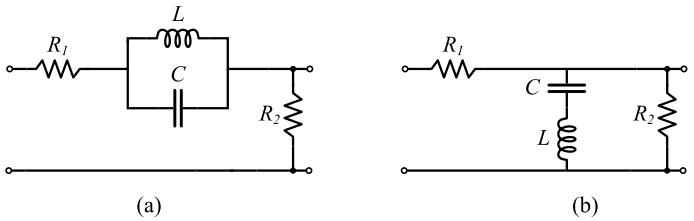

Fig. 10.19 Typical passive 2nd order band-reject circuits

Fig. 10.20 Pole-zeros diagram of the 2nd order AP function

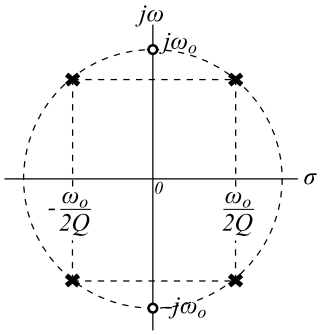

All-pass function has two poles in the left half s-plane and two zeros with identical frequencies and Q in the right hand s-plane, as seen in Fig. 10.20 for the case $Q > 0.5$. The magnitude frequency response can be found from (10.30):

$$G(\omega) = |H(j\omega)| = \frac{\sqrt{(\omega_o^2 - \omega^2)^2 + \frac{\omega_o^2}{Q^2}}}{\sqrt{(\omega_o^2 - \omega^2)^2 + \frac{\omega_o^2}{Q^2}}} = 1 \tag{10.31}$$

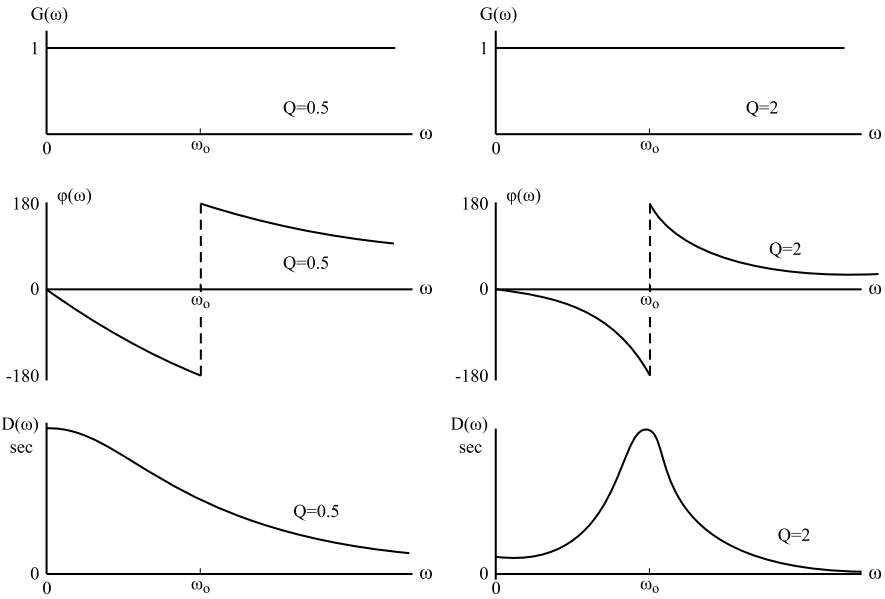

Fig. 10.21 Gain, phase and group delay plots of the 2nd order AP function

Equation (10.31) justifies the all-pass name since it shows that all frequencies pass with unity gain, i.e. no magnitude distortion occurs and therefore no filtering is performed. In a filtering environment, such transfer functions are employed beneficially not for their magnitude, but rather for their phase or group delay properties shown in Fig. 10.21.

Circuits with all-pass transfer function are referred to as all-pass filters and are used as phase or *delay equalizers*, i.e. as circuits connected to the output of a filter to correct phase and delay without altering the gain.

10.3 Second Order Active-RC Circuits

This is a large range of circuits that have been developed for the purpose of realizing second order transfer function. Very often these can be used as starting point for a realization better suited to a specific application. The most significant circuits are reviewed in this part and some further derivations are indicated.

10.3.1 Impedance and Frequency Scaling

Consider an inductorless active circuit that has only resistors and capacitors. According to impedance scaling as presented in Sect. 1.6.1, the transfer function of an RC circuit does not change if all resistor values are multiplied by a scalar factor

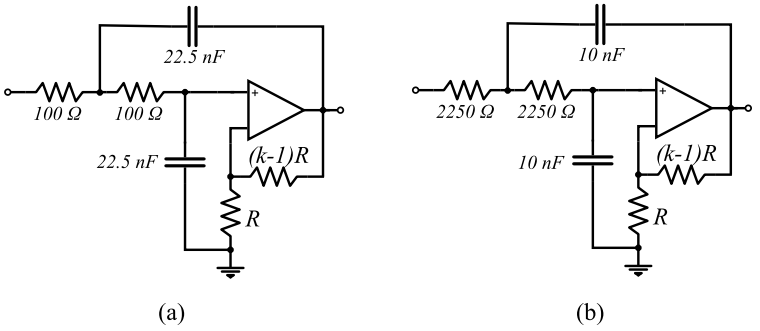

Fig. 10.22 Impedance scaling applied to an active-RC circuit

K and simultaneously all capacitor values are divided by the same factor. Such a scaling is clearly obvious, since in such RC-active circuits scaling the resistors and capacitors as indicated will not change the time constants RC. Impedance scaling is widely used in active filter design as a means of scaling the component elements to a desirable range of values. Scaling the circuit in Fig. 10.22a by $K = 2.25$ produces component values as indicated in Fig. 10.22b and the scaled circuit has the same transfer function.

It is observed here that resistors or capacitors used to set up a gain value through their ratio may not be scaled. In the circuit of Fig. 10.22, parametric resistor R in the feedback resistors R and $(k-1)R$ can have any convenient and suitable value. "Suitable" is of course a relative term that depends on some practical aspects. For implementations using operational amplifiers, for example, in order to avoid high currents, high resistor values are used. However, very high resistor values lead to very small currents and voltages comparable to the noise level. Hence, a compromise is made. In active-RC circuits with operational amplifiers, resistors with values of the order of 10 kOhms are preferred. This resistance level can also be used as a guide for impedance scaling.

Frequency scaling presented in Sect. 1.6.2, is easily applied to inductorless active-RC circuits simply by multiplying all resistor values or all capacitor values by a constant K. This is equivalent to multiplying all time constants RC by K and so dividing all frequencies by K. If for example in an active-RC filter with cutoff frequency ω_C, all resistors are multiplied by K, the cutoff frequency will be changed to $\frac{\omega_C}{K}$. The same result can be achieved by instead multiplying all capacitor values by K. Through frequency scaling the frequency characteristics of active-RC filters can be modified so as to suit the design requirements.

As an example, impedance and frequency scaling will be applied to the circuit of Fig. 10.23, which has a lowpass transfer function

$$H_{LP}(s) = \frac{V_3(s)}{E(s)} = -\frac{(R_6/R_5)/(R_2R_4C_1C_2)}{s^2 + s\frac{1}{R_1C_1} + \frac{R_6/R_5}{R_2R_3C_1C_2}}$$

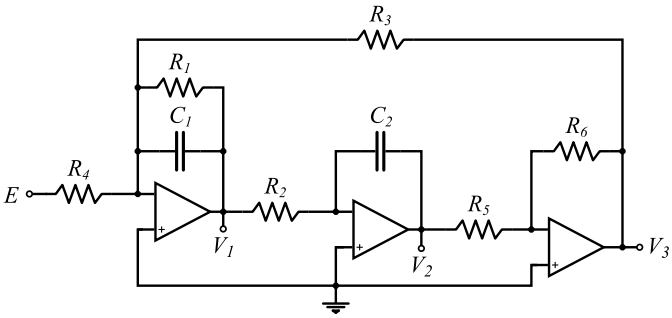

Fig. 10.23 An active-RC lowpass filter

with the obvious definitions

$$\omega_o = \sqrt{\frac{R_6/R_5}{R_2 R_3 C_1 C_2}} \qquad Q = \frac{R_1}{\sqrt{R_2 R_3}} \sqrt{\frac{R_6 C_1}{R_5 C_2}}$$

It can easily be seen that if all resistors are multiplied by a constant K and all capacitors are divided by the same constant K, the transfer function does not change since Q and ω_o do not change. However, if only the capacitors are divided by K, Q does not change but the pole frequency is multiplied by K becoming $K\omega_o$. Of course in this case the numerator of the transfer function is multiplied by K^2 but this does not affect the selectivity of the filter.

Finally, we note as a general rule that in order to change the operational frequency range of an active-RC filter, it is sufficient to change only the resistor or capacitor values. Moreover, in order to adjust the resistors and capacitors at a desirable level without altering the behavior of the filter, resistor and capacitor values must be treated in an inverse manner.

10.3.2 The RC-CR or LP-HP Transformation

Mitra proved in [10] that if in an active-RC circuit every resistor with resistance R (Ohm) is replaced by a capacitor with capacitance $1/R$ (F) and every capacitor with capacitance C (F) is replaced by a resistor with resistance $1/C$ (Ohm), then

i. All conductance functions $Y_o(s)$ of the initial circuit become $Y(s) = sY_o(\frac{1}{s})$
ii. All impedance functions $Z_o(s)$ of the initial circuit become $Z(s) = \frac{1}{s} Z_o(\frac{1}{s})$
iii. All transfer functions $H_o(s)$ of the initial circuit become $H(s) = H_o(\frac{1}{s})$

This called RC-CR transformation and transforms a lowpass filter to highpass and vice versa. Applying the RC-CR transformation to an active-RC lowpass filter with transfer function

$$H_{LP}(s) = \frac{A}{s^2 + s\frac{\omega_o}{Q} + \omega_o^2}$$

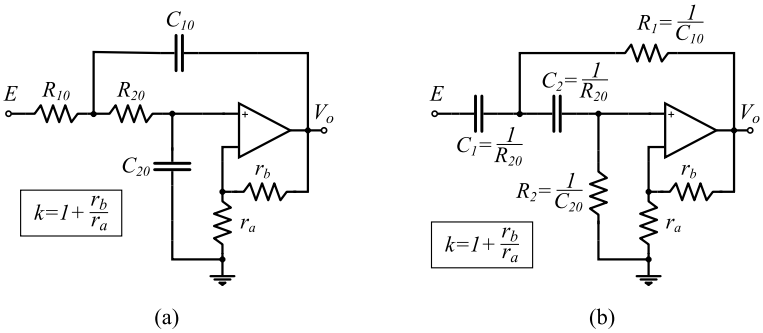

Fig. 10.24 (**a**) A lowpass filter. (**b**) RC-CR transformed circuit

a new transfer function will be obtained of the form

$$H_{HP}(s) = H_{LP}\left(\frac{1}{s}\right) = \frac{\omega_{HP}^2 A s^2}{s^2 + s\frac{\omega_{HP}}{Q} + \omega_{HP}^2} \quad \text{with } \omega_{HP} = \frac{1}{\omega_o}$$

Example 10.3 The RC-CR transformation is applied to the lowpass filter of Fig. 10.24a with voltage transfer function

$$H_{LP}(s) = \frac{V_o(s)}{E(s)} = \frac{\frac{k}{R_{10}R_{20}C_{10}C_{20}}}{s^2 + s(\frac{1}{R_{10}C_{10}} + \frac{1}{R_{20}C_{10}} + \frac{1-k}{R_{20}C_{20}}) + \frac{1}{R_{10}R_{20}C_{10}C_{20}}}$$

Accordingly, the transformed circuit of Fig. 10.24b will have the highpass transfer function

$$\begin{aligned} H_{HP}(s) &= H_{LP}\left(\frac{1}{s}\right) \\ &= \frac{ks^2}{s^2 + s(R_{20}C_{20} + R_{10}C_{20} + (1-k)R_{10}C_{10}) + R_{10}R_{20}C_{10}C_{20}} \end{aligned}$$

To verify this, the transformed circuit is analysed to yield:

$$H(s) = \frac{V_o(s)}{E(s)} = \frac{ks^2}{s^2 + s(\frac{1}{R_2C_2} + \frac{1}{R_2C_1} + \frac{1-k}{R_1C_1}) + \frac{1}{R_1R_2C_1C_2}}$$

which, on replacing components by their corresponding RC-CR transformation values, we obtain the same transfer function

$$H(s) = \frac{V_o(s)}{E(s)} = \frac{ks^2}{s^2 + s(R_{20}C_{20} + R_{10}C_{20} + (1-k)R_{10}C_{10}) + R_{10}R_{20}C_{10}C_{20}}$$

as expected.

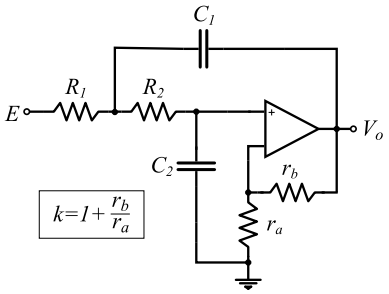

Fig. 10.25 Sallen-Key second order lowpass filter

It is noted that resistors r_a and r_b were not transformed since they are simply used to set up gain k by their ratio. If they had been transformed into capacitors C_a and C_b respectively, the gain k would be determined by their ratio: $k = 1 + \frac{C_a}{C_b}$.

If the circuit is not normalized, the element values of the transformed circuit are usually awkward and impedance scaling might be necessary (see Sect. 10.3.1).

The RC-CR transformation transforms a lowpass filter into a highpass filter and vice versa and for this reason it is also referred to as LP-HP transformation.

10.4 Sallen-Key Circuits

R.P. Sallen and E.I. Key of MIT proposed [11] some circuits with one operational amplifier for the implementation of second order voltage transfer functions. Such circuits employing a single operational amplifier are referred to as Single Amplifier Biquads (SAB). The Sallen-Key circuits are still very popular.

10.4.1 Sallen and Key Second Order Lowpass Filter

The voltage transfer function of the circuit of Fig. 10.25 is given by:

$$H(s) = \frac{V_o(s)}{E(s)} = \frac{\frac{k}{R_1 R_2 C_1 C_2}}{s^2 + s(\frac{1}{R_1 C_1} + \frac{1}{R_2 C_1} + \frac{1-k}{R_2 C_2}) + \frac{1}{R_1 R_2 C_1 C_2}} \tag{10.32}$$

with

$$\omega_o = \sqrt{\frac{1}{R_1 R_2 C_1 C_2}} \qquad Q = \frac{\sqrt{\frac{1}{R_1 R_2 C_1 C_2}}}{\frac{1}{R_1 C_1} + \frac{1}{R_2 C_1} + \frac{1-k}{R_2 C_2}} \tag{10.33}$$

The constant $k = 1 + \frac{r_b}{r_a} \geq 1$ is determined by the ratio of resistors r_a and r_b according to the requirements. In fact, the voltage divider formed by r_a and r_b imposes a feedback voltage $\frac{V_o(s)}{k}$ on the inverting input of the operational amplifier and k affects only the pole-Q.

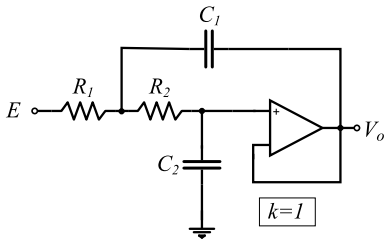

Fig. 10.26 Sallen-Key LP filter with $k = 1$ and equal resistors

In filter design, the element values R_1, R_2, C_1, C_2 of the circuit and k must be so calculated as to realize given ω_o and Q. The estimation of these five unknown values must be performed from the two design equations (10.33). Since there are only two equations, we can express two of the unknown five parameters in terms of the other three. Thus, given ω_o and Q, we can for example calculate R_1 and C_1 as functions of R_2, C_2 and k:

$$R_1 = \frac{k-1}{R_2 C_2^2 \omega_o^2} + \frac{1}{Q C_2 \omega_o} - R_2 \qquad C_1 = \frac{C_2}{(k-1) + \frac{R_2 C_2 \omega_o}{Q} - R_2^2 C_2^2 \omega_o^2} \tag{10.34}$$

From (10.34), R_1 and C_1 can be calculated for any value of R_2, C_2 and k that lead to positive R_1 and C_1. This freedom of arbitrary choice of three out of the five unknowns is equivalent to adding three more arbitrary design equations and this effectively leaves room for optimizing the final design.

For the particular lowpass Sallen-Key circuit, three design procedures are commonly used, each based on a different set of design assumptions.

Design I (Unit Gain Equal Resistors) Given ω_o and Q, the two basic design equations (10.33) with the additional equations: $R_1 = R$, $R_2 = R$ and $k = 1$ yield:

$$C_1 = \frac{2Q}{\omega_o R} \quad \text{and} \quad C_2 = \frac{1}{2\omega_o R Q} \tag{10.35}$$

The corresponding circuit is shown in Fig. 10.26. From (10.35), the capacitor value ratio can be calculated as $\frac{C_1}{C_2} = 4Q^2$, implying that for high Q values the capacitors value spread can be undesirably high, presenting difficulties in the implementation, especially in integrated technologies. This limits the usefulness of this design to those cases with low Q.

Design II (Equal Capacitors, Equal Resistors) Given ω_o and Q and setting $C_1 = C_2 = C$ and $R_1 = R_2 = R$, the two basic design equations (10.33) yield:

$$\omega_o = \frac{1}{RC} \quad \text{and} \quad Q = \frac{1}{3-k} \tag{10.36}$$

from which we get

$$k = 3 - \frac{1}{Q} \qquad RC = \frac{1}{\omega_o}$$

Constant k assumes a single value dependent on Q which must have a value $Q \geq 0.5$ in order that $k = 1 + \frac{r_b}{r_a} \geq 1$. As for the passive elements, any R and C values satisfying $RC = \frac{1}{\omega_o}$ may be selected.

Design III (Minimum Sensitivity) As mentioned above, for a given ω_o and Q, the two basic design equations (10.33) cannot be solved uniquely for R_1, R_2, C_1, C_2 and k unless we add three more equations. This design freedom makes it possible to optimize the circuit for some criterion. W. Saraga in [12] minimized the sensitivity of Q by setting $k = \frac{4}{3}$ and $R_1 C_1 = 3R_2 C_2$. These two equations combined with the basic design equations (10.33) can be solved for R_1, R_2, C_1, and k, leaving C_2 as a design parameter:

$$C_1 = \sqrt{3} Q C_2 \qquad R_1 = \frac{1}{\omega_o Q C_2} \qquad R_2 = \frac{1}{\sqrt{3}\omega_o C_2} \tag{10.37}$$

From (10.37) and selecting a value for C_2, all other circuit parameters can be calculated.

Example 10.4 Design a minimum sensitivity Sallen-Key circuit with transfer function

$$H(s) = \frac{A}{s^2 + s(4000\pi) + 4 \cdot 10^8 \pi^2}$$

and calculate its gain factor A. Finally, plot the magnitude frequency response.

From the transfer function, it is obvious that $\omega_o = 2\pi 10^4$ and $Q = \frac{\omega_o}{4000\pi} = 5$. Setting $k = \frac{4}{3}$ and selecting $C_2 = 10^{-8} = 10$ nF, the values of the rest of the passive elements are calculated from (10.37):

$$C_1 = \sqrt{3} \cdot 5 \cdot 10^{-8} = 86.6 \text{ nF} \qquad R_1 = \frac{1}{2\pi \cdot 10^4 \cdot 5 \cdot 10^{-8}} = 318.31 \text{ Ohm}$$

$$R_2 = \frac{1}{\sqrt{3} \cdot 2\pi \cdot 10^4 \cdot 10^{-8}} = 918.88 \text{ Ohm} \qquad A = \frac{1}{R_1 R_2 C_1 C_2} = 0.5264 \cdot 10^{10}$$

The frequency response is shown in Fig. 10.27.

10.4.2 Sallen and Key Second Order Highpass Filter

As we have seen, the RC-CR or LP-HP transformation transforms an active-RC lowpass filter into a highpass filter. In circuit (a) of Fig. 10.28, a Sallen-Key lowpass filter is transformed into the highpass circuit (b) simply by replacing resistors with capacitors and capacitors with resistors. The resistors r_a and r_b are not replaced, although they could be, since their actual values are irrelevant and only their ratio appears in the transfer function.

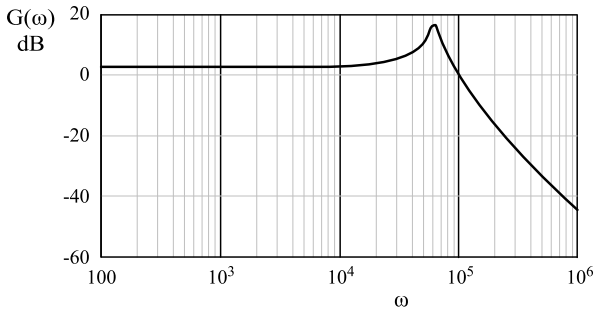

Fig. 10.27 Magnitude frequency response of example design

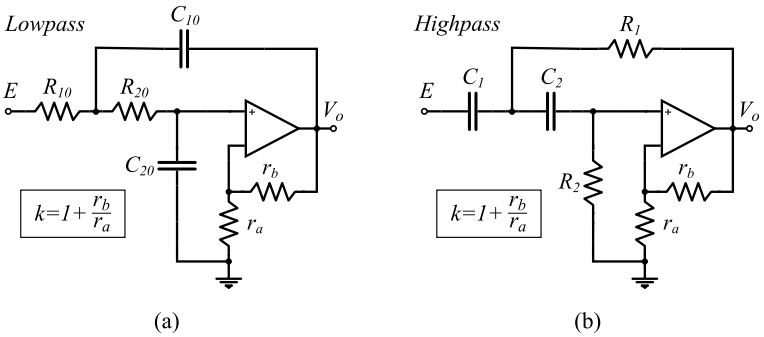

Fig. 10.28 (**a**) Lowpass circuit. (**b**) Highpass circuit via LP-HP transformation

The circuit of Fig. 10.28 is the Sallen-Key highpass filter and its voltage transfer function can be easily determined:

$$H(s) = \frac{V_o(s)}{E(s)} = \frac{ks^2}{s^2 + s(\frac{1}{R_2C_2} + \frac{1}{R_2C_1} + \frac{1-k}{R_1C_1}) + \frac{1}{R_1R_2C_1C_2}} \tag{10.38}$$

where $k = 1 + \frac{r_b}{r_a} \geq 1$. The corresponding design equations are given below:

$$\omega_o = \sqrt{\frac{1}{R_1R_2C_1C_2}} \qquad Q = \frac{\sqrt{\frac{1}{R_1R_2C_1C_2}}}{\frac{1}{R_2C_2} + \frac{1}{R_2C_1} + \frac{1-k}{R_1C_1}} \tag{10.39}$$

As in the LP Sallen-Key circuit, k is not involved in the expression for ω_o and affects only the value of Q.

10.4.3 Sallen and Key Second Order Bandpass Filter

Figure 10.29 shows the second order Sallen-Key bandpass circuit which has a transfer function

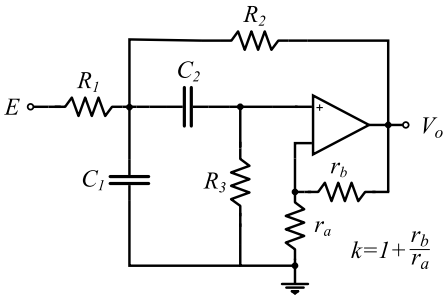

Fig. 10.29 Second order Sallen-Key bandpass circuit

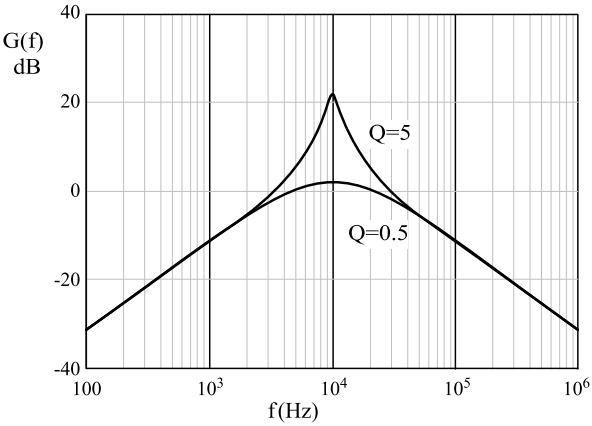

Fig. 10.30 Gain plot of the Sallen-Key bandpass circuit

$$H(s) = \frac{\frac{k}{R_1C_1}s}{s^2 + s(\frac{1}{R_1C_1} + \frac{1}{R_3C_2} + \frac{1}{R_3C_1} + \frac{1-k}{R_2C_1}) + \frac{R_1+R_2}{R_1R_2R_3C_1C_2}} \tag{10.40}$$

where $k = 1 + \frac{r_B}{r_A} \geq 1$ and

$$\omega_o = \sqrt{\frac{R_1 + R_2}{R_1R_2R_3C_1C_2}} \qquad Q = \frac{\sqrt{\frac{R_1+R_3}{R_1R_2R_3C_1C_2}}}{\frac{1}{R_1C_1} + \frac{1}{R_3C_2} + \frac{1}{R_3C_1} + \frac{1-k}{R_2C_1}} \tag{10.41}$$

Figure 10.30 shows a typical gain plot for $Q = 0.5$ and $Q = 5$. As in the LP and HP cases, the parameter k is used to adjust the value of Q and does not affect the pole frequency ω_o.

Example 10.5 The BP transfer function

$$H(s) = \frac{As}{s^2 + s(2\pi \cdot 10000/Q) + (2\pi \cdot 10000)^2}$$

with $\omega_o = 2\pi 10^4$ can be realized by a Sallen-Key circuit. On setting $R_1 = R_2 = R_3 = R$ and $C_1 = C_2 = C$, the design equations (10.41) yield

$$\omega_o = \frac{\sqrt{2}}{RC} \qquad Q = \frac{\sqrt{2}}{4-k}$$

from which $k = 4 - \frac{\sqrt{2}}{Q}$ and $RC = \frac{\sqrt{2}}{\omega_o}$.

Any arbitrary choice of $R = R_1 = R_2$ can be made and C can be calculated from $C = C_1 = C_2 = \frac{\sqrt{2}}{\omega_o R}$. If, for example, $R = R_1 = R_2 = 1$ kOhm $\rightarrow$ $C = 22.51$ nF.

The value of k depends solely on Q and for $Q = 0.5 \rightarrow k = 1.1716$ while for $Q = 5.0 \rightarrow k = 3.7172$.

The numerator coefficient A is given by $A = \frac{k}{RC} = \frac{k\omega_o}{\sqrt{2}} = (2\sqrt{2} - \frac{1}{Q})\omega_o$. For $Q = 0.5 \rightarrow A = 5.2052 \cdot 10^4$ and for $Q = 5 \rightarrow A = 16.5148 \cdot 10^4$.

10.5 Deliyannis Circuits

The basic Deliyannis circuit [5] of Fig. 10.31 is a single amplifier biquad that realizes a second order bandpass transfer function.

The circuit is based on the differentiator $C_1 - R_2$, with positive feedback provided by the voltage divider r_a/r_b. The transfer function of the circuit is

$$H(s) = \frac{V_o(s)}{E(s)} = -\frac{\frac{1}{R_1 C_2 (1-\frac{1}{k})} s}{s^2 + s(\frac{1}{R_2 C_1} + \frac{1}{R_2 C_2} - \frac{1}{(k-1)R_1 C_2}) + \frac{1}{R_1 R_2 C_1 C_2}} \tag{10.42}$$

from which the design equations are derived:

$$\begin{aligned} \omega_o &= \sqrt{\frac{1}{R_1 R_2 C_1 C_2}} \\ Q &= \frac{\sqrt{\frac{1}{R_1 R_2 C_1 C_2}}}{\frac{1}{R_2 C_1} + \frac{1}{R_2 C_2} - \frac{1}{(k-1)R_1 C_2}} = \frac{\sqrt{\frac{R_2}{R_1}}}{\sqrt{\frac{C_2}{C_1}} + \sqrt{\frac{C_1}{C_2}} - \frac{1}{(k-1)} \frac{R_2}{R_1} \sqrt{\frac{C_1}{C_2}}} \end{aligned} \tag{10.43}$$

The design of the Deliyannis BP circuit, i.e. the determination of its element values given ω_o and Q, can be performed in many ways, but in [5] an optimal procedure is proposed. According to this procedure, the capacitors are assigned an equal value, $C_1 = C_2 = C$, and the ratio R_2/R_1 is denoted by β: $\frac{R_2}{R_1} = \beta$. Under these conditions, the rest of the element values of the circuit are given by

$$R_1 = \frac{1}{\omega_o C \sqrt{\beta}} \qquad R_2 = \frac{\sqrt{\beta}}{\omega_o C} \qquad k = \frac{Q(\beta+2) - \sqrt{\beta}}{2Q - \sqrt{\beta}} \tag{10.44}$$

The value of β can be chosen arbitrarily but can be also calculated as to minimize the Q-sensitivity.

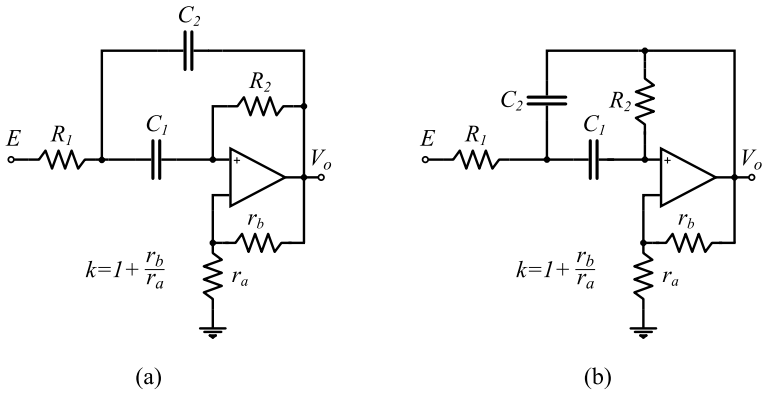

Fig. 10.31 The Deliyannis BP circuit

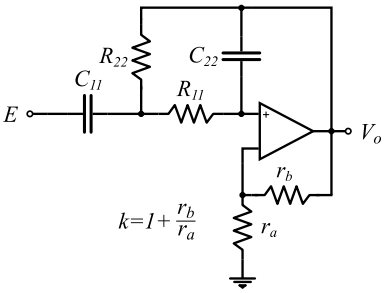

Fig. 10.32 RC-CR transformed Deliyannis BP circuit

Applying the RC-CR transformation to the circuit of Fig. 10.31, a new Deliyannis BP circuit is obtained, based on an integrator, as shown in Fig. 10.32. The determination of the transfer function of the circuit is left as an exercise.

Example 10.6 In order to design a Deliyannis bandpass circuit with pole frequency at 2 kHz and $Q = 10$, (10.44) will be used with $C_1 = C_2 = 10$ nF (arbitrary choice) and $\beta = 42$. The value of β could be any positive number but this particular value has been calculated so as to minimize the Q-sensitivity. Equations (10.44) give $R_1 = 1.23$ kOhm, $R_2 = 51.6$ kOhm and $k = 32.06$, i.e. $r_b/r_a = 31.06$. The logarithmic gain plot is shown in Fig. 10.33.

10.5.1 The Generalized Deliyannis Circuit

The circuit of Fig. 10.34 has been derived from the Deliyannis BP circuit of Fig. 10.31 by splitting resistor R_1 as shown ($\alpha \leq 1$) and feeding the input to the non-inverting input of the operational amplifier.

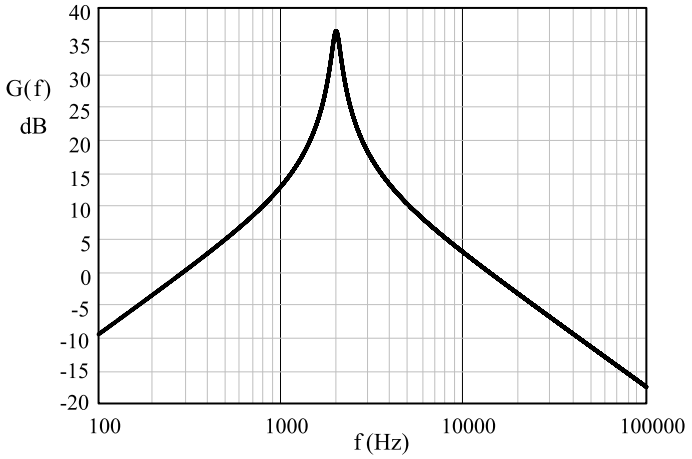

Fig. 10.33 RC-CR transformed Deliyannis BP circuit

Fig. 10.34 The generalized Deliyannis circuit

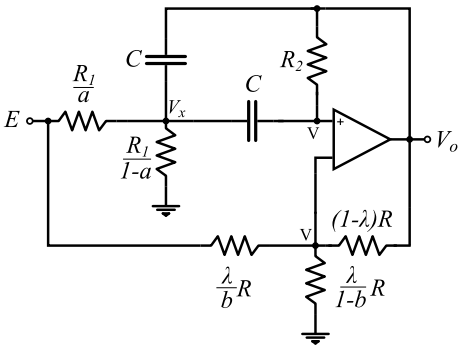

The transfer function of the new circuit is

$$H(s) = \frac{V_o(s)}{E(s)} = b \cdot \frac{s^2 + \frac{2}{CR_2}[1 + \frac{R_2}{2R_1}(1 - \frac{\alpha}{b(1-\lambda)})]s + \frac{1}{C^2R_1R_2}}{s^2 + \frac{2}{CR_2}[1 - \frac{\lambda}{2(1-\lambda)}\frac{R_2}{R_1}]s + \frac{1}{C^2R_1R_2}} \tag{10.45}$$

with $\alpha \leq 1$, $b \leq 1$ and $\lambda \leq 1$ in order that all resistor values are non-negative.

For $b = 0$, i.e. with no feeding of the input to the non-inverting input of the operational amplifier, the transfer function of (10.45) becomes BP

$$H(s) = \frac{V_o(s)}{E(s)} = \frac{-\frac{\alpha}{(1-\lambda)}\frac{1}{R_1C}s}{s^2 + \frac{2}{CR_2}[1 - \frac{\lambda}{2(1-\lambda)}\frac{R_2}{R_1}]s + \frac{1}{C^2R_1R_2}} \tag{10.46}$$

with

$$\omega_o = \frac{1}{C\sqrt{R_1 R_2}} \quad \text{and} \quad Q = \frac{\frac{1}{2}\sqrt{\frac{R_2}{R_1}}}{1 - \frac{\lambda}{2(1-\lambda)}\frac{R_2}{R_1}} \tag{10.47}$$

If in the generalized Deliyannis circuit the parameters are chosen in such a way as to satisfy

$$1 + \frac{R_2}{2R_1}\left(1 - \frac{\alpha}{b(1-\lambda)}\right) = 0 \quad \Leftrightarrow \quad \frac{\alpha}{b} = \left(1 - \lambda\right)\left(1 + \frac{2R_1}{R_2}\right) \tag{10.48}$$

the transfer function becomes notch filter.

$$\begin{aligned} H(s) = \frac{V_o(s)}{E(s)} &= b \times \frac{s^2 + \frac{1}{C^2 R_1 R_2}}{s^2 + \frac{2}{CR_2}[1 - \frac{\lambda}{2(1-\lambda)}\frac{R_2}{R_1}]s + \frac{1}{C^2 R_1 R_2}} \\ &= \frac{b(s^2 + \omega_o^2)}{s^2 + s\frac{\omega_o}{Q} + \omega_o^2} \end{aligned} \tag{10.49}$$

with

$$\omega_o = \frac{1}{C\sqrt{R_1 R_2}} \quad Q = \frac{\omega_o}{\frac{2}{CR_2}[1 - \frac{\lambda}{2(1-\lambda)}\frac{R_2}{R_1}]} = \frac{\sqrt{\frac{R_2}{R_1}}}{1 - \frac{\lambda}{2(1-\lambda)}\frac{R_2}{R_1}} \tag{10.50}$$

The generalized Deliyannis biquad can also realize allpass functions if the parameters are chosen to satisfy

$$1 + \frac{R_2}{2R_1}\left(1 - \frac{\alpha}{b(1-\lambda)}\right) = -\left(1 - \frac{\lambda}{2(1-\lambda)}\frac{R_2}{R_1}\right) \tag{10.51}$$

10.5.2 Friend's Biquad

Friend's biquad (Fig. 10.35) is in fact a modified generalized Deliyannis circuit with the input fed also to the inverting input of the operational amplifier.

The transfer function takes the form

$$H(s) = K\frac{ms^2 + cs + d}{s^2 + as + b}$$

with

$$R_{1A} = \frac{R_A R_{AA}}{R_A + R_{AA}} \qquad R_{2C} = \frac{R_C R_{CC}}{R_C + R_{CC}} \qquad R_{3B} = \frac{R_B R_{BB}}{R_B + R_{BB}}$$

$$K_1 = \frac{R_{AA}}{R_A + R_{AA}} \qquad K_2 = \frac{R_{CC}}{R_C + R_{CC}} \qquad K_3 = \frac{R_{BB}}{R_B + R_{BB}}K = 1 \qquad m = K_2$$

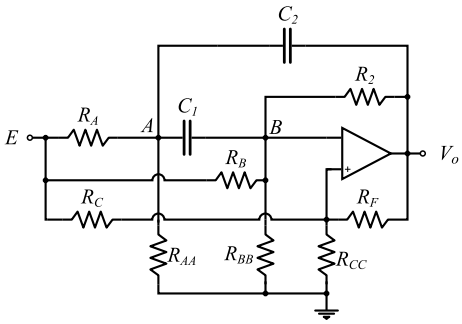

Fig. 10.35 The Friend's biquad

$$c = \frac{K_2}{C_2}\left(\frac{1}{R_1}+\frac{1}{R_2}+\frac{1}{R_{3B}}\right)+\frac{K_2}{C_1}\left(\frac{1}{R_2}+\frac{1}{R_{3B}}\right)-\frac{K_1}{R_{1A}C_2}\left(1+\frac{R_{2C}}{R_F}\right)$$
$$-\frac{K_3}{R_{3B}}\left(\frac{1}{C_1}+\frac{1}{C_2}\right)\left(1+\frac{R_{2C}}{R_F}\right)$$

$$d = \frac{1}{C_1C_2}\left[\frac{K_2}{R_{1A}}\left(\frac{1}{R_2}=\frac{1}{R_{3B}}\right)-\frac{K_3}{R_{1A}R_{3B}}\left(1+\frac{R_{2C}}{R_F}\right)\right]$$

$$a = \frac{C_1+C_2}{C_1C_2}\left(\frac{1}{R_2}-\frac{R_{2C}}{R_FR_{3B}}\right)-\frac{R_{2C}}{R_FR_{1A}C_2} \qquad b = \frac{1}{R_{1A}C_1C_2}\left(\frac{1}{R_2}-\frac{R_{2C}}{R_FR_{3B}}\right)$$

The design equations are very involved and the circuit does not presently offer any significant advantage over the generalized Deliyannis circuit.

10.6 Multiple Feedback (MF) Circuits

Multiple feedback single amplifier biquads are very similar in structure to the generalized Deliyannis circuit. They employ one operational amplifier in an inverting integrator or differentiator configuration with an additional feedback to the input of the circuit.

10.6.1 The Lowpass Multiple Feedback Circuit

The circuit of Fig. 10.36 is based on an inverting integrator with its output fed back to the input node through resistor R_2. The transfer function of the circuit is given by

$$H(s) = -\frac{\frac{1}{R_1R_3C_1C_2}}{s^2+s(\frac{1}{R_1}+\frac{1}{R_2}+\frac{1}{R_3})\frac{1}{C_1}+\frac{1}{R_2R_3C_1C_2}} \tag{10.52}$$

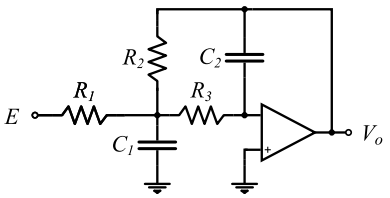

Fig. 10.36 The MF lowpass circuit

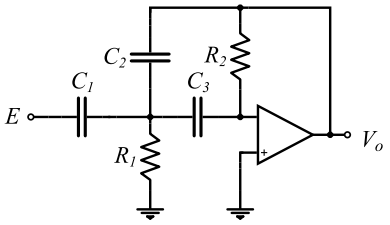

Fig. 10.37 The MF highpass circuit

The design equations are given below:

$$\omega_o = \frac{1}{\sqrt{R_2 R_3 C_1 C_2}} \qquad Q = \sqrt{\frac{\frac{C_1}{C_2}}{\sqrt{\frac{R_3}{R_2}} + \sqrt{\frac{R_2}{R_3}} + \sqrt{\frac{R_2 R_3}{R_1}}}} \tag{10.53}$$

Resistor R_1 is not involved in the expression for ω_o and therefore can be used for the adjustment of the Q value.

10.6.2 The Highpass Multiple Feedback Circuit

The circuit of Fig. 10.37 is obtained from the circuit of Fig. 10.36 via the LP-HP transformation. The voltage transfer function is found to be:

$$H(s) = -\frac{(C_1/C_2)s^2}{s^2 + s(\frac{C_1}{C_2 C_3} + \frac{1}{C_2} + \frac{1}{C_3})\frac{1}{R_2} + \frac{1}{R_1 R_2 C_2 C_3}} \tag{10.54}$$

The design equations in this case are given below:

$$\omega_o = \frac{1}{\sqrt{R_1 R_2 C_2 C_3}} \qquad Q = \sqrt{\frac{R_2/R_1}{\sqrt{\frac{C_3}{C_2}} + \sqrt{\frac{C_2}{C_3}} + \frac{C_1}{\sqrt{C_2 C_3}}}} \tag{10.55}$$

It should be noted that we again have frequency independent Q adjustment through capacitor C_1 as expected.

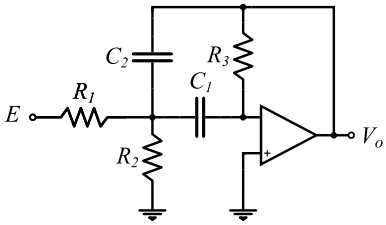

Fig. 10.38 The MF bandpass circuit

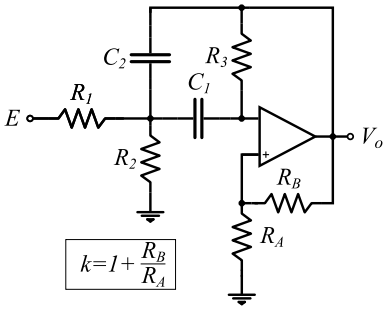

Fig. 10.39 The MF modified bandpass circuit

10.6.3 The Bandpass Multiple Feedback Circuit

This circuit is shown in Fig. 10.38 and its voltage transfer function is

$$H(s) = -\frac{\frac{1}{R_1 C_2} s}{s^2 + s(\frac{1}{C_1} + \frac{1}{C_2})\frac{1}{R_3} + \frac{1}{R_3 C_1 C_2}(\frac{1}{R_1} + \frac{1}{R_2})} \tag{10.56}$$

The design equations are

$$\omega_o = \sqrt{\frac{R_1 + R_2}{R_1 R_2 R_3 C_1 C_2}} \qquad Q = \sqrt{\frac{\frac{R_3}{R_2}(1 + \frac{R_2}{R_1})}{\sqrt{\frac{C_1}{C_2}} + \sqrt{\frac{C_2}{C_1}}}} \tag{10.57}$$

If the output is fed back to the non-inverting input of the operational amplifier through a voltage divider R_A/R_B, as in Fig. 10.39, the transfer function becomes

$$H(s) = -\frac{\frac{k}{(k-1)R_1 C_2} s}{s^2 + s[\frac{R_1+R_2}{R_1 R_2 C_2 (k-1)} - \frac{C_1+C_2}{C_1 C_2 R_3}] + \frac{R_1+R_2}{R_1 R_2 R_3 C_1 C_2}} \tag{10.58}$$

This circuit offers better control of the Q value through $k = 1 + \frac{R_B}{R_A}$. It should be noted that both multiple feedback bandpass circuits can be obtained from the generalized Deliyannis circuit by setting $b = 0$.

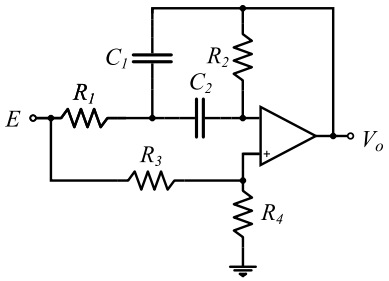

Fig. 10.40 The MF bandstop circuit

10.6.4 The Band-Reject Multiple Feedback Circuit

The circuit is shown in Fig. 10.40 and has a voltage transfer function:

$$H(s) = \frac{R_4}{R_3 + R_4} \frac{s^2 + s(\frac{1}{R_2C_1} + \frac{1}{R_2C_2} - \frac{R_3}{R_4}\frac{1}{R_1C_1}) + \frac{1}{R_1R_2C_1C_2}}{s^2 + s(\frac{1}{R_2C_1} + \frac{1}{R_2C_2}) + \frac{1}{R_1R_2C_1C_2}} \tag{10.59}$$

The pole (center) frequency and Q are given by

$$\omega_o = \frac{1}{\sqrt{R_1R_2C_1C_2}} \qquad Q = \frac{\sqrt{\frac{R_2}{R_1}}}{\sqrt{\frac{C_2}{C_1}} + \sqrt{\frac{C_1}{C_2}}} \tag{10.60}$$

In order for $H(s)$ of (10.59) to become a band-reject function, the coefficient of s in the numerator must be zero and therefore

$$\frac{1}{R_2C_1} + \frac{1}{R_2C_2} = \frac{R_3}{R_4}\frac{1}{R_1C_1} \tag{10.61}$$

This constraint can be met by adjusting the ratio $\frac{R_3}{R_4}$ without affecting ω_o and Q, as can be seen from (10.60).

Since the constant terms of the numerator and denominator in the expression of the transfer function of (10.59) are equal, the circuit can only realize notch type transfer functions (i.e. it cannot realize LP-notch and HP-notch functions).

However, by adding one more capacitor C_3, as in Fig. 10.41, the transfer function becomes

$$H(s) = b \cdot \frac{s^2 + s(\frac{R_1R_4(C_1+C_2+C_3) - R_2R_3C_2}{R_1R_2R_4C_2(C_1+C_3)}) + \frac{1}{R_1R_2C_1C_2 + R_1R_2C_2C_3}}{s^2 + s(\frac{C_1+C_2+C_3}{C_1C_2R_2}) + \frac{1}{R_1R_2C_1C_2}} \tag{10.62}$$

where

$$b = \frac{1 + \frac{C_3}{C_1}}{1 + \frac{R_3}{R_4}}$$

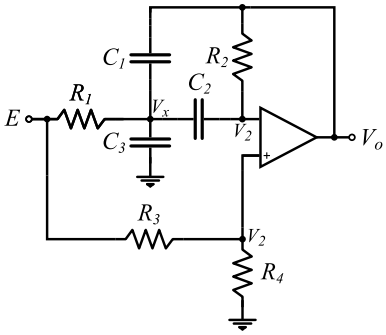

Fig. 10.41 The modified MF bandstop circuit

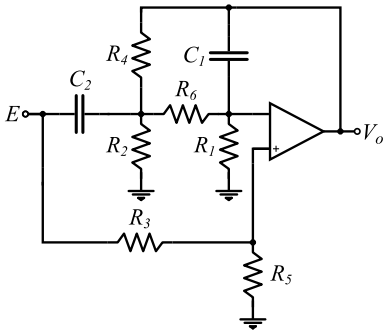

Fig. 10.42 The Boctor notch-LP circuit

For $R_1R_4(C_1 + C_2 + C_3) = R_2R_3C_2$, i.e. when

$$\frac{R_1R_4}{R_2R_3} = \frac{C_2}{C_1 + C_2 + C_3} \tag{10.63}$$

the transfer function becomes bandstop and can realize HP-notch transfer function since $\omega_{oz} < \omega_{op}$:

$$\omega_{oz} = \frac{1}{\sqrt{R_1R_2C_1C_2 + R_1R_2C_2C_3}} \qquad \omega_{op} = \frac{1}{\sqrt{R_1R_2C_1C_2}} \tag{10.64}$$

Notice that R_3 and R_4 are not involved in the expressions for the frequencies of the pole and zero, nor in the expression for Q of the denominator.

10.6.5 The Boctor Circuits

The voltage transfer function of the circuit shown in Fig. 10.42 [3] is given by

$$H(s) = k\frac{s^2 + s(\frac{1}{C_2R_6} + \frac{1}{C_2R_{24}} + \frac{1}{C_1R_1} - \frac{R_3}{C_1R_6R_5}) + \frac{R_1+R_{24}+R_6}{C_1C_2R_1R_{24}R_6}}{s^2 + s(\frac{1}{C_2R_6} + \frac{1}{C_2R_{24}}) + \frac{1}{C_1C_2R_4R_6}} \tag{10.65}$$

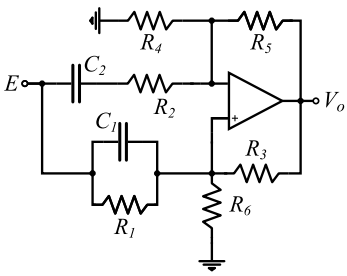

Fig. 10.43 The Boctor notch-HP circuit

where

$$k = \frac{R_5}{R_3 + R_5} < 1 \qquad R_{24} = \frac{R_2 R_4}{R_2 + R_4} \tag{10.66}$$

When the element values are chosen so that the coefficient of s in the numerator becomes zero, i.e.

$$\frac{1}{C_2 R_6} + \frac{1}{C_2 R_{24}} + \frac{1}{C_1 R_1} = \frac{R_3}{C_1 R_6 R_5}$$

the transfer function becomes

$$H(s) = k \frac{s^2 + \frac{R_1 + R_{24} + R_6}{C_1 C_2 R_1 R_{24} R_6}}{s^2 + s(\frac{1}{C_2 R_6} + \frac{1}{C_2 R_{24}}) + \frac{1}{C_1 C_2 R_4 R_6}} \tag{10.67}$$

This is an LP-notch transfer function since

$$\frac{R_1 + R_{24} + R_6}{R_1 R_{24}} > \frac{1}{R_4}$$

The design of the circuit, i.e. the calculation of 6 resistors and two capacitors from given ω_o and Q is very complicated and for this reason special algorithms are required like the one developed by J.M. Cioffi [16].

A circuit that realizes notch-HP transfer function was proposed in [3] and is shown in Fig. 10.43. It can be shown that in this circuit, $Q < \frac{1}{1-(\omega_z/\omega_o)^2}$. This additional constraint makes the design of the circuit more involved and renders the circuit unattractive given that it does not offer any particular advantage over other notch-HP circuits to be presented in the following sections.

10.7 Current Generalized Immittance Converter (CGIC) Circuits

The Antoniou CGIC circuit is shown in Fig. 10.44. The function of interest in this circuit is the driving-point input impedance which can be easily calculated:

$$Z_{IN}(s) = \frac{Z_1(s) Z_3(s) Z_5(s)}{Z_2(s) Z_4(s)} \tag{10.68}$$

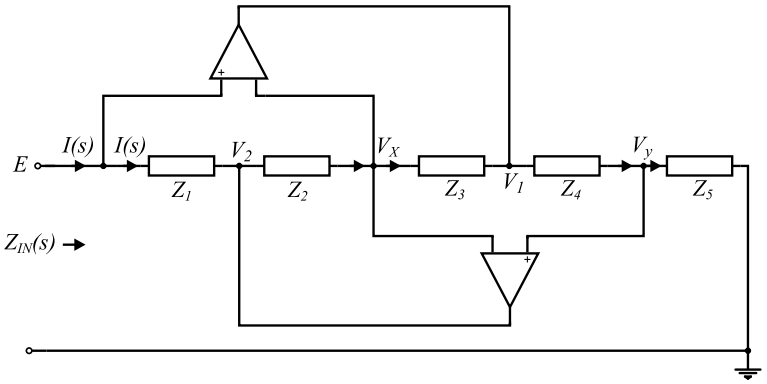

Fig. 10.44 Antoniou's CGIC

It is obvious that if $Z_2(s) = 1/sC_2$ (capacitor) and all other circuit elements are resistors, then (10.68) yields:

$$Z_{IN}(s) = s\frac{R_1 R_3 R_5}{R_4} C_2 \tag{10.69}$$

which implies that the input impedance of the circuit is equal to the impedance of an inductor with $L = \frac{R_1 R_3 R_5}{R_4} C_2$. This is the Antoniou's simulated inductor and we will return to this circuit in a later chapter.

The Antoniou's CGIC circuit is employed in various ways in circuits that realize inter alia biquadratic voltage transfer functions.

10.7.1 The Basic CGIC Biquad

Figure 10.45a shows an RC circuit ($R_o - C_1$) with a simulated Antoniou's inductor placed in parallel to C_1. Figure 10.45 shows the passive equivalent circuit with a buffer at the output. For the analysis of the circuit, the nodal equations are written with reference to Fig. 10.46:

$$\frac{E - V_1}{R_o} = \frac{V_1 - V_2}{R_1} + sV_1C_1$$

$$(V_2 - V_1)sC_2 = \frac{V_1 - V_o}{R_3}$$

$$\frac{V_o - V_1}{R_4} = \frac{V_1}{R_5}$$

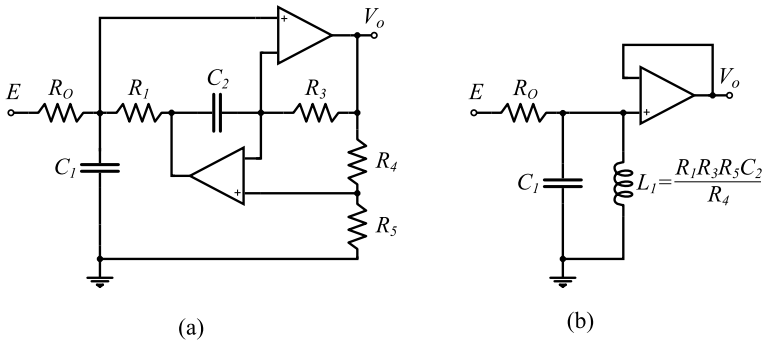

Fig. 10.45 (**a**) The CGIC biquad. (**b**) Equivalent circuit

Fig. 10.46 The CGIC biquad

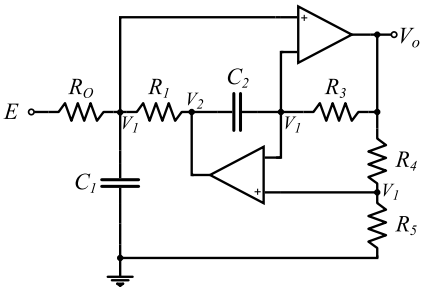

Solving the above system of equations for V_o, the voltage transfer function is obtained:

$$H(s) = \frac{V_o(s)}{E(s)} = \frac{s(R_4 + R_5)/(R_o R_5 C_1)}{s^2 + s\frac{1}{R_o C_1} + \frac{R_4}{R_1 R_3 R_5 C_1 C_2}} \tag{10.70}$$

Therefore, the circuit realizes a second order bandpass function with

$$\omega_o = \sqrt{\frac{R_4}{R_1 R_3 R_5 C_1 C_2}} \qquad Q = R_o \sqrt{\frac{C_1}{C_2}\frac{R_4}{R_1 R_3 R_5}} \tag{10.71}$$

With some minor modifications, as shown in Fig. 10.47, the circuit can realize band-reject functions. To calculate the transfer function, we write the nodal equations with reference to Fig. 10.47:

$$\frac{(E - V_1)\lambda}{QR} = \frac{V_1 - V_2}{R} + sV_1(1-k)C + \frac{(1-\lambda)V_1}{QR} + (V_1 - E)skC$$

$$(V_2 - V_1)sC = \frac{V_1 - V_o}{R}$$

$$\frac{V_o - V_1}{R} = \frac{(1-\mu)V_1}{R} + (V_1 - E)\frac{\mu}{R}$$

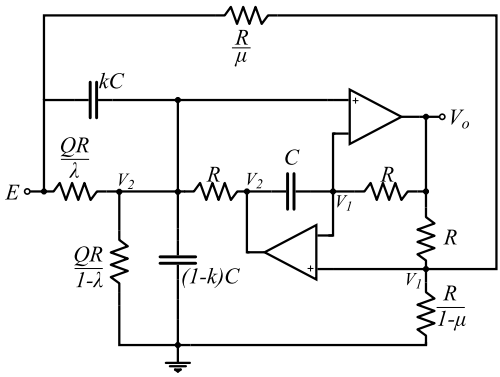

Fig. 10.47 Modified CGIC biquad

Solving for the system for V_o, the transfer function is obtained:

$$H(s) = \frac{(2k-\mu)(s^2 + \frac{2\lambda-\mu}{(2k-\mu)QRC}s + \frac{1}{(\frac{2k}{\mu}-1)C^2R^2})}{s^2 + s\frac{1}{QRC} + \frac{1}{R^2C^2}} \tag{10.72}$$

By selecting $\mu = 2\lambda$, the coefficient of s in the numerator becomes zero and the transfer function takes the form of the second order band-reject function:

$$H(s) = \frac{(2k-\mu)(s^2 + \frac{1}{(\frac{2k}{\mu}-1)C^2R^2})}{s^2 + s\frac{1}{QRC} + \frac{1}{R^2C^2}} \tag{10.73}$$

with pole quality factor Q and pole frequency $\omega_p = \frac{1}{RC}$.

The $j\omega$-axis zeros $\pm j\omega_z$ have

$$\omega_z = \frac{1}{RC\sqrt{\frac{2k}{\mu}-1}} = \frac{\omega_p}{\sqrt{\frac{2k}{\mu}-1}} \tag{10.74}$$

and therefore ω_z can take values lower, higher or equal to ω_p depending on the ratio $\frac{2k}{\mu}$ and provided that $2k > \mu$.

10.7.2 The Generalized (or 2-OA) CGIC Biquad

The Antoniou CGIC of Fig. 10.44 (repeated in Fig. 10.48a) can be redrawn as in Fig. 10.48b. When used as in Fig. 10.49, the circuit is referred to as the 2-OA CGIC biquad [4].

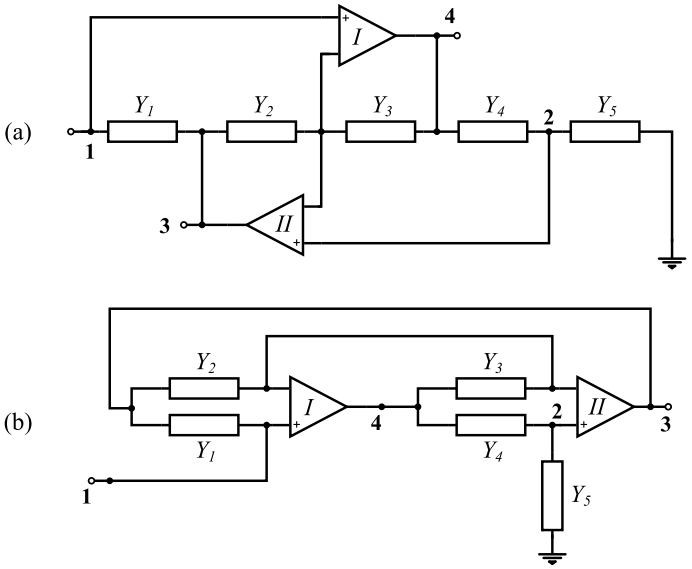

Fig. 10.48 Antoniou's CGIC: The two circuits are identical

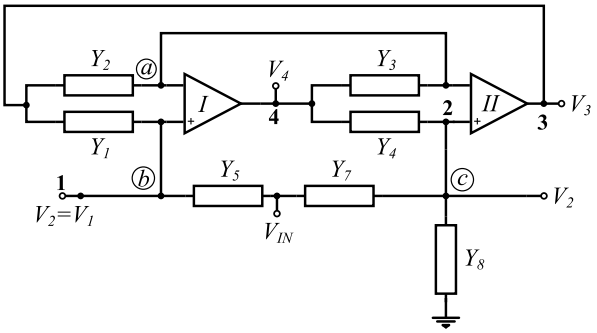

Fig. 10.49 The generalized or 2-OA CGIC biquad

Assuming ideal operational amplifiers, voltages V_1 and V_2 become equal, and therefore Kirchhof's current laws can be written for nodes a, b and c of Fig. 10.49 as follows:

$$\begin{aligned} &\text{Node a:} \quad (V_3 - V_2)Y_2 = (V_2 - V_4)Y_3 \\ &\text{Node b:} \quad (V_3 - V_2)Y_1 = V_2 Y_6 + (V_2 - V_{IN})Y_5 \\ &\text{Node c:} \quad (V_4 - V_2)Y_4 = V_2 Y_8 + (V_2 - V_{IN})Y_7 \end{aligned} \tag{10.75}$$

All voltages V_2, V_3 and V_4 can be used as outputs, and the corresponding transfer functions can be calculated from the above system of equations:

$$H_2(s) = \frac{V_2}{V_{IN}} = \frac{Y_5 + h(s)Y_7}{Y_5 + Y_6 + h(s)(Y_7 + Y_8)} \tag{10.76}$$

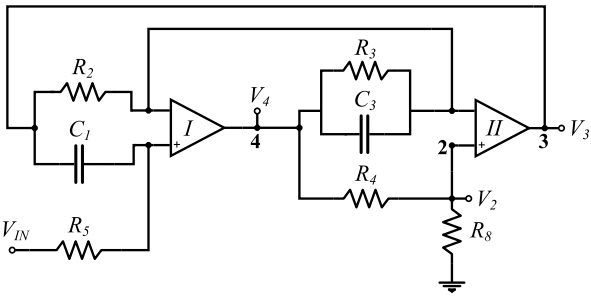

Fig. 10.50 Generalized CGIC lowpass biquad

$$H_3(s) = \frac{V_3}{V_{IN}} = \frac{Y_5 + h(s)[Y_7(1 + \frac{Y_6}{Y_1}) - \frac{Y_5 Y_8}{Y_1}]}{Y_5 + Y_6 + h(s)(Y_7 + Y_8)} \tag{10.77}$$

$$H_4(s) = \frac{V_4}{V_{IN}} = \frac{Y_5(1 + \frac{Y_8}{Y_4}) - \frac{Y_6 Y_7}{Y_4} + h(s)Y_7}{Y_5 + Y_6 + h(s)(Y_7 + Y_8)} \tag{10.78}$$

where the *conversion function* $h(s)$ is defined as

$$h(s) = \frac{Y_1 Y_3}{Y_2 Y_4} \tag{10.79}$$

As we will see in the next pages, with appropriate selection of conductances $Y_i(s)$ all second order functions can be obtained which share the following two properties [4]:

1. Due to the absence of negative signs in the denominator polynomials of the transfer functions, no low frequency unstable modes arise. Start-up instabilities therefore will not arise.
2. For the first order sensitivities of all critical quantities (pole Qs, poles and zeros frequencies), we have $0 \leq S_H^x \leq 1$.

10.7.2.1 Lowpass Biquad Based on the Generalized CGIC

One of the design choices that make $H_4(s)$ of (10.78) a lowpass function is $Y_1(s) = sC_1$, $Y_2(s) = \frac{1}{R_2}$, $Y_3(s) = \frac{1}{R_3} + sC_3$, $Y_4(s) = \frac{1}{R_4}$, $Y_5(s) = \frac{1}{R_5}$, $Y_6(s) = Y_7(s) = 0$ and $Y_8(s) = \frac{1}{R_8}$. In this case, shown in Fig. 10.50, (10.78) gives

$$H_4(s) = \frac{V_4(s)}{V_{IN}(s)} = \frac{\frac{R_4 + R_8}{R_2 R_4 R_5 C_1 C_3}}{s^2 + s\frac{1}{R_3 C_3} + \frac{R_8}{R_2 R_4 R_5 C_1 C_3}} \tag{10.80}$$

with

$$\omega_{op} = \sqrt{\frac{R_8}{R_2 R_4 R_5 C_1 C_3}} \qquad Q_p = R_3\sqrt{\frac{R_8 C_3}{R_2 R_4 R_5 C_1}} \tag{10.81}$$

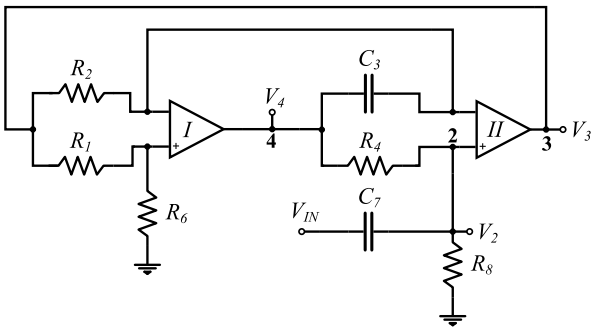

Fig. 10.51 Generalized CGIC highpass biquad

Since R_3 is not involved in the expression for ω_{op}, it can be used for frequency independent Q adjustment. By setting $R_1 = R_4 = R_5 = R_8 = R$ and $C_1 = C_3 = C$, (10.81) gives

$$R_3 = RQ_p \quad \text{and} \quad C = \frac{1}{\omega_{op} R} \tag{10.82}$$

and the transfer function (10.78) becomes

$$H_4(s) = \frac{V_4}{V_{IN}} = \frac{2\omega_p^2}{s^2 + s\frac{\omega_p}{Q_p} + \omega_p^2} \tag{10.83}$$

It should be noted that $H_2(s) = \frac{V_2(s)}{E(s)}$ is also lowpass but requires an additional operational amplifier (buffer) to isolate any load connected to the non-inverting input of opamp II.

10.7.2.2 Highpass Biquad Based on the Generalized CGIC

One of the design choices that make $H_3(s)$ of (10.78) a highpass function is $Y_1(s) = \frac{1}{R_1}$, $Y_2(s) = \frac{1}{R_2}$, $Y_3(s) = sC_3$, $Y_4(s) = \frac{1}{R_4}$, $Y_5(s) = 0$, $Y_6(s) = \frac{1}{R_6}$, $Y_7(s) = sC_7$ and $Y_8(s) = \frac{1}{R_8}$. This is shown in Fig. 10.51.

In this case, (10.78) gives

$$H_3(s) = \frac{V_3(s)}{V_{IN}(s)} = \frac{s^2(1 + \frac{R_1}{R_6})}{s^2 + s\frac{1}{R_8 C_7} + \frac{R_1}{R_2 R_4 R_6 C_3 C_7}} \tag{10.84}$$

with

$$\omega_{op} = \sqrt{\frac{R_1}{R_2 R_4 R_6 C_3 C_7}} \qquad Q_p = R_8\sqrt{\frac{R_1 C_7}{R_2 R_4 R_6 C_3}} \tag{10.85}$$

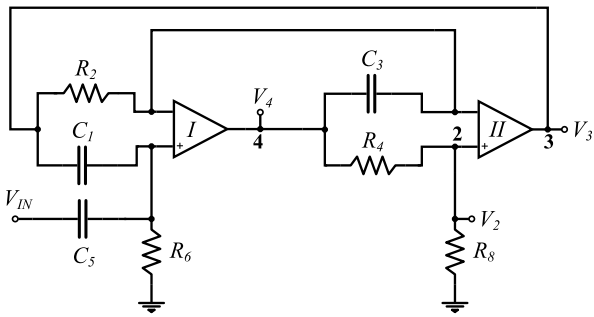

Fig. 10.52 Generalized CGIC bandpass biquad

Since R_8 is not involved in the expression for ω_{op} it can be used for frequency independent Q adjustment. By setting $R_1 = R_2 = R_4 = R_6 = R$ and $C_3 = C_7 = C$ we find

$$R_8 = RQ_p \quad \text{and} \quad C = \frac{1}{\omega_{op} R} \tag{10.86}$$

and (10.85) yields

$$H_3(s) = \frac{V_3}{V_{IN}} = \frac{2s^2}{s^2 + s\frac{\omega_{op}}{Q_p} + \omega_{op}^2} \tag{10.87}$$

As in the lowpass case, it should be noted that $H_2(s) = \frac{V_2(s)}{E(s)}$ is also a highpass transfer function but requires an additional operational amplifier (buffer) in order to isolate any load connected to the non-inverting input of opamp II.

10.7.2.3 Bandpass Biquad Based on the Generalized CGIC

The transfer function $H_4(s)$ of (10.78) can be made a bandpass function by setting $Y_1(s) = sC_1$, $Y_2(s) = \frac{1}{R_2}$, $Y_3(s) = sC_3$, $Y_4(s) = \frac{1}{R_4}$, $Y_5(s) = sC_5$, $Y_6(s) = \frac{1}{R_6}$, $Y_7(s) = 0$ and $Y_8(s) = \frac{1}{R_8}$. The corresponding circuit is shown in Fig. 10.52.

In this case, (10.78) gives

$$H_4(s) = \frac{sC_5(R_4 + R_8)/(C_1C_3R_2R_4)}{s^2 + s\frac{C_5R_8}{C_1C_3R_2R_4} + \frac{R_8}{C_1C_3R_2R_4R_6}} \tag{10.88}$$

with

$$\omega_p = \sqrt{\frac{R_8}{C_1C_3R_2R_4R_6}} \qquad Q_p = \frac{1}{C_5}\sqrt{\frac{C_1C_3R_2R_4}{R_6R_8}} \tag{10.89}$$

Frequency independent Q adjustment can be done by C_5, which is not involved in the expression for ω_p. Moreover, by setting $R_1 = R_2 = R_4 = R_6 = R_8 = R$ and $C_1 = C_3 = C$ we find

$$\omega_p = \frac{1}{RC} \qquad Q_p = \frac{C}{C_5} \quad \Rightarrow \quad C_5 = \frac{C}{Q_p} \quad \text{where } R = \frac{1}{\omega_p C} \tag{10.90}$$

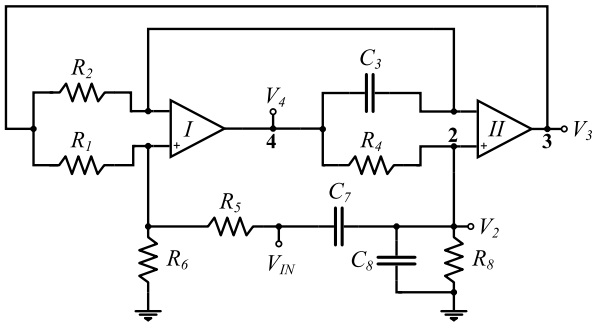

Fig. 10.53 Generalized CGIC band-reject biquad

and the bandpass transfer function becomes

$$H_4(s) = \frac{s\frac{2\omega_p}{Q_p}}{s^2 + s\frac{\omega_p}{Q_p} + \omega_p^2} \tag{10.91}$$

The output V_2 is also bandbass but requires an extra operational amplifier (buffer) in order to avoid loading.

10.7.2.4 Band-Reject Biquads Based on the Generalized CGIC

One design selection for transfer function $H_4(s)$ of (10.78) to become band-reject function is $Y_1(s) = \frac{1}{R_1}$, $Y_2(s) = \frac{1}{R_2}$, $Y_3(s) = sC_3$, $Y_4(s) = \frac{1}{R_4}$, $Y_5(s) = \frac{1}{R_5}$, $Y_6(s) = \frac{1}{R_6}$, $Y_7(s) = sC_7$ and $Y_8(s) = \frac{1}{R_8} + sC_8$. The corresponding circuit is shown in Fig. 10.53.

In this case, (10.78) gives

$$H_4(s) = \frac{s^2\frac{C_1C_3}{R_1} + s(\frac{C_8}{R_1R_5} - \frac{C_7}{R_2R_6}) + \frac{1}{R_2R_4R_5} + \frac{1}{R_2R_5R_8}}{(\frac{C_3C_8}{R_1} + \frac{C_3C_7}{R_1})s^2 + s\frac{C_3}{R_1R_8} + \frac{1}{R_2R_4R_5} + \frac{1}{R_2R_5R_6}} \tag{10.92}$$

For

$$\frac{C_8}{C_7} = \frac{R_1R_5}{R_2R_6} \tag{10.93}$$

the coefficient of s in the numerator becomes zero and the transfer function becomes band-reject:

$$H_4(s) = \frac{s^2\frac{C_1C_3}{R_1} + \frac{1}{R_2R_4R_5} + \frac{1}{R_2R_5R_8}}{(\frac{C_3C_8}{R_1} + \frac{C_3C_7}{R_1})s^2 + s\frac{C_3}{R_1R_8} + \frac{1}{R_2R_4R_5} + \frac{1}{R_2R_5R_6}}$$

or, after some rearrangement:

$$H_4(s) = \frac{\frac{C_7}{C_7+C_8}(s^2 + \frac{R_1(R_4+R_8)}{R_2R_4R_5R_8C_3C_7})}{s^2 + \frac{1}{R_8(C_7+C_8)}s + \frac{R_1(R_5+R_6)}{R_2R_4R_5R_6C_3(C_7+C_8)}} \tag{10.94}$$

The frequency of the zero is

$$\omega_z = \sqrt{\frac{R_1(R_4+R_8)}{R_2R_4R_5R_8C_3C_7}} \tag{10.95}$$

The pole frequency and Q are given by

$$\begin{aligned} \omega_p &= \sqrt{\frac{R_1(R_5+R_6)}{R_2R_4R_5R_6C_3(C_7+C_8)}} \\ Q_p &= R_8\sqrt{\frac{R_1(R_5+R_6)(C_7+C_8)}{R_2R_4R_5R_6C_3}} \end{aligned} \tag{10.96}$$

It can be easily found that

$$\frac{\omega_z}{\omega_p} = \sqrt{1+\frac{R_4}{R_8}} \tag{10.97}$$

i.e. the frequency of the zero is always higher than that of the pole and therefore this circuit can realize only lowpass-notch at output V_4.

However, for the same circuit $H_2(s)$ is:

$$H_2(s) = \frac{\frac{C_7}{C_7+C_8}(s^2+\frac{R_1}{R_2R_4R_5C_3C_7})}{s^2+\frac{1}{R_8(C_7+C_8)}s+\frac{R_1(R_5+R_6)}{R_2R_4R_5R_6C_3(C_7+C_8)}} \tag{10.98}$$

with

$$\omega_z = \sqrt{\frac{R_1}{R_2R_4R_5C_3C_7}} \tag{10.99}$$

and

$$\begin{aligned} \omega_p &= \sqrt{\frac{R_1(R_5+R_6)}{R_2R_4R_5R_6C_3(C_7+C_8)}} \\ Q_p &= R_8\sqrt{\frac{R_1(R_5+R_6)(C_7+C_8)}{R_2R_4R_5R_6C_3}} \end{aligned} \tag{10.100}$$

Resistor R_8 can be used for frequency independent Q adjustment.

Taking into account (10.93), the ratio ω_z/ω_p

$$\frac{\omega_z}{\omega_p} = \sqrt{\frac{1+\frac{C_8}{C_7}}{1+\frac{R_5}{R_6}}} = \sqrt{\frac{1+\frac{R_1R_5}{R_2R_6}}{1+\frac{R_5}{R_6}}}$$

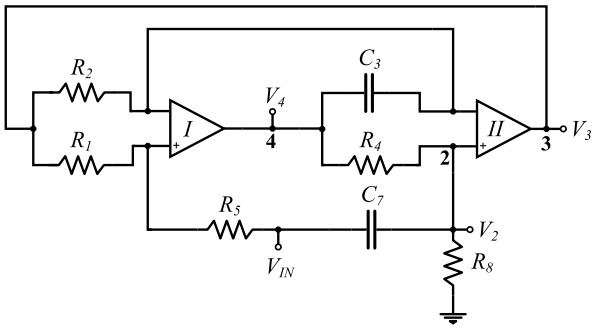

Fig. 10.54 Generalized CGIC band-reject biquad

can assume values greater or lower than unity and the particular circuit can realize, at output V_2, notch, lowpass-notch or highpass-notch functions by proper choice of the ratios $\frac{C_8}{C_7}$ and $\frac{R_5}{R_6}$. It should be remembered that in order to use output V_2, an extra operational amplifier is required as a buffer.

The circuit of Fig. 10.54 has been obtained from the generalized CGIC biquad by setting $Y_1(s) = \frac{1}{R_1}$, $Y_2(s) = \frac{1}{R_2}$, $Y_3(s) = sC_3$, $Y_4(s) = \frac{1}{R_4}$, $Y_5(s) = \frac{1}{R_5}$, $Y_6(s) = 0$, $Y_7(s) = sC_7$ and $Y_8(s) = \frac{1}{R_8}$

The transfer function $H_4(s)$ is found to be

$$H_4(s) = \frac{V_4}{V_{IN}} = \frac{s^2 + \frac{R_1(R_4+R_8)}{R_2R_4R_5R_8C_3C_7}}{s^2 + \frac{1}{R_8C_7} + \frac{R_1}{R_2R_4R_5C_3C_7}} \tag{10.101}$$

with

$$\omega_z = \sqrt{\frac{R_1(R_4+R_8)}{R_2R_4R_5R_8C_3C_7}} \qquad \omega_p = \sqrt{\frac{R_1}{R_2R_4R_5C_3C_7}}$$
$$Q_p = R_8\sqrt{\frac{C_7R_1}{C_3R_2R_4R_5}} \tag{10.102}$$

It can be found that

$$\frac{\omega_z}{\omega_p} = \sqrt{1 + \frac{R_4}{R_8}} > 1 \tag{10.103}$$

and therefore the circuit can realize only lowpass-notch functions.

$H_2(s)$ in this circuit is a notch transfer function:

$$H_2(s) = \frac{V_2}{V_{IN}} = \frac{s^2 + \frac{R_1}{R_2R_4R_5C_3C_7}}{s^2 + \frac{1}{R_8C_7} + \frac{R_1}{R_2R_4R_5C_3C_7}} \tag{10.104}$$

with

$$\omega_z = \sqrt{\frac{R_1}{R_2 R_4 R_5 C_3 C_7}} \qquad \omega_p = \sqrt{\frac{R_1}{R_2 R_4 R_5 C_3 C_7}}$$
$$Q_p = R_8 \sqrt{\frac{C_7 R_1}{C_3 R_2 R_4 R_5}} \tag{10.105}$$

Of particular interest is also the transfer function $H_3(s)$:

$$H_3(s) = \frac{V_3}{V_{IN}} = \frac{s^2 - \frac{R_1}{R_5 R_8 C_7} s + \frac{R_1}{R_2 R_4 R_5 C_3 C_7}}{s^2 + \frac{1}{R_8 C_7} + \frac{R_1}{R_2 R_4 R_5 C_3 C_7}} \tag{10.106}$$

which for $R_1 = R_5$ is a typical all-pass function with

$$\omega_z = \omega_p = \sqrt{\frac{1}{R_2 R_4 C_3 C_7}} \qquad Q_p = R_8 \sqrt{\frac{C_7}{C_3 R_2 R_4}} \tag{10.107}$$

10.8 Biquads with 3 Operational Amplifiers

The most popular biquads with 3 operational amplifiers, referred to as *3-OA biquads*, are presented in this section. Although the number of operational amplifiers employed in these circuits seems high, their features, especially the low sensitivity, very often make them attractive, particularly in demanding applications.

10.8.1 The Tow-Thomas Biquad

The circuit shown in Fig. 10.55 [14, 15] offers two buffered outputs, V_1 and V_3. Output V_2 is a scaled and opposite copy of V_3: $V_2 = -\frac{R_5}{R_6} V_3$. The output of the first operational amplifier, V_1, is the bandpass output, and V_3 is the lowpass output:

$$H_{BP}(s) = \frac{V_1(s)}{E(s)} = -\frac{\frac{s}{R_4 C_1}}{s^2 + s\frac{1}{R_1 C_1} + \frac{R_6/R_5}{R_2 R_3 C_1 C_2}} \tag{10.108}$$

$$H_{LP}(s) = \frac{V_3(s)}{E(s)} = -\frac{\frac{R_6/R_5}{R_2 R_4 C_1 C_2}}{s^2 + s\frac{1}{R_1 C_1} + \frac{R_6/R_5}{R_2 R_3 C_1 C_2}} \tag{10.109}$$

Both transfer functions share the same denominator and therefore have the same poles frequency and Q:

$$\omega_o = \sqrt{\frac{R_6/R_5}{R_2 R_3 C_1 C_2}} \qquad Q = \frac{R_1}{\sqrt{R_2 R_3}} \sqrt{\frac{R_6 C_1}{R_5 C_2}} \tag{10.110}$$

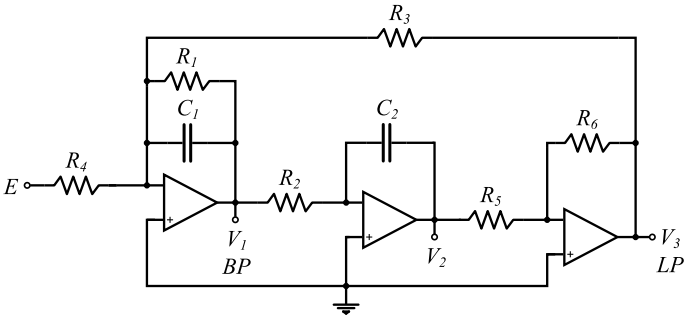

Fig. 10.55 Tow-Thomas 3-OA biquad

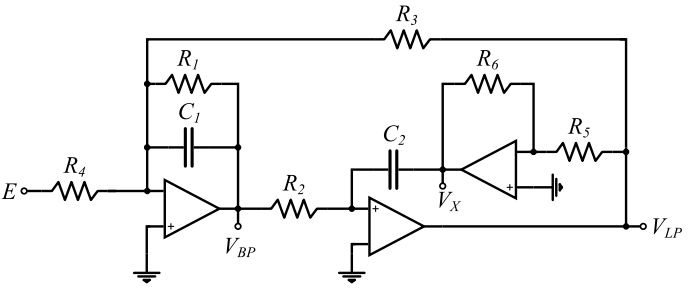

Fig. 10.56 Akerberg-Mossberg 3-OA biquad

The high operational amplifier overhead is compensated by the low Q sensitivity to changes of the passive elements and as a result high-Q biquads can be designed. The obvious way to adjust Q without affecting the poles frequency is by adjusting resistor R_1.

10.8.1.1 Akerberg-Mossberg 3-OA Biquad

A variation of the Tow-Thomas biquad is attributed to Akerberg-Mossberg, who placed the inverting voltage amplifier within the feedback path of the Miller integrator realized by the second operational amplifier. This non-inverting integrator with the inverting amplifier in the feedback path is presented in Chap. 9. The Akerberg-Mossberg biquad is shown in Fig. 10.56.

The transfer functions of the circuit are given below:

$$H_{LP}(s) = \frac{-\frac{R_5}{C_1C_2R_2R_4R_6}}{s^2 + s\frac{1}{C_1R_1} + \frac{R_5}{C_1C_2R_2R_3R_6}}$$
$$H_{BP} = \frac{-s\frac{1}{C_1R_4}}{s^2 + s\frac{1}{C_1R_1} + \frac{R_5}{C_1C_2R_2R_3R_6}} \tag{10.111}$$

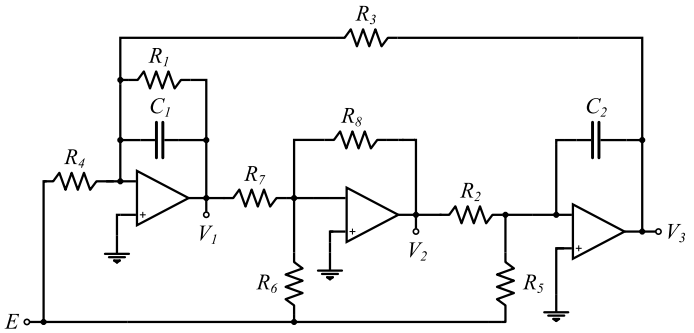

Fig. 10.57 A generalized 3-OA biquad

10.8.1.2 Band-Reject 3-OA Biquad

A more general form of the 3-OA biquad is shown in Fig. 10.57, where the input is also fed to the inverting inputs of the second and third operational amplifier.

The transfer function for output V_2 is:

$$H(s) = \frac{V_2(s)}{E(s)} = -\frac{R_8}{R_6} \frac{s^2 + s(\frac{1}{R_1 C_1} - \frac{R_6}{C_1 R_4 R_7}) + \frac{R_6}{C_1 C_2 R_3 R_5 R_7}}{s^2 + s\frac{1}{C_1 R_1} + \frac{R_8}{C_1 C_2 R_2 R_3 R_7}} \tag{10.112}$$

By proper selection of resistors R_1, R_4, R_6 and R_7 so as to satisfy $R_4 = R_1 R_6 / R_7$ the transfer function becomes

$$H(s) = \frac{V_2(s)}{E(s)} = -\frac{R_8}{R_6} \frac{s^2 + \frac{R_6/R_5}{C_1 C_2 R_3 R_7}}{s^2 + s\frac{1}{C_1 R_1} + \frac{R_8/R_2}{C_1 C_2 R_3 R_7}} \tag{10.113}$$

The circuit can realize all types of notch functions depending on the ratio $\frac{R_6 R_2}{R_5 R_8}$. For notch function, we can set $\frac{R_8}{R_2} = \frac{R_6}{R_5}$. Selecting for example $R_6 = R_8 = R_7$ and $R_2 = R_5$, the transfer function becomes

$$H(s) = \frac{V_2(s)}{E(s)} = -\frac{s^2 + \frac{1}{C_1 C_2 R_2 R_3}}{s^2 + s\frac{1}{C_1 R_1} + \frac{1}{C_1 C_2 R_2 R_3}} \tag{10.114}$$

Since the transfer function does not involve any of R_8, R_7, R_6, R_5 and R_2, they can all be equal with any convenient value. For this notch case, we have

$$\omega_o = \frac{1}{\sqrt{C_1 C_2 R_2 R_3}} \qquad Q = \frac{R_1}{\sqrt{R_2 R_3}} \sqrt{\frac{C_1}{C_2}} \tag{10.115}$$

and the bandwidth, i.e. the frequency band for which output power is lower than half the input power, is found to be $BW = \frac{\omega_o}{Q}$.

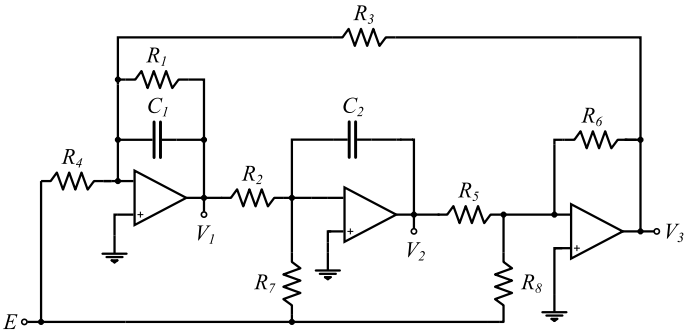

Fig. 10.58 Generalized Tow-Thomas 3-OA biquad

Figure 10.58 shows a generalized Tow-Thomas circuit, the transfer function of which is

$$\frac{V_3(s)}{E(s)} = -\left(\frac{R_6}{R_8}\right)\frac{s^2 + s(\frac{1}{R_1C_1} - \frac{R_8}{C_2R_5R_7}) + \frac{R_8}{C_1C_2R_5}(\frac{1}{R_2R_4} - \frac{1}{R_1R_5})}{s^2 + s\frac{1}{C_1R_1} + \frac{R_6}{C_1C_2R_2R_3R_5}} \tag{10.116}$$

Due to the negative signs within the coefficient of s and the constant term of the numerator, the circuit can be made to have highpass and band-reject behavior. If for example we set $R_1 = R_2 = R_4 = R_5 = R_6 = R_7 = R_8 = R$ and $C_1 = C_2 = C$, (10.116) gives

$$H(s) = \frac{V_3(s)}{E(s)} = -\frac{s^2}{s^2 + s\frac{1}{RC} + \frac{1}{RR_3C^2}} \tag{10.117}$$

with the evident definitions

$$\omega_o = \frac{1}{C\sqrt{RR_3}} \qquad Q = \sqrt{\frac{R}{R_3}}$$

If in (10.116) we set $\frac{1}{R_1C_1} = \frac{R_8}{C_2R_5R_7}$, the transfer function becomes

$$\frac{V_3(s)}{E(s)} = -\left(\frac{R_6}{R_8}\right)\frac{s^2 + \frac{R_8}{C_1C_2R_5}(\frac{1}{R_2R_4} - \frac{1}{R_1R_5})}{s^2 + s\frac{1}{C_1R_1} + \frac{R_6}{C_1C_2R_2R_3R_5}} \tag{10.118}$$

which can realize all types of notch functions.

10.8.2 The State Variable or KHN Circuit

The 3-OA circuit shown in Fig. 10.59 is referred to as the *state variable filter*. It is also known as KHN filter after the initials of its inventors [9]. The main characteristic of the circuit is that it employs two inverting Miller integrators and provides three useful outputs: a lowpass, a highpass and a bandpass.

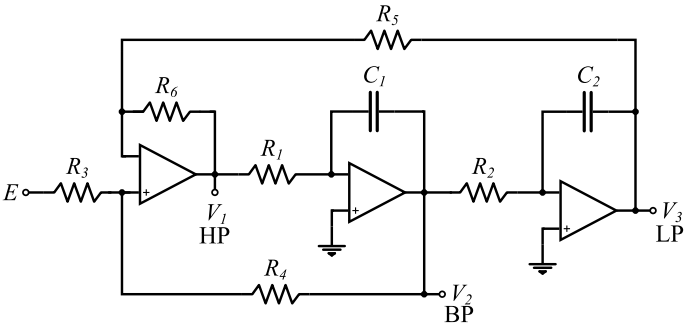

Fig. 10.59 The state variable filter

The corresponding transfer functions are given below:

$$H_{HP}(s) = \frac{V_1(s)}{E(s)} = -\frac{\frac{1+R_6/R_5}{R_1C_1(1+R_3/R_4)}s^2}{s^2 + s(\frac{1+R_6/R_5}{R_1C_1(1+R_4/R_3)}) + \frac{R_6/R_5}{R_1R_2C_1C_2}} \tag{10.119}$$

$$H_{BP}(s) = \frac{V_2(s)}{E(s)} = -\frac{1 + R_6/R_5/R_1C_1(1 + R_3/R_4)s}{s^2 + s(\frac{1+R_6/R_5}{R_1C_1(1+R_4/R_3)}) + \frac{R_6/R_5}{R_1R_2C_1C_2}} \tag{10.120}$$

$$H_{LP}(s) = \frac{V_3(s)}{E(s)} = -\frac{\frac{1+R_6/R_5}{R_1R_2C_1C_2(1+R_3/R_4)}}{s^2 + s(\frac{1+R_6/R_5}{R_1C_1(1+R_4/R_3)}) + \frac{R_6/R_5}{R_1R_2C_1C_2}} \tag{10.121}$$

10.8.3 The Universal Circuit

The *universal filter* shown in Fig. 10.60 is a variation of the state variable filter with some modification in the input section.

Although the characterization "universal" is somehow inappropriate, the truth is that the circuit was commercially available in packaged form for many years, ready for use with the addition of some external components to determine the poles frequency and Q-factor. More detailed information on the integrated universal filter can be found in the book by L.P. Huelsman [8] as well as in National Semiconductors' and Burr-Brown's literature.

Operation of the circuit with input 2 grounded ($E_2 = 0$) is referred to as *noninverting configuration*. When the input signal is applied to input 2, the corresponding circuit is called *inverting configuration*. The two configurations are presented below.

Noninverting Configuration By grounding input 2, as shown in Fig. 10.61, the three transfer functions are found to be:

$$H_{HP}(s) = \frac{V_1(s)}{E_1(s)} = \frac{(1 + K_3 + K_4)K_1s^2}{s^2 + (1 + K_3 + K_4)K_2\omega_1 s + K_3\omega_1\omega_2} \tag{10.122}$$

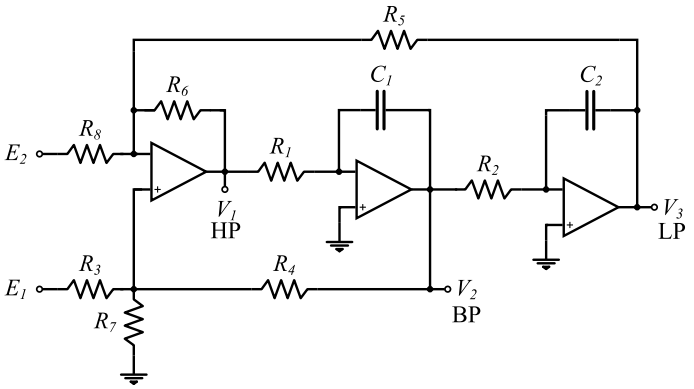

Fig. 10.60 The universal filter

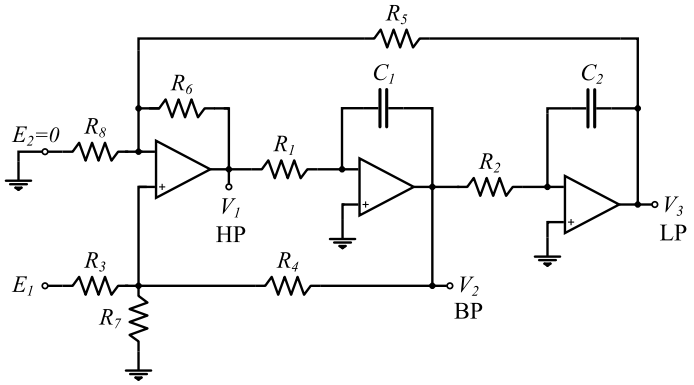

Fig. 10.61 The non-inverting configuration of the universal filter

$$H_{BP}(s) = \frac{V_2(s)}{E_1(s)} = \frac{-(1+K_3)K_1\omega_1 s}{s^2 + (1+K_3+K_4)K_2\omega_1 s + K_3\omega_1\omega_2} \tag{10.123}$$

$$H_{LP}(s) = \frac{V_3(s)}{E_1(s)} = \frac{(1+K_3)K_1\omega_1\omega_2}{s^2 + (1+K_3+K_4)K_2\omega_1 s + K_3\omega_1\omega_2} \tag{10.124}$$

where the following definitions have been used:

$$K_1 = \frac{1}{1+\frac{R_3}{R_4}+\frac{R_3}{R_7}} \qquad K_2 = \frac{1}{1+\frac{R_4}{R_3}+\frac{R_4}{R_7}} \qquad K_3 = \frac{R_6}{R_5} \qquad K_4 = \frac{R_6}{R_8} \tag{10.125}$$

$$\omega_1 = \frac{1}{R_1 C_1} \qquad \omega_2 = \frac{1}{R_2 C_2}$$

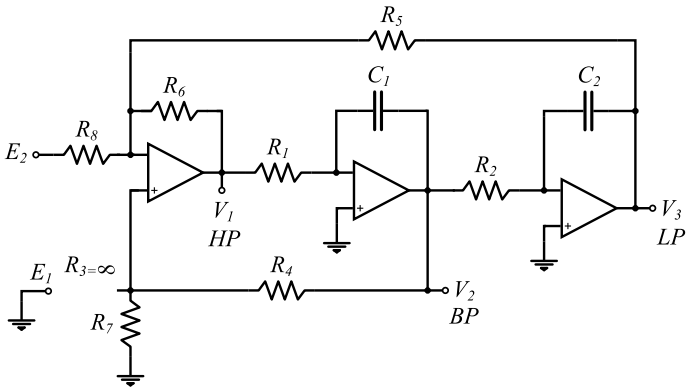

Fig. 10.62 The inverting configuration of the universal filter

All transfer functions share the same denominator and therefore have common poles frequency and Q given below:

$$\omega_o = \sqrt{\omega_1 \omega_2 K_3} = \sqrt{\frac{\frac{R_6}{R_5}}{R_1 R_2 C_1 C_2}}$$

$$Q = \frac{1}{(1+K_3)K_2}\sqrt{\frac{\omega_2 K_3}{\omega_1}} = \frac{1+\frac{R_4}{R_3}+\frac{R_4}{R_7}}{1+\frac{R_6}{R_5}}\sqrt{\frac{R_1 R_6 C_1}{R_2 R_5 C_2}}$$

A typical design is to set $K_3 = 0.1$, $C_1 = C_2 = 1$ nF, $R_4 = R_5 = 100$ kOhm, $R_6 = 10$ kOhm and $R_8 = \infty$. In this case:

$$\omega_o = \frac{316.2 \cdot 10^6}{\sqrt{R_1 R_2}} \qquad Q = 28748\left(\frac{1}{100\ \text{kOhm}} + \frac{1}{R_3} + \frac{1}{R_7}\right)\sqrt{\frac{R_1}{R_2}} \tag{10.126}$$

From these equations, it can be said that R_1 and R_2 determine the poles frequency and R_3 and R_7 determine the Q value.

Inverting Configuration In the inverting configuration, the input signal is applied to input 2 and input 1 is left free. This is equivalent to grounding input 1 and assuming $R_3 = \infty$ as shown in Fig. 10.62. Analysis of the circuit yields:

$$H_{HP}(s) = \frac{V_1(s)}{E(s)} = \frac{-K_4 s^2}{s^2 + (1+K_3+K_4)K_2\omega_1 s + K_3\omega_1\omega_2}$$

$$H_{BP}(s) = \frac{V_2(s)}{E(s)} = \frac{K_4\omega_1 s}{s^2 + (1+K_3+K_4)K_2\omega_1 s + K_3\omega_1\omega_2}$$

$$H_{BP}(s) = \frac{V_3(s)}{E(s)} = \frac{-K_4\omega_1\omega_2}{s^2 + (1+K_3+K_4)K_2\omega_1 s + K_3\omega_1\omega_2}$$

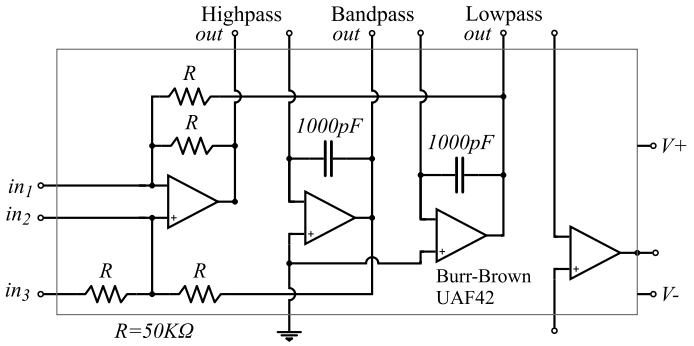

Fig. 10.63 Burr-Brown's UAF42 diagram

where

$$K_1 = \frac{1}{1 + \frac{R_3}{R_4} + \frac{R_3}{R_7}} \qquad K_2 = \frac{1}{1 + \frac{R_4}{R_3} + \frac{R_4}{R_7}} \qquad K_3 = \frac{R_6}{R_5} \qquad K_4 = \frac{R_6}{R_8}$$

$$\omega_1 = \frac{1}{R_1 C_1} \qquad \omega_2 = \frac{1}{R_2 C_2}$$

The common denominator implies common pole frequency and Q given by

$$\omega_o = \sqrt{\omega_1 \omega_2 K_3} = \sqrt{(R_6/R_5)/(R_1 R_2 C_1 C_2)}$$

$$Q = \frac{1}{(1 + K_3 + K_4) K_2} \sqrt{\frac{\omega_2 K_3}{\omega_1}} = \frac{1 + R_4/R_7}{1 + R_6/R_5 + R_6/R_8} \sqrt{\frac{R_1 R_6 C_1}{R_2 R_5 C_2}}$$

For a typical design, we can set $K_3 = 0.1$, $C_1 = C_2 = 1$ nF, $R_4 = R_5 = 100$ kOhm, $R_6 = 10$ kOhm and $R_8 = \infty$, in which case the above design equations become:

$$\omega_o = \frac{316.2 \cdot 10^6}{\sqrt{R_1 R_2}} \qquad Q = 0.3162 \left(\frac{1 + \frac{10^5}{R_7}}{1.1 + \frac{10^4}{R_8}} \right) \sqrt{\frac{R_1}{R_2}}$$

Given ω_o and Q, resistors R_1 and R_2 can be selected from the expression for ω_o, and R_7, R_8 from the expression for Q.

The universal filter is commercially available in IC form by Burr-Brown as UAF41 and UAF42 (Fig. 10.63) and by National Semiconductors as AF-100, AF-150 and AF-151 (Fig. 10.64). In both circuits, the two capacitors and R_1, R_5 and R_6 are within the IC and the rest are external and must be calculated.

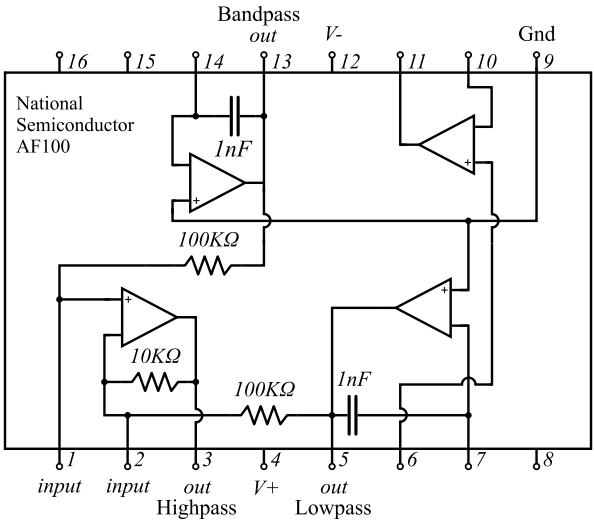

Fig. 10.64 National Semiconductors' AF-100 diagram

10.8.4 The 3-OA CGIC Biquad

The 3-OA CGIC biquad can be obtained from the generalized CGIC biquad of Fig. 10.49 by adding one operational amplifier and feeding the input to all noninverting inputs through voltage dividers, as shown in Fig. 10.65. All inverting inputs are connected to a common node.

For the analysis of the circuit, the KCL is written for the common inverting inputs node with voltage V_x, and for the noninverting input nodes of the three operational amplifiers:

$$\begin{aligned}
(V_3 - V_x)Y_{11} &= (V_x - V_1)Y_8 + (V_x - V_2)Y_{10} \\
(V_3 - V_x)Y_7 + (V_{IN} - V_x)Y_1 &= V_x Y_2 \\
(V_1 - V_x)Y_9 + (V_{IN} - V_x)Y_3 &= V_x Y_4 \\
(V_2 - V_x)Y_{12} + (V_{IN} - V_x)Y_5 &= V_x Y_6
\end{aligned} \tag{10.127}$$

The above system can be solved for the four unknowns V_x, V_1, V_2 and V_3 and the three transfer functions of interest $H_i(s) = \frac{V_i(s)}{V_{IN}(s)}$ $(i = 1 \ldots 3)$ can be calculated.

To make the results shorter, we set all Y_i for $i = 1, 2, \ldots, 10$ to be resistive ($Y_i = R_i^{-1}$ with $R_8 = R_9$), and only Y_{11} and Y_{12} to be capacitive ($Y_{11} = sC_{11}$ and $Y_{12} = sC_{12}$). The circuit is shown in Fig. 10.66. Under this design choice, the three transfer functions will share the same denominator polynomial $D(s)$:

$$D(s) = s^2 + s\frac{Y_7(Y_3 + Y_4)}{C_{11}(Y_1 + Y_2)} + \frac{Y_{10}Y_7(Y_5 + Y_6)}{C_{11}C_{12}(Y_1 + Y_2)} \tag{10.128}$$

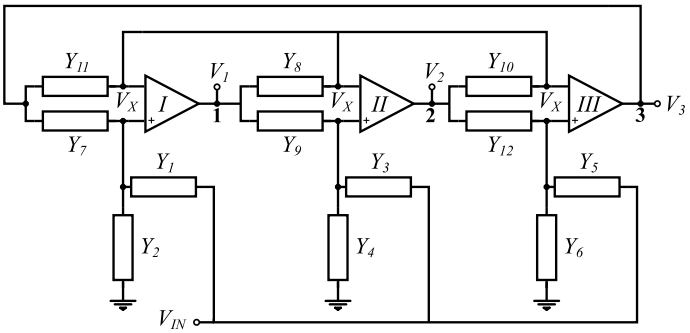

Fig. 10.65 The general 3-OA CGIC biquad

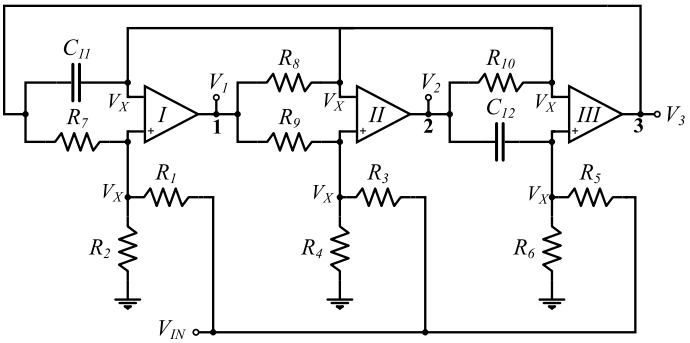

Fig. 10.66 The 3-OA CGIC biquad

Defining

$$Y_A = Y_1 + Y_1\frac{Y_4}{Y_9} - \frac{Y_2Y_3}{Y_9}$$

and

$$\omega_{Z1}^2 = \frac{Y_7Y_{10}(Y_5 + \frac{Y_4Y_5}{Y_9} - \frac{Y_3Y_6}{Y_9})}{C_{11}C_{12}Y_A} \qquad \omega_{Z2}^2 = \frac{Y_7(Y_3Y_6 + Y_5Y_{10} - Y_4Y_5)}{C_{11}C_{12}Y_1}$$

$$\omega_{Z3}^2 = \frac{Y_{10}(Y_5(Y_2 + Y_7) - Y_1Y_6)}{C_{11}C_{12}Y_1}$$

the three transfer functions will be

$$H_1(s) = \frac{V_1(s)}{V_{IN}(s)} = \frac{\frac{Y_A}{Y_1+Y_2}[s^2 + s\frac{Y_3Y_7}{C_{11}Y_A} + \omega_{Z1}^2]}{D(s)}$$

$$H_2(s) = \frac{V_2(s)}{V_{IN}(s)} = \frac{\frac{Y_1}{Y_1+Y_2}[s^2 + s\frac{Y_3Y_7+Y_1Y_6-Y_2Y_5}{C_{11}Y_1} + \omega_{Z2}^2]}{D(s)} \qquad (10.129)$$

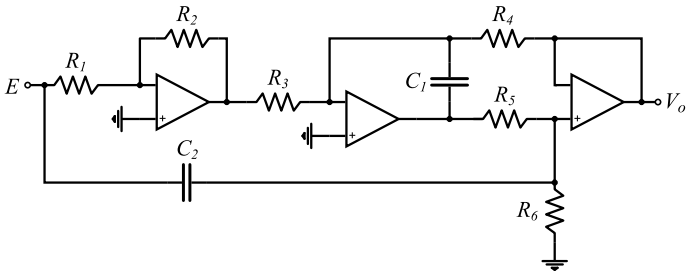

Fig. 10.67 The Bainter biquad

$$H_3(s) = \frac{V_3(s)}{V_{IN}(s)} = \frac{\frac{Y_1}{Y_1+Y_2}[s^2 + s\frac{Y_3Y_7+Y_2Y_3-Y_1Y_4}{C_{11}Y_1} + \omega_{Z3}^2]}{D(s)}$$

It should be remembered that all Y_i appearing in the transfer functions are resistive i.e. $Y_i = \frac{1}{R_i}$. With proper choice of the resistor values, the 3-OA CGIC circuit can realize all types of second order functions as follows:

$H_1(s)$: Bandpass when $Y_A = 0 \rightarrow Y_1(Y_4 + Y_9) = Y_2Y_3$ and $Y_5(Y_4 + Y_9) = Y_3Y_6$
Band-reject (all types) when $Y_3 = 0$
Highpass when $Y_3 = 0$ and $Y_5(Y_4 + Y_9) = Y_3Y_6$

$H_2(s)$: Lowpass when $Y_1 = 0$ and $Y_2Y_5 = Y_3Y_7$
Bandpass when $Y_1 = 0$ and $Y_5(Y_4 - Y_{10}) = Y_3Y_6$
Highpass when $Y_2Y_5 = Y_3Y_7 + Y_1Y_6$ and $Y_5(Y_4 - Y_{10}) = Y_3Y_6$
Band-reject (all types) when $Y_2Y_5 = Y_3Y_7 + Y_1Y_6$

$H_3(s)$: Highpass when $Y_1Y_4 = Y_3(Y_2 + Y_7)$ and $Y_1Y_6 = Y_5(Y_2 + Y_7)$
Band-reject (all types) when $Y_1Y_4 = Y_3(Y_2 + Y_7)$

10.8.5 The Bainter 3-OA Circuit

The Bainter circuit [2] of Fig. 10.67 has three discrete gain stages. The first is an inverting voltage amplifier, the second an inverting Miller integrator, and the third a voltage follower. This structure facilitates the analysis of the circuit and the transfer function can easily be calculated:

$$H(s) = \frac{V_o(s)}{E(s)} = \frac{s^2 + (R_2/R_1R_3R_5C_1C_2)}{s^2 + s\frac{R_5+R_6}{R_5R_6C_2} + \frac{1}{R_4R_5C_1C_2}} \tag{10.130}$$

This is a band-reject function and since $\frac{\omega_{oz}}{\omega_{op}} = \sqrt{\frac{R_2R_4}{R_1R_3}}$, the circuit can realize notch, lowpass-notch and highpass-notch functions by proper selection of the involved resistor ratios.

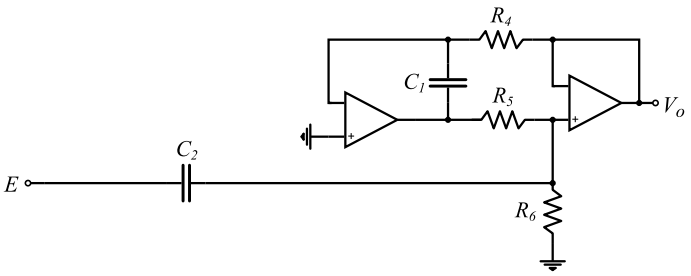

Fig. 10.68 The Bainter highpass filter

For $R_2 = 0$ the circuit is simplified, as shown in Fig. 10.68, and the transfer function becomes a highpass function:

$$H(s) = \frac{V_o(s)}{E(s)} = \frac{s^2}{s^2 + s\frac{R_5+R_6}{R_5R_6C_2} + \frac{1}{R_4R_5C_1C_2}} \tag{10.131}$$

10.9 Creation of Zeros

Notch transfer functions with $j\omega$-axis zeros are very useful in filter design, not only for the realization of band-reject filters, but also for the realization of certain types of lowpass and highpass filters, as for example inverse Chebyshev, inverse Pascal and elliptic filters.

Although all presented band-reject biquads offer these $j\omega$-axis zeros inherently, these can be also be created from all-pole circuits. One such method is to feed the input to some nodes, as has been done for example in Fig. 10.57.

A second method is to create the sum of appropriate voltages using a summing circuit. The Akerberg-Mossberg circuit, for example (Fig. 10.56), does not provide $j\omega$-axis zeros. However, by adding one more operational amplifier to add the input and the output of the first and the second amplifiers, as we have done in Fig. 10.69, the transfer function becomes

$$H(s) = \frac{V_o(s)}{E(s)} = k\frac{s^2 + s\frac{1-\frac{\lambda}{k}\frac{R_1}{R_4}}{CR_1} + \frac{1-\frac{\mu}{k}\frac{R}{R_4}}{C^2R^2}}{s^2 + s\frac{1}{CR_1} + \frac{1}{C^2R^2}} \tag{10.132}$$

This Akerberg-Mossberg circuit realizes bandpass transfer function at the output of the first operational amplifier, lowpass at the output of the second operational amplifier, and with the addition of the fourth operational amplifier can produce all three types of band-reject output for $\lambda/k = R_4/R_3$. It should also be noted that with proper selection of μ, the transfer function can be made highpass.

Moreover, $j\omega$-axis zeros can be created using a twin-T circuit as shown in Fig. 10.70.

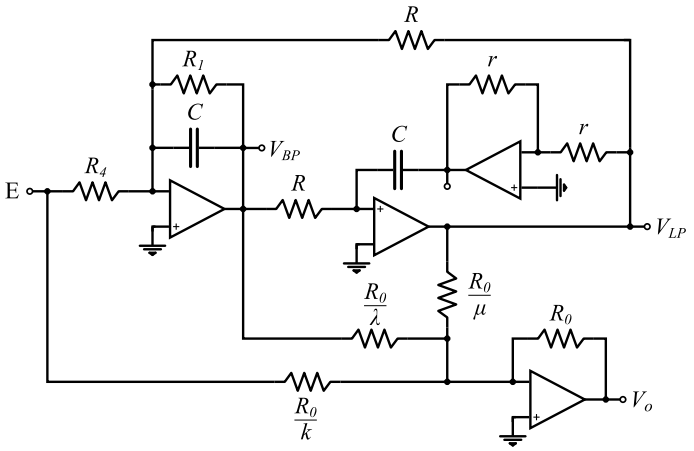

Fig. 10.69 Creating zeros by adding one more op amp

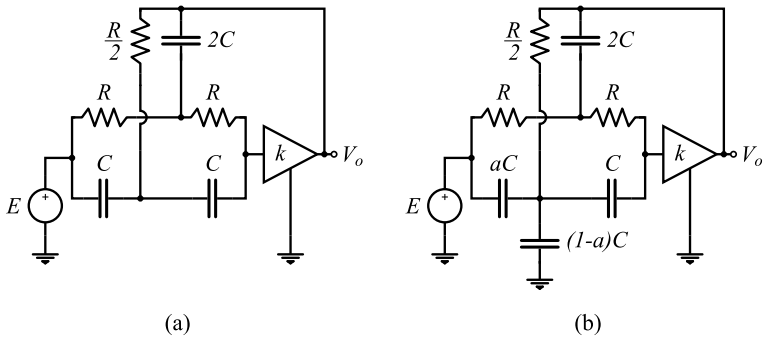

Fig. 10.70 Creating zeros using twin-T circuits

The transfer function of the circuit of Fig. 10.70a is

$$H_a(s) = \frac{k(s^2 + \frac{1}{R^2C^2})}{s^2 + s\frac{4(1-k)}{RC} = \frac{1}{R^2C^2}} \tag{10.133}$$

meaning that with $k < 1$, it realizes a stable notch output. The circuit of Fig. 10.70b has transfer function

$$H_b(s) = \frac{\alpha k(s^2 + \frac{1}{\alpha R^2C^2})}{s^2 + s\frac{4(1-k)}{RC} = \frac{1}{R^2C^2}} \tag{10.134}$$

i.e. for $k < 1$ and $\alpha < 1$, it realizes lowpass-notch output.

Fig. 10.71 Creating zeros

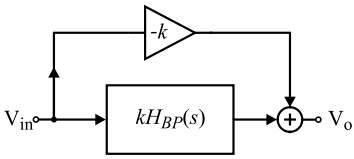

Finally, a more general method to create $j\omega$-axis zeros is based on Fig. 10.71, which uses a bandpass circuit with transfer function

$$H_{BP}(s) = \frac{As}{s^2 + s\frac{\omega_o}{Q} + \omega_o^2}$$

If we choose $k = \frac{QA}{\omega_o}$, then at the output of the adder we have:

$$H(s) = \frac{As}{s^2 + s\frac{\omega_o}{Q} + \omega_o^2} - \frac{AQ}{\omega_o} = \frac{\frac{AQ}{\omega_o}(s^2 + \omega_o^2)}{s^2 + s\frac{\omega_o}{Q} + \omega_o^2}$$

which is a notch transfer function.

10.10 Problems

10.1 Calculate the voltage transfer functions of the circuits shown in Fig. 10.7b and c and confirm that they are second order lowpass filters.

10.2 Calculate the voltage transfer functions of the circuits shown in Fig. 10.12 and confirm that they are second order highpass filters.

10.3 Apply the RC-CR transformation to a second order active BP filter (e.g. Sallen-Key) and study the transformed circuit.

10.4 Calculate the voltage transfer functions of the circuits shown in Fig. 10.15 and confirm that they are second order bandpass filters.

10.5 Prove that the Deliyannis circuit shown in Fig. 10.32 is a second order bandpass filter and find the expressions for the poles frequency and Q.

10.6 For the lowpass circuit of Sect. 10.7.2.1 (Fig. 10.50):

i. Prove that the transfer function $H_2(s) = \frac{V_2(s)}{V_{IN}(s)}$ is a second order lowpass function
ii. Design the circuit so as $H_2(s)$ has $\omega_p = 2\pi \cdot 10^4$ and $Q = 2$
iii. Explain what will happen if output V_2 is used to drive directly a load R_L

10.7 For the highpass circuit of Sect. 10.7.2.2 (Fig. 10.51):

i. Prove that the transfer function $H_2(s) = \frac{V_2(s)}{V_{IN}(s)}$ is a second order highpass function
ii. Design the circuit so as $H_2(s)$ has $\omega_p = 2\pi \cdot 10^4$ and $Q = 2$
iii. Explain what will happen if output V_2 is used to drive directly a load R_L

10.8 For the bandpass circuit of Sect. 10.7.2.3 (Fig. 10.52):
i. Prove that the transfer function $H_2(s) = \frac{V_2(s)}{V_{IN}(s)}$ is a second order bandpass function
ii. Design the circuit so as $H_2(s)$ has $\omega_p = 2\pi \cdot 10^4$ and $Q = 2$
iii. Explain what will happen if output V_2 is used to drive directly a load R_L

10.9 Apply the RC-CR transformation to the generalized CGIC BR filter of Fig. 10.53 and study the transformed circuit.

References[1]

1. Antoniou, A.: Realization of gyrators using operational amplifiers and their use in RC-Active network synthesis. Proc. IEEE **116**, 1838–1850 (1969)
2. Bainter, J.R.: Active filter has stable notch and response can be regulated. Electronics 115–117 (1975)
3. Boctor, S.A.: Single amplifier functionally tunable low-pass notch filter. IEEE Trans. Circuits Syst. **CAS-2**, 875–881 (1975)
4. Chen, W.-K.: Passive, Active and Digital Filters. The Circuits and Filters Handbook, vol. V. CRC Press, Boca Raton (2009)
5. Deliyannis, T.: High-Q factor circuit with reduced sensitivity. Electron. Lett. **4**, 567 (1968)
6. Deliyannis, T., Sun, Y., Fidler, J.K.: Continuous-Time Active Filter Design. CRC Press, Boca Raton (1999)
7. Graeme, J.G., Tobey, G.E., Huelsman, L.P.: Operational Amplifiers. McGraw-Hill, New York (1971)
8. Huelsman, L.P.: Active and Passive Analog Filter Design. McGraw-Hill, New York (1993), pp. 335–342
9. Kerwin, W.J., Huelsman, L.P., Newcomb, R.W.: State variable synthesis for insensitive integrated circuit transfer functions. IEEE J. Solid-State Circuits **SC-2**, 87–92 (1967)
10. Mitra, S.K.: A network transformation for active RC networks. Proc. IEEE **55**, 2021–2022 (1967)
11. Sallen, R.P., Key, E.L.: A practical method of designing RC active filters. IRE Trans. Circuit Theory **CT-2**, 74–85 (1955)
12. Saraga, W.: Sensitivity of 2-nd order Sallen-key-type active RC filters. IEE Electron. Lett. **3**, 442–44 (1971)
13. Schaumann, R., Van Valkenburg, M.E.: Design of Analog Filters. Oxford University Press, London (2001)
14. Thomas, L.C.: The biquad part I, some practical design considerations. IEEE Trans. Circuit Theory **CT-18**, 350–357 (1971)
15. Tow, J.: Design formulas for active RC filters using operational amplifiers. Electron. Lett. **5**, 339–341 (1969)
16. Van Valkenburg, M.E.: Analog Filter Design. Oxford University Press, London (1982)
17. Williams, A., Taylor, F.: Electronic Filter Design Handbook. McGraw-Hill, New York (2006)

[1] All references, whether or not cited within the text, are recommended for further reading.

Some Filter Design Mathematics

11

11.1 Polynomials

The network functions (transfer functions, driving-point functions etc.) of linear lumped circuits are rational functions of the complex frequency $s = \sigma + j\omega$, i.e. ratios of two polynomials in s with real coefficients. Therefore, it is not surprising that the mathematics involved in filter synthesis are mainly theory of polynomials and functions of complex variables. Circuit synthesis requires simple mathematics used in a correct manner and some useful concepts, definitions and methods are presented in this chapter.

Polynomials play an important role in filter synthesis since, as mentioned above, all driving-point functions, transfer functions and in general all functions of the lumped linear circuits are rational functions of the form

$$F(s) = \frac{N(s)}{D(s)}$$

where $N(s)$ and $D(s)$ are polynomials in s with real coefficients. The complete theory of polynomials can be found in the relevant mathematics books. In this section, only some useful theorems and methods will be presented in an engineering operational manner, i.e. without strict mathematical proofs.

A polynomial in s is a polynomial function of s of the form

$$P(s) = a_N s^N + a_{N-1} s^{N-1} + a_{N-2} s^{N-2} + \cdots + a_1 s^1 + a_0$$

where all coefficients a_k are real and the integer N is the *degree* of the polynomial. The independent variable s can be real or complex but in circuit theory is the variable of the Laplace transform $s = \sigma + j\omega$, the complex frequency.

The *roots* s_i of a polynomial are the values of the independent variable at which the polynomial assumes zero value, i.e. $P(s_i) = 0$. The calculation of the roots of a polynomial actually requires the solution of the equation

$$P(s) = 0 \quad \Leftrightarrow \quad a_N s^N + a_{N-1} s^{N-1} + a_{N-2} s^{N-2} + \cdots + a_1 s + a_0 = 0$$

H.G. Dimopoulos, *Analog Electronic Filters*, Analog Circuits and Signal Processing,
DOI 10.1007/978-94-007-2190-6_11, © Springer Science+Business Media B.V. 2012

and this is not a trivial task when $N > 2$. It is clear that a polynomial of degree N has N roots which can be real or complex. Complex roots come in conjugate pairs, i.e. when $z = a + jb$ is a complex root of $P(s)$ then its conjugate $z^* = a - jb$ is also a root of $P(s)$.

Polynomials of the form $P(s) = s^N - z$ are referred to as *binomials*. Constant z is in general complex, of the form $z = re^{j\theta}$ where r is its magnitude $r = |z|$ and θ its argument $\theta = \sphericalangle z$. If $z = a$ is a real positive constant, then $r = a$ and $\theta = 0$. If $z = -a$ with a a real positive constant, then $z = ae^{j\pi} \Rightarrow r = a$ and $\theta = \pi$.

The roots of a binomial $P(s) = s^N - re^{j\theta}$ are given by

$$z_k = r^{\frac{1}{N}} e^{j\left(\frac{2k\pi+\theta}{N}\right)} \quad \text{for } k = 0, 1, \ldots, (N-1) \tag{11.1}$$

As an example, the binomial

$$s^4 - 1 = s^4 - 1 \cdot e^{j0}$$

has the following roots:

$$z_0 = 1^{\frac{1}{4}} e^{j\left(\frac{0\cdot\pi+0}{4}\right)} = 1 \qquad z_1 = 1^{\frac{1}{4}} e^{j\left(\frac{2\cdot\pi+0}{4}\right)} = e^{j\frac{\pi}{2}} = j$$
$$z_2 = 1^{\frac{1}{4}} e^{j\left(\frac{4\cdot\pi+0}{4}\right)} = e^{j\pi} = -1 \qquad z_3 = 1^{\frac{1}{4}} e^{j\left(\frac{6\cdot\pi+0}{4}\right)} = e^{j\frac{3\pi}{2}} = -j$$

A polynomial of degree N with N roots s_i can be expressed as follows:

$$\begin{aligned} P(s) &= a_N s^N + a_{N-1} s^{N-1} + a_{N-2} s^{N-2} + \cdots + a_1 s + a_0 \\ &= a_N (s - s_1)(s - s_2) \cdots (s - s_N) \end{aligned}$$

It is clear that if s_k is a root of $P(s)$, then the division $\frac{P(s)}{s-s_k}$ leaves zero remainder. This is often used in order to factorize a polynomial when one or some of its roots are known since the division of two polynomials is expressed as

$$\frac{N(s)}{D(s)} = Q(s) + \frac{R(s)}{D(s)} \quad \Leftrightarrow \quad N(s) = Q(s)D(s) + R(s) \tag{11.2}$$

where $Q(s)$ is the quotient and $R(s)$ is the remainder of the division $N(s)/D(s)$.

Example 11.1 The polynomial $P(s) = s^3 + 6s^2 + 11s + 6$ has a root $s = -1$ and we expect zero remainder if divided by $s + 1$. Indeed, the division $\frac{P(s)}{s+1}$ yields quotient $Q(s) = s^2 + 5s + 6$ and remainder $R(s) = 0$. Therefore, the polynomial $P(s)$ can be expressed as

$$P(s) = Q(s)(s + 1) + R(s) = (s + 1)(s^2 + 5s + 6)$$

Example 11.2 Find k so that $s_1 = -1 + j$ is a root of the polynomial

$$P(s) = s^4 + 7s^3 + 18s^2 + 22s + k$$

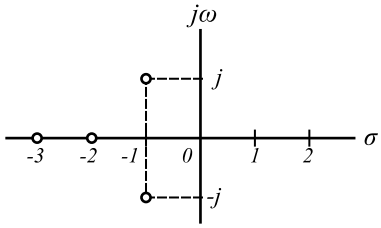

Fig. 11.1 Polynomial root diagram

Since $P(s)$ has a complex root $s_1 = -1 + j$, the conjugate $s_1^* = -1 - j$ is also a root and $P(s)$ contains the factor:

$$D(s) = (s - s_1)(s - s_1^*) = (s + 1 - j)(s + 1 + j) = s^2 + 2s + 2$$

Therefore, the remainder of the division $P(s)/D(s)$ must be zero. The division gives

$$P(s) = Q(s)(s^2 + 2s + 2) + R(s) \quad \text{where } Q(s) = s^2 + 5s + 6 \text{ and } R(s) = k - 12$$

and therefore, $R(s) = 0 \Leftrightarrow k = 12$.

Example 11.3 Find all the roots of the polynomial

$$P(s) = s^4 + 7s^3 + 18s^2 + 22s + 12$$

if we know that s_1 is one of its roots with $s_1 = -1 + j$.

Since $P(s)$ has a complex root $s_1 = -1 + j$, the conjugate $s_1^* = -1 - j$ is also a root and $P(s)$ contains the factor:

$$D(s) = (s - s_1)(s - s_1^*) = (s + 1 - j)(s + 1 + j) = s^2 + 2s + 2$$

The division $P(s)/D(s)$ gives

$$P(s) = Q(s)(s^2 + 2s + 2) + R(s) \quad \text{where } Q(s) = s^2 + 5s + 6 \text{ and } R(s) = 0$$

and therefore,

$$P(s) = s^4 + 7s^3 + 18s^2 + 22s + 12 = (s^2 + 5s + 6)(s^2 + 2s + 2)$$

The roots of $s^2 + 5s + 6$ are easily calculated: $s = -2$ and $s = -3$. The roots of a polynomial in s can be plotted in the s-plane (imaginary part on the vertical and real part on the horizontal axis). Figure 11.1, for example, shows the roots $\{-1 \pm j, -2, -3\}$ of the polynomial $P(s) = s^4 + 7s^3 + 18s^2 + 22s + 12$.

The Remainder Theorem The remainder theorem states that the value $P(s_1)$ of a polynomial $P(s)$ for $s = s_1$ equals $R(s_1)$, where $R(s)$ is the remainder of the division $\frac{P(s)}{s - s_1}$. To prove this simple theorem we use the fundamental equation of the division of (11.2) with divisor $D(s) = s - s_1$:

$$P(s) = Q(s)D(s) + R(s) = Q(s)(s - s_1) + R(s) \quad \Rightarrow \quad P(s_1) = R(s_1)$$

When s_1 is complex of the form $s = a + jb$, then the division $P(s)/(s - a - jb)$ is complicated and for this reason $P(s)$ is divided by

$$(s - s_1)(s - s_1^*) = (s - a)^2 + b^2 = s^2 - 2as + a^2 + b^2$$

In this case, we have:

$$\frac{P(s)}{(s - s_1)(s - s_1^*)} = Q(s) + \frac{R(s)}{(s - s_1)(s - s_1^*)}$$
$$\Rightarrow \quad P(s) = Q(s)(s - s_1)(s - s_1^*) + R(s)$$

It is apparent that

$$P(s_1) = R(s_1) \quad \text{and} \quad P(s_1^*) = R(s_1^*)$$

The usefulness of the remainder theorem can be demonstrated with the following example.

Example 11.4 Given $P(s) = s^4 - 4s^3 + 7s^2 - 24s + 36$, find $P(-1 + j2)$.

Substituting s with $-1 + j2$ in $P(s)$, the term $-1 + j2$ must be raised to the 4th, 3rd and 2nd order. Instead of this tedious task, it is simpler to divide $P(s)$ by $(s - s_1)(s - s_1^*) = s^2 + 2s + 5$ to find the remainder $R(s) = -22s - 34$, from which

$$P(-1 + j2) = R(-1 + j2) = -(22s + 34)_{s=-1+j2} = -12 - j44$$

11.1.1 Even and Odd Part of Polynomials

The *even part* of a polynomial $P(s)$ is the polynomial $P_e(s)$ which contains all the even order terms of $P(s)$. The *odd part* of a polynomial $P(s)$ is the polynomial $P_o(s)$ which contains all the odd order terms of $P(s)$ and therefore,

$$P(s) = P_e(s) + P_o(s) \tag{11.3}$$

Setting $s = j\omega$ with real ω, we have

$$P_e(j\omega) = \text{Re}[P(j\omega)] \quad \text{and} \quad P_o(j\omega) = j\,\text{Im}[P(j\omega)] \tag{11.4}$$

11.1.2 The Polynomial $P(-s)$

Polynomial $P(-s)$ is simply the polynomial $P(s)$ where s has been replaced by $-s$ as in the following example:

$$P(s) = s^4 + 7s^3 + 18s^2 + 22s + 12 \quad \Rightarrow \quad P(-s) = s^4 - 7s^3 + 18s^2 - 22s + 12$$

It can be shown that if s_o is a root of $P(s)$, then $-s_o$ is a root of $P(-s)$, i.e. $P(s)$ and $P(-s)$ have opposite roots. Moreover, $P(s)$ and $P(-s)$ have the same even part and opposite odd parts, i.e. if from (11.3), we have

$$P(s) = P_e(s) + P_o(s)$$

and

$$P(-s) = P_e(s) - P_o(s)$$

and therefore:

$$P(s)P(-s) = [P_e(s) + P_o(s)][P_e(s) - P_o(s)] = P_e^2(s) - P_o^2(s)$$

Using (11.4), we get

$$\begin{aligned} P(s)P(-s)|_{s=j\omega} &= P_e^2(j\omega) - P_o^2(j\omega) = (\mathrm{Re}[P(j\omega)])^2 + (\mathrm{Im}[P(j\omega)])^2 \\ &= |P(j\omega)|^2 \end{aligned}$$

and finally:

$$\begin{aligned} &P(s)P(-s)|_{s=j\omega} = |P(j\omega)|^2 \quad \text{and} \\ &|P(j\omega)|^2_{\omega^2=-s^2} = |P(j\omega)|^2_{\omega=-js} = P(s)P(-s) \end{aligned} \tag{11.5}$$

Equation (11.5) is very frequently used in filter synthesis since it relates $P(s)$ to the square of the magnitude $|P(j\omega)|^2$.

11.2 Hurwitz Polynomials

Polynomial with all their roots restricted in the closed left half s-plane, i.e. including the $j\omega$-axis, are very common in circuit theory and are referred to as *Hurwitz polynomials*. If all the roots of a polynomial are inside the left half s-plane excluding the $j\omega$-axis, then the polynomial is referred to as *strictly Hurwitz polynomial*. Hurwitz polynomials can have roots of two categories:
(a) k real roots of the form $s_i = -\gamma_i$ with $\gamma \geq 0$
(b) λ complex conjugate root pairs of the form $s_i = -\sigma_i \pm j\omega_i$ with $\sigma_i \geq 0$
Therefore, Hurwitz polynomials include factors of the form

$$\begin{aligned} &\prod_{i=1}^{k}(s + \gamma_i) \\ &\prod_{i=1}^{\lambda}(s - s_i)(s - s_i^*) = \prod_{i=1}^{\lambda}(s^2 + 2\sigma_i s + \sigma_i^2 + \omega_i^2) \end{aligned} \tag{11.6}$$

and can in general be expressed as

$$P(s) = (s+\gamma_1)\cdots(s+\gamma_k)(s^2+2\sigma_1 s+\sigma_1^2+\omega_1^2)\cdots(s^2+2\sigma_\lambda s+\sigma_\lambda^2+\omega_\lambda^2) \quad (11.7)$$

The order of the above Hurwitz polynomial is $N = k + 2\lambda$.

Using the form of Hurwitz polynomials of (11.7), some characteristic properties can be proved, which are also necessary conditions of Hurwitz polynomials:

1. Hurwitz polynomial coefficients are either all positive or all negative
2. Hurwitz polynomials are complete (no terms are missing), complete even (no even terms are missing) or complete odd (no odd terms are missing).
3. The roots of the even part of a Hurwitz polynomial are all located on the $j\omega$-axis
4. The roots of the odd part of a Hurwitz polynomial are all located on the $j\omega$-axis

It should be noted that the above conditions are only necessary but not sufficient and can be only used to classify some polynomials as non-Hurwitz.

11.2.1 The Continued-Fraction Property

Given a complete polynomial $P(s)$ of degree n and positive coefficients, for the even and odd parts $P_e(s)$ and $P_o(s)$ respectively, we have $P(s) = P_e(s) + P_o(s)$.

– When n is even, then $P_e(s)$ is of degree n and $P_o(s)$ of degree $n-1$
– When n is odd, then $P_o(s)$ is of degree n and $P_e(s)$ of degree $n-1$

We form the ratio $Q(s) = \frac{N(s)}{D(s)}$, where in the numerator polynomial $N(s)$ we put whichever of the polynomial $P_e(s)$ or $P_o(s)$ is of higher degree and in the denominator the other. $Q(s)$ can now be expanded in continued-fraction around infinity as follows:

$$Q(s) = \frac{N(s)}{D(s)} = q_1 s + \cfrac{1}{q_2 s + \cfrac{1}{q_3 s + \cfrac{1}{\cdots + \cfrac{1}{q_{n-1}s + \cfrac{1}{q_n s}}}}} \quad (11.8)$$

In Hurwitz polynomials, all coefficients q_i are positive and this property is referred to as the *continued-fraction property*.

The continued-fraction expansion around infinity is also called *long division*. The procedure starts with the first division which gives a partial quotient $q_1 s$ and a remainder $R_1(s)$ of degree $n-2$:

$$Q(s) = \frac{N(s)}{D(s)} = q_1 s + \frac{R_1(s)}{D(s)} = q_1 s + \frac{1}{\frac{D(s)}{R_1(s)}}$$

From the division $D(s)/R_1(s)$ we get a partial quotient $q_2 s$ and a remainder $R_2(s)$ of degree $n-3$:

$$\frac{D(s)}{R_1(s)} = q_2 s + \frac{R_2(s)}{R_1(s)} = q_2 s + \frac{1}{\frac{R_1(s)}{R_2(s)}}$$

$$\Rightarrow \quad Q(s) = \frac{N(s)}{D(s)} = q_1 s + \frac{R_1(s)}{D(s)} = q_1 s + \frac{1}{q_2 s + \frac{1}{\frac{R_1(s)}{R_2(s)}}}$$

The expansion continues making the division $R_1(s)/R_2(s)$ and so on until one of the following happens:

1. The long division produces n partial quotients q_i with the last $R_n(s) = 0$. If the initial polynomial $P(s)$ is Hurwitz, then all partial quotients q_i for $i = 1, 2..n$ are positive. If one of them is negative, then $P(s)$ is not Hurwitz.
2. The division ends prematurely with a zero remainder $R_k(s) = 0$ with $k < n$. In this case, the last non-zero remainder $R_{k-1}(s)$ is a common factor of $P_e(s)$ and $P_o(s)$:

$$P_e(s) = R_{k-1}(s)F_e(s) \quad \text{and} \quad P_o(s) = R_{k-1}(s)F_o(s)$$

If $R_{k-1}(s)$ were an odd polynomial, then $F_e(s)$ should be odd so that $R_{k-1}(s) \cdot F_e(s)$ is the even part $P_e(s)$ of $P(s)$. However, the product of two odd polynomials cannot give the constant term and therefore the even part $P_e(s)$ would not be complete. Therefore, if $P(s)$ is Hurwitz, $R_{k-1}(s)$ must be even and $P(s)$ can be expressed as

$$P(s) = P_e(s) + P_o(s) = R_{k-1}(s)F_e(s) + R_{k-1}(s)F_o(s) = R_{k-1}(s)F(s)$$

where the even factor $R_{k-1}(s)$ includes the $j\omega$-axis conjugate root pairs of $P(s)$ and $F(s)$ all the rest. For this reason $F(s)$ is a Hurwitz polynomial. It should also be noted that when $P(s)$ is a Hurwitz polynomial, all partial quotients q_i are positive.

The properties of the partial quotients q_i of the continued-fraction express a set of necessary and sufficient conditions for Hurwitz polynomials. More specifically:

- If for a polynomial $P(s)$ of degree n the continued-fraction expansion leads to n positive partial quotients q_i or
- if the procedure ends up prematurely giving $n - k$ positive partial quotients q_i and a common factor $R_{k-1}(s)$ with no roots in the right half s-plane,

then $P(s)$ is Hurwitz.

Example 11.5 Polynomial $P(s) = s^5 + 5s^4 + 11s^3 + 14s^2 + 10s + 4$ is complete with all its coefficients positive and therefore it may be Hurwitz. The ratio of its odd to its even parts is expanded to continued-fraction as follows:

$$Q(s) = \frac{s^5 + 11s^3 + 10s}{5s^4 + 14s^2 + 4} = \frac{1}{5}s + \cfrac{1}{\frac{25}{41}s + \cfrac{1}{\frac{1681}{1720}s + \cfrac{1}{\frac{59168}{37310}s + \cfrac{1}{\frac{910}{688}s}}}}$$

Since $n = 5$ and all 5 partial quotients are positive, polynomial $P(s)$ is Hurwitz. Indeed, if its roots are calculated, they are all in the closed left half s-plane: $\{-2\ -1 \pm j\ -0.5 \pm j0.8660\}$.

Example 11.6 Polynomial $P(s) = s^5 + 2s^4 + 3s^3 + 5s^2 + 5s + 2$ is complete with all its coefficients positive and therefore it may be Hurwitz. In order to test it, we use the continued-fraction property as follows:

$$Q(s) = \frac{s^5 + 3s^3 + 5s}{2s^4 + 5s^2 + 2} = 0.5s + \frac{0.5s^3 + 4s}{2s^4 + 5s^2 + 2}$$
$$\frac{2s^4 + 5s^2 + 2}{0.5s^3 + 4s} = 4s + \frac{-11s^2 + 2}{0.5s^3 + 4s}$$
$$\frac{0.5s^3 + 4s}{-11s^2 + 2} = -\frac{1}{22}s + \frac{\frac{43}{11}s}{-11s^2 + 2}$$

Since a negative partial quotient appears, the polynomial $P(s)$ is not Hurwitz, i.e. its roots are not restricted to the closed left s-plane. Indeed its roots are $\{-1\ -0.8296 \pm j0.48153\ 0.3296 \pm j1.4370\}$

Example 11.7 Polynomial $P(s) = s^5 + 4s^4 + 10s^3 + 20s^2 + 24s + 16$ is complete with all its coefficients positive and therefore it may be Hurwitz. In order to test it we use the continued-fraction property as follows:

$$Q(s) = \frac{s^5 + 10s^3 + 24s}{4s^4 + 20s^2 + 16} = 0.25s + \frac{5s^3 + 20s}{4s^4 + 20s^2 + 16} \qquad R_1(s) = 5s^3 + 20s$$
$$\frac{4s^4 + 20s^2 + 16}{5s^3 + 20s} = 0.8s + \frac{4(s^2 + 4)}{5s^3 + 20s} \qquad R_2(s) = 4(s^2 + 4)$$
$$\frac{5s^3 + 20s}{4s^2 + 16} = \frac{5}{4}s + \frac{0}{4s^2 + 16} \qquad R_3(s) = 0$$

Since the procedure ends prematurely with a zero remainder $R_3(s) = 0$, the term $R_2(s) = 4(s^2 + 4)$ is a common factor of the odd and the even parts of $P(s)$ and therefore $P(s) = 4(s^2 + 4)F(s)$. The fact that all partial quotients q_i are positive ensures that $F(s)$ is Hurwitz. Moreover, since the factor $R_2(s) = 4(s^2 + 4)$ has no roots in the right half s-plane makes $P(s)$ Hurwitz. Indeed, the roots of $P(s) = s^5 + 4s^4 + 10s^3 + 20s^2 + 24s + 16$ are: $\{-2 \pm j \pm j2\}$

Example 11.8 Polynomial $P(s) = s^7 + 2s^6 + 2s^5 + s^4 + 4s^3 + 8s^2 + 8s + 4$ is complete with all its coefficients positive and therefore it may be Hurwitz. In order to test it, we use the continued-fraction property as follows:

$$Q(s) = \frac{s^7 + 2s^5 + 4s^3 + 8s}{2s^6 + s^4 + 8s^2 + 4} = 0.5s + \frac{1.5s^5 + 6s}{2s^6 + s^4 + 8s^2 + 4} \qquad R_1(s) = 1.5s^5 + 6s$$

$$\frac{2s^6+s^4+8s^2+4}{1.5s^5+6s}=\frac{4}{3}s+\frac{s^4+4}{1.5s^5+6s} \qquad R_2(s)=s^4+4$$

$$\frac{1.5s^5+6s}{s^4+4}=1.5s+\frac{0}{s^4+4} \qquad R_3(s)=0$$

Since the procedure ends prematurely with a zero remainder $R_3(s)=0$, the term $R_2(s)=s^4+4$ is a common factor of the odd and the even parts of $P(s)$ and therefore $P(s)=(s^4+4)F(s)$. The fact that all partial quotients q_i are positive ensures that $F(s)$ is Hurwitz. However, since the factor $R_2(s)=s^4+4$ is not a complete even polynomial (term 2 is missing), it is not Hurwitz and has roots in the right half s-plane. Indeed, the roots of $P(s)=s^4+4$ are: $(-1\pm j)$ and $(+1\pm j)$, which makes

$$P(s)=s^7+2s^6+2s^5+s^4+4s^3+8s^2+8s+4=(s^4+4)F(s)$$

non-Hurwitz.

11.3 Strictly Hurwitz Polynomials—Routh's Criterion

Strictly Hurwitz polynomials are complete polynomials (no missing terms) with positive coefficients with all their roots inside the open left half s-plane, i.e. the real parts of all roots are negative. The continued-fraction property presented in the previous section sets the necessary and sufficient condition for strictly Hurwitz polynomials. As seen, we form the ratio $Q(s)=\frac{N(s)}{D(s)}$, where in the numerator polynomial $N(s)$ we put whichever of the polynomial $P_e(s)$ or $P_o(s)$ is of higher degree and in the denominator the other. $Q(s)$ can now be expanded in continued-fraction around infinity as follows:

$$Q(s)=\frac{N(s)}{D(s)}=q_1s+\cfrac{1}{q_2s+\cfrac{1}{q_3s+\cfrac{1}{\cdots+\cfrac{1}{q_{n-1}s+\cfrac{1}{q_ns}}}}}$$

$P(s)$ is strictly Hurwitz if, and only if, all n partial quotients q_i are positive, i.e. $q_i>0$ for $i=1,2,\ldots,n$. This is referred to as *Routh criterion*. If for any reason a zero remainder appears prematurely, then the polynomial is not strictly Hurwitz.

Example 11.9 Find the values of k for which the polynomial $P(s)=s^4+6s^3+11s^2+36s+k$ is strictly Hurwitz.

To use the Routh criterion, the rational function

$$Q(s)=\frac{s^4+11s^2+k}{6s^3+36s}$$

must be expanded in continued-fraction as follows:

$$Q(s) = \frac{s^4 + 11s^2 + k}{6s^3 + 36s} = \frac{1}{6}s + \cfrac{1}{\frac{6}{5}s + \cfrac{1}{\frac{25}{180-6k}s + \cfrac{1}{\frac{180-6k}{5k}s}}}$$

Four quotients q_i have been produced for the polynomial of degree $n = 4$ and in order $P(s)$ to be strictly Hurwitz, they must all be positive. The first two are positive and the last two are positive for $0 < k < 30$. Therefore for $k \leq 0$ or $k \geq 30$, polynomial $P(s)$ is not strictly Hurwitz.

Example 11.10 To check if polynomial $P(s) = s^6 + 3s^5 + 8s^4 + 15s^3 + 17s^2 + 12s + 4$ is strictly Hurwitz, the rational function

$$Q(s) = \frac{s^6 + 8s^4 + 17s^2 + 4}{3s^5 + 15s^3 + 12s}$$

must be expanded in continued-fraction as follows:

$$Q(s) = \frac{s^6 + 8s^4 + 17s^2 + 4}{3s^5 + 15s^3 + 12s} = \frac{1}{3}s + \frac{3s^4 + 13s^2 + 4}{3s^5 + 15s^3 + 12s}$$

$$R_1(s) = 3s^4 + 13s^2 + 4$$

$$\frac{3s^5 + 15s^3 + 12s}{3s^4 + 13s^2 + 4} = s + 2s^3 + 8s3s^4 + 13s^2 + 4 \qquad R_2(s) = 2s^3 + 8s$$

$$\frac{3s^4 + 13s^2 + 4}{2s^3 + 8s} = \frac{3}{2}s + s^2 + 42s^3 + 8s \qquad R_3(s) = s^2 + 4$$

$$\frac{2s^3 + 8s}{s^2 + 4} = 2s + \frac{0}{s^2 + 4} \qquad R_4(s) = 0$$

The procedure ends prematurely producing only four positive quotients q_i for the polynomial $P(s)$ of degree $n = 6$, and therefore $P(s)$ is not strictly Hurwitz. The premature appearance of the zero remainder $R_4(s) = 0$ implies that $R_3(s) = s^2 + 4$ is a factor of $P(s)$ which is of the form $P(s) = (s^2 + 4)F(s)$, with $j\omega$-axis roots $\pm j2$.

Routh and Hurwitz tests are specially developed systematic procedures to test a polynomial for the strictly Hurwitz property and are usually presented in more detail in control theory textbooks.

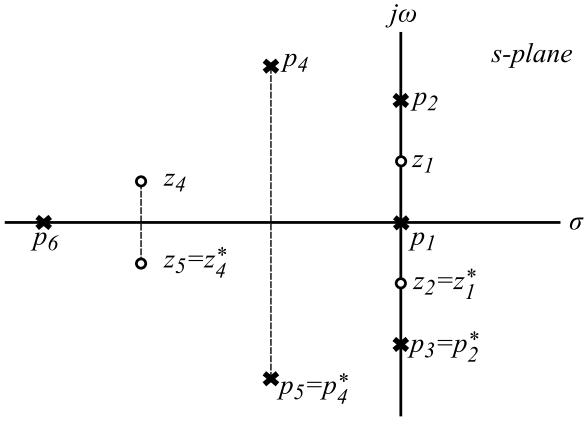

Fig. 11.2 Indicative pole-zero diagram

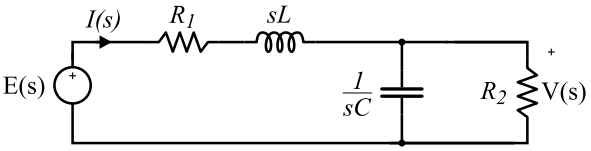

Fig. 11.3 A passive ladder circuit

11.4 Rational Functions

All functions of lumped linear circuits are rational functions of s of the form:

$$F(s) = \frac{N(s)}{D(s)} = \frac{a_n s^n + a_{n-1} s^{n-1} + \cdots + a_1 s + a_0}{b_m s^n + b_{m-1} s^{m-1} + \cdots + b_1 s + b_0}$$

Polynomial $N(s)$ can be expressed in terms of its n roots z_i, the zeros of $F(s)$. Polynomial $D(s)$ can be expressed in terms of its m roots p_i, the poles of $F(s)$:

$$F(s) = \frac{N(s)}{D(s)} = \frac{a_n}{b_m} \frac{(s - z_1)(s - z_2) \cdots (s - z_{n-1})(s - z_n)}{(s - p_1)(s - p_2) \cdots (s - p_{m-1})(s - p_m)}$$

Poles and zeros of a circuit function can be real or complex conjugate pairs and can be plotted in the complex plane, the s-plane, as is shown in Fig. 11.2 where zeros are represented by "o" and poles by "x". Such plots are referred to as pole-zero diagrams.

As an example, consider the circuit shown in Fig. 11.3. Its voltage transfer function can be calculated using any circuit analysis method and for $R_1 = R_2 = 1$, $C = 1$ and $L = 1$ it is

$$H(s) = \frac{V(s)}{E(s)} = \frac{1}{s^2 + 2s + 2}$$

with no zeros and a complex conjugate pole pair $s = -1 \pm j$, shown in the pole-zero diagram of Fig. 11.4.

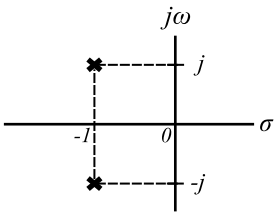

Fig. 11.4 Pole-zero diagram of $H(s)$ with $R_1 = R_2 = 1$, $C = 1$ and $L = 1$

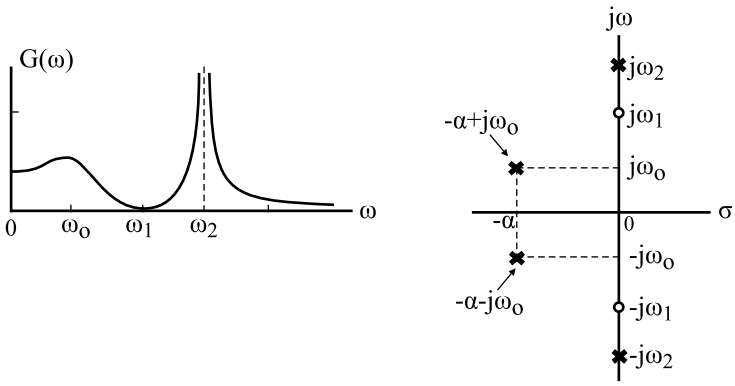

Fig. 11.5 Plot of the magnitude of a circuit function and the corresponding pole-zero diagram

It should be noted that a real frequency ω_x appears on the imaginary axis as $\pm j\omega_x$ according to Fig. 11.5, which shows the plot of the magnitude $G(\omega) = |G(j\omega)|$ of a circuit function $G(s)$ and the corresponding pole-zero diagram. A zero $j\omega_1$ on the $j\omega$-axis makes $G(\omega_1) = 0$ and a pole $j\omega_2$ on the $j\omega$-axis makes $G(\omega_2) = \infty$. A pole $-a \pm jb$ which is not located on the $j\omega$-axis, i.e. $a \neq 0$, cannot make $G(\omega)$ infinite.

There are some general rules concerning the location of poles and zeros of circuit functions in the s-plane but also special rules for each type of function. For stable circuits, for example, the poles of the corresponding transfer function must be located in the left half s-plane, i.e. the denominator polynomial $D(s)$ must be Hurwitz or strictly Hurwitz.

11.5 Sturm's Theorem

It is sometimes very useful in synthesis to be able to check the sign of the real part of a rational function $F(s)$ for $s = j\omega$, i.e. the sign of $\mathrm{Re}[F(j\omega)]$. Therefore, an appropriate systematic method would be desirable.

Let us assume the rational function $F(s) = \frac{N(s)}{D(s)}$, where $N(s)$ and $D(s)$ are polynomials with real coefficients. When s is replaced by $j\omega$ in $N(s)$, even order terms become real and contribute only to the real part of $N(j\omega)$, while odd terms contribute only to the imaginary part of $N(j\omega)$. In other words, the even part $N_e(s)$ of

$N(s)$ will give the real part of $N(j\omega)$ and the odd part $N_o(s)$ of $N(s)$ will give the imaginary part of $N(j\omega)$:

$$N_e(j\omega) = \text{Re}[N(j\omega)] \quad \text{and} \quad N_o(j\omega) = j\,\text{Im}[N(j\omega)]$$

Similarly,

$$D_e(j\omega) = \text{Re}[D(j\omega)] \quad \text{and} \quad D_o(j\omega) = j\,\text{Im}[D(j\omega)]$$

and therefore

$$F(j\omega) = \left.\frac{N_e(j\omega) + N_o(j\omega)}{D_e(j\omega) + D_o(j\omega)}\right|_{s=j\omega} = \frac{\text{Re}[N(j\omega)] + j\,\text{Im}[N(j\omega)]}{\text{Re}[D(j\omega)] + j\,\text{Im}[D(j\omega)]}$$

The real part of $F(j\omega)$ will be given by:

$$\text{Re}[F(j\omega)] = \frac{N_e(j\omega)D_e(j\omega) - N_o(j\omega)D_o(j\omega)}{D_e^2(j\omega) + D_o^2(j\omega)} = \frac{P(\omega^2)}{|D(j\omega)|^2}$$

where the denominator is non-negative and the sign of $\text{Re}[F(j\omega)]$ depends on

$$N_e(j\omega)D_e(j\omega) - N_o(j\omega)D_o(j\omega)$$

which is a polynomial in ω with only even terms and for this reason is denoted as $P(\omega^2)$. It is clear that the real part $\text{Re}[F(j\omega)]$ is an even rational function of ω with even numerator and denominator polynomials. The sign of $\text{Re}[F(j\omega)]$ depends on the sign of the function

$$P(x) = \gamma x^n + \gamma_{n-1}x^{n-1} + \cdots + \gamma_1 x + \gamma_0 \quad \text{where } x = \omega^2$$

In order for $\text{Re}[F(j\omega)]$ to be non-negative for all values of ω, $P(x)$ must be non-negative for $x \geq 0$. When all coefficients γ_i of $P(x)$ are positive, then it assumes positive values for all $x \geq 0$ and therefore $\text{Re}[F(j\omega)] \geq 0$. However, when one or more of the coefficients γ_i is negative, $P(x)$ may assume negative value for some value of $x \geq 0$.

If we want $P(x) \geq 0$, then γ_0 cannot be negative since $P(0) = \gamma_0$. Moreover, since the sign of $P(x)$ as $x \to \infty$ is the sign of γ_n, it must also be positive. Therefore if we want $P(x) \geq 0$, both γ_n and γ_0 must be positive.

If both γ_n and γ_0 are positive but one or more of the rest of the coefficients is negative, $P(x)$ may or may not be non-negative for all $x \geq 0$, depending on its roots, the calculation of which is not necessary. What we need in fact is the information whether $P(x)$ has one or more odd multiplicity roots. Even multiplicity roots make the curve to touch the x-axis without sign change, as shown in Fig. 11.6a, while odd multiplicity roots correspond to sign changes, as shown in Fig. 11.6b.

Sturm's theorem may give some interesting information about the positive roots of $P(x)$. The theorem is based on a sequence of polynomials, referred to as Sturm polynomials or functions. Sturm polynomials are derived as follows:

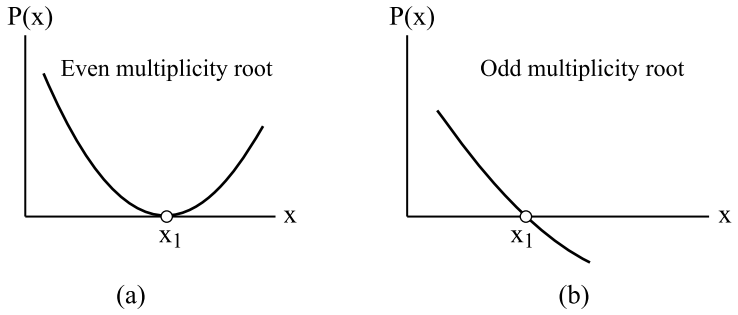

Fig. 11.6 (**a**) Even multiplicity. (**b**) Odd multiplicity

1. $P_1(x)$ is the derivative of $P(x)$

$$P_1(x) = \frac{d}{dx}P(x) \quad \text{of degree } n-1$$

2. $P(x)$ is divided by $P_1(x)$ until a quotient of the form $q_1 = a_1x + b_1$ is reached. The remainder of the division is $R_2(x)$ and the next Sturm's polynomial is $P_2(x) = -R_2(x)$ of degree $n-2$.
3. Polynomial $P_1(x)$ is divided by $P_2(x)$ until a quotient of the form $q_2 = a_2x + b_2$ is reached. The remainder of the division is $R_3(x)$ and the next Sturm's polynomial is $P_3(x) = -R_3(x)$ of degree $n-3$.
4. The procedure continues, dividing each previous polynomial by the next until a constant remainder $R_k(x) = R_k$ (of zero degree) is reached and the last Sturm's polynomial is $P_k(x) = -R_k$.

If all roots of $P(x)$ are simple, then $k = n$ and $R_n > 0$. In this case, we have $n+1$ Sturm's polynomials, including $P(x)$ and $P_n = -R_n$.

Sturm's theorem states that the number of simple roots of a polynomial $P(x)$ in the range $a \le x \le b$ (in our case $a = 0$ and $b = \infty$) is equal to the number of sign changes in the sequence

$$P(a),\ P_1(a),\ P_2(a), \ldots, P_n$$

reduced by the number of sign changes in the sequence

$$P(b),\ P_1(b),\ P_2(b), \ldots, P_n$$

Since in our case $a = 0$ and $b = \infty$, the first sequence is the sequence of the constant terms of the Sturm polynomials. The number of sign changes in the second sequence is the number of sign changes in the sequence of the higher order terms of the Sturm polynomials. A more detailed presentation of Sturm's theorem and its use can be found in [6] and [5] from where the following example has been borrowed.

Example 11.11 While examining the sign of the real part of a rational function, we found that it depends on the sign of

$$P(\omega^2) = \omega^8 - 15\omega^4 + 10\omega^2 + 24$$

Therefore, the sign of the polynomial

$$P(x) = x^4 - 15x^2 + 10x + 24$$

must be tested for $x \geq 0$. This will be done by checking if it has simple positive roots for $x \geq 0$ using Sturm's theorem. The first polynomial will be

$$P_1(x) = \frac{d}{dx}P(x) = 4x^3 - 30x + 10$$

If the remainder of the division $P(x)/P_1(x)$ is $R_2(x)$, then the second polynomial will be $P_2(x) = -R_2(x)$:

$$\frac{P(x)}{P_1(x)} = \frac{x^4 - 15x^2 + 10x + 24}{4x^3 - 30x + 10} = 0.25x + \frac{R_2(x)}{4x^3 - 30x + 10}$$

where

$$R_2(x) = -7.5x^2 + 7.5x + 24$$

and therefore

$$P_2(x) = -R_2(x) = 7.5x^2 - 7.5x - 24$$

The next polynomial will be the opposite of the remainder of the division $P_1(x)/P_2(x)$:

$$\frac{P_1(x)}{P_2(x)} = \frac{4x^3 - 30x + 10}{7.5x^2 - 7.5x - 24} = 0.5333x + 0.5333 + \frac{R_3(x)}{7.5x^2 - 7.5x - 24}$$

where

$$R_3(x) = -13.2x + 22.8 \quad \Rightarrow \quad P_3(x) = -R_3(x) = 13.2x - 22.8$$

The next and last polynomial will be the opposite of the remainder of the division:

$$\frac{P_2(x)}{P_3(x)} = \frac{7.5x^2 - 7.5x - 24}{13.2x - 22.8}$$

which is found

$$R_4(x) = -14.5785 \quad \Rightarrow \quad P_4(x) = -R_4(x) = 14.5785$$

The first sequence of Sturm's theorem will be:

$$[P(0) = 24 \; P_1(0) = 10 \; P_2(0) = -24 \; P_3(0) = -22.8 \; P_4(0) = 14.5785]$$

The sequence of the coefficients of the higher order terms of the same polynomials $P_i(x)$ is:

$$[1\ 4\ 7.5\ 13.2\ 14.5785]$$

The first sequence has two sign changes and the second zero sign changes and therefore $P(x)$ has $2-0=2$ simple positive roots for $x \geq 0$. The existence of these two simple roots means that $P(x)$ takes negative values in the region of these roots.

All the roots of $P(x)$ can of course be found using a mathematical software package. In this case, the roots of $P(x)$ are $\{-4\ -1\ 2\ 3\}$.

When polynomial $P(x)$ has one or more roots of multiplicity higher than 1, the derivation of Sturm's polynomials ends prematurely with $k < n$ and $P_k(x) = -R_k(x) = 0$. In this case, it can be shown that $P_{k-1}(x)$ is a common factor of $P_{k-2}(x)$ and all Sturm's polynomials, including $P_1(x)$ and $P(x)$. Polynomial $P(x)$ can therefore be expressed as:

$$P(x) = P_{k-1}(x)Q(x)$$

Polynomial $P_{k-1}(x)$ is of degree $n-k-1 < n$ and therefore it is easier to calculate its roots, which will also be roots of $P(x)$. Again, more details can be found in [5] and [6] although it must be noted that the sign of the real part of a particular rational function $F(s)$ for $s = j\omega$ can be examined using any of the modern very powerful computer software packages which make the old theoretical tools, like Sturm's theorem, seem of minor usefulness.

11.6 Retrieving Polynomial $P(s)$ from $|P(j\omega)|$

Given a polynomial $P(s)$, a very important relationship, which is very often used in synthesis, has been given in (11.5):

$$\begin{aligned} &P(s)P(-s)|_{s=j\omega} = |P(j\omega)|^2 \quad \text{and} \\ &|P(j\omega)|^2_{\omega^2=-s^2} = |P(j\omega)|^2_{\omega=-js} = P(s)P(-s) \end{aligned} \tag{11.9}$$

As an example, if $P(s) = s+1$ then $P(-s) = -s+1$ and

$$P(s)P(-s)|_{s=j\omega} = (s+1)(-s+1)|_{s=j\omega} = 1+\omega^2 = |P(j\omega)|^2$$

We have seen that if the roots of a polynomial of degree n

$$P(s) = a_n s^n + a_{n-1}s^{n-1} + \cdots + a_1 s + a_0$$

are ρ_k with $k = 1, 2, \ldots, n$, then the roots of the polynomial $P(-s)$ will be $-\rho_k$ for $k = 1, 2, \ldots, n$. Moreover, polynomial $B(s) = P(s)P(-s)$ can be expressed as

$$B(s) = P(s)P(-s) = a_n^2 \prod_{k=1}^{k=n}(s-\rho_k)(s+\rho_k) = a_n^2 \prod_{k=1}^{k=n}(s^2-\rho_k^2)$$

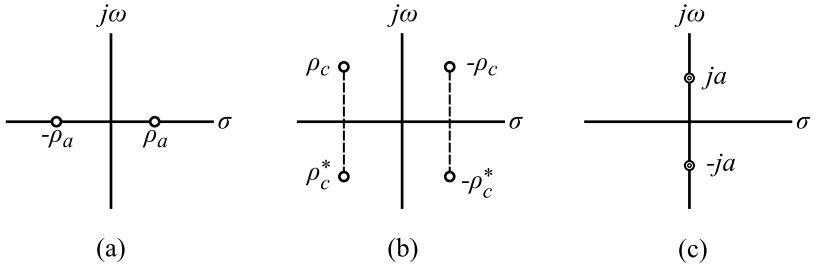

Fig. 11.7 Organization of the roots of $B(s)$

and therefore it is even with $2n$ roots $\pm\rho_k$ for $k = 1, 2, \ldots, n$ organized as follows:

1. If ρ_a is a real root of $P(s)$, then ρ_a and $-\rho_a$ will be roots of $B(s) = P(s)P(-s)$ (Fig. 11.7a).
2. If $\rho_C = a \pm jb$ is a root pair of $P(s)$, then ρ_C, ρ_C^*, $-\rho_C$ and $-\rho_C^*$ will be roots of $B(s) = P(s)P(-s)$ (Fig. 11.7b).
3. If $\pm ja$ is a root pair of $P(s)$, then $\pm ja$ will be a root pair of $B(s) = P(s)P(-s)$ with multiplicity 2 (Fig. 11.7c).

The roots of $B(s) = P(s)P(-s)$ are organized in three groups shown in Fig. 11.7. For the two real roots $\pm\rho_a$ of Fig. 11.7a, we know that one comes from $P(s)$ and its opposite from $P(-s)$. For the two complex root pairs $\{\rho_C, \rho_C^*\}$ and $\{-\rho_C, -\rho_C^*\}$ of Fig. 11.7b, one comes from $P(s)$ and its opposite from $P(-s)$. For the two identical imaginary root pairs $\{ja, -ja\}$ and $\{ja, -ja\}$ of Fig. 11.7c, we know that both $P(s)$ and $P(-s)$ have an imaginary pair of roots $\{ja, -ja\}$ and therefore both contain the factor $s^2 + a^2$.

In circuit synthesis it is very often necessary to retrieve a polynomial $P(s)$ from $|P(j\omega)|$ or $|P(j\omega)|^2$. It is clear that there is no unique solution to this problem, which is analogous to the determination of a complex number from its magnitude. A polynomial $P(s)$ can be determined from $|P(j\omega)|$ only if some additional information is available, as will be seen below.

Given $|P(j\omega)|^2$, which is an even polynomial in ω, from (11.9) we get

$$B(s) = P(s)P(-s) = |P(j\omega)|^2_{\omega^2=-s^2}$$

and the problem is now to separate $P(s)$ and $P(-s)$ from $B(s) = P(s)P(-s)$. Due to the above mentioned organization of the roots of $B(s) = P(s)P(-s)$, they can easily be allocated to one of the polynomials $P(s)$ or $P(-s)$ as follows:

1. When a real root ρ_a is allocated to $P(s)$ as a factor $(s - \rho_a)$, then $-\rho_a$ is allocated to $P(-s)$ as a factor $(s + \rho_a)$.
2. When a complex root pair $\{\rho_C, \rho_C^*\}$ is allocated to $P(s)$ as a factor $(s^2 - 2\,\mathrm{Re}[\rho_C]s + |\rho_C|^2)$, then the opposite root pair $\{-\rho_C, -\rho_C^*\}$ is allocated to $P(-s)$ as a factor $(s^2 - 2\,\mathrm{Re}[\rho_C]s + |\rho_C|^2)$.
3. When an imaginary root pair $\{ja, -ja\}$ is allocated to $P(s)$ as a factor $(s^2 + a^2)$, it is also allocated to $P(-s)$.

Since there is more than one combination of roots which can be allocated to $P(s)$, this procedure leads to more than one polynomial $P(s)$. However, if we know that $P(s)$ is Hurwitz, then the left half s-plane roots, including the $j\omega$-axis, will be allocated to $P(s)$ and the rest to $P(-s)$. If, for example

$$P(s)P(-s) = (s+2)(s-2)(s^2+2s+5)(s^2-2s+5)(s^2+6)^2$$

then $P(s)$ can be one of the following:

$$(s+2)(s^2+2s+5)(s^2+6) \qquad (s-2)(s^2+2s+5)(s^2+6)$$
$$(s+2)(s^2-2s+5)(s^2+6) \qquad (s-2)(s^2-2s+5)(s^2+6)$$

If, in addition, we know that $P(s)$ is a Hurwitz polynomial, then $P(s)$ could have been uniquely determined as $P(s) = (s+2)(s^2+2s+5)(s^2+6)$.

Example 11.12 Determine a Hurwitz polynomial $D(s)$ from $|D(j\omega)|^2 = 4\omega^6 + 4$.

We have

$$D(s)D(-s) = 4\omega^6 + 4|_{\omega^2=-s^2} = -4s^6 + 4 = 4(1-s^6)$$

According to (11.1), the roots of the binomial $1 - s^6$ are

$$s = e^{j\frac{2k\pi}{6}} \quad \text{for } k = 0, \ldots, 5$$
$$k = 0 \quad \rightarrow \quad s_1 = \cos(0) + j\sin(0) = 1$$
$$k = 1 \quad \rightarrow \quad s_2 = \cos(\pi/3) + j\sin(\pi/3) = 0.5 + j\frac{\sqrt{3}}{2}$$
$$k = 2 \quad \rightarrow \quad s_3 = \cos(2\pi/3) + j\sin(2\pi/3) = -0.5 + j\frac{\sqrt{3}}{2}$$
$$k = 3 \quad \rightarrow \quad s_4 = \cos(\pi) + j\sin(\pi) = -1$$
$$k = 4 \quad \rightarrow \quad s_5 = \cos(4\pi/3) + j\sin(4\pi/3) = -0.5 - j\frac{\sqrt{3}}{2}$$
$$k = 5 \quad \rightarrow \quad s_6 = \cos(5\pi/3) + j\sin(5\pi/3) = 0.5 - j\frac{\sqrt{3}}{2}$$

The roots of $1 - s^6$ are shown in Fig. 11.8.

Since a Hurwitz polynomial $D(s)$ must be determined, the left half s-plane roots must be allocated to $D(s)$ and their opposite to $D(-s)$:

$$D(s) = 2(s+1)\left(s + 0.5 - j\frac{\sqrt{3}}{2}\right)\left(s + 0.5 + j\frac{\sqrt{3}}{2}\right) = 2(s+1)(s^2+s+1)$$
$$D(-s) = 2(s-1)\left(s - 0.5 - j\frac{\sqrt{3}}{2}\right)\left(s - 0.5 + j\frac{\sqrt{3}}{2}\right) = 2(s-1)(s^2-s+1)$$

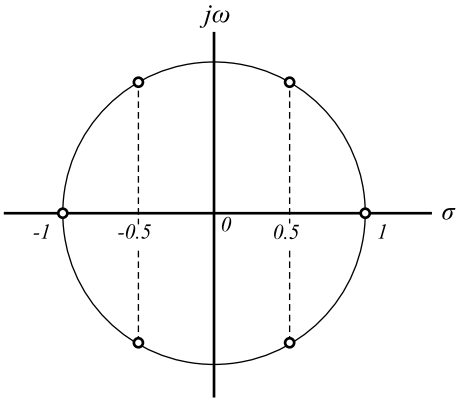

Fig. 11.8 The roots of $1 - s^6$

Example 11.13 Determine the polynomial $N(s)$ from $|N(j\omega)|^2 = \omega^6 + k^6$

We have

$$N(s)N(-s) = \omega^6 + k^6|_{\omega^2=-s^2} = k^6 - s^6 = (s+k)(s-k)(s^2+ks+k^2)(s^2-ks+k^2)$$

Since there are no restrictions for the location of the roots, $N(s)$ can be one of the following:

$$N_1(s) = (s+k)(s^2-ks+1) \qquad N_2(s) = (s+k)(s^2+ks+1)$$
$$N_3(s) = (s-k)(s^2-ks+1) \qquad N_4(s) = (s-k)(s^2+ks+1)$$

If $N(s)$ must be Hurwitz, then

$$\text{If } k > 0 \quad \Rightarrow \quad N(s) = (s+k)(s^2+ks+1)$$
$$\text{If } k < 0 \quad \Rightarrow \quad N(s) = (s-k)(s^2-ks+1)$$

Using the method presented above, a rational function $F(s) = \frac{N(s)}{D(s)}$ can also be determined from $|F(j\omega)|^2 = \frac{|N(j\omega)|^2}{|D(j\omega)|^2}$ by determining the numerator and denominator polynomials independently. If, for example, the transfer function $H(s) = \frac{N(s)}{D(s)}$ of a lumped linear circuit must be determined from

$$|H(j\omega)|^2 = \frac{\omega^6 + 2^6}{4\omega^6 + 4}$$

we will use

$$H(s)H(-s) = \frac{N(s)N(-s)}{D(s)D(-s)} = \left.\frac{\omega^6 + 2^6}{4\omega^6 + 4}\right|_{\omega^2=-s^2} = \frac{s^6 - 2^6}{4s^6 - 4}$$

The numerator and denominator polynomials can be determined independently from

$$N(s)N(-s) = s^6 - 2^6 \quad \text{and} \quad D(s)D(-s) = 4s^6 - 4$$

From Example 11.13 for $k = 2$, we have

$$N_1(s) = (s+2)(s^2 - 2s + 1) \qquad N_2(s) = (s+2)(s^2 + 2s + 1)$$
$$N_3(s) = (s-2)(s^2 - 2s + 1) \qquad N_4(s) = (s-2)(s^2 + 2s + 1)$$

Since there are no restrictions for the zeros of the transfer function, any of the above $N_i(s)$ can be used. However, the denominator of the transfer function must be Hurwitz and therefore according to Example 11.12, $D(s)$ can only be $D(s) = 2(s+1)(s^2 + s + 1)$. Finally, $H(s)$ can be one of the following:

$$H_1(s) = \frac{(s+2)(s^2 - 2s + 1)}{2(s+1)(s^2 + s + 1)} \qquad H_2(s) = \frac{(s+2)(s^2 + 2s + 1)}{2(s+1)(s^2 + s + 1)}$$
$$H_3(s) = \frac{(s-2)(s^2 - 2s + 1)}{2(s+1)(s^2 + s + 1)} \qquad H_4(s) = \frac{(s-2)(s^2 + 2s + 1)}{2(s+1)(s^2 + s + 1)}$$

11.7 Partial Fractions Expansion—Pole Residues

Rational functions with only simple poles are very common in circuit synthesis. Simple poles, i.e. poles with multiplicity $r = 1$, are also called first-order poles. In a rational function $F(s) = N(s)/D(s)$ with only simple poles, the degree of the numerator polynomial $N(s)$ may exceed the degree of the denominator polynomial $D(s)$ at most by 1, in which case $F(s)$ will have a simple pole at infinity.

Given a rational function $F(s) = N(s)/D(s)$ with only simple finite poles $s_1, s_2, \ldots, s_m$, it can be expanded into partial fractions as follows:

$$F(s) = \frac{N(s)}{D(s)} = \frac{k_1}{s - s_1} + \frac{k_2}{s - s_2} + \cdots + \frac{k_m}{s - s_m} \tag{11.10}$$

Coefficients $k_1, k_2, \ldots, k_m$ are the residues associated with the simple finite poles, i.e. the residues of $F(s)$ evaluated at its poles. Simple pole residues are determined by use of Heaviside's expansion theorem as follows:

$$k_i = (s - s_i)F(s)|_{s=s_i} \tag{11.11}$$

According to the above Heaviside's formula, $F(s)$ is first multiplied by $(s - s_i)$ and in the resulting function we let $s = s_i$. It can be shown that conjugate poles have conjugate residues and that simple pole residues can also be evaluated as follows:

$$k_i = \frac{N(s_i)}{\frac{d}{ds}D(s)|_{s=s_i}} \tag{11.12}$$

When the degree of the numerator polynomial $N(s)$ exceeds the degree of the denominator polynomial $D(s)$ by 1, then there is a simple pole at infinity ($s = \infty$) and its residue k_∞ is given by:

$$k_\infty = \left.\frac{F(s)}{s}\right|_{s\to\infty} \tag{11.13}$$

In this case, $F(s)$ is analyzed as follows:

$$F(s) = \frac{N(s)}{D(s)} = k_\infty s + \frac{k_1}{s - s_1} + \frac{k_2}{s - s_2} + \cdots + \frac{k_m}{s - s_m} \tag{11.14}$$

where s_i are the finite poles.

11.8 Positive Real (PR) Functions

Brune proved that if $F(s)$ is an *immitance function*, (i.e. impedance or admittance function) of a lumped linear RLCM circuit, then:

$$\mathrm{Re}[F(\sigma + j\omega)] \geq 0 \quad \text{when } \sigma \geq 0 \tag{11.15}$$

This *positive real property* of RLCM immitances is also referred to as Brune's theorem. Rational functions which possess the positive real property are referred to as *positive real functions* and play a significant role in passive circuit synthesis.

11.8.1 Positive Real Functions: Definition I

A rational function of s of the form

$$F(s) = \frac{a_n s^n + a_{n-1}s^{n-1} + \cdots + a_1 s + a_0}{b_m s^m + b_{m-1}s^{m-1} + \cdots + b_1 s + b_0}$$

with real coefficients a_i and b_i is positive real if and only if it has the positive real property, i.e.

$$\mathrm{Re}[F(\sigma + j\omega)] \geq 0 \quad \text{when } \sigma \geq 0 \tag{11.16}$$

Example 11.14 To check if $F(s) = \frac{2s+5}{s+2}$ is positive real, the real part of $F(\sigma + j\omega)$ must be checked:

$$F(\sigma + j\omega) = \frac{2\sigma + j2\omega + 5}{\sigma + j\omega + 2} = \frac{(2\sigma + 5)(\sigma + 2) + 2\omega^2}{(\sigma + 2) + \omega^2} - j\frac{\omega}{(\sigma + 2) + \omega^2}$$

$$\Rightarrow \quad \mathrm{Re}[F(\sigma + j\omega)] = \frac{(2\sigma + 5)(\sigma + 2) + 2\omega^2}{(\sigma + 2) + \omega^2}$$

which is positive for all $\sigma \geq 0$ and therefore $F(s)$ is positive real.

It can be shown that

(a) If $F_1(s)$ and $F_2(s)$ are positive real functions, then $F_1(F_2(s))$ and $F_2(F_1(s))$ are also positive real functions.

(b) If $F(s)$ is positive real, then $\frac{1}{F(s)}$ is also positive real.

When the definition of positive real functions given in (11.16), referred to as "definition I", is used to test a function for the positive real property, it may lead to very complex expressions and computations. For this reason, other more practical equivalent definitions have been developed.

11.8.2 Positive Real Functions: Definition II

A rational function of s of the form

$$F(s) = \frac{a_n s^n + a_{n-1} s^{n-1} + \cdots + a_1 s + a_0}{b_m s^m + b_{m-1} s^{m-1} + \cdots + b_1 s + b_0}$$

with real coefficients a_i and b_i is positive real if and only if:

(i) $\mathrm{Re}[F(j\omega)] \geq 0$ for all real values of ω

(ii) Denominator polynomial $D(s)$ is Hurwitz

(iii) $j\omega$-axis poles, including poles at zero and infinity, are simple with positive residues, i.e. if s_k is a $j\omega$-axis pole of $F(s)$, it must be simple and

$$k_k = (s - s_k)F(s)|_{s=s_k} \geq 0$$

The proof of the equivalence of this definition, referred to as *definition II*, to the basic definition is beyond the scope of this textbook.

As has been mentioned, when $F(s)$ is PR, then $1/F(s)$ is also PR and therefore the numerator polynomial $N(s)$ of $F(s)$ is also Hurwitz and $j\omega$-axis zeros, including zeros at zero and infinity, are simple. For example, function

$$F(s) = \frac{s+1}{s^3 + 4s^2 + 5s + 1}$$

is not positive real since it has a zero of multiplicity 2 on the $j\omega$-axis at $s = \infty$ (difference of the degrees of $D(s)$ and $N(s)$). Function

$$F(s) = \frac{(s+1)(s^2+4)^2}{s^4 + 3s^3 + s^2 + 5s + 1}$$

is not positive real since it has a pair of zeros at $a = \pm j2$ of multiplicity 2.

A practical set of necessary conditions for positive real functions can be created from the two definitions and is presented below.

1. All coefficients of the numerator $N(s)$ and denominator $D(s)$ polynomials are positive.
2. Both polynomials are complete, complete odd or complete even.
3. The difference of the degrees of $N(s)$ and $D(s)$ cannot exceed 1.

4. The difference of the orders of the lower order terms of the two polynomials cannot be higher than unity. If it is, then there is a pole or a zero at $s = 0$ of multiplicity higher than 1.
5. Both $N(s)$ and $D(s)$ are Hurwitz polynomials and if they have jω roots, they are simple.

Example 11.15 The rational function

$$F(s) = \frac{2s+5}{s+2}$$

meets all necessary conditions given above and therefore it may be positive real. For the real part, we have

$$\text{Re}[F(j\omega)] = \text{Re}\left[\frac{5+j2\omega}{2+j\omega}\right] = \frac{10+2\omega^2}{4+\omega^2} > 0 \quad \text{for all } \omega \geq 0$$

Therefore, $F(s)$ is positive real since it meets all the conditions of definition II.

Example 11.16 The rational function

$$F(s) = \frac{s^2+2s+25}{s+4}$$

has simple poles $s = -4$ and $s = \infty$ and a conjugate pair of zeros $-1 \pm j48$. Therefore, it meets all conditions of definition II and all the necessary conditions for positive real function and it is worth checking Re$[F(j\omega)]$:

$$\text{Re}[F(j\omega)] = \text{Re}\left[\frac{-\omega^2+25+j2\omega}{j\omega+4}\right] = \frac{100-2\omega^2}{\omega^2+16}$$

It is clear that Re$[F(j\omega)]$ can assume negative values for $\omega > \sqrt{50}$, which makes $F(s)$ non-PR.

Example 11.17 Check if the following functions are positive real:

$$F(s) = \frac{s^4+3s^2+2s+2}{s^3+6s^2+11s+6} \qquad Z(s) = \frac{s^4+3s^2+2}{s^3+6s^2+11s+6}$$

Since from the numerator polynomial of $F(s)$ only the term s^3 is missing, it cannot be Hurwitz and $F(s)$ cannot be positive real. In the numerator polynomial of $Z(s)$, all odd terms are missing and the polynomial is complete even. Both polynomials of $Z(s)$ satisfy the necessary conditions and the sign of Re$[Z(j\omega)]$ must be examined:

$$\text{Re}[Z(j\omega)] = \text{Re}\left[\frac{\omega^4-3\omega^2+2}{6-6\omega^2-j\omega(\omega^2-11)^2}\right] = \frac{-6(\omega^2-1)(\omega^2-2)}{36(\omega^2-1)^2+\omega^2(\omega^2-11)^2}$$

The above Re$[Z(j\omega)]$ assumes negative values for $\omega > \sqrt{2}$ and therefore $Z(s)$ is not positive real.

Example 11.18 Is $F(s) = \frac{s^3+2s}{s^2+1}$ positive real?

Both numerator and denominator are Hurwitz polynomials since the zeros are $s = 0, s = \pm j\sqrt{2}$ and the poles $s = \pm j, s = \infty$. According to definition II, in order for $F(s)$ to be PR, $\text{Re}[F(j\omega)] \geq 0$ for all $\omega \geq 0$ and the pole residues must be positive. In this case, $\text{Re}[F(j\omega)] = 0$ (non-negative) and for the residues of the $j\omega$-axis poles we have:

$$\text{Pole } s = \infty \qquad K_\infty = \left.\frac{F(s)}{s}\right|_{s\to\infty} = 1$$

$$\text{Pole } s = j \qquad K_j = (s-j)F(s)|_{s=j} = 0.5$$

$$\text{Pole } s = -j \qquad K_{-j} = (s+j)F(s)|_{s=-j} = 0.5$$

Therefore, since we have non-negative real part $\text{Re}[F(j\omega)]$ and the residues of all the $j\omega$-axis poles are positive, $F(s)$ is positive real.

11.8.3 Positive Real Functions: Definition III

A rational function $F(s) = \frac{N(s)}{Q(s)}$ is positive real if and only if

$$\begin{aligned} &\text{(i)} \quad \text{Re}[F(j\omega)] \geq 0 \quad \text{for all real } \omega \quad \text{and} \\ &\text{(ii)} \quad \text{Polynomial } Q(s) = N(s) + D(s) \quad \text{is strictly Hurwitz} \end{aligned} \tag{11.17}$$

This equivalent definition of positive real rational functions is often used due to the existence of appropriate mathematical tools which facilitate the test of the sign of the real part and the location of the roots of a polynomial.

Example 11.19 In order for $F(s) = \frac{s^3+2s}{s^2+1}$ to be positive real,
(i) $\text{Re}[F(j\omega)]$ must be non-negative for all real ω and
(ii) Polynomial $Q(s) = N(s) + D(s) = s^3 + s^2 + 2s + 1$ must be strictly Hurwitz
Since $\text{Re}[F(j\omega)] = \text{Re}[\frac{j\omega(2-\omega^2)}{1-\omega^2}] = 0$, the first condition of definition III is met. To check if polynomial $Q(s) = N(s) + D(s) = s^3 + s^2 + 2s + 1$ is strictly Hurwitz, the Routh criterion will be used and if three positive partial quotients are derived, then $Q(s)$ will be strictly Hurwitz. The odd part of $Q(s)$ is $s^3 + 2s$ of degree 3, and its even part is $s^2 + 1$ of degree 2. Therefore, for $\frac{s^3+2s}{s^2+1}$ we have:

$$\frac{s^3+2s}{s^2+1} = s + \frac{1}{s+\frac{1}{s}}$$

Since for this 3rd order rational function, three positive partial quotients are obtained, $Q(s) = s^3 + s^2 + 2s + 1$ is strictly Hurwitz and therefore, $F(s)$ is positive real.

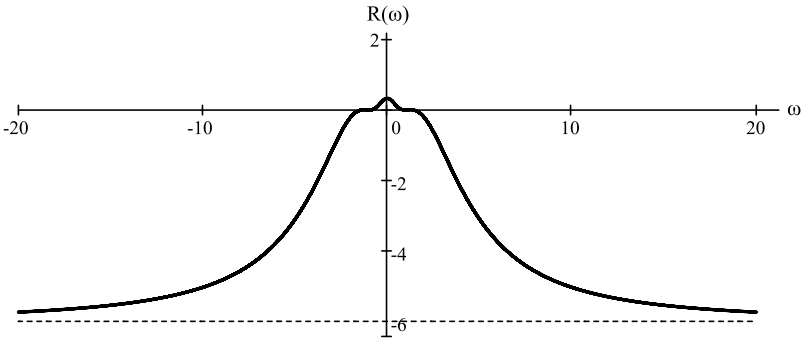

Fig. 11.9 Plot of the real part

Example 11.20 Given

$$F(s) = \frac{s^4 + 3s^2 + 2}{s^3 + 6s^2 + 11s + 6}$$

it will be positive real if

(i) $\mathrm{Re}[F(j\omega)]$ is non-negative for all real ω and

(ii) Polynomial $Q(s) = N(s) + D(s) = s^4 + s^3 + 9s^2 + 11s + 8$ is strictly Hurwitz

For the real part, we have:

$$\mathrm{Re}[F(j\omega)] = \mathrm{Re}\left[\frac{\omega^4 - 3\omega^2 + 2}{6 - 6\omega^2 - j\omega(\omega^2 - 11)}\right] = \frac{-6(\omega^2 - 1)(\omega^2 - 2)}{36(\omega^2 - 1)^2 + \omega^2(\omega^2 - 11)^2}$$

It is clear that $\mathrm{Re}[F(j\omega)]$ assumes negative values for $|\omega| > \sqrt{2}$ and therefore $F(s)$ is not positive real. A plot of $R(\omega) = \mathrm{Re}[F(j\omega)]$ is shown in Fig. 11.9.

Although the function is not positive real if it fails to satisfy one of the two criteria of definition III, we will continue by checking if $Q(s) = N(s) + D(s) = s^4 + s^3 + 9s^2 + 11s + 8$ is strictly Hurwitz. The even part of $Q(s)$ is of degree 4 and the odd part is of degree 3. Therefore, the rational function $G(s) = Q_e(s)/Q_o(s)$ will be expanded in continued fraction:

$$G(s) = \frac{s^4 + 9s^2 + 8}{s^3 + 11s} = s + \cfrac{1}{-0.5s + \cfrac{1}{-\frac{2}{15}s + \cfrac{1}{\frac{15}{8}s}}}$$

Since at least one of the partial quotients is negative, $Q(s)$ is not strictly Hurwitz and the given $F(s)$ fails to satisfy both conditions of definition III.

Example 11.21 Given

$$F(s) = \frac{s^4 + 6s^2 + 1}{s^3 + 4s^2 + 6s + 6}$$

it will be positive real if

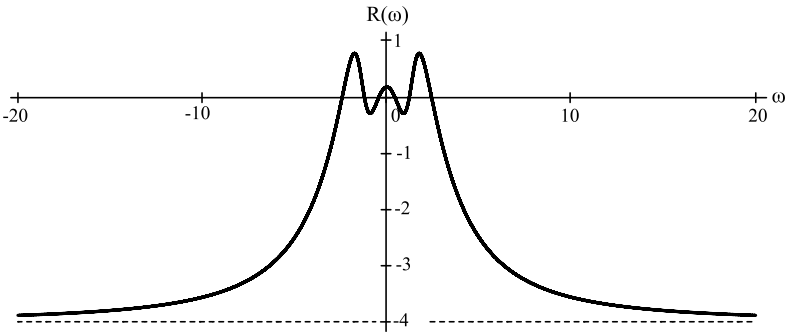

Fig. 11.10 Plot of the real part

(i) Re$[F(j\omega)]$ is non-negative for all real ω and
(ii) Polynomial $Q(s) = N(s) + D(s) = s^4 + s^3 + 10s^2 + 6s + 7$ is strictly Hurwitz
Let us first check if $Q(s) = N(s) + D(s) = s^4 + s^3 + 10s^2 + 6s + 7$ is strictly Hurwitz using Routh criterion:

$$G(s) = \frac{s^4 + 10s^2 + 7}{s^3 + 6s} = s + \frac{1}{0.25s + \frac{1}{\frac{16}{17}s + \frac{1}{\frac{17}{28}s}}}$$

Since all four partial quotients are positive, $Q(s)$ is strictly Hurwitz.

For the real part, we have

$$R(\omega) = \text{Re}[F(j\omega)] = \text{Re}\left[\frac{\omega^4 - 6\omega^2 + 1}{6 - 4\omega^2 - j\omega(\omega^2 - 6)}\right] = \frac{-4\omega^6 + 30\omega^4 - 40\omega^2 + 6}{(6 - 4\omega^2)^2 + \omega^2(6 - \omega^2)^2}$$

The denominator polynomial of $R(\omega)$ is non-negative and the sign of $R(\omega)$ depends on the sign of the numerator polynomial

$$P(\omega) = -4\omega^6 + 30\omega^4 - 40\omega^2 + 6 \qquad P(x) = -4x^3 + 30x^2 - 40x + 6$$

It is obvious that $P(\omega)$ assumes negative value as $\omega \to \infty$ since the coefficient of the highest order term is negative. This makes the real part $R(\omega)$ negative as $\omega \to \infty$ and the first condition of definition III is violated, making the given $F(s)$ non-positive real. Figure 11.10 shows the plot of $R(\omega) = \text{Re}[F(j\omega)]$.

Example 11.22 Is the following rational function $F(s)$ positive real?

$$F(s) = \frac{N(s)}{D(s)} = \frac{s^8 + 13s^7 + 21s^6 + 98s^5 + 95s^4 + 195s^3 + 95s^2 + 116s + 8}{s(s^2 + 4)(s^4 + 7s^3 + 8s^2 + 10s + 1)}$$

Using a mathematical software package, we find that the roots of the polynomial $Q(s) = N(s) + D(s)$ are:

$$-12.397 \quad -0.5 \pm j1.13 \quad -0.193 \pm j1.112 \quad -0.073 \pm j2.149 \quad -0.072$$

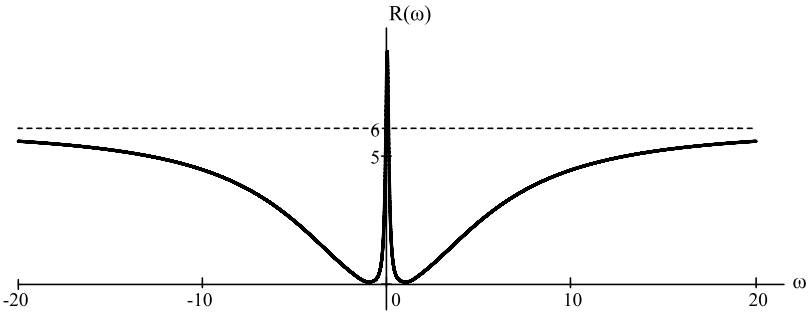

Fig. 11.11 Plot of the real part

The plot of the real part $R(\omega)$ is shown in Fig. 11.11. It is obvious that both conditions of definition III are satisfied and therefore the given rational function $F(s)$ is positive real.

11.9 Problems

11.1 If we know that $s = -1$ and $s = -2 + j$ are roots of the polynomial

$$s^5 + 6s^4 + 15s^3 + 19s^2 + 14s + 5$$

find all its roots.

11.2 Given

$$P(s) = s^4 + s^3 + 2s^2 + 3s + 1$$

find the value $P(-1 - j)$ using the remainder theorem.

11.3 Given

$$P(s) = s^2 + 3s + 1$$

find $|P(j\omega)|^2$ and $B(\omega) = .P(s)P(-s)|_{s=j\omega}$ and verify that $B(\omega) = |P(j\omega)|^2$.

11.4 Check if the polynomial

$$P(s) = s^5 + 6s^4 + 15s^3 + 19s^2 + 14s + 5$$

is Hurwitz. Use the continued-fraction property.

11.5 Check if the polynomial

$$P(s) = 2s^4 + 12s^3 + 22s^2 + 72s + 10$$

is strictly Hurwitz.

11.6 Determine the Hurwitz polynomial $P(s)$ from $|P(j\omega)|^2 = \omega^4 + 1$.

11.7 Determine the Hurwitz polynomial $P(s)$ from $|P(j\omega)|^2 = \omega^5 + 1$.

11.8 Prove that $F(s) = \frac{s^2+1}{s^3+2s}$ is positive real using definition II.

References[1]

1. Belevitch, V.: Classical Network Theory. Holden-Day, Oakland (1968)
2. Chen, W.-K. (ed.): Passive, Active and Digital Filters. The Circuits and Filters Handbook, vol. V. CRC Press, Boca Raton (2009)
3. Guillemin, E.A.: The Mathematics of Circuit Analysis. Wiley, New York (1949)
4. Guillemin, E.A.: Synthesis of Passive Networks. Krieger, Melbourne (1977)
5. Temes, G.C., LaPatra, J.W.: Introduction to Circuit Synthesis and Design. McGraw-Hill, New York (1977)
6. Van Valkenburg, M.E.: Introduction to Modern Network Synthesis. Wiley, New York (1966)
7. Van Valkenburg, M.E.: Analog Filter Design. Oxford University Press, London (1982)
8. Weinberg, L.: Network Analysis and Synthesis. McGraw-Hill, New York (1962)

[1] All references, whether or not cited within the text, are recommended for further reading.

Synthesis of RLCM One-Port Circuits

12

12.1 Pole Removals

If the driving point input impedance function $Z(s)$ of a passive RLCM one-port circuit is expressed as a sum of two functions $Z_1(s)$ and $Z_2(s)$

$$Z(s) = Z_1(s) + Z_2(s)$$

then it can be viewed as the series connection of impedances $Z_1(s)$ and $Z_2(s)$, as shown in Fig. 12.1a. The initial one-port circuit is of course equivalent to that of the series connection of $Z_1(s)$ and $Z_2(s)$.

Similarly, driving-point input admittance function $Y(s)$ of a passive RLCM one-port circuit can be expressed as a sum of two functions $Y_1(s)$ and $Y_2(s)$

$$Y(s) = Y_1(s) + Y_2(s)$$

and it can be viewed as the parallel connection of admittances $Y_1(s)$ and $Y_2(s)$ as shown in Fig. 12.1b. The initial circuit is of course equivalent to that of the parallel connection of $Y_1(s)$ and $Y_2(s)$.

Such an analysis of a driving-point function $F(s)$ into $F_1(s)$ and $F_2(s)$ can be considered as the *removal* of part $F_1(s)$ from $F(s)$ to leave $F_2(s) = F(s) - F_1(s)$, referred to as the *remainder* function.

It should be noted that the driving-point functions of lumped passive RLCM circuits are rational positive real (PR) functions, i.e. they possess the positive real property according to Chap. 11. The synthesis of a positive real rational function as a passive RLCM circuit is based on the removal of easily realizable PR parts in such a way as to leave PR (and hence realizable) remainder functions. It will be seen in the next sections that the $j\omega$-axis poles of the driving-point function $F(s)$ to be synthesized as an RLCM circuit are the reference points of such removals.

H.G. Dimopoulos, *Analog Electronic Filters*, Analog Circuits and Signal Processing,
DOI 10.1007/978-94-007-2190-6_12, © Springer Science+Business Media B.V. 2012

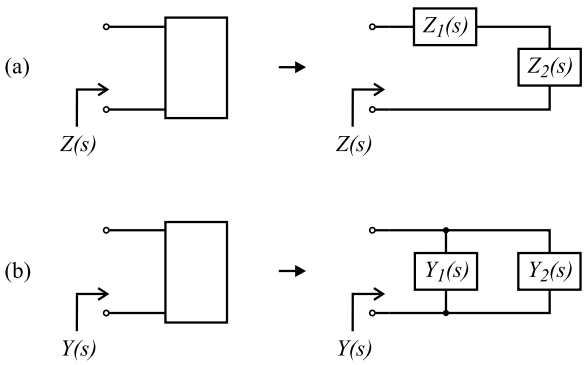

Fig. 12.1 Removal of a part from (**a**) an impedance (**b**) an admittance

12.1.1 Removal of Pole at $s = 0$

When a rational function $F(s)$ has a pole at $s = 0$, it is of the form

$$F(s) = \frac{N(s)}{D(s)} = \frac{a_N s^N + a_{N-1} s^{N-1} + \cdots + a_1 s + a_0}{b_m s^m + b_{m-1} s^{m-1} + \cdots + b_1 s} \tag{12.1}$$

without constant term b_0 in the denominator. In this case, $F(s)$ can also be expressed as

$$F(s) = \frac{N(s)}{D(s)} = \frac{a_N s^N + a_{N-1} s^{N-1} + \cdots + a_1 s + a_0}{s(b_m s^{m-1} + b_{m-1} s^{m-2} + \cdots + b_1)}$$

When $F(s)$ is positive real, the difference of the numerator and denominator polynomials $|N - m|$ can be at most equal to unity, i.e. $|N - m| \leq 1$. $F(s)$ can be analyzed as follows:

$$F(s) = \frac{k_0}{s} + \frac{\delta_{N-1} s^{N-1} + \cdots + \delta_1}{b_m s^{m-1} + b_{m-1} s^{m-2} + \cdots + b_1} = F_1(s) + F_2(s) \tag{12.2}$$

Constant k_0 is the residue of the pole $s = 0$ given by Heaviside's formula:

$$k_0 = sF(s)|_{s=0} \quad \text{or} \quad k_0 = \frac{N(0)}{\frac{d}{ds} D(s)|_{s=0}} \tag{12.3}$$

Equation (12.2) can be seen as the removal of the pole at $s = 0$, which leaves the remainder function

$$F_2(s) = F(s) - \frac{k_0}{s}$$

The degree of the numerator of $F_2(s)$ will be equal to the degree of $F(s)$ reduced by 1. Moreover, k_0 is positive since the residues of jω-axis poles of positive real functions are positive (see definition II of PR functions in Chap. 11). This makes $F_1(s) = \frac{k_0}{s}$ positive real. The remainder $F_2(s)$ is also positive real since:

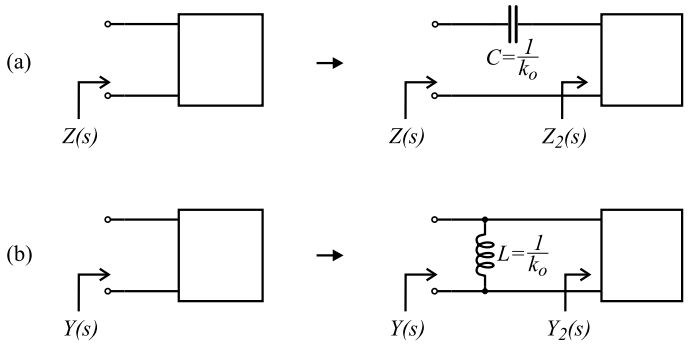

Fig. 12.2 Removal of pole at $s = 0$. (**a**) From impedance. (**b**) From admittance

1. The poles of $F_2(s)$ are in the left half s-plane including the $j\omega$-axis since $F_2(s)$ has the poles of $F(s)$ without the pole at $s = 0$, which has been removed.
2. The residues of these poles are positive since they are the residues of the same poles of the positive real $F(s)$.
3. $\text{Re}[F_2(j\omega)] = \text{Re}[F(j\omega)] - \text{Re}[\frac{k_0}{j\omega}] = \text{Re}[F(j\omega)] \geq 0$ since $F(s)$ is positive real.

Therefore, when a positive real $F(s)$ has a pole at $s = 0$, it can be analyzed in a sum of two positive real parts from which the first, k_0/s, corresponds to the pole $s = 0$ and the second, the remainder function $F_2(s)$, has all the poles of $F(s)$ except the removed pole at $s = 0$.

- When $F(s)$ is an impedance function $Z(s)$, then the removal of pole at $s = 0$ corresponds to the removal of a series arm capacitor with $C = \frac{1}{k_0}$, as shown in Fig. 12.2a.
- When $F(s)$ is an admittance function $Y(s)$, then the removal of pole at $s = 0$ corresponds to the removal of a shunt arm inductor with $L = \frac{1}{k_0}$, as shown in Fig. 12.2b.

Example 12.1 The rational function

$$F(s) = \frac{2s^3 + 3s^2 + s + 1}{2s^3 + 2s^2 + 2s}$$

has a pole at $s = 0$ and can be expressed as

$$F(s) = \frac{2s^3 + 3s^2 + s + 1}{2s^3 + 2s^2 + 2s} = \frac{k_0}{s} + F_2(s)$$

where

$$k_0 = sF(s)|_{s=0} = \left.\frac{2s^3 + 3s^2 + s + 1}{2s^2 + 2s + 2}\right|_{s=0} = \frac{1}{2}$$

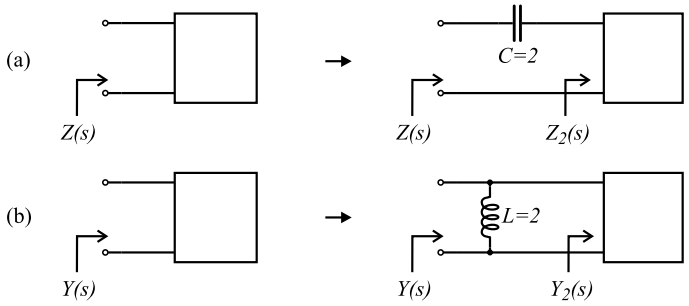

Fig. 12.3 Removal of pole $s = 0$ of from $F(s)$ of Example 12.1

The remainder function will be

$$F_2(s) = F(s) - \frac{k_0}{s} = \frac{2s^3 + 3s^2 + s + 1}{2s^3 + 2s^2 + 2s} - \frac{1}{2s} = \cdots = \frac{s(s+1)}{s^2 + s + 1}$$

- If $F(s)$ is an impedance function $Z(s) = F(s)$, then it can be synthesized as a series capacitor $C = 2$ in series with an one-port with driving-point input impedance $Z_2(s) = F_2(s)$ as shown in Fig. 12.3a.
- If $F(s)$ is an admittance function $Y(s) = F(s)$, then it can be synthesized as a shunt inductor $L = 2$ in parallel with an one-port with driving-point input admittance $Y_2(s) = F_2(s)$ as shown in Fig. 12.3b.

12.1.2 Removal of Pole at $s = \infty$

When a rational positive real function $F(s)$ has a pole at $s = \infty$ it means that the degree of the numerator polynomial is higher than the degree of the denominator polynomial and is of the form:

$$F(s) = \frac{N(s)}{D(s)} = \frac{a_N s^N + a_{N-1} s^{N-1} + \cdots + a_1 s + a_0}{b_m s^m + b_{m-1} s^{m-1} + \cdots + b_1 s + b_0} \tag{12.4}$$

with $N = m + 1$ since $F(s)$ is PR. In this case, $F(s)$ can also be expressed as

$$F(s) = k_\infty s + \frac{c_m s^m + c_{m-1} s^{m-1} + \cdots + c_1 s + c_0}{b_m s^m + b_{m-1} s^{m-1} + \cdots + b_1 s + b_0}$$

where $k_\infty = \frac{a_N}{b_m} > 0$ and the numerator polynomial of $F_2(s)$ is the first residue of the division $\frac{N(s)}{D(s)}$. Constant $k_\infty > 0$ can also be considered as the residue of the pole $s = \infty$ given by

$$k_\infty = \lim_{s \to \infty} \left(\frac{F(s)}{s} \right) > 0 \tag{12.5}$$

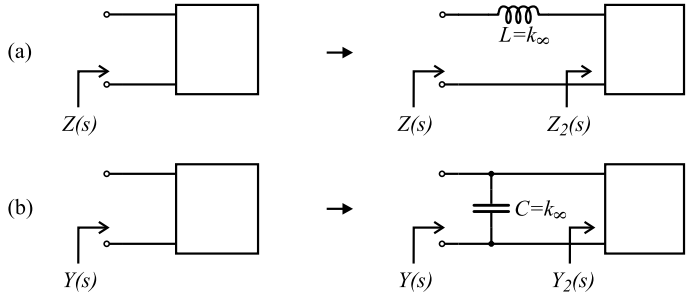

Fig. 12.4 Removal of pole $s = \infty$. (**a**) From an impedance $Z(s)$. (**b**) From an admittance $Y(s)$

The remainder function will be

$$F_2(s) = F(s) - k_\infty s$$

and the degree of the numerator polynomial of $F_2(s)$ will be equal to m, the degree of the denominator polynomial of $F(s)$. Moreover, k_∞ is positive since it is the residue of a $j\omega$-axis pole of a PR function. Therefore, $F_1(s) = k_\infty s$ is PR. The remainder function $F_2(s)$ is also positive real since:

1. The poles of $F_2(s)$ are in the left half s-plane including the $j\omega$-axis since $F_2(s)$ has the poles of $F(s)$ without the pole at $s = \infty$, which has been removed.
2. The residues of these poles are positive since they are the residues of the same poles of the positive real $F(s)$.
3. $\text{Re}[F_2(j\omega)] = \text{Re}[F(j\omega)] - \text{Re}[jk_\infty\omega] = \text{Re}[F(j\omega)] \geq 0$ since $F(s)$ is positive real.

We therefore analyzed a rational PR function with a pole at $s = \infty$ into two positive real parts from which the first, $F_1(s) = k_\infty s$, corresponds to the pole $s = \infty$ and the second, the remainder function $F_2(s)$, has all the remaining poles of $F(s)$.

- If $F(s)$ is an impedance function $Z(s) = F(s)$, then it can be synthesized as a series arm inductor $L = k_\infty$ in series with a one-port with driving-point input impedance $Z_2(s) = F_2(s)$, as shown in Fig. 12.4a.
- If $F(s)$ is an admittance function $Y(s) = F(s)$ then it can be synthesized as a shunt arm capacitor $L = k_\infty$ in parallel with an one-port with driving-point input admittance $Y_2(s) = F_2(s)$, as shown in Fig. 12.4b.

Example 12.2 The rational function

$$F(s) = \frac{s^3 + 2s^2 + 2s}{s^2 + s + 1}$$

has a pole at $s = \infty$ since the numerator is of higher degree than the denominator, and can be expressed as

$$F(s) = \frac{s^3 + 2s^2 + 2s}{s^2 + s + 1} = k_\infty + F_2(s)$$

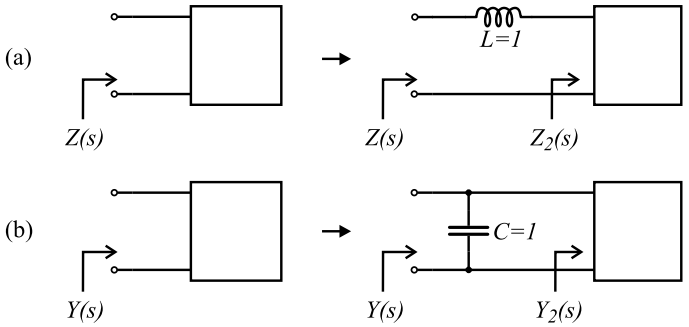

Fig. 12.5 Removal of pole $s = \infty$ from $F(s)$ of Example 12.2

where

$$k_\infty = \frac{a_N}{b_m} = \frac{1}{1} = 1$$

The remainder function will be

$$F_2(s) = F(s) - k_\infty s = \frac{s^3 + 2s^2 + 2s}{s^2 + s + 1} - s = \cdots = \frac{s(s+1)}{s^2 + s + 1}$$

- If $F(s)$ is an impedance function $Z(s) = F(s)$, then it can be synthesized as an inductor $L = k_\infty = 1$ in series with an one-port with driving-point input impedance $Z_2(s) = F_2(s)$, as shown in Fig. 12.5a.
- If $F(s)$ is an admittance function $Y(s) = F(s)$, then it can be synthesized as a capacitor $C = k_\infty = 1$ in parallel with an one-port with driving-point input admittance $Y_2(s) = F_2(s)$, as shown in Fig. 12.5b.

12.1.3 Removal of a Conjugate Pole Pair at $s = \pm j\omega_1$

When a rational positive real function $F(s)$ has an imaginary pole pair at $s = \pm j\omega_1$ it is of the form:

$$F(s) = \frac{N(s)}{(s^2 + \omega_1^2) D_2(s)} = \frac{N(s)}{(s + j\omega_1)(s - j\omega_1) D_2(s)} \tag{12.6}$$

$F(s)$ can be expanded in partial fractions as follows:

$$F(s) = \frac{k_1}{s - j\omega_1} + \frac{k_1^*}{s + j\omega_1} + \frac{N(s)}{D_2(s)} \tag{12.7}$$

where k_1 is real and therefore $k_1^* = k_1$ (see condition iii in definition II of PR functions in Chap. 11). For the calculation of the real pole residue k_1, Heaviside's formula can be used:

$$k_1 = (s - j\omega_1) F(s)|_{s=j\omega_1} = (s + j\omega_1) F(s)|_{s=-j\omega_1} \tag{12.8}$$

and therefore

$$F(s) = \frac{2k_1 s}{s^2 + \omega_1^2} + \frac{N(s)}{D_2(s)} = F_1(s) + F_2(s) \tag{12.9}$$

Function $F(s) = \frac{2k_1 s}{s^2+\omega_1^2}$ is positive real since $F_1(j\omega)$ has zero real part and its poles are located on the $j\omega$-axis. For $F_2(s)$ given by

$$F_2(s) = \frac{N(s)}{(s^2 + \omega_1^2)D_2(s)} - \frac{2k_1 s}{s^2 + \omega_1^2} = \frac{N(s) - 2k_1 s D_2(s)}{(s^2 + \omega_1^2)D_2(s)} \tag{12.10}$$

we observe that

I. Simple reasoning dictates that the numerator polynomial of $F_2(s)$ must have roots at $\pm j\omega_1$ (factor $(s^2 + \omega_1^2)$) in order to cancel out the roots of the denominator polynomial at $\pm j\omega_1$. If this pole-zero cancellation does not happen, $F_2(s)$ will still have the poles at $s = \pm j\omega_1$. Finally, the denominator polynomial of $F_2(s)$ will be $D_2(s)$.

II. The remainder $F_2(s)$ is positive real since:
   1. No new poles were introduced to $F_2(s)$.
   2. The residues of the poles of the $j\omega$-axis were not affected.
   3. $\text{Re}[F_2(j\omega)] = \text{Re}[F(j\omega)]$ since $\text{Re}[F_1(j\omega)] = 0$ and no real part has been deducted from $F(j\omega)$.

Equation (12.9) implies that

- If $F(s)$ is an impedance function $Z(s) = F(s)$, then it can be synthesized as a parallel resonant circuit in series with an one-port with driving-point input impedance $Z_2(s) = F_2(s)$, as shown in Fig. 12.6a.
- If $F(s)$ is an admittance function $Y(s) = F(s)$, then it can be synthesized as a series resonant circuit in parallel with an one-port with driving-point input admittance $Y_2(s) = F_2(s)$, as shown in Fig. 12.6b

In both cases the resonant circuits resonate at the pole frequency ω_1.

Example 12.3 The rational function

$$F(s) = \frac{s^4 + 3s^3 + 3s^2 + 3s}{(s^2 + 1)(s^2 + s + 1)}$$

has a pole pair at $s = \pm j$ and can be expressed as

$$F(s) = \frac{s^4 + 3s^3 + 3s^2 + 3s}{(s^2 + 1)(s^2 + s + 1)} = \frac{2k_1 s}{s^2 + 1} + F_2(s)$$

where

$$k_1 = (s - j)F(s)|_{s=j} = \cdots = 1$$

The remainder function will be

$$F_2(s) = F(s) - \frac{2k_1 s}{s^2 + 1} = \cdots = \frac{s(s + 1)}{s^2 + s + 1}$$

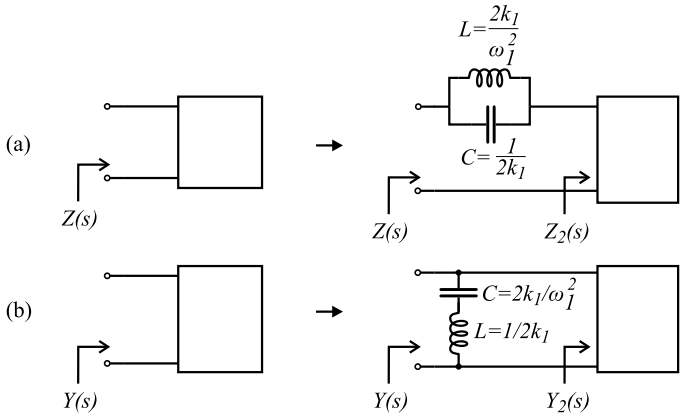

Fig. 12.6 Removal of pole pair at $s = \pm j\omega_1$. (**a**) From impedance $Z(s)$. (**b**) From admittance $Y(s)$

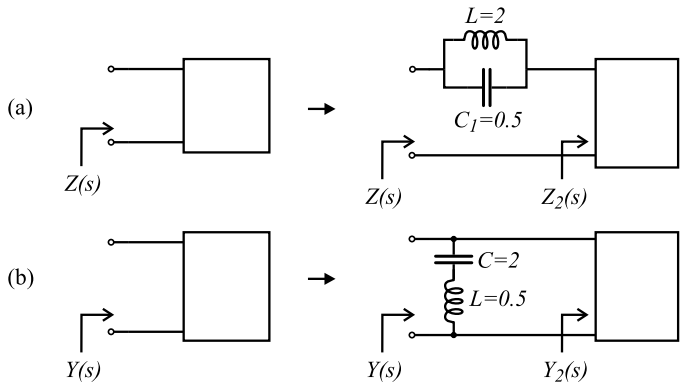

Fig. 12.7 Removal of pole pair at $s = \pm j\omega_1$ from $F(s)$ of Example 12.3

The corresponding realizations when $F(s)$ is an impedance or an admittance function are shown in Fig. 12.7a and b respectively.

12.1.4 Partial Pole Removal

Up to this point we have completely removed the $j\omega$-axis poles from a rational function. If the rational function $F(s)$ is expanded in partial fractions, a $j\omega$-axis pole removal, as presented, completely removes the associated fraction. If this partial fraction is denoted as $F_1(s)$, the remainder function is $F_2(s) = F(s) - F_1(s)$.

In partial pole removal, only a fraction $kF_1(s)$ of $F_1(s)$ is removed from $F(s)$ and the remainder function is $F_2(s) = F(s) - kF_1(s)$. If $F(s)$ is positive real, it can be shown that $F_2(s)$ is also positive real and has the same poles as $F(s)$. Partial pole

removal affects only the zeros of $F(s)$ and for this reason it is also referred to as *zero shifting*.

Example 12.4 The rational function

$$F(s) = \frac{s^3 + 2s^2 + 2s}{s^2 + s + 1}$$

has a pole at $s = \infty$ since the degree of the numerator polynomial is higher than the degree of the denominator polynomial, and can be expressed as

$$F(s) = \frac{s^3 + 2s^2 + 2s}{s^2 + s + 1} = k_\infty s + F_2(s) \quad \text{where } k_\infty = \frac{a_N}{b_m} = 1$$

The complete pole removal has been done in Example 12.4, where $F_1(s) = k_\infty s = s$ and the remainder function was

$$F_2(s) = F(s) - F_1(s) = \frac{s^3 + 2s^2 + 2s}{s^2 + s + 1} - s = \frac{s(s+1)}{s^2 + s + 1}$$

To partially remove the pole at $s = \infty$, we can for example use $k = 0.5$, in which case the remainder function will be:

$$F_2(s) = F(s) - 0.5F_1(s) = \frac{s^3 + 2s^2 + 2s}{s^2 + s + 1} - 0.5s = \frac{0.5s(s^2 + 3s + 3)}{s^2 + s + 1}$$

It should be observed that $F_2(s)$ has the same poles as $F(s)$ but different zeros. If $F(s)$ is an impedance function, it can be synthesized as an inductor $L = 0.5$ in series with an one-port with input impedance $F_2(s)$. If $F(s)$ is an admittance function, it can be synthesized as a capacitor $C = 0.5$ in parallel with an one-port with input admittance $F_2(s)$.

12.1.5 Removal of a Constant

RLCM driving-point functions $F(s)$ are positive real and therefore $\text{Re}[F(j\omega)] \geq 0$ for all real values of ω. If the real part $\text{Re}[F(j\omega)]$ has no real roots but it assumes a finite minimum value F_{MIN} at a frequency ω_1, as for example in Fig. 12.8, a constant $F_o \leq F_{MIN}$ can be removed from $F(s)$ leaving a positive real remainder function $F_2(s) = F(s) - F_o$.

If $F(s)$ is an impedance function then the removal of the constant corresponds to the removal of a series resistor of value $R = F_o$ as shown in Fig. 12.9a. If $F(s)$ is an admittance function then the removal of the constant corresponds to the removal of a parallel resistor of value $R = \frac{1}{F_o}$, as shown in Fig. 12.9b.

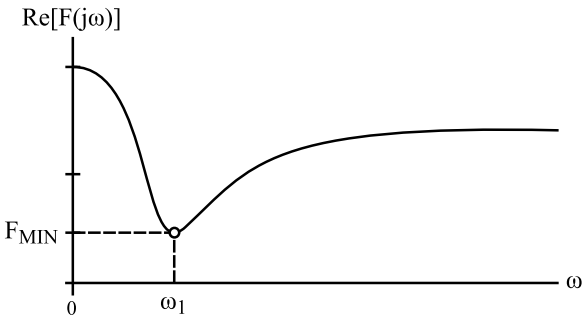

Fig. 12.8 Example of a real part with a minimum value

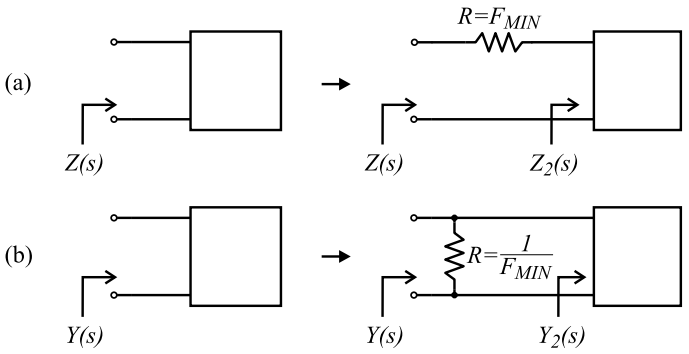

Fig. 12.9 Removal of a constant. (**a**) From an impedance. (**b**) From an admittance

12.2 Minimum Positive Real Functions

If all $j\omega$-axis poles are removed from a rational positive real driving-point function $F(s)$, the remainder function $F_a(s)$ will not have any such poles. If in addition, any $j\omega$-axis poles of $1/F_a(s)$ are removed, the remainder function $F_a(s)$ will have neither $j\omega$-axis poles nor $j\omega$-axis zeros. If $\mathrm{Re}[F_a(j\omega)]$ has a minimum value $F_{MIN} > 0$ at ω_1, a constant F_{MIN} can be removed according to Sect. 12.1.5 and the remainder function will have $\mathrm{Re}[F_a(j\omega_1)] = 0$.

Such rational positive real functions with no $j\omega$-axis poles and zeros and a frequency ω_1 at which the real part assumes zero value are referred to as *minimum positive real* functions. Minimum positive real functions have been defined by Hendrik W. Bode and are very important in RLCM circuit synthesis.

Definition of Minimum Positive Real Functions A rational positive real function $F(s)$ is defined as *minimum* if

i. $F(s)$ does not have any $j\omega$-axis poles and zeros, i.e. its numerator and denominator polynomials are strictly Hurwitz
ii. There exists a value ω_o of ω for which $\mathrm{Re}[F(j\omega_o)] = 0$ and $\mathrm{Im}[F(j\omega_o)] \neq 0$
iii. $F(s)$ assumes finite positive values for $s = 0$ and $s = \infty$

The term "minimum" is used to imply that no $j\omega$-axis poles or constants can be removed from a minimum positive real function. To minimize a positive real function $F(s)$, i.e. to make it minimum PR, all $j\omega$-axis poles must be removed from $F(s)$ and from $1/F(s)$ to satisfy condition (i.) and then the maximum possible constant must be removed to satisfy condition (ii.) of the definition. After removing any poles at $s = 0$ and $s = \infty$, condition (iii.) is automatically satisfied.

The synthesis of a positive real driving-point function $F(s)$ is in fact the procedure to minimize it by sequentially removing $j\omega$-axis poles from it or $1/F(s)$. When no more $j\omega$-axis poles and zeros exist in the remainder function $F_R(s)$, the maximum constant is removed in order to create a frequency ω_o at which for the new remainder function $F_a(s)$ we have $\text{Re}[F_a(j\omega_o)] = 0$. This synthesis procedure is demonstrated in the next example where it should be observed that $j\omega$-axis poles are removed from the more suitable function, i.e. $F_k(s)$ or $1/F_k(s)$.

Example 12.5 Synthesize the following input impedance function which has been found to be positive real:

$$Z(s) = \frac{N(s)}{D(s)} = \frac{s^8 + 13s^7 + 21s^6 + 98s^5 + 95s^4 + 195s^3 + 95s^2 + 116s + 8}{s(s^2 + 4)(s^4 + 7s^3 + 8s^2 + 10s + 1)}$$

$Z(s)$ has obvious $j\omega$-axis poles at $s = 0$, $s = \pm j2$. It also has a pole at $s = \infty$, since the degree of the numerator polynomial is 8 and that of the denominator polynomial is lower, namely 7.

1. Removal of Pole at $s = \infty$

$Z(s) = k_\infty s + Z_2(s)$ with $k_\infty = \frac{1}{1} = 1$ and therefore:

$$\begin{aligned} Z_2(s) &= Z(s) - s = \frac{N_1(s)}{D(s)} \\ &= \frac{6s^7 + 9s^6 + 60s^5 + 62s^4 + 155s^3 + 91s^2 + 116s + 8}{s(s^2 + 4)(s^4 + 7s^3 + 8s^2 + 10s + 1)} \end{aligned}$$

$Z_2(s)$ has the same denominator polynomial as $Z(s)$ but it has no pole at $s = \infty$ since this pole has been removed. This pole removal corresponds to the removal of an inductor with $L_1 = 1$ connected in series with a one-port with input impedance equal to the remainder $Z_2(s)$, as shown in Fig. 12.10a.

2. Removal of Pole at $s = 0$

The remainder impedance $Z_2(s)$ still has the pole at $s = 0$, which can be removed according to Sect. 12.1.1:

$$Z_2(s) = \frac{k_0}{s} + Z_3(s) \quad \text{where } k_0 = sZ_2(s)|_{s=0} = 2$$

$$\Rightarrow \quad Z_3(s) = Z_2(s) - \frac{2}{s} = \frac{6s^6 + 7s^5 + 46s^4 + 38s^3 + 79s^2 + 25s + 36}{(s^2 + 4)(s^4 + 7s^3 + 8s^2 + 10s + 1)}$$

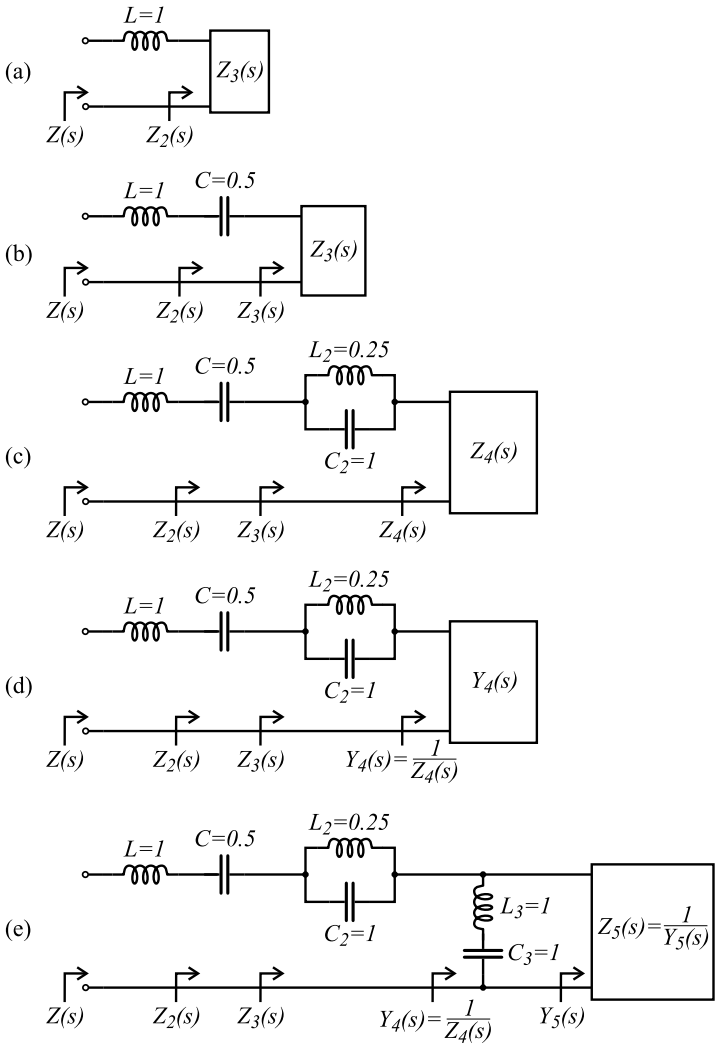

Fig. 12.10 Sequential pole removals

The $s = 0$ pole removal from an impedance function corresponds to a capacitor $C_1 = 1/k_0 = 1/2$ in series with a one-port with input impedance $Z_3(s)$, as shown in Fig. 12.10b.

3. Removal of Pole Pair at $s = \pm j2$

After removing poles $s = 0$ and $s = \infty$ from $Z(s)$, the remainder impedance function $Z_3(s)$ still has the conjugate pole pair $s = \pm j2$, which can be removed according to Sect. 12.1.3:

$$Z_3(s) = \frac{2ks}{s^2+4} + Z_4(s) \quad \text{where } k = (s-j2)Z_3(s)|_{s=j2} = 0.5$$

$$\Rightarrow \quad Z_4(s) = Z_3(s) - \frac{s}{s^2+4} = \frac{6s^6+6s^5+39s^4+30s^3+69s^2+24s+36}{(s^2+4)(s^4+7s^3+8s^2+10s+1)}$$

As expected, the numerator polynomial is exactly divided by (s^2+4), giving zero residue and quotient $6s^4+6s^3+15s^2+6s+9$ and therefore:

$$Z_4(s) = \frac{6s^4+6s^3+15s^2+6s+9}{s^4+7s^3+8s^2+10s+1}$$

The removal of the pole pair $s = \pm j2$ from the impedance function $Z_3(s)$ corresponds to a parallel resonant circuit with capacitor $C_2 = 1$ and $L_2 = 0.25$ in series with a one-port with input impedance $Z_4(s)$ as shown in Fig. 12.10c.

After the removal of the obvious $j\omega$-axis poles from $Z(s)$, impedance $Z_4(s)$ could be minimum with no $j\omega$-axis poles and zeros. This would require both numerator and denominator polynomials to be strictly Hurwitz. Applying Routh's criterion to the denominator polynomial, we find:

$$\frac{s^4+8s^2+1}{7s^3+10s} = \frac{1}{7} + \frac{1}{1.0652s + \frac{1}{0.7355s + \frac{1}{8.9348s}}}$$

Since for a 4th order denominator polynomial we get four positive partial residues, the denominator polynomial is strictly Hurwitz. Using Routh's criterion to check the numerator polynomial we get:

$$\frac{6s^4+15s^2+9}{6s^3+s} = s + \frac{9(s^2+1)}{6s(s^2+1)} = s + \frac{1}{\frac{2}{3}s}$$

Since we do not get four positive partial residues for the fourth order numerator polynomial, it is not strictly Hurwitz and it is exactly divided by s^2+1:

$$Z_4(s) = \frac{(s^2+1)(6s^2+6s+9)}{s^4+7s^3+8s^2+10s+1} \quad \Rightarrow \quad Y_4(s) = \frac{s^4+7s^3+8s^2+10s+1}{(s^2+1)(6s^2+6s+9)}$$

Therefore, $Z_4(s)$ is not minimum as it has a pair of zeros $s = \pm j$. Admittance function $Y_4(s) = 1/Z_4(s)$ has a pair of poles at $s = \pm j$, which can be removed according to Sect. 12.1.3.

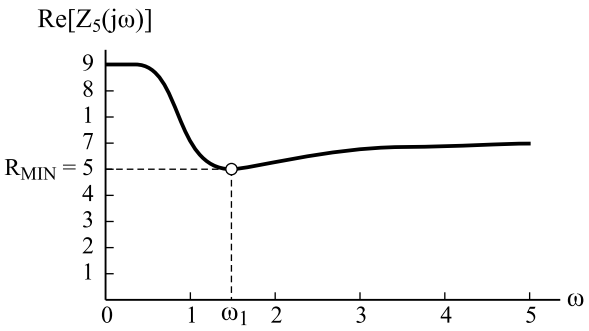

Fig. 12.11 Plot of the real part

4. Removal of Poles $s = \pm j$ from $Y_4(s)$

$$Y_4(s) = \frac{2k_4 s}{s^2+1} + Y_5(s) \quad \text{where } k_4 = (s-j)Y_4(s)|_{s=j} = \frac{-6+3j}{-12+6j} = 0.5$$

$$\Rightarrow \quad Y_5(s) = Y_4(s) - \frac{s}{s^2+1} = \frac{s^2+s+1}{6s^2+6s+9}$$

Admittance $\frac{s}{s^2+1}$ is a series resonant circuit with $L_3 = 1$ and $C_3 = 1$, as shown in Fig. 12.10e. The remainder admittance $Y_5(s)$ and impedance $Z_5(s)$ might be minimum as they have no poles or zeros on the $j\omega$-axis and assume finite positive values for $s = 0$ and $s = \infty$. The real part of $Z_5(j\omega)$ can easily be calculated (usage of $Y_5(s)$ would lead to similar results):

$$\mathrm{Re}[Z_5(j\omega)] = \mathrm{Re}\left[\frac{9-6\omega^2+j6\omega}{1-\omega^2+j\omega}\right] = \frac{6\omega^4-9\omega^2+9}{\omega^4-\omega^2+1}$$

The real part is of course non-negative for all positive ω values. For the derivative of $\mathrm{Re}[Z_5(j\omega)]$ we have

$$\frac{d}{d\omega}\mathrm{Re}[Z_5(j\omega)] = \frac{3\omega^2(\omega^2-2)}{(\omega^4-\omega^2+1)^2}$$

which assumes zero value for $\omega = 0$ and $\omega = \sqrt{2}$. Checking the second derivative, we find that for $\omega = 0$ the real part assumes maximum value 9 and for $\omega_1 = \sqrt{2}$ it assumes minimum value $R_{MIN} = 5$. The real part for $s \to \infty$ tends to 6. Figure 12.11 shows full details of this.

The absolute minimum value of $R_{MIN} = \mathrm{Re}[Z_5(j\omega_1) = 5$ can be removed from $Z_5(s)$ according to Sect. 12.1.5, and the remainder $Z_6(s)$ will be minimum positive real:

$$Z_6(s) = Z_5(s) - 5 = \frac{s^2+s+4}{s^2+s+1} \tag{12.11}$$

The final circuit is shown in Fig. 12.12.

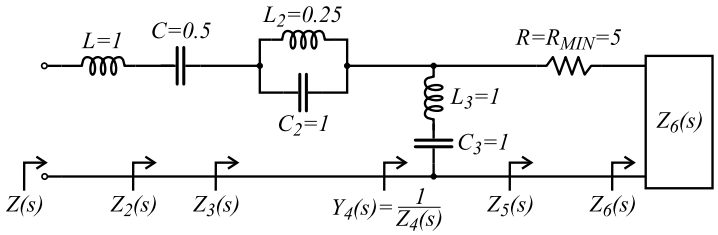

Fig. 12.12 The final circuit

Fig. 12.13 Removal of a negative inductor

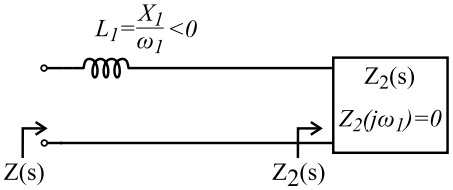

12.3 Synthesis of Minimum Positive Real Functions

When after removal of all $j\omega$-axis poles we have a minimum positive real function, special methods must be employed in order to continue the synthesis procedure. One of these methods, accredited to Brune, is presented in this section.

When a minimum positive real admittance function $Y(s)$ is given, Brune's method is applied to $Z(s) = 1/Y(s)$, which is also a minimum positive real function. For a minimum positive real impedance function $Z(s)$, for which $\mathrm{Re}[Z(j\omega_1)] = 0$, we have:

$$Z(j\omega_1) = \mathrm{Re}[Z(j\omega_1)] + j\,\mathrm{Im}[Z(j\omega_1)] = jX_1 \quad \text{where } X_1 = \mathrm{Im}[Z(j\omega_1)]$$

Quantity $X_1 = \mathrm{Im}[Z(j\omega_1)]$ is a constant which can be positive or negative. The two cases will be examined below.

12.3.1 Brune's Method with $X_1 < 0$

When $X_1 < 0$, impedance $Z(j\omega_1) = jX_1$ can be seen as a negative inductor with $L = \frac{X_1}{\omega_1}$. We can therefore see $Z(s)$ as a series connection of this negative inductor with impedance $Z_2(s)$ as follows:

$$Z(s) = \frac{X_1}{\omega_1}s + Z_2(s) \quad \Rightarrow \quad Z_2(s) = Z(s) - \frac{X_1}{\omega_1}s$$

This is shown in Fig. 12.13.

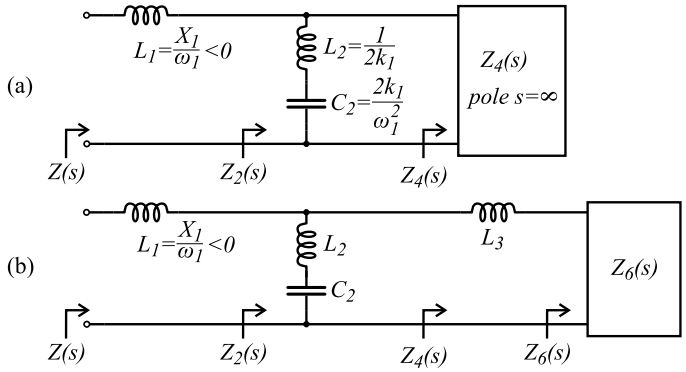

Fig. 12.14 Complete Brune's cycle

It is clear that the real part of impedance $Z_2(s)$ is equal to that of the positive real function $Z(s)$ since $-\frac{X_1}{\omega_1}s$ is added to the imaginary part of $Z(s)$. Therefore, $\mathrm{Re}[Z_2(s)]$ is positive for $\omega \geq 0$ and assumes zero value at $s = \pm j\omega_1$:

$$Z_2(j\omega_1) = Z(j\omega_1) - j\frac{X_1}{\omega_1}\omega_1 = jX_1 - jX_1 = 0$$

$Z_2(s)$ has a pole at $s = \infty$ due to the term sX_1/ω_1. Moreover, as a sum of positive real functions, $Z_2(s)$ is positive real and has a zero at $s = \pm j\omega_1$. Therefore, two pole removals are possible:

1. Removal of pole pair $s = \pm j\omega_1$ from admittance $Y_2(s) = 1/Z_2(s)$ which will give a series resonant LC circuit in parallel to the remainder admittance $Y_4(s)$ with a zero for $s = \infty$ due to the pole of $Z_2(s)$ at infinity.
2. Removal of pole $s = \infty$ from $Z_4(s) = 1/Y_4(s)$.

Removing the pole pair $s = \pm j\omega_1$ from $Y_2(s) = 1/Z_2(s)$, we get

$$Y_2(s) = \frac{1}{Z_2(s)} = \frac{2k_1 s}{s^2 + \omega_1^2} + Y_4(s)$$

where, according to (12.8), the positive quantity k_1 is the residue of the pole $s = +j\omega_1$ or $s = -j\omega_1$. The removal of the series LC circuit with admittance $\frac{2k_1 s}{s^2+\omega_1^2}$ is shown in Fig. 12.14a.

If the degree of the numerator of $Y_2(s)$ is n_4, the degree of the numerator of admittance $Y_4(s)$ will be $n_4 - 2$. Moreover, both $Y_2(s)$ and $Y_4(s)$ have zero at $s = \infty$ since $Z_2(s)$ has a pole at $s = \infty$. The pole at infinity of $Z_4(s) = 1/Y_4(s)$ can be removed as follows:

$$Z_4(s) = k_\infty s + Z_6(s) \quad \text{where } k_\infty = \left.\frac{Z_4(s)}{s}\right|_{s=\infty} = L_3 > 0$$

Since $Z_4(s)$ is PR, the pole residue $L_3 = k_\infty$ is positive and the remainder impedance $Z_6(s) = Z_4(s) - sk_\infty$ is positive real. The removal of the pole at infinity as an inductor L_3 is shown in Fig. 12.14b.

If the remainder impedance $Z_6(s)$ is not minimum, synthesis may continue by removing the $j\omega$-axis poles and any constants. If $Z_6(s)$ is minimum, the procedure must be repeated.

It must not be forgotten that the final circuit of Fig. 12.14b has a negative inductor $L_1 = \frac{X_1}{\omega_1}$, which cannot be realized with passive circuits. It can, however, be absorbed by the neighboring elements, as will be explained below.

From Fig. 12.14b we have:

$$Z(s) = sL_1 + \frac{1}{\frac{1}{sL_2+\frac{1}{sC_2}} + \frac{1}{sL_3+Z_6(s)}}$$

Impedance $Z_6(s)$ does not have a pole at infinity since it has been removed and therefore it assumes a finite value at infinity, making

$$\lim_{s\to\infty} (sL_3 + Z_6(s)) = sL_3$$

Moreover,

$$\lim_{s\to\infty} \left(sL_2 + \frac{1}{sC_2} \right) = sL_2$$

and under these conditions, we have:

$$Z(s \to \infty) = sL_1 + \frac{1}{\frac{1}{sL_2} + \frac{1}{sL_3}} = \frac{L_1L_2 + L_1L_3 + L_2L_3}{L_2 + L_3}\, s$$

Since $Z(s)$ is minimum positive real, $Z(s \to \infty)$ is finite. From the above expression, it is clear that this may happen if, and only if,

$$L_1L_2 + L_1L_3 + L_2L_3 = 0$$

Since $L_2 > 0$ and $L_3 > 0$, we have:

$$L_3 = -\frac{L_1L_2}{L_1 + L_2} \quad \Rightarrow \quad L_1 + L_2 > 0$$

$$L_2 = -\frac{L_1L_3}{L_1 + L_3} \quad \Rightarrow \quad L_1 + L_3 > 0$$

The equivalence of the circuits shown in Fig. 12.15 can be used to absorb the negative inductance introducing coupling, as shown, provided that $L_p = L_1 + L_2 > 0$, $L_s = L_2 + L_3 > 0$ and $k \leq 1$.

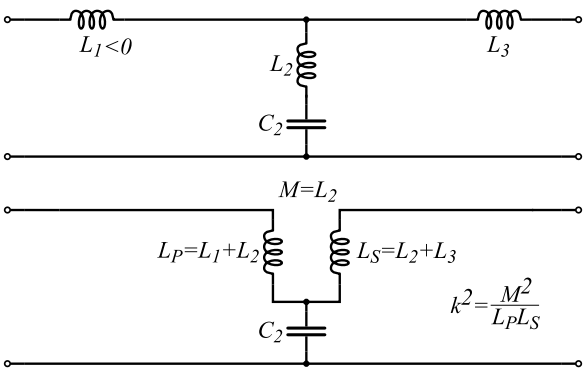

Fig. 12.15 An inductive T-circuit and its equivalent

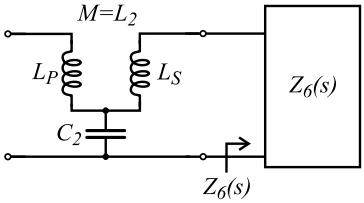

Fig. 12.16 The Brune's cycle circuit and the remainder impedance

The two first conditions have been proved above and we need only prove that $k = \frac{L_2}{\sqrt{L_p L_s}} \leq 1$:

$$k = \frac{L_2}{\sqrt{L_p L_s}} = \frac{L_2}{\sqrt{(L_1 + L - 2)(L_2 + L_3)}}$$
$$= \frac{L_2}{\sqrt{L_1 L_2 + L_1 L_3 + L_2 L_3 + L_2^2}} = \frac{L_2}{L_2} = 1$$

Therefore, all conditions are satisfied and the circuit requires an ideal transformer ($k = 1$).

The synthesis procedure until the circuit of Fig. 12.16 with the ideal transformer is reached is referred to as a *Brune cycle*. If the degrees of the numerator and denominator of the initial minimum PR impedance $Z(s)$ are N_n and N_d respectively, a Brune cycle leads to the remainder impedance $Z_6(s)$ with the degrees of both numerator and denominator polynomials reduced by 2, i.e. $N_n - 2$ and $N_d - 2$ respectively.

Example 12.6 We return to the minimum positive real impedance function of (12.11)

$$Z(s) = \frac{s^2 + s + 4}{s^2 + s + 1}$$

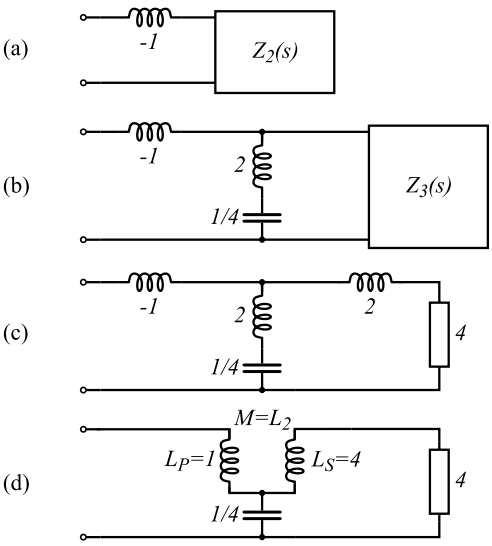

Fig. 12.17 Example Brune's synthesis

of Example 12.5. The real part $\mathrm{Re}[Z(j\omega)]$ assumes zero value for $\omega_1 = \sqrt{2}$ and $\omega_2 = -\sqrt{2}$ and

$$Z(j\omega_1) = Z(j\sqrt{2}) = -j\sqrt{2} \quad \Rightarrow \quad X_1 = -\sqrt{2} < 0$$

A negative inductor with $L_1 = \frac{X_1}{\omega_1} = -1$ can be removed as shown in Fig. 12.17a and the remainder impedance is:

$$Z_2(s) = Z(s) + s = \frac{s^3 + 2s^2 + 2s + 4}{s^2 + s + 1}$$

From the way it has been created, $Z_2(s)$ has a pair of zeros at $s = \pm j\omega_1 = \pm j\sqrt{2}$ and a pole at $s = \infty$.

Removal of pole pair $s = \pm j\sqrt{2}$ from $Y_2(s) = 1/Z_2(s)$ gives:

$$Y_2(s) = \frac{2ks}{s^2 + 2} + Y_3(s) \quad \text{where } k = (s + j\sqrt{2})Z(s)|_{s=-j\sqrt{2}} = \frac{1}{4}$$

$$\Rightarrow \quad Y_3(s) = Y_2(s) - \frac{0.5s}{s^2 + 2} = \frac{1}{2(s + 2)}$$

Therefore, $Y_2(s)$ is a series LC circuit with $L = 2$ and $C = 1/4$, as shown in Fig. 12.17b. Impedance $Z_3(s) = 1/Y_3(s) = 2s + 4$ is realized as shown in Fig. 12.17c. Finally, the negative inductance $L_1 = -1$ is absorbed using the equivalent circuit with the ideal transformer to give the final circuit of Fig. 12.17d.

12.3.2 Brune's Method with $X_1 > 0$

As we have seen, at frequency ω_1 where the real part of the minimum positive real impedance $Z(s)$ assumes zero value, i.e. $\mathrm{Re}[Z(j\omega_1)] = 0$, we have:

$$Z(j\omega_1) = j\,\mathrm{Im}[Z(j\omega_1)] = jX_1$$

The case $X_1 < 0$ has been examined in the previous section and here we consider $X_1 > 0$. At first glance, it seems that the procedure followed when $X_1 < 0$ can be repeated and a positive inductor $L_1 = \frac{X_1}{\omega_1}$ can be removed. However, since we have no way to ensure that the remainder function $Z_2(s) = Z(s) - \frac{X_1}{\omega_1}s$ is PR when $X_1 > 0$, it is better to start synthesizing the minimum PR function $Y(s) = 1/Z(s)$, which at ω_1 becomes:

$$Y(j\omega_1) = \frac{1}{\mathrm{Re}[Z(j\omega_1)] + j\,\mathrm{Im}[Z(j\omega_1)]} = \frac{1}{jX_1} = -j\frac{1}{X_1}$$

Therefore, $Y(j\omega_1)$ looks like a negative capacitor with $C_1 = -\frac{1}{\omega_1 X_1}$ and $Y(s)$ may be analyzed as shown in Fig. 12.18a with

$$Y_2(s) = Y(s) - sC_1 = Y(s) + \frac{1}{\omega_1 X_1}s \quad (X_1 > 0)$$

Admittance $Y_2(s)$, as a sum of two PR functions, is itself positive real and has a pole at $s = \infty$ and a pair of zeros $s = \pm j\omega_1$. These imaginary zeros can be removed as poles of $Z_2(s) = 1/Y_2(s)$:

$$Z_2(s) = \frac{1}{Y_2(s)} = \frac{2k_1 s}{s^2 + \omega_1^2} + Z_4(s)$$

This removal is shown in Fig. 12.18b where L_2 and C_2 are positive, since $k_1 > 0$ as the residue of the $j\omega$-axis pole of a PR function.

The pole $s = \infty$ of $Y_2(s)$ is inherited to $Z_2(s)$ and $Z_4(s)$ as zero at infinity and finally, $Y_4(s)$ has the pole $s = \infty$, which can be removed according to Sect. 12.1.2:

$$Y_4(s) = k_\infty s + Y_6(s) \quad \text{where } k_\infty > 0 \text{ from (12.5)}$$

Removal of pole $s = \infty$ from $Y_4(s)$ as a shunt capacitor $C_3 = k_\infty$ is shown in Fig. 12.18c.

The remainder $Y_6(s) = Y_4(s) - sk_\infty$ is a positive real admittance function. If $Y_6(s)$ is not minimum, synthesis may continue by removing the $j\omega$-axis poles and any constants. If $Y_6(s)$ is minimum, the Brune synthesis procedure must be repeated.

We must not forget that in the final circuit of Fig. 12.18c, there still exists a negative capacitor $C_1 = -\frac{1}{\omega_1 X_1}$, which makes the passive circuit non-realizable. Negative C_1 can, however, be absorbed by the neighboring elements as will be explained below.

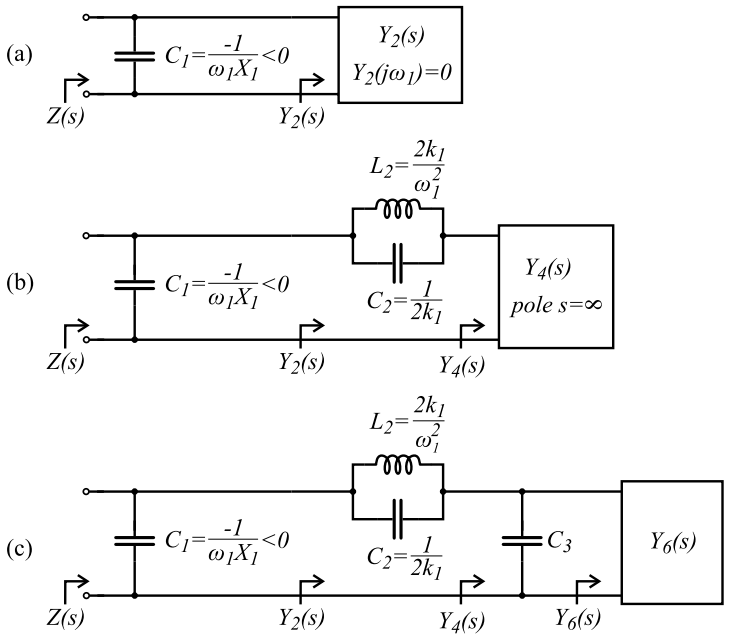

Fig. 12.18 Brune's cycle

From Fig. 12.18c, we have:

$$Y(s) = sC_1 + \frac{1}{\frac{1}{sC_2+\frac{1}{sL_2}} + \frac{1}{sC_3+Y_6(s)}}$$

Admittance $Y_6(s)$ does not have a pole at infinity since it has been removed, and therefore for $s \to \infty$ the quantity $\frac{1}{sL_2} \to 0$ and

$$Y(s \to \infty) = sC_1 + \frac{1}{\frac{1}{sC_2} + \frac{1}{sC_3}} = \frac{C_1C_2 + C_1C_3 + C_2C_3}{C_2 + C_3}\, s$$

Since $Y(s)$ is minimum positive real, $Y(s \to \infty)$ is finite. From the above expression, it is clear that this may happen if, and only if,

$$C_1C_2 + C_1C_3 + C_2C_3 = 0 \quad \Leftrightarrow \quad \frac{1}{C_1} + \frac{1}{C_2} + \frac{1}{C_3} = 0$$

Since $C_2 > 0$ and $C_3 > 0$, we have:

$$C_3 = -\frac{C_1C_2}{C_1 + C_2} > 0 \quad \Rightarrow \quad C_1 + C_2 > 0$$

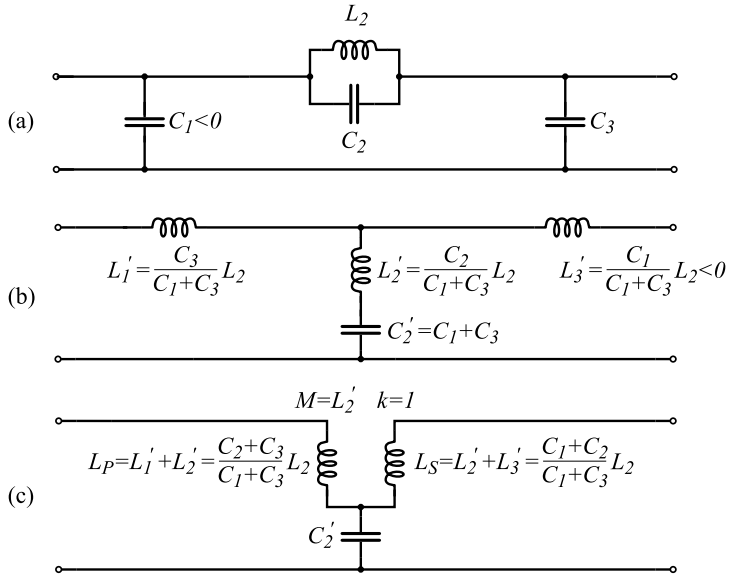

Fig. 12.19 Three equivalent circuits

Fig. 12.20 The Brune's cycle circuit and the remainder impedance

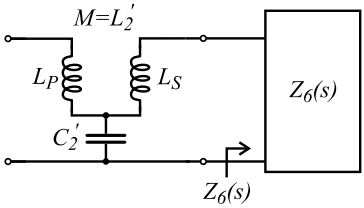

$$C_2 = -\frac{C_1 C_3}{C_1 + C_3} > 0 \quad \Rightarrow \quad C_1 + C_3 > 0$$

The above results can be combined with the equivalence of the three circuits shown in Fig. 12.19 in order to absorb the negative capacitance C_1. This, as is shown in Fig. 12.19c, introduces an ideal transformer as in the case of $X_1 < 0$.

The synthesis procedure until a circuit like the one shown in Fig. 12.20 with the ideal transformer is reached is a *Brune cycle*, and decreases the degree of both the numerator and the denominator polynomials of the initial minimum PR function $Y(s)$ by 2, leading to a PR remainder admittance $Y_6(s)$.

Final Conclusion Given a positive real impedance or admittance function $F(s)$, it can be synthesized as an RLCM circuit by removing all $j\omega$-axis poles from $F(s)$ and $1/F(s)$. When no more such poles exist in the remainder function, a constant is removed according to Sect. 12.1.5 in order to have a frequency ω_1 at which the real part of the remainder function assumes zero value. This minimum positive real func-

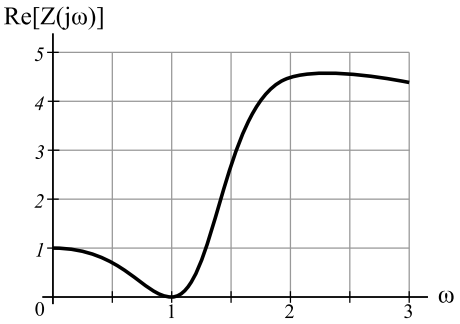

Fig. 12.21 Plot of the real part

tion can then be synthesized using Brune's method. It should be noted that Brune's method is not the only method to synthesize minimum PR driving-point functions. The Bott-Duffin method, for example, can be used to derive passive RLC circuits without transformers but their complexity makes the particular method unattractive.

Finally, in this section, it has been proven that any rational positive real function can be synthesized as a driving-point function of an one-port RLCM circuit.

Example 12.7 The rational impedance function

$$Z(s) = \frac{4s^2 + 2s + 2}{s^2 + s + 2}$$

is minimum positive real and for $\omega_1 = 1$, we have $\mathrm{Re}[F(j\omega_1)] = 0$ (see Fig. 12.21) and $\mathrm{Im}[F(j\omega_1)] = X_1 = 2$. Since $X_1 > 0$, synthesis must start from

$$Y(s) = \frac{s^2 + s + 2}{4s^2 + 2s + 2}$$

for which we have $Y(j\omega_1) = -j\frac{1}{X_1}$ and therefore $Y(s)$ can be seen as shown in Fig. 12.22a with $C_1 = -\frac{1}{\omega_1 X_1} = -\frac{1}{2}$, from which:

$$Y_2(s) = Y(s) - sC_1 = Y(s) + \frac{1}{2}s = \frac{s^3 + s^2 + s + 1}{2s^2 + s + 1}$$

$Y_2(s)$, as the sum of two PR functions is positive real. Moreover, it has a pole at infinity and a pair of zeros at $s = \pm j\omega_1 = \pm j$ which can be removed as poles of

$$Z_2(s) = \frac{2s^2 + s + 1}{s^3 + s^2 + s + 1} = \frac{2k_1 s}{s^2 + \omega_1^2} + Z_4(s) \quad \text{where } k_1 = (s - j)Z_2(s)|_{s=j} = \frac{1}{2}$$

This removal of the imaginary pole pair corresponds to a parallel LC circuit with $L_2 = 1$ and $C_2 = 1$ and is shown in Fig. 12.22b. The remainder impedance $Z_4(s)$ is

$$Z_4(s) = Z_2(s) - \frac{s}{s^2 + 1} = \frac{1}{s + 1}$$

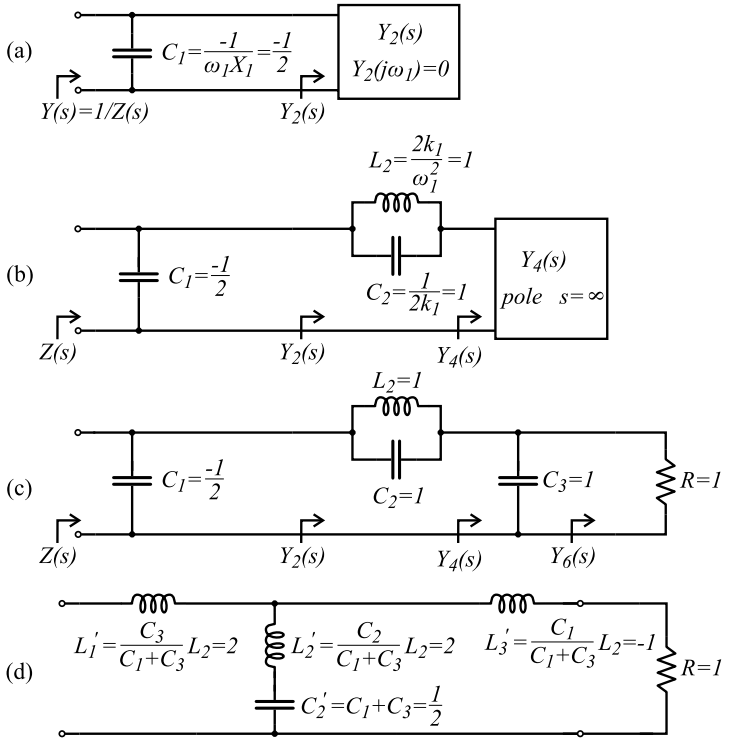

Fig. 12.22 Brune's synthesis

Fig. 12.23 Equivalent circuit

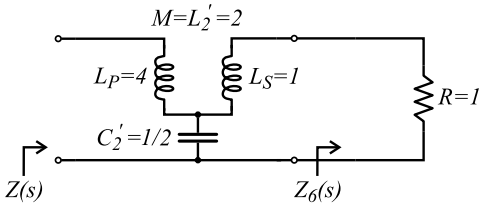

and $Y_4(s) = s + 1$ retains the pole $s = \infty$ of $Y_2(s)$, which is removed as shown in Fig. 12.22c, as a shunt capacitor $C_3 = 1$.

The Π-type circuit of Fig. 12.22c is equivalent to the T-type circuit shown in Fig. 12.22d, which has still a negative inductor. However, if for the inductor T-circuit the transformer equivalent is used with

$$L_p = \frac{C_2 + C_3}{C_1 + C_3} L_2 = 4 \qquad L_s = \frac{C_1 + C_2}{C_1 + C_3} L_2 = 1 \qquad M = \frac{C_2}{C_1 + C_3} L_2 = 2$$

we get the final circuit with a transformer, as shown in Fig. 12.23.

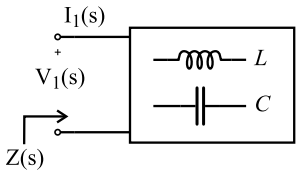

Fig. 12.24 LC one-port circuit

12.4 Synthesis of LC One-Ports

Passive lossless circuits consisting exclusively of inductors and capacitors are referred to as *LC circuits*. Due to the relatively simpler synthesis procedure, LC circuits constitute the favorite circuits category of filter designers.

12.4.1 Properties of the LC Functions

Referring to Fig. 12.24, the driving-point functions of the LC one-port circuit, $Z(s) = \frac{V_1(s)}{I_1(s)}$ and $Y(s) = 1/Z(s)$, are rational positive real functions.

The driving-point functions of LC one-port circuits have only simple $j\omega$-axis poles and zeros and both the numerator and denominator polynomials, $N(s)$ and $D(s)$ respectively, are of the form:

$$(s^2+\omega_1^2)(s^2+\omega_2^2)\cdots(s^2+\omega_n^2) \quad \text{or} \quad s(s^2+\omega_1^2)(s^2+\omega_2^2)\cdots(s^2+\omega_n^2)$$

Moreover, $Z(j\omega)$ and $Y(j\omega)$ are imaginary, with $\mathrm{Re}[Z(j\omega)] = 0$ and $\mathrm{Re}[Y(j\omega)] = 0$. From the above general expression of the numerator and denominator polynomials, it is clear that they cannot be both even or odd since this would lead to real $Z(j\omega)$ and $Y(j\omega)$. Therefore, LC driving-point functions have either even numerator and odd denominator polynomials or odd numerator and even denominator polynomials. This also implies that the difference of the degrees of the numerator and denominator polynomials is equal to 1.

Finally, the two possible forms of an LC driving-point function are given below:

$$F_{LC}(s) = \frac{(s^2+\omega_{z1}^2)(s^2+\omega_{z2}^2)\cdots(s^2+\omega_{zn}^2)}{s(s^2+\omega_{p1}^2)(s^2+\omega_{p2}^2)\cdots(s^2+\omega_{pn}^2)}$$

or

$$F_{LC}(s) = \frac{s(s^2+\omega_{z1}^2)(s^2+\omega_{z2}^2)\cdots(s^2+\omega_{zn}^2)}{(s^2+\omega_{p1}^2)(s^2+\omega_{p2}^2)\cdots(s^2+\omega_{pn}^2)}$$

It is apparent from these expressions that LC driving-point functions are odd functions, i.e. $F_{LC}(-s) = -F_{LC}(s)$.

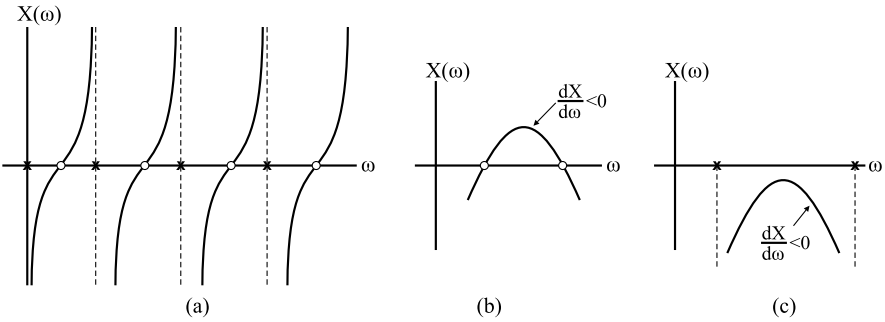

Fig. 12.25 (**a**) Reactance or susceptance plot (**b**) and (**c**) negative derivative values

Since LC driving-point functions have simple poles on the $j\omega$-axis, they can be expanded in partial functions as follows:

$$F_{LC}(s) = k_\infty s + \frac{k_0}{s} + \frac{sk_1}{s^2+\omega_{p1}^2} + \frac{sk_2}{s^2+\omega_{p2}^2} + \cdots + \frac{sk_m}{s^2+\omega_{pm}^2}$$

k_∞ and k_0 are the residues of poles at $s = \infty$ and $s = 0$ respectively and $\frac{1}{2}k_1, \frac{1}{2}k_2, \ldots, \frac{1}{2}k_m$ the residues of the imaginary poles. For $s = j\omega$, $F_{LC}(j\omega)$ can be written as:

$$\begin{aligned} F_{LC}(j\omega) &= j\left[k_\infty\omega - \frac{k_0}{\omega} + \frac{\omega k_1}{\omega_{p1}^2-\omega^2} + \frac{\omega k_2}{\omega_{p2}^2-\omega^2} + \cdots + \frac{\omega k_m}{\omega_{pm}^2-\omega^2}\right] \\ &= jX(\omega) \end{aligned} \tag{12.12}$$

$X(\omega)$ is a real function of ω referred to as the *reactance* function of the LC circuit when $F_{LC}(s)$ is an impedance, and as the *susceptance* function when $F_{LC}(s)$ is an admittance, in which case it is denoted by $B(\omega)$.

For the derivative of the reactance function, we have

$$\frac{dX(\omega)}{d\omega} = k_\infty + \frac{k_0}{\omega^2} + \frac{k_1(\omega_{p1}^2+\omega^2)}{(\omega_{p1}^2-\omega^2)^2} + \cdots \geq 0 \quad \text{for } \omega < \infty$$

and

$$\frac{dX(\omega)}{d\omega} \to k_\infty \quad \text{when } \omega \to \infty$$

Therefore, $X(\omega)$ is monotonically increasing. Taking into account that all poles and zeros are on the $j\omega$-axis, this is only possible if there is always a zero between two poles and a pole between two zeros. An indicative plot of reactance and susceptance of LC circuits is shown in Fig. 12.25a. Figures 12.25b and c show how the absence of a pole between two zeros or of a zero between two poles violates the condition for positive derivative.

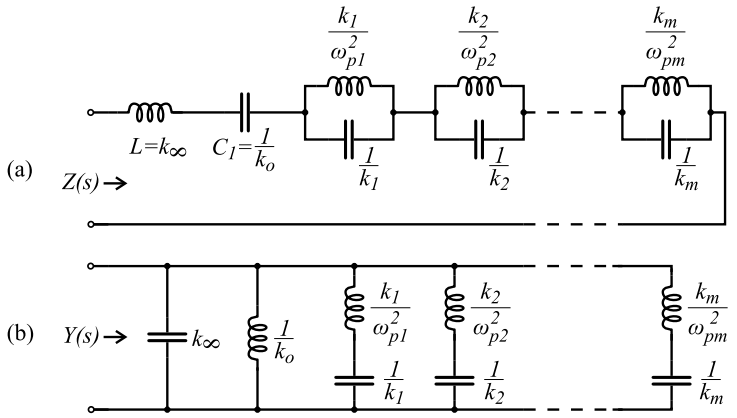

Fig. 12.26 Foster realizations

Necessary Conditions for LC Driving-Point Functions

1. LC driving-point functions are odd rational positive real functions. From the two polynomials involved, one is odd and the other is even. Both polynomials are complete, i.e. no terms are missing.
2. The difference of the degrees of the two polynomials is exactly 1.
3. All zeros and poles are simple and are located on the $j\omega$-axis.
4. There is always a pole or a zero at $s = 0$ and $s = \infty$.
5. There is a pole between two zeros and a zero between two poles.

12.4.2 Foster Realizations

LC functions can be expanded according to (12.12) as follows:

$$Z_{LC}(j\omega) = j\left[k_\infty \omega - \frac{k_0}{\omega} + \frac{\omega k_1}{\omega_{p1}^2 - \omega^2} + \frac{\omega k_2}{\omega_{p2}^2 - \omega^2} + \cdots + \frac{\omega k_m}{\omega_{pm}^2 - \omega^2}\right] = jX(\omega)$$

or

$$Y_{LC}(j\omega) = j\left[k_\infty \omega - \frac{k_0}{\omega} + \frac{\omega k_1}{\omega_{p1}^2 - \omega^2} + \frac{\omega k_2}{\omega_{p2}^2 - \omega^2} + \cdots + \frac{\omega k_m}{\omega_{pm}^2 - \omega^2}\right] = jB(\omega)$$

The above expressions suggest a straightforward synthesis method by realizing each partial fraction separately and appropriately connecting the corresponding circuits. If the function is an impedance $Z_{LC}(s)$, the circuits that correspond to each term will be connected in series, as shown in Fig. 12.26a. If the function is an admittance $Y_{LC}(s)$, the circuits that correspond to each term will be connected in parallel, as shown in Fig. 12.26b.

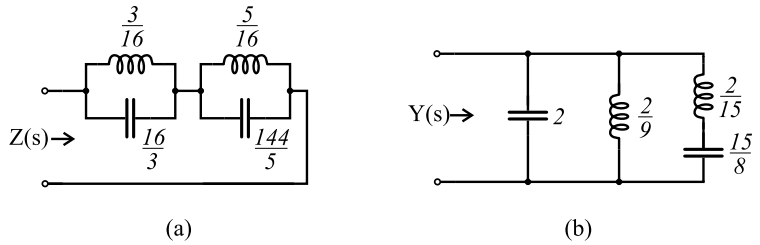

Fig. 12.27 Examples of Foster synthesis

This synthesis method, referred to as Foster's method, is in fact the sequential removal of all poles of the function and leads to the Foster realizations of Fig. 12.26, which are canonical in the sense that they employ as many lossless elements (L and C) as the degree of $Z_{LC}(s)$.

Example 12.8 Synthesize the following LC impedance function using Foster's method.

$$Z(s) = \frac{s(s^2+4)}{2(s^2+1)(s^2+9)} = \frac{s^3+4s}{2s^4+20s^2+18}$$

The poles of $Z(s)$ are $s = \pm j$ and $s = \pm j3$ and therefore it can be expanded in partial fractions as follows:

$$Z(s) = \frac{s(s^2+4)}{2(s^2+1)(s^2+9)} = \frac{k_1 s}{s^2+1} + \frac{k_2 s}{s^2+9}$$

$$k_1 = \frac{s^2+1}{s} Z(s)\Big|_{s^2=-1} = \frac{3}{16} \qquad k_2 = \frac{s^2+9}{s} Z(s)\Big|_{s^2=-9} = \frac{5}{16}$$

$$\Rightarrow \quad Z(s) = \frac{\frac{3}{16}s}{s^2+1} + \frac{\frac{5}{16}s}{s^2+9}$$

This can be realized as the series connection of two parallel resonant circuits, as shown in Fig. 12.27a.

If the driving-point admittance function

$$Y(s) = \frac{2(s^2+1)(s^2+9)}{s(s^2+4)} = \frac{2s^4+20s^2+18}{s^3+4s}$$

had been given, then

$$Y(s) = \frac{2s^4+20s^2+18}{s^3+4s} = \frac{2(s^2+1)(s^2+9)}{s(s^2+4)} = k_\infty s + \frac{k_0}{s} + \frac{k_1 s}{s^2+4}$$

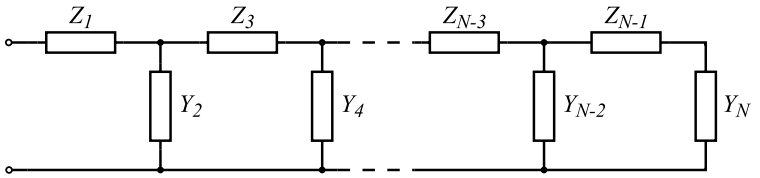

Fig. 12.28 Ladder passive LC circuit structure

where

$$k_\infty = \left.\frac{Y(s)}{s}\right|_{s\to\infty} = 2 \qquad k_0 = sY(s)|_{s=0} = 4.5 \qquad k_1 = \left.\frac{s^2+4}{s}Y(s)\right|_{s^2=-4} = 7.5$$

Finally

$$Y(s) = 2s + \frac{4.5}{s} + \frac{7.5}{s^2+4}$$

which can be realized as shown in Fig. 12.27b.

12.4.3 Cauer Realizations

Cauer methods for the synthesis of LC impedance or admittance functions are based on the sequential removal of poles at $s = \infty$ or $s = 0$ from a function $F(s)$ and $1/F(s)$. Each removal corresponds to a lossless element and finally the so-derived circuits have the ladder topology shown in Fig. 12.28.

12.4.3.1 Cauer Synthesis I: Sequential Removal of Poles $s = \infty$

Given an LC driving-point function $F(s)$, the higher order polynomial may be that of the numerator or the denominator. If the higher order polynomial is in the numerator, then $F(s)$ has a pole at $s = \infty$. If the denominator polynomial of $F(s)$ is of higher order, then in $1/F(s)$ the numerator polynomial will be of higher order and $1/F(s)$ will have a pole at $s = \infty$.

Cauer synthesis I (or first Cauer realization) starts from the function (impedance or admittance) with the pole $s = \infty$, which is removed, and in the remainder function $F_2(s)$, the degree of the denominator polynomial is higher than the degree of the numerator polynomial so that a pole $s = \infty$ can be removed from $1/F_2(s)$. This procedure continues until all arms of the ladder have been derived. If, for example, $Z(s)$ has a pole $s = \infty$ (higher degree polynomial in the numerator), it can be removed as an inductor $L_1 = k_{\infty 1}$ according to Sect. 12.1.2. This is shown in Fig. 12.29b. If in the given $Z(s)$, the higher order polynomial is in the denominator, then $Y(s) = 1/Z(s)$ has the pole $s = \infty$. This pole can be removed as a capacitor $C_1 = k_{\infty 1}$ in parallel with the remainder admittance $Y_2(s) = Y(s) - sC_1$, which is still an LC admittance (Fig. 12.29a).

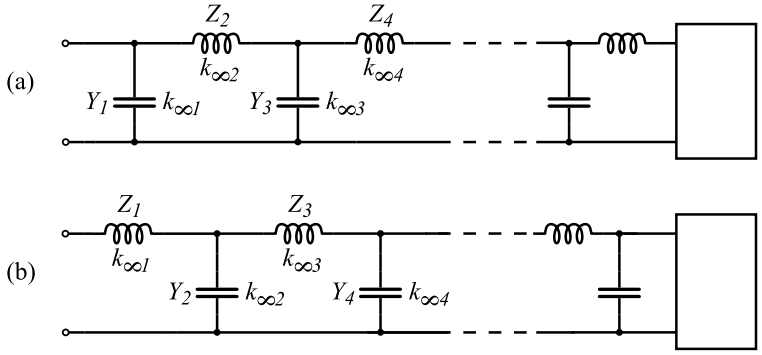

Fig. 12.29 Cauer ladder synthesis

Cauer synthesis I, as has been presented with the sequential removals of poles at $s = \infty$, is equivalent to expanding the function with the pole $s = \infty$ in continued-fraction around infinity as follows:

$$Z(s) = k_{\infty 1}s + \cfrac{1}{k_{\infty 2}s + \cfrac{1}{k_{\infty 3}s + \cfrac{1}{k_{\infty 4}s + \cdots}}} = Z_1(s) + \cfrac{1}{Y_2(s) + \cfrac{1}{Z_3(s) + \cfrac{1}{Y_4(s) + \cdots}}}$$

or

$$Y(s) = k_{\infty 1}s + \cfrac{1}{k_{\infty 2}s + \cfrac{1}{k_{\infty 3}s + \cfrac{1}{k_{\infty 4}s + \cdots}}} = Y_1(s) + \cfrac{1}{Z_2(s) + \cfrac{1}{Y_3(s) + \cfrac{1}{Z_4(s) + \cdots}}}$$

12.4.3.2 Cauer Synthesis II: Sequential Removal of Poles $s = 0$

Cauer synthesis II (or second Cauer realization) is based on sequential pole removals at $s = 0$ from alternating impedance and admittance functions. LC functions have a pole or a zero at $s = 0$. If the given function has the pole $s = 0$, the procedure starts from this function by removing the pole at zero. If the given function $F(s)$ does not have the pole at zero, then $1/F(s)$ will have it and the procedure starts from $1/F(s)$. If, for example, the given $Z(s)$ has the pole $s = 0$, then

$$Z(s) = \frac{k_{o1}}{s} + Z_2(s) \quad \left(\text{capacitor } C = \frac{1}{k_{o1}} \text{ in series with } Z_2(s)\right)$$

This procedure leads to a ladder circuit of the form shown in Fig. 12.30b. If $Z(s)$ has zero at $s = 0$, then $Y(s) = 1/Z(s)$ will have the pole $s = 0$, which can be removed:

$$Y(s) = \frac{k_{o1}}{s} + Y_2(s) \quad \left(\text{inductor } L = \frac{1}{k_{o1}} \text{ in parallel with } Y_2(s)\right)$$

The procedure leads to a ladder circuit of the form shown in Fig. 12.30a.

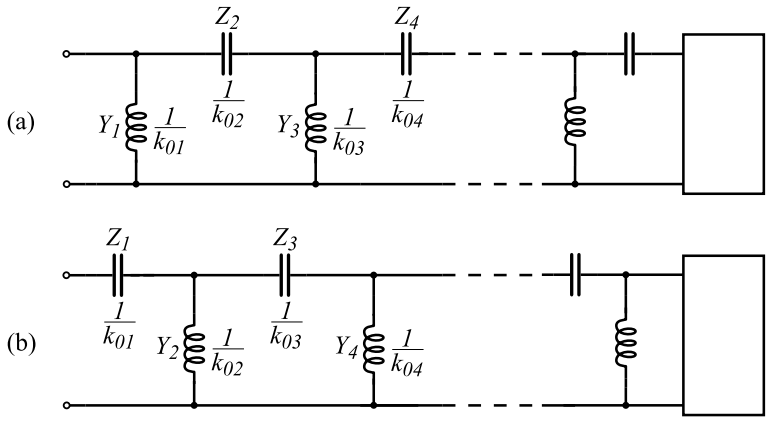

Fig. 12.30 Cauer synthesis II

Cauer synthesis II, as has been presented with the sequential removals of poles at $s = 0$, is equivalent to expanding the function with the pole $s = 0$ in continued-fraction around zero as follows:

$$Z(s) = \frac{k_{o1}}{s} + \cfrac{1}{\frac{k_{o2}}{s} + \cfrac{1}{\frac{k_{o3}}{s} + \cfrac{1}{\frac{k_{o4}}{s} + \cdots}}} = Z_1(s) + \cfrac{1}{Y_2(s) + \cfrac{1}{Z_3(s) + \cfrac{1}{Y_4(s) + \cdots}}}$$

or

$$Y(s) = \frac{k_{o1}}{s} + \cfrac{1}{\frac{k_{o2}}{s} + \cfrac{1}{\frac{k_{o3}}{s} + \cfrac{1}{\frac{k_{o4}}{s} + \cdots}}} = Y_1(s) + \cfrac{1}{Z_2(s) + \cfrac{1}{Y_3(s) + \cfrac{1}{Z_4(s) + \cdots}}}$$

Example 12.9 Use Cauer synthesis I and II to synthesize the LC impedance function

$$Z(s) = \frac{6s^5 + 20s^3 + 10s}{6s^4 + 17s^2 + 2}$$

Since $Z(s)$ has the pole at infinity required for Cauer synthesis I, it can be removed as follows:

$$Z(s) = k_{\infty 1}s + Z_2(s) \quad \text{where } k_{\infty 1} = \frac{6}{6} = 1 \quad \Rightarrow \quad Z_2(s) = \frac{3s^3 + 8s}{6s^4 + 17s^2 + 2}$$

Removal of the pole $s = \infty$ from $Z(s)$ gives an inductor $L_1 = k_{\infty 1} = 1$ connected in series to the remainder impedance $Z_2(s)$, which no longer has the pole at $s = \infty$. Synthesis must continue with

$$Y_2(s) = \frac{1}{Z_2(s)} = \frac{6s^4 + 17s^2 + 2}{3s^3 + 8s}$$

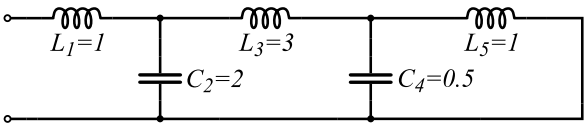

Fig. 12.31 Example Cauer synthesis I

by removing the pole at $s = \infty$:

$$Y_2(s) = k_{\infty 2}s + Y_3(s) \quad \text{where } k_{\infty 2} = \frac{6}{3} = 2 \quad \Rightarrow \quad Y_3(s) = \frac{s^2+2}{3s^3+8s}$$

Removal of the pole $s = \infty$ from $Y_2(s)$ gives a capacitor $C_2 = k_{\infty 2} = 2$ connected in parallel to the remainder admittance $Y_3(s)$, which has no pole at $s = \infty$, and synthesis must continue with

$$Z_3(s) = \frac{3s^3+8s}{s^2+2}$$

from which the pole at infinity is removed:

$$Z_3(s) = k_{\infty 3}s + Z_4(s) \quad \text{where } k_{\infty 3} = \frac{3}{1} = 3 \quad \Rightarrow \quad Z_4(s) = \frac{2s}{s^2+2}$$

Removal of the pole $s = \infty$ from $Z_3(s)$ gives an inductor $L_3 = k_{\infty 3} = 3$ connected in series to the remainder impedance $Z_4(s)$, which has no pole at $s = \infty$, and synthesis must continue with

$$Y_4(s) = \frac{s^2+2}{2s} = 0.5s + \frac{1}{s}$$

the realization of which is straightforward. The circuit that corresponds to the above presented Cauer I synthesis procedure is shown in Fig. 12.31.

The continuous fraction expansion of $Z(s)$ is given below:

$$Z(s) = s + \cfrac{1}{2s + \cfrac{1}{3s + \cfrac{1}{0.5s + \cfrac{1}{s}}}}$$

For the second Cauer realization, we need a pole at $s = 0$ to start with. Such a pole is available in

$$Y(s) = \frac{1}{Z(s)} = \frac{6s^4+17s^2+2}{6s^5+20s^3+10s}$$

and when removed yields:

$$Y(s) = \frac{k_{o1}}{s} + Y_2(s) \quad \text{where } k_{o1} = sY(s)|_{s=0} = \frac{1}{5}$$

The pole removal gives an inductor $L_1 = \frac{1}{k_{o1}} = 5$ connected in parallel to $Y_2(s)$

$$Y_2(s) = Y(s) - \frac{1}{5s} = \frac{24s^3 + 65s}{5(6s^4 + 20s^2 + 10)}$$

which does not have the pole at $s = 0$, and synthesis must continue with $Z_2(s)$, which has the required pole:

$$\begin{aligned} Z_2(s) &= \frac{1}{Y_2(s)} = \frac{5(6s^4 + 20s^2 + 10)}{24s^3 + 65s} \\ &= \frac{k_{o2}}{s} + Z_3(s) \quad \text{where } k_{o2} = sZ_2(s)|_{s=0} = \frac{10}{13} \end{aligned}$$

This is a capacitor $C_2 = \frac{1}{k_{o2}} = \frac{13}{10}$ in series with the remainder impedance $Z_3(s)$:

$$Z_3(s) = Z_2(s) - \frac{10}{13s} = \frac{5(78s^3 + 212s)}{13(24s^2 + 65)}$$

The pole $s = 0$ is now present in $Y_3(s) = 1/Z_3(s)$ and can be removed as follows:

$$Y_3(s) = \frac{13(24s^2 + 65)}{5(78s^3 + 212s)} = \frac{k_{o3}}{s} + Y_4(s) \quad \text{where } k_{o3} = sY_3(s)|_{s=0} = \frac{169}{212}$$

Therefore, $Y_3(s)$ is an inductor with

$$L_3 = \frac{1}{k_{o3}} = \frac{212}{169} = 1.2544$$

in parallel to the remainder admittance

$$Y_4(s) = Y_3(s) - \frac{169}{212s} = \frac{\frac{117}{1060}s}{39s^2 + 106}$$

The pole at $s = 0$ can now be removed from $Z_4(s) = 1/Y_4(s)$:

$$\begin{aligned} Z_4(s) &= \frac{39s^2 + 106}{\frac{117}{1060}s} = \frac{k_{o4}}{s} + Z_5(s) \\ &\text{where } k_{o4} = sZ_4(s)|_{s=0} = \frac{106 \cdot 1060}{117} = 960.3419 \end{aligned}$$

This pole removal yields a capacitor $C_4 = \frac{1}{k_{o4}} = 1/960.3419$ connected in series with the remainder impedance

$$Z_5(s) = Z_4(s) - \frac{1}{sC_5} = \frac{1060}{3}s$$

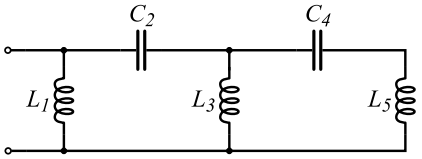

Fig. 12.32 Example Cauer synthesis II

which is an inductor with $L_5 = \frac{1060}{3} = 353.33$. The final circuit is shown in Fig. 12.32.

The corresponding continuous fraction expansion of $Y(s)$ is given below:

$$Y(s) = \frac{1}{5s} + \cfrac{1}{\frac{10}{13s} + \cfrac{1}{\frac{169}{212s} + \cfrac{1}{\frac{960.3419}{s} + \cfrac{1}{353.33s}}}}$$

It should be noted that the one-port circuits shown in Figs. 12.31 and 12.32 both have

$$Z(s) = \frac{6s^5 + 20s^3 + 10s}{6s^4 + 17s^2 + 2}$$

12.5 Problems

12.1 Synthesize impedance $Z(s) = \frac{s^2+2}{s^3+4s}$ using sequential removals of poles at $s = 0$.

12.2 Synthesize impedance $Z(s) = \frac{s^2+2}{s^3+4s}$ using sequential removals of poles at $s = \infty$.

12.3 Synthesize impedance $Z(s) = \frac{2s^4+4s^2+1}{s^3+s}$ using only removals of poles at $s = 0$.

12.4 Synthesize impedance $Z(s) = \frac{2s^4+4s^2+1}{s^3+s}$ using only removals of poles at $s = \infty$.

12.5 Synthesize impedance $Z(s) = \frac{2s^4+4s^2+1}{s^3+s}$ using only removals of complex conjugate pole pairs.

12.6 In Example 12.5, the $j\omega$-axis poles have been removed from the impedance function

$$Z(s) = \frac{N(s)}{D(s)} = \frac{s^8 + 13s^7 + 21s^6 + 98s^5 + 95s^4 + 195s^3 + 95s^2 + 116s + 8}{s(s^2+4)(s^4 + 7s^3 + 8s^2 + 10s + 1)}$$

in the order $s = \infty$, $s = 0$ and $s = \pm j2$. Remove the same poles in the reverse order to verify that the remainder function will be the same, namely:

$$Z_4(s) = \frac{6s^4 + 6s^3 + 15s^2 + 6s + 9}{s^4 + 7s^3 + 8s^2 + 10s + 1}$$

12.7 Synthesize

$$Y(s) = \frac{2(s^2 + 1)(s^2 + 9)}{s(s^2 + 4)} = \frac{2s^4 + 20s^2 + 18}{s^3 + 4s}$$

using Cauer synthesis I (sequential removals of poles at $s = \infty$).

12.8 Synthesize

$$Y(s) = \frac{2(s^2 + 1)(s^2 + 9)}{s(s^2 + 4)} = \frac{2s^4 + 20s^2 + 18}{s^3 + 4s}$$

using Cauer synthesis II (sequential removals of poles at $s = 0$).

12.9 Synthesize

$$Z(s) = \frac{s^2 + 0.6608s + 1.0108}{1.5296s + 1.0108}$$

by sequential removals of poles at infinity (Cauer I).

12.10 Synthesize

$$Z(s) = \frac{0.3824s + 0.2527}{s^2 + 0.6608s + 1.0108}$$

by sequential removals of poles at infinity (Cauer I).

12.11 Synthesize

$$Z(s) = \frac{1.2529s^2 + 0.7849s + 0.47713}{s^3 + 0.62646s^2 + 1.14245s + 0.47713}$$

by sequential removals of poles at infinity (Cauer I).

12.12 Synthesize

$$Z(s) = \frac{s^4 + 0.427707s^3 + 5.002818s^2 + 1.857231s + 2.30123}{6.268238s^3 + 2.680969s^2 + 9.520648s + 2.30123}$$

by sequential removals of poles at infinity.

References[1]

1. Belevitch, V.: Classical Network Theory. Holden-Day, Oakland (1968)
2. Chen, W.-K. (ed.): Passive, Active and Digital Filters. The Circuits and Filters Handbook, vol. V. CRC Press, Boca Raton (2009)
3. Daniels, R.W.: Approximation Methods for Electronic Filter Design. McGraw-Hill, New York (1974)
4. Guillemin, E.A.: The Mathematics of Circuit Analysis. Willey, New York (1949)
5. Guillemin, E.A.: Synthesis of Passive Networks. Krieger, Melbourne (1977)
6. Lutovac, M.D., Tosic, O., Dejan, V., Evans, B.L.: Filter Design for Signal Processing Using MATLAB and Mathematica. Prentice Hall, Upper Saddle River (2001)
7. Sedra, A., Bracket, P.O.: Filter Theory and Design: Active and Passive. Pitman, London (1978)
8. Temes, G.C., LaPatra, J.W.: Introduction to Circuit Synthesis and Design. McGraw-Hill, New York (1977)
9. Van Valkenburg, M.E.: Introduction to Modern Network Synthesis. Wiley, New York (1966)
10. Van Valkenburg, M.E.: Analog Filter Design. Oxford University Press, London (1982)
11. Weinberg, L.: Network Analysis and Synthesis. McGraw-Hill, New York (1962)

[1] All references, whether or not cited within the text, are recommended for further reading.

Index

0–9
3 dB frequency
  Butterworth filters, 46
  Chebyshev filters, 70
3-OA biquads, 493

A
AGM, *see* arithmetic-geometric mean
Akerberg-Mossberg biquad, 494
All-pole functions, 449
Allpass filter, 7
Amplitude distortion, 4
Approximating polynomial, 40
Approximation, 18, 37, 40
  all-pole, 103
  Butterworth, 19, 41
  Chebyshev, 19, 59
  elliptic, 19, 165
  inverse Chebyshev, 110
  inverse Pascal, 130
  Pascal, 19, 77
  polynomial, 103
  rational, 104
Arithmetic-geometric mean, 169
  calculation of elliptic integral, 169
  calculation of elliptic sine, 169
  definition, 170
Attenuation, 1
  effective, 263

B
Back-to-back connection, 370
Band-elimination, *see* band-reject
Band-reject, 11
  bandwidth, 238
  filter design, 213
Bandpass filter design, 213
Bandpass filters, 11
Bandstop, *see* band-reject
Bandwidth
  band-reject filter, 11, 238
  bandpass filter, 11, 227
Biquadratic form, 449
Biquads, 449
Brune cycle, 554, 558
Brune's method, 551
Brune's theorem, 529
Bruton L.T., 380
Buffer, *see* voltage follower
Butterworth, 41
  3 dB frequency, 46
  approximation, 41
  cut-off rate, 47
  fractional order, 44
  gain function, 42
  integer order, 42
  optimization, 44
  order, 42
  order equation, 44
  passive filters, 291
  prototype filters, 53
  transfer function, 49

C
Canonic circuits, 32
Canonical circuits, 298
Cauer
  realization, 565
  synthesis I, 565
  synthesis II, 566
Cauer approximation, *see* elliptic approximation
Center frequency
  band-reject filter, 11
  bandpass filter, 11
Center frequency of BP filter, 227
Center frequency of BR filter, 238
Characteristic function, 267

H.G. Dimopoulos, *Analog Electronic Filters*, Analog Circuits and Signal Processing,
DOI 10.1007/978-94-007-2190-6, © Springer Science+Business Media B.V. 2012

Chebyshev
3 dB frequency, 70
cut-off rate, 70
decimal order, 65
even order passive, 313
integer order, 65
modified approximation, 317
optimization, 67
order equation, 65
passive filters, 309
polynomial, 60
prototype filters, 73
prototype transfer functions, 94
transfer function, 71
Circuit order, 30
Common-Mode Gain, 444
Common-Mode Rejection Ratio, 444
Comparator, 444
Complete elliptic integral, 167
calculation, 169
Complex power, 254
Continued fraction property, 514
Conversion function, 487
Cross-cascade connection, 387
Current mirrors, 411
Cut-off frequency, 5
Cut-off rate
Butterworth, 47
Chebyshev, 70

D

Deboo integrator, 441
Decimal order
Butterworth, 42
Chebyshev, 65
elliptic, 182
Pascal, 86
Delay, 5
Delay equalizer, 464
Denormalization, 26
Differentiator, 424
Discrimination factor, 174
Distortion
amplitude, 4
group delay, 5
phase, 4

E

Effective attenuation, 263
Effective parameters, 261
Elliptic
even order passive, 359
Elliptic approximation, 165
design tables, 206
discrimination factor, 174
modified, 361
optimization, 184
order equation, 182
order nomograph, 204
passive filters, 351
poles and zeros, 190
transfer function, 190
Elliptic integral
complete, 167
non-complete, 168
Elliptic rational function, 172
definition, 172
poles and zeros, 172
properties, 173
Elliptic sine, 169
calculation, 169
ERF, *see* elliptic rational function
Even order
passive Chebyshev filters, 313
passive elliptic filters, 359
passive Pascal filters, 339

F

FDNR, 380
Feldtkeller's equation, 290, 336
Filter-appropriate Pascal polynomial, 80
Filters
active-RC, 14
continuous-time, 12
crystal, 14
current-mode, 14
discrete-time, 12
integrated, 14
mechanical, 14
microwave, 14
passive, 14
prototype, 29
sampled-data, 12
switched capacitor, 14
Floating inductor, 370
Foster method, 563
Fractional order
Butterworth, 44
Chebyshev, 65
elliptic, 182
Frequency dependent impedance scaling, 380
Frequency response
magnitude, 1
phase, 1
Frequency transformations, 213
lowpass to band-reject, 237
lowpass to bandpass, 227

Frequency transformations (*cont.*)
lowpass to highpass, 213
RC-CR, 218

G
Gain
function, 1
logarithmic, 1
plain, 1
plots, 3
Group delay, 5

H
Highpass
filter design, 213
filters, 10
notch, 462
transformation, 213
Hurwitz
continued fraction property, 514
polynomial, 513, 517
polynomial (strictly), 517
Hurwitz test, 518

I
Ideal filter
allpass, 7
band-reject, 6
bandpass, 6
highpass, 6
lowpass, 5
impulse response, 6
Ideal transmission, 4
Immitance function, 529
Impedance matching, 258
Insertion parameters, *see* effective parameters
Integer order
Butterworth, 42
Chebyshev, 65
Pascal, 86
Integrator, 435
Deboo, 441
inverting, 421, 436
loss, 424
lossy, 422
Miller, 421
non-inverting, 440
Inverse Chebyshev approximation, 110
Inverse Pascal approximation, 130
definition, 137
design, 140
design tables, 153
order, 141
transfer function, 146
Inverting voltage amplifier, 417

J
Jacobi elliptic sine, 169

K
KHN circuit, 496

L
Ladder filters, 15
Lattice filters, 15
LC circuits, 561
LC functions, 561
LC synthesis, 561
Leap-frog filters, 395
Linear Transformation Active Filters, 383
cross-cascade connection, 387
input termination, 388
output termination, 390
transformation matrix, 384
Load, 7
Logarithmic gain, 1
Lossy integrator, 422
Lowpass filters, 8
Lowpass to band-reject transformation, 237
Lowpass to bandpass transformation, 227
Lowpass to highpass transformation, 213
Lowpass-notch, 462
LP-BP transformation, 227
LP-BR transformation, 237
LP-HP transformation, 213
LTA, *see* Linear Transformation Active Filters

M
Matching, *see* impedance matching
Maximally flat, 43
Maximum power transfer theorem, 258
Minimum positive real, 546, 551
Modified Chebyshev approximation, 317
Modified Pascal approximation, 349
Modified transmission matrix, 384

N
Natural frequencies, 449
Negative impedance converter, 432
NIC, *see* negative impedance converter
Nome, 170
Normalization, 17, 22, 25
Notch, *see* band-reject, 462
Notch-highpass, 462
Notch-lowpass, 462

O
OA, *see* op amp
One-pole model, 409

Op amp
CMG, 444
CMRR, 444
current-mode, 411
imperfections, 442
integrator model, 410
one-pole model, 409
open-loop bandwidth, 409
open-loop gain, 405
slew rate, 443
voltage-mode, 404
Open-loop bandwidth, 409
Operational amplifier, *see* op amp
Order equation
Butterworth, 44
Chebyshev, 65
elliptic approximation, 182
Order of circuit, 30, 449

P
Partial fractions, 528
Pascal
approximation, 77
even order passive filters, 339
modified approximation, 349
optimization, 84
order calculation, 86
order nomograph, 86
passive filters, 332
polynomial, 80
transfer function, 86
Passband, 8
Passive filters
Butterworth, 291
Chebyshev, 309
elliptic, 351
Pascal, 332
Phase distortion, 4
Phase equalizer, 464
Phase response, 1
Plain gain, 1
Pole removals, 537
constant, 545
imaginary pole pair at $s = \pm j\omega_1$, 542
partial removal, 544
pole at $s = 0$, 538
pole at $s = \infty$, 540
Pole residue, 528
Pole-zero diagram, 519
Polynomial, 509
degree, 509
even part, 512
Hurwitz, 513
odd part, 512
remainder theorem, 511
roots, 509
strictly Hurwitz, 513, 517
Positive real
definition I, 529
definition II, 530
definition III, 532
function, 529
property, 529
Power
apparent, 255
average, 255
complex, 254
factor, 255
maximum transfer, 258
reactive, 255
real, 255
reflected, 265
Precise filter design method, 253
Prototype cutoff frequency, 453
Prototype filters, 29
Butterworth, 53
Chebyshev, 73

Q
Quality factor, 449

R
Rational approximations, 103
definition, 104
elliptic, 165
inverse Chebyshev, 110
inverse Pascal, 130
Rational functions, 519
RC-CR transformation, 218
Reactance, 562
Realizable
band-reject filter, 11
bandpass filter, 11
highpass filter, 10
lowpass filter, 8
Reflected power, 265, 266
Reflection coefficient, 265, 267
Reflectionless impedance matching, 258
Remainder function, 537
Remainder theorem, 511
Residue, *see* pole residue
Routh criterion, 517
Routh test, 518

S
SAB, 468
Scaling, 17, 22
frequency, 17, 24

Scaling (*cont.*)
impedance, 17, 23
normalization, 17
Second order functions, 451
Second order LP functions, 451
Selectivity, 8
Simulated inductor, 366
a general approach, 373
Antoniou's, 369
floating, 370
grounded, 367, 369, 377
Riordan's, 366
Simulation of
inductors, 366
ladder filters, 365
Single amplifier biquads, 468
Slew rate, 443
Source, 7
State variable filter, 496
Stopband, 8
Stopband edge frequency, 9
Strictly Hurwitz polynomial, 513, 517
Sturm's theorem, 521
Su Kendal L., 207
Subtractor, 425
Supercapacitor, *see* FDNR
Susceptance, 562

T
Theta functions, 171
Tow-Thomas, 493
Transfer function, 1, 7
Transimpedance, 412
Transmission
distortionless, 5
ideal, 4, 5
without distortion, 4
Transmission function, 7, 267
Transmission parameters, *see* effective parameters
Transmission zeros, 2, 103

U
Universal filter, 497

V
Voltage follower, 416

W
WAF, *see* Wave active filters
Wave active filters, 394

Z
Zero shifting, 545